FACULTY OF SCIENCES

From Sequence-Defined Macromolecules To Macromolecular Pin Codes

Joshua O'Connor Holloway

Promotor:
Prof. Dr Filip Du Prez

Academic year 2018-2019

Submitted to the Faculty of Sciences of Ghent University, in fulfilment of the requirements for the degree of Doctor of Science: Chemistry

GHENT UNIVERSITY

FACULTY OF SCIENCES

From Sequence-Defined Macromolecules To Macromolecular Pin Codes

Joshua O'Connor Holloway

Promotor: Prof. Dr Filip Du Prez

Academic year 2018-2019

Submitted to the Faculty of Sciences of Ghent University, in fulfilment of the requirements for the degree of Doctor of Science: Chemistry

GHENT UNIVERSITY

Exam commission

Prof. Dr Sandra Van Vlierberghe (Chair, Ghent University)

Dr Remzi Becer (University of Warwick)

Prof. Dr Bruno De Geest (Ghent University)

Prof. Dr Johan Winne (Ghent University)

Prof. Dr Richard Hoogenboom (Ghent University)

Prof. Dr Filip Du Prez (Promotor, Ghent University)





This project has received funding from the European Union's Horizon 2020 research and innovation programme under the Marie Skłodowska-Curie grant agreement No *642083.*

This project was also partially funded by the Ghent University Special Research Fund-ITN (BOF-ITN).

"In the long history of humankind (and animal kind, too)
those who learned to collaborate and improvise
most effectively have prevailed"

Charles Darwin, scientist and Salopian

1809-1882

Acknowledgements

After nearly four years since I started my PhD, I now find myself writing the most important part of my whole thesis, as I finally get the opportunity to thank the large number of people who contributed in various ways towards this work. Naturally, I would like to first and foremost thank Filip Du Prez, firstly for giving me the opportunity to do my PhD in the Polymer Chemistry Research group and for all his support over the last four years and for making the PCR group a great place to work. I would also like to thank the members of the exam commission for taking the time to read and evaluate my thesis and for their constructive comments and suggestions which have undoubtedly improved the quality of this manuscript.

Amongst the many people to thank, top of the list is Hannes. Your support and friendship as a colleague, housemate and travelling partner has been so important over the last four years, helping me through the highs and lows of PhD life. Since sharing an apartment together, I will admit that you have probably done more than your fair share of the cooking and I will put it here in writing that it was always delicious (maar ik zou ook graag jouw mama bedanken voor het lekker eten zoals de vispannetjes en vol-au-vent als ik Waregem bezocht), although I hope that I have made that up to you by chauffeuring you around the many countries that we have visited together, from Australia to Canada as well as all around Europe. You have constantly been there to help me whenever I have been struggling with work, either by helping me out in the lab, correcting my writing or discussing with me whilst sharing a few drinks at home. Dus wil ik nog eens zeggen, bedankt voor alles en nog succes met jouw carrière ook!

Working in the PCR group, here at Ghent University, has been an incredible experience, which is in no small part thanks to all the fantastic people that work here. Whilst it is almost impossible to mention everyone in the group by name, I will do my best to thank as many of you as possible here. I would first like to thank Bernhard. He keeps everything in the group organised and working, from the GPCs to the coffee machine and keeps us entertained with unique jokes and humorous emails. I would also like to thank Bastiaan, not only for also keeping things running and help in the lab, but also for the good times we have shared together, particularly on the many holidays and trips with others from the group. Furthermore, I wish to thank Christian for the fun time we had sharing the apartment whilst Hannes was in Australia and nice travels together in Iceland along with Hannes and Bastiaan. My time in the PCR group has certainly provided me with the chance to enjoy many nice group trips, both for business and pleasure as the people that I have worked with have proved to be not only been fantastic colleagues but also great friends. Vooral bedankt aan Chiel, Hannes, Bastiaan, Maarten en Niels voor de zeer leuke

skivakanties! I wish to thank all those from the sequence-defined team, in particular Nezha, Steven, Chiel and Resat, for the help given during my PhD and the nice time working together and sharing a lab. Additionally, thanks to the rest of those who have worked with me in Lab 1, both past and present, for making it a fun place to work en dankzij Martijn, Stef, Hannes, Maarten en Niels voor de leuke sfeer terwijl wij een bureau gedeeld hebben. Last, but certainly not least, I would like to thank Nezha, who has given me so much help and support over the last four years. Since starting together in the PCR group back in September 2015, you have helped me whenever asked in the lab, with my writing and in giving much needed advice. Moreover, your corrections have certainly improved both my articles and this PhD manuscript. Merci encore pour tout ton aide!

One of the great things about working in an academic research group, is the chance to work alongside and collaborate with other researchers from around the world, which is something that I have had the pleasure of doing during my PhD. My thanks go to Susanne for the nice time working next to each other and socialising during the first months of my PhD. I would like to thank Suzan, for the very nice and fun collaborations both in Ghent and in London and many thanks Remzi and his group for hosting me for the short research stays in London. I wish to also thank Resat for his help during this collaboration. I would also like to thank Katharina for the great collaboration and fun time working together and for introducing me to the nice curves that one can only achieve when using GPC! In all these instances, I had not only a fantastic time working together but I also gained some great friends too.

Ik ben ook heel blij dat ik de kans gekregen heb om een master student te begeleiden. Dus wil ik zeker Filip Van Lysebetten (aka Filip Jr) bedanken voor al zijn harde werk dat tot een mooi hoofdstuk van deze thesis heeft geleid. Bedankt ook voor de goede tijd in het labo met al de grapjes (samen met Matthieu en Elias). Additionally, I would like to thank both Hannah and Görkem whom I guided during their internships and for the hard work that they put in.

Naast die van de PCR-groep, zijn er ook vele anderen binnen onze vakgroep die ik wil bedanken. Dus, bedankt aan Jan Goeman, Tim Courtin en Jos Van den Begin om de instrumenten te laten werken waar ons onderzoek van afhangt. Bedankt aan iedereen van de administratie (Veerle, Queenie, Carine, Christel, Paul en Domien) voor alles wat ze doen om het dagelijkse leven in onze vakgroep gemakkelijker te maken.

Eén van mijn beste prestaties tijdens mijn verblijf hier in België was de kans om een nieuwe taal te kunnen leren. Daardoor moet ik zeker mijn Nederlandse lesgever Tom bedanken, want dankzij jou kan ik nu elke dag in het Nederlands lezen, schrijven en spreken. J'ai aussi eu la chance d'améliorer mon français grâce à Céline et je pense que ce sera très utile pour ma future carrière et vie en Belgique ou mes futures vacances !

Finally, I would like to thank all of my friends and family for their support during my PhD. In particular, thanks to Mum and Dad for all your help in getting me this far in my career and for making the numerous trips across the Channel not just for a holiday but also to visit me! Thanks to the rest of my family and friends who have supported me throughout my PhD in many ways and have made the journey to come and visit me from time to time in Belgium, whether it be from the UK, Switzerland or elsewhere.

Bedankt allemaal et merci à tout le monde!

Josh

Table of contents

Chapter I: Introduction and outline **1**

I.1 Introduction **1**

I.2 Aims and objectives **3**

I.3 Thesis outline **5**

I.4 References **6**

Chapter II: Theoretical overview: Sequence-defined macromolecules **11**

II.1 Introduction **11**

II.2 Sequence-controlled or sequence-defined? **12**

II.3 The synthetic toolbox for sequence-defined macromolecules **13**

II.3.1 Solid-phase synthesis 14

II.3.2 Solution-phase synthesis 14

II.4 Biologically and synthetically inspired sequence-controlled and sequence-defined synthesis strategies **15**

II.4.1 Biologically inspired synthesis routes 15

II.4.2 Synthetic chain and step-growth sequence-controlled/defined synthesis strategies 18

II.5 Click and click-like reactions in sequence-defined synthesis **21**

II.5.1 Introduction 21

II.5.2 Copper(I)-catalysed azide/alkyne cycloaddition reactions 23

II.5.3 Diels-Alder reactions 26

II.5.4 Thiol-X reactions 28

II.5.5 Thiolactone reactions 30

II.6 Multicomponent reactions in sequence-defined synthesis **34**

II.6.1 Introduction 34

II.6.2 Passerini three component reaction 35

II.6.3 Ugi four component reaction 39

II.7 1,2,4-Triazoline-3,5-dione chemistry **41**

II.7.1 Introduction 41

II.7.2 Synthesis routes towards TAD molecules 42
II.7.2.1 Urazole synthesis 42
II.7.2.2 Oxidation of urazoles to corresponding TADs 49
II.7.3 Reactivity of TAD compounds 52
II.7.4 Current applications in polymer chemistry 53
II.7.5 Potential in sequence-defined synthesis 54
II.8 Conclusions 54
II.9 References 56

Chapter III: Tailored modification of thioacrylates in a sequence-defined procedure ... 73
III.1 Introduction 73
III.2 Results and discussion 74
III.2.1 NMR model studies 74
III.2.2 The synthetic protocol 77
III.2.3 Kinetic studies 78
III.2.4 Analysis of synthesised sequence defined oligomers 81
III.3 Conclusion and outlook 88
III.4 Experimental details 89
III.4.1 Materials and separation techniques 89
III.4.2 Analytical methods 90
III.4.3 Synthesis of functional thiolactone compounds 91
III.4.3.1 Synthesis of thiolactone carboxylic acid 91
III.4.3.2 Synthesis of α-thiolactone-γ-isocyanate 92
III.4.3.3 Synthesis of ethyl thioacrylate 93
III.4.4 Manipulation of the solid support and general synthetic procedure 94
III.4.4.1 Loading of the 2-chlorotrityl chloride polystyrene resin 94
III.4.4.2 Manipulation of the solid-phase resin 95
III4.4.3 General procedure of sequence-defined protocol 95
III.4.5 NMR model studies 96

III.4.5.1 Amidation model reaction in THF-d_8 and $CDCl_3$ 96
III.4.5.2 Catalysed model amidation reaction in THF-d_8 97
III.4.5.3 Online ^{1}H NMR study of the reaction between ethanolamine and ethyl acrylate 97
III.4.5.4 Online ^{1}H NMR study of the reaction between ethanolamine and ethyl thioacrylate 97
III.5 Additional data 98
III.5.1 HRMS and NMR data for monomers synthesised 98
III.5.2 HRMS and NMR data for the oligomers synthesised 104
III.6 References 108

Chapter IV: Automated synthesis protocol of sequence-defined oligo-urethane-amides using thiolactone chemistry 111
IV.1 Introduction 111
IV.2 Results and discussion 113
IV.2.1 The protocol 113
IV.2.2 Manual solid-phase synthesis 113
IV.2.3 Automated solid-phase synthesis 116
IV.2.4 Alternative resins and loading 118
IV.3 Conclusion and outlook 120
IV.4 Experimental details 121
IV.4.1 Chemicals 121
IV.4.2 Analytical methods 122
IV.4.3 Synthesis of functional thiolactone compounds 124
IV.4.3.1 Synthesis of thiolactone-carboxylic acid 124
IV.4.3.2 Synthesis of α-thiolactone-γ-isocyanate 124
IV.4.4 Loading of the resins with thiolactone carboxylic acid molecule 124
IV.4.4.1 Loading of the rink-amide resin 124
IV.4.4.2 Loading of the Wang resin 124
IV.4.4.3 Loading of the 2-chlorotrityl chloride resin 125

IV.4.5 General procedure for the manual synthesis of sequence-defined oligomers: Synthesis of oligomer 1 125

IV.4.5.1 General procedure for thiolactone aminolysis – manual protocol step 1 125

IV.4.5.2 General procedure for the addition of α-thiolactone-γ-isocyanate – manual protocol step 2 125

V.4.5.3 NMR and HRMS characterisation of oligomer 1 126

IV.4.6 General procedure for the automated synthesis of sequence-defined oligomers: Synthesis of oligomers 2, 3 & 4 128

IV.4.6.1 NMR and HRMS characterisation of oligomer 2 129

IV.4.7 NMR and HRMS characterisation of sequence-defined hexamer 3 and nonamer 4 synthesised *via* the automated procedure IV.4.6 130

IV.4.7.1 Oligomer 3 131

IV.4.7.1 Oligomer 4 131

IV.5 References 132

Chapter V: Triazolinedione meets thiolactone chemistry in the pursuit of sequence-defined macromolecules 135

V.1 Introduction 135

V.2 Results and discussion 137

V.2.1 Orthogonality model studies 137

V.2.2 TAD-thiolactone synthesis 140

V.2.3 Implementation of TAD-thiolactone within a sequence-defined protocol 143

V.2.4 Alternative routes to urazole thiolactone synthesis 147

V.3 Conclusion and outlook 149

V.4 Experimental details 150

V.4.1 Materials and separation techniques 150

V.4.2 Analytical methods 151

V.4.3 Synthesis of thiolactone and urazole functional building blocks 151

V4.3.1 Synthesis of thiolactone carboxylic acid 151

V.4.3.2 Synthesis of hexa-2,4-diene acrylate 152

V.4.3.3 Synthesis of 4-butyl TAD 152
V.4.3.4 Synthesis of 4(4-aminophenyl) urazole 153
V.4.3.5 Synthesis of thiolactone pentafluorophenol 154
V.4.3.6 Synthesis of thiolactone phenyl urazole 155
V.4.4 Synthesis of sequence-defined oligomer 1 156
V.4.4.1 Manipulation of the solid-phase resin 156
V.4.4.2 Loading of the 2-chlorotrityl chloride resin with sorbic alcohol[8] 157
V.4.4.3 General solid-phase protocol 158
V.4.5 Analysis of sequence-defined oligomer 1 159
V.4.5.1 NMR analysis of oligomer 1 159
V.4.5.2 HRMS analysis of oligomer 1 160
V.5 References 160

Chapter VI: Direct comparison of solution and solid-phase sequence-defined synthesis using a combined click chemistry and multicomponent reaction approach 165
VI.1 Introduction 165
VI.2 Results and discussion 168
VI.2.1 Synthesis of AB-type linker molecules 168
VI.2.2 Solid-phase approach 169
VI.2.3 Solution-phase approach 174
VI.3 Conclusion and outlook 177
VI.4 Experimental details 179
VI.4.1 Chemicals 179
VI.4.2 Analytical methods 180
VI.4.3 Synthesis of linker molecules 182
VI.4.3.1 Synthesis of diene-isocyanide, L1 182
VI.4.3.2 Synthesis of 1,2,4-triazoline-3,5-dione hexanoic acid (TAD-COOH), L2 185
VI.4.4 Solid-phase synthesis of sequence-defined oligomers 188
VI.4.4.1 Manipulation of the solid-phase resin 188

VI.4.4.2 Loading of the 2-chlorotrityl chloride resin 188
VI.4.4.3 General solid-phase synthesis protocol 188
VI.4.5 HRMS analysis of the solid-phase synthesised sequence-defined oligomers 190
VI.4.6 NMR analysis of the solid-phase synthesised sequence-defined oligomers 192
VI.4.7 Solution-phase synthesis of sequence-defined nonamer 196
VI.4.7.1 1st P-3CR 196
VI.4.7.2 1st TAD Diels-Alder reaction 196
VI.4.7.3 2nd P-3CR 196
VI.4.7.4 2nd TAD Diels-Alder reaction 197
VI.4.7.5 3rd P-3CR 197
VI.4.7.6 3rd TAD Diels-Alder reaction 197
VI.4.7.7 4th P-3CR 198
VI.4.7.8 4th TAD Diels-Alder reaction 198
VI.4.7.9 5th P-3CR 198
VI.4.7.10 5th TAD Diels-Alder reaction 199
VI.4.7.11 6th P-3CR 199
VI.4.7.12 6th TAD Diels-Alder reaction 199
VI.4.7.13 7th P-3CR 200
VI.4.7.14 7th TAD Diels-Alder reaction 200
VI.4.7.15 8th P-3CR 200
VI.4.7.16 8th TAD Diels-Alder reaction 201
VI.4.7.17 9th P-3CR 201
VI.4.8 SEC-ESI-MS analysis of solution phase sequence-defined nonamer 17 203
IV.5 References 203

Chapter VII: Dynamic sequence-defined macromolecular pin codes: The next generation of data encryption 207

VII.1 Introduction 207

VII.2 Results and discussion 210

VII.2.1 Sequence-defined protocol 211
VII.2.2 Synthesis of indole position markers 213
VII.2.3 Synthesis of a four-digit molecular pin code 213
VII.2.4 Encryption and decryption of molecular pin codes 216
VII.2.5 Incorporation of dynamic sequences onto polymer materials 221
VII.2.6 Solid-phase synthesis of molecular pin codes 224
VII.2.7 Expanding the chemical toolbox with the U-4CR 225
VII.3 Conclusion and outlook 226
VII.4 Experimental details 227
VII.4.1 Chemicals 227
VII.4.2 Analytical methods 228
VII.4.3 Synthesis of multicomponent reaction building blocks 230
VII.4.3.1 Synthesis of 1,2,4-triazoline-3,5-dione hexanoic acid (TAD-COOH) 230
VII.4.3.2 Synthesis of 2-(4-chlorophenyl)-1*H*-indole 231
VII.4.3.3 Synthesis of 2-(4-bromophenyl)-1*H*-indole 232
VII.4.3.3 Synthesis of 2-(3,5-dibromophenyl)-1*H*-indole 233
VII.4.3.4 Synthesis of morpholinum trifluoroacetate salt 234
VII.4.3.5 Synthesis of 3-(2-phenyl-1*H*-indol-3-yl) propanal 235
VII.4.3.6 Synthesis of 3-(2-(4-chlorophenyl)-1*H*-indol-3-yl) propanal 236
VII.4.3.7 Synthesis of 3-(2-(4-bromophenyl)-1*H*-indol-3-yl) propanal 237
VII.4.3.8 Synthesis of 3-(2-(3,5-dibromophenyl)-1H-indol-3-yl) propanal 238
VII.4.4 Solid-phase synthesis of sequence-defined oligomers *via* the P-3CR 239
VII.4.4.1 Loading of the 2-chlorotrityl chloride resin 239
VII.4.4.2 Synthesis of 4-(((2E,4E)-hexa-2,4-dien-1-yl)oxy)-4-oxobutanoic acid 239
VII.4.4.3 Loading of the Rink-Amide resin 240
VII.4.4.4 Capping the loaded Rink Amide resin 241
VII.4.4.5 Manipulation of the solid-phase resin 241
VII.4.4.6 General procedure of the solid-phase protocol 241
VII.4.5 Solution synthesis of sequence-defined oligomers *via* the P-3CR 243

VII.4.5.1 Synthesis of (2E, 4E)-hexa-2,4-dien-1-yl stearate starting block (**1**) 243
VII.4.5.2 1st TAD addition 244
VII.4.5.3 1st P-3CR 245
VII.4.5.3 2nd TAD addition 246
VII.4.5.4 2nd P-3CR 247
VII4.5.5 3rd TAD addition 248
VII.4.5.6 3rd P-3CR 249
VII.4.5.7 4th TAD addition 250
VII.4.5.8 4th 3-PCR 251
VII.4.6 Solution synthesis of sequence-defined oligomers *via* the U-4CR 252
VII.4.6.1 1st TAD addition 252
VII.4.6.2 1st U-4CR 253
VII.4.7 Encryption and decryption model studies 254
VII.4.7.1 Encryption model study 254
VII.4.7.2 Decryption model study 254
VII.5 References 256

Chapter VIII: Conclusion and outlook 259
VIII.1 Conclusion 259
VIII.2 Outlook and future work 264
VIII.3 References 266

Hoofdstuk IX: Nederlandstalige samenvatting 269
IX.1 Inleiding 269
IX.2 Overzicht van de resultaten 272
IX.3 Conclusie en vooruitblik 274
IX.4 Referenties 276

List of publications 280

Abbreviations

AcOH	Acetic acid
AIBN	Azobis(isobutyronitrile)
ADMET	Acyclic Diene Metathesis
APT	Attached Proton Test
Ar	Aromatic
ATRA	Atom Transfer Radical Addition
ATRC	Atom Transfer Radical Coupling
ATRP	Atom Transfer Radical Polymerisation
a.u.	Arbitrary Units
B	Base
B-3CR	Biginelli Three-Component Reaction
CDI	Carbonyldiimidazole
$CHCl_3$	Chloroform
COOH	Carboxylic acid
COSY	Correlation Spectroscopy
CuAAC	Copper-catalysed Azide-Alkyne Click
Đ	Polydispersity
DCM	Dichloromethane
DCC	Dicyclohexylcarbodiimide
DIC	Diisopropylcarbodiimide
DIPEA	Diisopropylethylamine
DMF	Dimethylformamide
DMPP	Dimethylphenylphosphine
DNA	Deoxyribonucleic acid
DP	Degree of Polymerisation
DPPA	Diphenylphosphoryl acid
DSC	Differential Scanning Calorimetry
EDG	Electron Donating Group
ESI-MS	Electrospray Ionisation Mass Spectroscopy
EWG	Electron Withdrawing Group
FRP	Free Radical Polymerisation
F-SPE	Fluorous Solid-Phase Extraction
FTIR	Fourier Transform Infrared
GPC	Gel Permeation Chromatography

HDI	1,6-hexamethylene diisocyanate
HMBC	Heteronuclear Multiple-Bond Correlation spectroscopy
HNO_3	Nitric acid
HOMO	Highest Occupied Molecular Orbital
HRMS	High Resolution Mass Spectroscopy
HSQC	Heteronuclear Single-Quantum Correlation spectroscopy
Hz	Hertz
IUPCA	International Union of Pure and Applied Chemistry
J	Coupling Constant
KOH	Potassium hydroxide
LUMO	Lowest Unoccupied Molecular Orbital
M_n	Average Molecular Weight
MALDI-TOF	Matrix Assisted Laser Desorption/Ionisation – Time of Flight
MDI	4,4'-Methylene diphenyl diisocyanate
MCR	Multicomponent Reactions
MeOH	Methanol
MEHQ	4-Methoxyphenol
Mpt	Melting Point
MUMI	Multiple Unit Monomer Insertion
MW	Molecular Weight
NBS	*N*-bromosuccinimide
NHS	*N*-hydroxysuccinimide
NIPAM	*N*-isopropylacrylamide
NMP	Nitroxide Mediated Polymerisation
NMR	Nuclear Magnetic Resonance
Nu	Nucleophile
p	*para*
P-3CR	Passerini Three-Component Reaction
PEG	Polyethylene glycol
PET-RAFT	Photoinduced Electron/Energy Transfer – Reversible Addition Fragmentation Chain-Transfer
PFP	Pentafluorophenol
Ph	Phenyl
PhTAD	4-Phenyl-1,2,4-triazoline-3,5-dione
pK_a	Logarithmic Acid Dissociation Constant
PMA	Phosphomolybdic acid
PNA	Peptide nucleic acid

PPA	Polyphosphoric acid
ppm	Parts per Million
RAFT	Reversible Addition Fragmentation Chain-Transfer
R_F	Retention Factor
ROMP	Ring Opening Metathesis Polymerisation
RNA	Ribonucleic acid
SET-LRP	Single Electron Transfer - Living Radical Polymerisation
SEC	Size Exclusion Chromatography
SUMI	Single-Unit Monomer Insertion
TAD	1,2,4-Triazoline-3,5-dione
TCICA	Trichloroisocyanuric acid
TFA	Trifluoroacetic acid
T_d	Degradation Temperature
T_g	Glass Transition Temperature
TGA	Thermogravimetric Analysis
THF	Tetrahydrofuran
TLC	Thin Layer Chromatography
U-4CR	Ugi Four-Component Reaction

Chapter I
Introduction and outline

I.1 Introduction

In 1907, the development of world's first fully synthetic polymer - a phenolic-formaldehyde resin marketed as Bakelite® - by Ghent University alumnus, Leo Bakeland,[1] was the beginning of what is recognised today as the hugely important research field of polymer chemistry, which now underpins an enormous global industry. We use daily a vast quantity of polymer material, mostly in the form of packaging, but also in more complex and demanding applications such as within complicated electricals, personal transport and even in medical applications. As a result, the polymer industry is nowadays producing more than 340 million tonnes of plastic per year to satisfy the ever-increasing demand. This represents a vital part of the economy in Belgium and as such, intense research continues across our companies and universities, including here, at Ghent University.

The last 30 years has seen a great evolution in polymer chemistry research, from the synthesis of simple bulk materials, comprised of a simple, linear chain of monomers, to more complex and diverse structures such as block copolymers, graft polymers and dendrimers.[2] Whilst historically, many polymers were often synthesised *via* step-growth polymerisation or Free Radical Polymerisation (FRP), this gave little consideration to molecular weight, dispersity and structure.[3,4] However, the discovery of an number of living or radical polymerisations,[4–7] (*e.g.* Nitroxide Mediated Polymerisation (NMP),[8] Atom Transfer Radical Polymerisation (ATRP)[9,10] and Reversible Addition Fragmentation Transfer Polymerisation (RAFT)[11]), facilitated a breakthrough in polymer synthesis and an explosion in polymer chemistry research, leading to many more complex and interesting macromolecular structures.[2]

However, in comparison to the many biopolymers that occur in Nature, there is still quite some way to go for synthetic polymers to reach the same levels of control and precision. Arguably the most well-known biopolymer is deoxyribonucleic acid (DNA).[12] This highly complex, information-carrying biopolymer where the order and position of monomer units is precisely controlled, has a defined primary structure which contains our genetic code. The precise length and order of the monomer units within the strands of DNA, influences its structure-property relationships and is what gives it its remarkable ability to store vast amounts of genetic information.[13–17] In fact, it can be thought of as a biological hard drive. Within Nature, precise, folded biomacromolecules which act as biological catalysts (*i.e.*

enzymes) are yet another example of how careful biomacromolecular design can have a profound effect.[18] It is from the precision demonstrated in Nature with regard to macromolecular design that many chemists are now drawing their inspiration.[13–16,19–22] Researchers hope that through the exploration of how controlled macromolecular structure could affect properties, new and advanced applications of polymer science could be discovered and our understanding enhanced.[14,15,18,22]

First widely introduced to polymer chemistry in 2005,[21] and later cemented in 2010,[19] the desire to synthetically mimic Nature in terms of macromolecular control and design has led to the introduction of the field of *sequence control* within the area of polymer chemistry. Researchers have to date used a plethora of techniques to explore higher levels of control in macromolecular synthesis. This has been investigated not only through the use of bio-inspired reactions,[23–27] but also by a combination of efficient and chemoselective reactions.[22,28–30] Through this careful and selective design of macromolecules, potential applications have been explored, such as enhanced data storage,[31] anti-counterfeiting and product tagging,[32–35] antibacterial advances,[36] improved pharmaceuticals[37] or catalysis.[38,39] It is also hoped that, as can be observed in Nature, one can synthetically influence conformational properties such as folding and self-assembly.[14,15,18]

Within the umbrella term of sequence control, two subclasses have developed within this field: *sequence-controlled* and *sequence-defined macromolecules*. Whilst there are differences between their synthesis, levels of structural precision and applications (as further elaborated upon in Chapter II.2),[14,15,22,40] they have both seen keen interest from researchers and have both been significantly advanced by the introduction of "click" chemistry.[41] This name is given only to the most efficient and selective chemical reactions that satisfy a set of stringent criteria and has revolutionised chemical science.[42–46] The founders of click chemistry also took their lead from Nature, introducing these reactions as ones that *"...must be modular, wide in scope, give very high yields, generate only inoffensive by-products that can be removed by nonchromatographic methods, and be stereospecific (but not necessarily enantio- selective). The required process characteristics include simple reaction conditions (ideally, the process should be insensitive to oxygen and water), readily available starting materials and reagents, the use of no solvent or a solvent that is benign (such as water) or easily removed, and simple product isolation. Purification if required must be by nonchromatographic methods, such as crystallization or distillation, and the product must be stable under physiological conditions."*[41] Over time, the requirements of click chemistry have been further expanded to better fit to polymer chemistry.[47,48] The precise and often iterative nature of sequence-controlled and sequence-defined synthesis approaches, means that click chemistry, along with other highly efficient reactions ("click-like" or "click-inspired" chemistries) has become crucial within this field.[28,29]

Within the Polymer Chemistry Research group, here at Ghent University, two key click and click-like chemistries have been intensively explored in recent years: 1,2,4-triazoline-3,5-dione (TAD) and γ-thiolactone. Thiolactone chemistry has been reviewed[49,50] and explored by our research group within the context of polymer synthesis and modification[51–57] and more recently in the field of sequence-defined synthesis.[31,40,58–64] Thiolactone chemistry has presented itself as a highly efficient tool for sequence-defined synthesis on account of its ability to undergo a one-pot, double modification reaction.[49] This can be achieved by ring-opening the thiolactone with a primary amine, whereby the released thiol can undergo an immediate Michael addition with an acrylic group. Such a reaction is known as an amine-thiolactone-ene conjugation,[65] and has been explored within the research group in combination with solid-phase chemistry,[66] for the design of iterative protocols, yielding multi-functional, sequence-defined oligomers. This has eventually led to advances being made towards applications in data storage.[31] Within this thesis, the use of thiolactones in combination with solid-phase chemistry was further explored, in order to investigate the incorporation of alternative acrylics[64] and the use of alternative functional handles through which sequence-definition was introduced in both a manual and automated fashion.[63] Whilst TAD chemistry was discovered in 1894,[67] it was not until more than 50 years later that Cookson *et. al.* developed it extensively,[68–70] successfully isolating 4-phenyl-1,2,4-triazoline-3,5-dione. In 2014, our research group published the results of our first work with TADs.[71] Since then, this remarkable chemistry has been the focus of much research within our group as TAD chemistry holds much potential to polymer synthesis and modification.[71–79] TAD moieties can undergo ultrafast click reactions with a wide range of substrates, although the substrate and conditions have an effect upon the speed of the reaction.[72] Moreover, the reaction of TAD is accompanied by a visual feedback as the TAD substrate is red in colour but the adducts that it forms upon reaction are colourless.[72] The two key reactions which were explored in this thesis were the Diels-Alder reaction with a conjugated diene and the thermoreversible Alder-ene reaction with substituted indoles. Within this PhD thesis, TAD chemistry was introduced to the field of sequence control for the first time and enabled the development of new, sequence-defined synthesis protocols using functional TAD molecules and the Passerini and Ugi multicomponent reactions.[80,81]

I.2 Aims and objectives

The primary aim of this thesis was in the first instance to develop iterative protocols for the synthesis of sequence-defined oligomers. The starting point for this work was the use of thiolactone chemistry as the chemical handle and solid-phase as the tool for carrying out the synthesis as this had been published by our group.[59,60] Therefore, the protocol published by Martens *et. al.* (discussed in detail in Chapter II.5.5),[60] provided the first ideas to this PhD project, as this work introduced an automated, two-step,

solid-phase protocol, where the thiolactone unit was opened using an amino-alcohol and a range of acrylates were used to introduce sequence definition. Therefore, in this PhD, initially a variation of this protocol was investigated, using an alcohol functionalised acrylamide as both the Michael acceptor and chain-extender and commercially available primary amines to introduce the sequence functionality. This was also explored in both a manual and automated fashion in order to compare and contrast the two approaches (Chapter IV).[63] Concurrently, an alternative thiolactone-based four-step, iterative protocol was developed in collaboration with the Polymer Chemistry Laboratory, Queen Mary, University of London (Chapter III). Here, the incorporation of thioacrylates as an alternative class of acrylics was investigated along with their modification with primary amines.[64,82]

Existing expertise within our research group prompted the idea of combining TAD and thiolactone chemistry to develop an improved iterative protocol for sequence-defined synthesis. This presented a unique challenge to synthesise one molecule containing both functionalities. It was hoped that the easy double modification of thiolactone, combined with the ultrafast reactions of TAD would mean that this would far outstrip existing protocols, which were reliant on thiolactone isocyanate (often the slowest step in the protocol)[60] to reinstall the thiolactone functionality each time. However, difficulties experienced during this project, both in the synthesis of a TAD thiolactone molecule and the sequence-defined oligomer synthesis too, guided us more towards a solely TAD-based protocol.

Therefore, in a collaborative approach with the Karlsruhe Institute for Technology, Germany (KIT), TAD chemistry was combined with the Passerini three-component reaction (P-3CR), which was already a well-reported tool in sequence-defined chemistry,[83,84] to develop a new, two-step protocol. The objective was also to compare carrying out the same synthetic protocol both using solid-phase chemistry as well as in solution, as it was felt that whilst both techniques were widely used in the area of sequence-defined synthesis, a full comparison to highlight the advantages and disadvantages of both was lacking.

The final, more application orientated objective of this PhD thesis was to use the thermoreversible nature of the TAD-indole reaction to synthesise dynamic, sequence-defined tetramers. The synthesis of short oligomers was investigated with the potential application of product tagging and anti-counterfeiting in mind. The success of the collaborative protocol developed with KIT, meant that TAD in combination with multicomponent reactions was a logical choice. The aim was to synthesise code-carrying tetramers, which upon heating, would cause the disassociation of the TAD-indole bonds, liberating the four monomers, which would then form a disperse mixture of oligomers, scrambling the code and permanently encrypting the information. Upon heating again, in the presence of a conjugated

diene, the four different TAD moieties could be released and upon cooling would react irreversibly with the diene, forming 4 monomers, whose original order would only be readable to the desired person.

I.3 Thesis outline

Chapter II: This chapter introduces the development of polymer science, from its very beginnings to the introduction of controlled radical polymerisation techniques and how chemists have now delved beyond this to synthesise macromolecules of unprecedent structure and design, directly challenging what has until recently only been observed in Nature. Furthermore, within this chapter, the area of sequence-control is better defined by introducing and highlighting the differences between the two subclasses of macromolecules that exist within this field. The synthetic toolbox available to the sequence-defined chemist is introduced, with the differences between solid-phase and solution-phase synthesis and synthesis with and without a support discussed. As can be expected within this field, where inspiration has been drawn from Nature, a wide range of biologically inspired synthesis strategies are highlighted. The chapter then moves to discuss click and click-like chemistries and multicomponent reactions and their use within sequence-defined synthesis. Finally, TAD chemistry is introduced, from its synthesis to its remarkable reactivity and potential applications in polymer science today.

Chapter III: A collaborative project with Queen Mary, University of London, is introduced here, where thioacrylate chemistry was combined with thiolactone chemistry to enable us to develop an iterative protocol for the synthesis of multifunctional sequence-defined oligomers. The reactivity of thioacrylates in comparison to acrylates was studied along with their catalysed modification with primary amines. The unique reactivity of thioacrylates dictated the way the sequence-defined protocol was constructed and hence this was a four-step approach.[64]

Chapter IV: This chapter reports our continued efforts towards fully exploring the use of thiolactone chemistry for the development of solid-phase, sequence-defined synthesis protocols with an improved approach compared to the one described in Chapter III. Here, varying primary amines were directly incorporated into the sequence-defined protocol without the need for thioacrylate modification, thus reducing this to a two-step approach. Furthermore, the automation of this protocol is explored, using an adapted peptide synthesiser. Moreover, the manual and automated synthesis approaches are compared. A range of resins were used, although the resin of primary focus in this research was the rink-amide resin.[63]

Chapter V: TAD chemistry was combined with thiolactone chemistry in this chapter, with the synthesis of a TAD-thiolactone functionalised molecule. In the resulting protocol, sequence definition was again introduced by thiolactone aminolysis, but the reintroduction of new thiolactone units was *via* the TAD-

thiolactone molecule, thus rapidly decreasing the time required for this step. The challenging synthesis and implementation of the TAD-thiolactone molecule is discussed in detail.

Chapter VI: TAD chemistry was further implemented, but this time in combination with the Passerini three-component reaction (P-3CR). The synthesis of a TAD-carboxylic acid (TAD-COOH) molecule and a diene-functionalised isocyanide enabled a two-step, click-multicomponent protocol to be designed. This was carried out in tandem both on the solid-phase and in solution, allowing a direct comparison of the same chemistry being carried out using two different methods. High molecular weight (>7 kDa), monodisperse, sequence-defined oligomers resulted from both approaches, and they were compared in terms of yield, purity, scale, degree of polymerisation, purification and time.[40]

Chapter VII: Through the success of the work discussed in Chapter VI, the combination of TAD chemistry and multicomponent reactions was used to synthesise dynamic, thermoreversible, sequence-defined oligomers. Isocyanides were used to write the sequence-defined code when reacted together with TAD-COOH and indole-aldehydes in a P-3CR. As a result, TAD-indole chemistry was used because its thermoreversible nature meant that the oligomer could be heated and scrambled and only read back by those who knew the original order of the different indole marker compounds that were used. In addition to the P-3CR, the Ugi four-component reaction (U-4CR) was explored to introduce a double modification of each monomer in the sequence, thus exponentially increasing the potential amount of information that could be encoded. Solution phase synthesis was chosen as the primary synthetic tool in this work, enabling the scalable synthesis of oligomers. Therefore, their use on the surface of polymer banknotes was investigated to demonstrate the advantage of such a sequence-defined oligomer in product tagging and anti-counterfeiting applications.

Chapter VIII: A conclusion and outlook on the work carried out during this PhD is given, focusing on what were considered to be the most important results of this thesis and how they should be carried forward by future researchers working on this topic.

Chapter IX: A summary of this thesis is given in Dutch.

I.4 References

1 L. H. Baekeland, *J. Ind. Eng. Chem.*, 1909, **1**, 149–161.

2 J.-F. Lutz, J.-M. Lehn, E. W. Meijer and K. Matyjaszewski, *Nat. Rev. Mater.*, 2016, **1**, 1–14.

3 G. Odian, *Principles of polymerization*, Wiley-Interscience, 4th edn., 2004.

4 K. Matyjaszewski and T. P. Davis, Eds., *Handbook of Radical Polymerization*, John Wiley & Sons, 2003.

5 K. Matyjaszewski, *Advances in Controlled/Living Radical Polymerization*, American Chemical Society, Vol. 854., 2003.

6 W. A. Braunecker and K. Matyjaszewski, *Prog. Polym. Sci.*, 2007, **32**, 93–146.

7 K. Matyjaszewski, *Curr. Opin. Solid State Mater. Sci.*, 1996, **1**, 769–776.

8 G. Moad, E. Rizzardo and D. H. Solomon, *Macromolecules*, 1982, **15**, 909–914.

9 J.-S. Wang and K. Matyjaszewski, *J. Am. Chem. Soc.*, 1995, **117**, 5614–5615.

10 M. Kato, M. Kamigaito, M. Sawamoto and T. Higashimura, *Macromolecules*, 1995, **28**, 1721–1723.

11 John Chiefari, Y. K. (Bill) Chong, Frances Ercole, Julia Krstina, Justine Jeffery, Tam P. T. Le, Roshan T. A. Mayadunne, Gordon F. Meijs, Catherine L. Moad, G. Moad, E. Rizzardo and S. H. Thang, *Macromolecules*, 1998, **31**, 5559–5562.

12 J. D. Watson and F. H. C. Crick, *Nature*, 1953, **171**, 737–738.

13 J.-F. Lutz, T. Y. Meyer, M. Ouchi and M. Sawamoto, Eds., *Sequence-Controlled Polymers: Synthesis, Self-Assembly and Properties*, American Chemical Society, Washington DC, 2014.

14 J.-F. Lutz, *Macromol. Rapid Commun.*, 2017, **1700582**, 1–12.

15 J.-F. Lutz, in *Sequence-Controlled Polymers*, ed. J.-F. Lutz, Wiley VCH, Weinheim, 1st edn., 2018, pp. 1–26.

16 H. M. Colquhoun and J.-F. Lutz, *Nat. Chem.*, 2014, **6**, 455–456.

17 J.-F. Lutz, *Macromolecules*, 2015, **48**, 4759–4767.

18 M. A. R. Meier and C. Barner-Kowollik, *Adv. Mater.*, 2019, **31**, 1806027.

19 J.-F. Lutz, *Polym. Chem.*, 2010, **1**, 55–62.

20 N. Badi and J.-F. Lutz, *Chem. Soc. Rev.*, 2009, **38**, 3383–3390.

21 C. J. Hawker and K. L. Wooley, *Science*, 2005, **309**, 1200–1205.

22 J. A. De Neve, J. J. Haven, L. Maes and T. Junkers, *Polym. Chem.*, 2018, **9**, 4692–4705.

23 E. R. Kay and D. A. Leigh, *Angew. Chemie Int. Ed.*, 2015, **54**, 10080–10088.

24 J.-F. Ayme, J. E. Beves, D. A. Leigh, R. T. McBurney, K. Rissanen and D. Schultz, *Nat. Chem.*, 2012, **4**, 15–20.

25 S. N. Semenov, L. J. Kraft, A. Ainla, M. Zhao, M. Baghbanzadeh, V. E. Campbell, K. Kang, J. M. Fox and G. M. Whitesides, *Nature*, 2016, **537**, 656–660.

26 P. J. Bracher, P. W. Snyder, B. R. Bohall and G. M. Whitesides, *Orig. Life Evol. Biosph.*, 2011, **41**, 399–412.

27 V. R. Pattabiraman and J. W. Bode, *Nature*, 2011, **480**, 471–479.

28 S. Martens, J. O. Holloway and F. E. Du Prez, *Macromol. Rapid Commun.*, 2017, **38**, 1700469.

29 S. Martens, J. O. Holloway and F. E. Du Prez, in *Sequence-Controlled Polymers*, ed. J.-F. Lutz, Wiley VCH, Weinheim, 2018, pp. 379–416.

30 S. C. Solleder, R. V. Schneider, K. S. Wetzel, A. C. Boukis and M. A. R. Meier, *Macromol. Rapid Commun.*, 2017, **38**, 1600711.

31 S. Martens, A. Landuyt, P. Espeel, B. Devreese, P. Dawyndt and F. E. Du Prez, *Nat. Commun.*, 2018, **9**, 4451.

32 D. Karamessini, S. Poyer, L. Charles and J.-F. Lutz, *Macromol. Rapid Commun.*, 2017, **38**, 1700426.

33 U. S. Gunay, B. E. Petit, D. Karamessini, A. Al Ouahabi, J. A. Amalian, C. Chendo, M. Bouquey, D. Gigmes, L. Charles and J.-F. Lutz, *Chem*, 2016, **1**, 114–126.

34 D. Karamessini, T. Simon-yarza, S. Poyer, E. Konishcheva, L. Charles, D. Letourneur and J.-F. Lutz, *Angew. Chemie Int. Ed.*, 2018, **57**, 10574–10578.

35 A. C. Boukis, K. Reiter, M. Frölich, D. Hofheinz and M. A. R. Meier, *Nat. Commun.*, 2018, **9**, 1439.

36 M. Porel, D. N. Thornlow, C. M. Artim and C. A. Alabi, *ACS Chem. Biol.*, 2017, **12**, 715–723.

37 C. Lawatscheck, M. Pickhardt, A. Grafl, K. Linkert, F. Polster, E. Mandelkow and H. G. Börner, *Macromol. Biosci.*, 2017, **17**, 1700109.

38 L. Hartmann and H. G. Börner, *Adv. Mater.*, 2009, **21**, 3425–3431.

39 P. Chandra, A. M. Jonas and A. E. Fernandes, *J. Am. Chem. Soc.*, 2018, **140**, 5179–5184.

40 J. O. Holloway, K. S. Wetzel, S. Martens, F. E. Du Prez and M. A. R. Meier, *Polym. Chem.*, 2019, **10**, 3859–3867.

41 H. C. Kolb, M. G. Finn and K. B. Sharpless, *Angew. Chemie - Int. Ed.*, 2001, **40**, 2004–2021.

42 B. Helms, J. L. Mynar, C. J. Hawker and J. M. J. Fréchet, *J. Am. Chem. Soc.*, 2004, **126**, 15020–15021.

43 N. V. Tsarevsky, K. V. Bernaerts, B. Dufour, F. E. Du Prez and K. Matyjaszewski, *Macromolecules*, 2004, **37**, 9308–9313.

44 P. Wu, A. K. Feldman, A. K. Nugent, C. J. Hawker, A. Scheel, B. Voit, J. Pyun, J. M. J. Fréchet, K. B. Sharpless and V. V. Fokin, *Angew. Chemie Int. Ed.*, 2004, **43**, 3928–3932.

45 D. D. Díaz, S. Punna, P. Holzer, A. K. McPherson, K. B. Sharpless, V. V. Fokin and M. G. Finn, *J. Polym. Sci. Part A Polym. Chem.*, 2004, **42**, 4392–4403.

46 W. H. Binder and C. Kluger, *Macromolecules*, 2004, **37**, 9321–9330.

47 C. Barner-Kowollik, F. E. Du Prez, P. Espeel, C. J. Hawker, T. Junkers, H. Schlaad and W. Van Camp, *Angew. Chemie Int. Ed.*, 2011, **50**, 60–62.

48 P. Espeel and F. E. Du Prez, *Macromolecules*, 2015, **48**, 2–14.

49 P. Espeel and F. E. Du Prez, *Eur. Polym. J.*, 2015, **62**, 247–272.

50 P. Espeel and F. E. Du Prez, in *Multicomponent and Sequential Reactions in Polymer Science*, ed. P. Theato, Springer, Switzerland, 2015, pp. 105–132.

51 M. M. Stamenović, P. Espeel, E. Baba, T. Yamamoto, Y. Tezuka and F. E. Du Prez, *Polym. Chem.*, 2013, **4**, 184–193.

52 D. Frank, P. Espeel, S. Claessens, E. Mes and F. E. Du Prez, *Tetrahedron*, 2016, **72**, 6616–6625.

53 P. Espeel, F. Goethals, M. M. Stamenović, L. Petton and F. E. Du Prez, *Polym. Chem.*, 2012, **3**, 1007–1015.

54 S. Reinicke, P. Espeel and F. E. Du Prez, *Polym. Chem.*, 2014, **5**, 5461–5470.

55 F. Driessen, S. Martens, B. De Meyer, F. E. Du Prez and P. Espeel, *Macromol. Rapid Commun.*, 2016, **37**, 947–951.

56 G. B. Desmet, D. R. D'hooge, M. K. Sabbe, G. B. Marin, F. E. Du Prez, P. Espeel and M. F. Reyniers, *J. Org. Chem.*, 2015, **80**, 8520–8529.

57 D. Van Lysebetten, S. Felissati, E. Antonatou, L. Carrette, P. Espeel, E. Foquet, F. E. Du Prez and A. Madder, *ChemBioChem*, 2018, **19**, 641–646.

58 S. C. Solleder, S. Martens, P. Espeel, F. E. Du Prez and M. A. R. Meier, *Chem. - A Eur. J.*, 2017, **23**, 13906–13909.

59 P. Espeel, L. L. G. Carrette, K. Bury, S. Capenberghs, J. C. Martins, F. E. Du Prez and A. Madder, *Angew. Chemie - Int. Ed.*, 2013, **52**, 13261–13264.

60 S. Martens, J. Van Den Begin, A. Madder, F. E. Du Prez and P. Espeel, *J. Am. Chem. Soc.*, 2016, **138**, 14182–14185.

61 S. Celasun, D. Remmler, T. Schwaar, M. G. Weller, F. E. Du Prez and H. G. Börner, *Angew. Chemie Int. Ed.*, 2018, **58**, 1960–1964.

62 S. Celasun, F. E. Du Prez and H. G. Börner, *Macromol. Rapid Commun.*, 2017, **38**, 1700688.

63 J. O. Holloway, C. Mertens, F. E. Du Prez and N. Badi, *Macromol. Rapid Commun.*, 2019, **40**, 1800685.

64 J. O. Holloway, S. Aksakal, F. E. Du Prez and C. Remzi Becer, *Macromol. Rapid Commun.*, 2017, **38**, 1700500.

65 S. Martens, Ghent University, 2019.

66 R. B. Merrifield, *J. Am. Chem. Soc.*, 1963, **85**, 2149–2154.

67 J. Thiele and O. Stange, *Justus Liebig's Ann. der Chemie*, 1894, **283**, 1–46.

68 R. C. Cookson, S. S. H. Gilani and I. D. R. Stevens, *J. Chem. Soc. C*, 1967, 1905–1909.

69 R. C. Cookson, S. S. H. Gilani and I. D. R. Stevens, *Tetrahedron Lett.*, 1962, **3**, 615–618.

70 R. C. Cookson, S. S. Gupte, I. D. R. Stevens and C. T. Watts, *Org. Synth.*, 1971, **51**, 121–127.

71 S. Billiet, K. De Bruycker, F. Driessen, H. Goossens, V. Van Speybroeck, J. M. Winne and F. E. Du Prez, *Nat. Chem.*, 2014, **6**, 815–821.

72 K. De Bruycker, S. Billiet, H. A. Houck, S. Chattopadhyay, J. M. Winne and F. E. Du Prez, *Chem. Rev.*, 2016, **116**, 3919–3974.

73 N. Van Herck and F. E. Du Prez, *Macromolecules*, 2018, **51**, 3405–3414.

74 O. Türünç, S. Billiet, K. De Bruycker, S. Ouardad, J. M. Winne and F. E. Du Prez, *Eur. Polym. J.*, 2015, **65**, 286–297.

75 G. Becker, L. Vlaminck, M. M. Velencoso, F. E. Du Prez and F. R. Wurm, *Polym. Chem.*, 2017, **8**, 4074–4078.

76 O. Roling, K. De Bruycker, B. Vonhören, L. Stricker, M. Körsgen, H. F. Arlinghaus, B. J. Ravoo and F. E. Du Prez, *Angew. Chemie - Int. Ed.*, 2015, **54**, 13126–13129.

77 S. Chattopadhyay and F. E. Du Prez, *Eur. Polym. J.*, 2016, **81**, 77–85.

78 H. A. Houck, K. De Bruycker, S. Billiet, B. Dhanis, H. Goossens, S. Catak, V. Van Speybroeck, J. M. Winne and F. E. Du Prez, *Chem. Sci.*, 2017, **8**, 3098–3108.

79 H. A. Houck, F. E. Du Prez and C. Barner-Kowollik, *Nat. Commun.*, 2017, **8**, 1869.

80 M. Passerini, *Gazz. Chim. Ital.*, 1921, **51**, 126–129.

81 I. K. Ugi, *Angew. Chemie*, 1959, **71**, 373–388.

82 S. Aksakal and C. R. Becer, *Polym. Chem.*, 2016, **7**, 7011–7018.

83 S. C. Solleder and M. A. R. Meier, *Angew. Chemie - Int. Ed.*, 2014, **53**, 711–714.

84 S. C. Solleder, D. Zengel, K. S. Wetzel and M. A. R. Meier, *Angew. Chemie - Int. Ed.*, 2016, **55**, 1204–1207.

Abstract

Whilst the field of polymer chemistry has grown exponentially over recent decades, one particular area that, until recently, received little to no attention was the synthesis of precisely defined macromolecular structures. Advances in controlled polymerisation techniques have led to the synthesis of more controlled polymeric architectures with a narrow dispersity, but compared to natural biopolymers, such as DNA, these still lack a certain amount of precision. As such, the last decade has seen more and more research attention shift towards the synthesis of so-called sequence defined macromolecules. These are monodisperse macromolecules, often synthesised *via* iterative synthesis techniques. This chapter focuses on introducing the wealth of different techniques and chemistries used to synthesise these macromolecules, with particular focus on click, click-like and multicomponent reactions and the introduction of thiolactone and 1,2,4-triazoline-3,5-dione chemistries.

Parts of this chapter have been discussed in the following review:

S. Martens, J. O. Holloway and F. E. Du Prez, *Macromol. Rapid. Comm.*, 2017, **38**, 1700469.

Chapter II
Theoretical overview: Sequence-defined macromolecules

II.1 Introduction

In 1907, Leo Baekeland, who began his scientific career at Ghent University, developed the world's first synthetic polymer – Bakelite.[1] A phenolic-formaldehyde resin whose unique material properties at the time meant that it rapidly became a commercial success and as such, the field of synthetic polymer chemistry was born. Since then, polymer chemistry has continued to grow exponentially, as consumer demand has increased rapidly over recent decades. Today polymer chemistry sits at the forefront of science and represents a large global industry. Research in this field has expanded and evolved too, with countless different polymers developed to satisfy an ever-growing demand for materials of unprecedented structure and design as they are used in more and more ever-changing applications.[2]

Traditionally, the synthesis of many commercial, bulk polymers was carried out via step-growth (such as in the case of Bakelite) or chain-growth polymerisations (e.g. Free Radical Polymerisation - FRP). Although more complex polymer architectures can be obtained *via* these routes, these types of polymerisations typically gave little control with respect to average molecular weight, dispersity and chain structure.[3,4] However, one of the major advancements in polymer science has been the development of living or controlled polymerisation techniques,[4–7] (ionic polymerisations and Reversible Deactivation Radical Polymerisations - RDRP). Three key examples of these RDRP techniques are Nitroxide Mediated Polymerisation (NMP),[8] Atom Transfer Radical Polymerisation (ATRP)[9,10] and Reversible Addition Fragmentation Transfer Polymerisation (RAFT),[11] and were developed between 1982 and 1998. These methods all proceed *via* different mechanistic routes but have all led the way towards more control in polymer architectures. The resulting structures from these polymerisations have a much more controlled and defined average molecular weight and a narrower dispersity (Đ = ca. <1.3). They also present themselves as interesting polymerisation techniques, which have allowed the direct polymerisation and incorporation of many functional monomers,[12] the synthesis of a wide range of structures in addition to the classical linear topology and higher control over the polymer end group.[13,14]

However, when one considers the concept of controlled polymerisations and macromolecular synthesis, then one should look no further than to Nature. Highly complex biopolymers are present throughout the

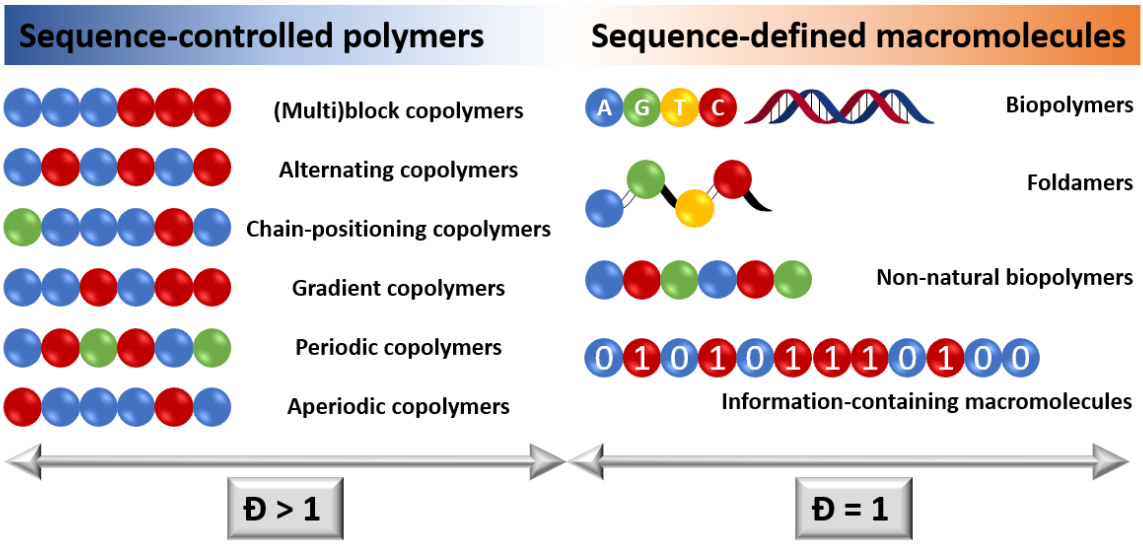
natural world and the most celebrated of these is arguably DNA[15] alongside other biologically important macromolecules such as RNA and proteins. This highly complex chain of coded, sequenced monomers contains all the vital genetic information that defines who we are, as well as having a strong influence on structure-property relationships.[16] It is from this very concept that polymer chemists worldwide are drawing their inspiration to develop the next generation of highly controlled macromolecules.[16–23]

Although first highlighted to Hawker and Wooley in 2005,[20] it was further emphasised by Jean-François Lutz in 2010 that sequence-controlled polymerisations hold the potential to be the next "holy grail" in polymer chemistry.[18] Indeed, since then, polymer chemists have strived to synthesise (complex) macromolecules which can now rival natural biopolymers in terms of their precise, sequenced order of monomers within the polymer chain through various strategies, many of which will be highlighted within this chapter. This tailored synthesis of macromolecules is enabled through a series of highly efficient and chemoselective reactions,[24,25] often *via* biologically inspired chemistries.[26–30] Today, the field of sequence-controlled chemistry has developed into one of the hot-topics of polymer chemistry and as a result of this, new applications of polymer science are now on the horizon.

II.2 Sequence-controlled or sequence-defined?

When discussing the area of sequence-controlled polymers, it is important to distinguish between two pieces of terminology. The two different terms of *"sequence-controlled"* and *"sequence-defined"* which are used to describe macromolecules within this field, are sometimes used interchangeably, although they have subtle but distinct differences (see *Scheme II.1*).[21–23,31] Sequence-controlled refers to macromolecules/polymers which have control to a greater extent than other polymers. The sequenced order of monomers is typically regulated, such as in aperiodic polymers (where the monomer sequence distribution is irregular but follows the same pattern in all chains),[32] yet the resulting structure is disperse as a result of synthesis *via*, for example, RDRP techniques.[21–23,31,33] The latter, sequence-defined, is the more precise of the two as it describes macromolecules of one discrete chain length, which have a perfectly controlled sequence of monomers and it is clear where exactly along the macromolecular chain a particular functionality is situated.[21–23,31] The majority of sequence-defined macromolecules tend to be the length of oligomers as opposed to polymers as a result of the limits of current iterative synthesis approaches,[31] although the synthesis of a sequence-defined polymer with a DP of over 100 using a DNA synthesiser was reported by Lutz and co-workers.[34] Whilst some arguably describe sequence-defined macromolecules as a subclass of sequence-controlled polymers,[21,22] others (and also within this thesis) class them separately because of their differing synthesis routes and potential applications.

The work presented within this thesis focuses on the synthesis of *sequence-defined macromolecules*, primarily from click and similarly efficient chemistries, using iterative synthesis approaches. This doctoral work was carried out within the framework of the "*Eurosequences*" European Union Innovative Training Network (ITN), comprising of 15 researchers across 8 European universities together with PSA Peugeot-Citroën (France) and Ionera (Freiburg, Germany) as industrial partners. This ITN stimulated movement, collaboration and training within this group of universities. The theoretical background discussed hereunder will highlight predominantly iterative sequence-defined synthesis approaches that are currently used worldwide (Section II.4) along with an introduction to the specific chemistries used with this doctoral work, namely thiolactone chemistry (Section II.5.3), multicomponent reactions (Section II.6) and 1,2,4-triazoline-3,5-dione chemistry (Section II.7).



Scheme II 1: Overview to demonstrate the range of controlled polymer structures and to highlight the difference between sequence-controlled and sequence-defined. Figure adapted from Lutz, 2017. [22]

II.3 The synthetic toolbox for sequence-defined macromolecules

A plethora of different synthetic routes and strategies have been developed over the last decade for the synthesis of sequence-defined macromolecules. Importantly, reactions can be carried out using either solid-phase or solution-phase methods, which, in combination with several different chemical strategies, have facilitated the synthesis of sequence-defined oligomers and are highlighted within this section. Solution-phase synthesis can even be further subdivided into whether it uses a soluble support or not. The choice of which chemical method to opt for is dependent on a range of factors, including the chemistry and application in question, although a full comparative study is currently lacking. However, a detailed comparison of the same chemistry carried out *via* two different techniques is discussed in Chapter VI.

II.3.1 Solid-phase synthesis

Solid-phase synthesis was first introduced by Merrifield in 1963 to the area of peptide chemistry.[35] Using a cross-linked polymer resin, functionalised with a cleavable linker, one can very easily carry out multi-step or iterative synthesis protocols, achieving very high conversion. Although this technique was initially foreseen for peptide synthesis,[35–39] in more recent years it has become a highly attractive technique in the development of protocols leading to sequence-defined macromolecules.[40–49] In order to synthesise perfectly monodisperse, multifunctional macromolecular structures, one often has to adopt an iterative synthesis approach. The repetitive nature of such a synthesis strategy means that simple purification steps and 100 % conversion after each reaction are desired in order to ensure structural monodispersity. Solid-phase synthesis is advantageous in this, as one can use a high excess of reagents which not only helps to achieve high conversion, but also enables faster reaction kinetics by creating a higher effective concentration.[31,43] Another advantage of solid-phase synthesis, is that one has the potential to automate the protocol by using peptide synthesisers.[41,43] This allows one to generate multiple, varying sequences concurrently, whilst saving time and labour. Disadvantages to solid-phase synthesis, often in terms of limited scale (although in certain instances large-scale approaches have been reported),[50] have led to the exploration of alternative synthesis routes.

II.3.2 Solution-phase synthesis

Classical synthesis in solution (without a support) is still the choice of many researchers in the field of sequence-defined chemistry. Solleder *et. al.* have reported much success with the Passerini and Ugi multicomponent reactions (Section II.6) *via* solution-phase procedures, that require purification after each iterative cycle using column chromatography.[31,51–54] Whilst time-consuming, high purity and high-yields were reported.[54] In this context, the experimental Chapter VI will highlight the comparison between solid-phase and solution-phase synthesis *via* a combined Passerini three-component reaction and click chemistry approach.

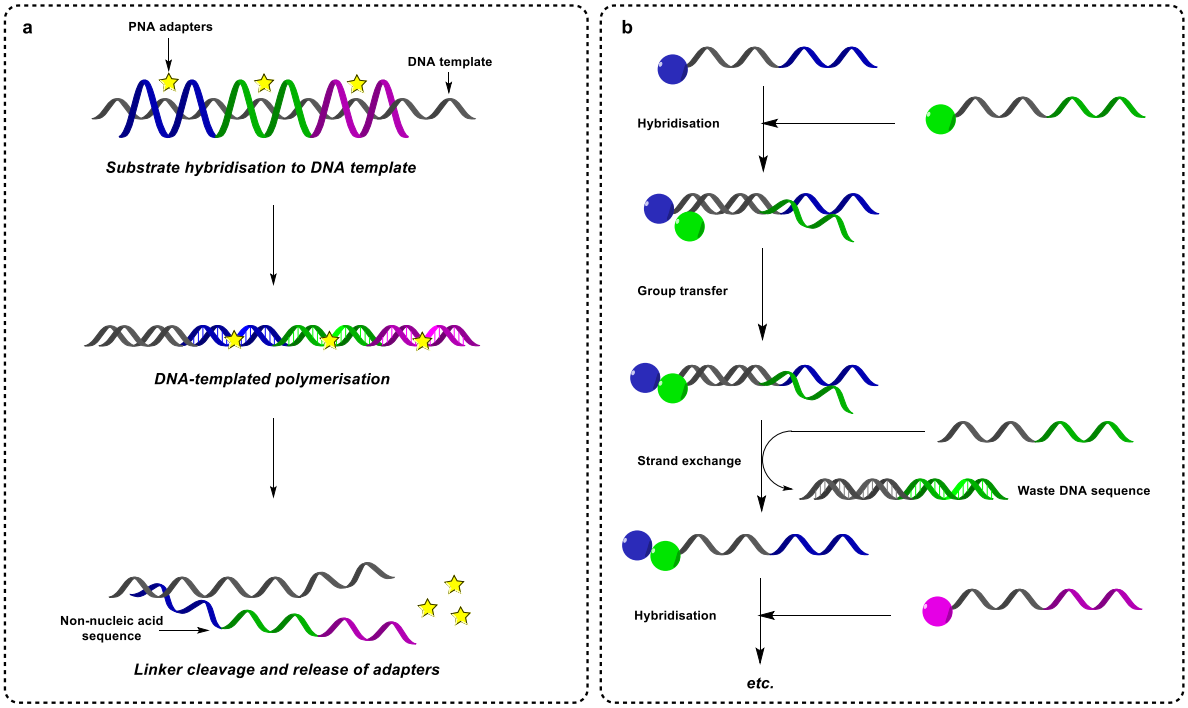
Alternatively, the use of soluble supports appears to offer the best of both techniques. This approach uses a soluble polymer support, such as polystyrene, which is end-functionalised with a cleavable linker molecule (similar to the solid-phase approach). From this functional group, the sequence is grown iteratively, with intermediate purifications being carried out using precipitation.[55–59] This synthesis tool facilitates a larger scale synthesis than with solid-phase chemistry and the purification can be seen as relatively straightforward compared to column chromatography, although precipitation can be equally

time-consuming and not always as high yielding as chromatographic techniques. Moreover, the commercial availability of some linkers can be more restricted with respect to functionalised polystyrene resins.[43]

II.4 Biologically and synthetically inspired sequence-controlled and sequence-defined synthesis strategies

II.4.1 Biologically inspired synthesis routes

A range of chemical strategies have been explored (in combination with any of the above-mentioned synthesis methods) to prepare sequence-defined macromolecules.[22,60] Some of these take inspiration from Nature, much like the field of macromolecular precision synthesis itself. Indeed, chemists have taken inspiration from *in vivo* DNA synthesis whose defined sequence of nucleotide monomers contains all of our genetic information.[15]



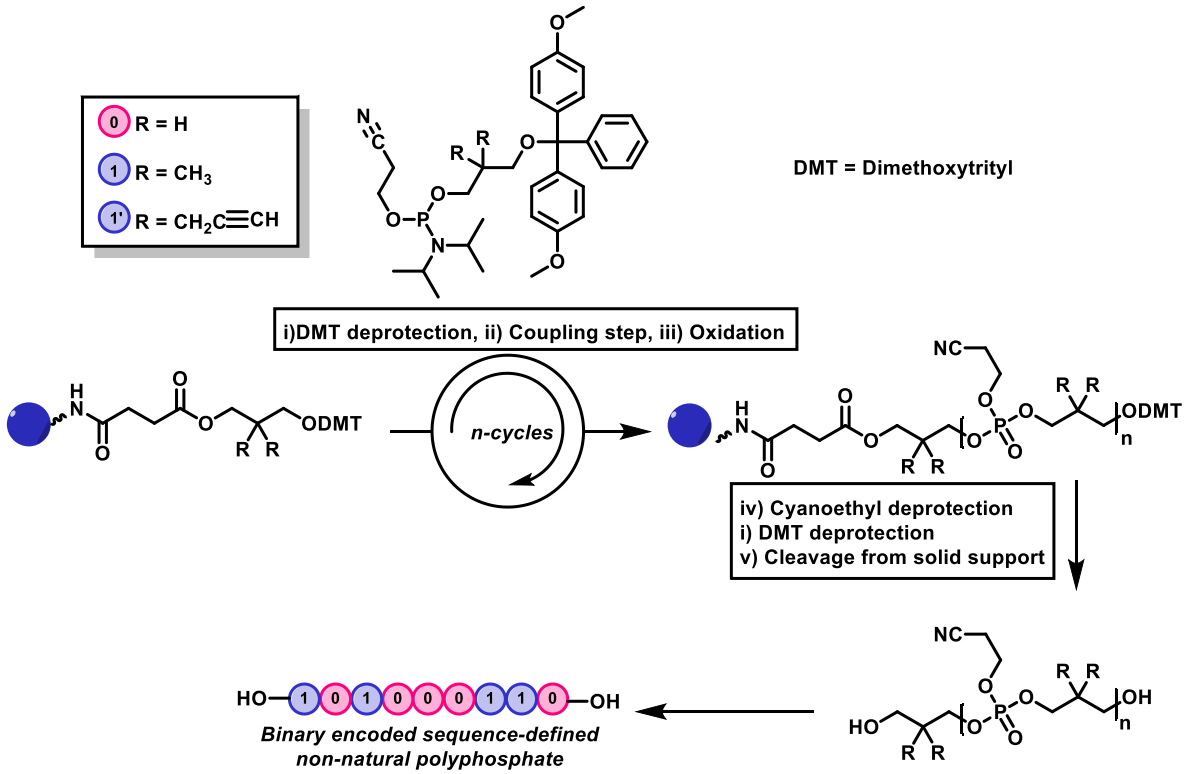
Scheme II 2: a) Enzyme-free DNA-templated approach to synthesise sequence-defined non-nucleic acid oligomers.[61,62] *b) DNA-templated synthesis* via *incomplete hybridisation and waste DNA expulsion approach.*[63]

For example, Liu and co-workers have extensively worked on the sequence-specific polymerisation of lysine-containing peptide nucleic acid (PNA) building blocks *via* a DNA templated, enzyme-free approach (as shown in *Scheme II 2a*).[61,62] This was achieved by using a pentameric PNA adapter (which mimics the function of an *in vivo* transfer RNA adapter) to cognate or hybridise a non-nucleic acid

substrate to the DNA template in a defined order. These substrates then underwent a sequence-defined polymerisation *via* an efficient coupling chemistry with the resulting sequence structure bearing no resemblance to the DNA template. The incorporation of a cleavable linker (in this instance a disulfide bond) enabled the subsequent release of the PNA adapters.[61] This technique was also translated by O'Reilly and co-workers towards the creation of truly synthetic sequence-defined macromolecules whose structure was also unrelated to that of the nucleic acid template, also by harnessing a bio-inspired approach for the synthesis of non-biological sequences. This alternative DNA-templated approach entails an incomplete hybridisation reaction between the DNA strands which carry the first monomers of the sequence (see *Scheme II 2b*).[63] The two monomer-containing strands join to begin the sequence. Another DNA strand is then inserted, complementing one of the previous DNA strands and so they hybridise and are expelled as waste DNA. This leaves the dimer as another monomer-containing strand joins *via* an incomplete hybridisation and so the cycle continues.[63] The acyl transfer reaction of functionalised DNA strands was later optimised by altering the reactions conditions – notably by changing the pH.[64] In 2012, the same research group further reported efforts towards DNA templated synthesis approaches,[65] including the optimised and high-yielding (85 % per coupling step) synthesis of sequence-defined decamers with tuneable monomer sequences[66] and even a one-pot, multistep approach where multiple reaction sequences could be programmed in parallel in the same reaction vessel thanks to the use of different chemical adapters.[67] More recently, the use of synthetic molecular machines in autonomous cascade DNA hybridisation reactions to synthesise sequence-defined oligomers was reported.[68]

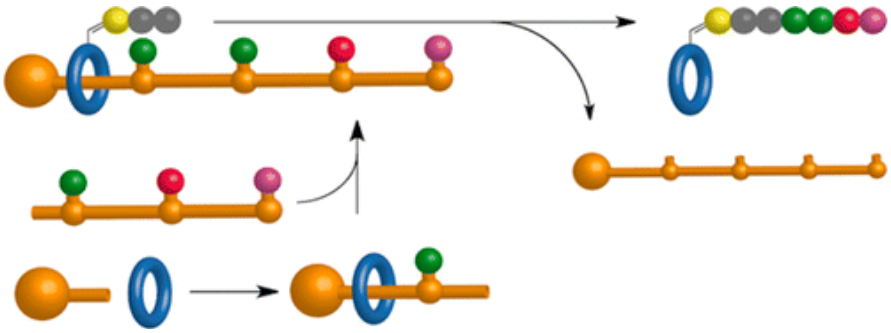
As mentioned above, solid-phase chemistry was originally used in the area of peptides and since then protocols for the preparation of oligopeptides have served as biological inspiration for synthetic sequence-defined oligomers.[2,19] Lutz and co-workers reported the use of soluble polystyrene supports (synthesised *via* ATRP), which were functionalised with an acid-cleavable linker, to facilitate the up-scalable synthesis of oligopeptides[56] and leading also to the synthesis of peptide-polymer bioconjugates.[57] The group then used this soluble support method,[55,69,70] along with solid-phase approaches,[45–47,71–75] for the synthesis of non-peptide derived sequence-defined oligomers, *via* a range of chemistries. The use of sequence-defined peptides has also been found in the synthesis of macro-RAFT agents which were used for the synthesis of well-defined peptide-polymer conjugates.[76] Solid-phase approaches have also been extended to oligonucleotide synthesis, which has served as biological inspiration for sequence-defined synthesis, most notably in the area of phosphoramidite chemistry.[19] Lutz and co-workers have worked extensively on utilising the phosphoramidite coupling reaction in combination with solid-phase synthesis and succeeded in synthesising a sequence-defined polymer with a DP of >100 using a DNA synthesiser.[34] Their work in this area has led them to synthesise many non-nucleoside phosphoramidite monomers, which have been used to synthesise binary encoded, non-

natural sequence-defined oligomers (*Scheme II 3*).[77] The close similarity of these structures with DNA, means that analysis and read-out is possible using protein-based nanopore sequencing.[77] Alternatively, the coupling of an alkyl bromide functionalised phosphoramidite monomer to a hydroxy functionalised nitroxide resulted in a phosphate bond. The alkyl bromide could then be activated with copper bromide to give a radical-radical coupling step. The iterative combination of these two coupling reactions using solid-phase synthesis resulted in sequence-defined oligo(alkoxyamine phosphodiester)s, which contained an easily cleavable alkoxyamine bond that enabled analysis *via* tandem mass spectrometry (MS/MS) as it leads to predictable, computer readable fragmentation patterns.[48]



Scheme II 3: Solid-phase phosphoramidite-based iterative protocol to synthesise sequence-defined non-natural polyphosphates.[77]

Ribosomes have also been used as biological inspiration for the synthesis of sequence-defined structures, as demonstrated by Leigh and co-workers (see *Scheme II 4*).[78,79] They used rotaxane-based molecular machines to synthesise sequence-defined oligopeptides in an iterative manner *via* the movement of a ring along a 'polymer track', which could 'pick-up' and assemble amino-acid building blocks as it travelled. Alternatively, Sawamoto and co-workers developed a complex single monomer addition approach based upon iterative intramolecular cyclisation *via* a radical intermediate and subsequent regeneration to introduce vinyl monomers one by one.[80] An initiating monomer contains both an alkene functionality and a radical generating site, to facilitate the iterative process. A metal catalyst and dilute reaction conditions ensure cyclisation rather than chain-growth polymerisation.[23,80]



Scheme II 4: c) Graphic showing the molecular machines synthesis of sequence-defined oligopeptides where the rotaxane travels along a 'polymer track'.[79] *Reproduced with permission from the American Chemical Society, Copyright 2014.*

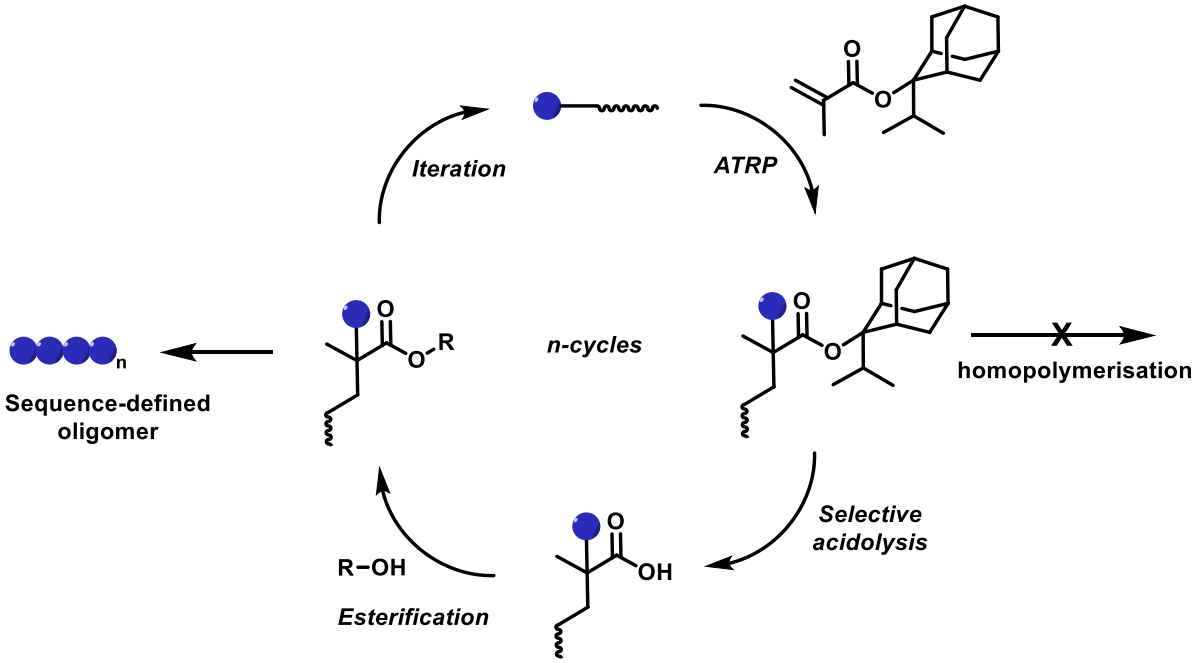
II.4.2 Synthetic chain and step-growth sequence-controlled/defined synthesis strategies

Despite the success of biologically inspired approaches, chemists have been mostly in pursuit of less expensive, purely synthetic methods to synthesise sequence-defined macromolecules. This has led to an emerging range of structures and synthesis routes, broadening the scope of sequence-controlled and sequence-defined chemistry.[22] In the following, chain and step-growth approaches will be discussed as certain step-growth approaches are highly relevant to the work discussed within this thesis.

Chain-growth polymerisations, either ionic or radical, have been reported to facilitate the synthesis of sequence-controlled polymers.[22,23] Unlike free-radical polymerisations, the development of RDRP (Section II.1) has led to greater control in polymer dispersity and structure. Perrier and co-workers have used RAFT polymerisation to synthesise sequence-controlled polymers in a rapid and one-pot fashion.[33] Alternatively, controlled structures have been achieved using Ring Opening Metathesis Polymerisation (ROMP)[81] and a similar strategy was employed by Hawker and co-workers for the synthesis of sequence-defined macrocycles, which upon ring-opening, gave the resulting linear polymers.[82] ATRP, NMP and RAFT polymerisation techniques, amongst others, have all proved successful in the copolymerisation of functional maleimides, styrene and maleic anhydride.[83–87] However, in almost all cases they result in sequence-controlled rather than sequence-defined structures (Section II.2), owing to the disperse (albeit narrow, *i.e.* Đ <1.3) character of the aforementioned polymerisation techniques.

Recently, Sawamoto and co-workers were able to bypass the dispersity challenge through a radical addition approach using bulky monomers to synthesise short, sequence-defined structures.[88] *Via* a four-step iterative cycle which combined ATRP, selective acidolysis and esterification, bulky adamantane

and isopropyl functionalised methacrylate monomers were incorporated into sequence-defined structures (see *Scheme II 5*). The steric hindrance, introduced by the monomer, was crucial to prevent subsequent homopolymerisation and instead facilitated selective modification and subsequent iterative addition of a new monomer.[23,89] This method of inserting the desired monomer into the growing sequence chain is a type of Single-Unit Monomer Insertion (SUMI).



Scheme II 5: Reaction scheme of an iterative radical addition SUMI approach to synthesise sequence-defined macromolecules using bulky monomers to prevent homopolymerisation.[89]

The use of SUMI in combination with RAFT polymerisation hoped to bring new insight to the synthesis of sequence-defined structures *via* controlled chain-growth polymerisation techniques. Further kinetic studies into RAFT polymerisation[90,91] culminated with Klumperman and co-workers discovering that selective initiation occurs during the initial consumption of the RAFT agent as opposed to inhibition.[92] These kinetic studies inspired the concept of using SUMI to achieve sequence-defined macromolecules, which was demonstrated by the design of functionalised RAFT agents with photoactive macromolecules.[23,93] By purposely opting for an equimolar ratio of RAFT agent to monomer, single chromophore units were inserted into the RAFT agent. Moad and co-workers further developed this technique to synthesise trithiocarbonate and dithiobenzoate macro RAFT agents *via* the respective single unit insertions of styrene and *N*-isopropylacrylamide (NIPAM).[94] Photoactivated SUMI reactions were also reported by using Photoinduced Electron/Energy Transfer RAFT (PET-RAFT), initiated by visible light in order to achieve sequence-defined trimers. The resulting oligomers could then be coupled together and grafted onto polymers as sequence-defined hexameric brushes,[95] or transformed into pentamers by means of post-modification, *e.g.* thiol-ene or esterification.[96,97] Arguably, the biggest

advancement in the SUMI-RAFT approach towards sequence-defined oligomeric structures was established by Junkers and co-workers, who investigated the polymerisation kinetics *via* online Electrospray Ionisation Mass Spectroscopy (ESI-MS).[98] Moreover, preparative Recycling Size Exclusion Chromatography (reSEC) was utilised to obtain monodisperse structures following the SUMI-RAFT polymerisation of acrylate monomers.[99] Continuous optimisation and screening eventually led to the synthesis of the largest sequence-defined decamer obtained *via* RDRP so far.[100] RAFT, in combination with SUMI and Multiple Unit Monomer Insertion (MUMI) resulted in decamers which were purified *via* automated column chromatography as opposed to reSEC.[23,100] Chain length could further be increased by coupling together oligomers through disulfide formation.[100]

In contrast to chain-growth techniques, the well-known class of step-growth polymerisations also presents itself as an alternative strategy within the context of sequence-controlled and sequence-defined synthesis. Despite their limited control in terms of polymeric structure and molecular weight, two strategies have emerged to prepare polymers with well-defined structures.[22] Starting from end-functionalised sequence-defined macromonomers, one has either an AB-type or AA'-type monomer, which can be polymerised, or alternatively an AA-type monomer which can be copolymerised with a complimentary BB-monomer. Acyclic Diene Metathesis (ADMET) has been used to synthesis polyolefins with well-defined side-chain functionalities.[101] In other cases, Atom Transfer Radical Addition (ATRA) was used to synthesise defined monomers, which were then polymerised *via* various routes to yield periodic copolymers, including, ATRA [102] and Atom Transfer Radical Coupling (ATRC).[103] Radical Addition Coupling Polymerisation (RACP) was also used to synthesise periodic copolymers.[104]

An important strategy that has been explored for the step-growth synthesis within the area of sequence-controlled polymers is click chemistry, as it enables a fast and efficient build-up of monomers (or sequence-defined macromonomers) in a highly controlled manner.[22] Other similarly efficient reactions, commonly referred to as click-like transformations, have also been reported as suitable chemistries for iterative, defined growth.[24,25] Click chemistry and efficient reactions within the context of sequence-defined synthesis have thus been explored in the current doctoral work and are hence described in greater detail in the separate section; Section II.5. Another approach to achieve truly sequence-defined structures is based on iterative strategies, which are referred to as multi-step-growth synthetic protocols. These are often used in combination with solid-phase chemistry, as discussed earlier (Section II.3.1). Similarly, one-pot multicomponent reactions (MCRs) have been reported for the step-by-step growth of sequence-defined oligomers, most notably by Meier and co-workers.[105] Section II.6 is therefore dedicated to a detailed discussion of the relevant MCRs.

II.5 Click and click-like reactions in sequence-defined synthesis

II.5.1 Introduction

In order to achieve a high order of macromolecular precision and control, it is advisable to use the most efficient reaction classes, particularly when considering iterative approaches and the introduction of multiple functionalities. Whilst solid-phase peptide-inspired synthesis has traditionally been one such way of synthesising well-defined multifunctional macromolecules, a wider range of more efficient, protecting-group free approaches, which can introduce many different functionalities have been considered. The concept of "click chemistry" (and similarly efficient reactions) has really enabled the field of sequence-controlled and sequence-defined synthesis to grow. This topic has been comprehensively highlighted by us in recent publications.[24,25] The key uses of click and click-like chemistries in sequence-controlled/defined synthesis are discussed within this section.

The concept of click chemistry was first introduced by Sharpless and co-workers in 2001,[106] and since then, it has had a large global impact on organic and polymer chemistry research and many applied fields of research (e.g. drug discovery).[107–116] Click reactions are ones which fit a series of crucial criteria:

⇒ *Stereospecific*
⇒ *Wide in scope*
⇒ *Modular*
⇒ *Only form inoffensive by-products (which can be easily removed via non-chromatographic techniques)*
⇒ *High yielding*
⇒ *Begin from readily available start materials*
⇒ *Simple reaction conditions (e.g. ideally not water/oxygen sensitive reactions)*
⇒ *The use of no solvent or a benign solvent or a solvent which can be easily removed*
⇒ *Stable reaction products*
⇒ *Preferably a single reaction trajectory*

Since 2001, click chemistry has become rapidly implemented in global research[117–121] and also widely throughout polymer chemistry.[115,122] The introduction of this concept has driven the synthesis of a range of unprecedented macromolecular structures on a larger scale and in a more straightforward manner.[20,123–135] In 2011, the click chemistry requirements were further refined with regard to polymer

synthesis.[136] Our group, in collaboration with others, outlined the following additional criteria that are important to enable efficient polymer-polymer coupling reactions:

⇒ *Equimolarity*

⇒ *Large-scale purification*

⇒ *Fast time-scale*

The term "click" chemistry has been applied to several classes of chemical reactions, which are considered efficient enough to satisfy the criteria (although there is some debate amongst chemists as to whether some reactions are click or simply click-like). Below are some examples of reactions that are arguably defined as click, which are discussed in more detail within this section with respect to their applicability to sequence-defined synthesis:

⇒ *[3+2] azide/alkyne cycloaddition reactions (e.g.* copper(I)-catalysed azide/alkyne cycloaddition*)*

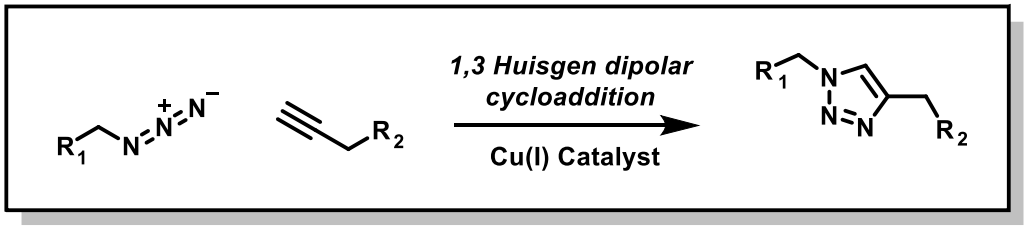
⇒ *Diels-Alder reaction*

⇒ *Thiol-ene reactions (e.g. nucleophilic thiol-ene)*

Furthermore, click chemistry has crucially been introduced to many sequence-defined areas of synthesis, including that of oligopeptides and oligonucleotides,[111,113,137–139] where chemoselective and efficient small-scale reactions are important and has also facilitated labelling and post-modification,[137,140–146] cyclisation[147–153] and bioconjugation reactions of sequence-defined structures.[154–163] In addition, click chemistry has facilitated the synthesis of peptide/protein-polymer conjugates[138,164–175] and oligonucleotide/DNA-polymer hybrid structures[138,176–178] for ranging applications, predominantly in a pharmaceutical and biomedical context.[166,175,176,179–181] However, sequence-defined synthesis extends beyond the area of bio-applications, reaching into the fields of data-storage[40,47,48,182,183] and single-chain folding.[87,184–187] Click(-inspired) reactions have been crucial to the advancement of this field, not only in terms of synthesis, but also post-modification and cyclisation of these precision polymers, which has resulted in a wide range of macromolecular architectures. Within this section, in addition to highlighting the range of click chemistries and related efficient reactions that have been used in the synthesis of sequence-defined macromolecules, special attention is devoted to the role of click chemistry in the context of sequence-defined synthesis within our own research group, which has inspired some of the work described within this doctoral thesis.

II.5.2 Copper(I)-catalysed azide/alkyne cycloaddition reactions

The copper(I)-catalysed azide/alkyne cycloaddition (CuAAC) reaction is not only the first but also arguably the most well-known of all click reactions.[106,188–190] It was independently reported by both Sharpless,[106] as well as by Meldal and co-workers,[189] as an improvement of the well-known Huisgen 1,3-dipolar cycloaddition (see *Scheme II 6*)[191,192] through the use of Cu (I) as a catalyst, leading to its widespread use in polymer synthesis and post-modification.[115,127,193–196] The usefulness and efficiency of CuAAC reactions led to its rapid implementation in sequence-defined synthesis as click reactions can be crucial in this field as iterative strategies are often implemented which are reliant on a 100 % conversion, time-efficient reactions and easy purifications. Although, a disadvantage of CuAAC compared with other click chemistries is the removal of the copper catalyst (*vide infra*).



Scheme II 6: General scheme of the 1,3-dipolar cycloaddition reaction.

CuAAC has been implemented in numerous sequence-defined, iterative protocols, using both solution and solid-phase approaches. Hawker and co-workers used this chemistry in a divergent-convergent approach where orthogonal deprotection of a monomer was followed by end-group coupling of a new protected monomer, resulting in a step-wise increase of chain length.[197] Hence, sequence-defined oligo(triazole)s were made available from oligoethers,[198,199] sugars,[200–202] epoxides,[203,204] nucleotides,[205] polymers,[206] or hydrocarbon building blocks containing protected alkynes, and functional groups which, upon deprotection, could be converted to their corresponding azide.[207–210] This synthesis route was even semi-automated and upscaled to multi-gram dimer synthesis by Johnson and co-workers.[210] Alternatively, Lutz and co-workers developed CuAAC- and amidation-based, iterative and orthogonal "AB + CD" protocols (see *Figure II 1*),[55] which were carried out on both solid[75] and liquid supports[211] and even later extended to peptide synthesis.[44,72] Importantly, the devised AB + CD protocol is protecting group-free as a result of the chemoselective reactivity of an alkyne "A" with an azide "D", in the presence of a carboxylic acid "B", which selectively reacts with an amine "C".[55,75,211,212]

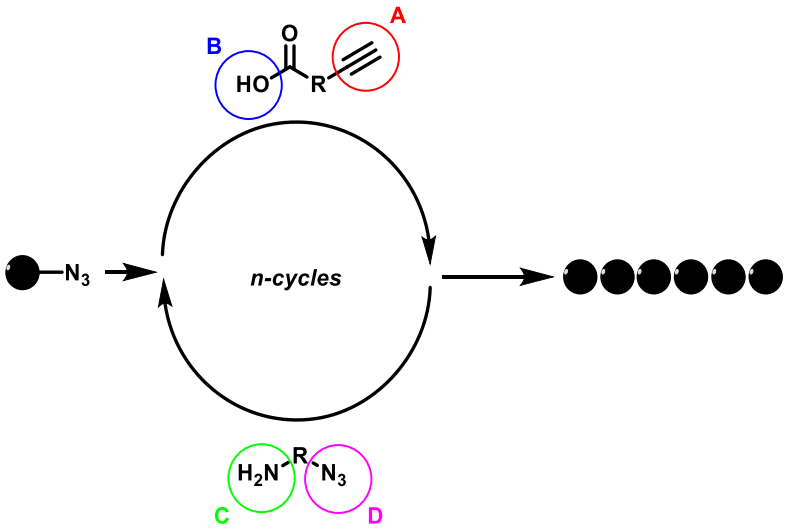
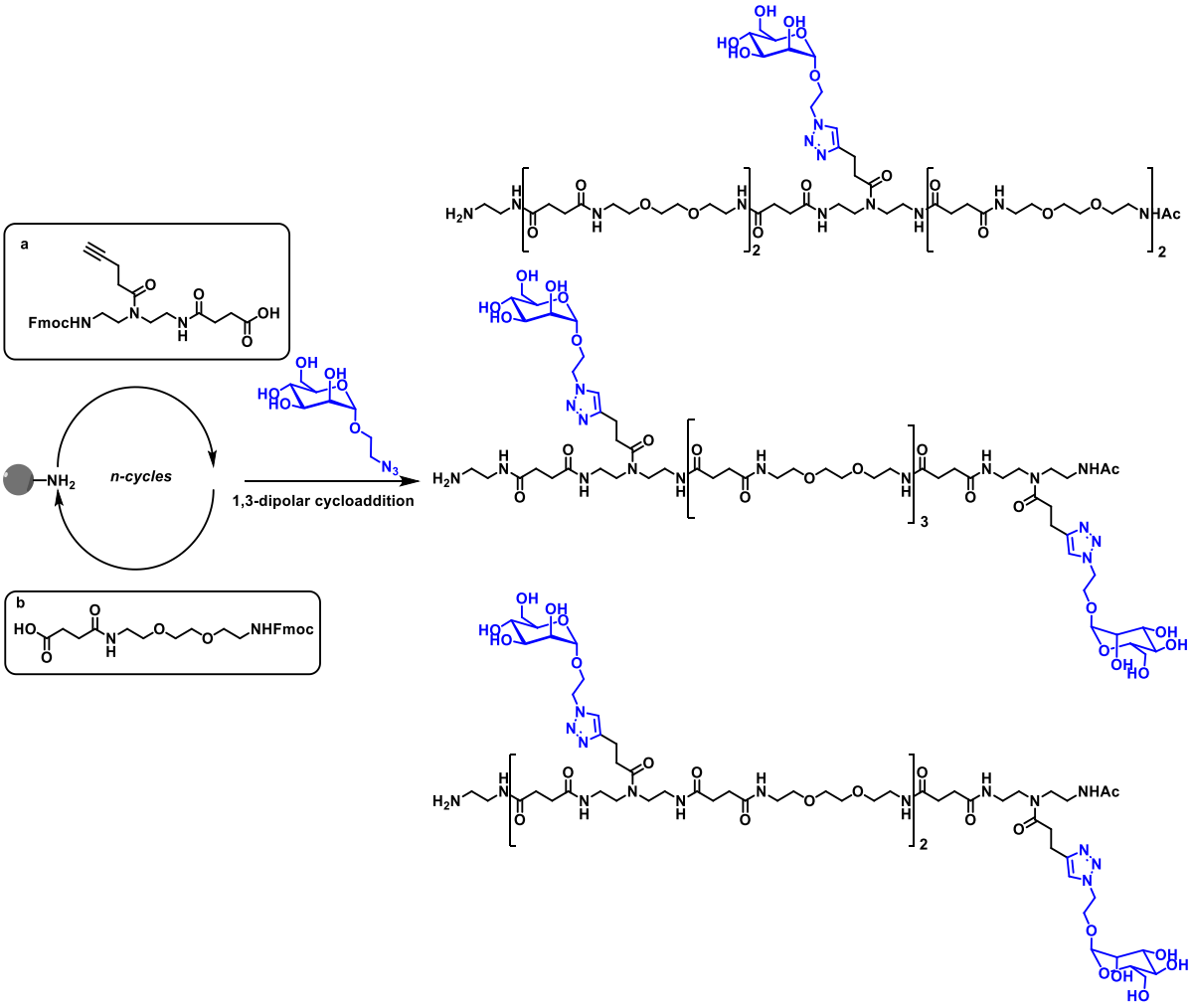


Figure II 1: Schematic representation of an "AB + CD" solid-phase approach for the orthogonal, protecting group-free, iterative synthesis of sequence-defined oligo(triazole)s.[24,25] *Adapted and reproduced with permission from John Wiley and Sons.*[24]

Another CuAAC-mediated sequence-defined synthesis example is found in the polyaddition of terminal alkynes and heterotelechelic azides, which was explored for the formation of *β*-turn mimics (*i.e.* molecules that replace amino acid residues in proteins that have adopted globular structures to act as folding nucleators)[213] as a result of the triazole ring formed between two oligopeptides.[214,215] This approach showed how sequence-controlled chemistry can have an effect on structure-property relationships as defined oligopeptides with secondary structures of either *β*-sheets or *β*-turns could be obtained.[216,217] This route was also utilised for the synthesis of high molecular weight, degradable sequence-controlled poly(amido-amine)s.[218] An alternative use of CuAAC chemistry to obtain specific secondary structures in high molecular weight, periodic copolymers was investigated by Lutz and co-workers, who synthesised well-defined, functional heterotelechelic *α*-alkyne, *ω*-azido poly(styrene-co-*N*-substituted maleimide) precursors.[219] The precursors were synthesised *via* ATRP using a protected alkyne and bromine-containing initiator. Following substitution of the bromine end group into an azide and deprotection of the alkyne, a controlled step-growth polymerisation was thus initiated.[219] Furthermore, not only have triazole units been shown to control secondary structures, but they have also been reported to control tertiary amide isomerism, with triazoliums having a more significant effect, although in both cases, the *cis*-conformation was favoured.[220]

Finally, CuAAC has been used in the post-modification, functionalisation and even cyclisation of precision macromolecules, by incorporating pendant azide or alkyne side-groups.[24,25] An elegant use is found in the facile installation of sugar moieties at well-defined positions along the macromolecular chain, (see *Scheme II 7*) which has been explored by many,[221–224] but notably by Hartmann and co-

workers [225–227] and by Becer and co-workers.[228–232] Other side groups that have been added utilising CuAAC post-modification reactions include, deoxyribonucleoside,[148,233] fluorophores,[233] oligopeptoids,[113,233] polyethylene glycol (PEG) units,[77,234,235] polystyrene,[236] hydroxyproline-based building blocks,[233] or metal complexes.[237] In addition to post-modification, cyclisation has also been successfully reported, most notably of oligopeptides[238,239] oligosaccharides, [240–242] polystyrene [243,244] and oligo(ether)s.[198]

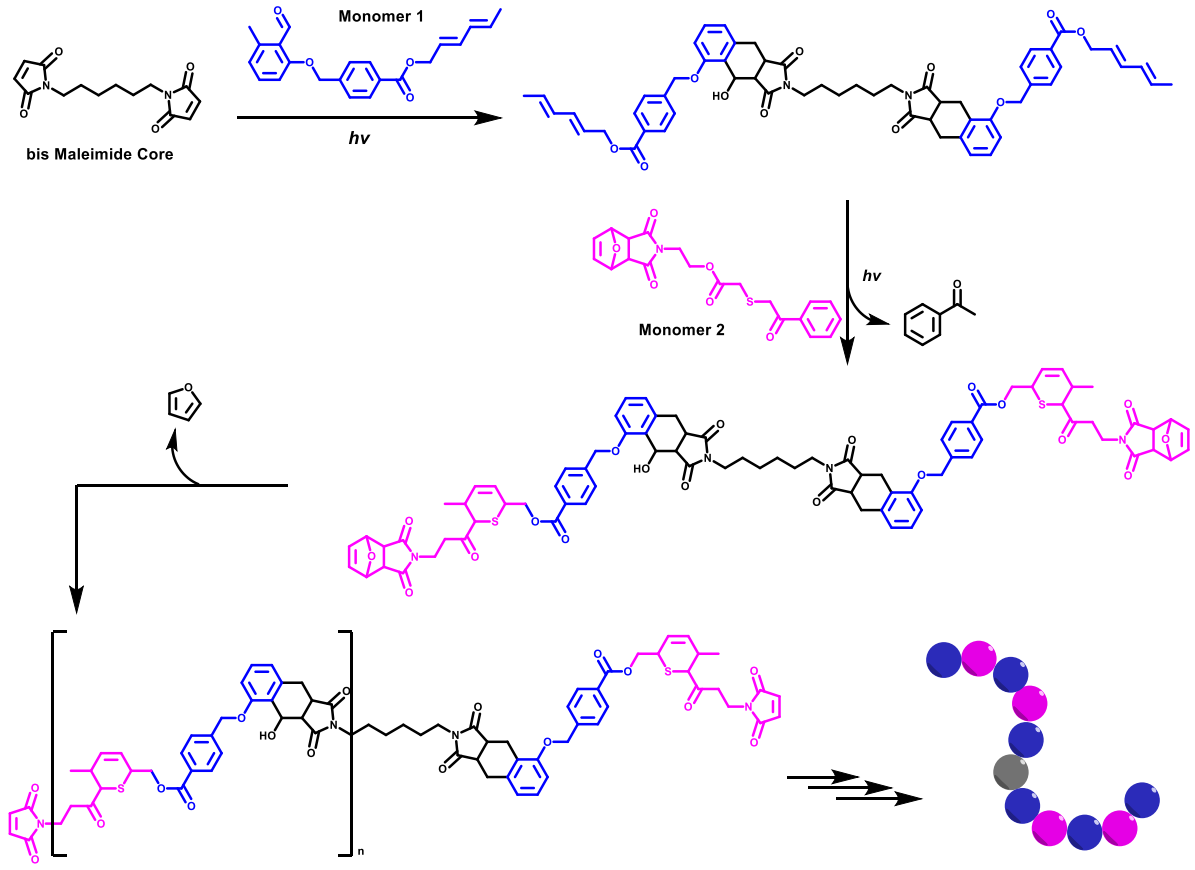


Scheme II 7: Iterative synthesis of alkyne-functionalised sequence-defined oligomers and their subsequent post-modification with mannose-azide moieties.[225]

However, despite the wide-ranging applications and the obvious advantages, using CuAAC-based click chemistry does have its disadvantages. The use of low molecular weight azides (such as NaN_3) can be explosive and also the copper can form complexes with the triazole moiety,[243,244] making it difficult to remove, which can be problematic, given the potential toxicity of copper. However, metal-free azide-alkyne click approaches such as strain-promoted or fluorine-activated are possible.[245,246]

II.5.3 Diels-Alder reactions

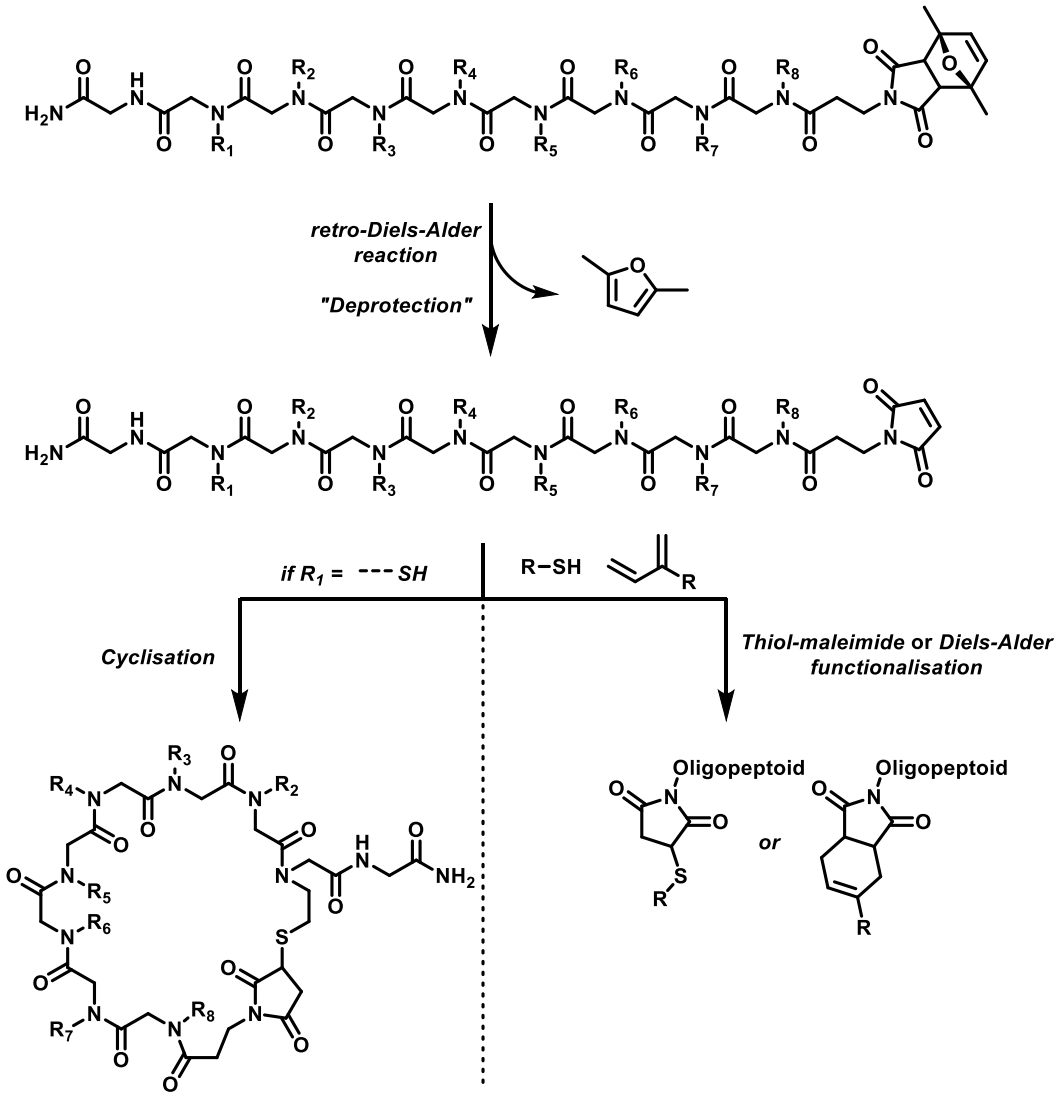
An alternate click chemistry is the Diels-Alder reaction, which was discovered in 1925[247] and its use in sequence-defined or sequence-controlled applications has remained fairly limited.[24,25] In 2015, Barner-Kowollik and co-workers first reported the use of Diels-Alder reactions for the photochemical synthesis of sequence-defined macromolecules.[248,249] Such photochemically triggered click reactions present themselves as interesting tools to access precisely defined macromolecules without the need for a high excess of reagents or high temperatures and so offers a potentially cost-effective route to synthesis.



Scheme II 8: Reaction scheme of photochemically triggered approach towards the synthesis of symmetrical sequence-defined oligomers using Diels-Alder chemistry.[249] *Adapted and reproduced with permission from the Royal Society of Chemistry, Copyright 2015.*

Perfectly monodisperse, high molecular weight decamers were synthesised by means of the light-induced Diels-Alder reaction as shown in *Scheme II 8*. This iterative route offers a more time-efficient approach towards sequence-defined synthesis than other strategies that use cleavable soluble supports.[55,57] However, the protection and deprotection of the maleimide functionalities with furan are a disadvantage as they add an extra synthetic step and require heating (at 80 °C). The route commences with a bis-maleimide functional core and is grown outwards in both directions, reacting with the first

of the photoreactive monomers, which carries a diene moiety *via* light radiation at λ = 350 nm. The second photoreactive monomer then reacts with the diene in another photoinduced Diels-Alder reaction and then the reaction cycle commences again. The resulting oligomer is therefore always symmetrical, which although interesting, could be a limitation too. A follow up report of this approach targeted a data-storage application of this chemistry with the data being read out by tandem mass-spectroscopy techniques, although, a limiting factor of this approach is the lack of ability to introduce various functionalities which could limit its information carrying potential.[248] The use of photochemistry and Diels-Alder reactions has also been reported recently by Ji *et. al.*,[250] also using a furan-protected maleimide substrate. Barner-Kowollik and co-workers have more recently reported a photo-induced Diels-Alder approach that is protecting group free because of orthogonal reactions, again using a symmetrical core unit.[251] They also reported the use of Diels-Alder reactions in combination with photoflow chemistry in order to synthesise 800 mg of sequence-defined oligomer.[252]



Scheme II 9: Retro-Diels-Alder deprotection of maleimide functionalised oligopeptoids and their subsequent cyclisation or functionalisation through thiol-maleimide or Diels-Alder chemistries.[148,253] *Adapted and reproduced with permission from John Wiley and Sons.*[24]

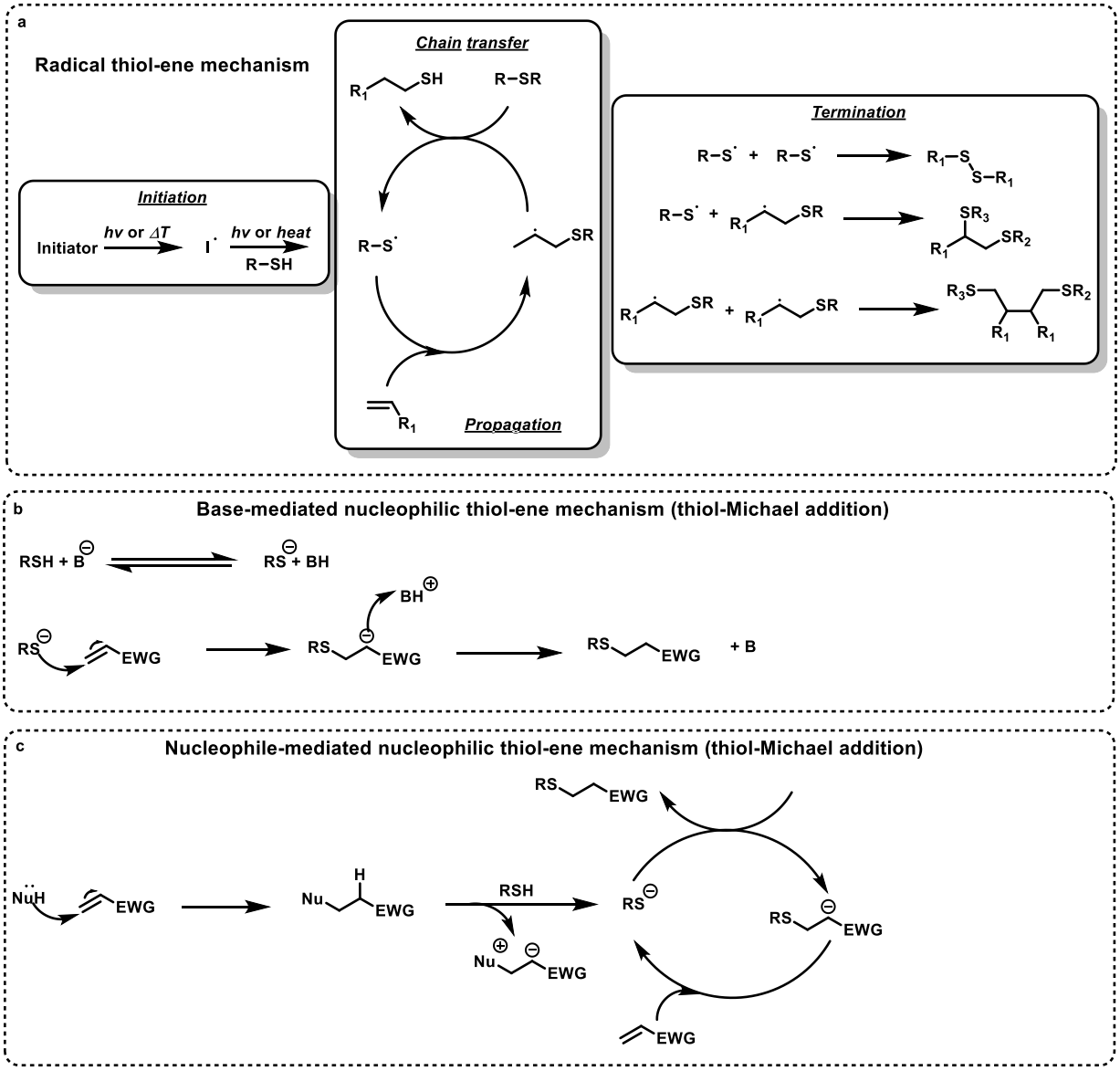
Finally, Grandas and co-workers use thermally initiated retro-Diels-Alder reactions in combination with thiol-ene or Diels-Alder reactions to either functionalise[253] or cyclise[141,154] oligopeptoids. The oligopeptoids were end-capped with 2,5-dimethylfuran protected maleimides, whereby deprotection under thermal conditions allowed for the cyclisation of the maleimide with a thiol present in the oligopeptoid side chain (see *Scheme II 9*). Alternatively, a thiol or diene could allow conjugation reactions to occur for further structural modification with oligonucleotides.

II.5.4 Thiol-X reactions

In addition to CuAAC and Diels-Alder click reactions, thiol-X reactions have gained a lot of interest in the field of sequence-defined synthesis. The most relevant of these are thiol-ene reactions, where thiol moieties readily react with a wide range of alkenes, can be carried out in either a nucleophilic or radical fashion. The radical thiol-ene reaction was first reported by Posner in 1905[254] and the radical reactivity of thiols can be explained by the weak S-H bond, which easily forms thiyl radicals, whereas the relatively high nucleophilic reactivity (with respect to alcohols and amines) is a result of the larger atomic size (compared with oxygen or nitrogen) and polarisability of the sulfur atom. Radical thiol-ene reactions are typically initiated thermally (*e.g.* azobis(isobutyronitrile) (AIBN)) or photochemically (*e.g.* 2,2-dimethoxy-2-phenylacetophenone) which react to form thiyl radicals (see *Scheme II 10a*). Alternatively, the nucleophilic thiol-ene reactions – or Michael additions – can be catalysed either by the nucleophile itself or with a base, proceeding *via* two plausible mechanisms (see *Scheme II 10b, c*).[255,256] In the base-catalysed approach, the thiol is first deprotonated and the resulting thiolate anion attacks the *β*-carbon of the alkene. In the nucleophilic approach, a strong base is first generated *in situ* as a result of nucleophilic attack of the activated alkene. Structure, catalyst and solvent polarity have been reported to have an effect on the rate of reaction.[257]

Although thiol-X reactions should not be classified as click as a single reaction trajectory is not always likely because side-reactions such as disulfide formation can occur, they are arguably referred to as click-like. [24,25] However, it should be noted that radical thiol-ene reactions should not even be classified as click-like, particularly when referring to polymer-polymer couplings,[258] despite widespread reports describing this as a click reaction.[259] On the other hand, nucleophilic thiol-ene reactions do comply with many of the click criteria, as they are insensitive to water and acid, wide in scope, fast and high yielding, hence their description as click-like.[24,25] Within polymer chemistry, they have been applied in a vast range of applications, including yet not limited to, polymer post-modification, coatings, adhesives and optical lenses.[24,25,259–261] The efficiency of the thiol-ene reaction therefore presents itself as the perfect partner in sequence-defined synthesis.

The combination of both radical and nucleophilic thiol-ene reactions within the area of sequence-defined synthesis was reported by the introduction of fluorous tags on oligoether-amides using an iterative method.[262–265] Fluoro-functionalised allyl acrylamides react orthogonally *via* both nucleophilic and photoinitiated, radical thiol-ene reactions to yield sequence-defined oligomers, which were even cyclised to replicate antimicrobial peptides.[262] Bowman and co-workers have also used both types of thiol-ene reactions in an orthogonal manner for the synthesis of sequence-defined oligomers, from nucleobase-functionalised, protected thiol-containing acrylamide and alkene monomers, which were eventually polymerised to result in sequence-controlled polymers.[266]

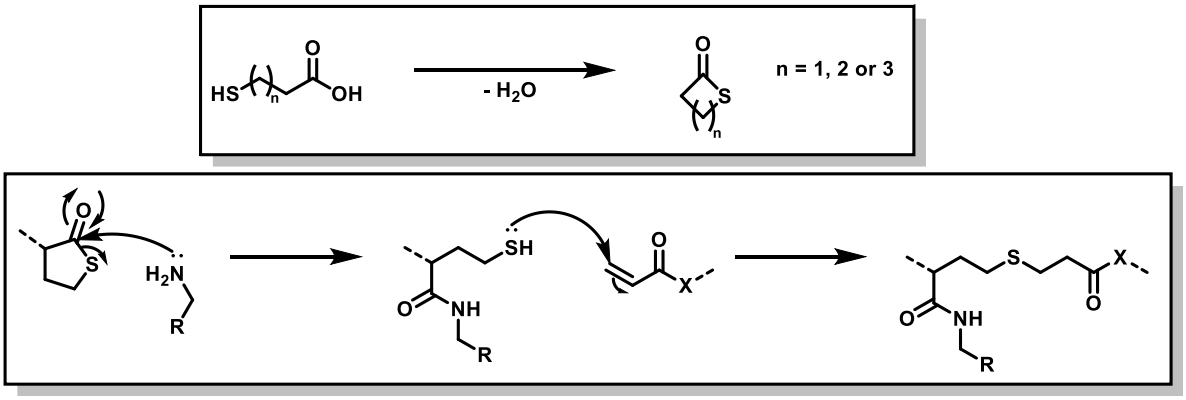


Scheme II 10: a) Outline of the mechanism of the radical thiol-ene reaction.[259,267] *b) Outline of the base-catalysed nucleophilic thiol-ene reaction mechanism.*[256] *c) Outline of the nucleophile-mediated nucleophilic thiol-ene reaction mechanism.*[256]

As with CuAAC, one of the key applications of thiol-X chemistry that is relevant to the current thesis is the post-modification or cyclisation of sequence-defined structures. Again, a functional handle, *e.g.*, an end-standing alkene, can readily be incorporated at defined positions along the macromolecular chain.[24,25,105,145,203,220,228,268,269] The incorporation of sugar moieties, for example, along the chain.[231,232,270–274] has led to the synthesis of various sequence-defined glycomacromonomers functionalised with an alkene at each end and with a varying numbers of pendant mannose side-groups. Polymerisation of these macromonomers with hydrophilic, dithiol spacer units enabled the study of the binding efficiency of these glycopolymers with the lectin, Concanavalin A (Con A).[275] Whilst the polymer length had no effect on the binding, the number of sugar units correlated to the Con A binding and clustering efficiency. In other research, the synthesis of alternating co-oligoesters which contained allyl and isobutyl side-chains was reported.[276] The allyl pendant groups could be selectively modified by either thioglycolic acid, mercaptoethanol or cysteamine to examine the effect on their folding behaviour. Furthermore, Johnson and co-workers focused on the post-modification of chiral oligomers with allyl side-chains in a scalable (ca. 1 g) approach.[203] The cyclisation of peptoids with a thiol side-group and protected maleimide end-group was also reported using a thermally induced retro-Diels-Alder reaction to release the maleimide, which underwent a subsequent thiol-ene reaction with the thiol side-group thereby cyclising the peptoid.[148,154]

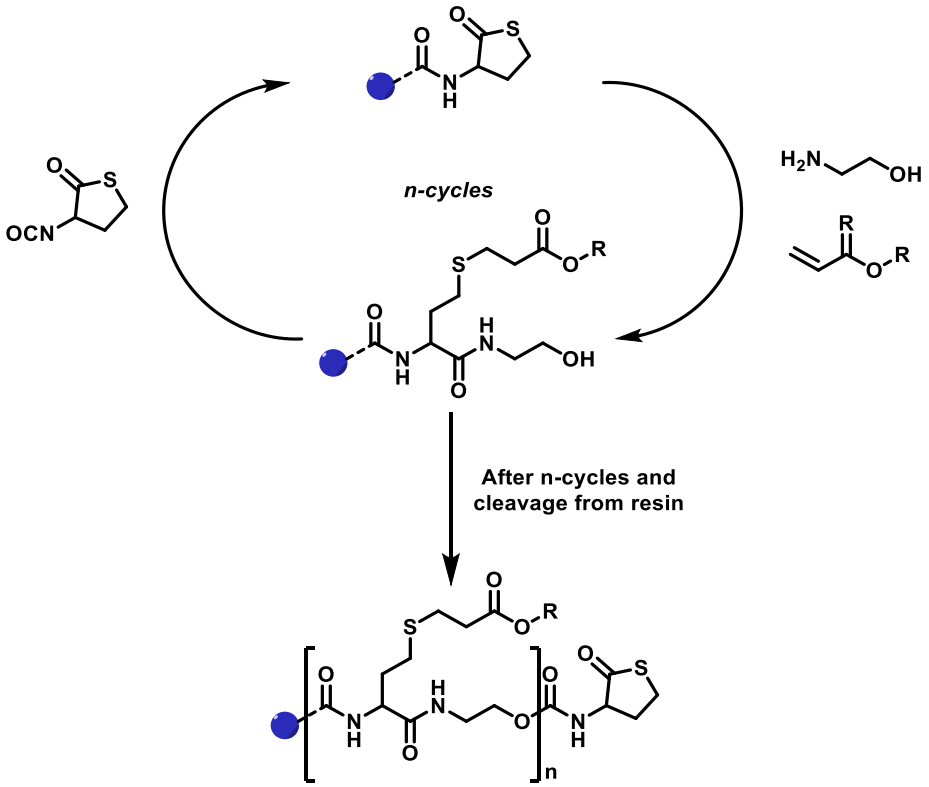
II.5.5 Thiolactone reactions

As demonstrated above, thiol-X reactions are highly useful tools in sequence-defined oligomeric synthesis (and also the subsequent polymerisation of these oligomers). However, the downside of using thiols is their rather poor shelf-life, limited commercial availability and unpleasant odour.[24,25] As a result, means to generate or release thiols *in situ* were highly desired. Whilst numerous routes exist to use protected thiols,[277] thiolactone chemistry has risen to prominence within our group's sequence-defined research. Thiolactones enable the efficient, one-pot, double modification *via* a nucleophilic ring-opening reaction with primary amines, whereby the *in situ* released thiol can subsequently undergo a Michael addition with, for example, acrylates (see *Scheme II 11*) .[278–282] Although, 4-, 5- and 6-membered thiolactones have been introduced,[281] the 5-ring analogue – γ thiolactone – has been reported as being the most favourable substrate.[281] Moreover, this analogue is derived from D,L-homocysteine, which is itself an abundant, bio-based building block.[283]



Scheme II 11: Top) General reaction scheme showing the formation of three thiolactone analogues from their respective mercapto acid. Bottom) A mechanistic overview of the aminolysis and subsequent thiol-ene (Michael) addition of γ-thiolactone.[281]

Whilst our group was the first to report a thiolactone-based, sequence-defined synthesis approach, only tetramers of moderate purity were obtained initially.[284] Indeed, upon opening of the thiolactone moiety by a primary amine, the released thiols were found to react with one another, leading to disulfide by-products. Hence, treatment with dimethylphenylphosphine (DMPP) was desired, which both simultaneously reduced the disulfide bonds and catalysed the subsequent Michael addition with a thiolactone acrylamide moiety.[284] Later, Martens *et. al.*, developed a one-pot, solid-phase iterative protocol (see *Scheme II 12*) to yield multifunctional, sequence-defined oligomers of high purity.[41] Starting from thiolactone functionalised solid-phase resins, ethanolamine and acrylates with varying functionality were applied to give the desired sequence-defined oligomers. The use of ethanolamine is crucial, as it provides a functional handle to install an isocyanate-containing thiolactone moiety to initiate the next cycle. Sequences were made both manually and *via* an automated approach using an adapted peptide synthesiser, whereby the purity was higher for the manually synthesised oligomers, although more laborious to synthesise. In other words, the time-saving advantage of automated solid-phase protocols was clearly established. Moreover, the ability to work with multiple reactions in parallel enabled the synthesis of a library of multifunctional, sequence-defined oligomers. It should be noted that the main advantage of using thiolactone-based protocols is that, in contrast to peptide synthesis, no protecting groups are required.

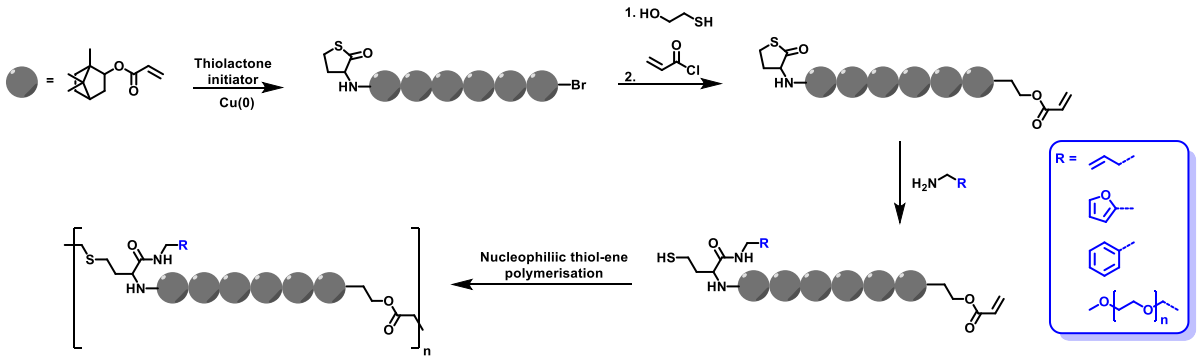


Scheme II 12: General overview of the iterative, solid-phase, sequence-defined protocol developed in our research group. This protocol was carried out both manually and in an automated fashion to yield multi-functional, sequence-defined oligomers.[41]

In a collaborative project with Becer and co-workers (Queen Mary, University of London),[42] the monomer scope of our solid-phase sequence-defined protocol was further expanded to thioacrylates and their further post-modification, as discussed in detail in the work in Chapter III. This work was improved upon further and is described in Chapter IV.[43] Thiolactone chemistry in combination with sequence-defined synthesis has also been used by our group, in collaboration with Börner and co-workers.[285] PEG was end-functionalised with thiolactone-derived sequence-defined oligomers to target biomedical applications (drug delivery) or applications in other fields such as anti-fouling coatings.[285]

Other collaborative works from our group have led to the combination of thiolactone chemistry with the Passerini three-component reaction in a convergent approach to synthesise a large library of sequence-defined oligomers which could be prepared on a multi gram scale.[53] The Passerini reaction in combination with amine thiolactone-ene-reactions in a one-pot synthesis approach, was also reported by Yang *et. al.*[269] They used the Passerini reaction to synthesise di-methacrylate species, which were then reacted with either monoamines and bis thiolactone compounds or diamines and mono thiolactone compounds to result in sequence-controlled polymers.[269] In an alternative approach, our group has also used thiolactone chemistry to generate sequence-defined, heterotelechelic, polyisobornyl acrylate

precursors with thiolactone and acrylate end-groups which were synthesised *via* a Cu(0)-mediated polymerisation with a thiolactone initiator.[270] The bromine end group was converted to an alcohol (using a thio-bromo reaction with 2-mercaptoethanol) and further modified with acryloyl chloride to provide the acrylate end functionality. The addition of various primary amines facilitated the ring-opening of the thiolactone-acrylate pre-polymers, which could then self-polymerise, with the pendant side groups installed at defined positions on the polymer backbone (see *Scheme II 13*). This approach enabled the synthesis of amphiphilic graft co-polymers with PEG-amine or sugar moieties (using allyl amine which could be post-modified with thiol-sugar species). The sequence-defined precursors allowed the grafted PEG- or glycosylated-arms to be spaced at precise intervals along the polymer chain. Alternatively, Van Lysebetten *et. al.* introduced thiolactone moieties at each end of oligopeptides, which were then cyclised *via* ring-opening with primary amines which enabled disulfide formation upon release of the thiols.[286]



Scheme II 13: Synthesis of α-thiolactone, ω-acrylate terminated polyisobornyl acrylate prepolymer and its subsequent modification with functional primary amines and nucleophilic thiol-ene polymerisation, resulting in sequence-controlled thiolactone-derived polymers.[270]

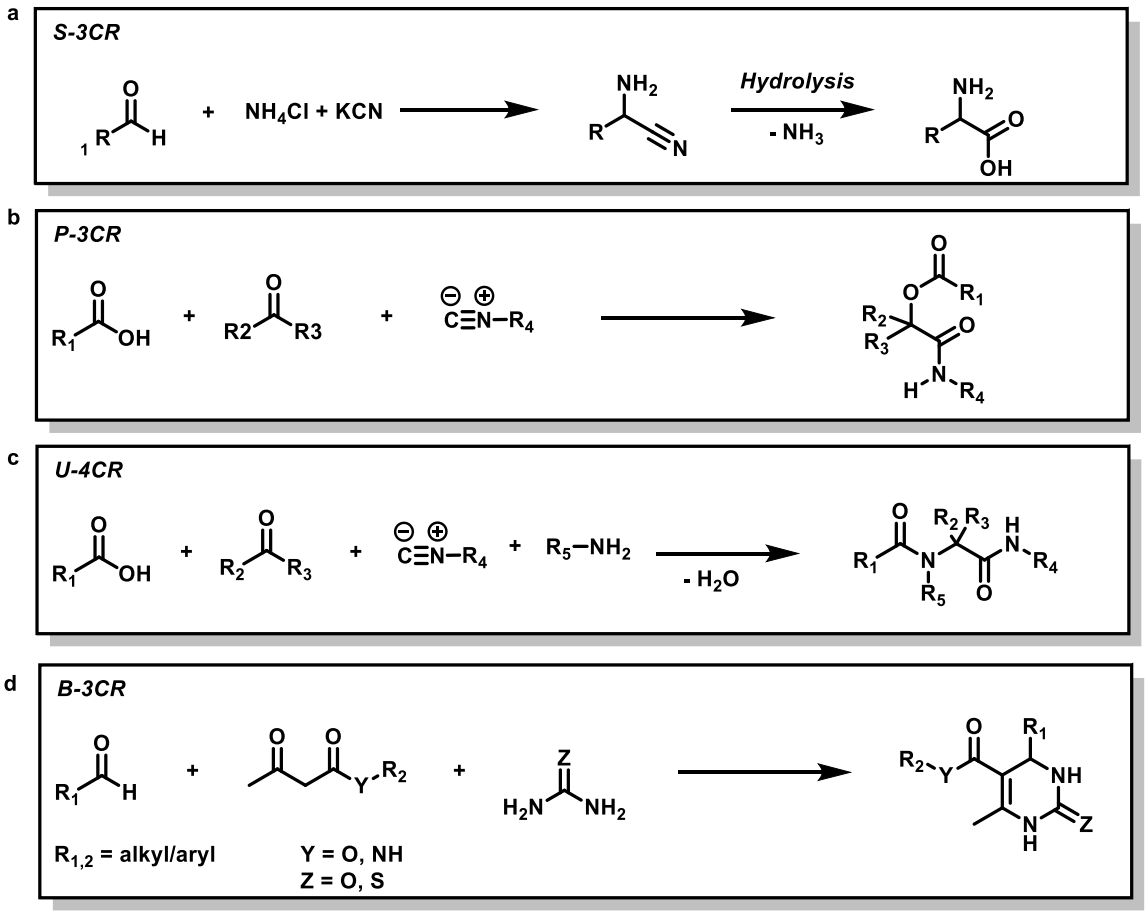
Many other research groups have used thiolactone chemistry to synthesise sequence-controlled polymers, utilising the thiolactone aminolysis reaction to facilitate the sequential addition of monomers, affording control over the sequence order.[268,269,287–289] A number of approaches were explored, the first of which resulted in sequences *via* a combination of thiolactone aminolysis followed by either nucleophilic and radical thiol-ene reactions, or just nucleophilic.[268,287,289] A thio-bromo reaction was also explored to synthesise alternative sequence-controlled polymers using dibromo and bromo-maleimide species.[287] Hong and co-workers have further investigated the thiolactone moieties in combination with diamine species and alkyne-methacrylates to generate dialkyne moieties. These could then undergo a subsequent reaction with sulfonylazides and either a diamine or a dithiol.[288] Alternatively, alkyne-amine species were used in combination with the sulfonylazide to result in sequences of a different monomer order within the sequence.[290]

Whilst thiol-ene (Michael) addition reactions were proven to be interesting click-like reactions in sequence-controlled and sequence-defined synthesis protocols, the use of thiolactones as protected thiols serves as a valuable expansion to the synthetic toolbox as they facilitate one-pot, double modification reactions. Therefore, thiolactone chemistry forms an important part of the current doctoral work, which was used to develop solid-phase, iterative protocols that were refined and automated, as will be discussed in Chapters III and IV.

II.6 Multicomponent reactions in sequence-defined synthesis

II.6.1 Introduction

A wide range of multicomponent reactions (MCRs) have been reported in organic chemistry, many of them around a century ago, including the Strecker multicomponent reaction (S-3CR, *Scheme II 14a*) for amino acid synthesis (which was the first reported MCR in 1850),[291,292] the Biginelli three-component reaction (B-3CR, *Scheme II 14b*),[293,294] Passerini three-component reaction (P-3CR, *Scheme II 14c*),[295] and Ugi four-component reaction (U-4CR, *Scheme II 14d*).[296] Many other examples of MCRs have also been developed since, which are generally categorised into metal-catalysed, isocyanide-based or non-isocyanide-based reactions.[297] Amongst these multicomponent reactions, the isocyanide-based routes are considered to be the most investigated, with the P-3CR and U-4CR having become the most relevant in polymer science and more specifically, in sequence-defined synthesis.[297] Hence, the Passerini and Ugi MCRs, which have been used in the current doctoral work (*cf.* Chapter VI and VII, respectively), will be discussed in more detail.

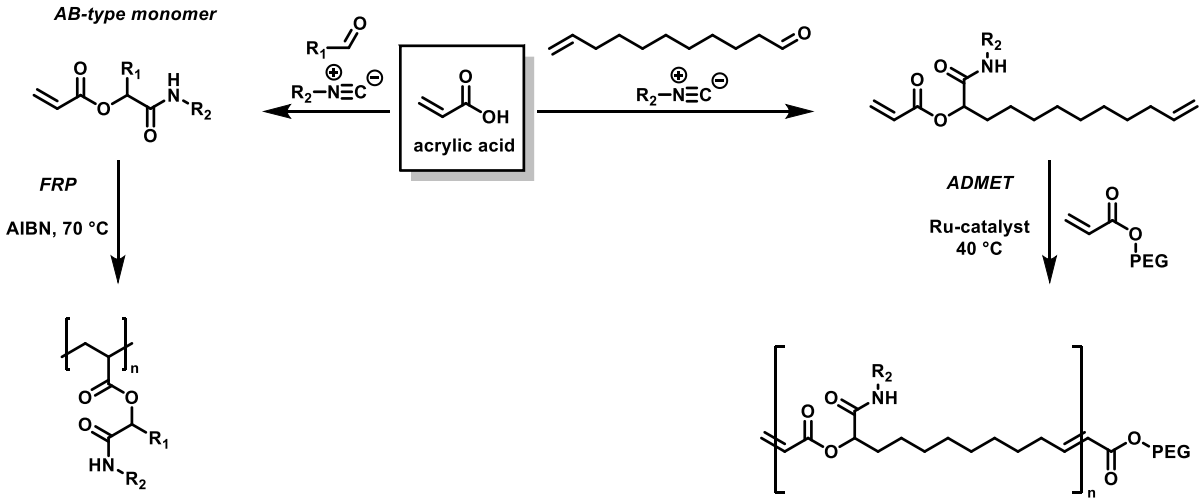


Scheme II 14: Examples of multicomponent reactions. a) Strecker multicomponent reaction, [291,292,297] *b) Passerini three-component reaction,*[295,298] *c) Ugi four-component reaction,*[296,298] *d) Biginelli three-component reaction.*[293,294,299]

II.6.2 Passerini three component reaction

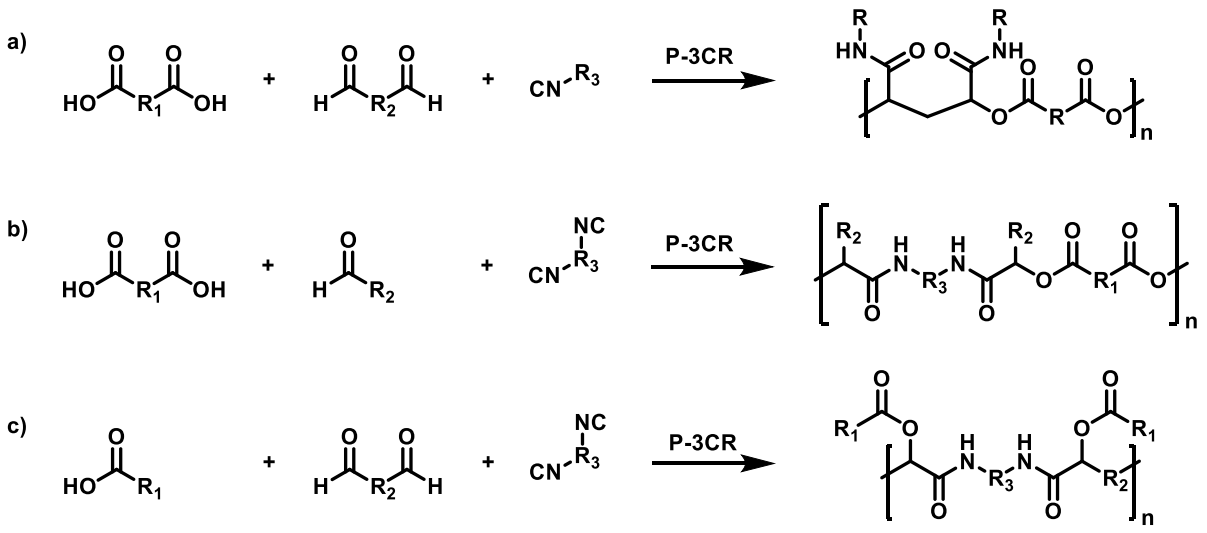
The P-3CR was first discovered by Mario Passerini in 1921 and involves the one-pot addition of a carboxylic acid, to an aldehyde or ketone and an isocyanide.[295] Its use within the context of polymer science has been well reported since.[298] The synthesis of monomers *via* the P-3CR was first reported in 2010 by Rubinshtein *et. al.*,[300] and in the same year, Meier and co-workers synthesised partially bio-based P-3CR monomers that are susceptible towards ADMET polymerisation, resulting in a highly efficient, one-pot avenue towards high molecular weight polymers (ca. M_n = 22 kDa).[101,301,302] In many of these approaches, 10-undecanal and 10-undecenoic acid can be employed to provide the required functionalities to affect metathesis polymerisation. However, acrylic acid was also used as a convenient building block in ADMET polymerisations, since the P-3CR between acrylic acid, 10-undecenal and an isocyanide resulted in unsymmetrical dienes (see *Scheme II 15*, right).[303] The latter could then be copolymerised with PEG-acrylate to yield amphiphilic block copolymers. Alternatively, the P-3CR of acrylic acid with an aldehyde and isocyanide can result in the formation of an alkene moiety, which can

be subjected to a Free Radical Polymerisation (FRP)[304] (see *Scheme II 15*, left). In addition, RAFT polymerisation has also been reported using P-3CR derived acrylate monomers, yielding homopolymers, statistical copolymers and block copolymers.[303]



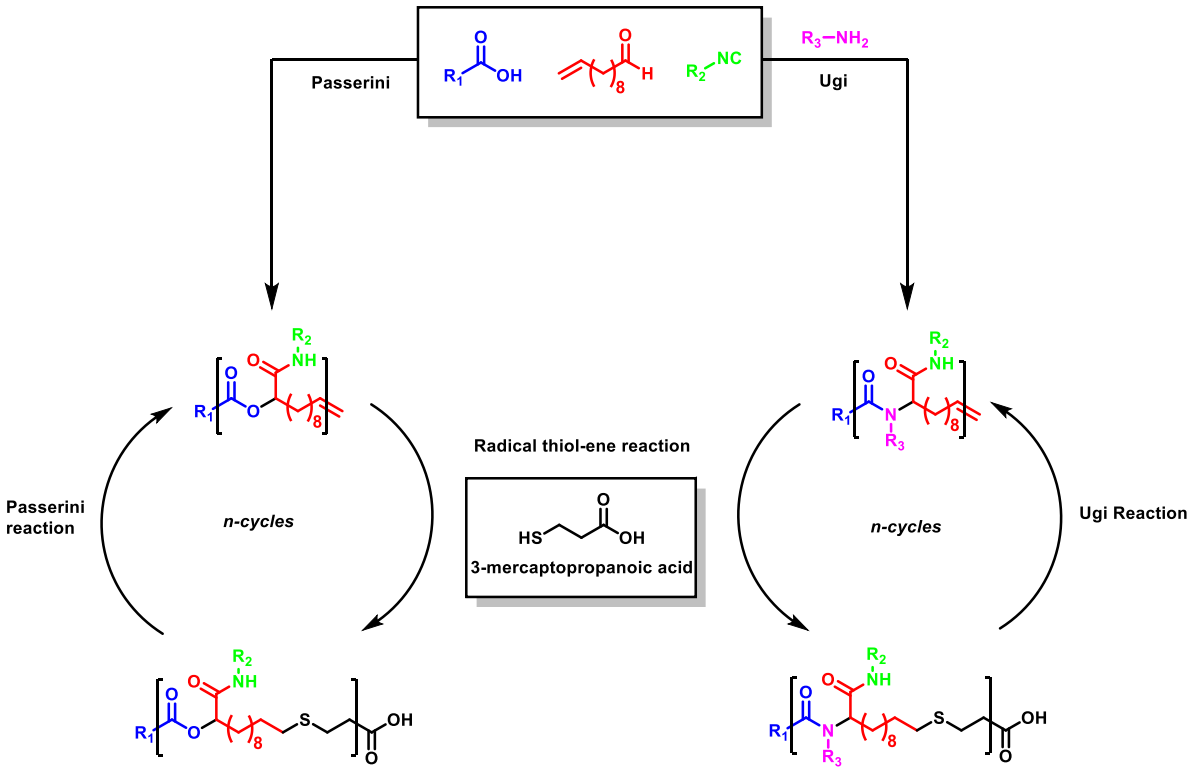
Scheme II 15: P-3CR polymerisation of acrylic acid via ADMET [303] *or FRP* [304] *techniques.*[298]

Besides radical polymerisations, step-growth addition polymerisations *via* the P-3CR are also feasible and have been successfully reported to yield linear and cyclic polymer products (depending on reaction concentration).[305] Importantly, two of the three components applied in the P-3CR need to be bifunctional and one monofunctional (AA + BB + AB-type monomers), and depending on the combination chosen, polyesters, poly(ester-amide)s or polyamides were possible products (see *Scheme II 16*).[298] Meier and co-workers reported the synthesis of α-amide-substituted polyesters of average molecular weights (M_n) up to 56 kDa, starting from a dicarboxylic acid, dialdehyde and mono-isocyanide.[302] In a similar manner, Li and co-workers investigated the addition polymerisation of diisocyanides and dicarboxylic acids in the presence of mono-aldehydes.[306] Furthermore, the *in-situ* generation of aldehydes from their corresponding alcohol during the P-3CR has been investigated.[307] A wide variety of more complex macromolecular structures have also possible been made accessible using the P-3CR, as illustrated by the convergent synthesis of dendrimers.[308]



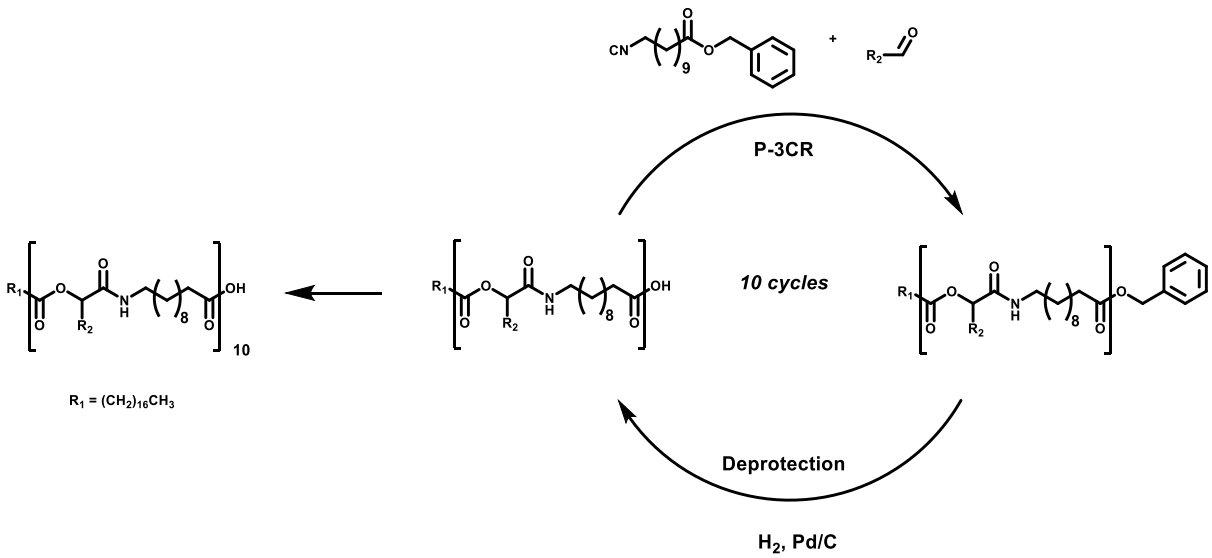
Scheme II 16: Passerini addition polymerisation possibilities using a combination of two bifunctional monomers and one monofunctional one in one-pot, yielding a) α-amide substituted polyesters, b) alternating poly(ester-amide)s and c) polyamides with pendant ester side-chains.[298]

Whereas the application of the P-3CR within the field of polymer science is vast,[298] it has recently gained much attention for the synthesis of sequence-defined oligomers, which was pioneered by Meier and co-workers in 2014.[51] In their initial report, monodisperse, sequence-defined tetramers (M_w = 1.6 kDa) were obtained in a two-step iterative procedure through the combination of the P-3CR with radical thiol-ene chemistry (see *Scheme II 17* left).[51] This approach was later extended to the U-4CR and is discussed in the following section (Section II.6.3).[52] In both cases, the multicomponent reaction utilises one component that is also functionalised with an end-standing alkene. This can then subsequently undergo radical thiol-ene reactions with 3-mercaptopropanoic acid to facilitate the following multicomponent reaction. Moreover, by using a PEG acid substrate in the Passerini reaction, an end functionalised sequence-defined pentamer block could be obtained. The advantage in the latter protocol was the simplified purification by means of precipitation over column chromatography. A crucial aspect of the use of multicomponent reactions is that it provides a protecting group-free strategy for an iterative synthetic protocol, which moreover facilitates the incorporation of numerous side-group functionalities. Additionally, this Passerini and thiol-ene combination was also reported by Zhang *et. al.* but using 1,6-diisocyanohexane, 10-undecylic acid and varying monoaldehydes.[309]



Scheme II 17: General overview showing the Passerini three-component reaction and the Ugi four-component reaction in combination with radical thiol-ene chemistry to result in both singly and doubly modified sequence-defined oligomers, respectively.[24,25]

The Meier group further optimised their original procedure into a more scalable and higher yielding approach, resulting in the gram-scale synthesis of a monodisperse, sequence-defined 20-mer (M_w = 7050 Da).[54] However, the 20-mer was derived from a tailored isocyanide carrying a benzyl-protected carboxylic acid whereby variation in the side-group functionality was now introduced by alteration of the aldehyde substrate (see *Scheme II 18*). Thus, a protecting group had to be introduced within the protocol in order to achieve the desired scalability. The result of this improved strategy was that on the level of a trimer, a 63 % yield was achieved and the synthesis was carried out on a 15-gram scale and an overall yield of 44 % was achieved for the decamer (compared with 26 % for the tetramer previously reported).[51] The introduction of a cis-double bond in the 10th iterative cycle facilitated a self-metathesis reaction to result in the sequence-defined 20-mer.



Scheme II 18: Iterative cycle for the scalable, high-yielding synthesis of sequence-defined oligomers via the P-3CR, starting from a protected isocyanide moiety.[54]

Solleder *et. al.* later reported the combination of the P-3CR with thiolactone chemistry (*vide supra*, Section II.5.5) in collaboration with our own research group to develop a convergent approach, which can be regarded as a variation of the protocol depicted in Scheme II 17.[53] By simply replacing the plain carboxylic acid moiety used in the initial P-3CR with a thiolactone-modified one, a functional handle could hence be introduced which could subsequently be derivatised through ring-opening aminolysis in the presence of an acrylate isocyanide. The resulting telechelic isocyanide and alkene-containing reaction product could finally be coupled via a P-3CR and thiol-ene reaction in order to rapidly expand the sequence.[53] Hence, the synthesis of thiolactone-derived sequences on gram-scale could be achieved, in contrast to the previously reported solid-phase synthesis of oligomers that could only be isolated in a few miligrams.[40–43,284] Barner-Kowollik and Meier also demonstrated an approach which combines P-3CR with Diels-Alder chemistry in a two-step protocol using a functional maleimide-isocyanide, α-methyl benzyl aldehyde and a carboxylic acid as an alternative combination of efficient chemistries to synthesise sequence-defined macromolecules.[310]

II.6.3 Ugi four component reaction

In addition to the Passerini MCR, the Ugi four component reaction (U-4CR) has also been used within polymer science, albeit to a lesser extent.[298] It differs from the P-3CR in that an amine and the aldehyde/ketone are first reacted with each other to form the corresponding imine, which only then is combined with the carboxylic acid and isocyanide substrates (*vide supra*, *Scheme II 14c*).[296,298] The first use of the U-4CR in polymer science dates back to 1999 when it was exploited in the crosslinking of

polysaccharides.[311] In 2003, Wright and co-workers described the first monomer synthesis via the Ugi reaction, which upon ROMP was transformed into high molecular weight polymers (*i.e.* $M_n \leq 50$ kDa).[298,312] Nonetheless, the U-4CR remained little explored since, until its monomer synthesis was re-investigated into more detail by Meier and co-workers - in parallel to their research concerning the P-3CR - to obtain structurally diverse polyamides *via* ADMET polymerisation.[298,313] Alternatively, a five-component version of the Ugi reaction (U-5CC) was also introduced whereby an alcohol and CO_2 were used to generate the acid *in situ*.[298,314] As a result, di-carbamate monomers became accessible which after a step-growth polymerisation afforded a range of functional polymers (*i.e.* polyurethanes, polyurethane-polycarbonates and polyamides). In a further example, the polycondensation of monomers synthesised by the U-4CR have also been examined, which is only possible making use of two AA-type or one AB-type monomers.[298] In addition, Wessjohann and co-workers observed that high concentrations were required to suppress macrocylisation.[315,316] The U-4CR has also been successfully used in PEGylation reactions for the conjugation onto a protein surface.[317]

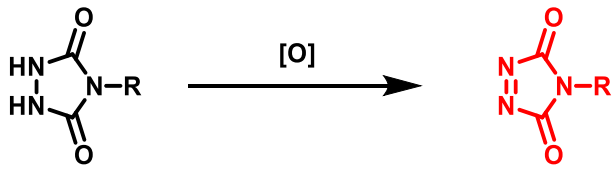
As mentioned in the previous section, Meier and co-workers introduced the Ugi MCR to sequence-defined synthesis in combination with the radical thiol-ene reaction (see *Scheme II 17* right). Through variation of both the isocyanide and the amine building blocks, a monodisperse, sequence-defined pentamer with 10 different functional side groups was hence obtained.[52,105] It should be noted that, as with the P-3CR, the U-4CR has been explored into a much greater extent within the field of polymer synthesis than the few examples outlined here.[298] For a more detailed overview, the interested reader is therefore referred to the relevant literature.[298]

Whereas both the Passerini and Ugi reaction are similar in terms of the components used (differing only by one additional reagent in the latter reaction), the U-4CR offers a significant advantage to the design of sequence-defined macromolecules as it enables the introduction of dual side-chain functionality. Related to the use of sequence defined oligomers in data storage, for instance, the introduction of different functionalities at once can lead to a significant expansion in information storage capacity. Indeed, when comparing the two approaches, a dimer synthesised *via* the P-3CR approach has the capacity of encoding 2^2 pieces of information, whereas a dimer obtained *via* the U-4CR can contain information up to 2^4. And yet, the use of the Ugi MCR for the synthesis of sequence-defined macromolecules is much more limited compared to the Passerini reaction. This might be attributed to the lower yields observed by Meier and co-workers for the Ugi-inspired synthesis of a decamer compared to its corresponding Passerini route (ca. 15 % compared with 44 %).[52,54,105] Nonetheless, the potential application of the U-4CR in the area of coding information for secret communication was elegantly demonstrated.[318]

II.7 1,2,4-Triazoline-3,5-dione chemistry

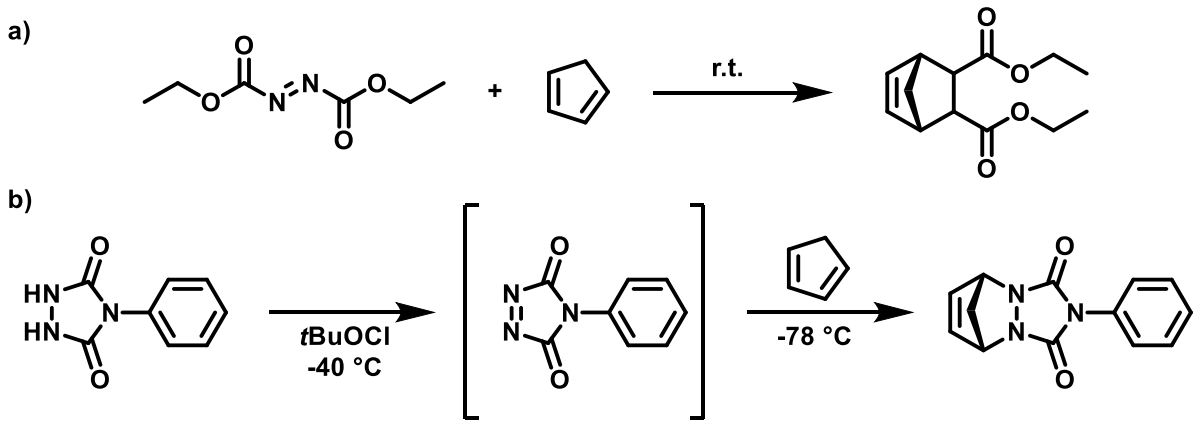
II.7.1 Introduction

1,2,4-Triazoline-3,5-diones - commonly referred to as triazolinediones or TADs - are a class of cyclic azocompounds that possess an extremely high reactivity towards electron-rich substrates, such as conjugated as well as isolated olefins (*vide infra*).[319–321] Although first reported by Thiele and Stange in 1894,[322] TAD reagents only found real interest in the 1960s following the first successful isolation of 4-phenyltriazolinedione (PhTAD) as carmine red crystals by Cookson *et. al.*.[319,320,323] The highly reactive TAD species typically showcase a rather limited stability and are therefore generated upon oxidation of their corresponding, bench-stable urazole compound (see *Scheme II 19*). This oxidation is accompanied by a colour change as the TAD species, unlike the urazole, has a bright red/pink colour. This can later provide a visual feedback during subsequent reaction as the vivid colour is then lost.[321] Recently, our own research group examined the click chemistry characteristics of triazolinediones upon reaction with (conjugated) alkenes[324] and re-introduced TADs as highly enabling tools for the low-temperature modification and crosslinking of unsaturated polymers.[321,324,325] A comprehensive discussion concerning the synthesis, reactivity and application of TAD compounds within polymer science is provided in a recent (2016) review by our group.[321]



Scheme II 19: Synthesis of triazolinediones through the oxidation of their corresponding bench-stable urazole precursor.

Principally, the reactivity of triazolinediones is centred around the nitrogen-nitrogen double bond. A similar bond configuration is also found in diethyl azodicarboxylate, which was already reported in 1925 by Otto Diels *et. al.*[247] to be highly reactive towards conjugated dienes with the quantitative formation of a cycloadduct at room temperature (see *Scheme II 20 a*). Together with Kurt Alder, this transformation later became known as the Diels-Alder reaction.[326] As TAD compounds also contain a nitrogen-nitrogen double bond, their Diels-Alder reactivity with cyclopentadiene was examined by Cookson and co-workers, who found that the cycloaddition proceeds instantaneous, even at very low temperatures (*i.e.* -78 °C, see *Scheme II 20 b*).[319,321,323]



Scheme II 20: a) Diels-Alder reaction between diethyl azidocarboxylate and cyclopentadiene with the quantitative formation of the cycloadduct at room temperature. b) In situ *formation of 4-phenyltriazolinedione from its corresponding urazole precursor in the presence of cyclopentadiene converts TAD instantaneous into its Diels-Alder product.*[319,321]

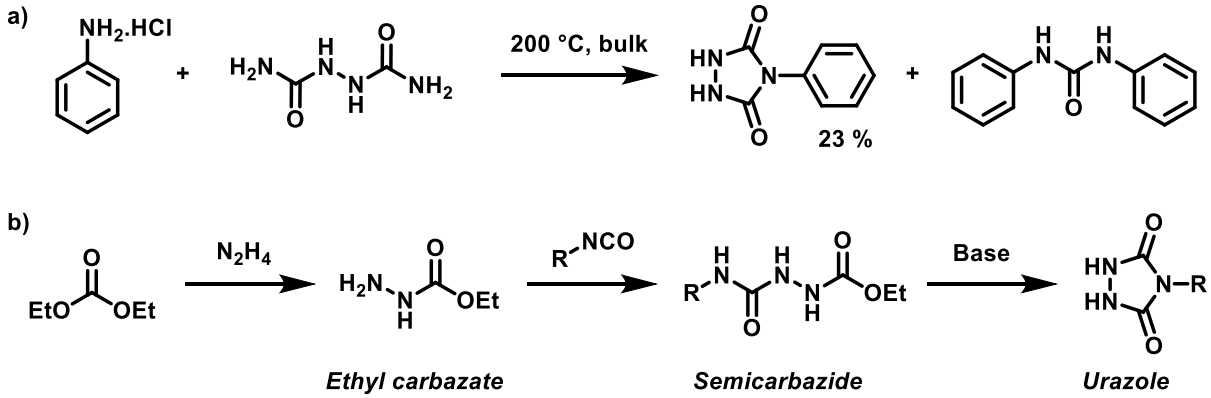
The remarkable reactivity of TADs sparked what would become decades of research into this unique class of cyclic compounds and this has grown into an area of intense research within our own Polymer Chemistry Research group at Ghent University. Within the current doctoral work, TAD-based click chemistry, for the first time, has been introduced into the field of sequence-defined oligomers and has played a pivotal role in the design of synthetic protocols towards these precision macromolecules. As a result, the first part of the current section (II.6.2) will outline some conventional synthesis strategies to generate triazolinedione reagents, which today all proceed *via* the oxidation of a suitable urazole precursor. Hence, not only the preparation of these urazole moieties will be discussed in more detail (II.6.2.1), but also different oxidants that can affect the crucial final TAD synthesis step will be highlighted (II.6.2.2). Following an overview of their synthesis, the unique and remarkable reactivity of TADs will be outlined (II.6.3) and the use of TADs within contemporary polymer science will briefly be discussed (II.6.4). Finally, the potential use of TAD moieties within sequence-defined synthesis on account of their unique reactivity properties will be presented (II.6.5).

II.7.2 Synthesis routes towards TAD molecules

II.7.2.1 Urazole synthesis

The first synthesis of a 4-substituted urazole was reported, when 4-phenylurazole was obtained upon heating a mixture of aniline hydrochloride salt (in order to prevent unwanted side reactions from using the pure amine)[322,327] and bis-urea in bulk at 200 °C (see *Scheme II 21a*).[322] However, in many subsequent cases, the bis-urea synthesis route was reported to be tedious and rather limited in scope.[321] Variations involving 1-substituted [321,328–330] or 1,6-substituted [321,330,331] bis-urea which are cyclised into

the urazole have also been reported along with procedures that involved the direct condensation of an amine with an unsubstituted urazole to introduce functionalities at the 4-position.[321,322,332–334]



Scheme II 21: a) First reported synthesis of 4-phenyl urazole.[321,322] *b) Zinner and Deunecker approach to urazole synthesis via an ethyl carbazate and semicarbazide intermediate. This was later utilised by Cookson to synthesise phenyl-TAD.* [320,321,335]

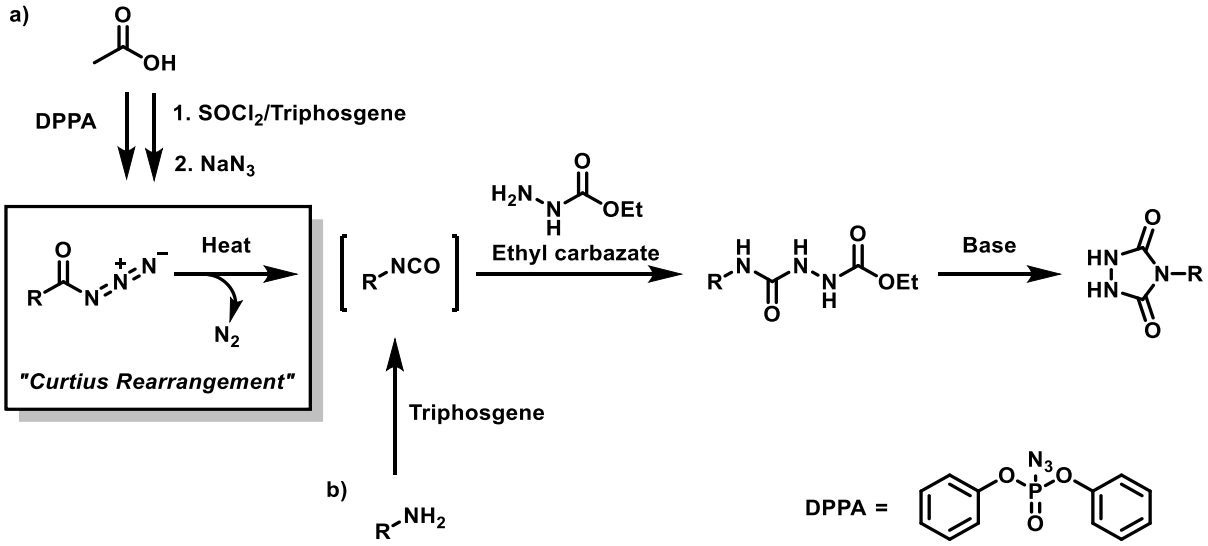
Over the 20th century, the original urazole synthesis approach was improved upon, notably by Zinner and Deucker in 1961 (*Scheme II 21b*), who first synthesised ethyl carbazate (now commercially available), which upon reaction with an isocyanate resulted in the 1-(ethoxycarbonyl)semicarbazide intermediates.[335] Subsequent ring-closure of this semicarbazide eventually afforded the corresponding urazole under much milder conditions. The introduction of this class of intermediates, commonly referred to as *semicarbazides*, paved the way for many modern synthesis routes towards 4-substituted urazoles.[321] 10 years later, Cookson *et. al.* utilised the Zinner-Deucker urazole synthesis for the first efficient isolation of 4-phenyl-1,2,4-triazoline-3,5-dione (phenyl-TAD), which was obtained following a subsequent oxidation of the respective urazole moieity.[320] Literature over the following decades has acknowledged the breakthrough method outlined here by Cookson *et. al.*, referring to phenyl-TAD as Cookson's reagent [336,337] and the synthesis thereafter became known as the Cookson method.[321,338]

The defining work of Zinner, Deucker and Cookson revealed the intermediate class of semicarbazides to be a crucial aspect in urazole synthesis. By simple alteration of the isocyanate substrate (a relatively large offering of varying structures and functionalities exists commercially), one can yield semicarbazides with a desired substituent and thus directly influence the structure of the resulting urazole and ultimate TAD compound.[321,339,340] The reactivity of isocyanate compounds towards ethyl carbazate, even at room temperature, means that semicarbazides can be easily obtained in high yields and often without the need for purification.[321] Indeed, when hydrophobic solvents are utilised, the semicarbazide precipitates and can be readily isolated through filtration. It has even been demonstrated that 4-phenyl urazole can be prepared on an industrial scale, with a good yield (> 90 % on a 4 kg

scale).[321,341] A key advancement in the use of isocyanates for semicarbazide (and urazole) synthesis was the introduction of bifunctional isocyanates, such as 4,4'-methylene diisocyanate (MDI) and 1,6-hexamethylene diisocyanate (HDI), which in turn enabled the preparation of bisTAD compounds.[321,342–345] This is of particular interest for material applications as bisTAD moieties can be used as highly efficient and ultrafast crosslinking agents, for example, the crosslinking of plant oils into transparent foils (see Section II.7.4).[346,347]

Despite the high efficiency and practicality associated with the Cookson method, a key limitation is found in its dependence on the commercial availability of isocyanates. As a result, many variations of the Cookson method have been investigated, most notably by generating the substituted isocyanate *in situ*, starting with, for instance, carboxylic acids,[321] which can be readily converted into an acyl azide in a one or two-step approach.[348–351] Treatment of a carboxylic acid with thionyl chloride, followed by a nucleophilic substitution with sodium azide, for example, readily gives the corresponding acyl azide. Upon heating, this will undergo a Curtius rearrangement, yielding the desired isocyanate (see *Scheme II 22 a*).[321,349–353] The combination of the Curtius rearrangement with Cookson's original procedure have become better known as the extend Cookson method and is seen as a great improvement to Cookson's original procedure.[321] This method, however, requires careful handling, owing to the explosive nature of NaN_3 along with the volatile and toxic nature of the highly reactive $SOCl_2$. Mallakpour and co-workers later examined the use of activated carboxylic acid species to obtain a structurally diverse scope of aryl-substituted semicarbazide intermediates which could be subsequently converted into the urazole targets in a high-yielding, multi-step strategy.[321,350]

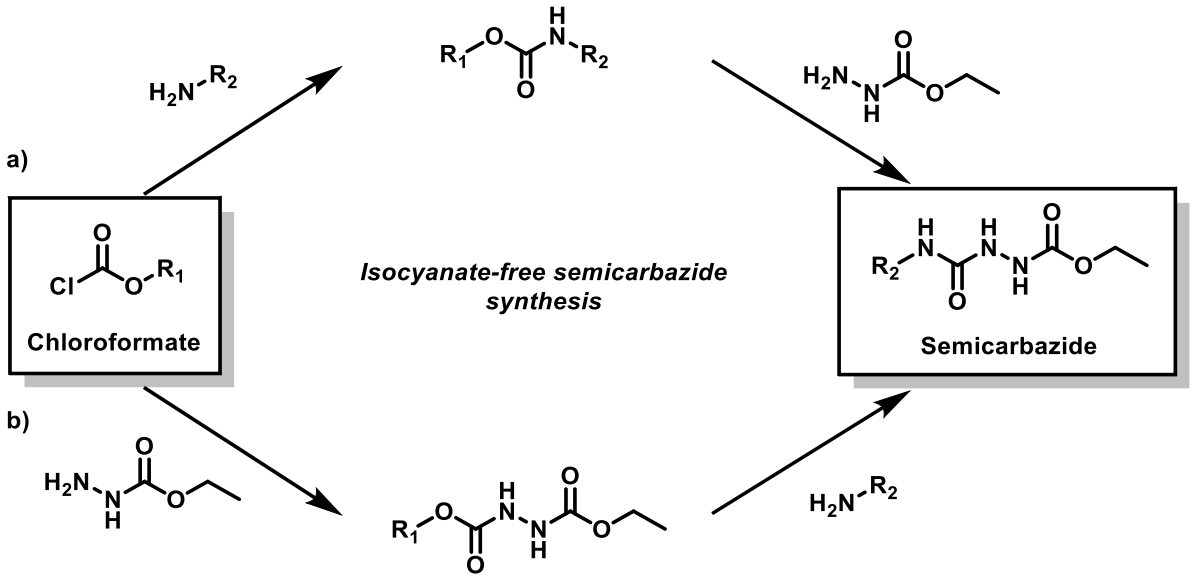
Next to carboxylic acids, primary amines can also be transformed into isocyanates upon phosgene addition (see *Scheme II 22 b*),[354,355] as well as *via* more moderate phosgene analogues.[356] In fact, the large commercial availability of primary amines, and their relatively inexpensive price, makes them ideal starting reagents for the synthesis of TAD compounds. However, the drawback of such an approach is the use of phosgene (or its derivatives) which is also notably toxic and thus must be handled appropriately, although di-[357] and triphosgene[358] can be regarded as a safer alternative to the more lethal, gaseous phosgene. Nonetheless, Paquette and co-workers demonstrated the advantage of the extended substrate scope with the synthesis of enantiomerically pure TAD species from chiral amines.[359,360]



Scheme II 22: Extended Cookson method. a) Carboxylic acid is converted to an acyl azide in a one-step approach using DPPA,[351] *or in a two-step approach using either triphosgene,*[348] *or thionyl chlorides*[350] *followed by treatment with sodium azide.*[350] *Subsequent heating results in a Curtius rearrangement. b) A primary amine is converted into an isocyanate by treatment with triphosgene, for example. The resulting isocyanate is treated as an intermediate, rather than being isolated and undergoes an* in situ *reaction with ethyl carbazate. The structure of the original carboxylic acid used dictates the final structure of the resulting urazole (and later TAD) molecule.*

Although the extended Cookson method has proved fruitful in TAD synthesis, the generation of isocyanates, albeit *in situ*, arguably remains unfavourable by some (notably in industry), because of their toxicity. Generally, throughout the chemical industry, isocyanate-free synthesis approaches are emerging - for example, in polyurethane production. Along with the fact that most routes following the extended Cookson method use other hazardous reagents (*e.g.* phosgene or derivatives thereof, sodium azide and thionyl chloride) to generate isocyanates *in situ*, alternative isocyanate-free approaches have also been investigated with respect to the synthesis of semicarbazides.[321]

Two notable isocyanate-free routes both start from chloroformates, although differing somewhat in their synthetic design (*Scheme II 23*).[321] The first route, depicted in *Scheme II 23a*, proposed by Mallakpour and co-workers,[361] involved the reaction of *p*-nitrophenyl chloroformate with aniline derivatives to give a phenyl-substituted carbamate derivative. The reactivity of the resulting carbamate in the follow-up reaction with ethyl carbazate is dependent on the chloroformate used, with ethyl chloroformate leading to significantly lower yields of the semicarbazide target. Nonetheless, all urazoles reported were obtained in high yields (> 89 %).[361,362]



Scheme II 23: Two proposed isocyanate-free semicarbazide synthesis routes, both commencing with chloroformates as start material. a) Reaction of chloroformate (R_1 = p-nitrophenyl [361], ethyl [362]) with primary amines (aniline derivatives) to form the corresponding carbamate followed by subsequent reaction with ethyl carbazate to yield desired semicarbazide.[361,362] *b) Direct reaction of chloroformate (R_1 = Ph) with ethyl carbazate, before reaction with primary amine to yield semicarbazide. Figure adapted from Chem. Soc. Rev., 2016.*[321]

In 2014, a second isocyanate-free strategy towards semicarbazides was introduced (*Scheme II 23b*).[338] Again, phenyl chloroformate was applied as the starting reagent, only this time reacted first with ethyl carbazate to obtain the ethyl phenyl hydrazine-1,2-dicarboxylate, which was subsequently combined with various primary amines at room temperature to afford the corresponding semicarbazides in high yields (> 76 %), except with aniline, which did not result in the corresponding phenyl-substituted intermediate, even after prolonged reaction times (*i.e.* > 24 h).[321,338] Both isocyanate-free routes were later condensed into a one-pot synthesis routes by Barbas and co-workers, leading to a range of differently functionalised TAD compounds that were of interest in TAD-based bioconjugation of peptides.[363,364] A one-pot synthesis approach towards azide-containing TAD species was also reported by Hu and co-workers when investigating further interesting applications of the glycoconjugation (of vaccines).[365,366]

Within our own research group, isocyanate free approaches have also been developed, ultimately leading to a more sustainable route towards urazole synthesis.[367] This synthesis route focussed upon the use of primary amines (which were cheaper and more readily abundant than isocyanates) as starting compounds together with diphenyl carbonate. They were implemented in a mostly solvent-free, high yielding and equimolar manner, yielding a range of urazole compounds.[367] In the present doctoral work, this newly introduced strategy was utilised for the synthesis of an aliphatic carboxylic acid functionalised TAD compound, which was a valuable click reagent that could be combined with

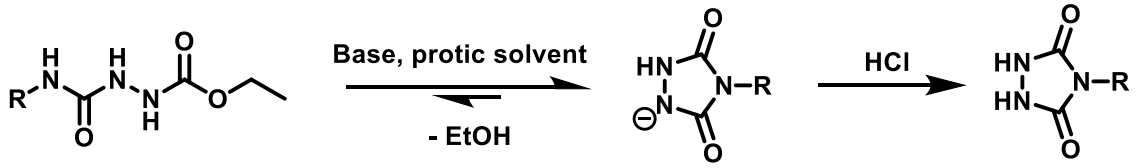
multicomponent reactions in the pursuit of sequence-defined oligomers (*cf.* Chapters VI and VII). Additionally, Little *et. al.* demonstrated the potential of carbonyl diimidazole (CDI) coupling agents to modify a range of amines, including aniline, into their 4-substituted urazole derivatives.[349] Alternative, older 'isocyanate-free' approaches to synthesise semicarbazides are also known, using both aliphatic and fluorinated amines. However, these pathways still require phosgene to generate the necessary intermediates, which is much more hazardous.[368,369]

A final point regarding semicarbazide synthesis is the possibility to post-modify an existing structure. The use of sodium azide to access azide-containing semicarbazides has been proposed,[321,370] for instance, while Mallakpour reported the tin(II)-catalysed reduction of *p*-nitrophenyl semicarbazide to its corresponding aniline.[371] Nonetheless, the introduction of additional functionalities on the semicarbazide level can often result in chemoselectivity issues, owing to the basic reaction conditions that are required during the cyclisation step (*vide infra*).[321]

As discussed so far, semicarbazides are important precursors in the synthesis of 4-substituted urazoles and numerous synthetic procedures to obtain these valuable intermediates have been reported. In contrast to this, the ring-closure of a semicarbazide into a urazole typically only proceeds *via* a limited number of relatively straightforward pathways, *i.e.* under alkaline or thermal conditions.[321] In general, the preferred ring-closure route is base catalysed (*e.g.* with potassium hydroxide) in a protic solvent, as in Zinner and Deucker's original procedure,[335] although potassium carbonate is also reported as an alternative base (see, *Scheme II 24*).[368] In the original Cookson synthesis of PhTAD, cyclisation was also achieved by refluxing the semicarbazide in aqueous KOH. The resulting solution containing the urazole-potassium salt was then acidified to pH ≈ 1, isolating the desired neutral urazole compound by means of precipitation.[320,321] However, refluxing in KOH can be considered as quite harsh conditions and can therefore result in the formation of side products.[321] Bulky or electron-withdrawing functionalities on the urazole, for instance, have been reported to suffer from competitive hydrolysis and decarboxylation as opposed to cylisation.[349] In addition, refluxing KOH has been observed to enable nucleophilic aromatic substitution of 4-pentafluorophenylurazole.[368] Nonetheless, this ring-closure approach is still widely used since many urazoles (particularly 4-aryl substituted ones)[368] easily precipitate from the reaction mixture upon acidification.[321]

Sodium ethoxide in combination with refluxing ethanol is a potentially milder option for the ring closure of semicarbazides, although the process is typically slower compared to the KOH-mediated cyclisation. In this case, the urazole needs to be isolated using a non-aqueous work-up, which is more suitable for

urazoles that tend to precipitate less readily in aqueous media (*e.g.* aliphatic substituted ones).[349,372] An even milder alternative can be found in potassium carbonate, although this again reduces reaction times of the cyclisation.[321,368] In addition to alcoholic solvents, water is also a possibility.[349,368,373] Alternatively, Mallakpour reported the use of triethylamine in combination with acetone.[362]



Scheme II 24: Base-catalysed ring-closure of a semicarbazide into a urazole.

Next to base-mediated cyclisation, the original method used by Thiele and Stange can also be applied to convert semicarbazides into their urazole derivatives.[322] Here, simply heating the semicarbazide above 200 °C is sufficient to complete ring closure. Today, however, this method is exclusively applied to those cases where the aforementioned base-catalysed approaches are found to be unsuitable.[321] However, with urazole synthesis, unlike that of semicarbazides, there is a wide range of possibilities with respect to the post-modification of the urazole structure prior to oxidation in order to greatly expand the range of functionalities and structures that can be incorporated onto the final TAD moiety. Modification can either be achieved during the semicarbazide cyclisation,[374,375] *via* hydrogenation and hydride addition of a suitable urazole compound,[324,364,373,376] or through electrophilic aromatic substitution[377] and click-type modification (*i.e. via* CuAAC).[363,364,378]

Finally, an important aspect of urazole synthesis that is relevant to this doctoral work, is that amine, hydroxyl and (activated) carboxylic acid groups suffer from chemoselectivity issues during the aforementioned synthesis routes, but instead can be easily introduced *via* a post-modification of other functional urazoles.[321] For example, Chapter V discusses the synthesis of an unprecedented thiolactone-functionalised TAD compound. Here the ring-closure of a thiolactone-semicarbazide was not possible whilst preserving the thiolactone unit. Instead, a functional thiolactone compound and 4-aniline urazole were synthesised separately and coupled together in a final step. 4-Aniline urazole is a very versatile substrate in post-modification reactions,[324,346] and was already used for the synthesis of imide derivatives such as 1,8-naphthalimidophenyl urazole,[379,380] azo derivatives when reacted with nitrosobenzene,[381] or an ATRP-initiator when coupling with an acid bromide.[324,382] Whilst the synthesis of alcohol containing urazoles has been barely explored, a greater number of examples exist for the reaction of activated carboxylic acid moieties with amino-urazoles. A common example is the activation of a carboxylic acid with *N*-hydroxysuccinimide (NHS), which can then be coupled to an amino-containing urazole.[321,363–365]

As can be seen in this sub-section, a wide range of synthesis routes have already been explored to generate functional urazole moieties, despite some being somewhat tedious. Notably, the synthesis of 4-substituted urazole derivatives and bifunctional urazole compounds has been easily accessible from cheap, commercial starting products and even in an isocyanate-free manner.

II.7.2.2 Oxidation of urazoles to corresponding TADs

To date, all TAD compounds are synthesised *via* oxidation of their corresponding urazoles. As with urazole synthesis, there is more than one oxidation route available, and in many cases, the choice of oxidant can strongly depend upon the compatibility with substituents on the urazole. Thus, high chemoselectivity is a crucial parameter to select the right oxidation method, along with orthogonality between the oxidant and the formed TAD species. Equally important is the ability to easily recover the TAD molecule from the resulting oxidation mixture. Indeed, given the high reactivity of TAD, one does not wish to extensively purify the final product after oxidation. Hence, simple filtration of formed salts followed by solvent removal *in vacuo* is often the preferred method for TAD isolation. Alternatively, an *in situ* oxidation is desired in some cases as this circumvents the need of one having to isolate the TAD product. Whilst urazole precursors are typically bench stable (*i.e.* > 2 years), the stability of TAD compounds can vary from minutes to days and months. As such, one often only oxidises urazoles shortly before the corresponding TAD is required.[321]

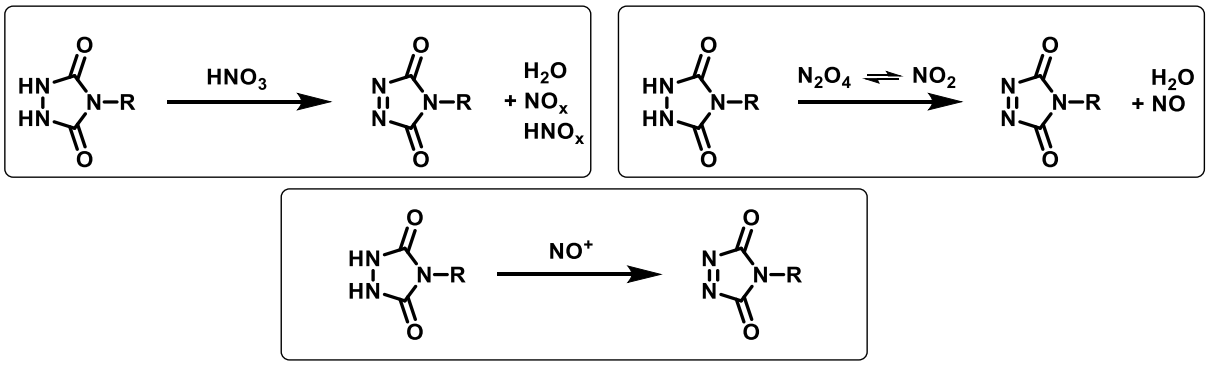
There is no fixed rule as to which urazole oxidation method is the most suitable, thus often some trial-and-error in the laboratory is required before the best one is found. *Table II 1* outlines a range of available oxidation methods of which the most relevant are the nitrogen and halogen mediated-routes.[321] These will be discussed in more detail below, whereas activated DMSO/selenic acid routes, metal-ion/metal-oxide and electrochemical oxidation routes fall outside the scope of this thesis. A complete overview of the possible routes to transform urazoles into TADs is presented in the recent review by De Bruycker *et.al.*[321]

Table II 1: General overview of the multitude of urazole oxidation routes to obtain TAD compounds. The ones in bold will be discussed further in this section.

Nitrogen (IV) and (V) Oxide-based			**Halogen (X) -mediated**				**Activated DMSO/ Selenic acid**	**Metal-ion/oxide**	**Electro-chemical**
HNO_3	**NO_2/ N_2O_4**	**N(IV) oxide**	**Cl_2/ Br_2**	**Hypo-chlorite**	***In situ***	**Catalytic**			

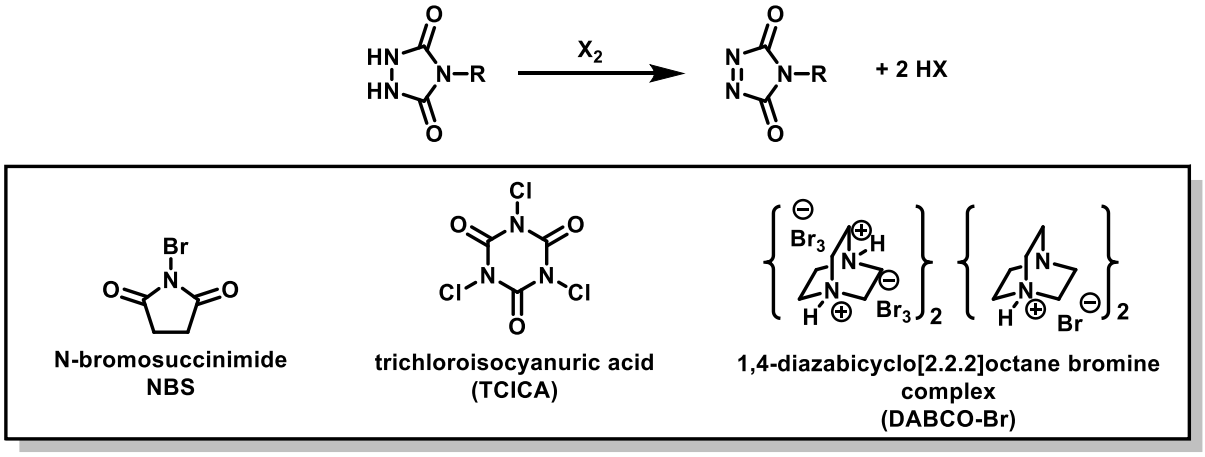
A range of nitrogen-based oxidation routes exist, as shown below in *Scheme II 25*. Nitric acid (HNO_3) was first utilised by Thiele and Stange as an oxidant,[322] but the limited shelf-life of PhTAD in the obtained reaction mixture meant that the oxidised product could never be isolated. The same oxidation method was later explored and optimised by Furdik *et.al.*, who applied fuming HNO_3 to the urazole suspended in chloroform to obtain 4-alkyl- and 4-benzyl-TADs, although again having a short life time.[383] This method was also later adopted for the successful oxidation of the bifunctional MDI-urazole derivatives which had better (although still limited) stability but the work up was somewhat tedious.[345] A few years later, Read and Lim developed the approach even further, resulting in both a good yield and a red stable crystalline PhTAD product.[384]

Although a cheap and readily available starting material, alternatives to HNO_3 were investigated as the aqueous work up (which can lead to TAD hydrolysis) and reaction by-products limited the TAD yields.[321] N_2O_4 was proposed by Stickler and Pirkle as a water and acid-free alternative to nitric acid and was also employed for the TAD synthesis described in Chapter VI of the current thesis.[31,385] Existing as a gas above 20 °C in an equilibrium with NO_2,[386] this oxidant readily and quantitatively converts urazoles to their respective TAD moieties, which are then easily isolatable following a quick filtration and removal of the solvent (of which a wide range are compatible).[31,387] Water is formed as an oxidation by-product, thus a drying agent such as magnesium sulfate is typically added.[31,321] One drawback to using N_2O_4 is its acute toxicity to humans and high cost, although an alternative set-up was developed by Mallakpour to generate N_2O_4 *in situ* from lead nitrate.[388] Nonetheless gaseous N_2O_4 is a very widely used oxidation technique for many urazole structures,[321] it has been known to cause side reactions when oxidising certain electron-rich aryl-substituted urazoles since undesired electrophilic aromatic nitration can also occur.[321,374] As a less hazardous alternative to N_2O_4 and also to reduce the amount of toxic waste, heterogeneous N-mediated oxidation routes have also been investigated.[321] Examples of such alternative routes include solid supports for nitrogen(VI)[389–392] species and the *in situ* generation of nitrogen (IV) from inorganic salts[392–401] or solid-supported acids.[392,402–405]



Scheme II 25: Overview of nitrogen-mediated urazole oxidation routes.[321]

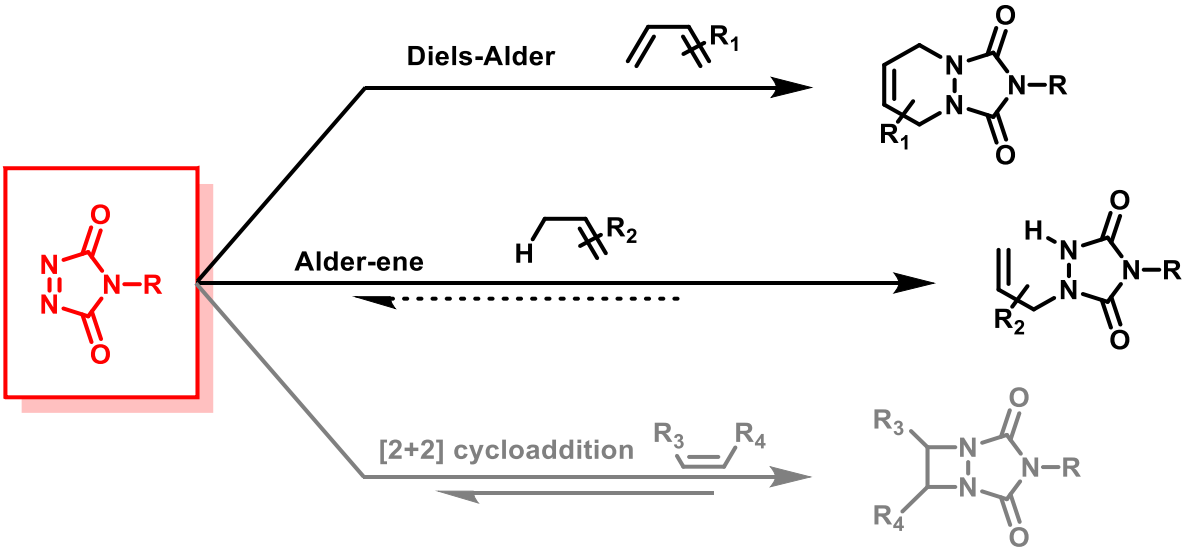
The key class of halogen-mediated oxidation methods are also relevant to the TAD synthesis within this thesis. Both elemental chlorine[406] and bromine[407] have been reported to oxidise 4-subsituted urazoles to TAD, although the yields and chemoselectivity were unfavourable. Hypochlorites are an alternative halogen-derived oxidation route and were even reported by Cookson for the oxidation of *tert*-butyl urazole in dry acetone at < -50 °C.[319] Changing the solvent later optimised this reaction, first with 1,4-dioxane [323] and later with ethyl acetate,[320] although the solubility of urazoles is often a limiting factor. Unlike with the N_2O_4 approach, the range of potential urazole substrates also includes electron-rich aromatic structures.[374] Nonetheless, as with the N_2O_4 approach, the use of a toxic gas is less than ideal and so again methods have been explored for *in situ* halogen generation (see *Scheme II 26*).[321] As well as solid-supported halide compounds such as silica-supported iodinemonochloride,[407] more well-known oxidants such as *N*-bromosuccinimide (NBS) (*Scheme II 26*) have been well reported.[408,409] Normally, extensive work-up of this method would be required, but as will be discussed in Chapter V, the crude reaction mixture can also be used directly, for example, in combination with solid-phase synthesis. An alternative, inexpensive and safer[410] oxidant is trichloroisocyanuric acid (TCICA) (*Scheme II 26*), which results in the formation of TAD moieties in high yields.[411] Moreover, TCICA is readily soluble in organic solvents, whereas its oxidation by-products are not and can be easily removed *via* filtration.[410] The use of TCICA will further be highlighted in Chapter VII as a safer and milder alternative to N_2O_4. DABCO-Br – a tetrameric 1,4-diazobicyclo[2.2.2]octane-bromine complex – is also an effective oxidant and has been used in urazole-functionalised polymer applications in our own research group,[324] but unlike TCICA is not commercially available. A final point to mention on halogen-mediated oxidation routes is the possibility of using catalytically generated halogen species, for example with halide salts (*e.g.* KBr).[321,412]



Scheme II 26: Halogen-mediated urazole oxidation routes, together with some commonly used examples of in situ *halogen generating oxidants to yield triazolinediones.*[321]

II.7.3 Reactivity of TAD compounds

The unique reactivity of TAD is why it was of great interest to our research group as it is ultrafast, chemoselective (and often irreversible) and provides a visual feedback (through the disappearance of the red colour upon reaction). Its reactivity is similar to that of singlet oxygen and also readily undergoes Diels-Alder, Alder-ene and [2+2] cycloaddition reactions (see *Scheme II 27*).[413,414] Indeed, with respect to orbital theory, both TAD and singlet oxygen have similar arrangements and energies of the filled and empty antibonding p-orbitals. They both have similar high energy π* HOMOs and low energy π* LUMOs and the orbitals are geometrically orthogonal to one another.[321,415]



Scheme II 27: Overview of the three principle reactions of TAD.[321] *The one which is greyed out, are outside of the scope of this doctoral thesis and so are not discussed in detail here .*

Scheme II 27 outlines the key reaction pathways of TAD that are of particular interest within this thesis (*cf.* Chapters V, VI and VII), namely the Diels-Alder and Alder-ene reactions, which proceed so rapidly and selectively, even at room temperature (or even below).[321] The third type of TAD-addition reaction, [2+2] cycloaddition, is beyond the scope of this doctoral dissertation and is therefore not discussed here.

TAD species undergo Diels-Alder reactions in an irreversible fashion almost instantaneously with many non-activated conjugated systems at room temperature, earning them the reputation of exceptional dienophiles.[319,321,415] Whereas normally Diels-Alder reactions proceed at elevated temperatures or require a catalyst to enable sufficient reaction rates,[416] even less reactive conjugated dienes such as anthracene and styrene are successful TAD-based Diels-Alder reaction partners at room temperature.[323] Moreover, with anthracene an equilibrium exists at ambient temperature, thus exhibiting reversibility.[417]

Alternatively, TAD-Alder-ene reactions[418] also readily occur at room temperature, with the TAD compound acting as an enophile. In such a reaction, the C=C π-bond shifts one position and a new C-C σ-bond is formed.[321] The Alder-ene reaction in general has been less explored than the Diels-Alder reaction because with most enophiles the rather poor orbital overlap and high activation barrier provides more constraints in the reaction.[419] With TAD, however, the reaction proceeds more readily, demonstrated by its high reactivity towards simple alkenes, first reported in 1967.[385] What is key in the reactivity and thus rate of TAD-Alder-ene reaction is the substitution of the alkene (*Figure II 2*).[420] As a result, it allows one to selectively control the TAD-alkene reaction kinetics, if desired.[346]

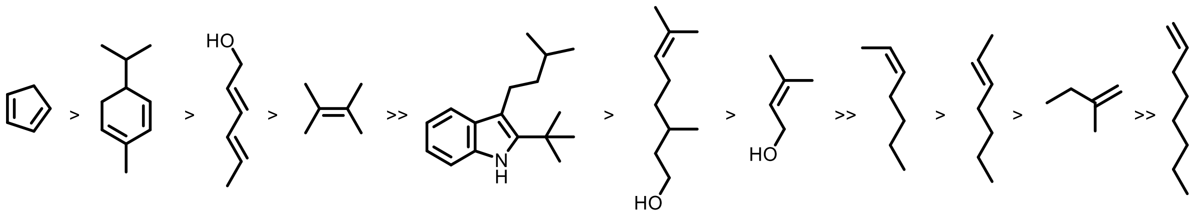
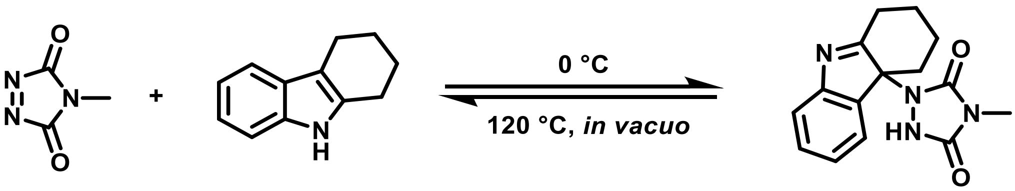


Figure II 2: Relative order of TAD-reactivity of substituted diene and alkene containing moieties.[420]

An important aspect of the Alder-ene reactivity of TAD that should be highlighted within the context of this thesis, is its thermoreversible addition to indole compounds (*Scheme II 28*). This interesting feature was first introduced in 2003 by Baran *et. al.*,[421] who, by heating at methyl-TAD-indole adduct at 120 °C, *in vacuo*, was able to re-isolate the initial indole starting compound. This reversible TAD-indole chemistry has since been explored by our research group to develop triggered TAD-based reactions and to transclick (*i.e*. reversibly click) TAD reagents.[324,422,423]



Scheme II 28: Thermoreversible TAD-Indole reaction, as reported by Baran et. al.[421]

II.7.4 Current applications in polymer chemistry

As discussed in the above sections, the area of TAD chemistry is one of interest within the field of organic chemistry. In our research group, we have sought to utilise this highly enabling synthetic tool within polymer science to facilitate polymer synthesis, modification and applications. One striking example of the use of TAD-click chemistry in material science is the ability to access bisfunctional TAD moieties (*vide II.6.2*) for the crosslinking of polydienes (*e.g.* polybutadiene)[424] and plant oils at

room temperature.[346,347] Furthermore, De Bruycker *et. al.*, successfully synthesised fluorinated TAD compounds for the modification of polybutadiene-containing surfaces to study the effect on their surface-wetting properties.[425] Mono- and bis-functional TADs were also successfully used by our group to post-modify ROMP- and ADMET-derived polymers.[425–427] In addition, TAD compounds have also been applied in the area of bioconjugation, with Barbas and co-workers being the first to report this conjugation with a polymeric end-functional TAD substrate.[363] Börner and co-workers recently investigated the transformation of *N*-terminal amino groups of peptides into reactive TAD moieties in order to click the resulting peptides onto diene end-capped polymers.[428] Finally, our group has also been developed the dynamic TAD-indole chemistry to create healable and recyclable polyurethane materials, via the reversible crosslinking of polyurethanes,[324] which through thermally-assisted shape-memory recovery can heal up to 1 mm deep cuts.[429]

II.7.5 Potential in sequence-defined synthesis

This thesis describes for the first time the use of triazolinedione chemistry in the synthesis of sequence-defined macromolecules. Therefore, one can only comment on its potential contribution to this field. What can be seen from the literature discussed within this chapter is that click chemistry holds a vital role in the synthesis of sequence-defined macromolecular systems. Its high efficiency and orthogonality correlates well with iterative synthesis approaches that target precise, well-defined macromolecules. Thus, as a highly efficient and remarkably interesting click chemistry as a result of its reversible and irreversible reactions and visual feedback systems, TAD chemistry contains much potential as a click chemistry that could be more widely used in sequence-defined synthesis. Furthermore, its coupling-agent free, thermoreversible nature and ultra-fast (<1 s) reactions with a wide range of alkene-containing substrates which are accompanied by a visual response, means that it could be considered to be superior to other click or efficient reactions.

II.8 Conclusions

The current chapter has highlighted the wealth of research that has been carried out within a relatively short space of time within the field of sequence-controlled and sequence-defined macromolecular synthesis. It has demonstrated the range of synthetic chemical methods and chemistry strategies that are commonly utilised within the pursuit of precision macromolecular design. Polymer science has clearly evolved rapidly in recent decades, with many advances in controlled polymerisation. However, the last 10 years has seen, perhaps, the greatest advancement in the field since the introduction of the first RDRP

technique in 1982. The state-of-the-art discussed within this chapter has shown the range of complex, multifunctional, monodisperse, macromolecular architectures that now exist and the ingenious approaches that have brought them into existence. The use of click, click-like and multicomponent reactions within sequence-defined synthesis has certainly been the organic chemistry of choice for many research groups. The subsequent chapters in this thesis will highlight the use and combination of such chemistries, *i.e.* thiolactone, 1,2,4-triazoline-3,5-dione chemistry and multicomponent reactions, to generate monodisperse macromolecules, not only for the purpose of investigating new protocols, but also to compare different chemical methods (*i.e.* solid-phase vs. solution-phase synthesis).

Whilst click chemistry has become an invaluable tool to the sequence-defined chemist, one notable click chemistry, that has so far been absent from this field is that of TAD chemistry. However, its ultrafast, chemoselective reactivity towards specific substrates means that it holds much potential for use within sequence-defined protocols and could be more advantageous than other click chemistries currently used in this field. Within the context of this thesis, we have not only sought to combined it with thiolactone chemistry in one molecule (*cf.* Chapter V), but we have also successfully married it with another efficient chemical platform – multicomponent reactions – as outlined in Chapters VI and VII. Through the synthesis of functional TAD species and corresponding reaction partners, we have introduced this click chemistry to both the P-3CR and U-4CR in an irreversible and reversible fashion, to bring click and multicomponent reactions together.

Finally, whilst this chapter has highlighted the progress made into sequence-defined synthesis, there also currently remain many challenges within this field that still need to be addressed. Whilst much fundamental research has taken place to date, scientists in this field need to now focus their attention towards considering the potential commercial applications of sequence-defined macromolecules (as proposed by the proof-of-concept presented in Chapter VII). Therefore, it could be said that the biggest challenge yet is to still prove the importance of synthesising such precise structures and whether they provide a significant advantage that is worth the added synthetic effort. A recent mini-review by Meier and Barner-Kowollik hinted towards some of the newly emerging applications of sequence-defined macromolecules,[430] such as data storage,[70,182,431] molecular tagging,[46,74,432,433] cryptography[40,318] or biomedical applications.[434] Further investigation on the effect of chain length and monomer unit spacing is also an important challenge to be addressed. This could influence which synthesis approaches are used, especially if they can better control atomic distances between functionalities and even show us how much control is required. Such concepts are being investigated, for example, with respect to the effect of the spacing of sugar functionalities on the binding efficiencies of sequence-defined glycomacromolecules with Concanavalin A and Lectin.[275,435,436] When considering potential

applications such as data storage and cryptography, then one of the greatest challenges has also to be efficient analysis or 'read-out' of sequence-defined macromolecules and the information contained within. This is discussed in more detail in Chapter VII. Other challenges to this field are the continuing efforts towards improving the efficiency and up-scalability of sequence-defined synthesis, either through the investigation of more efficient or robust chemistries (such as TAD chemistry), better handling or automation. This is something that is highlighted throughout the experimental chapters of this PhD thesis.

II.9 References

1 L. H. Baekeland, *J. Ind. Eng. Chem.*, 1909, **1**, 149–161.

2 J.-F. Lutz, J.-M. Lehn, E. W. Meijer and K. Matyjaszewski, *Nat. Rev. Mater.*, 2016, **1**, 1–14.

3 G. Odian, *Principles of polymerization*, Wiley-Interscience, 4th edn., 2004.

4 K. Matyjaszewski and T. P. Davis, Eds., *Handbook of Radical Polymerization*, John Wiley & Sons, 2003.

5 K. Matyjaszewski, *Advances in Controlled/Living Radical Polymerization*, American Chemical Society, Vol. 854., 2003.

6 W. A. Braunecker and K. Matyjaszewski, *Prog. Polym. Sci.*, 2007, **32**, 93–146.

7 K. Matyjaszewski, *Curr. Opin. Solid State Mater. Sci.*, 1996, **1**, 769–776.

8 G. Moad, E. Rizzardo and D. H. Solomon, *Macromolecules*, 1982, **15**, 909–914.

9 J.-S. Wang and K. Matyjaszewski, *J. Am. Chem. Soc.*, 1995, **117**, 5614–5615.

10 M. Kato, M. Kamigaito, M. Sawamoto and T. Higashimura, *Macromolecules*, 1995, **28**, 1721–1723.

11 John Chiefari, Y. K. (Bill) Chong, Frances Ercole, Julia Krstina, Justine Jeffery, Tam P. T. Le, Roshan T. A. Mayadunne, Gordon F. Meijs, Catherine L. Moad, G. Moad, E. Rizzardo and S. H. Thang, *Macromolecules*, 1998, **31**, 5559–5562.

12 S. Aksakal and C. R. Becer, *Polym. Chem.*, 2016, **7**, 7011–7018.

13 S. Wallyn, Z. Zhang, F. Driessen, J. Pietrasik, B. G. De Geest, R. Hoogenboom and F. E. Du Prez, *Macromol. Rapid Commun.*, 2014, **35**, 405–411.

14 H. G. Börner, K. Beers, K. Matyjaszewski, S. S. Sheiko and M. Moeller, *Macromolecules*, 2001, **34**, 4375–4383.

15 J. D. Watson and F. H. C. Crick, *Nature*, 1953, **171**, 737–738.

16 J.-F. Lutz, T. Y. Meyer, M. Ouchi and M. Sawamoto, Eds., *Sequence-Controlled Polymers: Synthesis, Self-Assembly and Properties*, American Chemical Society, Washington DC, 2014.

17 H. M. Colquhoun and J.-F. Lutz, *Nat. Chem.*, 2014, **6**, 455–456.

18 J.-F. Lutz, *Polym. Chem.*, 2010, **1**, 55–62.

19 N. Badi and J.-F. Lutz, *Chem. Soc. Rev.*, 2009, **38**, 3383–3390.

20 C. J. Hawker and K. L. Wooley, *Science*, 2005, **309**, 1200–1205.

21 J.-F. Lutz, in *Sequence-Controlled Polymers*, ed. J.-F. Lutz, Wiley VCH, Weinheim, 1st edn., 2018, pp. 1–26.

22 J.-F. Lutz, *Macromol. Rapid Commun.*, 2017, **38**, 1700582.

23 J. A. De Neve, J. J. Haven, L. Maes and T. Junkers, *Polym. Chem.*, 2018, **9**, 4692–4705.

24 S. Martens, J. O. Holloway and F. E. Du Prez, *Macromol. Rapid Commun.*, 2017, **38**, 1700469.

25 S. Martens, J. O. Holloway and F. E. Du Prez, in *Sequence-Controlled Polymers*, ed. J.-F. Lutz, Wiley VCH, Weinheim, 2018, pp. 379–416.

26 E. R. Kay and D. A. Leigh, *Angew. Chemie Int. Ed.*, 2015, **54**, 10080–10088.

27 J.-F. Ayme, J. E. Beves, D. A. Leigh, R. T. McBurney, K. Rissanen and D. Schultz, *Nat. Chem.*, 2012, **4**, 15–20.

28 S. N. Semenov, L. J. Kraft, A. Ainla, M. Zhao, M. Baghbanzadeh, V. E. Campbell, K. Kang, J. M. Fox and G. M. Whitesides, *Nature*, 2016, **537**, 656–660.

29 P. J. Bracher, P. W. Snyder, B. R. Bohall and G. M. Whitesides, *Orig. Life Evol. Biosph.*, 2011, **41**, 399–412.

30 V. R. Pattabiraman and J. W. Bode, *Nature*, 2011, **480**, 471–479.

31 J. O. Holloway, K. S. Wetzel, S. Martens, F. E. Du Prez and M. A. R. Meier, *Polym. Chem.*, 2019, **10**, 3859–3867.

32 J.-F. Lutz, *ACS Macro Lett.*, 2014, **3**, 1020–1023.

33 G. Gody, T. Maschmeyer, P. B. Zetterlund and S. Perrier, *Nat. Commun.*, 2013, **4**, 2505–2514.

34 A. Al Ouahabi, M. Kotera, L. Charles and J.-F. Lutz, *ACS Macro Lett.*, 2015, **4**, 1077–1080.

35 R. B. Merrifield, *J. Am. Chem. Soc.*, 1963, **85**, 2149–2154.

36 R. B. Merrifield, *Adv. Enzymol. Relat. Areas Mol. Biol.*, 1969.

37 E. Biron and H. Kessler, *J. Org. Chem.*, 2005, **70**, 5183–5189.

38 H. Rink, *Tetrahedron Lett.*, 1987, **28**, 3787–3790.

39 R. B. Merrifield, *J. Am. Chem. Soc.*, 1972, **1067**, 3102–3107.

40 S. Martens, A. Landuyt, P. Espeel, B. Devreese, P. Dawyndt and F. E. Du Prez, *Nat. Commun.*, 2018, **9**, 4451.

41 S. Martens, J. Van Den Begin, A. Madder, F. E. Du Prez and P. Espeel, *J. Am. Chem. Soc.*, 2016, **138**, 14182–14185.

42 J. O. Holloway, S. Aksakal, F. E. Du Prez and C. Remzi Becer, *Macromol. Rapid Commun.*, 2017, **38**, 1700500.

43 J. O. Holloway, C. Mertens, F. E. Du Prez and N. Badi, *Macromol. Rapid Commun.*, 2019, **40**, 1800685.

44 D. Chan-Seng and J.-F. Lutz, in *Sequence-Controlled Polymers: Synthesis, Self-Assembly, and Properties*, American Chemical Society, Washington DC, 2014, pp. 103–118.

45 T. T. Trinh, C. Laure and J.-F. Lutz, *Macromol. Chem. Phys.*, 2015, **216**, 1498–1506.

46 D. Karamessini, B. E. Petit, M. Bouquey, L. Charles and J.-F. Lutz, *Adv. Funct. Mater.*, 2017, **27**, 1604595.

47 C. Laure, D. Karamessini, O. Milenkovic, L. Charles and J.-F. Lutz, *Angew. Chemie - Int. Ed.*, 2016, **55**, 10722–10725.

48 G. Cavallo, S. Poyer, J.-A. Amalian, F. Dufour, A. Burel, C. Carapito, L. Charles and J.-F. Lutz, *Angew. Chemie Int. Ed.*, 2018, **130**, 6374–6377.

49 N. F. König, A. Al Ouahabi, S. Poyer, L. Charles and J.-F. Lutz, *Angew. Chemie - Int. Ed.*, 2017, **56**, 7297–7301.

50 B. L. Bray, *Nat. Rev. Drug Discov.*, 2003, **2**, 587–593.

51 S. C. Solleder and M. A. R. Meier, *Angew. Chemie - Int. Ed.*, 2014, **53**, 711–714.

52 S. C. Solleder, K. S. Wetzel and M. A. R. Meier, *Polym. Chem.*, 2015, **6**, 3201–3204.

53 S. C. Solleder, S. Martens, P. Espeel, F. E. Du Prez and M. A. R. Meier, *Chem. - A Eur. J.*, 2017, **23**, 13906–13909.

54 S. C. Solleder, D. Zengel, K. S. Wetzel and M. A. R. Meier, *Angew. Chemie - Int. Ed.*, 2016, **55**, 1204–1207.

55 S. Pfeifer, Z. Zarafshani, N. Badi and J.-F. Lutz, *J. Am. Chem. Soc.*, 2009, **131**, 9195–9197.

56 M. I. Amrane, D. Chouikhi, N. Badi and J.-F. Lutz, *Macromol. Chem. Phys.*, 2014, **215**, 1984–1990.

57 A. Meszynska, N. Badi, H. G. Börner and J.-F. Lutz, *Chem. Commun.*, 2012, **48**, 3887–3889.

58 D. J. Gravert, A. Datta, P. Wentworth and K. D. Janda, *J. Am. Chem. Soc.*, 1998, **120**, 9481–9495.

59 M. Landa, M. Kotera, J. S. Remy and N. Badi, *Eur. Polym. J.*, 2016, **84**, 338–344.

60 J.-F. Lutz, M. Ouchi, D. R. Liu and M. Sawamoto, *Science*, 2013, **341**, 1238149.

61 J. Niu, R. Hili and D. R. Liu, *Nat. Chem.*, 2013, **5**, 282–292.

62 R. E. Kleiner, Y. Brudno, M. E. Birnbaum and D. R. Liu, *J. Am. Chem. Soc.*, 2008, **130**, 4646–4659.

63 M. L. McKee, P. J. Milnes, J. Bath, E. Stulz, A. J. Turberfield and R. K. O'Reilly, *Angew. Chemie - Int. Ed.*, 2010, **49**, 7948–7951.

64 M. L. McKee, A. C. Evans, S. R. Gerrard, R. K. O'Reilly, A. J. Turberfield and E. Stulz, *Org. Biomol. Chem.*, 2011, **9**, 1661.

65 R. K. O'Reilly, A. J. Turberfield and T. R. Wilks, *Acc. Chem. Res.*, 2017, **50**, 2496–2509.

66 P. J. Milnes, M. L. McKee, J. Bath, L. Song, E. Stulz, A. J. Turberfield and R. K. O'Reilly, *Chem. Commun.*, 2012, **48**, 5614.

67 M. L. McKee, P. J. Milnes, J. Bath, E. Stulz, R. K. O'Reilly and A. J. Turberfield, *J. Am. Chem. Soc.*, 2012, **134**, 1446–1449.

68 W. Meng, R. A. Muscat, M. L. McKee, P. J. Milnes, A. H. El-Sagheer, J. Bath, B. G. Davis, T. Brown, R. K. O'Reilly and A. J. Turberfield, *Nat. Chem.*, 2016, **8**, 542–548.

69 R. Szweda, C. Chendo, L. Charles, P. N. W. Baxter and J.-F. Lutz, *Chem. Commun.*, 2017, **53**, 8312–8315.

70 R. K. Roy, A. Meszynska, C. Laure, L. Charles, C. Verchin and J.-F. Lutz, *Nat. Commun.*, 2015, **6**, 7237–7239.

71 T. T. Trinh, C. Laure and J.-F. Lutz, *Macromol. Chem. Phys.*, 2015, **216**, 1498–1506.

72 D. Chan-Seng and J.-F. Lutz, *ACS Macro Lett.*, 2014, **3**, 291–294.

73 G. Cavallo, A. Al Ouahabi, L. Oswald, L. Charles and J.-F. Lutz, *J. Am. Chem. Soc.*, 2016, **138**, 9417–9420.

74 D. Karamessini, S. Poyer, L. Charles and J.-F. Lutz, *Macromol. Rapid Commun.*, 2017, **38**, 1700426.

75 T. T. Trinh, L. Oswald, D. Chan-Seng and J.-F. Lutz, *Macromol. Rapid Commun.*, 2014, **35**, 141–145.

76 Mattijs G. J. ten Cate, Hartmut Rettig, A. Kaj Bernhardt and H. G. Börner*, *Macromolecules*, 2005, **38**, 10643–10649.

77 A. Al Ouahabi, L. Charles and J.-F. Lutz, *J. Am. Chem. Soc.*, 2015, **137**, 5629–5635.

78 B. Lewandowski, G. De Bo, J. W. Ward, M. Papmeyer, S. Kuschel, M. J. Aldegunde, P. M. E. Gramlich, D. Heckmann, S. M. Goldup, D. M. D'Souza, A. E. Fernandes and D. A. Leigh, *Science*, 2013, **339**, 189–193.

79 G. De Bo, S. Kuschel, D. A. Leigh, B. Lewandowski, M. Papmeyer and J. W. Ward, *J. Am. Chem. Soc.*, 2014, **136**, 5811–5814.

80 Y. Hibi, M. Ouchi and M. Sawamoto, *Nat. Commun.*, 2016, **7**, 11064.

81 J. Zhang, M. E. Matta and M. A. Hillmyer, *ACS Macro Lett.*, 2012, **1**, 1383–1387.

82 W. R. Gutekunst and C. J. Hawker, *J. Am. Chem. Soc.*, 2015, **137**, 8038–8041.

83 S. Pfeifer and J.-F. Lutz, *J. Am. Chem. Soc.*, 2007, **129**, 9542–9543.

84 J.-F. Lutz, B. V. K. J. Schmidt and S. Pfeifer, *Macromol. Rapid Commun.*, 2011, **32**, 127–135.

85 D. Chan-Seng, M. Zamfir and J.-F. Lutz, *Angew. Chemie - Int. Ed.*, 2012, **51**, 12254–12257.

86 G. Moriceau, G. Gody, M. Hartlieb, J. Winn, H. Kim, A. Mastrangelo, T. Smith and S. Perrier, *Polym. Chem.*, 2017, **8**, 4152–4161.

87 R. K. Roy and J.-F. Lutz, *J. Am. Chem. Soc.*, 2014, **136**, 12888–12891.

88 D. Oh, M. Ouchi, T. Nakanishi, H. Ono and M. Sawamoto, *ACS Macro Lett.*, 2016, **5**, 745–749.

89 D. Oh, M. Ouchi, T. Nakanishi, H. Ono and M. Sawamoto, *ACS Macro Lett.*, 2016, **5**, 745–749.

90 B. Quiclet-Sire, G. Revol and S. Z. Zard, *Tetrahedron*, 2010, **66**, 6656–6666.

91 P. Delduc, C. Tailhan and S. Z. Zard, *J. Chem. Soc. Chem. Commun.*, 1988, **0**, 308.

92 J. B. McLeary, F. M. Calitz, J. M. McKenzie, M. P. Tonge, R. D. Sanderson and B. Klumperman, *Macromolecules*, 2004, **37**, 2383–2394.

93 M. Chen, K. P. Ghiggino, A. W. H. Mau, E. Rizzardo, W. H. F. Sasse, S. H. Thang and G. J. Wilson, *Macromolecules*, 2004, **37**, 5479–5481.

94 S. Houshyar, D. J. Keddie, G. Moad, R. J. Mulder, S. Saubern and J. Tsanaktsidis, *Polym. Chem.*, 2012, **3**, 1879.

95 J. Xu, C. Fu, S. Shanmugam, C. J. Hawker, G. Moad and C. Boyer, *Angew. Chemie Int. Ed.*, 2017, **56**, 8376–8383.

96 J. Xu, S. Shanmugam, C. Fu, K.-F. Aguey-Zinsou and C. Boyer, *J. Am. Chem. Soc.*, 2016, **138**, 3094–3106.

97 C. Fu, Z. Huang, C. J. Hawker, G. Moad, J. Xu and C. Boyer, *Polym. Chem.*, 2017, **8**, 4637–4643.

98 J. J. Haven, J. Vandenbergh and T. Junkers, *Chem. Commun.*, 2015, **51**, 4611–4614.

99 J. Vandenbergh, G. Reekmans, P. Adriaensens and T. Junkers, *Chem. Commun.*, 2013, **49**, 10358.

100 J. J. Haven, J. A. De Neve and T. Junkers, *ACS Macro Lett.*, 2017, **6**, 743–747.

101 H. Mutlu, L. M. de Espinosa and M. A. R. Meier, *Chem. Soc. Rev.*, 2011, **40**, 1404–1445.

102 K. Satoh, S. Ozawa, M. Mizutani, K. Nagai and M. Kamigaito, *Nat. Commun.*, 2010, **1**, 1–6.

103 C.-H. Wang, Z.-Y. Song, X.-X. Deng, L.-J. Zhang, F.-S. Du and Z.-C. Li, *Macromol. Rapid Commun.*, 2014, **35**, 474–478.

104 C. Zhang, J. Ling and Q. Wang, *Macromolecules*, 2011, **44**, 8739–8743.

105 S. C. Solleder, R. V. Schneider, K. S. Wetzel, A. C. Boukis and M. A. R. Meier, *Macromol. Rapid Commun.*, 2017, **38**, 1600711.

106 H. C. Kolb, M. G. Finn and K. B. Sharpless, *Angew. Chemie - Int. Ed.*, 2001, **40**, 2004–2021.

107 Y. Jiang, J. Chen, C. Deng, E. J. Suuronen and Z. Zhong, *Biomaterials*, 2014, **35**, 4969–4985.

108 A. Marechal, R. El-Debs, V. Dugas and C. Demesmay, *J. Sep. Sci.*, 2013, **36**, 2049–2062.

109 D. L. Alge, M. A. Azagarsamy, D. F. Donohue and K. S. Anseth, *Biomacromolecules*, 2013, **14**, 949–953.

110 B. J. Adzima and C. N. Bowman, *AIChE J.*, 2012, **58**, 2952–2965.

111 A. H. El-Sagheer and T. Brown, *Chem. Soc. Rev.*, 2010, **39**, 1388.

112 C. D. Hein, X.-M. Liu and D. Wang, *Pharm. Res.*, 2008, **25**, 2216–2230.

113 J. E. Moses and A. D. Moorhouse, *Chem. Soc. Rev.*, 2007, **36**, 1249–1262.

114 J. M. Baskin and C. R. Bertozzi, *QSAR Comb. Sci.*, 2007, **26**, 1211–1219.

115 P. Espeel and F. E. Du Prez, *Macromolecules*, 2015, **48**, 2–14.

116 J.-F. Lutz and Z. Zarafshani, *Adv. Drug Deliv. Rev.*, 2008, **60**, 958–970.

117 B. Helms, J. L. Mynar, C. J. Hawker and J. M. J. Fréchet, *J. Am. Chem. Soc.*, 2004, **126**, 15020–15021.

118 N. V. Tsarevsky, K. V. Bernaerts, B. Dufour, F. E. Du Prez and K. Matyjaszewski, *Macromolecules*, 2004, **37**, 9308–9313.

119 P. Wu, A. K. Feldman, A. K. Nugent, C. J. Hawker, A. Scheel, B. Voit, J. Pyun, J. M. J. Fréchet, K. B. Sharpless and V. V. Fokin, *Angew. Chemie Int. Ed.*, 2004, **43**, 3928–3932.

120 D. D. Díaz, S. Punna, P. Holzer, A. K. McPherson, K. B. Sharpless, V. V. Fokin and M. G. Finn, *J. Polym. Sci. Part A Polym. Chem.*, 2004, **42**, 4392–4403.

121 W. H. Binder and C. Kluger, *Macromolecules*, 2004, **37**, 9321–9330.

122 C. Barner-Kowollik and A. J. Inglis, *Macromol. Chem. Phys.*, 2009, **210**, 987–992.

123 W. Xi, T. F. Scott, C. J. Kloxin and C. N. Bowman, *Adv. Funct. Mater.*, 2014, **24**, 2572–2590.

124 C. J. Hawker, V. V. Fokin, M. G. Finn and K. B. Sharpless, *Aust. J. Chem.*, 2007, **60**, 381.

125 D. Fournier, R. Hoogenboom and U. S. Schubert, *Chem. Soc. Rev.*, 2007, **36**, 1369.

126 W. H. Binder and R. Sachsenhofer, *Macromol. Rapid Commun.*, 2007, **28**, 15–54.

127 M. J. Robb and C. J. Hawker, in *Materials Science and Technology*, Wiley-VCH Verlag GmbH & Co. KGaA, Weinheim, Germany, 2012, pp. 923–972.

128 A. B. Lowe, *Polymer*, 2014, **55**, 5517–5549.

129 K. Kempe, A. Krieg, C. R. Becer and U. S. Schubert, *Chem. Soc. Rev.*, 2012, **41**, 176–191.

130 P. L. Golas and K. Matyjaszewski, *Chem. Soc. Rev.*, 2010, **39**, 1338–1354.

131 B. S. Sumerlin and A. P. Vogt, *Macromolecules*, 2010, **43**, 1–13.

132 R. K. Iha, K. L. Wooley, A. M. Nyström, D. J. Burke, M. J. Kade and C. J. Hawker, *Chem. Rev.*, 2009, **109**, 5620–5686.

133 C. R. Becer, R. Hoogenboom and U. S. Schubert, *Angew. Chemie Int. Ed.*, 2009, **48**, 4900–4908.

134 W. H. Binder and R. Sachsenhofer, *Macromol. Rapid Commun.*, 2008, **29**, 952–981.

135 H. Nandivada, X. Jiang and J. Lahann, *Adv. Mater.*, 2007, **19**, 2197–2208.

136 C. Barner-Kowollik, F. E. Du Prez, P. Espeel, C. J. Hawker, T. Junkers, H. Schlaad and W. Van Camp, *Angew. Chemie Int. Ed.*, 2011, **50**, 60–62.

137 H. Li, R. Aneja, I. Chaiken, H. Li, R. Aneja and I. Chaiken, *Molecules*, 2013, **18**, 9797–9817.

138 W. Tang and M. L. Becker, *Chem. Soc. Rev.*, 2014, **43**, 7013–7039.

139 J.-F. Lutz and H. G. Börner, *Prog. Polym. Sci.*, 2008, **33**, 1–39.

140 A. Meyer, M. Noël, J.-J. Vasseur and F. Morvan, *European J. Org. Chem.*, 2015, **2015**, 2921–2927.

141 O. Brun, X. Elduque, E. Pedroso and A. Grandas, *J. Org. Chem.*, 2015, **80**, 6093–6101.

142 L. Karmann and U. Kazmaier, *European J. Org. Chem.*, 2013, **2013**, 7101–7109.

143 L. Markey, S. Giordani and E. M. Scanlan, *J. Org. Chem.*, 2013, **78**, 4270–4277.

144 M. D. Best, *Biochemistry*, 2009, **48**, 6571–6584.

145 N. Franz, L. Menin and H.-A. Klok, *Org. Biomol. Chem.*, 2009, **7**, 5207.

146 F. Morvan, A. Meyer, G. Pourceau, S. Vidal, Y. Chevolot, E. Souteyrand and J.-J. Vasseur, *Nucleic Acids Symp. Ser.*, 2008, **52**, 47–48.

147 E. Scanlan, V. Corcé, A. Malone, E. M. Scanlan, V. Corcé and A. Malone, *Molecules*, 2014, **19**, 19137–19151.

148 X. Elduque, E. Pedroso and A. Grandas, *J. Org. Chem.*, 2014, **79**, 2843–2853.

149 A. Sánchez, E. Pedroso and A. Grandas, *Chem. Commun.*, 2013, **49**, 309–311.

150 C. J. White and A. K. Yudin, *Nat. Chem.*, 2011, **3**, 509–524.

151 A. A. Aimetti, R. K. Shoemaker, C.-C. Lin and K. S. Anseth, *Chem. Commun.*, 2010, **46**, 4061.

152 A. Le Chevalier Isaad, A. M. Papini, M. Chorev and P. Rovero, *J. Pept. Sci.*, 2009, **15**, 451–454.

153 Rushia A. Turner, A. Allen G. Oliver and R. S. Lokey, *Org. Lett.*, 2007, **9**, 5011–5014.

154 C. Paris, O. Brun, E. Pedroso, A. Grandas, C. Paris, O. Brun, E. Pedroso and A. Grandas, *Molecules*, 2015, **20**, 6389–6408.

155 F. J. Flett, J. G. A. Walton, C. L. Mackay and H. Interthal, *Anal. Chem.*, 2015, **87**, 9595–9599.

156 A. Meyer, J.-J. Vasseur and F. Morvan, *European J. Org. Chem.*, 2013, **2013**, 465–473.

157 A. Ahmad Fuaad, F. Azmi, M. Skwarczynski, I. Toth, A. A. H. Ahmad Fuaad, F. Azmi, M. Skwarczynski and I. Toth, *Molecules*, 2013, **18**, 13148–13174.

158 C. P. R. Hackenberger and D. Schwarzer, *Angew. Chemie Int. Ed.*, 2008, **47**, 10030–10074.

159 V. Marchan, S. Ortega, D. Pulido, E. Pedroso and A. Grandas, *Nucleic Acids Res.*, 2006, **34**, e24.

160 A. D. de Araújo, J. M. Palomo, J. Cramer, O. Seitz, K. Alexandrov and H. Waldmann, *Chem. - A Eur. J.*, 2006, **12**, 6095–6109.

161 R. Franke, C. Doll and J. Eichler, *Tetrahedron Lett.*, 2005, **46**, 4479–4482.

162 K. W. Hill, J. Taunton-Rigby, J. D. Carter, E. Kropp, K. Vagle, Wolfgang Pieken, D. P. C. McGee, G. M. Husar, M. Leuck, D. J. Anziano and D. P. Sebesta, *J. Org. Chem.*, 2001, **66**, 5352–5358.

163 S. S. Ghosh, P. M. Kao, A. W. McCue and H. L. Chappelle, *Bioconjug. Chem.*, 1990, **1**, 71–76.

164 J. Nicolas, G. Mantovani and D. M. Haddleton, *Macromol. Rapid Commun.*, 2007, **28**, 1083–1111.

165 I. W. Hamley, *Biomacromolecules*, 2014, **15**, 1543–1559.

166 Y. Qi and A. Chilkoti, *Polym. Chem.*, 2014, **5**, 266–276.

167 Bryan Parrish, A. Rebecca B. Breitenkamp and T. Emrick, *J. Am. Soc.*, 2005, **127**, 7404–7410.

168 M. A. Gauthier and H.-A. Klok, *Chem. Commun.*, 2008, 2591–2611.

169 H.-A. Klok, *Macromolecules*, 2009, **42**, 7990–8000.

170 H. Robson Marsden and A. Kros, *Macromol. Biosci.*, 2009, **9**, 939–951.

171 L. A. Canalle, D. W. P. M. Löwik and J. C. M. van Hest, *Chem. Soc. Rev.*, 2010, **39**, 329–353.

172 S. Dehn, R. Chapman, K. A. Jolliffe and S. Perrier, *Polym. Rev.*, 2011, **51**, 214–234.

173 R. M. Broyer, G. N. Grover and H. D. Maynard, *Chem. Commun.*, 2011, **47**, 2212.

174 R. P. Johnson, J. V. John and I. Kim, *Eur. Polym. J.*, 2013, **49**, 2925–2948.

175 D. E. Borchmann, T. P. Carberry and M. Weck, *Macromol. Rapid Commun.*, 2014, **35**, 27–43.

176 T. Schnitzler and A. Herrmann, *Acc. Chem. Res.*, 2012, **45**, 1419–1430.

177 C. Troiber and E. Wagner, *Bioconjug. Chem.*, 2011, **22**, 1737–1752.

178 M. Kwak and A. Herrmann, *Angew. Chemie Int. Ed.*, 2010, **49**, 8574–8587.

179 J. M. Harris and R. B. Chess, *Nat. Rev. Drug Discov.*, 2003, **2**, 214–221.

180 R. Duncan, *Nat. Rev. Drug Discov.*, 2003, **2**, 347–360.

181 W. Zhao, F. Liu, Y. Chen, J. Bai and W. Gao, *Polymer*, 2015, **66**, A1–A10.

182 A. C. Boukis and M. A. R. Meier, *Eur. Polym. J.*, 2018, **104**, 32–38.

183 J.-F. Lutz, *Macromolecules*, 2015, **48**, 4759–4767.

184 M. Ouchi, N. Badi, J.-F. Lutz and M. Sawamoto, *Nat. Chem.*, 2011, **3**, 917–924.

185 R. Kudirka, H. Tran, B. Sanii, K. T. Nam, P. H. Choi, N. Venkateswaran, R. Chen, S. Whitelam and R. N. Zuckermann, *Biopolymers*, 2011, **96**, 586–595.

186 J. Steinkoenig, T. Nitsche, B. T. Tuten and C. Barner-kowollik, *Macromolecules*, 2018, **51**, 3967–3974.

187 J. P. Cole, J. J. Lessard, K. J. Rodriguez, A. M. Hanlon, E. K. Reville, J. P. Mancinelli and E. B. Berda, *Polym. Chem.*, 2017, **8**, 5829–5835.

188 V. V. Rostovtsev, L. G. Green, V. V. Fokin and K. B. Sharpless, *Angew. Chemie Int. Ed.*, 2002, **41**, 2596–2599.

189 C. W. Tornøe, C. Christensen and M. Meldal, *J. Org. Chem.*, 2002, **67**, 3057–3064.

190 M. Meldal and C. W. Tornøe, *Chem. Rev.*, 2008, **108**, 2952–3015.

191 R. Huisgen, *Angew. Chemie Int. Ed. English*, 1963, **2**, 565–598.

192 R. Huisgen, *Angew. Chemie Int. Ed. English*, 1963, **2**, 633–645.

193 J.-F. Lutz, *Angew. Chemie - Int. Ed.*, 2008, **47**, 2182–2184.

194 M. Meldal, *Macromol. Rapid Commun.*, 2008, **29**, 1016–1051.

195 G. Delaittre, N. K. Guimard and C. Barner-Kowollik, *Acc. Chem. Res.*, 2015, **48**, 1296–1307.

196 N. V. Sokolova and V. G. Nenajdenko, *RSC Adv.*, 2013, **3**, 16212.

197 S. Binauld, D. Damiron, L. A. Connal, C. J. Hawker and E. Drockenmuller, *Macromol. Rapid Commun.*, 2011, **32**, 147–168.

198 S. Binauld, C. J. Hawker, E. Fleury and E. Drockenmuller, *Angew. Chemie Int. Ed.*, 2009, **48**, 6654–6658.

199 G. Lu, S. Lam and K. Burgess, *Chem. Commun.*, 2006, 1652–1654.

200 M. Lo Conte, A. Marra, A. Chambery, S. S. Gurcha, G. S. Besra and A. Dondoni, *J. Org. Chem.*, 2010, **75**, 6326–6336.

201 M. Lo Conte, A. Chambery, A. Marra and A. Dondoni, *Synlett*, 2009, **2009**, 2679–2681.

202 P. Cheshev, A. Marra and A. Dondoni, *Org. Biomol. Chem.*, 2006, **4**, 3225–3227.

203 Y. Jiang, M. R. Golder, H. V.-T. Nguyen, Y. Wang, M. Zhong, J. C. Barnes, D. J. C. Ehrlich and J. A. Johnson, *J. Am. Chem. Soc.*, 2016, **138**, 9369–9372.

204 J. C. Barnes, D. J. C. Ehrlich, A. X. Gao, F. A. Leibfarth, Y. Jiang, E. Zhou, T. F. Jamison and J. A. Johnson, *Nat. Chem.*, 2015, **7**, 810–815.

205 H. Isobe, T. Fujino, N. Yamazaki, M. Guillot-Nieckowski and E. Nakamura, *Org. Lett.*, 2008, **10**, 3729–3732.

206 F. Amir, Z. Jia and M. J. Monteiro, *J. Am. Chem. Soc.*, 2016, **138**, 16600–16603.

207 O. D. Montagnat, G. Lessene and A. B. Hughes, *J. Org. Chem.*, 2010, **75**, 390–398.

208 N. G. Angelo and P. S. Arora, *J. Org. Chem.*, 2007, **72**, 7963–7967.

209 O. D. Montagnat, G. Lessene and A. B. Hughes, *Tetrahedron Lett.*, 2006, **47**, 6971–6974.

210 F. A. Leibfarth, J. A. Johnson and T. F. Jamison, *Proc. Natl. Acad. Sci. U. S. A.*, 2015, **112**, 10617–22.

211 T. T. Trinh, L. Oswald, D. Chan-Seng, L. Charles and J.-F. Lutz, *Chem. - A Eur. J.*, 2015, **21**, 11961–11965.

212 Z. Zhang and E. Fan, *Tetrahedron Lett.*, 2006, **47**, 665–669.

213 A. A. Fuller, D. Du, F. Liu, J. E. Davoren, G. Bhabha, G. Kroon, D. A. Case, H. J. Dyson, E. T. Powers, P. Wipf, M. Gruebele and J. W. Kelly, *Proc. Natl. Acad. Sci.*, 2009, **106**, 11067 LP – 11072.

214 K. Oh and Z. Guan, *Chem. Commun.*, 2006, 3069–3071.

215 J. K. Pokorski, L. M. M. Jenkins, H. Feng, S. R. Durell, Y. Bai and D. H. Appella, *Org. Lett.*, 2007, **9**, 2381–2383.

216 Y. Chen and Z. Guan, *J. Am. Chem. Soc.*, 2010, **132**, 4577–4579.

217 T.-B. Yu, J. Z. Bai and Z. Guan, *Angew. Chemie*, 2009, **121**, 1117–1121.

218 M. F. Ebbesen, C. Gerke, P. Hartwig and L. Hartmann, *Polym. Chem.*, 2016, **7**, 7086–7093.

219 M. G. J. Cate, H. Rettig, K. Bernhardt and H. G. Börner, *Macromolecules*, 2005, **38**, 10643–10649.

220 C. Caumes, O. Roy, S. Faure and C. Taillefumier, *J. Am. Chem. Soc.*, 2012, **134**, 9553–9556.

221 A. Norgren, C. Budke, Z. Majer, C. Heggemann, T. Koop and N. Sewald, *Synthesis (Stuttg).*, 2009, **3**, 488–494.

222 D. Fürniss, T. Mack, F. Hahn, S. B. L. Vollrath, K. Koroniak, U. Schepers and S. Bräse, *Beilstein J. Org. Chem.*, 2013, **9**, 56–63.

223 N. Baradel, S. Fort, S. Halila, N. Badi and J.-F. Lutz, *Angew. Chemie*, 2013, **125**, 2391–2395.

224 T. Szekely, O. Roy, S. Faure and C. Taillefumier, *European J. Org. Chem.*, 2014, **2014**, 5641–5657.

225 D. Ponader, F. Wojcik, F. Beceren-Braun, J. Dernedde and L. Hartmann, *Biomacromolecules*, 2012, **13**, 1845–1852.

226 D. Ponader, P. Maffre, J. Aretz, D. Pussak, N. M. Ninnemann, S. Schmidt, P. H. Seeberger, C. Rademacher, G. U. Nienhaus and L. Hartmann, *J. Am. Chem. Soc.*, 2014, **136**, 2008–2016.

227 D. Ponader, S. Igde, M. Wehle, K. Märker, M. Santer, D. Bléger and L. Hartmann, *Beilstein J. Org. Chem.*, 2014, **10**, 1603–12.

228 Q. Zhang, J. Colins, A. Anastasaki, R. Wallis, D. A. Mitchell, C. P. W. Remzi Becer and D. M. Haddleton, in *Sequence-Controlled Polymers: Synthesis, Self-Assembly, and Properties*, eds. J.-F. Lutz, T. Y. Meyer, M. Ouchi and M. Sawamoto, American Chemical Society, Washington DC, 2014, pp. 327–348.

229 G. Yilmaz and C. R. Becer, *Eur. Polym. J.*, 2013, **49**, 3046–3051.

230 Q. Zhang, J. Collins, A. Anastasaki, R. Wallis, D. A. Mitchell, C. R. Becer and D. M. Haddleton, *Angew. Chemie*, 2013, **125**, 4531–4535.

231 Y. Abdouni, G. Yilmaz and C. R. Becer, *Macromol. Rapid Commun.*, 2017, **38**, 1700212.

232 Y. Abdouni, G. Yilmaz and C. R. Becer, in *Sequence-Controlled Polymers*, ed. J.-F. Lutz, Wiley VCH, Weinheim, 1st edn., 2018, vol. 38, pp. 229–256.

233 Hangjun Jang, Aaron Fafarman, A. Justin M. Holub and K. Kirshenbaum, *Org. Lett.*, 2005, **7**, 1951–1954.

234 S. Srichan, H. Mutlu, N. Badi and J.-F. Lutz, *Angew. Chem., Int. Ed.*, 2014, **53**, 9231–9235.

235 C. Zhou, L. Deng, F. Yao, L. Xu, J. Zhou and G. D. Fu, *Ind. Eng. Chem. Res.*, 2014, **53**, 19239–19248.

236 A. M. Rosales, B. L. McCulloch, R. N. Zuckermann and R. A. Segalman, *Macromolecules*, 2012, **45**, 6027–6035.

237 J. M. Holub, H. Jang and K. Kirshenbaum, *Org. Biomol. Chem.*, 2006, **4**, 1497.

238 R. Jagasia, J. M. Holub, M. Bollinger, K. Kirshenbaum and M. G. Finn, *J. Org. Chem.*, 2009, **74**, 2964–2974.

239 J. M. Holub, H. Jang and K. Kirshenbaum, *Org. Lett.*, 2007, **9**, 3275–3278.

240 V. K. Tiwari, B. B. Mishra, K. B. Mishra, N. Mishra, A. S. Singh and X. Chen, *Chem. Rev.*, 2016, **116**, 3086–3240.

241 Kyle D. Bodine, D. Y. Gin and M. S. Gin, *Org. Lett.*, 2005, **7**, 4479–4482.

242 Kyle D. Bodine, D. Y. Gin and M. S. Gin, *J. Am. Chem. Soc.*, 2004, **126**, 1638–1639.

243 M. Zamfir, P. Théato and J.-F. Lutz, *Polym. Chem.*, 2012, **3**, 1796–1802.

244 B. V. K. J. Schmidt, N. Fechler, J. Falkenhagen and J.-F. Lutz, *Nat. Chem.*, 2011, **3**, 234–238.

245 Q. Wang, H. Li, Q. Wei, J. Z. Sun, J. Wang, X. A. Zhang, A. Qin and B. Z. Tang, *Polym. Chem.*, 2013, **4**, 1396–1401.

246 J.-F. Lutz, *Angew. Chemie Int. Ed.*, 2008, **47**, 2182–2184.

247 O. Diels, J. H. Blom and W. Koll, *Justus Liebigs Ann. Chem.*, 1925, **443**, 242–262.

248 N. Zydziak, W. Konrad, F. Feist, S. Afonin, S. Weidner and C. Barner-Kowollik, *Nat. Commun.*, 2016, **7**, 1–10.

249 N. Zydziak, F. Feist, B. Huber, J. O. Mueller and C. Barner-Kowollik, *Chem. Commun.*, 2015, **51**, 1799–1802.

250 Y. Ji, L. Zhang, X. Gu, P. W. Zhang, P. N. Zhou and P. Z. Zhang, *Angew. Chemie Int. Ed.*

251 W. Konrad, C. Fengler, S. Putwa and C. Barner-Kowollik, *Angew. Chemie Int. Ed.*, 2019, **58**, 7133–7137.

252 J. P. Blinco, M. Van De Walle, T. Junkers, C. Barner-Kowollik and K. De Bruycker, *ChemPhotoChem*, 2019, **3800**, 1–5.

253 X. Elduque, A. Sánchez, K. Sharma, E. Pedroso and A. Grandas, *Bioconjug. Chem.*, 2013, **24**, 832–839.

254 T. Posner, *Dtsch. Chem. Ges.*, 1905, **38**, 646–657.

255 J. W. Chan, J. Shin, C. E. Hoyle, C. N. Bowman and A. B. Lowe, *Macromolecules*, 2010, **43**, 4937–4942.

256 Y. Sun, H. Liu, L. Cheng, S. Zhu, C. Cai, T. Yang and P. Ding, *Polym. Int.*, 2018, **67**, 25–31.

257 G.-Z. Li, R. Randev, A. H. Soeriyadi, G. J. Rees, C. Boyer, Z. Tong, C. R. Becer and D. M. Haddleton, *Polym. Chem.*, 2010, **1**, 1196–1204.

258 S. P. S. Koo, M. M. Stamenović, R. A. Prasath, A. J. Inglis, F. E. Du Prez, C. Barner-Kowollik, W. Van Camp and T. Junkers, *J. Polym. Sci. Part A - Polym. Chem.*, 2010, **48**, 1699–1713.

259 C. E. Hoyle and C. N. Bowman, *Angew. Chemie Int. Ed.*, 2010, **49**, 1540–1573.

260 C. Resetco, B. Hendriks, N. Badi and F. E. Du Prez, *Mater. Horiz.*, 2017, **4**, 1041–1053.

261 C. E. Hoyle, T. Y. Lee and T. Roper, *J. Polym. Sci. Part A Polym. Chem.*, 2004, **42**, 5301–5338.

262 M. Porel, D. N. Thornlow, N. N. Phan and C. A. Alabi, *Nat. Chem.*, 2016, **8**, 590–596.

263 M. Porel, J. S. Brown and C. A. Alabi, *Synlett*, 2015, **26**, 565–571.

264 M. Porel, D. N. Thornlow, C. M. Artim and C. A. Alabi, *ACS Chem. Biol.*, 2017, **12**, 715–723.

265 M. Porel and C. A. Alabi, *J. Am. Chem. Soc.*, 2014, **136**, 13162–13165.

266 W. Xi, S. Pattanayak, C. Wang, B. Fairbanks, T. Gong, J. Wagner, C. J. Kloxin and C. N. Bowman, *Angew. Chemie - Int. Ed.*, 2015, **54**, 14462–14467.

267 A. B. Lowe, *Polym. Chem.*, 2010, **1**, 17–36.

268 Z. Zhang, Y. Z. You, D. C. Wu and C. Y. Hong, *Polym. (United Kingdom)*, 2015, **64**, 221–226.

269 L. Yang, Z. Zhang, B. Cheng, Y. You, D. Wu and C. Hong, *Sci. China Chem.*, 2015, **58**, 1734–1740.

270 F. Driessen, F. E. Du Prez and P. Espeel, *ACS Macro Lett.*, 2015, **4**, 616–619.

271 F. Wojcik, D. Ponader, S. Mosca and L. Hartmann, in *Sequence-Controlled Polymers: Synthesis, Self-Assembly, and Properties*, eds. J.-F. Lutz, T. Y. Meyer, M. Ouchi and M. Sawamoto, American Chemical Society, Washington DC, 2014, pp. 85–102.

272 F. Wojcik, S. Lel, A. G. O'Brien, P. H. Seeberger and L. Hartmann, *Beilstein J. Org. Chem.*, 2013, **9**, 2395–403.

273 F. Wojcik, A. G. O'Brien, S. Götze, P. H. Seeberger and L. Hartmann, *Chem. - A Eur. J.*, 2013, **19**, 3090–3098.

274 D. Comegna and F. De Riccardis, *Org. Lett.*, 2009, **11**, 3898–3901.

275 C. Gerke, M. F. Ebbesen, D. Jansen, S. Boden, T. Freichel and L. Hartmann, *Biomacromolecules*, 2017, **18**, 787–796.

276 N. Franz, L. Menin and H.-A. Klok, *European J. Org. Chem.*, 2009, **2009**, 5390–5405.

277 F. Goethals, D. Frank and F. E. Du Prez, *Prog. Polym. Sci.*, 2017, **64**, 76–113.

278 P. Espeel, F. Goethals, M. M. Stamenović, L. Petton and F. E. Du Prez, *Polym. Chem.*, 2012, **3**, 1007–1015.

279 P. Espeel, F. Goethals, F. Driessen, L.-T. T. Nguyen and F. E. Du Prez, *Polym. Chem.*, 2013, **4**, 2373–2616.

280 F. Driessen, S. Martens, B. De Meyer, F. E. Du Prez and P. Espeel, *Macromol. Rapid Commun.*, 2016, **37**, 947–951.

281 P. Espeel and F. E. Du Prez, *Eur. Polym. J.*, 2015, **62**, 247–272.

282 P. Espeel and F. E. Du Prez, in *Multicomponent and Sequential Reactions in Polymer Science*, ed. P. Theato, Springer, Switzerland, 2015, pp. 105–132.

283 D. Frank, P. Espeel, S. Claessens, E. Mes and F. E. Du Prez, *Tetrahedron*, 2016, **72**, 6616–6625.

284 P. Espeel, L. L. G. Carrette, K. Bury, S. Capenberghs, J. C. Martins, F. E. Du Prez and A. Madder, *Angew. Chemie - Int. Ed.*, 2013, **52**, 13261–13264.

285 S. Celasun, F. E. Du Prez and H. G. Börner, *Macromol. Rapid Commun.*, 2017, **38**, 1700688.

286 D. Van Lysebetten, S. Felissati, E. Antonatou, L. Carrette, P. Espeel, E. Foquet, F. E. Du Prez and A. Madder, *ChemBioChem*, 2018, **19**, 641–646.

287 J.-J. Yan, D. Wang, D.-C. Wu and Y.-Z. You, *Chem. Commun. (Camb).*, 2013, **49**, 6057–9.

288 Z. Zhang, Y. You, D. Wu and C. Y. Hong, *Macromolecules*, 2015, **48**, 3414–3421.

289 L. Yu, L.-H. Wang, Z.-T. Hu, Y.-Z. You, D.-C. Wu and C.-Y. Hong, *Polym. Chem.*, 2015, **6**, 1527–1532.

290 Z. Zhang, Z.-B. Tan, C.-Y. Hong, D.-C. Wu and Y.-Z. You, *Polym. Chem.*, 2016, **7**, 1468–1474.

291 A. Strecker, *Ann. der Chemie und Pharm.*, 1850, **75**, 27–45.

292 A. Strecker, *Ann. der Chemie und Pharm.*, 1854, **91**, 349–351.

293 P. Biginelli, *Berichte der Dtsch. Chem. Gesellschaft*, 1891, **24**, 1317–1319.

294 P. Biginelli, *Berichte der Dtsch. Chem. Gesellschaft*, 1891, **24**, 2962–2967.

295 M. Passerini, *Gazz. Chim. Ital.*, 1921, **51**, 126–129.

296 I. K. Ugi, *Angew. Chemie*, 1959, **71**, 373–388.

297 R. Kakuchi, in *Multicomponent and Sequential Reactions in Polymer Science*, ed. P. Théato, Springer, Switzerland, 2015, pp. 1–16.

298 A. Sehlinger and M. A. R. Meier, in *Multicomponent and Sequential Reactions in Polymer Science*, ed. P. Théato, Springer, Switzerland, 2015, pp. 61–86.

299 L. Tao, C. Zhu, Y. Wei and Y. Zhao, in *Multicomponent and Sequential Reactions in Polymer Science*, ed. P. Théato, Springer, Switzerland, 2015, pp. 43–30.

300 M. Rubinshtein, C. R. James, J. L. Young, Y. J. Ma, Y. Kobayashi, N. C. Gianneschi and J. Yang, *Org. Lett.*, 2010, **12**, 3560–3563.

301 H. Mutlu and M. A. R. Meier, *Eur. J. Lipid Sci. Technol.*, 2010, **112**, 10–30.

302 O. Kreye, T. Tóth and M. A. R. Meier, *J. Am. Chem. Soc.*, 2011, **133**, 1790–1792.

303 A. Sehlinger, L. M. de Espinosa and M. A. R. Meier, *Macromol. Chem. Phys.*, 2013, **214**, 2821–2828.

304 A. Sehlinger, O. Kreye and M. A. R. Meier, *Macromolecules*, 2013, **46**, 6031–6037.

305 F. Leon, D. G. Rivera and L. A. Wessjohann, *J. Org. Chem.*, 2008, **73**, 1762–1767.

306 X.-X. Deng, L. Li, Z.-L. Li, A. Lv, F.-S. Du and Z.-C. Li, *ACS Macro Lett.*, 2012, **1**, 1300–1303.

307 X.-W. Kan, X.-X. Deng, F.-S. Du and Z.-C. Li, *Macromol. Chem. Phys.*, 2014, **215**, 2221–2228.

308 J.-A. Jee, L. A. Spagnuolo and J. G. Rudick, *Org. Lett.*, 2012, **14**, 3292–3295.

309 J. Zhang, X.-X. Deng, F.-S. Du and Z.-C. Li, in *Sequence-Controlled Polymers: Synthesis, Self-Assembly, and Properties*, eds. J.-F. Lutz, T. Y. Meyer, M. Ouchi and M. Sawamoto, American Chemical Society, Washington DC, 2014, pp. 223–234.

310 W. Konrad, F. R. Blößer, K. S. Wetzel, A. C. Boukis, M. A. R. Meier and C. Barner-Kowollik, *Chem. - A Eur. J.*, 2018, **24**, 3413–3419.

311 A. E. J. De Nooy, G. Masci and V. Crescenzi, *Macromolecules*, 1999, **32**, 1318–1320.

312 C. V. Robotham, C. Baker, B. Cuevas, K. Abboud and D. L. Wright, *Mol. Divers.*, 2000, **6**, 237–244.

313 O. Kreye, O. Türünç, A. Sehlinger, J. Rackwitz and M. A. R. Meier, *Chem. - A Eur. J.*, 2012, **18**, 5767–5776.

314 A. Sehlinger, R. V. Schneider and M. A. R. Meier, *Macromol. Rapid Commun.*, 2014, **35**, 1866–1871.

315 L. A. Wessjohann, D. G. Rivera and O. E. Vercillo, *Chem. Rev.*, 2009, **109**, 796–814.

316 A. R. Puentes, M. C. Morejón, D. G. Rivera and L. A. Wessjohann, *Org. Lett.*, 2017, **19**, 4022–4025.

317 B. Yang, Y. Zhao, S. Wang, Y. Zhang, C. Fu, Y. Wei and L. Tao, *Macromolecules*, 2014, **47**, 5607–5612.

318 A. C. Boukis, K. Reiter, M. Frölich, D. Hofheinz and M. A. R. Meier, *Nat. Commun.*, 2018, **9**, 1439.

319 R. C. Cookson, S. S. H. Gilani and I. D. R. Stevens, *Tetrahedron Lett.*, 1962, **3**, 615–618.

320 R. C. Cookson, S. S. Gupte, I. D. R. Stevens and C. T. Watts, *Org. Synth.*, 1971, **51**, 121–127.

321 K. De Bruycker, S. Billiet, H. A. Houck, S. Chattopadhyay, J. M. Winne and F. E. Du Prez, *Chem. Rev.*, 2016, **116**, 3919–3974.

322 J. Thiele and O. Stange, *Justus Liebig's Ann. der Chemie*, 1894, **283**, 1–46.

323 R. C. Cookson, S. S. H. Gilani and I. D. R. Stevens, *J. Chem. Soc. C*, 1967, 1905–1909.

324 S. Billiet, K. De Bruycker, F. Driessen, H. Goossens, V. Van Speybroeck, J. M. Winne and F. E. Du Prez, *Nat. Chem.*, 2014, **6**, 815–821.

325 O. Türünç, S. Billiet, K. De Bruycker, S. Ouardad, J. Winne and F. E. Du Prez, *Eur. Polym. J.*, 2015, **65**, 286–297.

326 O. Diels and K. Alder, *Justus Liebig's Ann. der Chemie*, 1928, **460**, 98–122.

327 T. Tsuji, *Pharm. Bull.*, 1954, **2**, 403–411.

328 L. F. Audrieth, E. B. Mohr, E. Davis and W. R. Tomlinson, in *Inorganic Syntheses*, John Wiley & Sons, New York, 1953, pp. 29–32.

329 G. Pellizzari and C. Massa, *Gazz. Chim. Ital.*, 1896, **26**, 413–429.

330 F. Eloy and C. Moussebois, *Bull. des Sociétés Chim. Belges*, 2010, **68**, 432–436.

331 A. M. Munro and F. J. Wilson, *J. Chem. Soc.*, 1928, **1928**, 1257–1261.

332 US4323687, 1982, 1–8.

333 EP0044417, 1982, 1–27.

334 US4433085, 1984, 1–26.

335 G. Zinner and W. Deucker, *Arch. Pharm.*, 1961, **294**, 370–372.

336 K. Shimada, T. Oe and T. Mizuguchi, *Analyst*, 1991, **116**, 1393–1397.

337 S. Ogawa, S. Ooki, M. Morohashi, K. Yamagata and T. Higashi, *Rapid Commun. Mass Spectrom.*, 2013, **27**, 2453–2460.

338 G. W. Breton and M. Turlington, *Tetrahedron Lett.*, 2014, **55**, 4661–4663.

339 V. P. Arya and S. J. Shenoy, *Indian J. Chem. - Sect. B Org. Med. Chem.*, 1976, **14**, 883–886.

340 A. Kiriazis, T. Rüffer, S. Jäntti, H. Lang and J. Yli-Kauhaluoma, *J. Comb. Chem.*, 2007, 263–266.

341 B. Chandrasekhar, G. B. Kumar, S. Mallela and S. B. Bhirud, *Org. Prep. Proced. Int.*, 2004, **36**, 469–472.

342 K. A. Matyjaszewski, K. B. Wagener and G. B. Butler, *J. Polym. Sci. Polym. Lett. Ed.*, 1979, **17**, 65–77.

343 Y.-C. Lai and G. B. Butler, *J. Macromol. Sci. Part A - Chem.*, 1985, **22**, 1443–1461.

344 K. B. Wagener, S. R. Turner and G. B. Butler, *J. Polym. Sci. Polym. Lett. Ed.*, 1972, **10**, 805–816.

345 B. Saville, *J. Chem. Soc. D Chem. Commun.*, 1971, 635–636.

346 O. Türünç, S. Billiet, K. De Bruycker, S. Ouardad, J. M. Winne and F. E. Du Prez, *Eur. Polym. J.*, 2015, **65**, 286–297.

347 S. Chattopadhyay and F. E. Du Prez, *Eur. Polym. J.*, 2016, **81**, 77–85.

348 V. K. Gumaste, B. M. Bhawal and A. R. A. S. Deshmukh, *Tetrahedron Lett.*, 2002, **43**, 1345–1346.

349 T. Little, J. Meara, F. Ruan, M. Nguyen and M. Qabar, *Synth. Commun.*, 2002, **32**, 1741–1749.

350 S. E. Mallakpour and Z. Rafiee, *Polymer*, 2007, **48**, 5530–5540.

351 K. Shimada and T. Oe, *Anlaytical Sci.*, 1990, **6**, 461–463.

352 T. Curtius, *Berichte der Dtsch. Chem. Gesellschaft*, 1890, **23**, 3023–3033.

353 T. Curtius, *J. für Prakt. Chemie*, 1894, **50**, 275–294.

354 H. J. Twitchett, *Chem. Soc. Rev.*, 1974, **3**, 209.

355 S. Ozaki, *Chem. Rev.*, 1972, **72**, 457–496.

356 H. W. I. Peerlings and E. W. Meijer, *Tetrahedron Lett.*, 1999, **40**, 1021–1024.

357 G. Read and N. R. Richardson, *J. Chem. Soc. Perkin Trans. 1*, 1996, 167–174.

358 A. Ghorbani-Choghamarani, M. Nikoorazm and G. Azadi, *Chinese Chem. Lett.*, 2014, **25**, 451–454.

359 L. A. Paquette and R. F. Doehner, *J. Org. Chem.*, 1980, **45**, 5105–5113.

360 J. M. Gardlik and L. A. Paquette, *Tetrahedron Lett.*, 1979, **20**, 3597–3600.

361 S. E. Mallakpour and Z. Rafiee, *Synth. Commun.*, 2007, **37**, 1927–1934.

362 S. E. Mallakpour and Z. Rafiee, *Synlett*, 2007, 1255–1256.

363 H. Ban, M. Nagano, J. Gavrilyuk, W. Hakamata, T. Inokuma and C. F. Barbas, *Bioconjug. Chem.*, 2013, **24**, 520–532.

364 H. Ban, J. Gavrilyuk and C. F. Barbas, *J. Am. Chem. Soc.*, 2010, **132**, 1523–1525.

365 WO2013009564, 2013.

366 Q.-Y. Hu, M. Allan, R. Adamo, D. Quinn, H. Zhai, G. Wu, K. Clark, J. Zhou, S. Ortiz, B. Wang, E. Danieli, S. Crotti, M. Tontini, G. Brogioni and F. Berti, *Chem. Sci.*, 2013, **4**, 3827.

367 L. Vlaminck, B. Van De Voorde and F. E. Du Prez, *Green Chem.*, 2017, **19**, 5659–5664.

368 T. J. Gilbertson and T. Ryan, *Synthesis (Stuttg).*, 1982, **1982**, 159–160.

369 C. D. Hurd and F. F. Cesark, *J. Am. Chem. Soc.*, 1967, **89**, 1417–1422.

370 JP04005287, 1992.

371 S. E. Mallakpour and H. Nasr-Isfahani, *Indian J. Chem. - Sect. B Org. Med. Chem.*, 2002, **41**, 169–174.

372 S. Alakurtti, T. Heiska, A. Kiriazis, N. Sacerdoti-Sierra, C. L. Jaffe and J. Yli-Kauhaluoma, *Bioorg. Med. Chem.*, 2010, **18**, 1573–1582.

373 M. Shimizu, T. Takahashi, S. Uratsuka and S. Yamada, *J. Chem. Soc. Chem. Commun.*, 1990, **0**, 1416.

374 J. Burgert and R. Stadler, *Chem. Ber.*, 1987, **120**, 691–694.

375 C. Hilger and R. Stadler, *Die Makromol. Chemie*, 1990, **191**, 1347–1361.

376 D. M. Bauer, I. Ahmed, A. Vigovskaya and L. Fruk, *Bioconjug. Chem.*, 2013, **24**, 1094–1101.

377 J. F. W. Keana, A. P. Guzikowski, D. D. Ward, C. Morat and F. L. Van Nice, *J. Org. Chem.*, 1983, **48**, 2654–2660.

378 A. Nilo, M. Allan, B. Brogioni, D. Proietti, V. Cattaneo, S. Crotti, S. Sokup, H. Zhai, I. Margarit, F. Berti, Q.-Y. Hu and R. Adamo, *Bioconjug. Chem.*, 2014, **25**, 2105–2111.

379 S. E. Mallakpour and Z. Rafiee, *Iran. Polym. J.*, 2004, **13**, 225–234.

380 S. E. Mallakpour and Z. Rafiee, *J. Appl. Polym. Sci.*, 2003, **90**, 2861–2869.

381 U. Seidel, J. Hellman, D. Schollmeyer, C. Hilger and R. Stadler, *Supramol. Sci.*, 1995, **2**, 45–50.

382 O. Roling, K. De Bruycker, B. Vonhören, L. Stricker, M. Körsgen, H. F. Arlinghaus, B. J. Ravoo and F. E. Du Prez, *Angew. Chemie - Int. Ed.*, 2015, **54**, 13126–13129.

383 M. Furdik, S. Mikulase, M. Livar and S. Priehrad, *Chem. Zvesti*, 1967, **21**, 427–442.

384 W. Ried and S.-H. Lim, *Justus Liebigs Ann. Chem.*, 1973, **1973**, 129–133.

385 J. C. Stickler and W. H. Pirkle, *J. Org. Chem.*, 1966, **31**, 3444–3445.

386 J. L. Riebsomer, *Chem. Rev.*, 1945, **36**, 157–233.

387 J. E. Herweh and R. M. Fantazier, *Tetrahedron Lett.*, 1973, **14**, 2101–2104.

388 S. E. Mallakpour, *J. Chem. Educ.*, 1992, **69**, 238.

389 M. A. Zolfigol, M. H. Zebarjadian, G. Chehardoli, S. E. Mallakpour and M. Shamsipur, *Tetrahedron*, 2001, **57**, 1627–1629.

390 G. Chehardoli, M. A. Zolfigol, E. Ghaemi, E. Madrakian, K. Niknam and S. E. Mallakpour, *J. Heterocycl. Chem.*, 2012, **49**, 596–599.

391 M. A. Zolfigol, E. Ghaemi, E. Madrakian and K. Niknam, *J. Chinese Chem. Soc.*, 2008, **55**, 704–711.

392 M. A. Zolfigol, M. K. Borazjani, S. E. Mallakpour and H. Nasr-isfahani, *Synth. Commun.*, 2000, **30**, 2573–2585.

393 M. A. Zolfigolo and S. E. Mallakpour, *Synth. Commun.*, 1999, **29**, 4061–4069.

394 M. A. Zolfigol, S. E. Mallakpour, E. Madrakian and E. Ghaemi, *Indian J. Chem. - Sect. B Org. Med. Chem.*, 2000, **39**, 308–310.

395 M. A. Zolfigol, M. Bagherzadeh, G. Chehardoli and S. E. Mallakpour, *Synth. Commun.*, 2001, **31**, 1149–1154.

396 M. A. Zolfigol, G. Chehardoli, F. Shirini, S. E. Mallakpour and H. Nasr-Isfahani, *Synth. Commun.*, 2001, **31**, 1965–1970.

397 G. Chehardoli, M. A. Zolfigol, T. Faal-Rastegar, S. E. Mallakpour and A. Ghorbani-Choghamarani, *J. Chem. Sci.*, 2009, **121**, 441–447.

398 G. Chehardoli, M. A. Zolfigol, M. Rasouli and S. E. Mallakpour, *Org. Chem. Int.*, 2011, **2011**, 1–3.

399 A. Ghorbani-Choghamarani, M. A. Zolfigol, M. Hajjami and S. E. Mallakpour, *J. Iran. Chem. Soc.*, 2010, **7**, 834–839.

400 A. Ghorbani-Choghamarani, M. Hajjami, H. Goudarziafshar, M. Nikoorazm, S. E. Mallakpour, F. Sadeghizadeh and G. Azadi, *Monatshefte für Chemie - Chem. Mon.*, 2009, **140**, 607–610.

401 M. Nikoorazm, A. Ghorbani-Choghamarani, H. Goudarziafshar and S. E. Mallakpour, *Bull. Korean Chem. Soc.*, 2010, **31**, 2389–2391.

402 M. Ali Zolfigol, G. Chehardoli and S. E. Mallakpour, *Synth. Commun.*, 2003, **33**, 833–841.

403 A. Ghorbani-Choghamarani, Z. Chenani and S. E. Mallakpour, *Synth. Commun.*, 2009, **39**, 4264–4270.

404 M. A. Zolfigol, M. Torabi and S. E. Mallakpour, *Tetrahedron*, 2001, **57**, 8381–8384.

405 A. Ghorbani-Choghamarani, M. Hajjami, M. Norouzi and A. Amiri, *Bulg. Chem. Commun.*, 2014, **46**, 384–388.

406 G. Read and N. R. Richardson, *J. Chem. Soc., Perkin Trans 1*, 1996, 167–174.

407 J. Sauer and B. Schröder, *Chem. Ber.*, 1967, **100**, 678–684.

408 H. Bock, G. Rudolph and E. Baltin, *Chem. Ber.*, 1965, **98**, 2054–2055.

409 H. Wamhoff and K. Wald, *Org. Prep. Proced. Int.*, 1975, **7**, 251–253.

410 U. Tilstam and H. Weinmann, *Org. Process Res. Dev.*, 2002, **6**, 384–393.

411 M. A. Zolfigol, E. Madrakian, E. Ghaemi and S. E. Mallakpour, *Synlett*, 2002, **2002**, 1633–1636.

412 T. C. Celius, *J. Chem. Educ.*, 2010, **87**, 1236–1237.

413 W. Adam and O. De Lucchi, *Tetrahedron Lett.*, 1981, **22**, 929–932.

414 P. S. Baran, C. A. Guerrero and E. J. Corey, *Org. Lett.*, 2003, **5**, 1999–2001.

415 A. G. Leach and K. N. Houk, *Chem. Commun.*, 2002, 1243–1255.

416 P. Yates and P. Eaton, *J. Am. Chem. Soc.*, 1960, **82**, 4436–4437.

417 N. Roy and J.-M. Lehn, *Chem. - An Asian J.*, 2011, **6**, 2419–2425.

418 K. Alder, F. Pascher and A. Schmitz, *Berichte der Dtsch. Chem. Gesellschaft*, 1943, **76**, 27–53.

419 H. M. R. Hoffmann, *Angew. Chemie Int. Ed. English*, 1969, **8**, 556–577.

420 C. C. Cheng, C. A. Seymour, M. A. Petti, F. D. Greene and J. F. Blount, *J. Org. Chem.*, 1984, **49**, 2910–2916.

421 Phil S. Baran, A. Carlos A. Guerrero and E. J. Corey, *Org. Lett.*, 2003, **5**, 1999–2001.

422 H. A. Houck, F. E. Du Prez and C. Barner-Kowollik, *Nat. Commun.*, 2017, **8**, 1869.

423 H. A. Houck, K. De Bruycker, S. Billiet, B. Dhanis, H. Goossens, S. Catak, V. Van Speybroeck, J. M. Winne and F. E. Du Prez, *Chem. Sci.*, 2017, **8**, 3098–3108.

424 L. L. de Lucca Freitas, M. M. Jacobi and R. Stadler, *Polym. Bull.*, 1984, **11**, 407–414.

425 K. De Bruycker, M. Delahaye, P. Cools, J. Winne and F. E. Du Prez, *Macromol. Rapid Commun.*, 2017, **38**, 1700122.

426 L. Vlaminck, S. Lingier, A. Hufendiek and F. E. Du Prez, *Eur. Polym. J.*, 2017, **95**, 503–513.

427 G. Becker, L. Vlaminck, M. M. Velencoso, F. E. Du Prez and F. R. Wurm, *Polym. Chem.*, 2017, **8**, 4074–4078.

428 P. Wilke, T. Kunde, S. Chattopadhyay, N. ten Brummelhuis, F. E. Du Prez and H. G. Börner, *Chem. Commun.*, 2017, **53**, 593–596.

429 N. Van Herck and F. E. Du Prez, *Macromolecules*, 2018, **51**, 3405–3414.

430 M. A. R. Meier and C. Barner-Kowollik, *Adv. Mater.*, 2019, **31**, 1806027.

431 R. K. Roy, C. Laure, D. Fischer-Krauser, L. Charles and J.-F. Lutz, *Chem. Commun.*, 2015, **51**, 15677–15680.

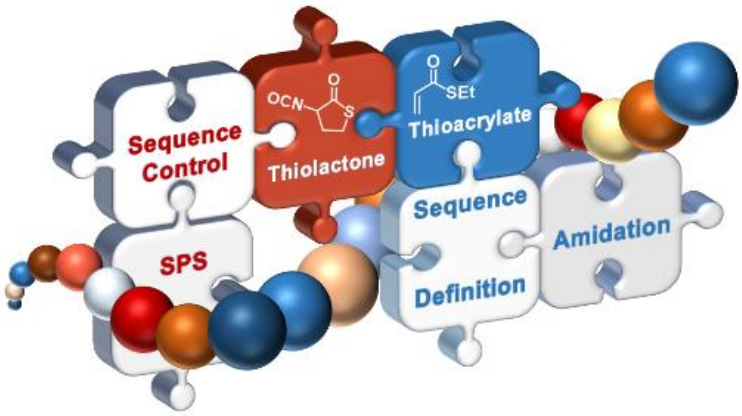
432 U. S. Gunay, B. E. Petit, D. Karamessini, A. Al Ouahabi, J. A. Amalian, C. Chendo, M. Bouquey, D. Gigmes, L. Charles and J.-F. Lutz, *Chem*, 2016, **1**, 114–126.

433 D. Karamessini, T. Simon-yarza, S. Poyer, E. Konishcheva, L. Charles, D. Letourneur and J.-F. Lutz, *Angew. Chemie Int. Ed.*, 2018, **57**, 10574–10578.

434 C. Lawatscheck, M. Pickhardt, A. Grafl, K. Linkert, F. Polster, E. Mandelkow and H. G. Börner, *Macromol. Biosci.*, 2017, **17**, 1700109.

435 S. Igde, S. Röblitz, A. Müller, K. Kolbe, S. Boden, C. Fessele, T. K. Lindhorst, M. Weber and L. Hartmann, *Macromol. Biosci.*, 2017, **17**, 1700198.

436 C. Gerke, F. Jacobi, L. E. Goodwin, F. Pieper, S. Schmidt and L. Hartmann, *Macromolecules*, 2018, **51**, 5608–5619.



This chapter is adapted with permission from:

J.O. Holloway, S. Aksakal, F.E. Du Prez and C.R. Becer, *Macromol. Rapid. Comm.*, 2017, **38**, 1700500.

Abstract

This chapter discusses a strategy for the synthesis of sequence-defined oligomers *via* a selective side-group insertion approach through means of thiophenol-catalysed amidation reactions. In this context, a new thiolactone-based, multistep, iterative protocol was designed, which, for the first time combines thioacrylates with solid-phase synthesis to yield sequence-defined oligomers. Sequence definition and structure variation are introduced by substituting the thioacrylate side groups with a wide variety of primary amines through a carefully constructed modification step. The step-by-step growth of the oligomers was followed by liquid chromatography–mass spectrometry and high-resolution mass spectroscopy to determine both conversion and purity along with ^{1}H and ^{13}C NMR to confirm structure.

Chapter III
Tailored modification of thioacrylates in a sequence-defined procedure

III.1 Introduction

As outlined in Chapter II, the field of sequence-defined synthesis is one that has been growing rapidly over the last decade, with many synthetic protocols proposed.[1–5] The synthesis of monodisperse, sequence-defined macromolecules, often requires an iterative approach, especially when one wishes to install multiple functionalities systematically along the oligomeric backbone. One promising chemical platform for the synthesis of sequence-defined oligomers is thiolactone chemistry, as discussed in Chapter II.5.5.[6–12] Thiolactones, which are essentially a protected thiol, allow a one-pot, double modification *via* ring-opening and thiol-ene conjugation reactions. Solid-phase chemistry was used as the tool to carry out this synthesis, as it offers many advantages in an iterative approach, such as, ease of purification, straightforward handling and time-saving.[11] In 2016, an iterative protocol for the synthesis of sequence-defined oligomers was reported, whereby the introduction of side-group functionality was enabled by a large library of acrylates.[7]

As the field of sequence-defined oligomers moves towards potential applications,[1] the need to expand the monomer alphabet has increased. Whilst approaches limited to simple binary codes have proved popular amongst Lutz and co-worker,[13–22] previously reported thiolactone-based, sequence-defined approaches have resulted in the synthesis of multifunctional oligomers with a diverse enough monomeric alphabet to write basic sentences and even encrypt and decrypt data in the form of a QR-code.[7,12] This approach was almost entirely limited to the use of acrylates and the incorporation of acrylamides was limited *via* this approach.[7] Therefore, in order to expand the monomer toolbox further for the synthesis of sequence-defined oligomers, the use of thioacrylates within a thiolactone-based, iterative protocol was investigated through this collaborative project.[10] Thioacrylates are a somewhat forgotten class of monomers, first discovered in 1956,[23] but not investigated for some decades since.[24] However, these molecules were more recently studied by Aksakal and Becer, who used them as monomers for RAFT polymerisations, yielding a range of homopolymers of varying degrees of polymerisation as well as to synthesise block co-polymers with ethyl acrylate.[24,25] The polymers were extensively investigated and characterised *via* NMR, SEC, DSC, TGA and water contact angle measurements. Therefore, within this present work, thioacrylates were proposed as a tuneable side group to not only increase the range of available monomers but because they also offered the possibility

to further modify the resulting thioester structure with a broad range of primary amines, to result in an amide (*Figure III 1*).[26] A multistep, protecting group-free, solid-phase protocol, based upon both thiolactone chemistry and the incorporation and modification of thioacrylates was therefore developed, resulting in multifunctional, sequence-defined oligomers.

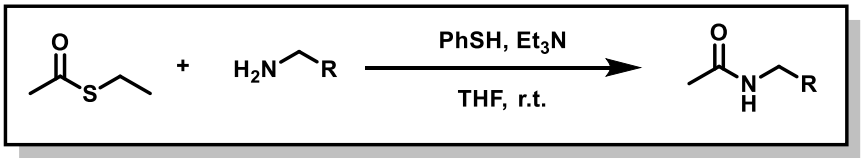


Figure III 1: General reaction scheme showing the modification of a thioester-containing structure with a primary amine. This reaction was the basis for this herein discussed sequence-defined approach.

III.2 Results and discussion

III.2.1 NMR model studies

Model studies and compatibility tests were first carried out to assess and optimise the amidation modification reaction and to confirm that thioacrylates were compatible Michael acceptors in a thiolactone-based, sequence-defined protocol. The first investigations were based upon experiments reported by Nicolaÿ and co-workers,[26] whereby a thioester containing moiety and a primary amine were used to study the proposed amidation reaction. ^{1}H NMR and Gas Chromatography (GC) measurements of both starting material (*S*-ethyl thioacetate and butylamine) and resulting amidation products were carried out, to compare first the effect of solvent (THF-d_8 and $CDCl_3$) (Experiment III.4.5.1) *via* ^{1}H NMR and subsequently the effect of thiophenol as a catalyst[27] was analysed *via* GC because the precipitate formed made online NMR analysis more difficult (Experiment III.4.5.2). During Experiment III.4.5.1, a measurement was taken every 6 mins and between measurements the sample was continuously spinning inside the instrument (sample spin rate = 20Hz) to replicate the stirring effect as carried out in Experiment III.4.5.2. The NMR data obtained was then used to plot the conversion of the thioester to the corresponding amide as a function of time (*Figure III 2*). From this study, it was shown that using THF as solvent, compared to chloroform, resulted in a slightly faster rate of reaction, but the addition of thiophenol had a more dramatic effect on the rate of reaction and conversion. Moreover, the study proved that a thioester containing moiety could be converted to an amide, upon reaction with a primary amine, thus confirming the potential that thioacrylates held as substituents that could be selectively modified.

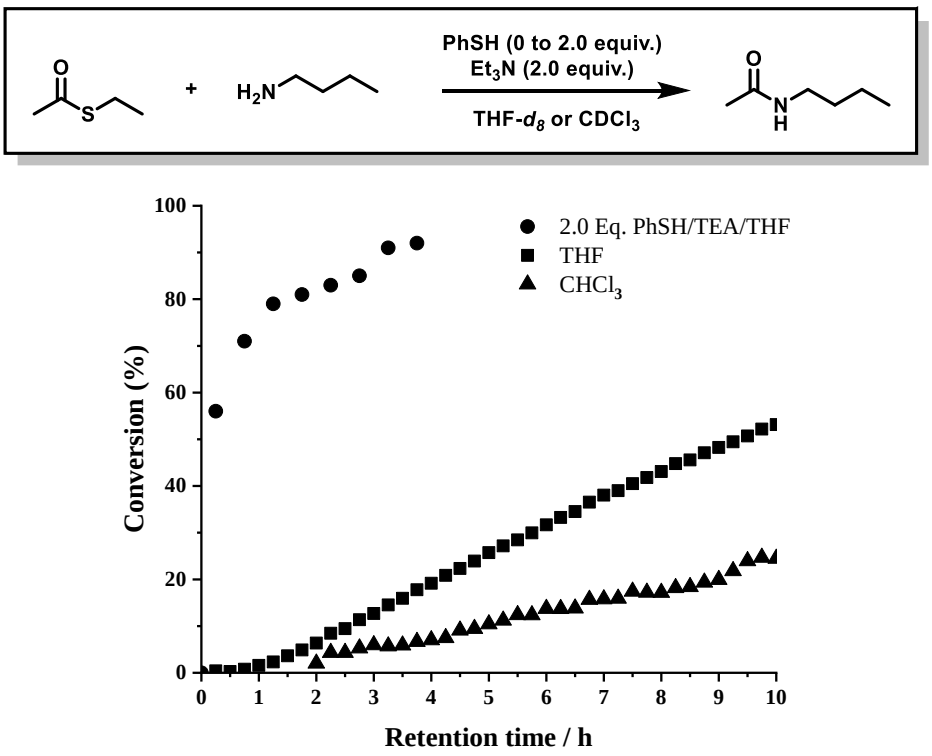


Figure III 2: Graph showing the influence of solvent (Experiment III.4.5.1) and thiophenol on catalysing the amidation reaction (Experiment III4.5.2) between a primary amine (butylamine) and a thioester.

In previously reported thiolactone-based protocols, the thiolactone ring-opening step and subsequent Michael addition reaction were carried out in one pot.[7] This enabled the immediate thiol-ene reaction between the acrylate and the newly released thiol, avoiding the potential side reaction of disulfide formation. The different electronic properties of the sulfur heteroatom of the thioacrylate, in comparison with that of the oxygen in acrylates, meant that there was a potential that the aza-Michael reaction, which can occur between an amine and an acrylate, could be more preferential than the thiolactone aminolysis in a one-pot reaction. To compare the two different acrylate species in such a reaction and assess the chemoselectivity of the primary amine within the protocol,[28] an online NMR study was carried out, comparing the reaction of ethanolamine with ethyl acrylate (Experiment III.4.5.3) and ethyl thioacrylate (Experiment III.4.5.4) over a period of two hours (see *Figure III 3*). Whilst a slow aza-Michael coupling can be observed between ethanolamine and ethyl acrylate over the two-hour period, as confirmed by a 23 % upfield shift in the alkyl proton resonances adjacent to the ester (O=C-O-C**H**$_2$), this is sufficiently slow so as not to interfere with the thiolactone aminolysis reaction (as an excess of reagents were used). On the other hand, the reaction between ethanolamine and ethyl thioacrylate proceeded very rapidly and could be attributed to the lower pK_a and thus higher reactivity of a thioester compared to an ester. This was shown by the complete disappearance of the acrylic proton resonances within 18 minutes. Therefore, it was clear that the aminolysis and Michael addition reactions must be separated within the protocol.

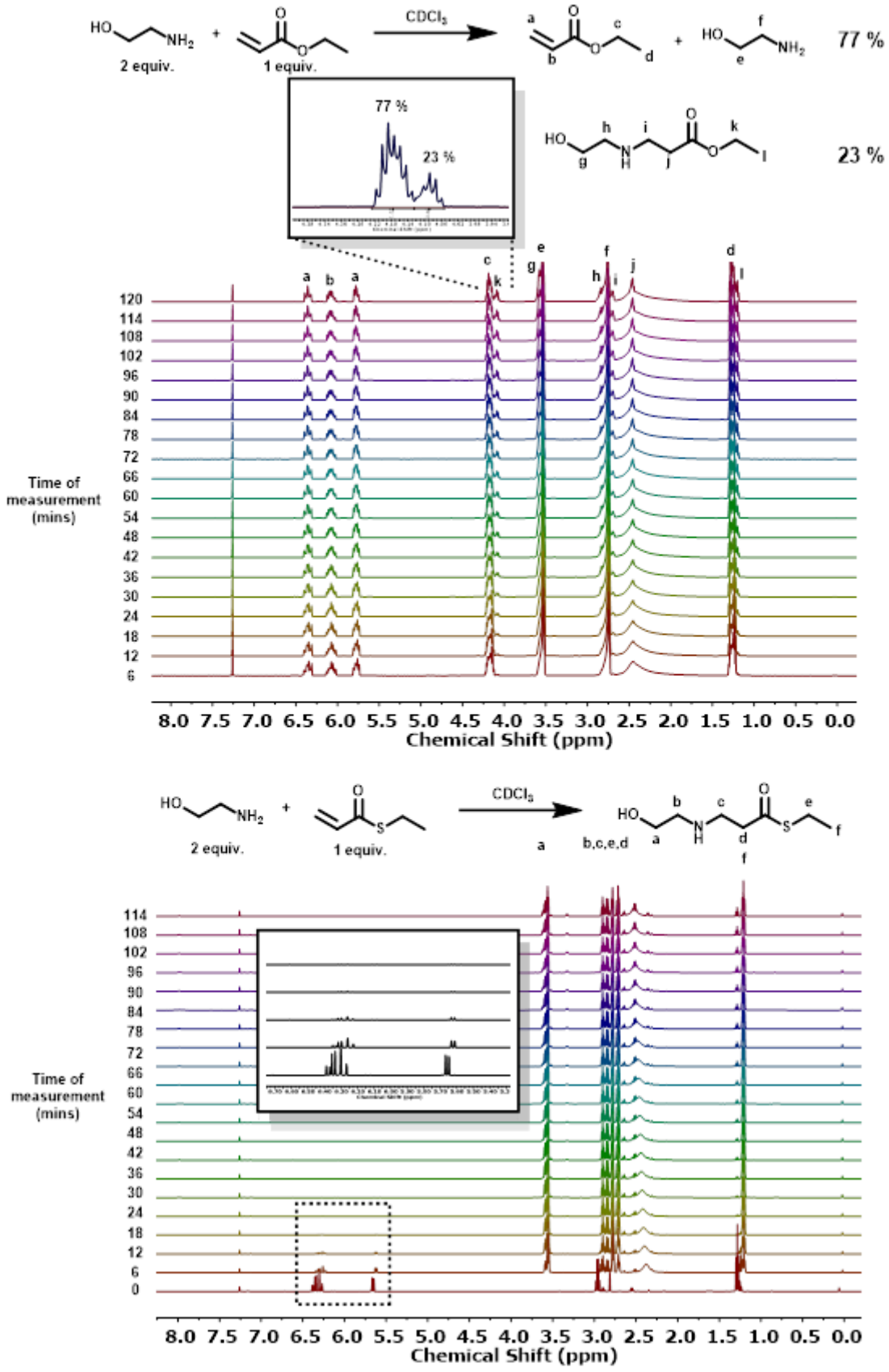


Figure III 3: Top) ^{1}H NMR spectra recorded every 6 minutes to compare the reactivity of ethanolamine with ethyl acrylate. Bottom) ^{1}H NMR spectra recorded every 6 minutes to compare the reactivity of ethanolamine with ethyl thioacrylate. Measurement at t=0 is also included because of the fast reaction between ethyl thioacrylate and ethanolamine.

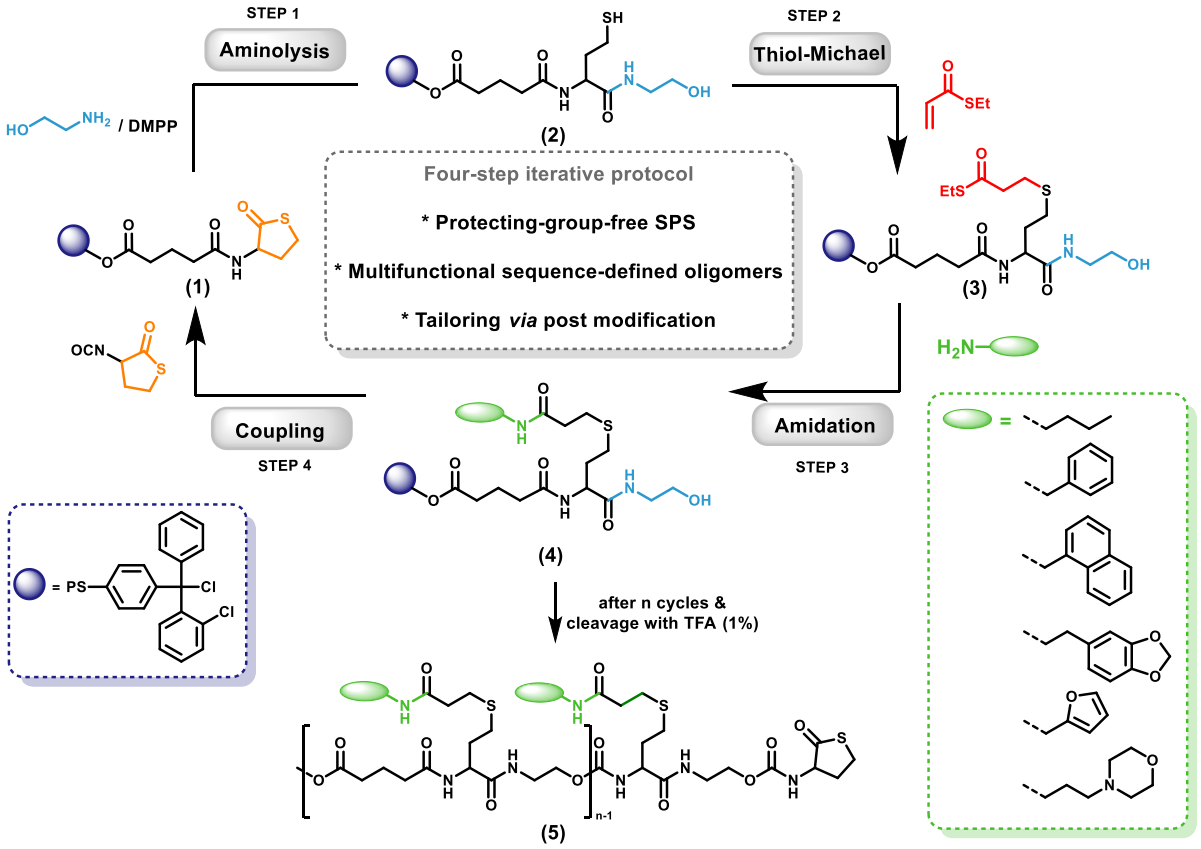
III.2.2 The synthetic protocol

Whilst the model studies performed demonstrated that thioacrylates could be modified in a thiophenol catalysed amidation reaction, the online NMR experiment to compare the reactivity of thioacrylates compared with acrylates towards ethanolamine highlighted one of the challenges that using thioacrylates presented in a thiolactone-based protocol. Nonetheless, a four-step protocol (see *Scheme III 1*) was carefully developed which enabled the ring-opening of thiolactone, incorporation of ethyl thioacrylate, the subsequent thiophenol catalysed amidation reaction of the thioester moiety with a range of functional primary amines and finally the reinstallation of a thiolactone unit to facilitate the next iterative cycle. The synthesis strategy was developed for Merrifield-inspired, solid-phase chemistry,[29] as this is the most straightforward chemical tool to enable a complex, multistep, iterative protocol (see Chapter II, Section II.3.1).[9,11] 2-Chlorotrityl chloride polystyrene resin, functionalised with a thiolactone carboxylic acid molecule, was used in this instance. The use of solid-phase chemistry meant that a high excess of reagents could be used during each reaction step to ensure 100 % conversion and enabled easy purification *via* washing with solvents.

The combination of thiolactone aminolysis and subsequent Michael addition in one-step was not possible, so these two reactions had to be split into two steps, however, the ring-opening of thiolactone in the absence of a Michael acceptor resulted in disulfide formation.[6] Therefore, in the first step of the protocol, rather than subsequently treating the disulfide bonds with a reducing agent - dimethylphenylphosphine (DMPP) - the aminolysis was carried out in the presence of DMPP to reduce the disulfide bonds as they formed, which was less challenging than previously reported.[6] It was not possible to carry out a one-pot reaction within the presence of DMPP to simultaneously reduce any disulfide formation and to catalyse the thiol-Michael addition,[30] allowing it to favourably compete with the aza-Michael coupling, as it was observed that the DMPP catalysed a further side reaction between the alcohol group of ethanolamine and the ethyl thioacrylate. Therefore, in the second step, no catalyst was used during the reaction between the free thiol group with ethyl thioacrylate. However, *N,N'*-dimethylformamide (DMF) was used as the reaction solvent as it provided the perfect combination of being a good swelling solvent for the polystyrene resin,[31] and being a highly polar solvent, which has been reported to have had a beneficial solvent effect on a thiol-Michael addition.[30]

A wide variety of functional primary amines were then used in the third step of the iterative cycle for the thiophenol catalysed amidation reaction, to demonstrate the versatility of this approach. In the final step of the cycle, the thiolactone moiety was re-introduced to the oligomer *via* the reaction of α-thiolactone-γ-isocyanate with the alcohol group of the ethanolamine, as done in previously reported

iterative, thiolactone-based, sequence-defined strategies.[7,9] The protocol in this work was designed in such a way that each step was orthogonal to one another, thus avoiding the need for protecting groups.



Scheme III 1: Solid-phase, iterative protocol for the preparation of multifunctional, sequence-defined oligomers.

III.2.3 Kinetic studies

The kinetics of each step in the protocol were investigated using Liquid Chromatography Mass Spectroscopy (LCMS) as the preferred analysis tool as it quantitatively showed the reaction conversion. This technique only required ca. 2 mg of resin to be taken (reactions were carried out on a 40 mg scale) at predetermined time intervals so that the oligomer could be recovered from the resin with the mild treatment of acid (see Section III.4.4.2). Moreover, an NMR kinetic study would not be feasible in this instance as the reaction conversion would be unclear in such complex spectra and would require too much material for analysis. However, analysis of the reaction kinetics of both the thiolactone ring-opening and thiol-Michael addition (steps one and two) was much more difficult than anticipated. In both instances, no visible change was observable over the measured period in the LCMS spectra (see *Figure III 4a* and *b*).

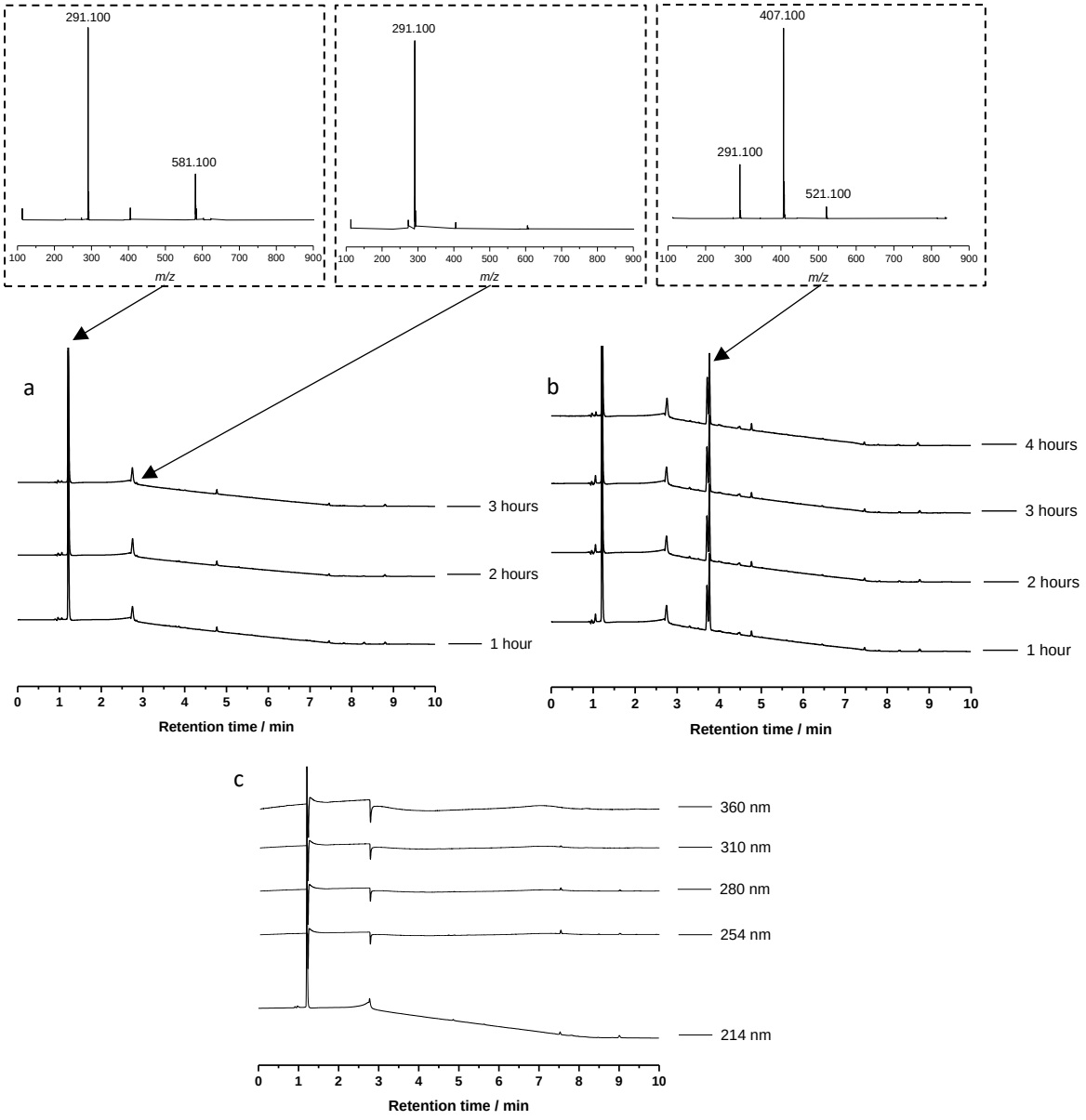


Figure III 4: LCMS chromatograms at λ = 214 nm of the reaction kinetics of a) the thiolactone ring-opening step, b) the thiol-Michael addition reaction and c) an injection of pure acetonitrile (the solvent used for the LCMS-analysis reported here) at all possible analysis wavelengths to show the effect of solvent injection on the chromatogram.

The retention time of the thiol-containing product, or possible undesired disulfide side-product, had retention times which coincided with the solvent injection peak (*Figure III 4c*). The ESI MS spectra of the largest peak at 3 hours in *Figure III 4a*, indicated the presence of the desired thiol product along with some disulfide side-product, despite the use of phosphines during the reaction. However, the ratio of disulfide species present, compared to free thiol moieties, was unclear as MS itself is not a quantitative technique. Nonetheless, proceeding after 4 hours of aminolysis with the subsequent reaction step showed no obvious side reaction or unwanted by-product.

Again, for the thiol-Michael addition step, the LCMS results displayed no apparent change over a period of 4 hours (*Figure III 4b*). The peak at the retention time of 3.75 minutes is that of the desired product, initially indicating that it is formed within the first hour. However, the thiol containing moiety from the first step is, as described above, difficult to distinguish from the solvent injection peak, thus making it difficult to be sure when the thiol-Michael reaction was complete. Nonetheless, selecting again a reaction time of 4 hours, seemed to yield no obvious side reactions or problems during synthesis.

A point to highlight when analysing the LCMS spectra, is that in addition to the peaks from the solvent injection, a small impurity peak was visible in all LCMS chromatograms at λ = 214 nm (for example, see *Figure III 4b*) and is accountable to an impurity from the LCMS instrument itself, with the mass of 278 Da.[10]

The kinetics of the thiophenol catalysed amidation step was much easier to quantify by LCMS (see *Figure III 5*) when compared with the first two steps of the protocol. Benzylamine was selected as the primary amine for this kinetic study, as previously reported studies showed that the chosen primary amine affects the rate of reaction.[32] Of the amines used in this study, benzylamine was known to have the slowest rate of reaction (except for 1-naphthylmethylamine, but the supply of this was more limited and the cost much higher). The experiment showed 100 % conversion of the previous step between 4 and 6 hours, thus 6 hours was decided upon as the suitable reaction time for this step. The reaction kinetics of the addition of α-thiolactone-γ-isocyanate in the fourth step of the protocol to the free alcohol moiety were already previously reported and so were not reinvestigated.[7]

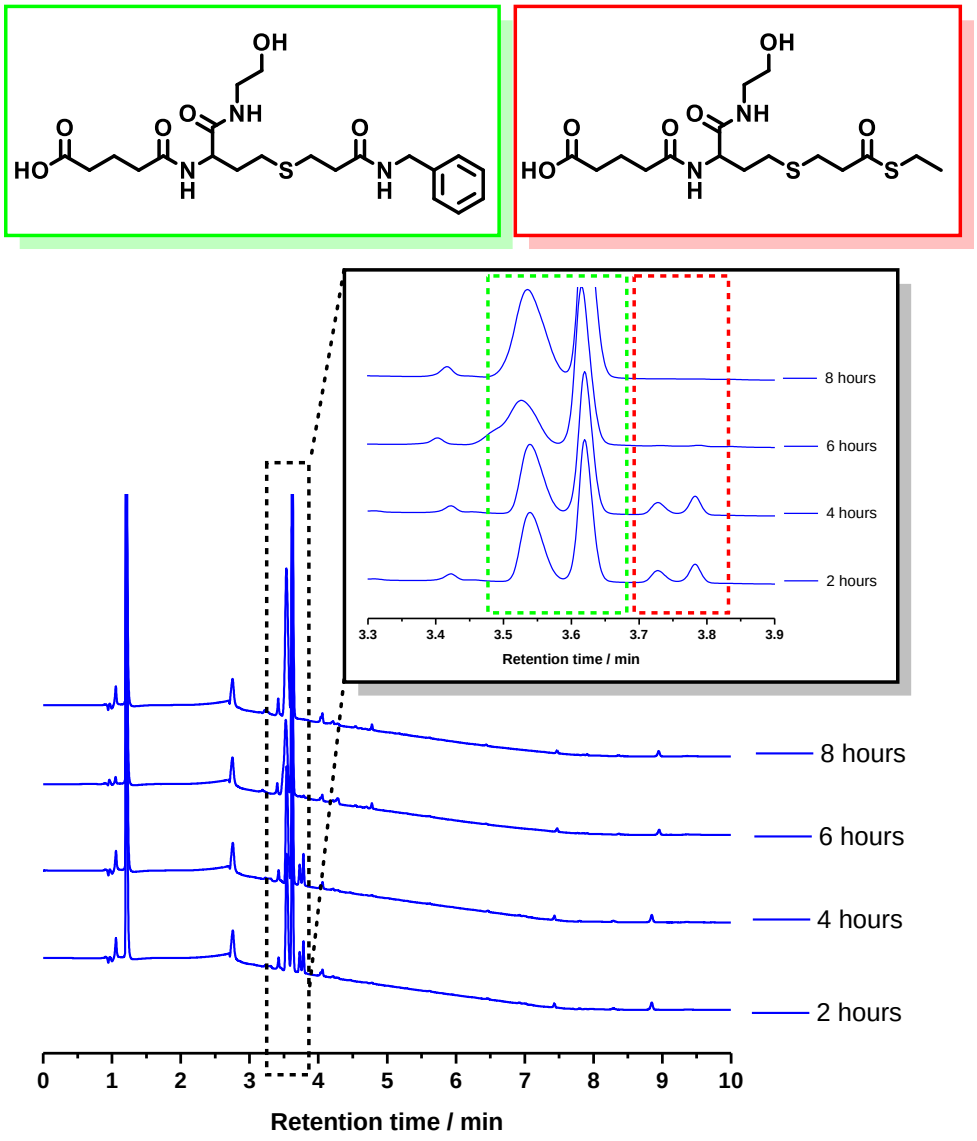


Figure III 5: LCMS chromatograms at λ = 214 nm showing the kinetics of the thiophenol catalysed amidation reaction with benzylamine over 8 hours. The thioester amidation can be observed to be fully complete within 6 hours.

III.2.4 Analysis of synthesised sequence defined oligomers

A range of six different functional primary amines were selected (*vide infra*, *Table III 1*) for this protocol. They were first used individually to synthesise six different monomers, to check both their compatibility within the protocol, to prove its versatility and to allow for full characterisation of these structures by LCMS, HRMS and NMR spectroscopy (see Section III.5.1 for the HRMS and NMR data). Characterisation by ^{1}H and ^{13}C NMR techniques was aided with COSY, HSQC and HMBC to enable full assignment of the monomer structures (an example is shown in *Figure III 6* and described below). In addition to the backbone, the carefully selected functional side groups could be easily identified in

the ^{1}H NMR spectrum. The assigned NMR spectra of the monomers were very useful for the more difficult analysis of the oligomers that were later synthesised (see Section III.5.2), as the full assignment of the backbone was then known. This also aided the side-group assignment, particularly for the multifunctional sequence-defined oligomer **3**, where a wide range of functionalities were installed there.

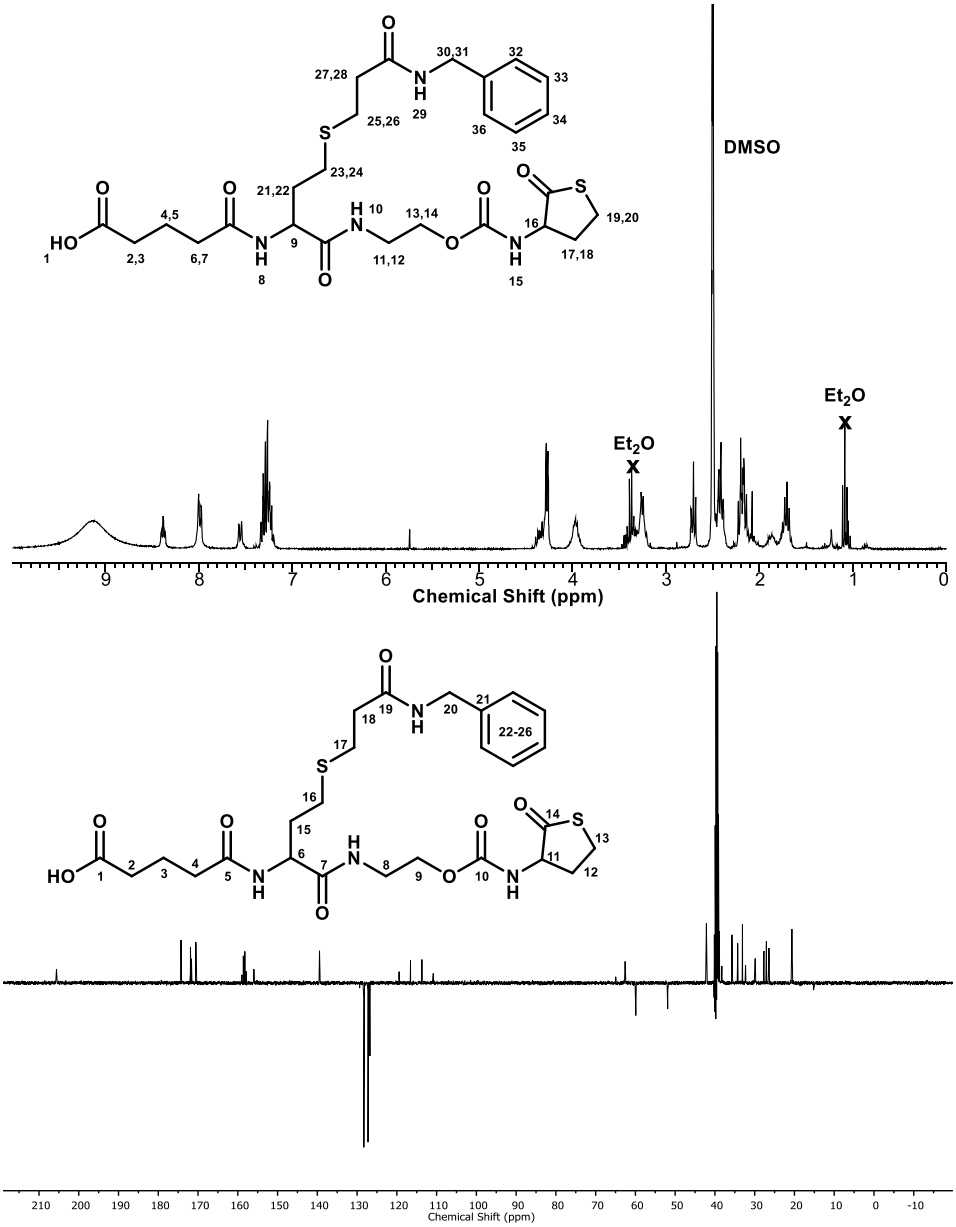


Figure III 6: ^{1}H (top) and ^{13}C (bottom) NMR spectra of a benzyl functionalised monomer. Full assignment of the structure can be found in section III.5.1.

As can be seen in the example in *Figure III 6*, there is a broad, shifting resonance in the ^{1}H NMR spectra of these monomers (see also Section III.5.1). This is most probably because of traces of trifluoroacetic acid (TFA) remaining in the sample, following cleavage from the resin, although all samples were dried for several hours under vacuum to remove as much solvent as possible. The carboxylic acid proton

resonance was not visible in the ^{1}H NMR spectrum, which is possible for spectra measured in DMSO-*d*$_6$. The proton resonances of the benzyl functionality (H_{32-36}) were easily identifiable as they gave a multiplet from 7.39-7.15 ppm, which lies in the characteristic range for aromatic groups. The amide protons ($H_{8,10,16,29}$) were also easily assignable as they too were in the usual shift range for these functionalities (5-9 ppm) and gave no corresponding cross-peak in the HSQC spectrum but corresponded to the carbonyl carbon resonances in the HMBC spectrum. The amide proton in the benzyl side-chain (H_{29}) was assignable in part because it gave a triplet but also because in COSY analysis it coupled with the proton resonances of the C**H$_2$** group adjacent to the aromatic ring. The proximity of this C**H$_2$** group to the aromatic ring caused a downfield shift of this resonance to 4.46-4.19 ppm. This resulted as a multiplet because of overlap with the signals of two protons from the thiolactone ring (one of the α-protons and the γ-proton). A shift of approximately 4.5 ppm is typical for resonance of the C**H** proton of γ-substituted thiolactone. Attached Proton Transfer (APT) ^{13}C NMR was used to help distinguish the seven **C**H groups of the structure. Signals at 128.29, 127.25 and 126.76 ppm (C_{22-26}) corresponded to the aromatic ring (coupling with the appropriate proton resonances in the HSQC spectrum) and C_8 and C_{11} were identified by the corresponding proton resonance that they coupled to in the HSQC spectrum. Once all easily distinguishable proton and carbon environments were assigned, the combination of 1D and 2D techniques were used to assign the remaining signals of the ^{1}H and ^{13}C spectra along with logical assignment based upon appropriate chemical shifts and splitting patterns. For example, the highest field multiplet (1.79-1.63 ppm) in the ^{1}H NMR spectrum corresponded to the C**H$_2$** protons ($H_{4,5,22}$) which were the least influenced by adjacent functional groups.

Analysis of the monomer structures (following one complete cycle of the protocol) by LCMS, revealed the conversion and purity of the structures (*Figure III 7*). In all cases, the main peak corresponded to that of the desired product. To the left of this, a small side peak is observable in most instances (as highlighted in *Figure III 7*) and is attributable to a partial oxidation of the thioether in the structure because of the cleavage with 1 % TFA solution, resulting in the mass of the product +16 Da to be observed in the MS spectrum.[10] This consequence of cleavage is something that has been reported in previous thiolactone protocols and requires future investigation to mitigate the occurrence of this side reaction,[7,9,10] however, in this protocol the amount of oxidation was negligible and was not considered further as it occurs during cleavage rather than during reaction itself. Aside from the aforementioned observable system peaks (solvent injection and instrument impurity), no other significant impurities were visible, except in the 1-naphthylmethyl structure, where the final thiolactone-isocyanate addition was observed to be not quite 100 % complete, suggesting that the limited shelf life of this isocyanate species[7] had reduced the effectiveness of this reaction step. Therefore, a new batch was synthesised for the following experiments.

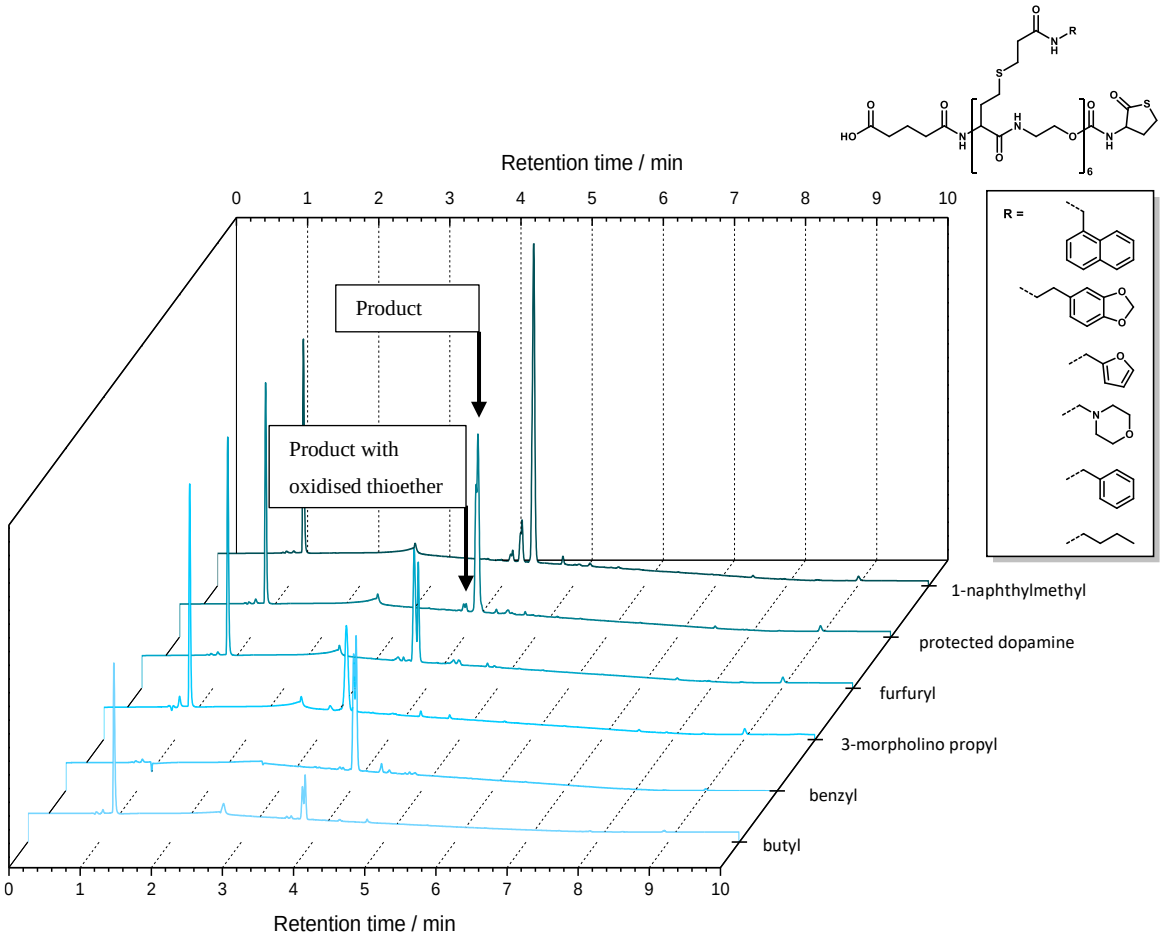


Figure III 7: Stacked LCMS chromatograms (λ = 214 nm) of the 6 different monomers synthesised. The peak at 1 minute is because of the solvent injection. The main peak seen at around 4 minutes in each chromatogram corresponds to the desired product and the small peak to the left of this corresponds the product with oxidised thioether.

Following these initial monomer tests of the protocol, sequence-defined oligomers were synthesised. Firstly, two opposite AB-type alternating octamers (**1** and **2**) were produced. The growth of these oligomers was followed principally throughout using LCMS as a visual and quantitative check of conversion and purity of the reaction, as shown below in *Figure III 8*. The complete shift in retention time as the oligomer size increased, showed that 100 % conversion was reached after each cycle and the final oligomers were obtained with a good purity. Again, as with the monomers analysed in *Figure III 7*, a small amount of thioether oxidation was observed at each step. Additionally, HRMS measurements were taken after each step in the cycle, as one can use the sample used for LCMS analysis (see Section III.5.2), however, because of limited material, NMR analysis was only possible for the final oligomer (see Section III.5.2).

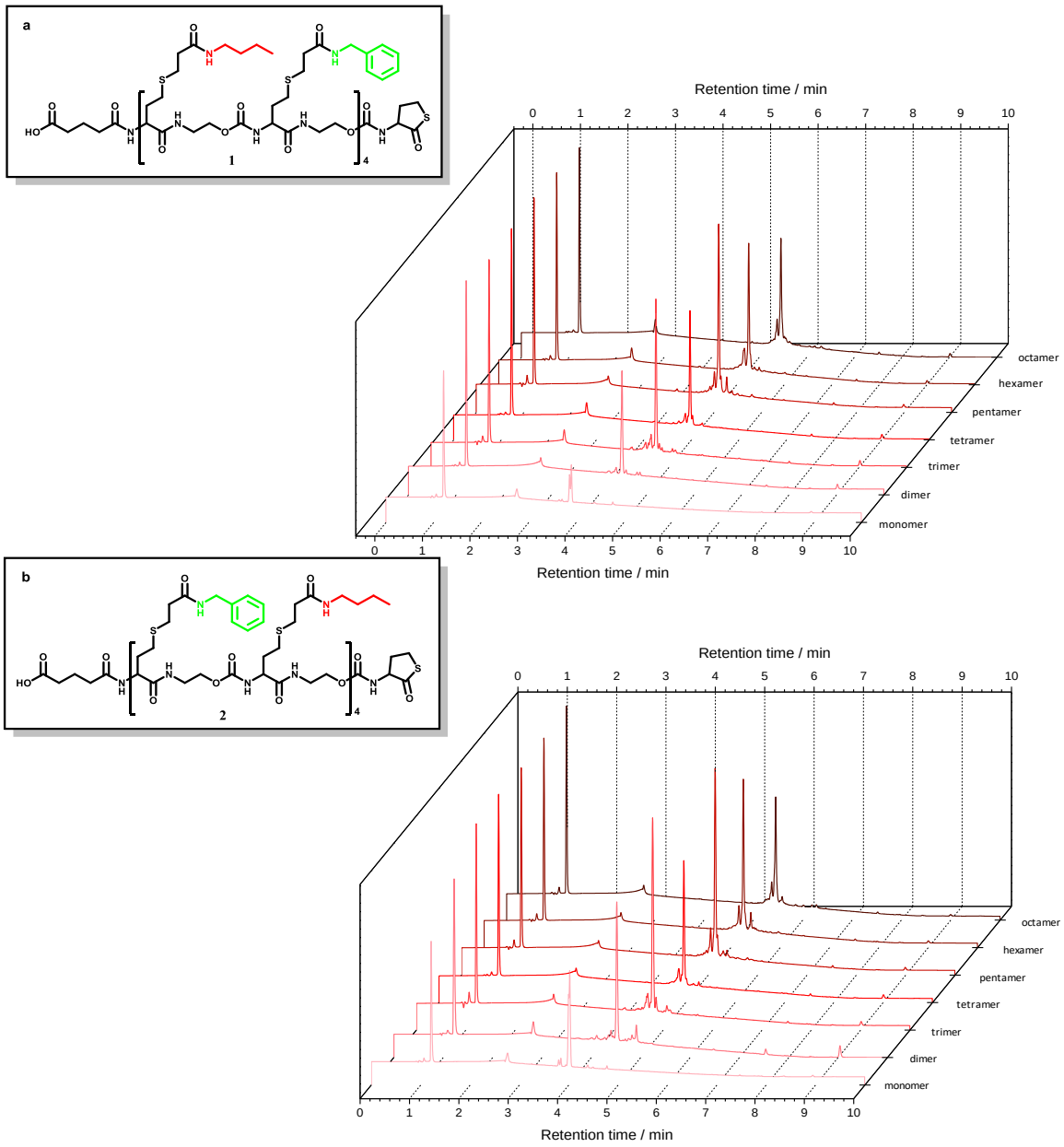


Figure III 8: Stacked LCMS chromatograms (λ = 214 nm) of alternating a) butyl-benzyl and b) benzyl-butyl functionalised octamers from monomer through to octamer. Note, no intermediate analysis between the 6th and 8th cycles.

A final, multifunctional oligomer, **3** was synthesised, incorporating all of the functionalities tested and shown in *Figure III 7* (*vide supra*). This was again followed cycle after cycle by LCMS (and HRMS), as shown below in *Figure III 9*. The final oligomer was also characterised by NMR spectroscopy (*Figure III 10*), where all functional side-groups of the oligomer were assignable, along with the rest of the structure.

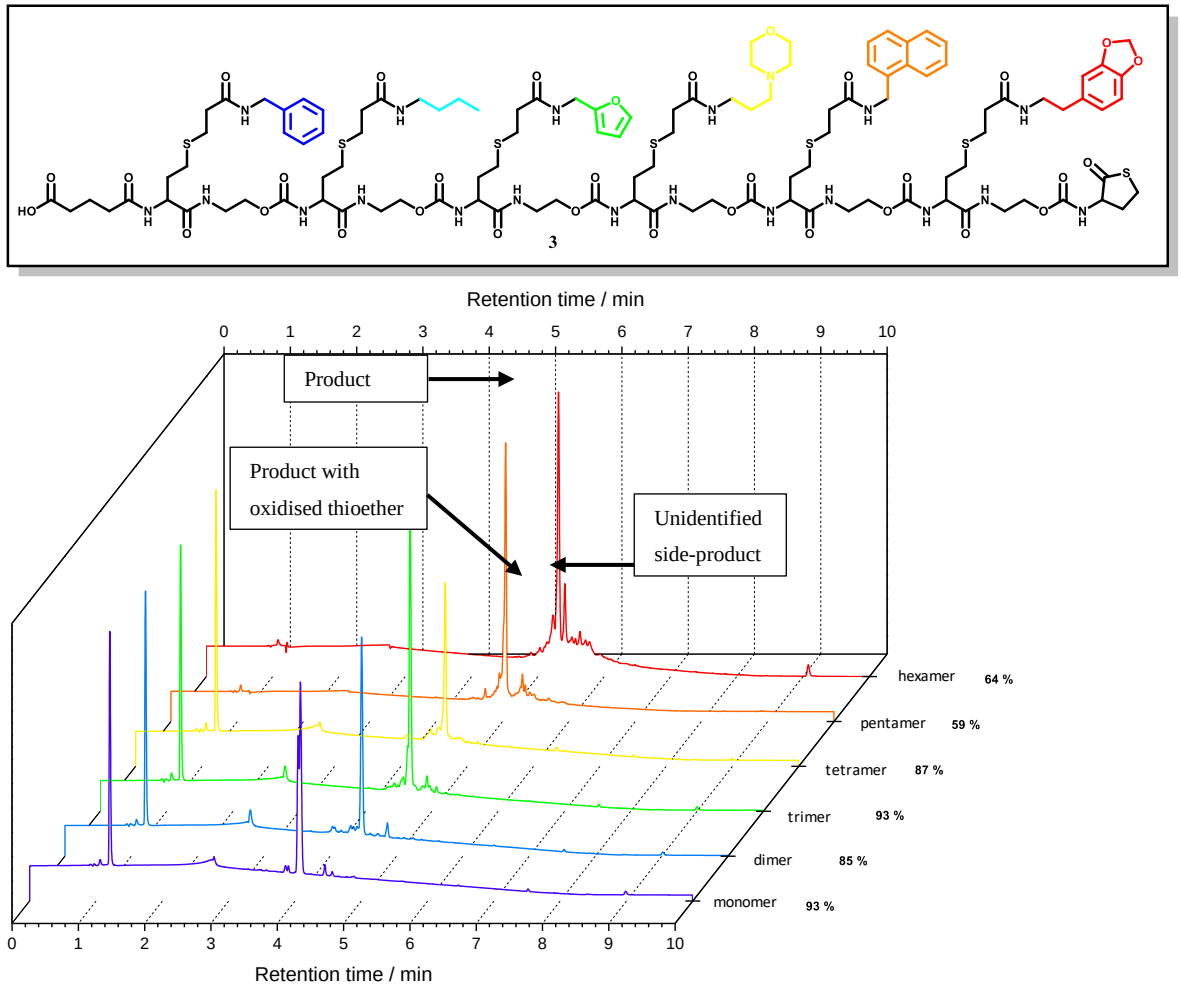


*Figure III 9: Stacked LCMS chromatograms (λ = 214 nm) of oligomer **3**. Purity of each oligomer is included on the z-axis as a percentage and was determined* via *integration of the chromatograms.*

Figure III 10 (*vide infra*) shows the ^{1}H spectrum of oligomer **3**. Full assignment of this spectra is detailed in Section III.5.2. However, as can be seen in the spectra in *Figure III 6*, the broad resonance between 10-9 ppm can most probably be attributed to residual traces of TFA. The carboxylic acid proton resonance was again not visible in the ^{1}H NMR spectrum. The assignment of the structure was very complicated because of the wide variety of proton and carbon environments, which caused much resonance overlap. However, it was possible because of the assignment of the previously synthesised monomers containing separately each of the functionalities of this oligomer, which helped to not only assign the functional side groups of oligomer **3**, but also confirm the backbone structure too. (This was also the case for the NMR assignment of oligomers **1** and **2** – *vide infra*, Section III.5.2). For example, in the ^{1}H NMR spectrum of *Figure III 10*, the multiplet at 7.38-7.17 corresponded to the benzyl side group and the proton resonances of the naphthyl side group were split over two multiplets at 8.15-7.76 ppm and 7.61-7.36 ppm. The proton (H_{36}) adjacent to the ether bond of the furfuryl side group was amongst the multiplet from 7.61-7.36 ppm and the other two alkene protons ($H_{34,35}$) gave two distinct

peaks - a doublet of doublets and a doublet at 6.37 and 6.23 ppm respectively. The protected dopamine functionality was easily assignable. The three aromatic protons of this group (H_{55-57}) gave a multiplet at 6.87-6.72 ppm and a doublet of doublets at 6.64 ppm. The C**H₂** (H_{58}) of the protecting group gave a distinct, sharp singlet at 5.94 ppm, as expected. The tertiary amine of the 3-morpholino side group, however, became protonated during the acidic cleavage, resulting in an extra proton. In the 3-morpholino monomer spectrum, (Section III.5.1) this proton resulted in a singlet at 9.63 ppm, however, in the spectrum in *Figure III 10*, this coincides with the broad shift of the residual TFA. The other protons of this side group can be found in the multiplet resonances (overlapping with other CH_2 proton signals) at 4.10-3.82 ppm and 3.45-2.95 ppm, except the two protons (one from each C**H₂**) closest to the oxygen atom ($H_{42',43'}$) which correspond to a small, but distinct triplet at 3.64 ppm. Finally, the aliphatic butyl side group was mostly difficult to distinguish from other upfield C**H₂** resonances, however, the C**H₃** protons resulted in a triplet with the most upfield shift of 0.85 ppm. COSY, HSQC and HMBC were again used to help assign the rest of the structure, helped also by the assigned NMR spectra of the monomers synthesised. APT ^{13}C NMR was used to help distinguish the **C**/**C**H_2 and the **C**H/**C**H_3 resonances and was assigned with the use of 2D NMR (see *Figure III 22*, Section II.5.2).

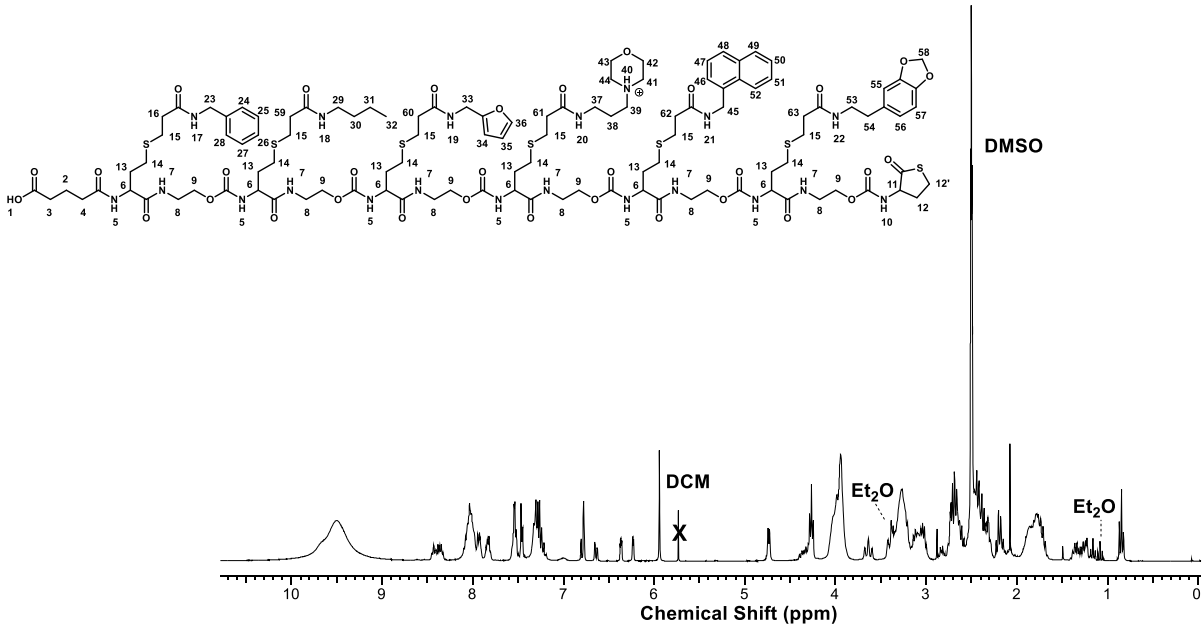


*Figure III 10: ^1H NMR spectrum of multifunctional sequence-defined hexamer **3**. Full assignment of the structure can be found in section III.5.2.*

Whilst the synthesis of the multifunctional hexamer was successful, *Figure III 9* shows that the purity (as indicated on the z-axis) is lower than that of the octamers **2** and **3** displayed in *Figure III 8* (*vide supra*). One possible explanation is that despite individually all working within the protocol (see *Figure III 7*), when together, unforeseen interactions between the side groups, such as folding, may occur which limit the efficiency of the protocol. An effect of the folding behaviour of precision macromolecules on

their synthesis is well known in the area of oligopeptides, for example. However, when considering the iterative growth of oligomer **3**, one can see from the LCMS chromatograms in *Figure III 9* that up until the level of tetramer, the purity remains high and that it is only in the final two cycles that a large decrease in purity is observed. Therefore, either the purity of the 1-napthylmethylamine or the protected dopamine or their interactions with the other groups of the oligomer could be a plausible explanation for this, although this was not further investigated. Alternatively, the washing steps may not have been enough alone to remove all excess reagents, thus influencing the end-purity after several cycles.

Improvement of the purity of oligomers resulting from this protocol could also be possible *via* further optimisation and potentially automation of the reaction. Automation would remove human error and improve reproducibility, although in a complex four-step cycle like this one, automation may prove challenging. Alternatively, the crude oligomers could be purified after *via* preparative High-Performance Liquid Chromatography (prep-HPLC), as is typically performed in peptide chemistry, in a similar way to organic compounds are also usually purified post-synthesis *via*, for example, column chromatography.

III.3 Conclusion and outlook

The protocol developed within this collaborative project, enabled both the inclusion of a new class of acrylics – thioacrylates – within an iterative protocol for sequence-defined oligomer synthesis, as well as the synthesis of multifunctional oligomers *via* the thiophenol catalysed modification of this newly introduced side-group. This work showed the compatibility of two sulfur-based functional compounds, thiolactones and thioacrylates. The protocol was carefully constructed following ^{1}H NMR model studies, analysis of the reaction kinetics and examination of the compatibility of certain reactions to ensure an efficient, protecting group-free protocol. Whilst developing the protocol, certain limitations and issues of using thioacrylates in an amine-thiolactone-ene conjugation reaction became evident. Considering their increased reactivity compared to acrylates, the ring-opening and subsequent Michael addition using thioacrylates could not be carried out in one-step. This increase in reaction steps led to an increase in reaction time and complexity per cycle, thus limiting the possibility of automating the procedure. Furthermore, unlike acrylates, thioacrylate compounds are not commercially available and thus extensive synthesis efforts can be required to obtain them. Nonetheless, by using this protocol, several multifunctional, sequence-defined oligomers were synthesised (up to the length of an octamer), demonstrating the versatility of this approach in terms of the ability to install a wide range of functional groups through the thiophenol catalysed amidation step. This method also showcases the advantage of

using solid-phase chemistry in an iterative approach, as despite the complex, multi-step protocol reported here, purification following each step was relatively easy as well as the handling of the reactions. Whilst just a selection of functional primary amines was examined here, the scope of this protocol could be extended beyond these, as the commercial availability of primary amines is vast and the use of a multitude of side groups enables one to target applications such as data storage.[12] The inclusion of more targeted groups, such as bioactive functionalities, could hold potential to some of the unique applications that sequence-defined synthesis has begun to unlock within polymer science.

III.4 Experimental details

This work was carried out jointly with Dr Suzan Aksakal as this was collaborative project with the Polymer Chemistry Laboratory, Queen Mary, University of London.

III.4.1 Materials and separation techniques

All chemicals were used as supplied, unless otherwise stated. THF-d_8 ≥ 99.5 %, DMSO-d_6 ≥ 99.8 % and $CDCl_3$, ≥ 99.8 % were purchased from Euriso-top. D,L-Homocysteine thiolactone hydrochloride, 99 % was purchased from Haihang Industry (Jinan City, China). Magnesium sulfate, dried, ≥ 99 %, potassium carbonate, ≥ 99 %, sodium hydrogen carbonate, ≥ 99 % and sodium chloride, ≥ 99 % were purchased from Carl Roth. Hydrochloric acid, 36 % was purchased from Chem Lab NV. Trifluoroacetic acid, peptide grade and 2-chlorotrityl chloride resin (100-200 mesh, 1 % DVB, 1.6 mmol/g) were purchased from Iris Biotech GmbH. Anhydrous dichloromethane, 99.8 %, anhydrous *N,N'*-dimethylformamide, 99.8 %, anhydrous tetrahydrofuran, 99.5 %, extra dry, over molecular sieves, anhydrous pyridine, 99.5 %, extra dry, benzene, 99 %, calcium hydride, ca. 93 %, extra pure, 0.20 mm grain size, 1,4-dioxane, ≥ 99 %, dichloromethane, *N,N'*-dimethylformamide, extra pure, dicyclohexylcarbodiimide (DCC), 99 %, hydroquinone inhibitor, pyridine, ≥ 99 %, extra pure and triphenylphosphine, 99 % were purchased from Acros Organics. Benzylamine, ReagentPlus®, 99 %, anhydrous diisopropylethylamine (DIPEA), 99.5 %, purified by redistillation, ethyl acrylate, 99.5 % stabilized with 10 - 20 ppm 4-Methoxyphenol, *S*-Ethyl thioacetate, ≥ 98 %, ethanolamine, ACS reagent grade > 99.0 %, ethanethiol, 97%, 3-morpholinopropylamine, dimethylphenylphosphine (DMPP), 99 %, furfurylamine, ≥ 99 %, glutaric anhydride, 95 %, paraformaldehyde, reagent grade and thiophenol, 97 %, were purchased from Sigma Aldrich. Chloroform and Methanol, HPLC grade, 99.9 % were also purchased from Sigma Aldrich. Bromoacetic acid, butylamine > 99.0 %, dibutyltin dilaurate (DBTL), dimethylaminopyridine (DMAP), >99.0 % and triphosgene, 98.0 % were purchased from the Tokyo Chemical Industry (Europe). 1-Naphthylmethylamine, 98 % was purchased from Alfar Aesar. 3,4-Methylene-dioxyphenethylamine, 95 % was purchased from Fluorochem Ltd. Acetonitrile, HPLC grade, and Toluene, ≥99.8 % were purchased from Fischer Scientific. Acetone and diethyl ether, HPLC

grade, HiPerSolv CHROMANORM were purchased from VWR. Pentane, technical grade was purchased from Univar. When anhydrous chloroform was required, HPLC grade chloroform, from Sigma Aldrich was dried over calcium hydride. Water, when used in the synthesis, was de-ionised. Silicagel (60 Å, 40-63 μm) was supplied by ROCC and used for purification of compounds by column chromatography. Thin Layer Chromatography (TLC) was performed using Merck Kieselgel 60 F_{254} coated aluminium plates.

III.4.2 Analytical methods

Nuclear Magnetic Resonance (NMR): ^{1}H and ^{13}C Attached Proton Test (APT) spectra were recorded on a Bruker Avance 300, a Bruker Avance 400 and a Bruker Avance 500. Chemical shifts are presented in parts per million (δ) relative to DMSO-d_6 or $CHCl_3$-d (2.50 ppm or 7.26 ppm in ^{1}H- and 39.51 ppm or 77.24 ppm in ^{13}C-NMR respectively). Coupling constants (J) are reported in Hertz (Hz). Full assignment of monomers and oligomer structures was aided by use of 2D NMR techniques (COSY, HSQC and HMBC). Nuclear magnetic resonance (NMR) spectra were also recorded on a Bruker AV-III 400 for ^{1}H- and ^{13}C NMR measurements. $CDCl_3$ was used as solvent and the resonance signal at 7.26 ppm (^{1}H) and 77.16 ppm (^{13}C) served as reference for the chemical shift δ. All measurements were performed at 25 °C and MestReNova NMR Processor or ACD/NMR Processor Academic Edition was used for the processing of all data.

Liquid Chromatography-Mass Spectrometry (LCMS): was record on an Agilent technologies 1100 series LC/MSD system equipped with a diode array detector and single quad MS detector (VL) with an electrospray source (ESI-MS) was used for classic reversed phase LCMS and MS analysis. Analytic reversed phase HPLC (high-performance liquid chromatography) was performed with a Phenomenex Kmetex C18 (2) column with a solid core at 35 °C and a flow rate of 1.5 mL/min (5 μ, 150 x 4.6 mm) using a solvent gradient (0 → 100 % acetonitrile in H_2O in 6 min) and the eluting compounds were detected via UV-detection (λ = 214 nm). LCMS spectra were analysed using ACD/Spectrus software and the purity of compounds was assessed by integrating the LC peaks (λ = 214 nm) using the in-software function.

High Resolution Mass Spectroscopy (HRMS): was collected using an Agilent 6220 Accurate-Mass time-of-flight (TOF) equipped with a multimode ionization (MMI) source.

Gas Chromatography – Flame Ionization Detection (GC-FID): analysis was performed using an Agilent Technologies 7820A. An Agilent J&W HP-5 capillary column of 30 m x 0.320 mm, film thickness 0.25 μm was used. The oven temperature was programmed as follows: 40 °C (hold for 1 minute) increase at 30 °C min^{-1} to 300 °C (hold for 2.5 minutes). The injector was operated at 250 °C

and the FID was operated at 320 °C. Nitrogen was used as carrier gas at a flow rate of 6.5 mL min^{-1} and a split ratio of 1:1 was applied. Chromatographic data was processed using OpenLab CDS ChemStation Edition, version C.01.05. Conversions were obtained by the comparing the integral of starting material (*S*-Ethyl thioacetate) or primary amine with integral of solvent or internal standard.

UV-Vis spectroscopy: was recorded on an Analytikjena Specord 200 at λ = 254 nm using 1 cm quartz cuvettes.

Solid-phase reactions: were carried out using a manual peptide shaker (see *Figure III 11*).

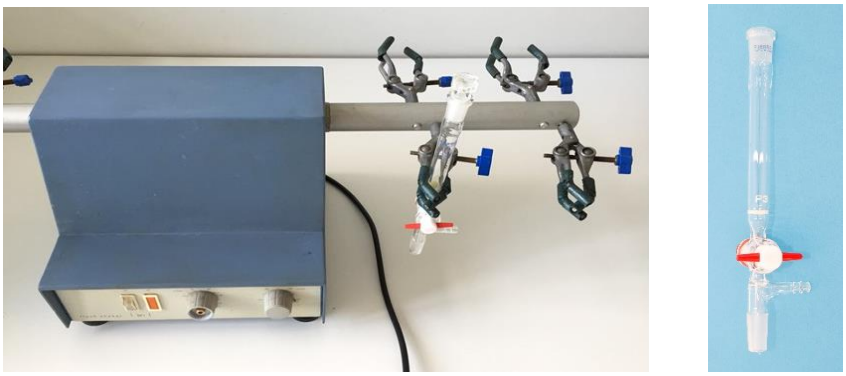
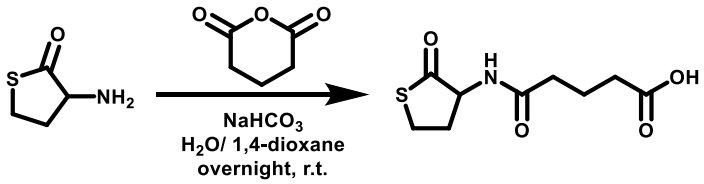


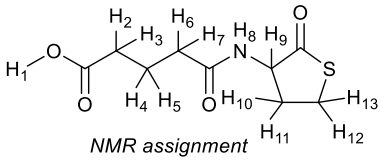
Figure III 11: Left) Manual peptide shaker,[7] right) glass solid-phase reaction vessel.

III.4.3 Synthesis of functional thiolactone compounds

III.4.3.1 Synthesis of thiolactone carboxylic acid

Thiolactone-carboxylic acid was prepared by a modified version of the previously reported procedure.[6]



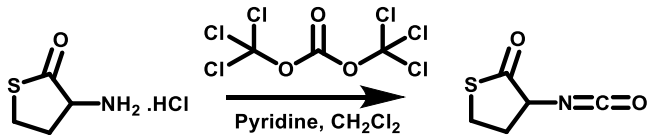


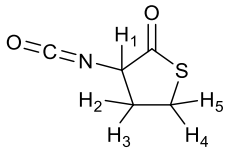
D,L-homocysteine thiolactone hydrochloride (7.013 g, 45.6 mmol) was dissolved in an ice-cooled solution of H_2O/1,4-dioxane (1:1 100 mL). $NaHCO_3$ (19.15 g, 0.2279 mol) was added and the reaction was stirred for 30 minutes at 0 °C. Glutaric anhydride (10.41 g, 91.2 mmol) was added in several portions to the reaction mixture and the reaction was allowed to reach room temperature and left to stir overnight. To adjust the pH to 1, 12 M HCl solution was added dropwise. Brine solution (100 mL) was added and the reaction mixture extracted with ethyl acetate (3 x 200 mL). The combined organic fractions were dried over $MgSO_4$, filtered and evaporated *in vacuo*. The crude was a white, crystalline solid, and analysis by LCMS spectroscopy. This indicated good purity, with only a small presence of the di-acid of glutaric anhydride as a side-product. The crude was purified by recrystallisation in minimum volume of acetone, yielding a white, crystalline solid. Yield = 79.7 %, (m = 8.404 g).

Characterisation was in good accordance with the literature. **^{1}H NMR (300 MHz, DMSO-d_6):** δ = 12.04 (s, 1H, H_1), 8.16 (d, J = 8.3 Hz, 1H, H_8), 4.59 (ddd, J = 12.6, 8.4, 7.0 Hz, 1H, H_9), 3.55-3.13 (m, 2H, $H_{12,13}$), 2.46-2.33 (m, 1H, H_{10}) 2.27-1.97 (m, 5H, $H_{2,3,6,7,11}$), 1.71 (p, J = 7.5 Hz, 2H, $H_{4,5}$); **^{13}C NMR (75 MHz, DMSO-d_6):** δ = 206.51 (C), 174.18 (C), 171.85, (C), 58.11 (CH), 34.29 (CH_2), 32.82 (CH_2), 30.13 (CH_2), 26.73 (CH_2), 20.57(CH_2). **IR** (ATR platinum diamond): ν [cm^{-1}] = 3290 (N-H), 3000-2100 (O-H), 1688 & 1606 (C=O), 1569 (N-H), 1439 (O-H), 1367 & 1323 (C-H), 1232 (C-O), 1018, 923, 713. **HRMS (ESI) *m/z*:** $[M + H]^+$ calculated for $C_9H_{14}NO_4S^+$, 232.0638; found, 232.0644.

III.4.3.2 Synthesis of α-thiolactone-γ-isocyanate

Thiolactone-isocyanate was prepared according to the procedure previously reported.[7]



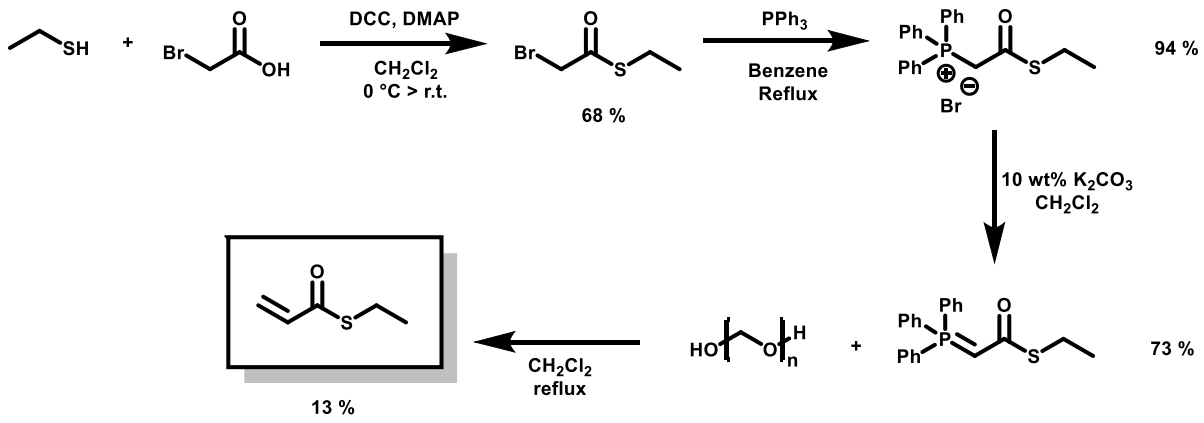


NMR assignment

Triphosgene (50.0 g, 0.168 mol) was dissolved in ice-cooled CH_2Cl_2 (500 mL) and then a further 400 mL of CH_2Cl_2 was added. DL-homocysteine thiolactone hydrochloride (74.0 g, 0.480 mol), dried by azeotropic evaporation 3 times with toluene and then under vacuum for at least 3 hours, was added gently to the reaction mixture. Anhydrous pyridine (128.22 mL, 1.584 mol) was added dropwise to the cooled reaction mixture. After 1 hour, the ice-bath was removed and the reaction stirred for a further 4 hours at room temperature. The aqueous work-up was performed quickly to avoid degradation of the isocyanate formed. The pyridinium hydrochloride salt formed during the reaction was filtered directly into a separating funnel. The salt was rinsed with CH_2Cl_2 (300 mL) and washed with cooled 2M $HCl_{(aq)}$ (500 mL), ice-water (500 mL) and brine solution (500 mL). The aqueous phase was extracted with CH_2Cl_2 (200 mL) The organic phases were collected and dried over $MgSO_4$, filtered and the solvent removed in vacuo. The product was purified by vacuum distillation (85-95 °C, 0.08 mbar), yielding a colourless liquid, however, the yield was not quantified. **^{1}H NMR (300 MHz, $CDCl_3$):** δ = 4.22 (dd, J = 12.7, 6.8 Hz, 1H, H_1), 3.40-3.13 (m, 2H, $H_{4,5}$), 2.74-2.52 (m, 1H, H_2), 2.21-1.90 (m, 1H, H_3); **^{13}C NMR (75 MHz, $CDCl_3$):** δ = 203.33 (C), 127.56 (C), 62.62 (CH), 30.13 (CH_2), 27.03 (CH_2). **IR** (ATR platinum diamond): ν [cm^{-1}] = 2224 (N=C=O), 1690 (C=O), 1337 (C-H). Characterisation was in good accordance with previously reported.[7]

III.4.3.3 Synthesis of ethyl thioacrylate

Ethyl thioacrylate was prepared according to the procedure previously reported.[24]



Bromoacetic acid (64.14 g, 0.462 mol, 1.0 equiv.), ethanethiol (36.6 mL, 0.508 mol, 1.0 equiv.) and DMAP (5.644 g, 0.0462 mol, 0.1 equiv.) were solubilised in CH_2Cl_2 (500 mL) and cooled to 0 °C under a nitrogen atmosphere. Dicyclohexylcarbodiimide (DCC) (100 g, 0.485 mol, 1.05 equiv.) was diluted in 200 mL of CH_2Cl_2 and added dropwise to the reaction solution. The reaction was allowed to warm to room temperature and stirred overnight. The solution was then filtered over silica and the filter cake was washed several times with CH_2Cl_2. The filtrate was washed with saturated $NaHCO_3$ solution, water and brine and then dried over Mg_2SO_4. The solvent was removed *in vacuo*, yielding a yellowish oil (57.028 g, 68 %). This was then refluxed with triphenylphosphine (106.22 g, 0.405 mol, 1.3 equiv.) in benzene (300 mL) under nitrogen overnight. The reaction was then filtered and washed with toluene and the solvent was then removed *in vacuo*, yielding white crystals (129.525 g, 94 %). These were then dissolved in CH_2Cl_2 (250 mL) and stirred vigorously with 10 % $K_2CO_{3\,(aq)}$ (100 mL) for 30 min. The organic phase was separated and the aqueous phase was twice extracted with CH_2Cl_2. The organic phases were combined, dried over Mg_2SO_4 and then the solvent was partially removed *in vacuo*, before the addition of pentane. After 24 hours, light brown crystals formed (83.029 g, 73 %). This 83.029 g of product (0.228 mol, 1.0 equiv.), was finally dissolved in CH_2Cl_2 (300 mL) and paraformaldehyde (34.24 g, 1.14 mol, 5.0 equiv.) was added and the reaction was refluxed for 1 h, before evaporation *in vacuo*, suspended in cold pentane (250 mL) and filtered over silica. The filter cake was washed with cold 1:9 Et_2O:Pentane. Hydroquinone inhibitor was added and the solution was distilled over CaH (2 g L^{-1}) at reduced pressure (11 mbar, 80 °C), yielding a colourless oil. Yield = 13 %, (m = 3.5 g). The poor yield was attributed to difficulties during the reflux, where a completely inert atmosphere was not achieved. **^{1}H NMR (400 MHz, $CDCl_3$):** δ = 6.32 (dd, J = 17.2, 9.7 Hz, C**H$_2$**CH), 6.28 (dd, J = 17.2, 1.6 Hz, C**H$_2$**CH), 5.59 (dd, J = 9.8, 1.6 Hz, CH_2C**H**), 2.89 (q, J = 7.4 Hz, C**H$_2$**CH_3), 1.21 (t, J = 7.4 Hz, CH_2C**H$_3$**); **^{13}C NMR (100 MHz, CDCl3):** δ = 190.1 (C), 135.1 (CH), 125.9 (CH_2), 23.1 (CH_2), 14.6 (CH_3). Characterisation was in good accordance with previously reported.[24]

III.4.4 Manipulation of the solid support and general synthetic procedure

III.4.4.1 Loading of the 2-chlorotrityl chloride polystyrene resin

Loading of the resin was carried out according to a previously reported procedure.[6]

2-chlorotrityl chloride resin (2.999g, 1.6 mmol g^{-1}, 1.0 equiv.) and thiolactone carboxylic acid (862 mg, 0.8 equiv.) were dissolved in anhydrous-CH_2Cl_2 (30 mL), anhydrous-DMF (3 mL) and anhydrous-DIPEA (5 mL) in a solid-phase reactor. The reaction was left to shake vigorously at room temperature for 3 h. The reaction was then filtered and washed with 17:2:1 CH_2Cl_2:MeOH:DIPEA (3 x 30 mL), shaking for 15 mins each time, to cap unreacted 2-chlorotrityl chloride groups on the resin. The reaction was then washed with CH_2Cl_2 (3 x 30 mL), DMF (2 x 30 mL), CH_2Cl_2 (2 x 30 mL) and Et_2O (3 x 30 mL). The product was then dried under vacuum for 3 hours. A 2 mg sample of the resin was prepared for LCMS analysis (*vide infra*, Section III.4.4.2). This sample was analysed by LCMS (*Figure III 12*).

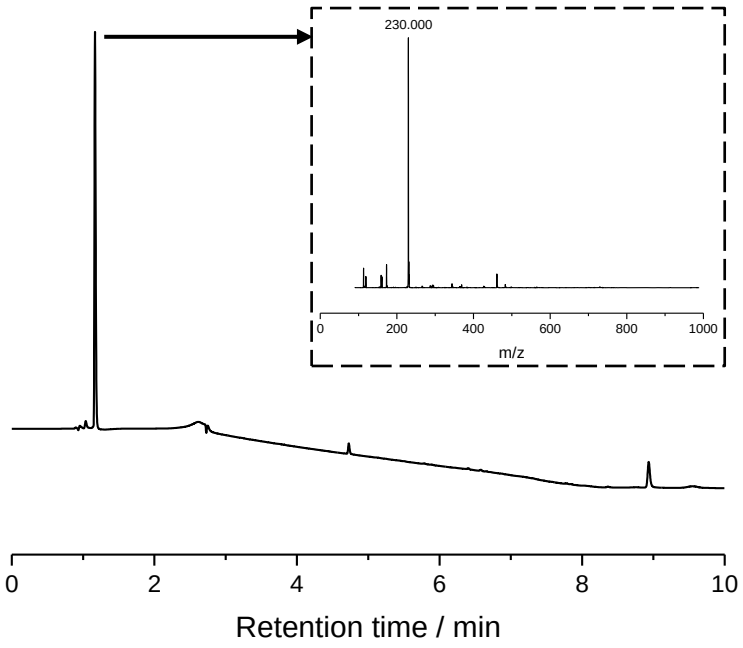


Figure III 12: LCMS chromatogram of thiolactone carboxylic acid.

The loading efficiency was determined by UV-Vis spectroscopy at 254 nm with a calibration curve prepared (*Figure III 13*) for the thiolactone carboxylic acid as previously described.[6] The loading was determined to be 0.705 mmol of thiolactone carboxylic acid per gram of resin, giving a loading efficiency of 44%.

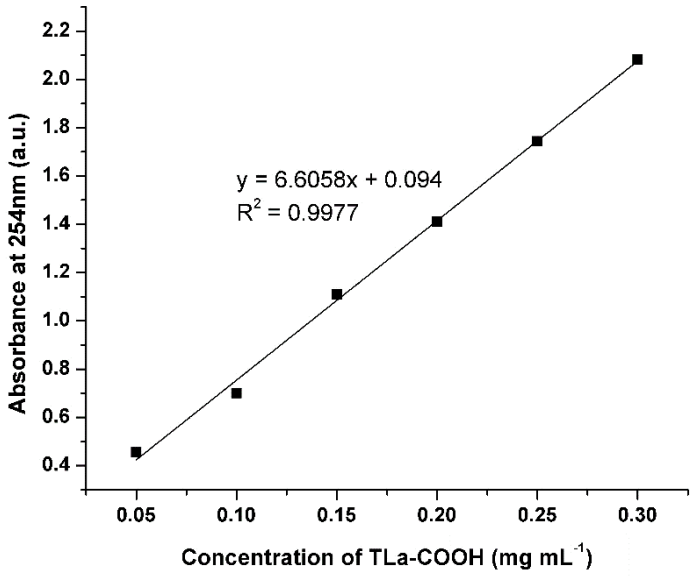


Figure III 13: UV-calibration curve of the thiolactone carboxylic acid linker.

III.4.4.2 Manipulation of the solid-phase resin

Swelling: The resin for each reaction was swollen for at least 10 minutes in the reaction solvent (1 mL of solvent per 100 mg of resin).

Washing: The solid phase resin was extensively washed, under filtration, after each reaction to ensure removal of remaining unreacted starting chemicals or unwanted side-products formed such as precipitates. Washing was done sequentially with DMF (x4), MeOH (x4), $CHCl_3$ (x4) and Et_2O (x4).

Cleavage: For analysis by LCMS, the sequence was cleaved from the resin by suspension in a solution of 1% TFA (trifluoroacetic acid) in CH_2Cl_2 for 5 minutes before filtration of the sample and then concentration by evaporation. During cleavage, a colour change of the beads could be observed from yellow to red because of the trityl cation formed on the resin.

Analysis: This was predominantly carried out using LCMS and HRMS. Once the complete oligomer was synthesised, the remainder of the compound was recovered from the resin and diluted in DMSO-d_6 for ^{1}H NMR and ^{13}C analysis.

III4.4.3 General procedure of sequence-defined protocol

Step 1 - Aminolysis with ethanolamine: Thiolactone carboxylic acid, immobilised on a resin (*vide supra*) (loading = 0.705 mmol g^{-1}) (40.00 mg, 1.0 equiv.) was swollen in $CHCl_3$ (see section III.4.4.2). Then, ethanolamine (86.1 µL, 50.0 equiv.), DMPP (8.0 µL, 2.0 equiv.) and 1 drop of water were added.

The reaction was shaken vigorously for at least 4 hours at room temperature. The reaction was then filtered and the resin washed (see Section III.4.4.2)

Step 2 - Thiol-Michael Addition with ethyl thioacrylate: The resin was then swollen in anhydrous-DMF. Ethyl thioacrylate, (32.8 mg, 10.0 equiv.) was added and the reaction was shaken vigorously for at least 4 hours at room temperature. The resin was then filtered and washed.

Step 3 - Thiophenol catalysed amidation: The resin was then swollen in anhydrous-THF. The desired primary amine (see *Table III 1*) (25.0 equiv.) and thiophenol (57.5 µL, 20.0 equiv.) were added and the reaction shaken vigorously for at least 6 hours at room temperature. Usually, addition of the primary amine resulted in the immediate formation of a white precipitate, but with some amines, this took longer during the reaction time to form. The resin was then filtered and washed.

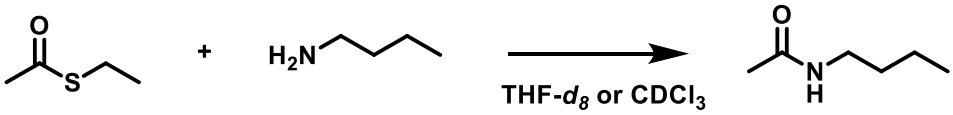
Table III 1: Table of different amines used for the thiophenol catalysed amidation step.

Primary Amine	Mw (g mol^{-1})	mg/µL used	Density (g mL^{-1})
Benzylamine	107.16	77.00 µL	0.981
Butylamine	73.14	69.70 µL	0.740
3-morpholino propylamine	144.21	103.00 µL	0.987
Furfurylamine	97.12	62.30 µL	1.099
1-napthylmethylamine	157.21	103.10 µL	1.073
3,4-methylenedioxyphenethylamine	165.19	116.46 mg	n/a

Step 4 - Chain extension: The resin was then swollen in anhydrous-$CHCl_3$. Then, α-thiolactone-γ-isocyanate, (61.2 µL, 20.0 equiv.) was added followed by a catalytic amount of dibutyltin dilaurate (~3 drops). The reaction was shaken vigorously at room temperature for at least 1 hour. The resin was then filtered and washed.

III.4.5 NMR model studies

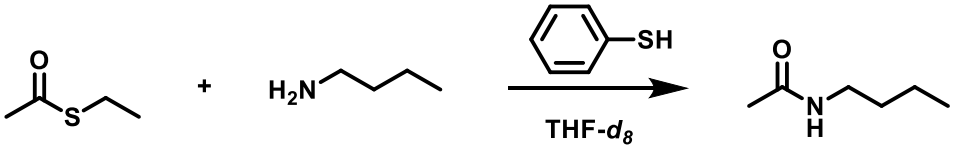
III.4.5.1 Amidation model reaction in THF-d_8 and $CDCl_3$



S-Ethyl thioacetate (16.00 µL, 0.15 mmol, 1.0 equiv.) was dissolved in 0.75 mL of solvent (THF-d_8 or $CDCl_3$) and a ^{1}H NMR was measured as t_0. Then, butylamine (37.00 µL, 0.37 mmol, 2.5 equiv.) was

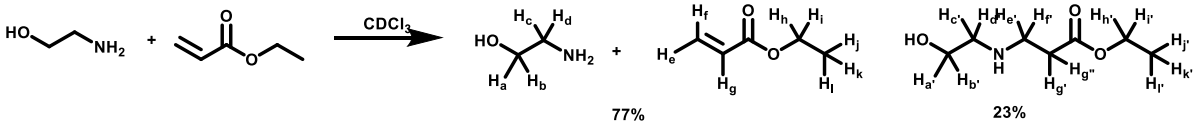
added and NMR spectra were measured every 6 minutes to follow the reaction while constantly spinning inside the NMR instrument (sample spin rate = 20 Hz).

III.4.5.2 Catalysed model amidation reaction in THF-d_8



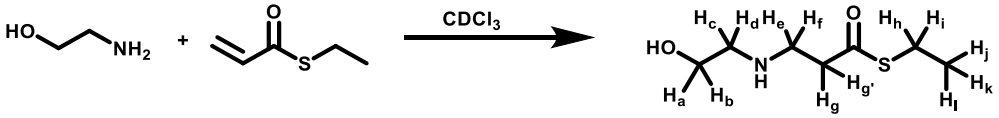
S-Ethyl thioacetate (160.00 µL, 1.5 mmol) was dissolved in THF-d_8 (7.5 mL). Then, butylamine (370.00 µL, 3.70 mmol, 2.5 equiv.), triethylamine (420.00 µL, 3.00 mmol) and thiophenol (306 µL, 3.00 mmol) were added to the solution sequentially. The mixture was stirred at room temperature and NMR spectra were recorded at 30-minute intervals to follow the reaction.

III.4.5.3 Online ^{1}H NMR study of the reaction between ethanolamine and ethyl acrylate



To an NMR tube, ethanolamine (21.34 µL, 0.3443 mmol) was added to ethyl acrylate (18.3 µL, 0.1721 mmol). 0.75 mL of $CDCl_3$ was added and a ^{1}H NMR measurement was taken every 6 mins at 500 MHz during the reaction for a period of 2 hours. **^{1}H NMR (120 mins)(500 MHz, $CDCl_3$):** δ = 6.35 (td, J = 17.1, 16.7, 3.9 Hz, 1H, H_f), 6.17-5.99 (m, 1H, H_g), 5.77 (td, J = 10.7, 3.4 Hz, 1H, H_e), 4.27-4.04 (m, 4H, $H_{h,i}$, $H_{h',i'}$), 3.64-3.49 (m, 4H, $H_{a,b}$, $H_{a',b'}$), 2.91-2.67 (m, 6HH, $H_{c,d}$, $H_{c',d'}$, $H_{e',f'}$), 2.50-2.43 (m, 4H, $H_{g',g''}$) 1.33-1.16 (m, 6H, $H_{j,k,l}$, $H_{j',k',l'}$).

III.4.5.4 Online ^{1}H NMR study of the reaction between ethanolamine and ethyl thioacrylate



To an NMR tube, ethyl thioacrylate (20.0 mg, 0.1721 mmol) was added along with 0.75 mL of $CDCl_3$ and a ^{1}H NMR measurement was taken. Ethanolamine (21.34 µL, 0.3433 mmol) was added and a ^{1}H NMR measurement was taken every 6 mins at 500 MHz during the reaction for a period of 2 hours. **^{1}H NMR (120 mins)(500 MHz, $CDCl_3$):** δ = 3.67-3.54 (m, 2H, $H_{a,b}$), 2.90 (t, J = 6.5 Hz, 2H, $H_{h,i}$), 2.88-2.81 (m, 2H, $H_{e,f}$), 2.80-2.76 (m, 2H, $H_{c,d}$), 2.74-2.69 (m, 2H, $H_{g,g'}$), 1.25-1.18 (m, 3H, $H_{j,k,l}$).

III.5 Additional data

III.5.1 HRMS and NMR data for monomers synthesised

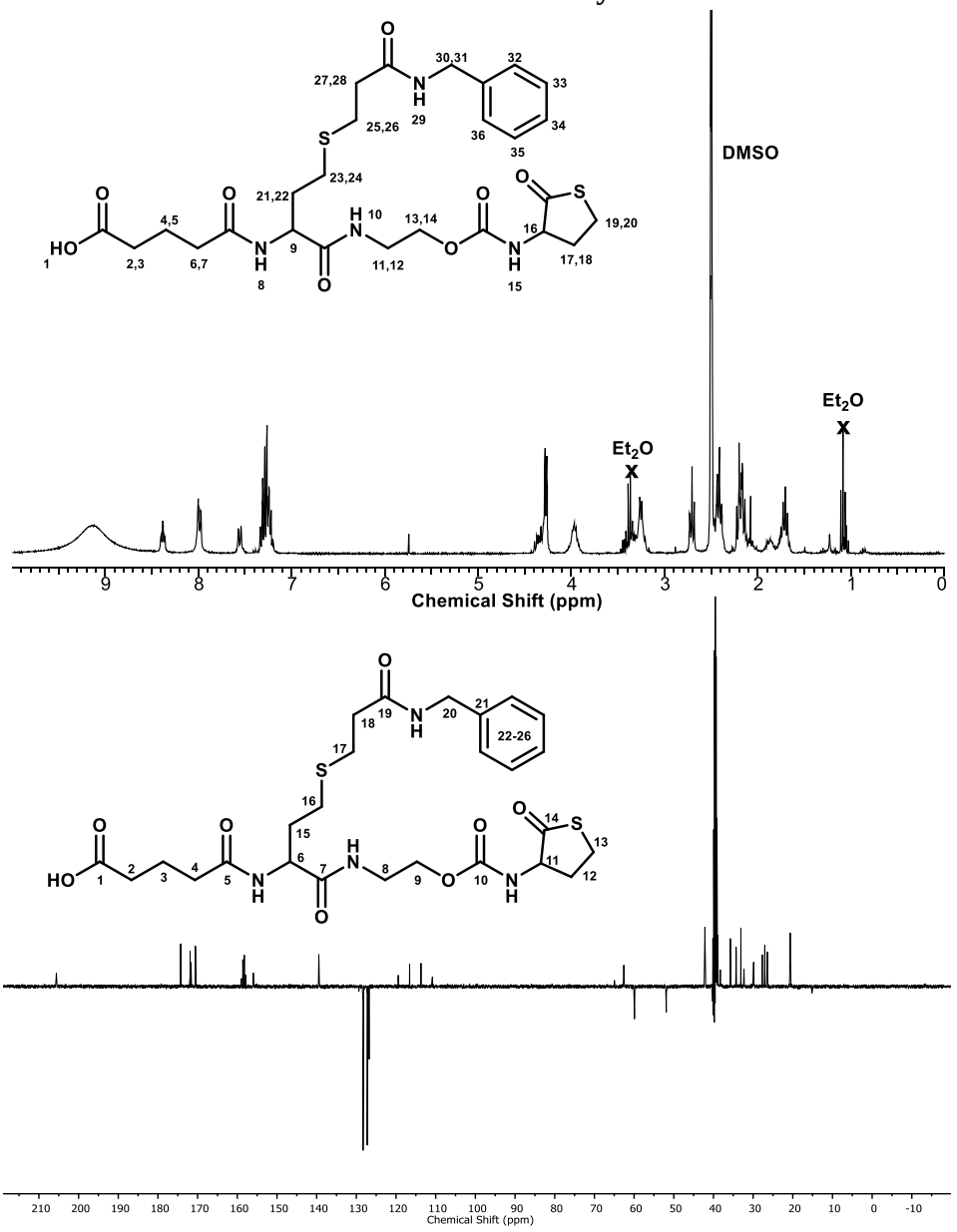


Figure III 14: Top) [1]H NMR spectrum and Bottom) [13]C NMR spectrum of benzyl-functionalised monomer.

^{1}H NMR (300 MHz, DMSO-d_6): δ = 8.38 (t, J = 5.9 Hz, 1H, H_{29}), 7.99 (d, J = 8.0 Hz, $H_{8,10}$), 7.55 (d, J = 8.6 Hz, 1H, H_{15}), 7.39-7.15 (m, 5H, $H_{32\text{-}36}$), 4.46-4.19 (m, 4H, $H_{9,16,30,31}$), 4.10-3.86 (m, 2H, $H_{13,14}$), 3.50-3.14 (m, 4H, $H_{11,12,19,20}$), 2.71 (t, J = 7.3 Hz, 2H, $H_{25,26}$), 2.49-2.31 (m, 5H, $H_{17,23,24,27,28}$), 2.26-2.00 (m, 5H, $H_{2,3,6,7,18}$) 1.97-1.81(m, 1H, H_{21}) 1.79-1.63 (m, 3H, $H_{4,5,22}$). **^{13}C NMR (100 MHz, DMSO-d_6):** δ = 205.61 (C_{14}, C), 174.17 (C_1, C), 171.90 (C_7, C), 171.66 (C_5, C), 170.56 (C_{19}, C), 155.96 (C_{10}, C), 139.44 (C_{21}, C), 128.29, 127.25, 126.76 ($C_{22\text{-}26}$, C_{ar}), 64.96 (C_9, CH_2), 59.90 (C_{11}, CH), 51.87 (C_6, CH), 42.14 (C_{20}, CH_2), 38.26 (C_8, CH_2), 35.73 (C_{12}, CH_2), 34.28, 33.08 ($C_{2,4}$, CH_2), 32.30 (C_{15}, CH_2), 29.87 (C_{18}, CH_2), 27.69 (C_{16}, CH_2), 27.06 (C_{17}, CH_2), 26.42 (C_{13}, CH_2), 20.65 (C_3, CH_2). **HRMS (ESI) *m/z*:** $[M + H]^+$ calculated for $C_{26}H_{37}N_4O_8S_2^+$, 597.1975; found, 597.2058.

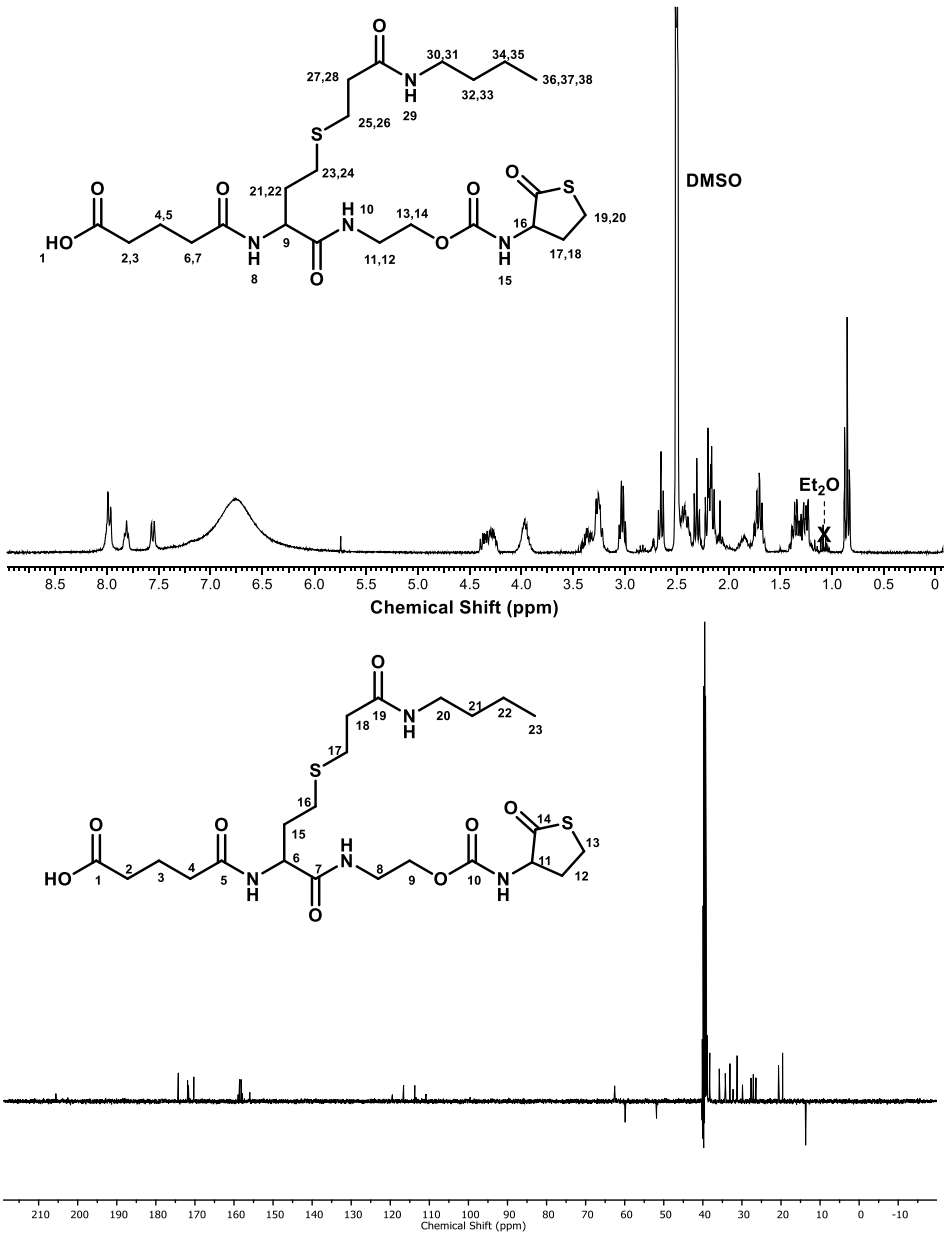


Figure III 15: Top) [1]H NMR spectrum and Bottom) [13]C NMR spectrum of butyl-functionalised monomer.

^{1}H NMR (300 MHz, DMSO-*d*$_6$): δ = 7.98 (d, *J* = 8.0 Hz, 2H, $H_{8,10}$), 7.81 (t, *J* = 5.6 Hz, 1H, H_{29}), 7.56 (d, *J* = 8.7 Hz, 1H, H_{15}), 4.44-4.21 (m, 2H, $H_{9,16}$), 4.06-3.87 (m, 2H, $H_{13,14}$), 3.48-3.16 (m, 4H, $H_{11,12,19,20}$) 3.03 (q, *J* = 6.9, 6.6 Hz, 2H, $H_{30,31}$), 2.65 (t, *J* = 7.3 Hz, 2H, $H_{25,26}$), 2.48-2.36 (m, 3H, $H_{17,23,24}$), 2.31 (t, *J* = 7.4 Hz, 2H, $H_{27,28}$), 2.25-2.06 (m, 5H, $H_{2,3,6,7,18}$), 1.95-1.80 (m, 1H, H_{21}), 1.70 (p, *J* = 7.5, 7.3 Hz, 3H, $H_{4,5,22}$), 1.43-1.20 (m, 4H, H_{32-35}), 0.86 (t, *J* = 7.1 Hz, 3H, H_{36-38}). **^{13}C NMR (100 MHz, DMSO-*d*$_6$):** δ = 205.59 (C_{14}, C), 174.26 (C_1, C), 171.88 (C_7, C), 171.64 (C_5, C), 170.28 (C_{19}, C), 155.94 (C_{10}, C), 62.57 (C_9, CH_2), 59.89 (C_{11}, CH), 51.85 (C_6, CH), 38.22 ($C_{8,20}$, CH_2), 35.80 (C_{12}, CH_2), 34.26, 33.06 ($C_{2,4}$, CH_2), 32.26 (C_{15}, CH_2), 31.23 (C_{21}, CH_2), 29.86 (C_{18}, CH_2), 27.66 (C_{16}, CH_2), 27.08 (C_{17}, CH_2), 26.41 (C_{13}, CH_2), 20.63 (C_3, CH_2), 19.59 (C_{22}, CH_2), 13.96 (C_{23}, CH_3). **HRMS (ESI) *m/z*:** $[M + H]^+$ calculated for $C_{23}H_{39}N_4O_8S_2^+$, 563.2131; found, 563.2220.

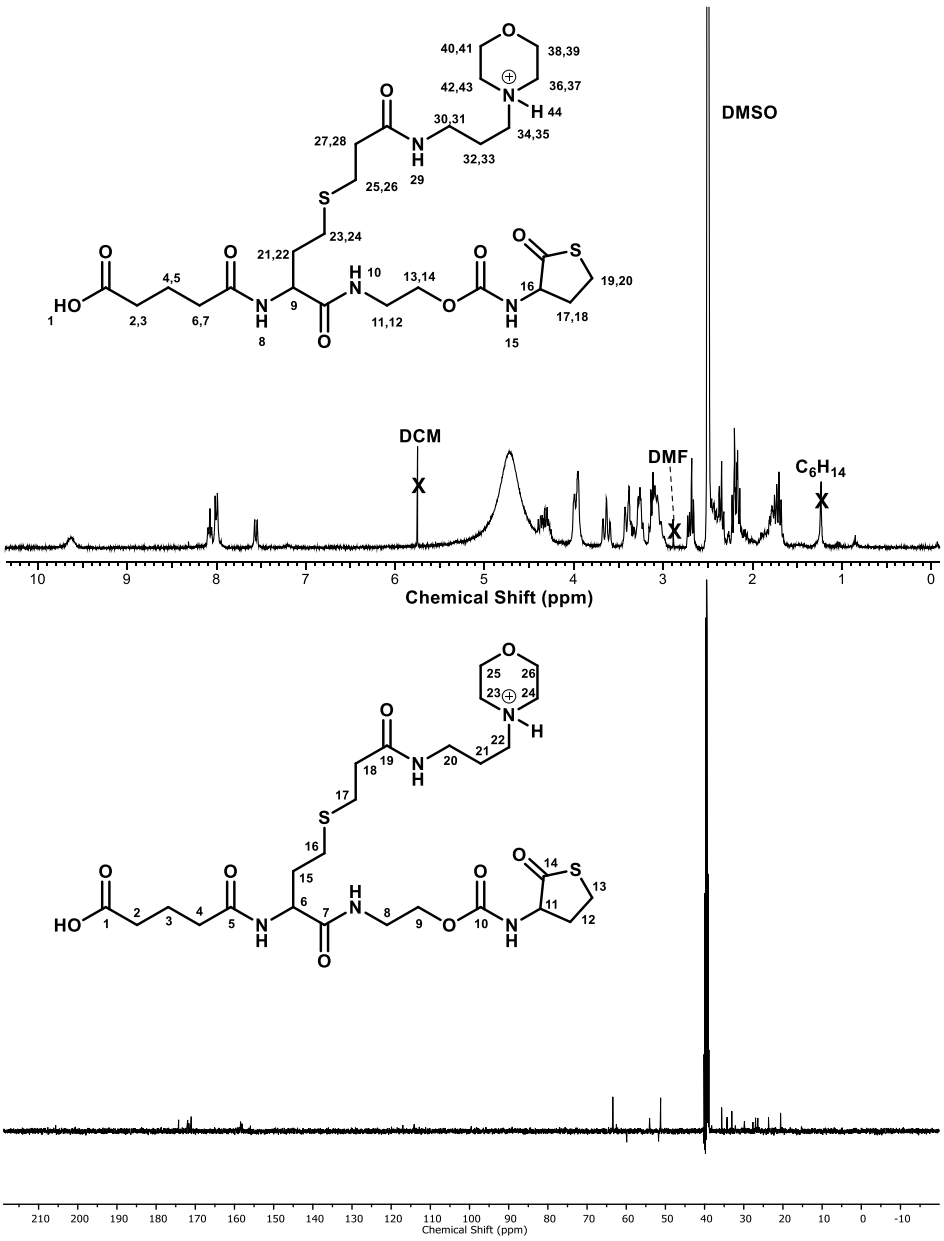


Figure III 16: Top) [1]H NMR spectrum and Bottom) [13]C NMR spectrum of morpholino-functionalised monomer.

^{1}H NMR (300 MHz, DMSO-*d*$_6$): δ = *9.63 (s, 1H, H_{44}), 8.08 (t, *J* = 5.9 Hz, 1H, H_{29}), 8.00 (d, *J* = 7.7 Hz, 2H, $H_{8,10}$), 7.56, (d, *J* = 8.6 Hz, 1H, H_{15}), 4.44-4.18 (m, 2H, $H_{9,16}$), 3.98 (d, *J* = 11.6 Hz, 4H, $H_{13,14,39,40}$), 3.64 (t, *J* = 12.2 Hz, 2H, $H_{38,41}$), 3.48-2.93 (m, 12H, $H_{11,12,19,20,30,31,34,35,36,37,42,43}$), 2.75-2.62 (m, 2H, $H_{25,26}$), 2.47-2.29 (m, 5H, $H_{17,23,24,27,28}$), 2.25-2.03 (m, 5H, $H_{2,3,6,7,18}$), 1.95-1.61 (m, 6H, $H_{4,5,21,22,32,33}$). *The acidic cleavage from the resin, results in protonation of the nitrogen atom here. **^{13}C NMR (100 MHz, DMSO-*d*$_6$):** δ = 205.62 (C_{14}, C), 174.24 (C_1, C), 171.92 (C_7, C), 171.64 (C_5, C), 171.04 (C_{19}, C), 155.92 (C_{10}, C), 63.42 ($C_{25,26}$, CH_2), 62.52 (C_9, CH_2), 59.87 (C_{11}, CH), 54.04 (C_{22}, CH_2), 51.73 (C_6, CH), 51.21 ($C_{23,24}$, CH_2), 138.17 ($C_{8,}$ CH_2), 35.65 (C_{12}, CH_2), 34.25, 33.04 ($C_{2,4}$, CH_2), 32.15 (C_{15}, CH_2), 29.83 (C_{18}, CH_2), 27.66 (C_{16}, CH_2), 26.98 (C_{17}, CH_2), 26.40 (C_{13}, CH_2), 23.68 (C_{21}, CH_2), 20.60 (C_3, CH_2). * Not visible because of DMSO peak ($C_{8,}$ CH_2). **HRMS (ESI) *m/z*:** $[M + H]^+$ calculated for $C_{26}H_{44}N_5O_9S_2^+$, 634.2502; found, 634.2595.

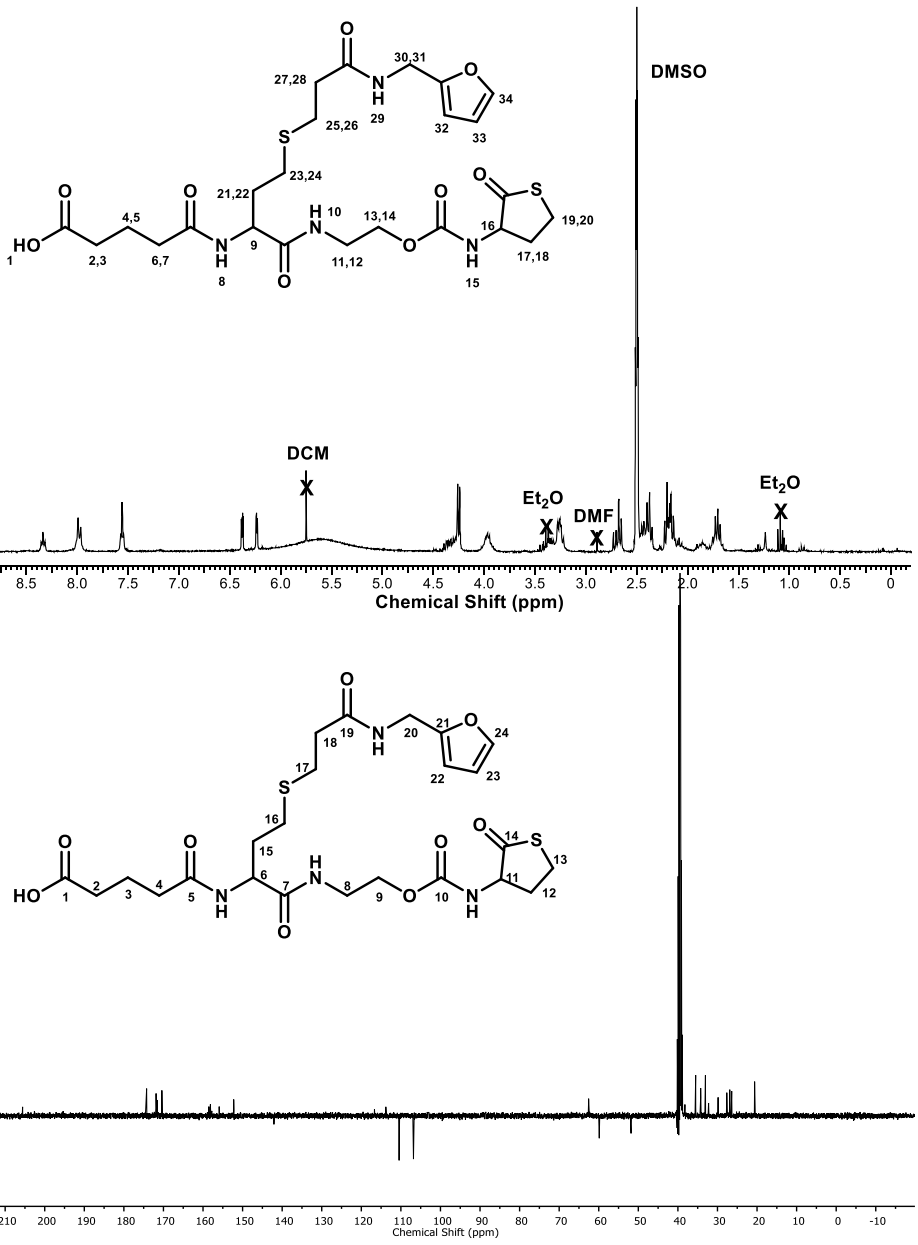


Figure III 17: Top) [1]H NMR spectrum and Bottom) [13]C NMR spectrum of furfuryl-functionalised monomer.

^{1}H NMR (300 MHz, DMSO-*d*$_6$): δ = 8.34 (t, *J* = 5.7 Hz, 1H, H_{29}), 7.98 (d, *J* = 8.0 Hz, 2H, $H_{8,10}$), 7.62-7.51 (m, 2H, $H_{15,34}$), 6.38 (dd, *J* = 3.2, 1.9 Hz, 1H, H_{33}), 6.24 (dd, *J* – 3.2, 0.9 Hz, 1H, H_{32}), 4.44-4.19 (m, 4H, $H_{9,16,30,31}$), 4.07-3.86 (m, 2H, $H_{13,14}$), 3.49-3.16 (m, 4H, $H_{11,12,19,20}$), 2.70 (dd, *J* = Hz, 8.2, 7.3 Hz, 2H, $H_{25,26}$), 2.49-2.31 (m, 5H, $H_{17,23,24,27,28}$), 2.27-1.99 (m, 5H, $H_{2,3,6,7,18}$), 1.95-1.80 (m, 1H, H_{21}), 1.71 (q, *J* = 7.7, 7.4 Hz, 3H, $H_{4,5,22}$). **^{13}C NMR (100 MHz, DMSO-*d*$_6$):** δ = 205.59 (C_{14}, C), 174.24 (C_1, C), 171.85 (C_7, C), 171.61 (C_5, C), 170.38 (C_{19}, C), 152.24 (C_{10}, C),142.08 (C_{24}, CH), 110.45 (C_{23}, CH), 106.81 (C_{22}, CH) 62.55 (C_9, CH_2), 59.87 (C_{11}, CH), 51.83 (C_6, CH), 38.23 (C_8, CH_2), 35.57 (C_{12}, CH_2), 35.50 (C_{20}, CH_2), 34.24, 33.04 ($C_{2,4}$, CH_2), 32.24 (C_{15}, CH_2), 29.84 (C_{18}, CH_2), 27.63 (C_{16}, CH_2), 26.88 (C_{17}, CH_2), 26.39 (C_{13}, CH_2), 20.63 (C_3, CH_2). C_{21}, C is not visible. **HRMS (ESI) *m/z*:** $[M + H]^+$ calculated for $C_{24}H_{35}N_4O_9S_2^+$, 587.1767; found, 587.1852.

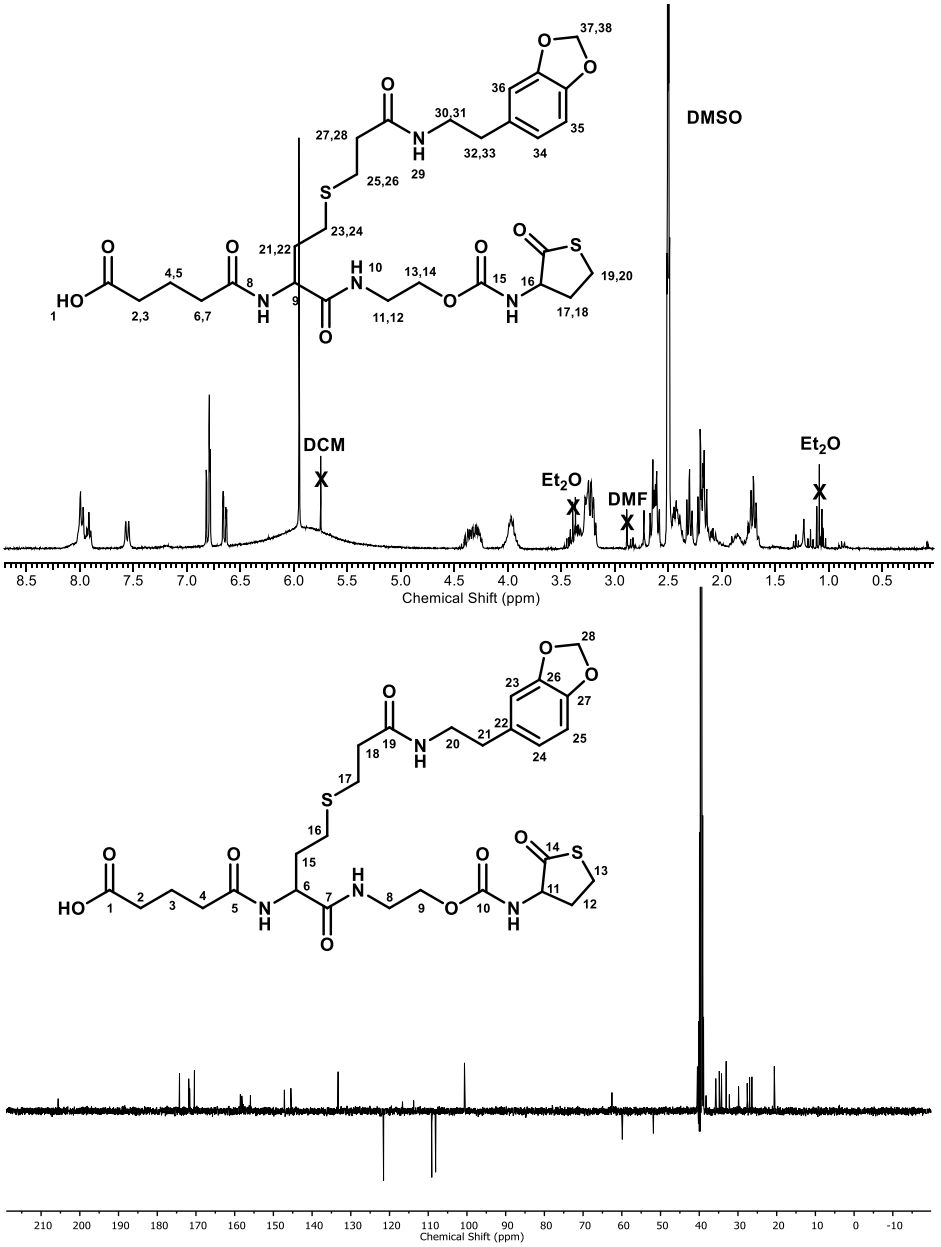


Figure III 18: Top) ^{1}H NMR spectrum and Bottom) ^{13}C NMR spectrum of 3,4-methylenedioxyphenethyl-functionalised monomer.

^{1}H NMR (300 MHz, DMSO-d_6): δ = 7.98 (d, J = 8.2 Hz, 1H, $H_{8,10}$), 7.92 (t, J = 5.6 Hz, 1H, H_{29}), 7.56 (d, J = 8.7 Hz, 1H, H_{15}), 6.85-6.75 (m, 2H, $H_{35,36}$), 6.65 (dd, J = 7.9, 1.7 Hz, 1H, H_{34}), 5.95 (s, 2H, $H_{37,38}$), 4.46-4.22 (m, 2H, $H_{9,16}$), 4.07-3.87 (m, 2H, $H_{13,14}$), 3.45-3.13 (m, 6H, $H_{11,12,19,20,30,31}$), 2.63 (dt, J = 11.2, 7.3 Hz, 4H, $H_{25,26,32,33}$), 2.47-2.35 (m, 3H, $H_{17,23,24}$), 2.30 (t, J = 7.3 Hz, 2H, $H_{27,28}$), 2.26-2.01 (m, 5H, $H_{2,3,6,7,18}$), 1.95-1.79 (m, 1H, H_{21}), 1.80-1.62 (m, 3H, $H_{4,5,22}$). **^{13}C NMR (100 MHz, DMSO-d_6):** δ = 205.59 (C_{14}, C), 174.25 (C_1, C), 171.86 (C_7, C), 171.63 (C_5, C), 170.39 (C_{19}, C), 155.92 (C_{10}, C), 147.16 (C_{26}, C), 145.49 (C_{27}, C), 133.28 (C_{22}, C), 121.54 (C_{24}, CH), 109.08 (C_{25}, CH), 108.09 (C_{23}, CH), 100.64 (C_{28}, CH_2), 62.56 (C_9, CH_2), 59.87 (C_{11}, CH), 51.83 (C_6, CH), 40.46 (C_{20}, CH_2), 38.23 (C_8, CH_2), 35.71 (C_{18}, CH_2), 34.83, (C_{21}, CH_2), 34.25, 33.05 ($C_{2,4}$, CH_2), 32.28 (C_{15}, CH_2),

29.85 (C_{12}, CH_2), 27.62 (C_{16}, CH_2), 27.00 (C_{17}, CH_2), 26.40 (C_{13}, CH_2), 20.61 (C_3, CH_2). **HRMS (ESI) *m/z*:** $[M + H]^+$ calculated for $C_{28}H_{39}N_4O_{10}S_2^+$, 655.2029; found, 655.2096.

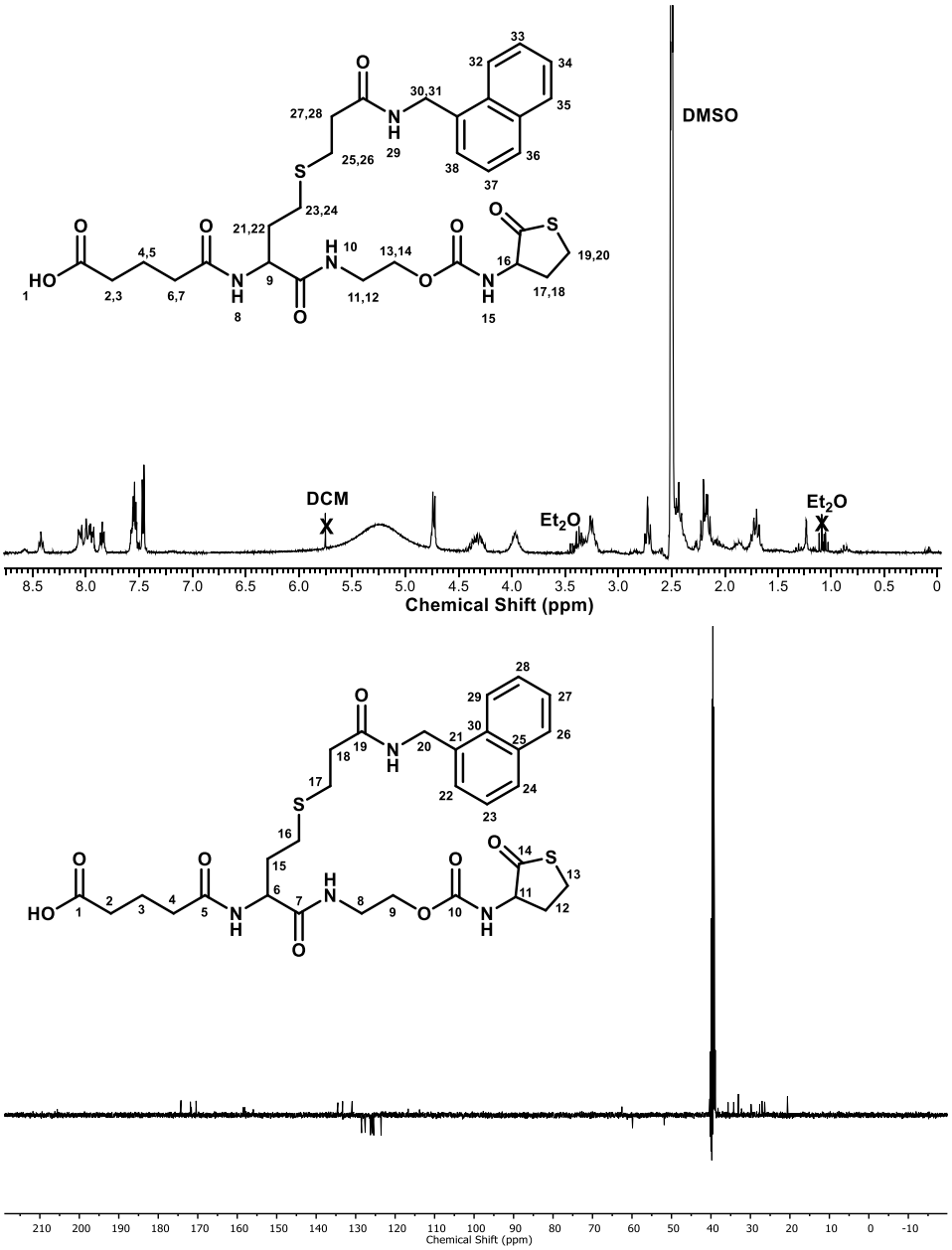


Figure III 19: Top) [1]H NMR spectrum and Bottom) [13]C NMR spectrum of naphthyl-functionalised monomer.

^{1}H NMR (300 MHz, DMSO-d_6): δ = 8.42 (t, *J* = 5.7 Hz, 1H, H_{29}), 8.14-7.91 (m, 4H, $H_{8,10,32,35}$), 7.85 (t, *J* = 4.8 Hz 1H, H_{37}), 7.64-7.49 (m, 3H, $H_{15,33,34}$), 7.47 (d, *J* = 5.5 Hz, 2H, $H_{36,38}$), 4.73 (d, *J* = 5.4 Hz, 2H, $H_{30,31}$), 4.42-4.23 (m, 2H, $H_{9,16}$), 4.05-3.86 (m, 2H, $H_{13,14}$), 3.48-3.17 (m, 4H, $H_{11,12,19,20}$), 2.72 (t, *J* = 7.2 Hz, 2H, $H_{25,26}$), 2.48-2.32 (m, 5H, $H_{17,23,24,27,28}$), 2.26-1.99 (m, 5H, $H_{2,3,6,7,18}$), 1.96-1.79 (m, 1H, H_{21}), 1.79-1.63 (m, 3H, $H_{4,5,22}$). **^{13}C NMR (100 MHz, DMSO-d_6):** δ = 205.58 (C_{14}, C), 174.25 (C_1, C), 171.86 (C_7, C), 171.62 (C_5, C), 170.43 (C_{19}, C), 155.51 (C_{10}, C), 134.50, 133.30 ($C_{25,30}$, C), 130.89 (C_{21}, C), 128.49, 127.58, 126.24, 125.82, 125.54, 125.42, 123.55 ($C_{22\text{-}24,26\text{-}29}$ CH_{ar}), 62.56 (C_9, CH_2), 59.87 (C_{11}, CH), 51.84 (C_6, CH), 40.30 (C_{20}, CH_2), 38.22 (C_8, CH_2),

35.66 (C_{12}, CH_2), 34.24, 33.04 ($C_{2,4}$, CH_2), 32.27 (C_{15}, CH_2), 29.83 (C_{18}, CH_2), 27.65 (C_{16}, CH_2), 27.05 (C_{17}, CH_2), 26.39 (C_{13}, CH_2), 20.61 (C_3, CH_2). **HRMS (ESI) *m/z*:** $[M + H]^+$ calculated for $C_{30}H_{39}N_4O_8S_2^+$, 647.2131; found, 647.2227.

III.5.2 HRMS and NMR data for the oligomers synthesised

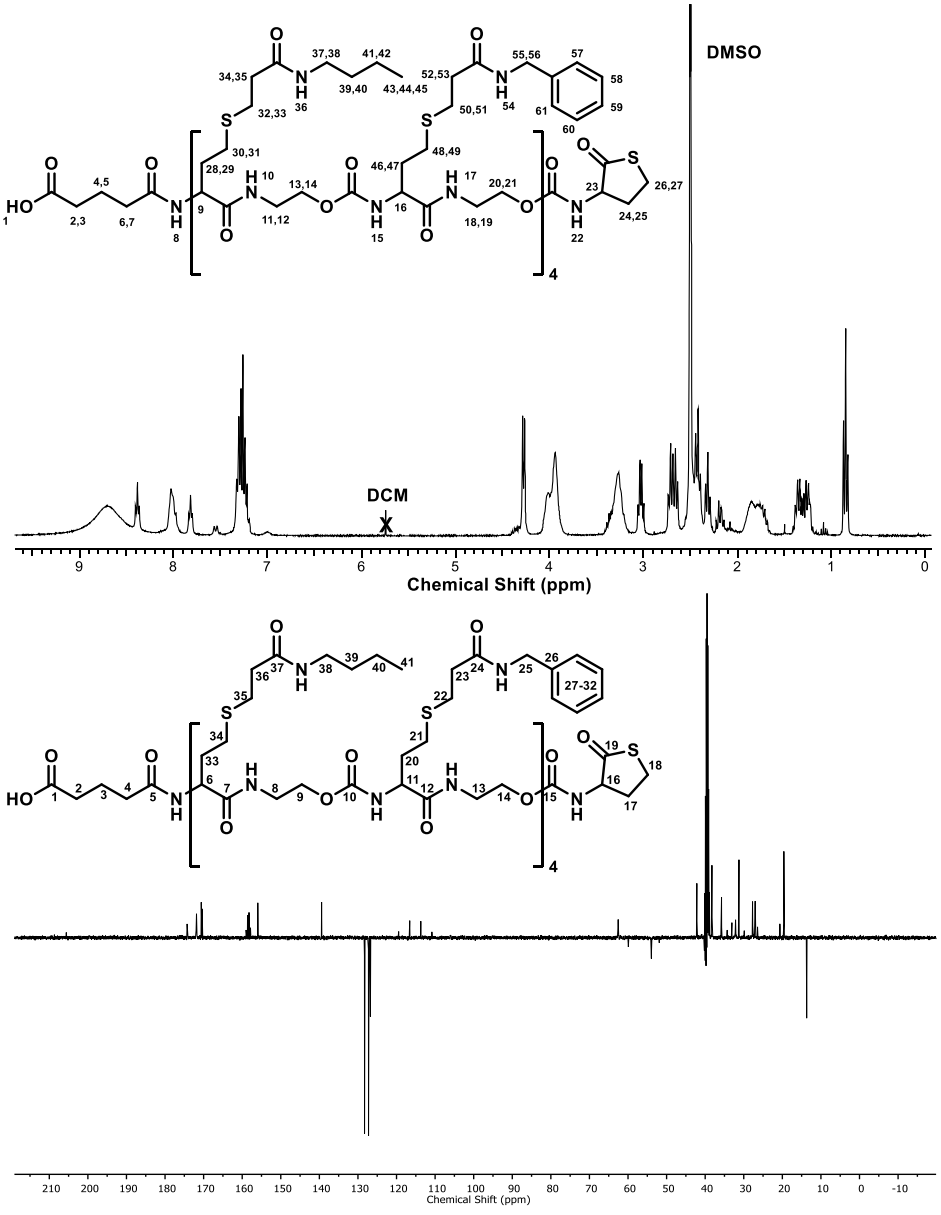


*Figure III 20: Top) [1]H NMR spectrum and Bottom) [13]C NMR spectrum of oligomer **1**.*

[1]H NMR (300 MHz, DMSO-*d*$_6$): δ = 8.38 (t, *J* = 5.9 Hz, 4H, H_{54}), 8.09-7.93 (m, 9H, $H_{8,10,17}$), 7.82 (t, *J* = 5.6 Hz, 4H, H_{36}), 7.55 (d, *J* = 8.6 Hz, 1H, H_{22}), 7.37-7.17 (m, 24H, $H_{15,57-61}$), 4.35-4.22 (m, 9H, $H_{23,55,56}$), 4.10-3.84 (m, 24H, $H_{9,13,14,16,20,21}$), 3.43-3.17 (m, 18H, $H_{11,12,18,19,26,27}$), 3.03 (q, *J* = 6.5, 6.4 Hz, 8H, $H_{37,38}$), 2.68 (dt, *J* = 15.5, 7.2 Hz, 16H, $H_{32,33,50,51}$), 2.48-2.36 (m, 25H, H $_{24,30,31,48,49,52,53}$), 2.31 (t, *J* = 7.3 Hz, 8H, $H_{34,35}$), 2.23-2.06 (m, 5H, $H_{2,3,6,7,25}$), 1.95-1.63 (m, 18H, $H_{4,5,28,29,46,47}$), 1.41-1.19 (m, 16H, H_{39-42}), 0.85 (t, *J* = 7.0 Hz, 12H, H_{43-45}). **[13]C NMR**

(100 MHz, DMSO-d_6): $\delta =$ 205.60 (C_{19}, C), 174.28 (C_1, C), 171.85 (C_5, C), 170.62, 170.38, 170.33 ($C_{7,12,24,37}$, C), 155.96 ($C_{10,15}$, C), 139.42 (C_{26}, C), 128.29, 127.25, 126.77 ($C_{27\text{-}32}$, CH_{ar}), 62.54 ($C_{14,9}$, CH_2), 59.91 (C_{16}, CH), 53.95 ($C_{6,11}$, CH), 42.16 (C_{25}, CH_2), 38.25 ($C_{8,13,38}$, CH_2), 35.84 (C_{17}, CH_2), 34.29, 33.07 ($C_{2,4}$, CH_2), 32.13 ($C_{20,33}$, CH_2), 31.24 (C_{39}, CH_2), 29.87 ($C_{23,36}$, CH_2), 27.72 ($C_{21,34}$, CH_2), 27.07 ($C_{22,35}$, CH_2), 26.43 (C_{18}, CH_2), 20.65 (C_3, CH_2), 19.65 (C_{40}, CH_2), 13.69 (C_{41}, CH_3).

HRMS (ESI) *m/z*:

	Ion	Structure	Mass calculated	Mass found
Monomer	$[M + H]^+$	$C_{23}H_{39}N_4O_8S_2^+$	563.2131	563.2220
Dimer	$[M + H]^+$	$C_{40}H_{62}N_7O_{12}S_3^+$	928.3540	928.3650
Trimer	$[M + H]^+$	$C_{54}H_{87}N_{10}O_{16}S_4^+$	1259.5106	1259.5231
Tetramer	$[M + H]^+$	$C_{71}H_{110}N_{13}O_{20}S_5^+$	1624.6515	1624.6609
Pentamer	$[M + H]^+$	$C_{85}H_{135}N_{16}O_{24}S_6^+$	1955.8081	1955.8204
Hexamer	$[\frac{M+2H}{2}]^{2+}$	$C_{102}H_{159}N_{19}O_{28}S_8^{2+}$	1160.6475	1160.9838
Octamer	$[\frac{M+2H}{2}]^{2+}$	$C_{133}H_{207}N_{25}O_{36}S_9^{2+}$	1509.1233	1509.1289

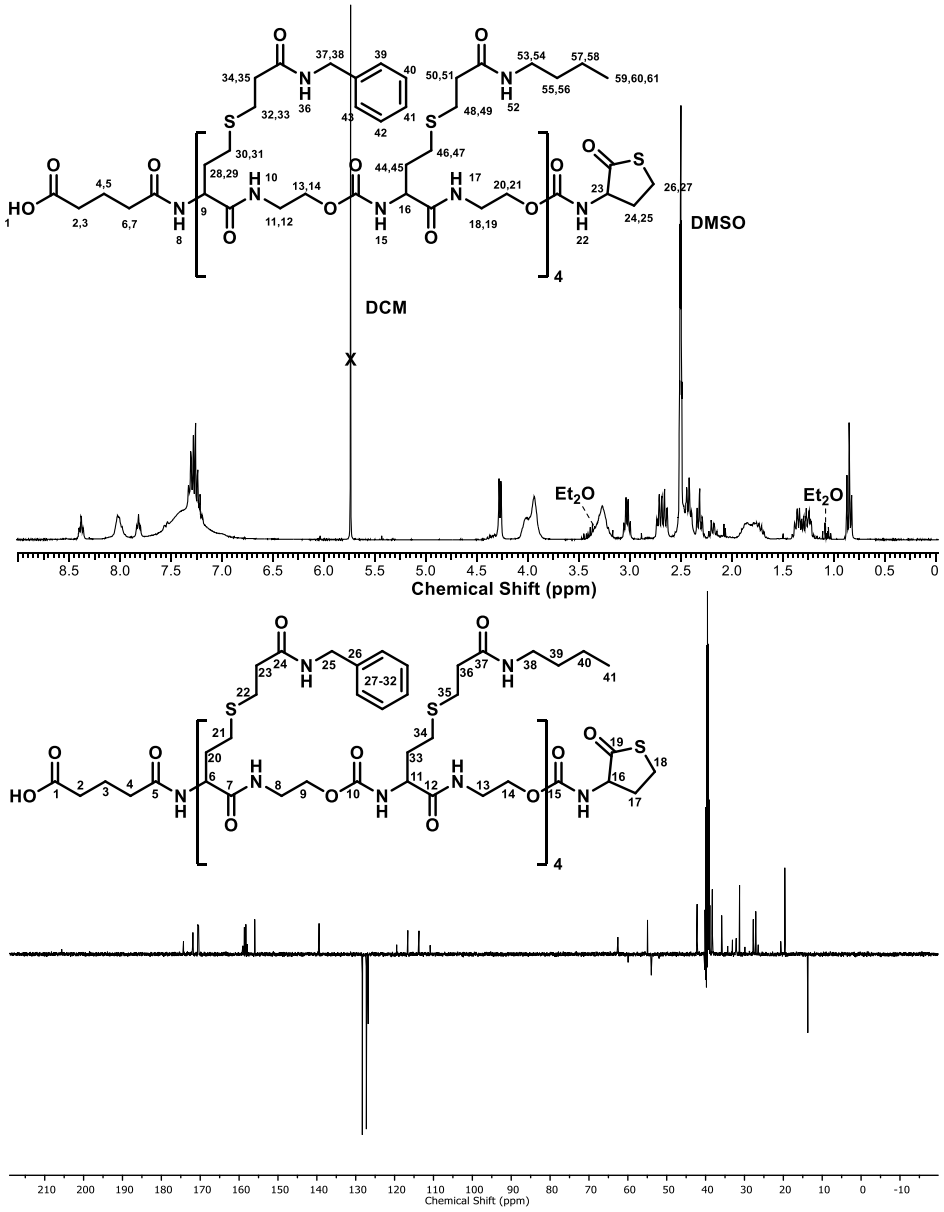


*Figure III 21: Top) [1]H NMR spectrum and Bottom) [13]C NMR spectrum of oligomer **2**.*

^{1}H NMR (300 MHz, DMSO-*d*$_6$): δ = 8.38 (t, *J* = 5.9 Hz, 4H, H_{36}), 8.09-7.91 (m, 9H, $H_{8,10,17}$), 7.82 (t, *J* = 5.6 Hz, 4H, H_{52}), 7.58-7.49 (m, 1H, H_{22}), 7.35-7.18 (m, 24H, $H_{15,39-43}$), 4.37-4.22 (m, 9H, $H_{23,37,38}$), 4.13-3.80 (m, 24H, $H_{9,13,14,16,20,21}$), 3.40-3.13 (m, 18H, $H_{11,12,18,19,26,27}$), 3.03 (q, *J* = 6.5, 6.4 Hz, 8H, $H_{53,54}$), 2.68 (dt, *J* = 15.3, 7.1 Hz, 16H, $H_{32,33,48,49}$), 2.49-2.36 (m, 25H, H $_{24,30,31,34,35,46,47}$), 2.31 (t, *J* = 7.3 Hz, 8H, $H_{50,51}$), 2.24-2.10 (m, 5H, $H_{2,3,6,7,25}$), 1.97-1.63 (m, 18H, $H_{4,5,28,29,44,45}$), 1.43-1.20 (m, 16H, H_{53-58}), 0.85 (t, *J* = 7.2, 6.9 Hz, 12H, H_{59-61}). **^{13}C NMR (100 MHz, DMSO-*d*$_6$):** δ = 205.63 (C_{19}, C), 174.31 (C_1, C), 172.00 (C_5, C), 170.65, 170.61, 170.342 ($C_{7,12,24,37}$, C), 155.98 ($C_{10,15}$, C), 139.43 (C_{26}, C), 128.31, 127.27, 126.79 (C_{27-32}, CH_{ar}), 62.57 ($C_{14,9}$, CH_2), 59.93 (C_{16}, CH), 53.96 ($C_{6,11}$, CH), 42.18 (C_{25}, CH_2), 38.27 ($C_{8,13,38}$, CH_2), 35.86 (C_{17}, CH_2), 34.31, 33.09 ($C_{2,4}$, CH_2), 32.13 ($C_{20,33}$, CH_2), 31.26 (C_{39}, CH_2), 29.89 ($C_{23,36}$, CH_2), 27.73 ($C_{21,34}$, CH_2), 27.09 ($C_{22,35}$, CH_2), 26.46 (C_{18}, CH_2), 20.67 (C_3, CH_2), 19.62 (C_{40}, CH_2), 13.70 (C_{41}, CH_3).

HRMS (ESI) *m/z*:

	Ion	Structure	Mass calculated	Mass found
Monomer	$[M + H]^+$	$C_{26}H_{37}N_4O_8S_2^+$	597.1975	597.2058
Dimer	$[M + H]^+$	$C_{40}H_{62}N_7O_{12}S_3^+$	928.3540	928.3647
Trimer	$[M + H]^+$	$C_{57}H_{85}N_{10}O_{16}S_4^+$	1293.4950	1293.5077
Tetramer	$[M + H]^+$	$C_{71}H_{110}N_{13}O_{20}S_5^+$	1624.6515	1624.6573
Pentamer	$[M + H]^+$	$C_{88}H_{133}N_{16}O_{24}S_6^+$	1989.7925	1989.8078
Hexamer	$[\frac{M+2H}{2}]^{2+}$	$C_{102}H_{159}N_{19}O_{28}S_8^{2+}$	1160.6475	1160.9827
Octamer	$[\frac{M+2H}{2}]^{2+}$	$C_{133}H_{207}N_{25}O_{36}S_9^{2+}$	1509.1233	1509.1283

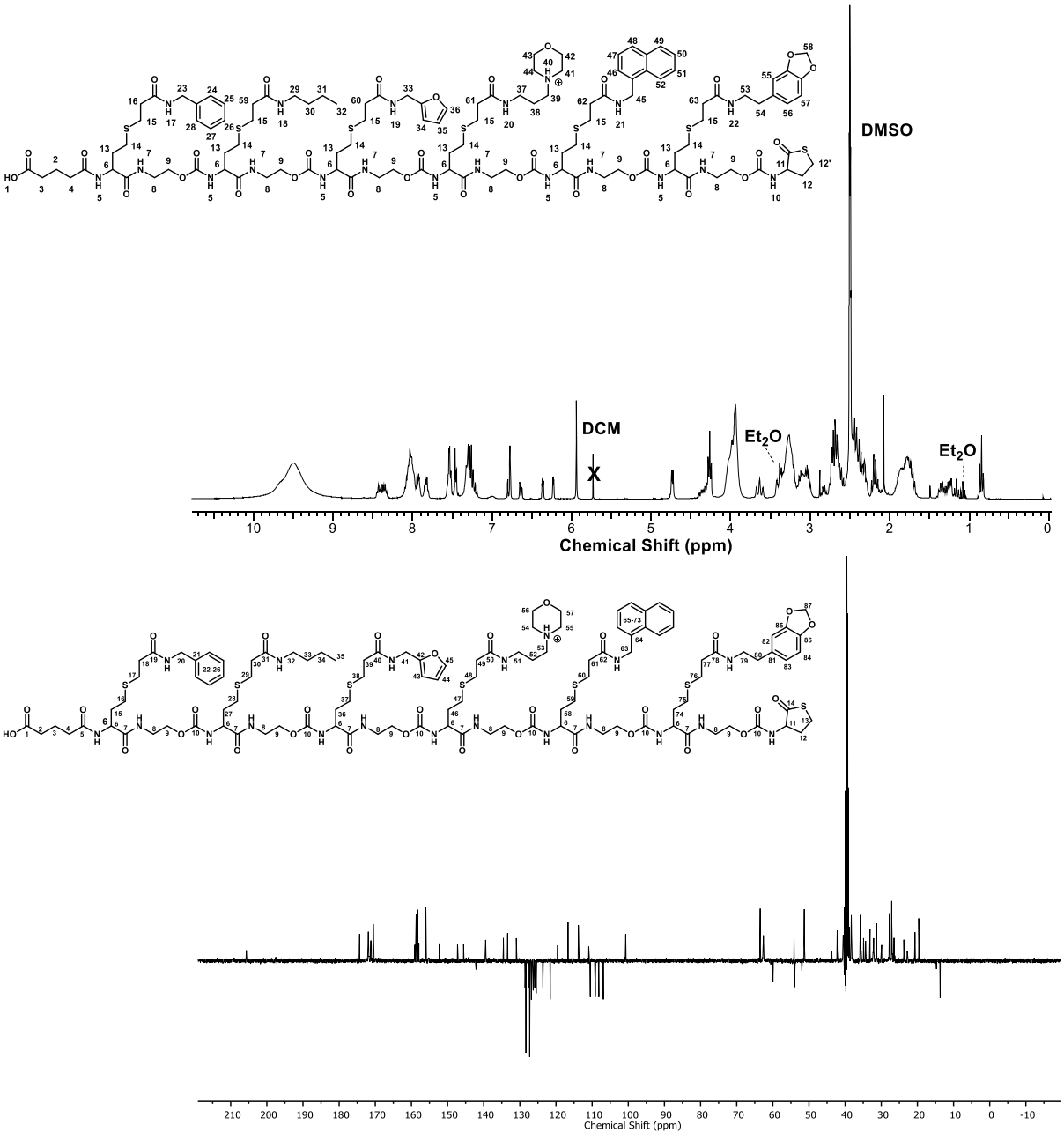


*Figure III 22: Top) ^{1}H NMR spectrum and Bottom) ^{13}C NMR spectrum of oligomer **3**.*

^{1}H NMR (300 MHz, DMSO-d_6): δ = 8.49-8.29 (m, 3H, $H_{17,19,21}$), 8.15-7.76 (m, 15H, $H_{5,7,47,49,52}$), 7.61-7.36 (m, 6H, $H_{10,36,46,48,50,51}$), 7.38-7.17 (m, 8H, $H_{18,20,22,24-28,}$), 6.87-6.72 (m, 2H, $H_{55,57}$), 6.64 (dd, *J* = 7.9, 1.7 Hz, 1H, H_{56}), 6.37 (dd, *J* = 3.2, 1.8 Hz, 1H, H_{35}), 6.23 (d, *J* = 3.1 Hz, 1H, H_{34}), 5.94 (s, 1H, H_{58}), 4.73 (d, *J* = 5.5 Hz, 2H H_{45}), 4.38-4.19 (m, 5H, $H_{11,23,33}$), 4.10-3.82 (m, 20H, $H_{6,9,42,43}$), 3.64 (t, *J* = 11.8 Hz, 2H, $H_{42',43'}$), 3.45-2.95 (m, 26H, $H_{8,16,29,37,39,41,44,54,}$), 2.78-2.58 (m, 14H, $H_{15,53}$), 2.48-2.27 (m, 22H, $H_{14,59-63}$), 2.25-2.10 (m, 5H, $H_{3,4,12}$), 1.9-1.63 (m, 15H, $H_{12',13,38}$), 1.42-1.14 (m, 6H, $H_{30,31,2}$), 0.85 (t, *J* = 7.1 Hz, H_{32}). **^{13}C NMR (100 MHz, DMSO-d_6):** δ = 205.66 (C_{14}, C), 174.33 (C_1, C), 172.02 (C_5, C), 171.92, 171.81, 171.22, 170.63, 170.59, 170.56, 170.44 ($C_{7,19,31,40,50,62,78}$, C), 156.01 (C_{10}, C), 152.30 (C_{42}, C), 147.24 (C_{85}, C), 145.57 (C_{86}, C), 142.12 (C_{45}, CH), 139.47 (C_{21}, C), 134.55, 133.38 (C_{65-74}, C) 133.34 (C_{81}, C), 130.97 (C_{64}, C), 128.32, 127.29, 126.80 (C_{22-26}, CH_{ar}), 128.56, 127.66, 126.30, 125.88, 125.63, 125.47, 123.61 (C_{65-73}, CH_{ar}), 121.60 (C_{83}, CH), 110.50 (C_{44}, CH), 109.14 (C_{82}, CH), 108.14 (C_{84}, CH), 106.89 (C_{43}, CH), 100.71 (C_{87}, CH_2), 63.49 ($C_{56,57}$, CH_2), 62.59 (C_9, CH_2), 59.96 (C_{11}, CH), 54.14 (C_{53}, CH_2), 53.96 (C_6, CH), 51.30 ($C_{54,55}$, CH_2), 43.67 (C_{20}, CH_2), 38.29 ($C_{8,32}$, CH_2), 35.88, 35.77 ($C_{41,80}$, CH_2), 34.90 (C_{12}, CH_2), 34.34, 33.11 ($C_{2,4}$, CH_2), 32.13 ($C_{15,27,36,46,58,74}$, CH_2), 31.27 ($C_{33,63}$, CH_2), 29.91 ($C_{18,30,39,49,61,77}$, CH_2), 27.75 ($C_{16,28,37,47,59,75}$, CH_2), 27.11 ($C_{17,29,38,48,60,76}$, CH_2), 26.47 (C_{13}, CH_2), 23.76 (C_{52}, CH_2), 20.69 (C_3, CH_2), 19.64 (C_{34}, CH_2), 13.71 (C_{35}, CH_3). * Not visible because of DMSO peak ($C_{15,27,36,46,58,74,79,}$ CH_2).

HRMS (ESI) *m/z*:

	Ion	Structure	Mass calculated	Mass found
Monomer	$[M + H]^+$	$C_{26}H_{37}N_4O_8S_2^+$	597.1975	597.2088
Dimer	$[M + H]^+$	$C_{40}H_{62}N_7O_{12}S_3^+$	928.3540	928.3631
Trimer	$[M + H]^+$	$C_{55}H_{83}N_{10}O_{17}S_4^+$	1283.4742	1283.4842
Tetramer	$[M + H]^+$	$C_{72}H_{113}N_{14}O_{22}S_5^+$	1685.6679	1685.6820
Pentamer	$[M + H]^+$	$C_{83}H_{138}N_{17}O_{26}S_6^+$	2100.8245	2100.8299
Hexamer	$[M + H]^+$	$C_{112}H_{163}N_{20}O_{32}S_7^+$	2523.97090	2523.8999

III.6 References

1 M. A. R. Meier and C. Barner-Kowollik, *Adv. Mater.*, 2019, **31**, 1806027.

2 S. Martens, J. O. Holloway and F. E. Du Prez, *Macromol. Rapid Commun.*, 2017, **38**, 1700469.

3 S. Martens, J. O. Holloway and F. E. Du Prez, in *Sequence-Controlled Polymers*, ed. J.-F. Lutz, Wiley VCH, Weinheim, 2018, pp. 379–416.

4 S. C. Solleder, R. V. Schneider, K. S. Wetzel, A. C. Boukis and M. A. R. Meier, *Macromol. Rapid Commun.*, 2017, **38**, 1600711.

5 J. A. De Neve, J. J. Haven, L. Maes and T. Junkers, *Polym. Chem.*, 2018, **9**, 4692–4705.

6 P. Espeel, L. L. G. Carrette, K. Bury, S. Capenberghs, J. C. Martins, F. E. Du Prez and A. Madder, *Angew. Chemie - Int. Ed.*, 2013, **52**, 13261–13264.

7 S. Martens, J. Van Den Begin, A. Madder, F. E. Du Prez and P. Espeel, *J. Am. Chem. Soc.*, 2016, **138**, 14182–14185.

8 S. C. Solleder, S. Martens, P. Espeel, F. E. Du Prez and M. A. R. Meier, *Chem. - A Eur. J.*, 2017, **23**, 13906–13909.

9 J. O. Holloway, C. Mertens, F. E. Du Prez and N. Badi, *Macromol. Rapid Commun.*, 2019, **40**, 1800685.

10 J. O. Holloway, S. Aksakal, F. E. Du Prez and C. Remzi Becer, *Macromol. Rapid Commun.*, 2017, **38**, 1700500.

11 J. O. Holloway, K. S. Wetzel, S. Martens, F. E. Du Prez and M. A. R. Meier, *Polym. Chem.*, 2019, **10**, 3859–3867.

12 S. Martens, A. Landuyt, P. Espeel, B. Devreese, P. Dawyndt and F. E. Du Prez, *Nat. Commun.*, 2018, **9**, 4451.

13 G. Cavallo, S. Poyer, J.-A. Amalian, F. Dufour, A. Burel, C. Carapito, L. Charles and J.-F. Lutz, *Angew. Chemie Int. Ed.*, 2018, **130**, 6374–6377.

14 J. A. Amalian, T. T. Trinh, J.-F. Lutz and L. Charles, *Anal. Chem.*, 2016, **88**, 3715–3722.

15 T. T. Trinh, L. Oswald, D. Chan-Seng and J.-F. Lutz, *Macromol. Rapid Commun.*, 2014, **35**, 141–145.

16 J.-F. Lutz, *Macromolecules*, 2015, **48**, 4759–4767.

17 A. Al Ouahabi, M. Kotera, L. Charles and J.-F. Lutz, *ACS Macro Lett.*, 2015, **4**, 1077–1080.

18 C. Laure, D. Karamessini, O. Milenkovic, L. Charles and J.-F. Lutz, *Angew. Chemie - Int. Ed.*, 2016, **55**, 10722–10725.

19 D. Karamessini, B. E. Petit, M. Bouquey, L. Charles and J.-F. Lutz, *Adv. Funct. Mater.*, 2017, **27**, 1604595.

20 R. K. Roy, A. Meszynska, C. Laure, L. Charles, C. Verchin and J.-F. Lutz, *Nat. Commun.*, 2015, **6**, 7237–7239.

21 R. K. Roy, C. Laure, D. Fischer-Krauser, L. Charles and J.-F. Lutz, *Chem. Commun.*, 2015, **51**, 15677–15680.

22 G. Cavallo, A. Al Ouahabi, L. Oswald, L. Charles and J.-F. Lutz, *J. Am. Chem. Soc.*, 2016, **138**, 9417–9420.

23 C. S. Marvel, S. L. Jacobs, W. K. Taft and B. G. Labbe, *J. Polym. Sci.*, 1956, **19**, 59–72.

24 S. Aksakal and C. R. Becer, *Polym. Chem.*, 2016, **7**, 7011–7018.

25 S. Aksakal, R. Aksakal and C. R. Becer, *Polym. Chem.*, 2018, **9**, 4507–4516.

26 M. Le Neindre, B. B. Magny and R. Nicolaÿ, *Polym. Chem.*, 2013, **4**, 5577–5584.

27 N. Stuhr-Hansen, N. Bork and K. Strømgaard, *Org. Biomol. Chem.*, 2014, **12**, 5745.

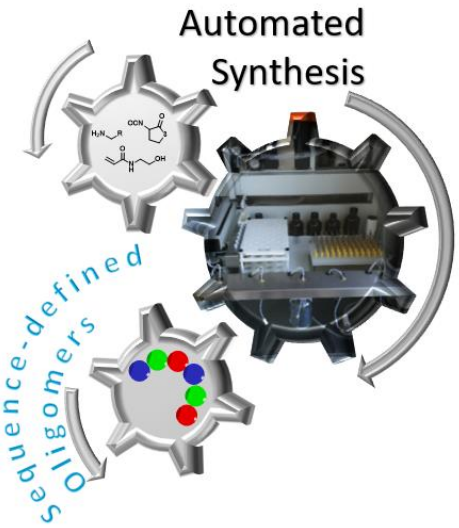
28 P. Espeel and F. E. Du Prez, *Eur. Polym. J.*, 2015, **62**, 247–272.

29 R. B. Merrifield, *J. Am. Chem. Soc.*, 1963, **85**, 2149–2154.

30 G.-Z. Li, R. Randev, A. H. Soeriyadi, G. J. Rees, C. Boyer, Z. Tong, C. R. Becer and D. M. Haddleton, *Polym. Chem.*, 2010, **1**, 1196–1204.

31 Swelling Volumes of Polystyrene Resins, http://www.rapp-polymere.com/index.php?id=1218, (accessed 1 April 2017).

32 P. Espeel, F. Goethals, F. Driessen, L.-T. T. Nguyen and F. E. Du Prez, *Polym. Chem.*, 2013, **4**, 2373–2616.



This chapter is adapted with permission from:

J. O. Holloway, C. Mertens, F. E. Du Prez and N. Badi, *Macromol. Rapid. Comm.*, 2019, **40**, 1800685.

Abstract

Thiolactone chemistry was used, in combination with solid-phase synthesis to develop a two-step iterative protocol, where sequence-functionalisation was achieved using commercially available, primary amines. This method was first optimised manually before being transferred to an automated synthesiser, resulting in monodisperse, sequence-defined oligomers of up to the length of nonamers. Both reaction time and purity were compared with the manual synthesis and also a wider range of acid-labile resin types were tested to demonstrate the versatility of this approach.

Chapter IV
Automated synthesis protocol of sequence-defined oligo-urethane-amides using thiolactone chemistry

IV.1 Introduction

The wide range of applications that are now being targeted by sequence-defined research, such as information storage,[1–3] biological mimicking[4] and anticounterfeiting technologies,[5,6] mean that many synthesis routes containing a strategic combination of highly efficient and orthogonal reactions towards sequence-defined macromolecules have been proposed,[7–15] including the use of thiolactone chemistry.[16–20] For example, growing interest in the area of the chemical encoding of data has led to the development of sequence-defined macromolecules with the ability to contain varying functional side groups in order to increase the amount of encrypted information.[3,7,21–25] More importantly, such data-management problems require large libraries of sequence-defined macromolecules, thus highlighting the need for automated synthesis.[20]

As with the study presented in Chapter III, the synthesis described in this chapter was carried out using a Merrifield-inspired, thiolactone-based, solid-phase approach.[26] Solid-phase chemistry was chosen because it allowed the use of a high excess of reagents (thus high concentration to improve kinetics and chance of 100 % conversion) and easy purification after each step. It also offered the potential to automate the approach. Automation was of interest because it was not only time and labour-saving but also opened the possibility to synthesise vast libraries of sequences. This is something that has already been investigated by our group for the use of sequence-defined oligomers to store data in the form of a QR-code.[20] Whilst the work described in Chapter III was the successful result of a collaboration with Becer and co-workers and yielded diverse, multifunctional oligomers, the resulting protocol was a four-step cycle, whereby sequence-definition was achieved by the catalysed modification of thioacrylates with primary amines.[19] However, the aminolysis and thiol-ene reactions could not be carried out in one-pot because the thioacrylate reacted directly with the amine. Thus, the complexity of this protocol hampered automation and therefore, resulted in a time-consuming process.

Thiolactone chemistry has already been well reported as a highly useful tool for polymer functionalisation and post-modification.[27–33] It circumvents many of the problems that arise from directly using thiols such as poor commercial availability, short shelf-life and unpleasant smell.[31,34] As

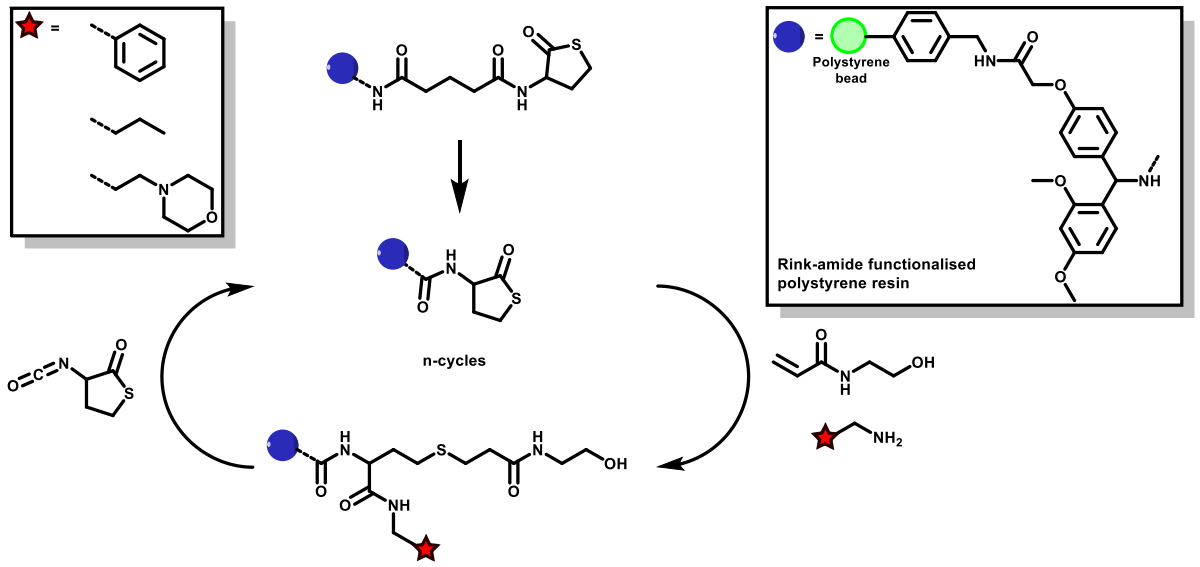
discussed in detail in Chapter II.5.5, thiolactones can undergo a double modification by aminolysis and subsequent Michael-thiol-ene conjugations[29,31,35,36] in an efficient "click-like" fashion.[14,37,38] This has led to it becoming used, notably by our group, to synthesise multifunctional, sequence-defined oligomers.[16–20,39] Initial research from our group, reported the synthesis of short oligomers (tetramers) of moderate purity,[17] whereby sequence definition was introduced *via* thiolactone aminolysis, followed by a nucleophilic thiol-ene reaction with a thiolactone acrylamide.[17] The moderate purity was attributed to disulfide bond formation and the subsequent reduction of this bond using dimethylphenylphosphine.[17,40] Alternatively, a thiolactone-based, two-step protocol using (mostly) acrylates as a functional handle instead of amines, was later introduced and more importantly, was eventually automated.[16] However, the crude purity of the resulting sequence-defined decamer was less than that of the oligomers synthesised manually and further purification was not explored. Moreover, this work was limited exclusively to the use of a 2-chlorotrityl chloride resin, because of the necessary mild cleavage conditions (1 % TFA solution) required for the ester-bond containing structures. Nonetheless, interest in the incorporation of primary amines as the functional handles, within a thiolactone-derived sequence remained. This was partly because of the comparatively wide ranging commercially availability of these compounds and the possibility to reduce the length of the side-chains, thus limiting their flexibility which could be potentially important for applications such as cell interaction, where optimal binding is achieved through the precise spacing of interacting units.[41]

Therefore, the work reported within this chapter represents a much simpler, two-step strategy, compared to the protocol outlined in Chapter III. Primary amines were used to directly open the thiolactone moieties and *N*-hydroxyethyl acrylamide as an alcohol containing Michael-acceptor. Thiolactone was again reintroduced using α-thiolactone-γ-isocyanate, which could be made *via* a scalable synthesis route (ca. 150 g).[27] This was in contrast to the previously mentioned approach that used varying acrylates as Michael acceptor and functional handle and an alcohol functionalised amine (ethanolamine) to both ring-open the thiolactone and provide a functional site for the isocyanate addition.[16] This new, simplified procedure enabled automation, which not only improved purity and saved time, but also provided the scope for enhanced throughput and up-scaling because of the possibility for the robot to handle up to 72 reactions in parallel. Moreover, automation in general has already been shown to be a highly effective, scalable, labour-saving technique for iterative, solid-phase methods.[8,16,42–45] The work presented here can also be seen as an alternative to existing thiolactone-based routes since it explores not only a different route to sequence-functionalisation (*i.e. via* primary amines instead of acrylates) but also the use of a variety of resins with different cleavage conditions, loadings and purification techniques (*via* preparative HPLC).

IV.2 Results and discussion

IV.2.1 The protocol

The protocol developed here (*Scheme IV 1*), was first developed manually using a laboratory shaker. Short oligomers (trimers) were synthesised, so that the experimental conditions could be checked and optimised (equivalents, kinetics etc.) before the protocol was taken to an automated peptide synthesiser, where trimers were again synthesised for optimisation before longer oligomers were considered.



Scheme IV 1: Two-step, iterative, solid-phase, sequence-defined oligomer synthetic protocol.

The protocol starts with the immobilisation of thiolactone on a solid-support by coupling thiolactone carboxylic acid (see Chapter III.1) onto the resin (rink-amide resin was mainly used). The thiolactone ring could then be opened with a primary amine. *N*-hydroxyethyl acrylamide was added simultaneously, allowing the newly released thiol to undergo a thiol-ene conjugation. The pendant hydroxy-group of the acrylamide facilitated the reinstallation of a new thiolactone unit for the following cycle of the sequence *via* reaction with α-thiolactone-γ-isocyanate. The general synthesis procedure of the protocol both manually and automated is described in sections IV.4.5 and IV.4.6 respectively.

IV.2.2 Manual solid-phase synthesis

During initial experiments, the aminolysis step was left overnight to check if the reaction was at all successful before the step was better refined by investigating the reaction kinetics. An ABC-type functional trimer (where A, B, and C represent three different functional side chains) was synthesised

(see section IV.1) and conversion was followed by liquid chromatography mass spectrometry (LCMS) (*Figure IV 1a* and *b*). LCMS is an effective technique for analysing the conversion and purity of the obtained sequences.[16,19] At a wavelength of 214 nm, one can quantitatively see the disappearance of the starting material, the formation of product and eventually, appearance of side-products.

The reaction kinetics of the aminolysis step were also followed by LCMS (*Figure IV 1c*). Every 2 hours, a 2 mg sample of resin was removed from the reaction, washed as described in the experimental section and prepared for LCMS analysis. Benzylamine was used as it is known that the kinetics of thiolactone ring-opening depends on the chosen amine, as this is the rate-dependant step.[31,46] With respect to the three amines used in this study, this one has the slowest rate of reaction, according to literature.[46] It should also be noted that the acrylic used also affects the rate of the Michael addition, depending on the heteroatom and substitution of the structure (as discussed in Chapter III).[19,47] The kinetics showed that within 6 hours, the reaction was complete as can be seen by the disappearance of the peak of the unopened thiolactone in *Figure IV 1c* (peak at 2.9 minutes), although after 4 hours barely any unopened thiolactone remained. It should also be noted that as the reaction proceeded towards completion, there was a drastic improvement in purity, suggesting the disappearance of side-products and intermediates.

A second kinetic experiment (*Figure IV 1d*) was conducted whereby the reaction was again followed over six hours, but after every 2 hours the reaction was worked-up, a 2 mg sample was removed for LCMS analysis and fresh-reagents were added. This approach has been previously used and is common in solid-phase synthesis to further guarantee reaction completion.[16,19] The kinetics of the thiolactone isocyanate addition step were already previously reported.[16] Regarding the LCMS spectra in *Figure IV 1*, the peaks between 1 and 3 minutes of the LC chromatograms were from the solvent injection into the system and the small peaks observed in *Figure IV 1a*, *c* and *d* at retention times of 5 minutes and above were unassignable to any product or by-product and so were assumed to be system peaks. The small signal sometimes observed to the left of the main product peak is a result of a partial oxidation of the thioether in the structure, which occurs during cleavage from the resin with TFA (trifluoroacetic acid), resulting in the mass of the product + 16 Da.[19] This oxidation was controlled and kept to a minimum by sealing the vial during cleavage to reduce contact with the air. Cleavage in completely inert conditions should circumvent this totally. The peak observed at 4.8 minutes of *Figure IV 1d* was present in each chromatogram of that experiment and was also not attributable to any product or by-product. Thus, it was assumed to be a contaminant on the LC column.

As the results from the reactions carried out manually were promising and the structure of the manually synthesised trimer was also confirmed by ^{1}H, ^{13}C NMR and ESI-MS (see section IV.4.4), the protocol was transferred to a liquid-handling robot (*Figure IV 6*), originally developed for peptide synthesis, to further explore the synthesis of longer oligomers using an automated approach.

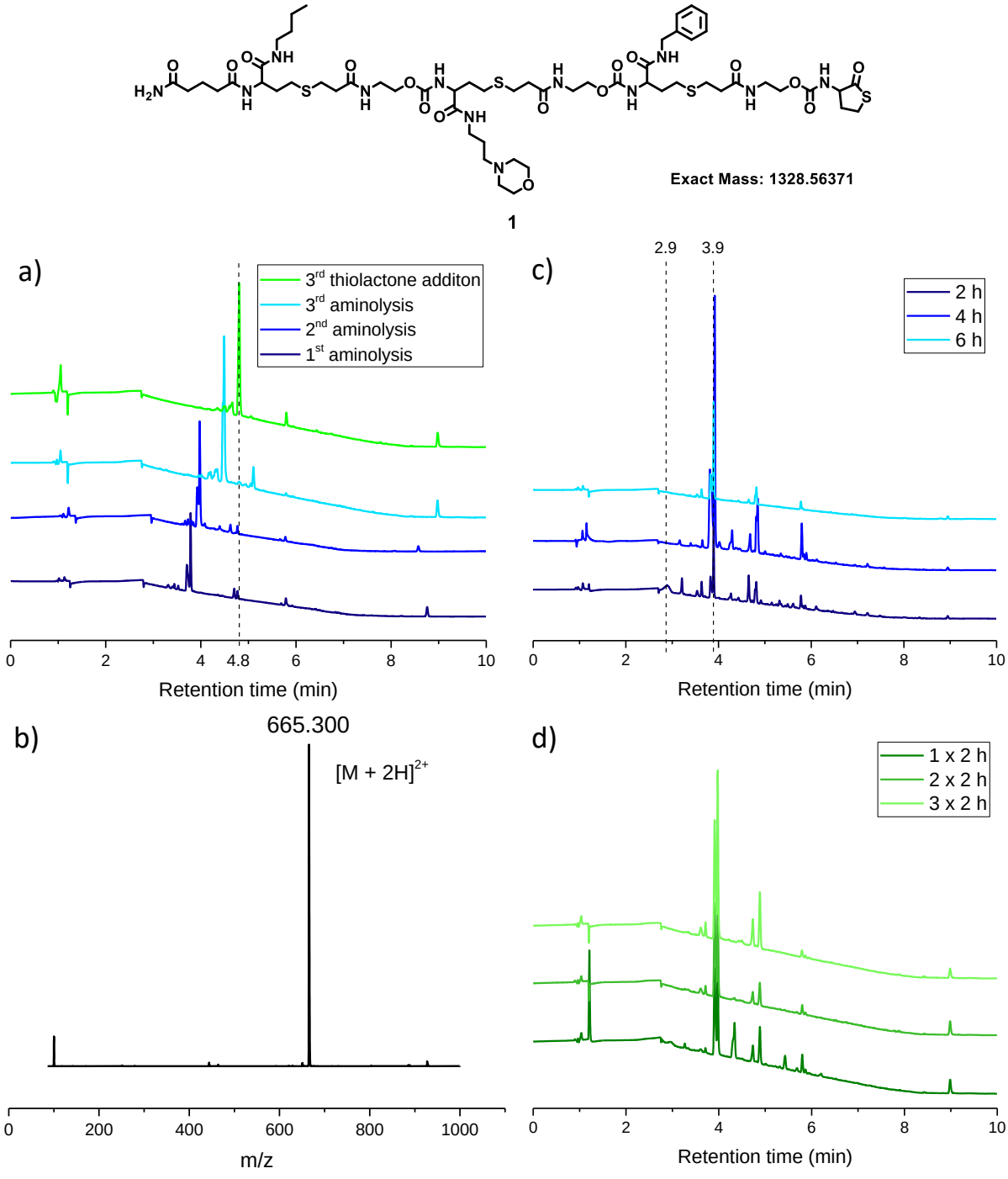


*Figure IV 1: Manual synthesis of oligomer **1** a) LCMS chromatograms (λ=214 nm) of each aminolysis step and the final thiolactone isocyanate addition. b) ESI-MS spectrum of the main peak (4.8 mins) of Figure 2a, corresponding to oligomer **1**. c) LCMS chromatograms (λ=214 nm) of the thiolactone aminolysis kinetics with benzylamine over 6 hours. Peak corresponding to the desired reaction product has a retention time of 3.9 minutes and that of the start material is at 2.9 minutes. d) LCMS chromatograms (λ=214 nm) of the thiolactone aminolysis kinetics with benzylamine over 6 hours but with the reaction worked-up and fresh reagents added every 2 hours.*

IV.2.3 Automated solid-phase synthesis

Using an automated peptide synthesiser (for pictures, see *Figure IV 6*), an ABC-type trimer (oligomer **2**) was again synthesised to optimise the reaction settings as this instrument works in a very different way to the manual set-up. The robot uses a needle and syringe to add all reagents to the reaction column, therefore, all reagents were made up into stock solutions of a determinate concentration. The concentrations of 2 M and 4 M were tested for the *N*-hydroxyethyl acrylamide and amines, respectively and 1.5 M and 0.5 M for the α-thiolactone-γ-isocyanate and dibutyltin dilaurate (DBTL). Initially, the reaction equivalents were kept the same as those used in the manual synthesis, thus also resulting in a total reaction volume of approximately 500 µL. These were indeed found to be the optimum reaction conditions (see section IV.4.5).

Alternative conditions were also evaluated whereby the reaction volume was doubled to approximately 1000 µL, but they were less optimal. A larger reaction volume was investigated to try and reduce the effect of partial evaporation of the chloroform during the reaction which occurred because the reaction vessels in the automated set-up were open to the atmosphere, unlike with the manual synthesis. The higher reaction volume was achieved by using either lower molar concentrations, thus increasing the reaction volume, but this was found to be too dilute and the reaction was slower, or, by keeping the same molar concentrations but increasing the equivalents used (40 and 20 equivalents for the acrylamide and amine respectively, instead of 20 and 10, for example). This also increased the reaction volume to 1000 µL but resulted in the stock solutions becoming apparently too viscous for the needle to handle.

Thus, after finding suitable concentrations of the stock solutions for the automated synthesis, a pure, sequence-defined trimer (oligomer **2**) was synthesised (*Figure IV 2*). Previously, a problem was observed with a similar automated, thiolactone-based protocol when it came to the thiolactone-isocyanate addition step.[16] This was found to be a result of isocyanate hydrolysis on account of the open reaction vessels in the robot.[16] This problem was solved in this work by adding the thiolactone-isocyanate, shaking for 1 hour, then washing away any formed dithiolactone urea with DMF before adding fresh thiolactone isocyanate for a further 1 hour, to mitigate the effects of any reagent degradation in the reaction vessel. The thiolactone isocyanate stock solution was stored under an inert atmosphere in the robot, preventing it from rapid degradation.

The purity of the oligomer **2** (93 %) (*Figure IV 2*) was comparable to that of the trimer synthesised manually (88 %) (*Figure IV 1b*). The oligomer was fully characterised by ^{1}H, ^{13}C NMR and ESI-MS

(see section IV.4.5). Purity was assessed by comparing the integration of all comparable LCMS peaks.[39] The yield was notably higher *via* the automated route and the time saving was impressive – 20 hours and 15 mins when compared to 2-3 days manually. After the optimisation of the reaction conditions, the sequence was continued for another 3 and 6 cycles to synthesise both a hexamer **3** and a nonamer **4**, respectively.

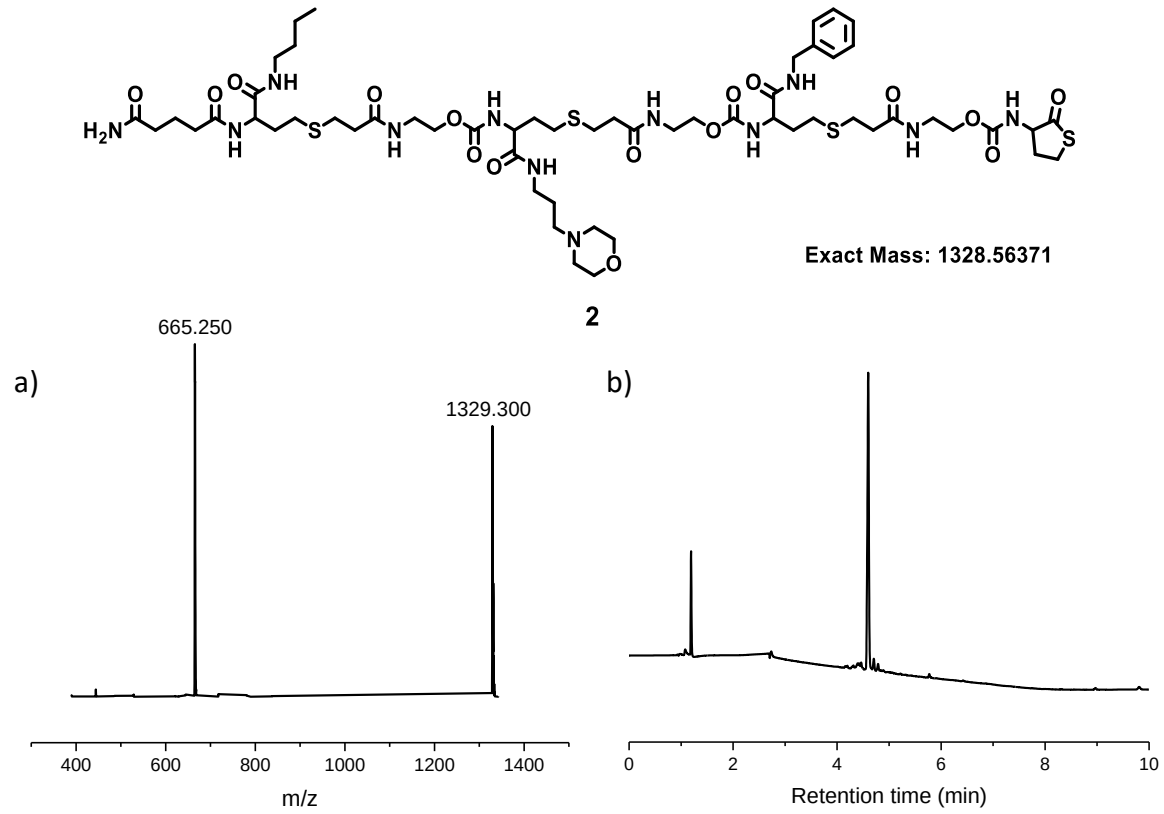


*Figure IV 2: Automatically synthesised sequence-defined trimer **2** a) ESI-MS spectrum of **2** from the LC-peak at retention time 4.6 minutes b) LCMS chromatogram (λ=214 nm) of **2**. The peaks at around 1 minute relate to solvent injection on the LC column.*

LCMS analysis of both oligomers (**3** and **4**) showed the presence of a small fraction of oligomer from the thiolactone aminolysis step of the previous cycle (*i.e.* pentamer and octamer respectively). The number of times that the aminolysis step was repeated in each cycle (*i.e.* to allow fresh addition of reagents in the system) was therefore increased to reduce or completely avoid the formation of these truncated structures. An increase from 3 to 4 additions of fresh reagents saw a slight reduction in the side product, while an increase from 4 to 5 fresh additions showed no additional benefit. Therefore, it is unlikely that this is a result of inefficient reactions, as a whole range of side peaks of numerous incomplete steps (*i.e.* a mix of trimer, tetramer, pentamer and hexamer etc.) were not observed by LCMS.

Although the crude purity of oligomers **3** and **4** was still relatively high (82 and 74 % respectively), they were successfully purified by preparative HPLC. *Figure IV 3* displays the structures of the hexamer and nonamer obtained from the robot and the resulting LCMS chromatograms, both before and after preparative HPLC purification. It shows that after preparative HPLC, the obtained oligomers were of very high purity (>97%), which was much higher than those obtained manually and of course obtained in a much faster time scale. Following purification, products were characterised by ^{1}H NMR and ESI-MS (see section IV.4.7). However, it should be noted that purification by preparative HPLC may not always be necessary in the future, as the required purity is dependent upon the desired application and can range from 70-98 %. [48,49]

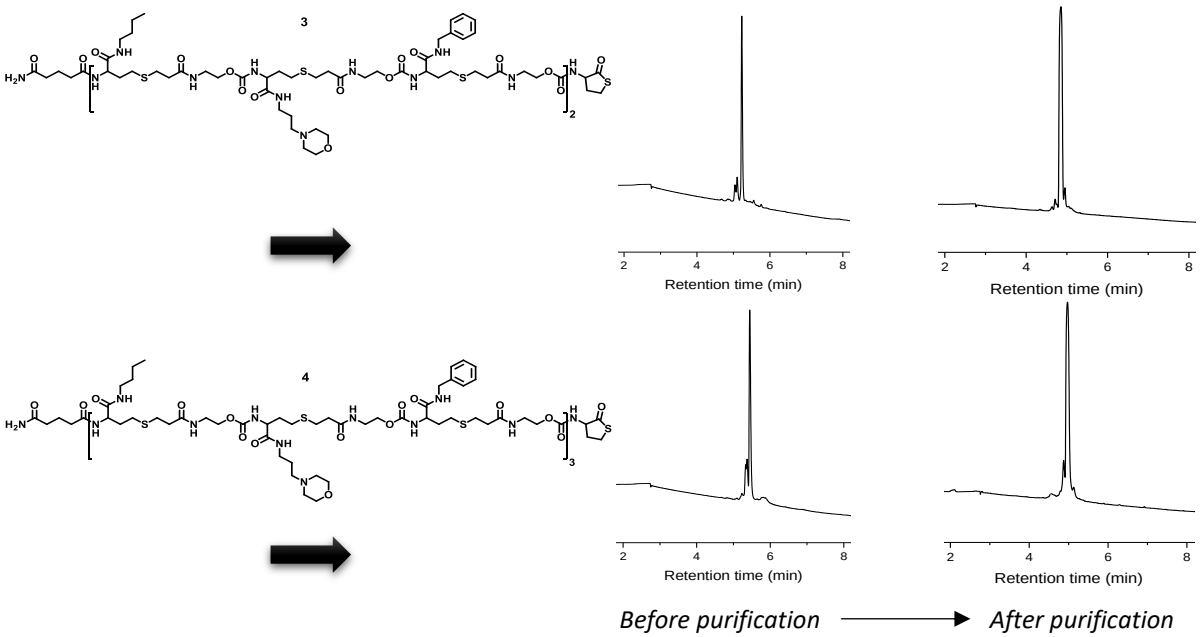


*Figure IV 3: Top) Hexamer **3** obtained from automated synthesis with LCMS chromatogram (λ=214 nm) both before (left) and after (right) preparative HPLC. Bottom) Nonamer **4** obtained from automated synthesis with LCMS chromatogram (λ=214 nm) both before (left) and after (right) preparative HPLC.*

IV.2.4 Alternative resins and loading

Whilst this study focused essentially on the use of rink amide resin, it is important to note that unlike in previously published works of our group,[16,17,19] trimers of identical sequences were also synthesised using the robot from thiolactone immobilised on other acid-labile resins to further demonstrate the versatility of our strategy (*Figure IV 4*). Both 2-chlorotrityl chloride and Wang resins were tested. The first resin can be cleaved in very weak acidic medium (1% TFA in CH_2Cl_2 typically) while for the Wang resin, stronger conditions are needed (50-95% TFA in CH_2Cl_2). On both resins, trimers of high crude-purity were obtained.

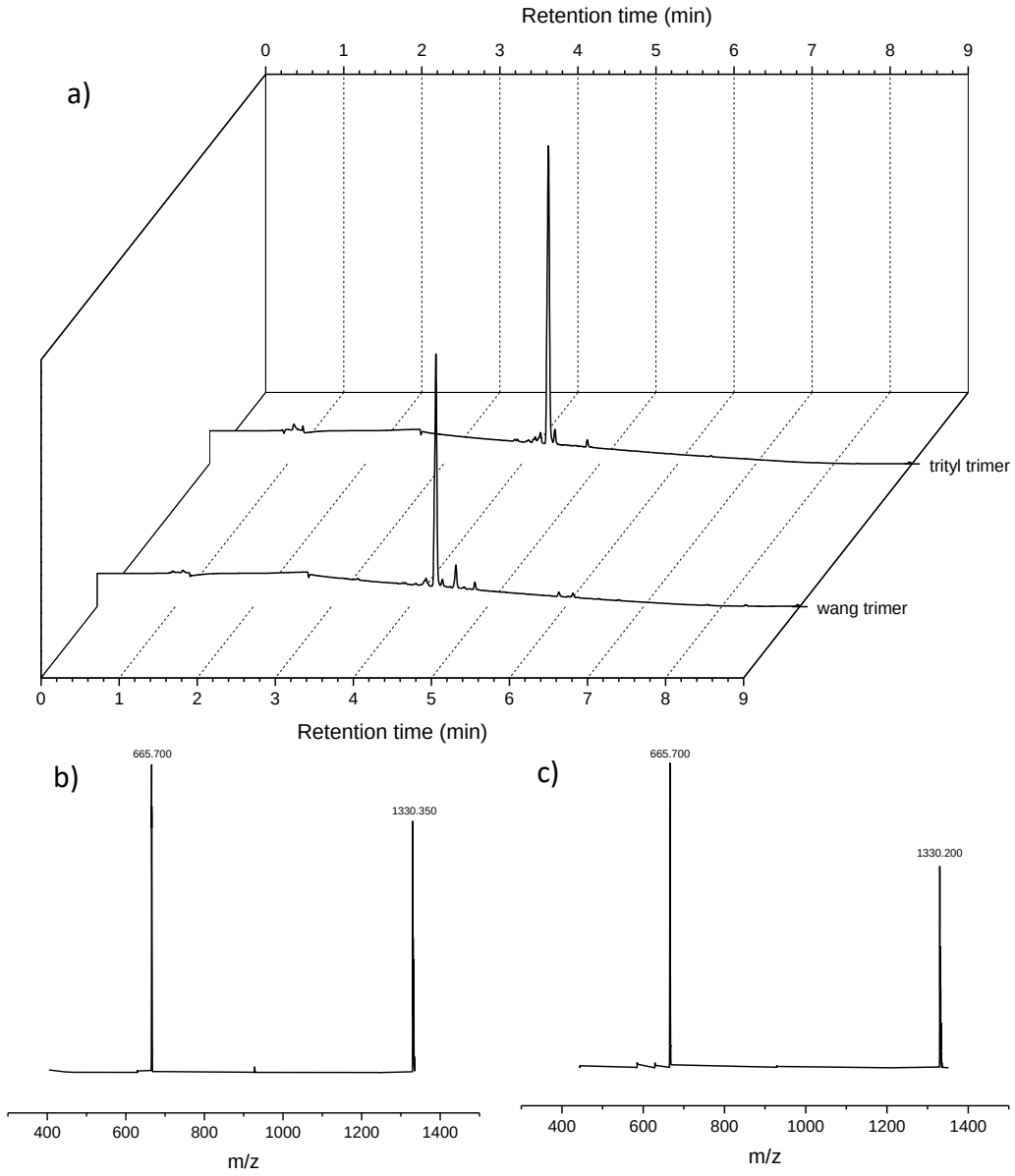


*Figure IV 4: a) LCMS chromatograms (λ = 214 nm) of trimers synthesised (identical in structure to oligomers **1** and **2** using 2-chlorotrityl chloride resin and Wang resin, b and c) ESI-MS spectra of the trimers obtained using 2-chlorotrityl chloride resin, and Wang resin, respectively.*

These results suggest that the choice of resin can be adapted to the acid sensitivity of the selected side groups or backbones, or to the targeted end-group functionality, thus increasing the scope of this protocol. The resins are also commercially available with different mesh sizes and loading capacities, thus allowing one even more variation when it comes to solid-phase synthesis, depending on the desired application. To demonstrate this, the robot was also used to synthesise a trimer (**5**) on a rink-amide resin with a lower loading capacity (0.40 mmol/g, compared to 0.74 mmol/g). The resulting trimer was of the same purity, according to LCMS (*Figure IV 5*), as oligomer **1** (93 %), however when longer sequences were attempted, the purity dropped significantly and investigations with different loading capacities were thus not further pursued.

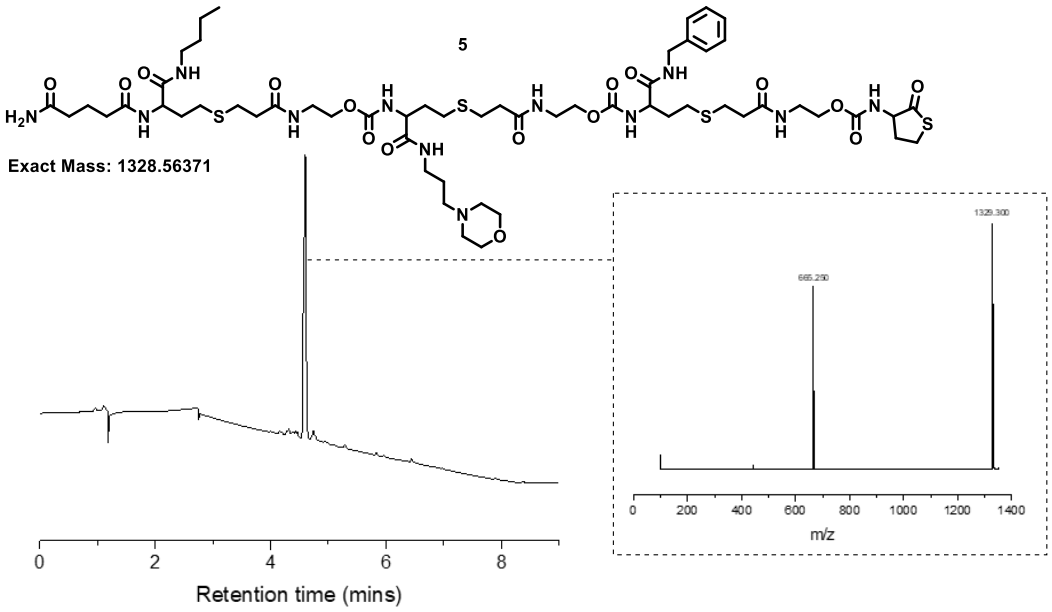


*Figure IV 5: LCMS of trimer **5**, synthesised using a Rink-amide resin with a lower loading capacity (0.4 mmol/g).*

IV.3 Conclusion and outlook

Whilst this study nicely demonstrates the wide range of possibilities and advantages of solid-phase synthesis, it also highlights both the advantages and disadvantages of an automated synthesis approach (as shown in *Table IV 1*). Solid-phase synthesis was again shown to be a useful tool in sequence-defined synthesis, with the use of a large excess of reagents to ensure high conversion and easy purification by simple washing with solvents. However, certain limitations with solid-phase synthesis regarding scale and the ability to follow the reaction with online-analysis were evident. The method discussed in this chapter shows how thiolactone chemistry, immobilised on different acid-labile solid-phase resins, could be easily adapted into a two-step, iterative protocol with side chain functionality being introduced using commercially available primary amines. Whilst the study was limited to just three different amines, many more are available, as demonstrated in the work described in Chapter III. The synthesis of multifunctional, sequence-defined macromolecules was significantly advanced by the automation of this method. The use of an automated peptide synthesiser showed the potential of the increased speed and throughput that is possible as one can carry out up to 72 reactions in parallel, thus side-stepping some of the limitations of scale when normally using solid-phase chemistry. As a result, the option to synthesise longer sequences and large libraries of monodisperse macromolecules could be realised by a parallel, automated approach in a comparatively short time-frame. It was also calculated that on a 50 mg reaction scale, the robot can handle up to 3.6 g of resin at any one time, thus holding the potential to yield a respectable amount of sequence-defined oligomer. However, certain disadvantages and limitations of an automated approach, compared with a manual one, became evident during this project.

Optimisation of the automated protocol, particularly with respect to the concentrations of the stock solutions, was more tedious as the set-up and preparation time required was much more than that of the manual synthesis. Therefore, for a totally new chemical protocol, it is first advisable to optimise manually before considering automated synthesis, even though further optimisation will then be required. Furthermore, the automated synthesis resulted in more chemical wastage of the stock solutions required because of the dead volume in each storage flask. The inability to seal the reaction vessels also led to complications when working with volatile and/or air-sensitive reagents. Nonetheless, once fully optimised, the time and labour-saving advantage of an automated approach became immediately apparent. One possible future study could be to further examine how structural changes, such as backbone composition and side-chain length, further influence structure-property relationships, such as folding and biological interaction using biologically active functional side groups.

Table IV 1: Overview of the advantages and disadvantages of automated solid-phase synthesis compared with a manual approach.

Advantages of automation	Disadvantages of automation
Time-saving synthesis	More time-consuming for optimisation
Labour-saving approach	More chemical waste
Multiple reactions/sequences possible in parallel	Inability to close reaction vessels can lead to problems with air sensitivity
Can operate 24/7 and can be controlled remotely	All reagents need to be added as stock solutions

IV.4 Experimental details

IV.4.1 Chemicals

All chemicals were used as supplied, unless otherwise stated. MeCN-d_3 ≥ 99.5 %, DMSO-d_6 ≥ 99.8 % and $CDCl_3$ ≥ 99.8 % were purchased from Euriso-top. D,L-Homocysteine thiolactone hydrochloride 99 % was purchased from Haihang Industry (Jinan City, China). Magnesium sulfate, dried ≥ 99 %, sodium hydrogen carbonate ≥ 99 % and sodium chloride ≥ 99 % were purchased from Carl Roth. Hydrochloric acid 36 wt% was purchased from Chem Lab NV. Trifluoroacetic acid, peptide grade, fmoc-protected rink-amide resin (100-200 mesh, 1 % DVB, 0.72 mmol/g and 0.4 mmol/g), 2-chlorotrityl chloride resin (100-200 mesh, 1 % DVB, 1.6 mmol/g) and Wang resin (100-200 mesh, 1 % DVB, 1.0-2.0 mmol/g) were purchased from Iris Biotech GmbH. Fmoc-protected rink-amide resin (100-200 mesh, 1 % DVB, 0.72 mmol/g) was also purchased from Merck – Novabiochem. Anhydrous dichloromethane 99.8 % and *N,N'*-dimethylformamide 99.8 % extra dry, over molecular sieves, calcium hydride ca. 93 %, extra pure, 0.20 mm grain size, pyridine 99 %+, extra pure and piperidine 99

%, extra pure were purchased from Acros Organics. Acetic anhydride, benzylamine 99 %, ReagentPlus®, dicyclohexylcarbodiimide 99 %, 3-morpholinopropylamine 98 % and *N*-hydroxyethyl acrylamide, 1000 ppm MEHQ inhibitor, 97 %. Acetonitrile 99.9 %, gradient grade, chloroform and methanol, HPLC grade, were also purchased from Sigma Aldrich. Butylamine > 99.0 %, 4-dimethylaminopyridine (DMAP), and dibutyltin dilaurate (DBTL) were purchased from Tokyo Chemical Industry (Europe). Diethyl ether, analytical reagent grade and *N,N'*-dimethylformamide 99.8 % laboratory reagent grade were purchased from Fischer Scientific. Acetone, HPLC grade HiPerSolv CHROMANORM was purchased from VWR. When anhydrous chloroform was required, HPLC grade chloroform was dried over calcium hydride. Water, when used in the synthesis, was de-ionised.

IV.4.2 Analytical methods

Nuclear Magnetic Resonance (NMR): ^{1}H- and ^{13}C-NMR Attached Proton Test (APT) spectra were recorded on a Bruker Avance 300, a Bruker Avance 400, Bruker Avance 500 or a Bruker Avance II 700. Chemical shifts are presented in parts per million (δ) relative to DMSO-d_6, $CDCl_3$ or MeCN-d_3 (2.50 ppm, 7.26 ppm or 1.94 ppm in ^{1}H- and 39.51 ppm, 77.24 ppm or 118.26 ppm in ^{13}C-NMR respectively) as internal standard. Coupling constants (J) are reported in Hertz (Hz). All measurements were recorded in a standard fashion at 25 °C unless otherwise stated. Full assignment of structures was aided by 2D NMR analysis (COSY, HSQC and HMBC).

High Performance Liquid Chromatography (HPLC): HPLC was carried out using two Agilent Prepstar pumps, one pumping acetonitrile and the other pumping water (+0.1 % TFA) to run at a gradient over 15 mins from 100 % water to 100 % acetonitrile. An Agilent Prostar UV-detector was used (λ = 214 nm). For the separation, two Luna C18 columns were used with 5µm particle size, diameter of 21.2 mm and length of 250 mm.

Electrospray Ionisation Mass Spectrometry (ESI-MS) and Liquid Chromatography Mass Spectrometry (LCMS): An Agilent technologies 1100 series LC/MSD system equipped with a diode array detector and single quad MS detector (VL) with an electrospray source (ESI-MS) was used for classic reversed phase LCMS and MS analysis. Analytic reversed phase HPLC (high-performance liquid chromatography) was performed with a Phenomenex Kmetex C18 (2) column with a solid core at 35 °C and a flow rate of 1.5 mL/min (5 µ, 150 x 4.6 mm) using a solvent gradient (0 → 100 % acetonitrile in H_2O in 6 min) and the eluting compounds were detected via UV-detection (λ = 214 nm). LCMS spectra were analysed using ACD/Spectrus software and the purity of compounds was assessed by integrating the LC peaks (λ = 214 nm) using the in-software function.

High Resolution Mass Spectroscopy (HRMS): HRMS spectra were collected using an Agilent 6220 Accurate-Mass time-of-flight (TOF) equipped with a multimode ionization (MMI) source.

Infrared: Spectra were recorded with Attenuated Total Reflection (ATR) with a PIKE Miracle ATR unit and a Perkin Elmer FTIR SPECTRUM 1000 spectrometer.

Automated peptide synthesiser layout: The robot used in the automated experiments was a 72-reactor block INTAVIS MultiPep CF synthesiser, with open 5 mL reaction columns equipped with vortexing unit. The speed of vortexing was 700 rpm. The robot is shown below in *Figure IV 6*.

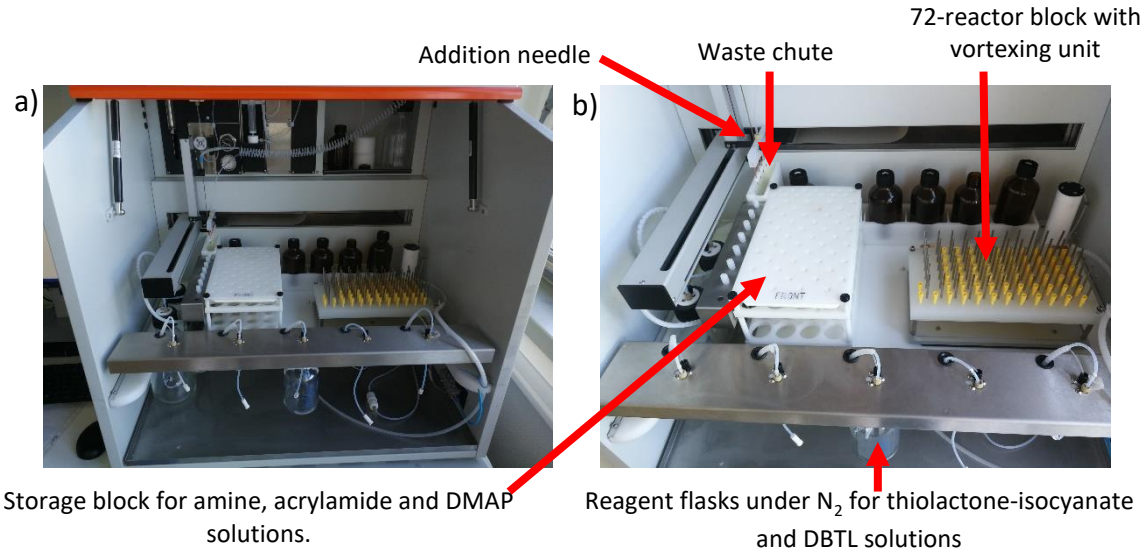
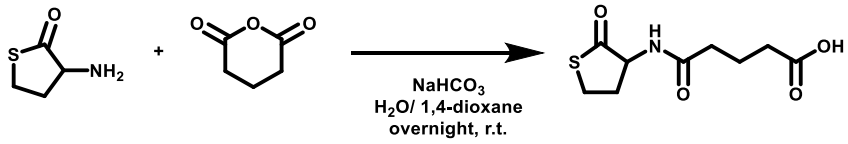


Figure IV 6: a) INTAVIS MultiPep CF Synthesiser. b) Close-up of INTAVIS MultiPep CF Synthesiser.

IV.4.3 Synthesis of functional thiolactone compounds

IV.4.3.1 Synthesis of thiolactone-carboxylic acid

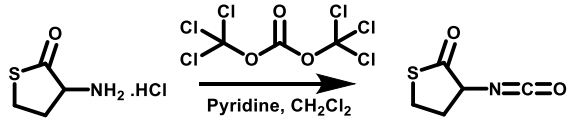
Thiolactone-carboxylic acid was prepared by a modified version of the previously reported procedure.[17]



See Chapter III.4.3.1 for experimental procedure and full characterisation.

IV.4.3.2 Synthesis of α-thiolactone-γ-isocyanate

Thiolactone-isocyanate was prepared according to the procedure previously reported.[16]



See Chapter III.4.3.2 for experimental procedure and full characterisation.

IV.4.4 Loading of the resins with thiolactone carboxylic acid molecule

IV.4.4.1 Loading of the rink-amide resin

Fmoc-protected rink-amide resin (100-200 mesh, 1 % DVB, 0.72 mmol/g) (2.5 g, 1.0 equiv.) was swollen for 5 mins in 20 mL anhydrous CH_2Cl_2. The solvent was then filtered off and the resin was washed twice with CH_2Cl_2. A 20 % piperidine in CH_2Cl_2 solution (20 mL) was added and the reaction mixture was shaken vigorously at room temperature for 4 hours to remove the fmoc protecting group. The reaction was then filtered and the resin washed with DMF (3 x 30 mL) and CH_2Cl_2 (3 x 30 mL). The resin was again swollen for 5 minutes in anhydrous CH_2Cl_2 (16 mL). The thiolactone-carboxylic acid molecule (2.08 g, 5.0 equiv.), *N,N'*-dicyclohexylcarbodiimide (DCC) (1.86 g, 5.0 equiv.), 4-dimethylaminopyridine (DMAP) (23 mg, 0.1 equiv.) and anhydrous DMF (4 mL) were added. The reaction was shaken vigorously at room temperature for 36 hours. The resin was then filtered and washed with CH_2Cl_2 (3 x 30 mL), DMF (3 x 30 mL) and diethyl ether (3 x 30 mL) before drying under vacuum at room temperature for 2 hours.

IV.4.4.2 Loading of the Wang resin

This was carried out according to a modified version of the previously reported procedure.[50] Wang resin (100-200 mesh, 1 % DVB, 1.0-2.0 mmol/g) (3.005 g, 2.04 mmol) was suspended in a 9:1 anhydrous

CH_2Cl_2:DMF solution (45 mL). In a separate flask, thiolactone carboxylic acid (2.361 g, 10.2 mmol) was dissolved in anhydrous DMF (4 mL) and was then added to the reaction. DCC (2.104 g, 0.68 mmol) and DMAP (24.9 mg, 0.204 mmol) were dissolved in anhydrous DMF (60 µL) and added to the reaction. The reaction was shaken vigorously at room temperature for 24 hours. The reaction was then filtered and the unreacted end-groups were capped by shaking for 20 minutes with a 9:1 solution of pyridine:acetic anhydride (50 mL). The resin was dried under vacuum for 3 hours.

IV.4.4.3 Loading of the 2-chlorotrityl chloride resin

2-Chlorotrityl chloride resin was loaded with the thiolactone carboxylic acid molecule according to the procedure described in *Chapter II.4.4.1* which was previously reported by Espeel *et. al.*[17]

IV.4.5 General procedure for the manual synthesis of sequence-defined oligomers: Synthesis of oligomer 1

IV.4.5.1 General procedure for thiolactone aminolysis – manual protocol step 1

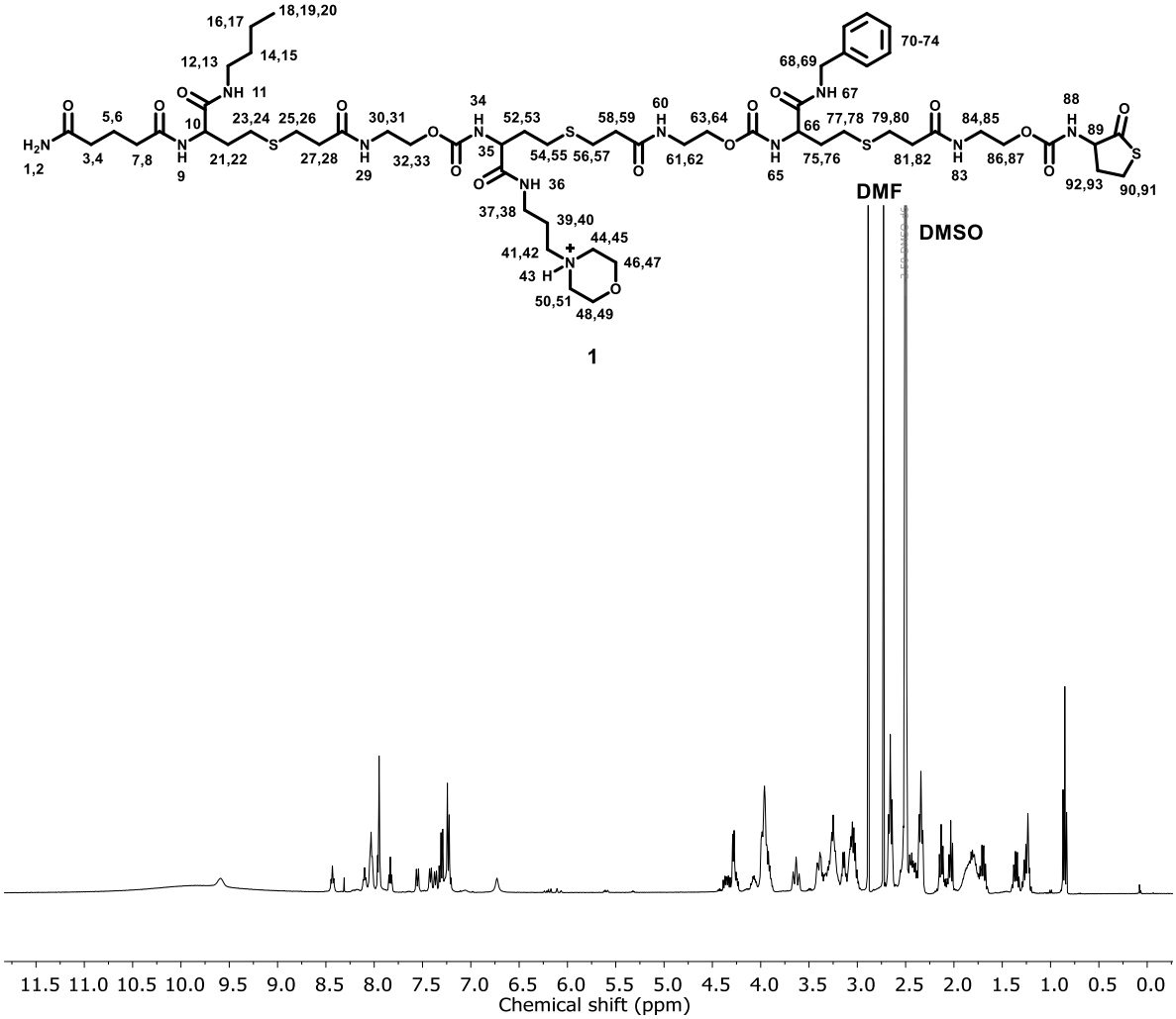
Fmoc-protected rink-amide resin (100-200 mesh, 1 % DVB, 0.72 mmol/g), functionalised with thiolactone carboxylic acid (50.0 mg, 1 equiv.) was swollen for at least 10 mins in chloroform (0.5 mL). N-hydroxyethyl acrylamide (80 µL, 20.0 equiv.), butylamine, 3-morpholino propylamine or benzylamine (10.0 equiv.) and DMAP (4.5 mg, 1.0 equiv.) were added. The reaction was left to shake vigorously at room temperature for 6 hours. The reaction was then filtered and the resin was washed with DMF (4x), MeOH (4x), $CHCl_3$ (4x) and Et_2O (4x). A sample was then prepared for analysis by LCMS to check reaction conversion: 2 mg of resin from the reaction was suspended for 25 minutes in a 10 % TFA in CH_2Cl_2solution (0.5 mL) with a sealed lid. The cleaved resin turned red as a result of the ion formed during the cleavage. The cleaved resin was filtered off by passing the solution through a syringe filter. The solvent was removed by evaporation and the sample then diluted in acetonitrile.

IV.4.5.2 General procedure for the addition of α-thiolactone-γ-isocyanate – manual protocol step 2

The thiolactone-functionalised resin, modified as described above in step 1, was swollen for at least 10 minutes in anhydrous chloroform (0.5 mL). Then, α-thiolactone-γ-isocyanate (80 µL, 20.0 equiv.) and dibutyltin dilaurate (3 drops) were added and the reaction was shaken vigorously at room temperature for 2 hours. A white precipitate – thiolactone urea [16] – was formed as a by-product during the reaction. The reaction was filtered and the resin was washed with DMF (4x), MeOH (4x), $CHCl_3$ (4x) and Et_2O

(4x). A sample was then prepared for analysis by LCMS. 2 mg of resin from the reaction was suspended for 25 minutes in a 10 % TFA in CH_2Cl_2 solution (0.5 mL) with a sealed lid. The cleaved resin was filtered off by passing the solution through a syringe filter. The solvent was removed by evaporation and the sample then diluted in acetonitrile. Steps 1 and 2 were repeated two more times to yield the final trimer (Oligomer **1**) which was cleaved from the resin as described for the LCMS sample preparation. The resulting colourless film was dried for at least 4 hours under vacuum. m = 21.3 mg, yield = 43 %. The oligomer is fully characterised below.

V.4.5.3 NMR and HRMS characterisation of oligomer 1



1

*Figure IV 7: [1]H NMR spectrum of oligomer **1** and structure with assignments.*

[1]H NMR (400 MHz, DMSO-*d*$_6$): δ = 9.59 (s, 1H, H_{43} $N^+\underline{H}$)*, 8.43 (t, *J* = 6.03 Hz, 1H, H_{67} O=CN$\underline{H}$), 8.10 (t, *J* = 6.42 Hz, 1H, H_{11} O=CN$\underline{H}$), 8.07-7.99 (m, 2H, $H_{29,60}$ O=CN$\underline{H}$), 7.99-7.93 (m, 2H, $H_{9,36}$ O=CN$\underline{H}$), 7.83 (t, *J* = 5.68 Hz, 1H, H_{83} O=CN$\underline{H}$), 7.55 (d, *J* = 8.68 Hz, 1H, H_{88} OC=ON$\underline{H}$), 7.42 (d, *J* = 7.45, 1H, H_{65} OC=ON$\underline{H}$),

7.37 (d, *J* = 8.00, 1H, H_{34} OC=ONH), 7.35-7.18 (m, 5H, $H_{70\text{-}74}$ Ph), 6.73 (s, 2H, $H_{1,2}$ H_2NCO)§, 4.40-4.31 (m, 1H, H_{89} Tl-H_α), 4.31-4.22 (m, 2H, $H_{68,69}$ CH_2Ph), 4.17-3.85 (m, 11H, $H_{10,32,33,35,46,48,63,64,66,86,87}$ H_2COC), 3.63 (t, *J* = 12.5 Hz, 2H, $H_{47,49}$ H_2COC), 3.45-2.97 (m, 18H, $H_{12,13,30,31,37,38,41,42,44,45,50,51,61,62,84,85,90,91}$ CONHCH_2 | CH_2N$^+$R$_3$ | Tl-H_γ) 2.67 (t, *J* = 7.78 Hz, 6H, $H_{25,26,56,57,79,80}$ CH_2SCH_2), 2.58-2.28 (m, 14H, $H_{23,24,27,28,54,55,58,59,77,78,81,82,92,93}$ CH_2SCH_2 | CH_2CONH | Tl-H_β), 2.13 (t, *J* = 7.37 Hz, 2H, $H_{7,8}$ CH_2CONH), 2.03 (t, *J* = 7.48 Hz, 2H, $H_{3,4}$ H_2NCOCH_2), 1.97-1.64 (m, 10H, $H_{5,6,21,2239,40,52,53,75,76}$ CH_2C$H_2$$CH_2$ | CHC$H_2$$CH_2$), 1.36 (p, *J* = 7.80, 7.80, 7.30, 6.40, 2H, $H_{14,15}$ CH_2C$H_2$$CH_2$$CH_3$), 1.31-1.18 (m, 2H, $H_{16,17}$ $CH_2$$CH_2CH_2$$CH_3$), 0.85 (t, *J* = 7.28 Hz, 3H, $H_{18,19,20}$ CH_3). * Cleavage from the solid-phase resin with 1% TFA solution resulted in protonation of the morpholino group, hence this extra proton and a broadening of the baseline gives a larger than expected integration. § Integration is lower than expected here, most probably because of proton exchange with the solvent.

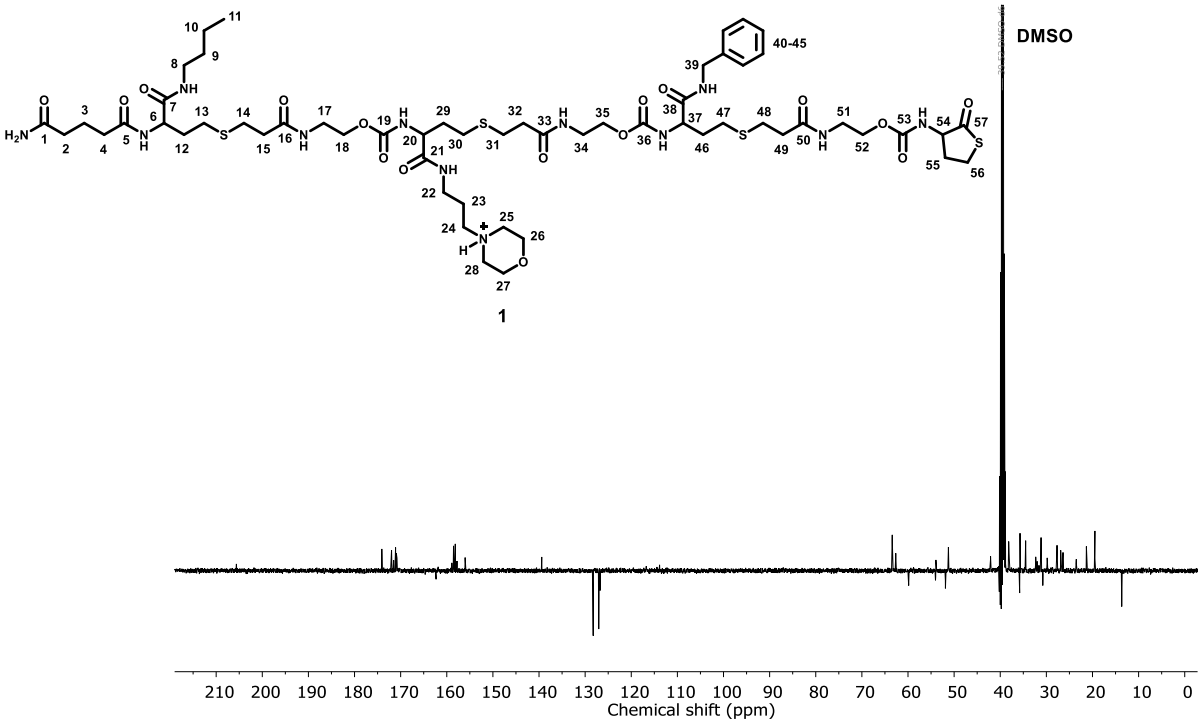


*Figure IV 8: ^{13}C NMR spectrum of oligomer **1** and structure with assignments.*

^{13}C NMR APT (100 MHz, DMSO-*d*$_6$): δ = 205.60 (C_{56}, C), 174.07 (C_1, C), 172.02, 171.96 ($C_{5,38}$, C), 171.51 (C_{21}, C), 171.09 (C_7, C), 170.92, 170.89, 170.79 ($C_{16,33,50}$, C), 156.01, 155.89 ($C_{19,36,53}$, C), 139.41 (C_{40}, CH), 128.25, 127.04, 126.73 ($C_{41\text{-}45}$, CH), 63.41 ($C_{26,27}$, CH_2), 62.69 ($C_{18,35,52}$, CH_2), 59.85 (C_{54}, CH), 53.95 (C_{24}, CH_2), 51.88 ($C_{6,20,37}$, CH), 51.23 ($C_{25,28}$, CH_2), 42.10 (C_{39}, CH_2), 38.17 ($C_{17,34,51}$, CH_2), 35.72 ($C_{8,55,13,30,47}$, CH_2), 34.56, 34.49 ($C_{2,4,22}$, CH_2), 32.31, 31.98 ($C_{12,29,46}$, CH_2), 31.15 (C_9, CH_2), 27.71 ($C_{15,32,49}$, CH_2), 26.39 (C_{56}, CH_2), 26.90 ($C_{14,31,48}$, CH_2), 23.51 (C_{23}, CH_2), 21.32 (C_3, CH_2), 19.48 (C_{10}, CH_2), 13.66 (C_{11}, CH_3)

HRMS (ESI) *m/z*:

	Ion	Structure	Mass calculated	Mass found
Monomer	$[M + H]^+$	$C_{23}H_{36}N_5O_7S_2^+$	562.2364	562.2377
Dimer	$[M + H]^+$	$C_{40}H_{71}N_9O_{12}S_3^+$	964.4301	964.4325
Trimer	$[M + H]^+$	$C_{57}H_{97}N_{12}O_{16}S_4^+$	1329.5710	1329.5696

IV.4.6 General procedure for the automated synthesis of sequence-defined oligomers: Synthesis of oligomers 2, 3 & 4

Stock solutions of all reagents were prepared in $CHCl_3$ as they were added to the reaction by a needle. For the thiolactone isocyanate and DBTL stock solutions, anhydrous chloroform was used and these solutions were stored under N_2 on the robot. Fmoc-protected rink-amide resin (100-200 mesh, 1 % DVB, 0.72 mmol/g), functionalised with thiolactone carboxylic acid (50.0 mg, 1 equiv.) was weighed into plastic reaction vessels designed for the automated peptide synthesiser (Figure S10). The resin was swollen on the robot for 10 minutes by addition of chloroform (500 µL). The solvent was then filtered off via the extraction pump and then the robot added solutions of hydroxyethyl acrylamide (307 µL, 2M in $CHCl_3$, 20 equiv.), butylamine, 3-morpholino propylamine or benzylamine (92.5 µL, 4M in $CHCl_3$, 10 equiv.) and DMAP solution (18.5 µL, 2M in $CHCl_3$, 1.0 equiv.). The reaction was shaken for 1 hour, then the mixture was filtered by the extraction pump, and fresh reagents were added and the system shaken for another hour. This was repeated twice more for the first three cycles and thrice more for the subsequent cycles (up to nonamer) before the reaction was filtered by the extraction pump and washed with DMF (4 x 500 µL), MeOH (4 x 500 µL) and $CHCl_3$ (4 x 500 µL). The needle was automatically rinsed with DMF. The resin was swollen on the robot for 10 minutes by addition of chloroform (500 µL). The solvent was filtered off via the extraction pump and then the robot added solutions of α-thiolactone-γ-isocyanate (490 µL, 1.5 M in $CHCl_3$, 20 equiv.) and DBTL (30 µL, 0.5 M, 0.4 equiv.). The reaction was shaken for 1 hour, then the mixture was filtered by the extraction pump, and fresh reagents were added and the system shaken for another hour. The reaction was filtered by the extraction pump and washed with DMF (4 x 500 µL), MeOH (4 x 500 µL) and $CHCl_3$ (4 x 500 µL). This procedure was repeated n times. After the n^{th} cycle, the resins were washed once manually with DMF (4x), MeOH (4x), $CHCl_3$ (4x) and Et_2O (4x) and then the oligomers were cleaved from the resin as described above in the manual synthesis, yielding a colourless film which was then dried under vacuum.

*Table IV 2: Table of reaction times per step and cumulative reaction times for the synthesis of oligomer **2**.* Time doesn't include swelling and washing of the resin.*

Number of Reaction Step	Reaction type	Reaction time per step* / h	Cumulative reaction time* / h
1	Aminolysis	4	4
2 (monomer)	Thiolactone isocyanate addition	2	6
3	Aminolysis	4	10
4 (dimer)	Thiolactone isocyanate addition	2	12
5	Aminolysis	4	16
6 (trimer)	Thiolactone isocyanate addition	2	18

IV.4.6.1 NMR and HRMS characterisation of oligomer 2

Oligomer **2**, m = 37.3 mg, yield = 76 %. The oligomer is fully characterised below.

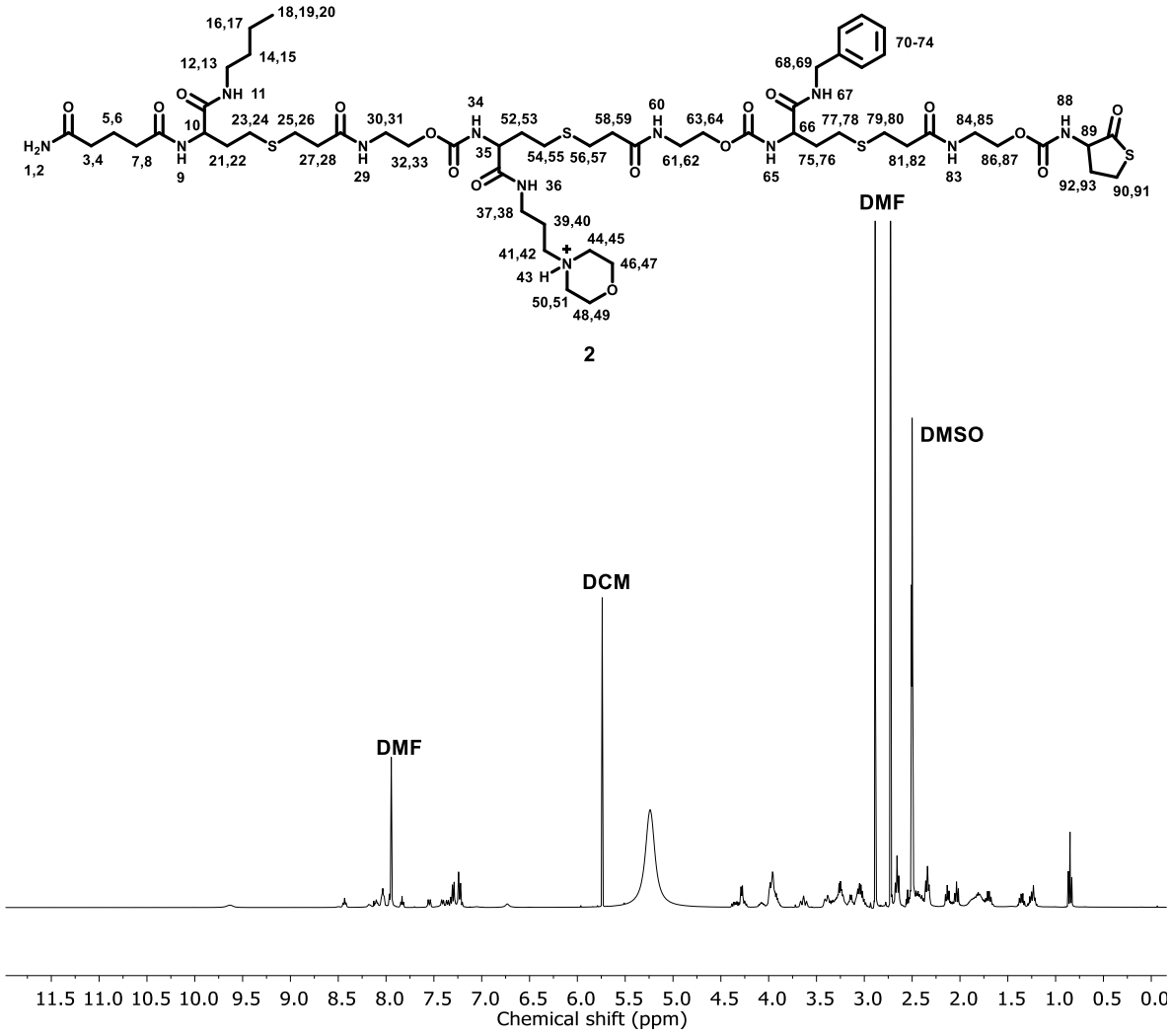


*Figure IV 9: ^{1}H NMR spectrum of oligomer **2** and structure with assignments.*

^{1}H NMR (400 MHz, DMSO-d_6): δ = 9.63 (s, 1H, H_{43} $N^{+}H$)*, 8.43 (t, J = 6.02 Hz, ^{1}H, H_{67} O=CN<u>H</u>), 8.10 (t, J = 7.44 Hz, 1H, H_{11} O=CN<u>H</u>), 8.03 (t, J = 5.49, 2H, $H_{29,60}$ O=CN<u>H</u>), 7.98-7.92 (m, 2H, $H_{9,36}$ O=CN<u>H</u>), 7.83 (t, J = 5.71 Hz, 1H, H_{83} O=CN<u>H</u>), 7.55 (d, J = 8.65 Hz, 1H, H_{88} OC=ON<u>H</u>), 7.41 (d, J = 7.49, 1H, H_{65} OC=ON<u>H</u>), 7.36 (d, J = 7.95, 1H, H_{34} OC=ON<u>H</u>), 7.33-7.18 (m, 5H, $H_{70\text{-}74}$ <u>Ph</u>), 6.73 (s, 2H, $H_{1,2}$ $\underline{H_2}$NCO)§, 4.40-4.30 (m, 1H, H_{89} Tl-$\underline{H_{\alpha}}$), 4.30-4.21 (m, 2H, $H_{68,69}$ C$\underline{H_2}$Ph), 4.14-3.85 (m, 11H, $H_{10,32,33,35,46,48,63,64,66,86,87}$ $\underline{H_2}$COC), 3.63 (t, J = 12.37 Hz, 2H, $H_{47,49}$ $\underline{H_2}$COC), 3.44-2.98 (m, 18H, $H_{12,13,30,31,37,38,41,42,44,45,50,51,61,62,84,85,90,91}$ $CONH_2C\underline{H_2}$ | $C\underline{H_2}N^{+}R_3$ | Tl-$\underline{H_{\gamma}}$) 2.67 (t, J = 7.15 Hz, 6H, $H_{25,26,56,57,79,80}$ $CH_2SC\underline{H_2}$), 2.57-2.29 (m, 14H, $H_{23,24,27,28,54,55,58,59,77,78,81,82,92,93}$ $C\underline{H_2}SCH_2$ | $C\underline{H_2}CONH$ | Tl-$\underline{H_{\beta}}$), 2.13 (t, J = 7.39 Hz, 2H, $H_{7,8}$ $C\underline{H_2}CONH$), 2.04 (t, J = 8.07 Hz, 2H, $H_{3,4}$ $H_2NCOC\underline{H_2}$), 1.95-1.62 (m, 10H, $H_{5,6,21,2239,40,52,53,75,76}$ $CH_2C\underline{H_2}CH_2$ | $CHC\underline{H_2}CH_2$), 1.42-1.31 (m, 2H, $H_{14,15}$ $CH_2C\underline{H_2}CH_2CH_3$), 1.30-1.19 (m, 2H, $H_{16,17}$ $CH_2CH_2C\underline{H_2}CH_3$), 0.85 (t, J = 7.27 Hz, 3H, $H_{18,19,20}$ $C\underline{H_3}$).

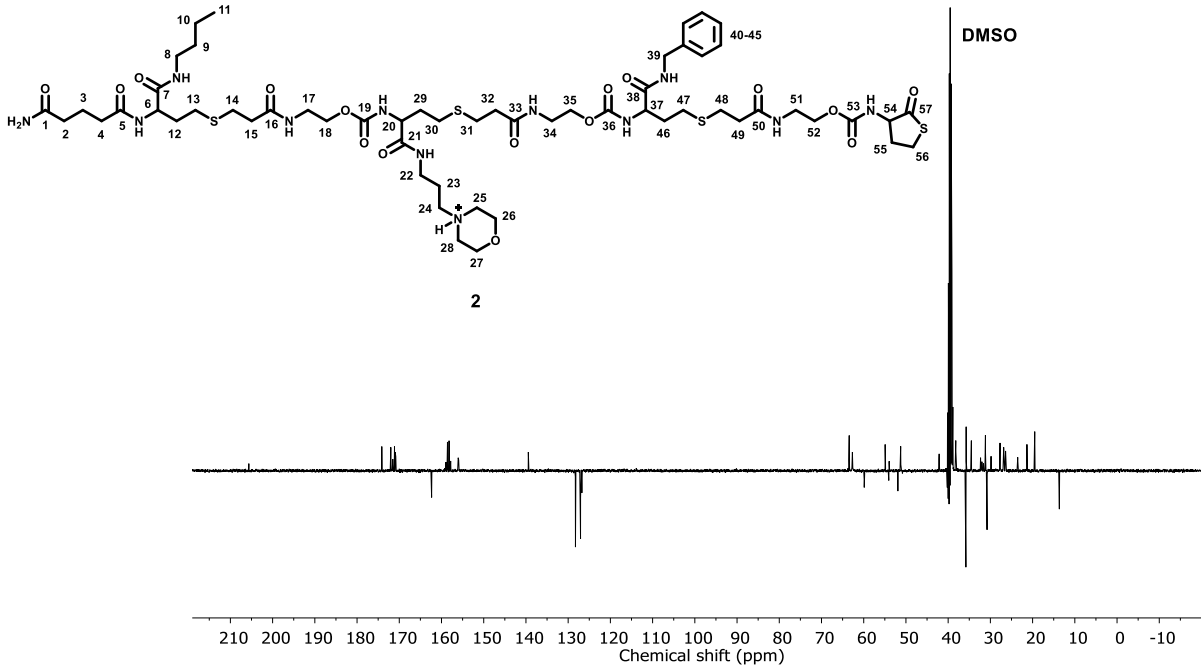


*Figure IV 10: ^{13}C NMR spectrum of oligomer **2** and structure with assignments.*

^{13}C NMR APT (100 MHz, DMSO-d_6): δ = 205.63 (C_{56}, C), 174.14 (C_1, C), 172.06 ($C_{5,7,21}$, C), 172.01 (C_{38}, C), 171.55, 171.13,170.97 ($C_{16,33,50}$, C), 156.05, 156.01, 155.93 ($C_{19,36,53}$, C), 139.44 (C_{40}, CH), 128.27, 127.07, 126.75 ($C_{41\text{-}45}$, CH), 63.43 ($C_{26,27}$, CH_2), 62.72 ($C_{18,35,52}$, CH_2), 59.88 (C_{54}, CH), 54.06 ($C_{6,20}$, CH_2), 51.91 (C_{37}, CH), 51.24 (C_{24}, CH_2), 42.26 (C_{39}, CH_2), 38.20 ($C_{17,34,51}$, CH_2), 35.74 ($C_{8,55,13,30,47}$, CH_2), 34.51 ($C_{2,4,22}$, CH_2), 31.17 ($C_{12,29,46}$, CH_2), 29.84 (C_9, CH_2), 27.73 ($C_{15,32,49}$, CH_2), 26.92 (C_{56}, CH_2), 26.85 ($C_{14,31,48}$, CH_2), 23.52 (C_{23}, CH_2), 21.35 (C_3, CH_2), 19.50 (C_{10}, CH_2), 13.66 (C_{11}, CH_3)**.**

HRMS (ESI) *m/z*: $[M+H]^+$ calculated for $C_{57}H_{97}N_{12}O_{16}S_4^+$, 1329.5710; found, 1329.5694.

IV.4.7 NMR and HRMS characterisation of sequence-defined hexamer 3 and nonamer 4 synthesised *via* the automated procedure IV.4.6

The NMR spectra of oligomer **3** (*Figure IV 11*) and oligomer **4** (*Figure IV 12*), both purified by preparative HPLC, were too difficult to fully assign because of the limited amount of material available, particularly for ^{13}C NMR. The characteristic broadening of the proton resonances associated with the NMR of a polymer reduces the resolution of the spectrum. Nonetheless, the functional side groups were visible.

IV.4.7.1 Oligomer 3

Crude yield = 30 % (m = 26.6 mg). Product was purified by prep-HPLC: yield = 16 % (m = 14 mg).

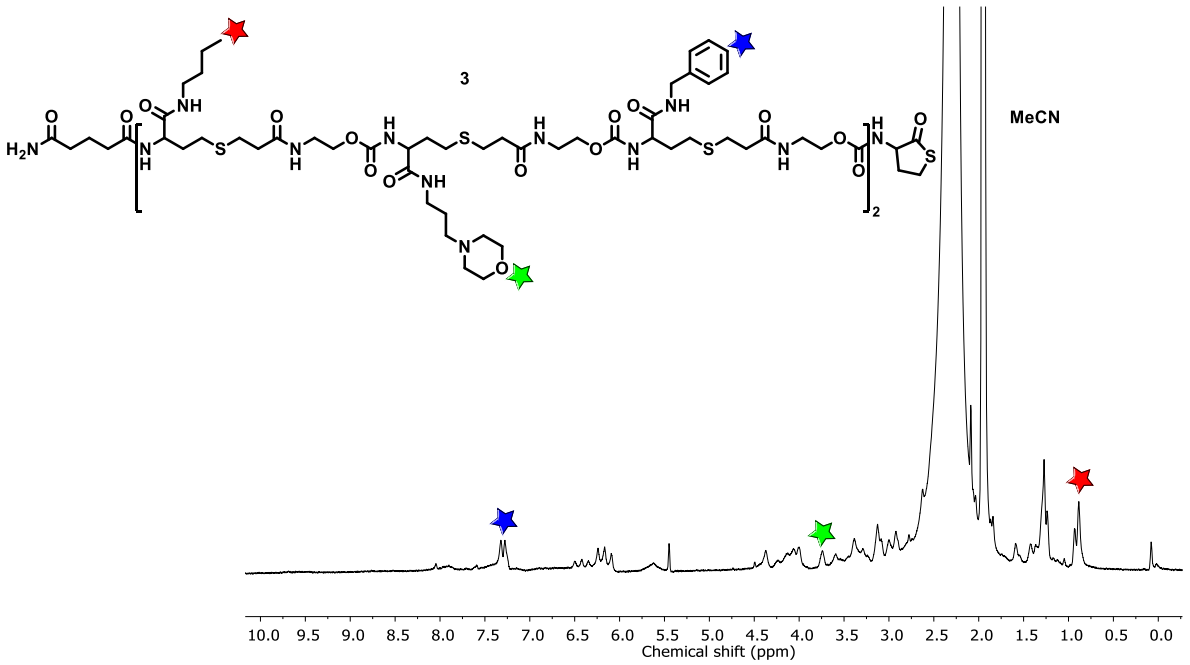


*Figure IV 11: ^{1}H NMR spectrum (700MHz, MeCN-d3) of oligomer **3** and structure with assignments.*

HRMS (ESI) m/z: $[\frac{M+2H}{2}]^{2+}$ calculated for $C_{105}H_{172}N_{22}O_{29}S_7^{2+}$, 1215.0364; found, 1214.5378.

IV.4.7.1 Oligomer 4

Crude yield = 26 % (m = 33.7 mg). Product was purified by prep-HPLC: yield = 19 % (m = 25 mg).

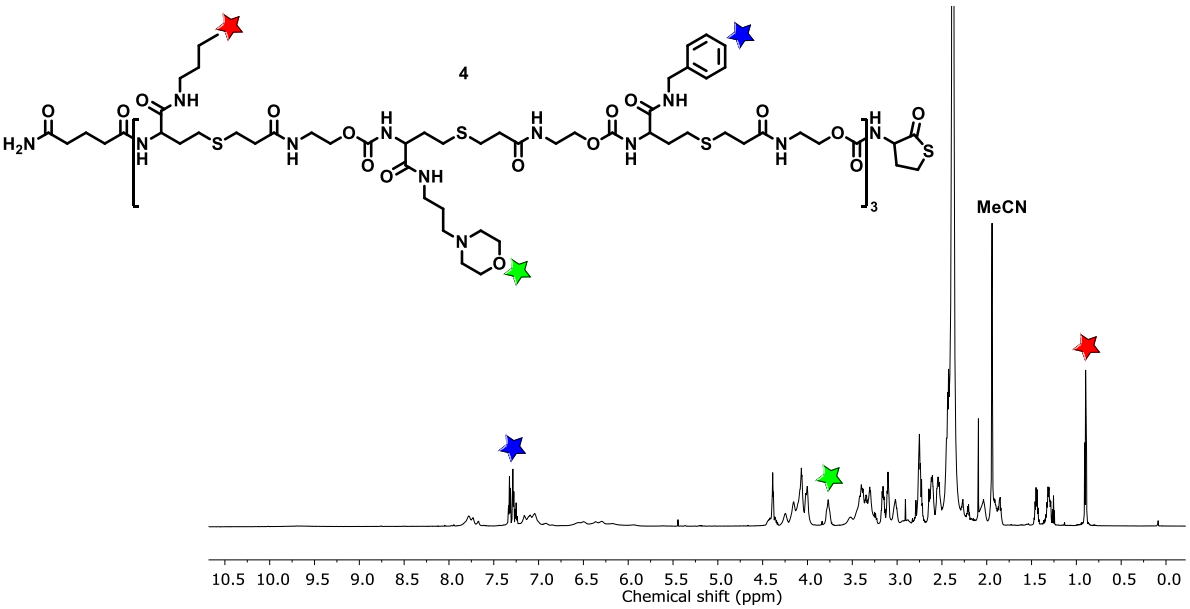


*Figure IV 12: ^{1}H NMR spectrum (700MHz, MeCN-d3 at 45 °C) of oligomer **4** and structure with assignments.*

HRMS (ESI) m/z: $[\frac{M+2H}{2}]^{2+}$ calculated for $C_{153}H_{250}N_{32}O_{42}S_{10}^{2+}$, 1764.2820; found, 1763.782.

IV.5 References

1 J.-F. Lutz, *Acc. Chem. Res.*, 2013, **46**, 2696–2705.

2 H. M. Colquhoun and J.-F. Lutz, *Nat. Chem.*, 2014, **6**, 455–456.

3 J.-F. Lutz, *Macromolecules*, 2015, **48**, 4759–4767.

4 C. Gerke, M. F. Ebbesen, D. Jansen, S. Boden, T. Freichel and L. Hartmann, *Biomacromolecules*, 2017, **18**, 787–796.

5 R. K. Roy, A. Meszynska, C. Laure, L. Charles, C. Verchin and J.-F. Lutz, *Nat. Commun.*, 2015, **6**, 7237–7239.

6 D. Karamessini, S. Poyer, L. Charles and J.-F. Lutz, *Macromol. Rapid Commun.*, 2017, **38**, 1700426.

7 L. Charles, C. Laure, J.-F. Lutz and R. K. Roy, *Macromolecules*, 2015, **48**, 4319–4328.

8 A. Al Ouahabi, M. Kotera, L. Charles and J.-F. Lutz, *ACS Macro Lett.*, 2015, **4**, 1077–1080.

9 S. C. Solleder, K. S. Wetzel and M. A. R. Meier, *Polym. Chem.*, 2015, **6**, 3201–3204.

10 S. C. Solleder and M. A. R. Meier, *Angew. Chemie - Int. Ed.*, 2014, **53**, 711–714.

11 N. Zydziak, F. Feist, B. Huber, J. O. Mueller and C. Barner-Kowollik, *Chem. Commun.*, 2015, **51**, 1799–1802.

12 J. Lawrence, S. H. Lee, A. Abdilla, M. D. Nothling, J. M. Ren, A. S. Knight, C. Fleischmann, Y. Li, A. S. Abrams, B. V. K. J. Schmidt, M. C. Hawker, L. A. Connal, A. J. McGrath, P. G. Clark, W. R. Gutekunst and C. J. Hawker, *J. Am. Chem. Soc.*, 2016, **138**, 6306–6310.

13 J.-F. Lutz, in *Sequence-Controlled Polymers*, ed. J.-F. Lutz, Wiley VCH, Weinheim, 1st edn., 2018, pp. 1–26.

14 S. Martens, J. O. Holloway and F. E. Du Prez, *Macromol. Rapid Commun.*, 2017, **38**, 1700469.

15 S. C. Solleder, R. V. Schneider, K. S. Wetzel, A. C. Boukis and M. A. R. Meier, *Macromol. Rapid Commun.*, 2017, **38**, 1600711.

16 S. Martens, J. Van Den Begin, A. Madder, F. E. Du Prez and P. Espeel, *J. Am. Chem. Soc.*, 2016, **138**, 14182–14185.

17 P. Espeel, L. L. G. Carrette, K. Bury, S. Capenberghs, J. C. Martins, F. E. Du Prez and A. Madder, *Angew. Chemie - Int. Ed.*, 2013, **52**, 13261–13264.

18 S. C. Solleder, S. Martens, P. Espeel, F. E. Du Prez and M. A. R. Meier, *Chem. - A Eur. J.*, 2017, **23**, 13906–13909.

19 J. O. Holloway, S. Aksakal, F. E. Du Prez and C. Remzi Becer, *Macromol. Rapid Commun.*, 2017, **38**, 1700500.

20 S. Martens, A. Landuyt, P. Espeel, B. Devreese, P. Dawyndt and F. E. Du Prez, *Nat. Commun.*, 2018, **9**, 4451.

21 C. Laure, D. Karamessini, O. Milenkovic, L. Charles and J.-F. Lutz, *Angew. Chemie - Int. Ed.*, 2016, **55**, 10722–10725.

22 N. Zydziak, W. Konrad, F. Feist, S. Afonin, S. Weidner and C. Barner-Kowollik, *Nat. Commun.*, 2016, **7**, 1–10.

23 T. T. Trinh, L. Oswald, D. Chan-Seng and J.-F. Lutz, *Macromol. Rapid Commun.*, 2014, **35**, 141–145.

24 A. C. Boukis and M. A. R. Meier, *Eur. Polym. J.*, 2018, **104**, 32–38.

25 A. Al Ouahabi, L. Charles and J.-F. Lutz, *J. Am. Chem. Soc.*, 2015, **137**, 5629–5635.

26 R. B. Merrifield, *J. Am. Chem. Soc.*, 1963, **85**, 2149–2154.

27 D. Frank, P. Espeel, S. Claessens, E. Mes and F. E. Du Prez, *Tetrahedron*, 2016, **72**, 6616–6625.

28 S. Reinicke, P. Espeel and F. E. Du Prez, *Polym. Chem.*, 2014, **5**, 5461–5470.

29 P. Espeel, F. Goethals, M. M. Stamenović, L. Petton and F. E. Du Prez, *Polym. Chem.*, 2012, **3**, 1007–1015.

30 M. M. Stamenović, P. Espeel, E. Baba, T. Yamamoto, Y. Tezuka and F. E. Du Prez, *Polym. Chem.*, 2013, **4**, 184–193.

31 P. Espeel and F. E. Du Prez, *Eur. Polym. J.*, 2015, **62**, 247–272.

32 S. Montolio, O. Zagorodko, R. Porcar, M. Isabel Burguete, S. V. Luis, H. Tenhu and E. García-Verdugo, *Polym. Chem.*, 2017, **8**, 4789–4797.

33 S. Mommer, K. Truong, H. Keul and M. Möller, *Polym. Chem.*, 2016, **7**, 2291–2298.

34 F. Goethals, D. Frank and F. E. Du Prez, *Prog. Polym. Sci.*, 2017, **64**, 76–113.

35 F. Driessen, S. Martens, B. De Meyer, F. E. Du Prez and P. Espeel, *Macromol. Rapid Commun.*, 2016, **37**, 947–951.

36 T. Posner, *Dtsch. Chem. Ges.*, 1905, **38**, 646–657.

37 P. Espeel and F. E. Du Prez, *Macromolecules*, 2015, **48**, 2–14.

38 S. Martens, J. O. Holloway and F. E. Du Prez, in *Sequence-Controlled Polymers*, ed. J.-F. Lutz, Wiley VCH, Weinheim, 2018, pp. 379–416.

39 J. O. Holloway, C. Mertens, F. E. Du Prez and N. Badi, *Macromol. Rapid Commun.*, 2019, **40**, 1800685.

40 G.-Z. Li, R. Randev, A. H. Soeriyadi, G. J. Rees, C. Boyer, Z. Tong, C. R. Becer and D. M. Haddleton, *Polym. Chem.*, 2010, **1**, 1196–1204.

41 D. Ponader, F. Wojcik, F. Beceren-Braun, J. Dernedde and L. Hartmann, *Biomacromolecules*, 2012, **13**, 1845–1852.

42 A. S. Knight, E. Y. Zhou, M. B. Francis and R. N. Zuckermann, *Adv. Mater.*, 2015, **27**, 5665–5691.

43 F. A. Leibfarth, J. A. Johnson and T. F. Jamison, *Proc. Natl. Acad. Sci.*, 2015, **112**, 10617–10622.

44 L. Hartmann, E. Krause, M. Antonietti and H. G. Borner, *Biomacromolecules*, 2006, **7**, 1239–1244.

45 B. L. Bray, *Nat. Rev. Drug Discov.*, 2003, **2**, 587–593.

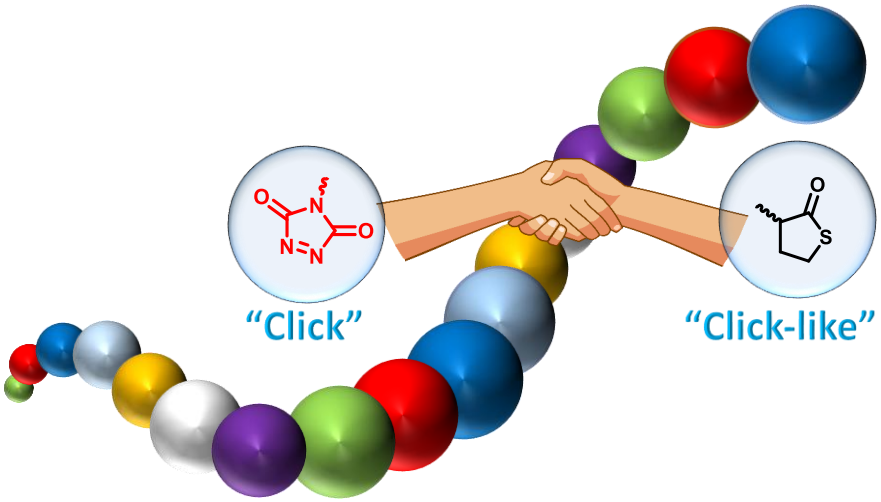
46 P. Espeel, F. Goethals, F. Driessen, L.-T. T. Nguyen and F. E. Du Prez, *Polym. Chem.*, 2013, **4**, 2373–2616.

47 D. P. Nair, M. Podgórski, S. Chatani, T. Gong, W. Xi, C. R. Fenoli and C. N. Bowman, *Chem. Mater.*, 2014, **26**, 724–744.

48 Recommended Peptide Purity Guidelines, www.genscript.com/recommended_peptide_purity.html, (accessed 20 July 2018).

49 Peptide Synthesis Application and Recommended Purity, www.peptide2.com/peptide_synthesis_application.php, (accessed 20 July 2018).

50 U. S. Gunay, B. E. Petit, D. Karamessini, A. Al Ouahabi, J. A. Amalian, C. Chendo, M. Bouquey, D. Gigmes, L. Charles and J.-F. Lutz, *Chem*, 2016, **1**, 114–126.



Abstract

Thiolactone and 1,2,4-triazoline-3,5-dione (TAD) chemistries have evolved over the past decade to be highly efficient tools in polymer synthesis. Whilst the former has also been well-explored within the context of sequence-defined synthesis, TAD chemistry has currently only been used for polymer modification and crosslinking. Within this chapter, TAD is introduced to the field of sequence-defined synthesis for the first time *via* the combination of thiolactone and TAD moieties onto one molecule, enabling the design of a new, efficient and fast iterative protocol, designed for solid-phase chemistry. This chapter describes the synthesis and challenges in synthesising such a multifunctional molecule and its implementation in a sequence-defined protocol. It also highlights how the incorporation of TAD chemistry opened the door to new potential sequence-defined synthesis routes as a result of its ultrafast, selective and dynamic reactivity, which are explored and discussed in more detail in Chapters VI and VII.

Chapter V
Triazolinedione meets thiolactone chemistry in the pursuit of sequence-defined macromolecules

V.1 Introduction

As introduced in the previous two chapters, thiolactone chemistry has demonstrated not only its use in polymer functionalisation and post-modifications,[1–7] but also as a chemical platform for the iterative synthesis of multifunctional, sequence-defined structures.[8–11] This protected thiol is spring-loaded for double modification *via* ring-opening by aminolysis and subsequent thiol-ene reactions.[5,12] Although being a highly efficient, one-pot combination of reactions, the modification of thiolactones has the potential for too many side reactions (particularly disulfide bond formation) to be truly classified as a "click" reaction and therefore is better defined as a "click-like" reaction.[13–15]

Since its introduction in 2001,[16] click chemistry has been seen by many as the most desirable class of chemical reactions. The handful of efficient chemistries that satisfy all of its criteria have gained much attention within the areas of organic[14,17–20] and polymer chemistry,[13,21–29] and have also branched into areas including pharmaceutical research[30] and separation science.[31] In 2011, these criteria were further adapted and expanded to become better applicable to polymer science, taking into account the typically larger scale of polymer coupling reactions.[29] Moreover, click chemistry has since been recognised as one of the key reactions within the sequence-defined chemistry toolbox.[14,15] Indeed, the pursuit of highly precise macromolecules and the repetitive and sometimes complex nature of the reactions undertaken, means that highly efficient and effective chemistries are often desired.

One of the many chemical reactions that have been defined as "click" is the Diels-Alder reaction. Although this chemistry was discovered almost a century before the term "click" was introduced,[32] its use to date within the context of sequence-defined chemistry remains rather limited.[14,15] Existing examples of the use of Diels-Alder chemistry in this field come from Barner-Kowollik and co-workers, who used photochemically triggered Diels-Alder reactions to build symmetrical, sequence-defined oligomers from a bifunctional core.[33,34] Alternatively, a thermally induced retro-Diels-Alder approach combined with thiol-ene chemistry was demonstrated by Grandas and co-workers, whereby sequence-defined oligopeptoids were either functionalised[35] or cyclised.[36,37]

In 2014, our group published work on 1,2,4-triazoline-3,5-diones (TADs),[38] sparking a renewed interest in this fascinating and highly reactive chemistry.[39] Although in existence since 1894,[40] and extensively worked upon by Cookson *et. al.* in the 1960's and 1970's,[41–43] the use of this remarkable class of molecules was relatively underexplored within the field of polymer chemistry. However, the last few years has seen TAD chemistry grow into an area of intense research activity within polymer science, not only fuelled by the interesting and ultra-fast, irreversible click reactions that TADs can undergo, but also by reversible conjugations with certain substrates.[38,44–49] One of the two key reaction types of TADs are the Diels-Alder and Alder-ene reactions (summarised in *Figure V 1*). Through these reactions, TADs can efficiently and reliably undergo reactions with certain substrates in seconds or even less,[39,50] making this class of molecules an ideal candidate to explore in sequence-defined chemistry.

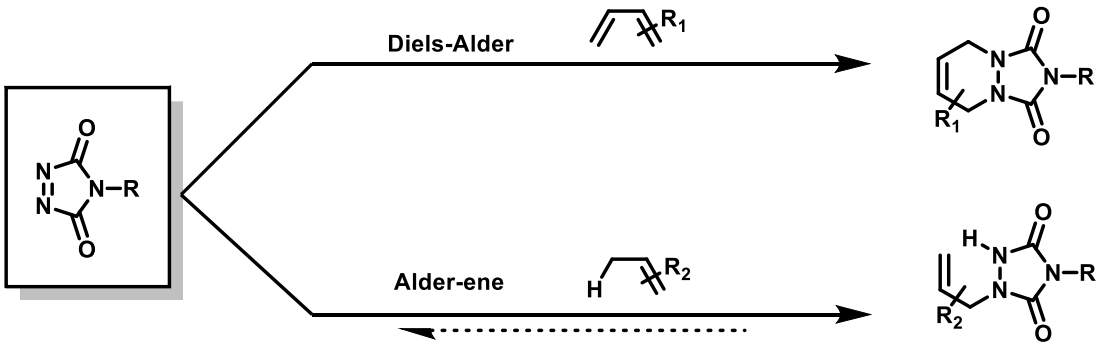


Figure V 1: General overview of the TAD-based irreversible Diels-Alder (top) and reversible Alder-ene (bottom) reactions.

We therefore aimed to combine thiolactone and triazolinedione chemistries to synthesise one multi-functional molecule that could undergo two different, efficient orthogonal chemical reactions, thus facilitating the iterative growth of a multifunctional, sequence-defined macromolecule *via* a new TAD-thiolactone based protocol. Such a molecule would benefit from the click and click-like reactions that these two different functional groups enable and would allow us to further explore the advantages of using the Diels-Alder reaction in sequence-defined synthesis.

The synthesis of TAD compounds carrying a further reactive handle or chemical functionality is relatively unexplored on account of the difficulties in synthesising the functional urazoles (the precursor to TAD compounds – see Chapter II.7.2.1 for details on urazole synthesis).[39] The typical route of semicarbazide synthesis followed by ring closure is often incompatible with specific functionalities.[39] Therefore urazole functionalisation is typically carried out by a post-cyclisation – *i.e.* the coupling of a urazole and another functional compound together. A few routes to urazole modification are known, such as hydrogenation and hydride addition,[38,51–53] electrophilic aromatic substitution[54] or click-type modification (*e.g.* azide-alkyne reactions).[51,55,56]

V.2 Results and discussion

V.2.1 Orthogonality model studies

Prior to synthesising a molecule functionalised with both TAD and thiolactone, several model studies were conducted to assess whether incorporating TAD and thiolactone into one molecule was feasible. These studies (displayed below in *Figure V 2*) aimed to investigate a) the compatibility of TAD and thiolactone moieties when present together, b) whether a urazole species could be oxidised into a TAD in the presence of a thiolactone and c) whether thiolactone moieties would influence the TAD click reaction with a conjugated diene.

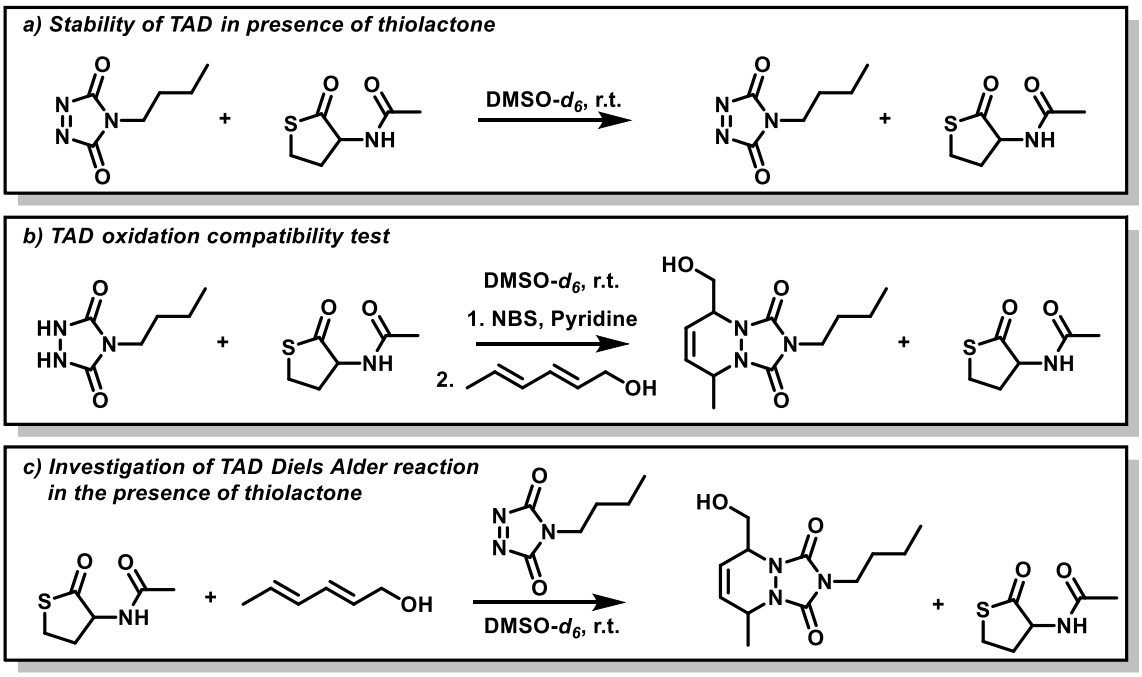


Figure V 2: Overview of the model studies conducted to investigate a) stability, b) oxidation compatibility and c) follow up reaction of a provisional TAD-thiolactone compound.

The first model study (*Figure V 2a*) was conducted to see whether the TAD and thiolactone functionalities were compatible with one another. A 1:1 equivalent ratio of 4-*n*-butyl-1,2,4-triazoline-3,5-dione and D,L-acetylhomocysteine thiolactone were solubilised separately in DMSO-d_6 and added to one another. A ^{1}H NMR measurement was taken after 1 hour and 24 hours and the two spectra were compared, as shown below in *Figure V 3* together with reference spectra of each model compound. After 1 hour, no observable change was visible in the NMR spectrum and the red colour of the solution, arising from the TAD, persisted. After 24 hours, the red colour had disappeared, indicating degradation of the TAD species, which was further evidenced by the increase in the NH proton resonance of the urazole precursor. As the stability of TAD is known to be problematic, it was assumed that the water

content of the deuterated DMSO assisted the TAD hydrolysis. Importantly, no side products arising from thiolactone degradation could be observed. Nevertheless, from this first model experiment it was concluded that TAD and thiolactone were compatible with one another, certainly for at least one hour, which was much longer than required, as the urazole thiolactone would be oxidised and used almost immediately within the planned synthesis approach.

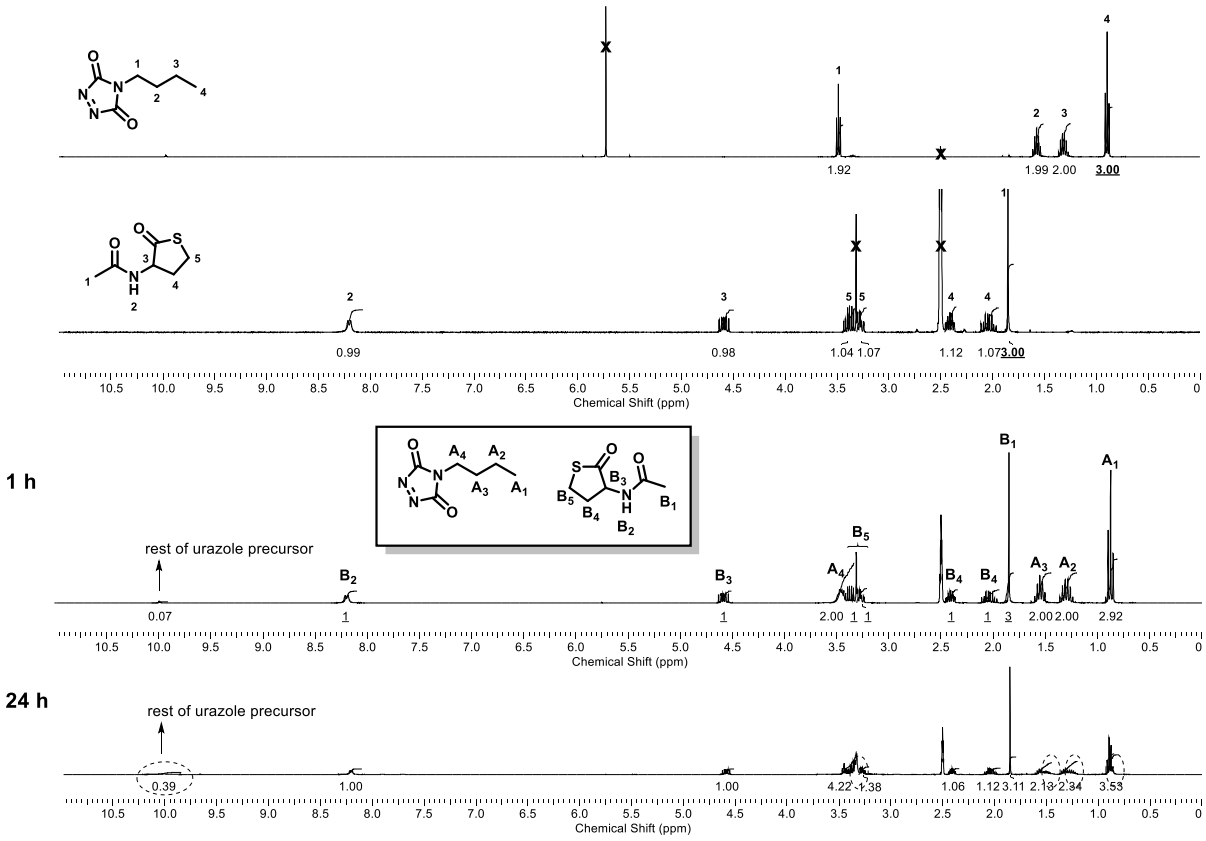


Figure V 3: ^{1}H NMR spectra of stability study of n*-butyl TAD and D,L-*N*-acetylhomocysteine thiolactone. Top) Reference ^{1}H NMR spectra of* n*-butyl TAD and D,L-*N*-acetylhomocysteine thiolactone. Bottom) ^{1}H NMR spectrum of reaction after 1 hour and 24 hours.*

The second model study (*Figure V 2b*) was designed to see whether the thiolactone unit would survive during the oxidation of the urazole into its respective TAD species. The oxidation of the urazole thiolactone molecule would be carried out using *N*-bromosuccinimide (NBS) and pyridine, which was previously reported[51,57] for the conversion of a highly functional urazole into its TAD derivative. Thus, butyl urazole was oxidised *via* this method (the urazole, NBS and pyridine were added in a 1:1:1 ratio) in the presence of 1 equivalent of DL-*N*-acetylhomocysteine thiolactone. A red/pink colour was rapidly observed and the oxidation was left for 10 minutes. Subsequently, 1.2 equivalents of hexa-2,4-dien-1-ol was added to irreversibly react with the newly formed TAD molecule in order to form a stable adduct that could be subjected to analysis. The products of the reaction were analysed both by ^{1}H NMR (*Figure V 4a*) and LCMS (*Figure V 4b*).

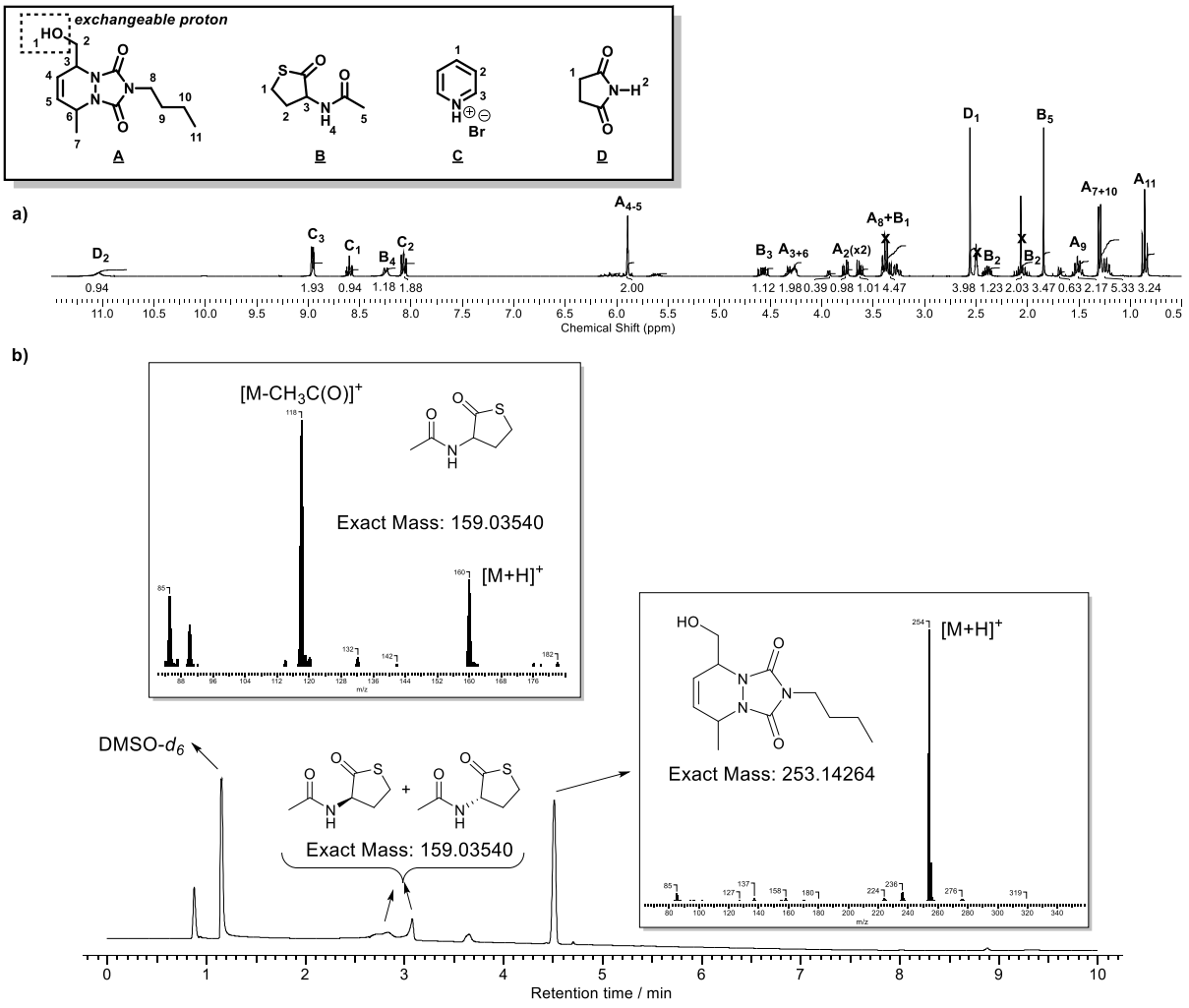


Figure V 4: a) [1]H NMR spectrum of products following the oxidation of butyl TAD in the presence of DL-N-acetylhomocysteine thiolactone and subsequent the addition of hexa-2,4-dien-1-ol. b) LCMS chromatogram at λ = 214 nm of the products of the butyl TAD oxidation model study in the presence of an equimolar amount of thiolactone.

The NMR spectrum shows that the TAD was successfully oxidised, as it immediately reacted with the hexa-2,4-dienol to form a stable Diels-Alder adduct, whilst the thiolactone remained unaffected by the reaction. The oxidation by-products were also visible in the NMR. However, for the envisioned sequence-defined synthesis, the oxidation mixture would be directly added to the solid-phase resin, whereby these oxidation by-products would be removed by repetitive washing steps. LCMS analysis (*Figure V 4b*) corresponded with the masses of the products identified in the NMR spectrum, further confirming that the anticipated TAD adduct was formed and the thiolactone was unaffected by the oxidation. It should be noted that an alternative oxidation route using DABCO-Br in the presence of thiolactone was also attempted, but this was unsuccessful, as it led to a range of unidentified side products.

The final model study (*Figure V 2c*) investigated whether the presence of thiolactone would influence the TAD Diels-Alder reaction. DL-*N*-acetylhomocysteine thiolactone and hexa-2,4-dienol were dissolved in a 1:1 equivalent ratio in DMSO-d_6. Butyl TAD (1 equivalent) was added, the reaction was stirred at room temperature for 5 minutes and the pink colour of the TAD was observed to almost completely disappear. The resulting reaction mixture was analysed by ^{1}H NMR spectroscopy, as shown below in *Figure V 5*, which confirmed the desired TAD Diels-Alder adduct formation, unaffected by the presence of the thiolactone unit.

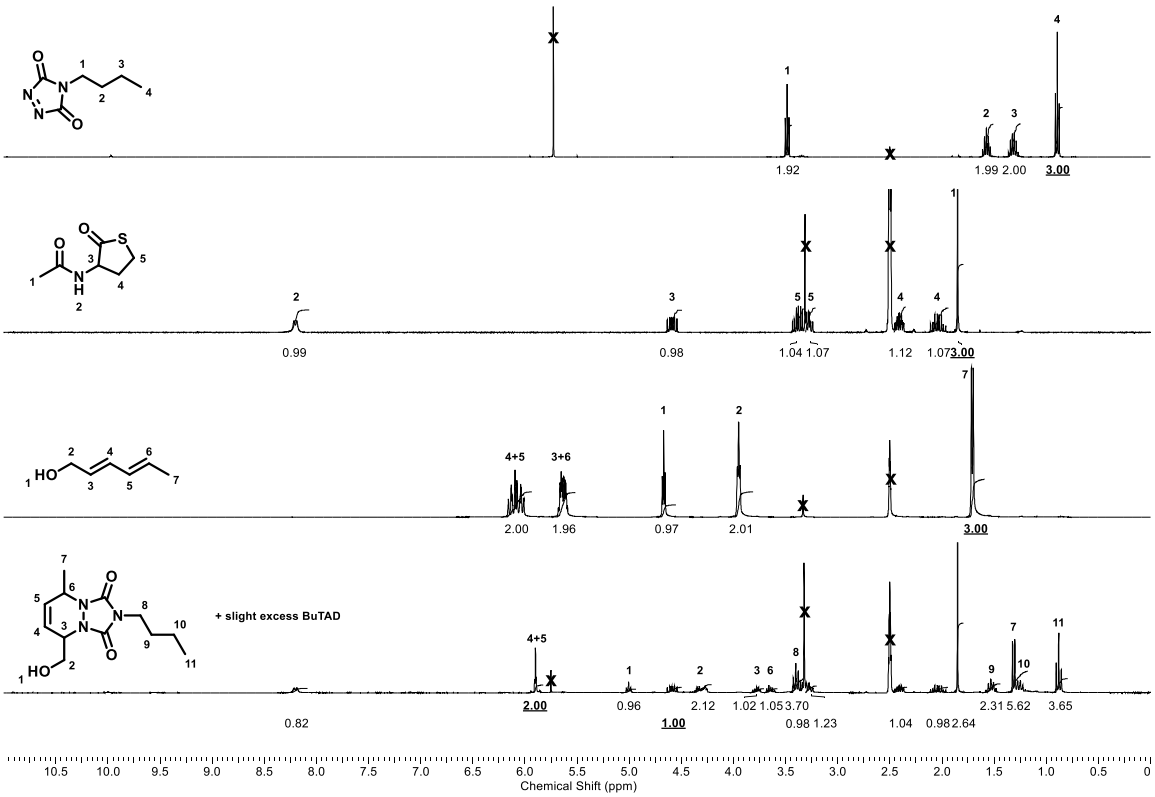


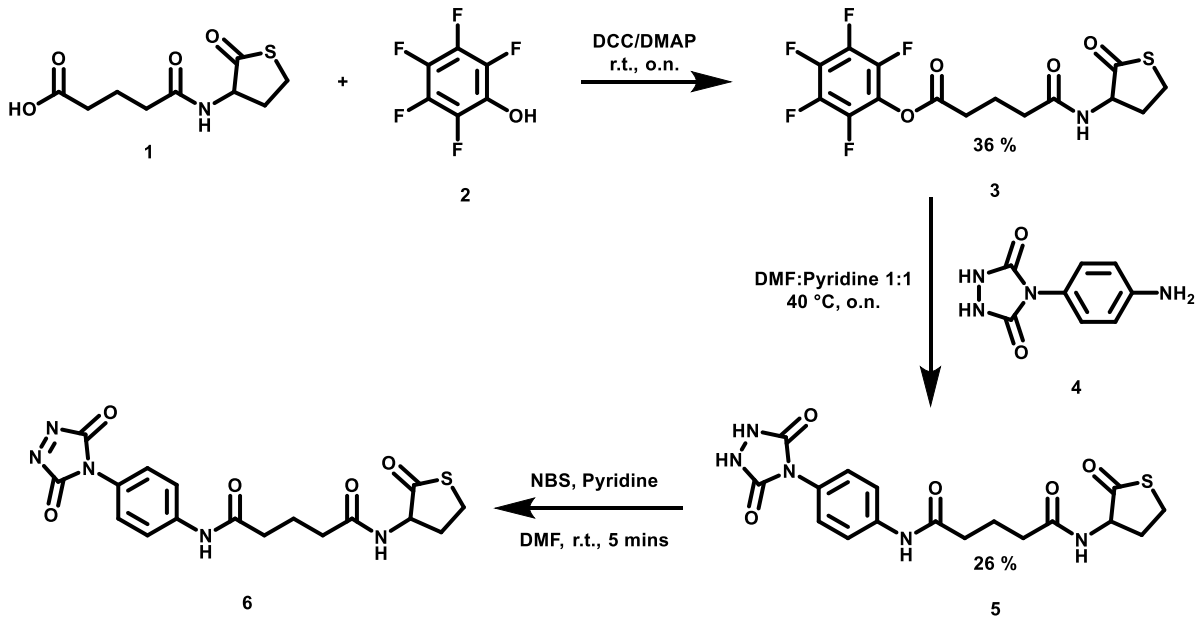
Figure V 5: ^{1}H NMR spectrum of the formed TAD Diels-Alder adduct (bottom) along with reference spectra of the start materials.

V.2.2 TAD-thiolactone synthesis

Following the successful model studies that indicated the possibility of incorporating a TAD and a thiolactone moiety in a single molecule, its synthesis was next explored. However, the synthesis of a functional urazole compound (and its subsequent oxidation to its corresponding TAD molecule) is not always straightforward, as urazole modification is known to be somewhat difficult and limited.[39] Urazoles are formed from the ring-closure of their corresponding semicarbazide (*cf.* Chapter II.7.2.1), and whilst numerous routes towards semicarbazides with a wide range of structural variation exist,[39] the subsequent cyclisation step is principally limited to being performed under thermal or basic

conditions.[39] The compatibility of this reaction step with the sensitive thiolactone functionality meant that post-cyclisation modification needed to be carried out to target the TAD-thiolactone molecule.[39] As such, bringing the two distinct functionalities of thiolactone and TAD together in one molecule presented a unique synthetic challenge.

Within our research group, we have developed and worked with a number of different functional thiolactone building blocks, both in the area of sequence-control but also in the wider context of polymer chemistry.[8,58,59] For this work, the same thiolactone carboxylic acid molecule (**1**) described in previous chapters of this thesis (see Chapter III.4.3.1 for synthesis details) was selected as most suitable building block and modified using pentafluorophenol (**2**) in order to create an activated thiolactone ester (**3**) with a good leaving group (see *Scheme V 1*). This then allowed us to perform a coupling reaction with 4-aniline urazole (**4**). The resulting compound could then be oxidised using NBS to the TAD-thiolactone molecule (**5**) and added directly to the solid-phase resin for use in the sequence-defined synthesis.



Scheme V 1: General overview of the synthesis of TAD-thiolactone by coupling a pentafluorophenol thiolactone and aniline. Overall yield = 9 %, assuming 100 % efficiency of the oxidation step. The experimental details and synthesis of the individual thiolactone and urazole starting components are detailed below in Section V.4.3.

During the synthesis, the purification of both pentafluorophenol (PFP) thiolactone molecule (**3**) and urazole thiolactone (**5**) presented some difficulties. For both products, column chromatography was necessary for purification. For the PFP thiolactone, whilst pure product could be obtained *via* column chromatography, a yield of only 36 % was achieved, because the desired product began to co-elute with an unknown side-product (see *Figure V 6*). The fraction that contained both product and side-product represented a further 49 % of the yield of the column, hence the low overall yield of this reaction.

Analysis by COSY NMR (see *Figure V 6*) showed that the unwanted side-product in this fraction was more than just a contaminant, but chemically bonded to a product of similar structure (possibly an ethanol adduct of the PFP activated compound). The similar polarity of the two products prevented their separation during column chromatography, despite a range of different solvent conditions being investigated. Recrystallisation in a minimum volume of hot toluene was also attempted but was unsuccessful. Other by-products of the reaction, which were removed more successfully during column chromatography, included dicyclohexylurea. However, the simplicity of the PFP thiolactone reaction, combined with the fact that the thiolactone carboxylic acid starting compound could be produced on a large scale (ca. 60 g) and that PFP was commercially available, meant that the low yield of the reaction was not of that great significance.

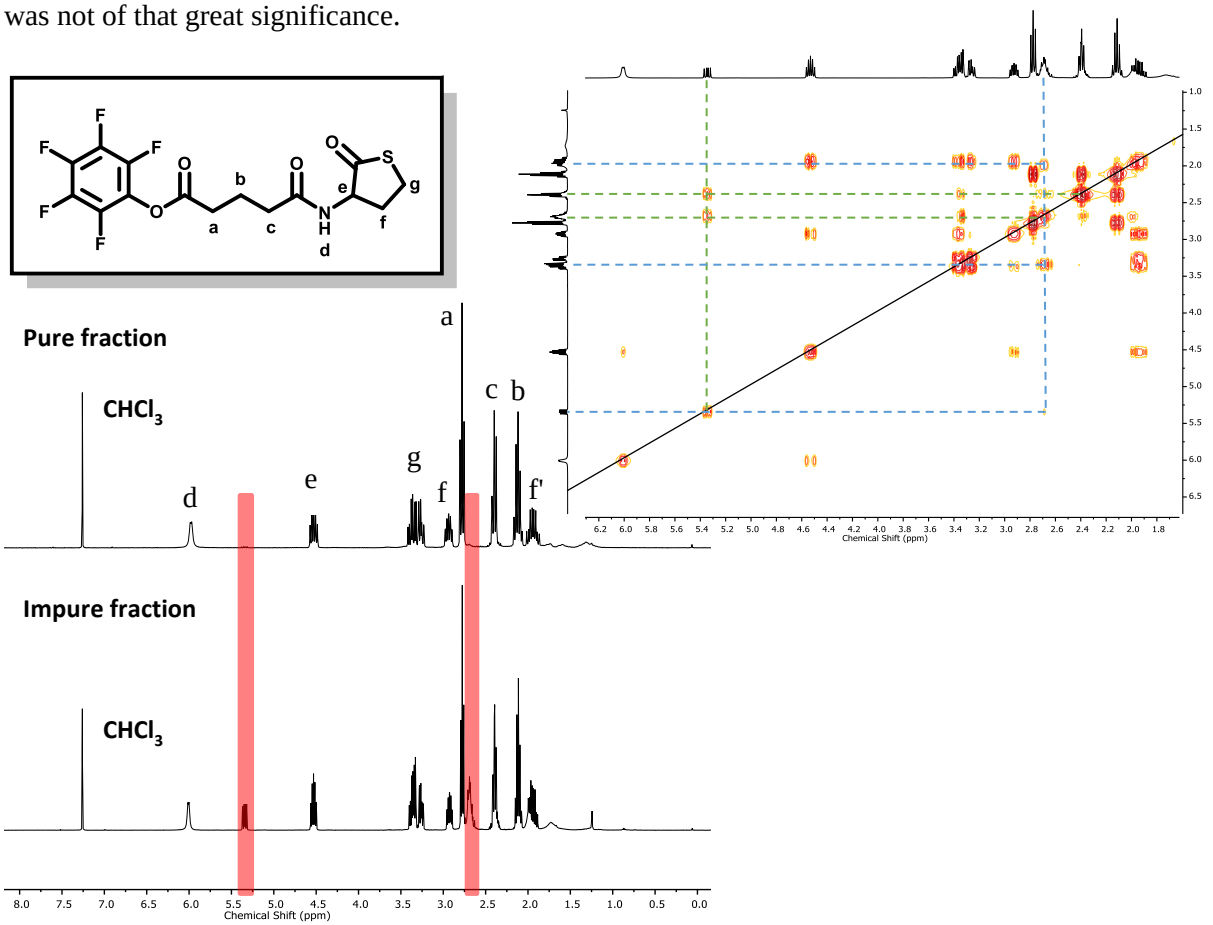
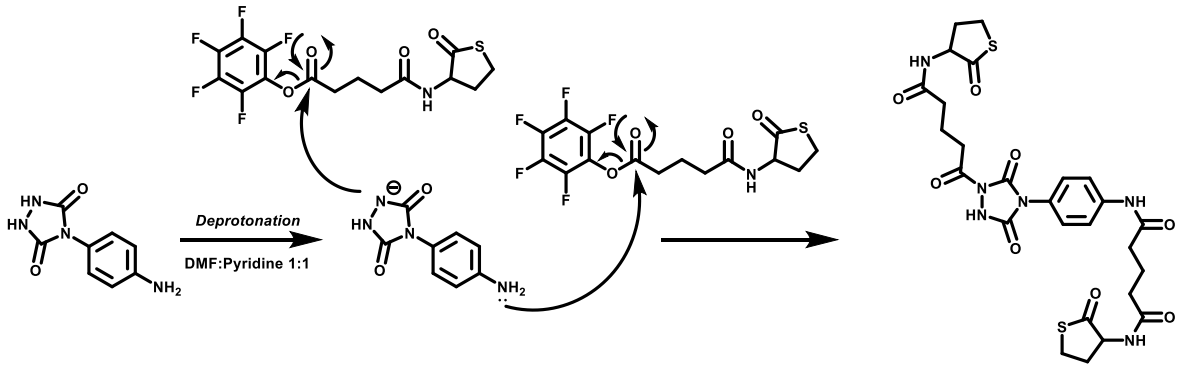


Figure V 6: Top) COSY NMR spectrum of overlapped fraction. Bottom) ^{1}H NMR spectra showing both the pure and overlapped fractions obtained from the column chromatography of the PFP thiolactone.

The following step in the synthesis was to couple the activated PFP thiolactone ester (**3**) with aniline urazole (**4**). Although less nucleophilic than other aliphatic amine-derived urazoles because of the mesomeric effect (caused by the close proximity of the free electron of the nitrogen atom to the aromatic ring), this urazole was chosen because it was much simpler to synthesise than its aliphatic analogues and the resulting TAD-thiolactone molecule could be isolated as a neutral molecule rather than a hydrochloride salt (*vide infra*, Section V.2.4). The potential for side reactions caused by an excess of

either the thiolactone or urazole component meant that they were added in a 1:1 ratio to reduce this. However, double addition of the thiolactone species to the 4-aniline urazole compound did still occur. This is because the pyridine used in the reaction could also deprotonate one of the N-H groups of the urazole, thus enabling an additional nucleophilic attack of the PFP ester (*Scheme V 2*). The presence of traces of this double adduct along with the desired urazole-thiolactone adduct (**5**) was of little concern, as this could not be oxidised further and thus would be washed away following the solid-phase synthesis.



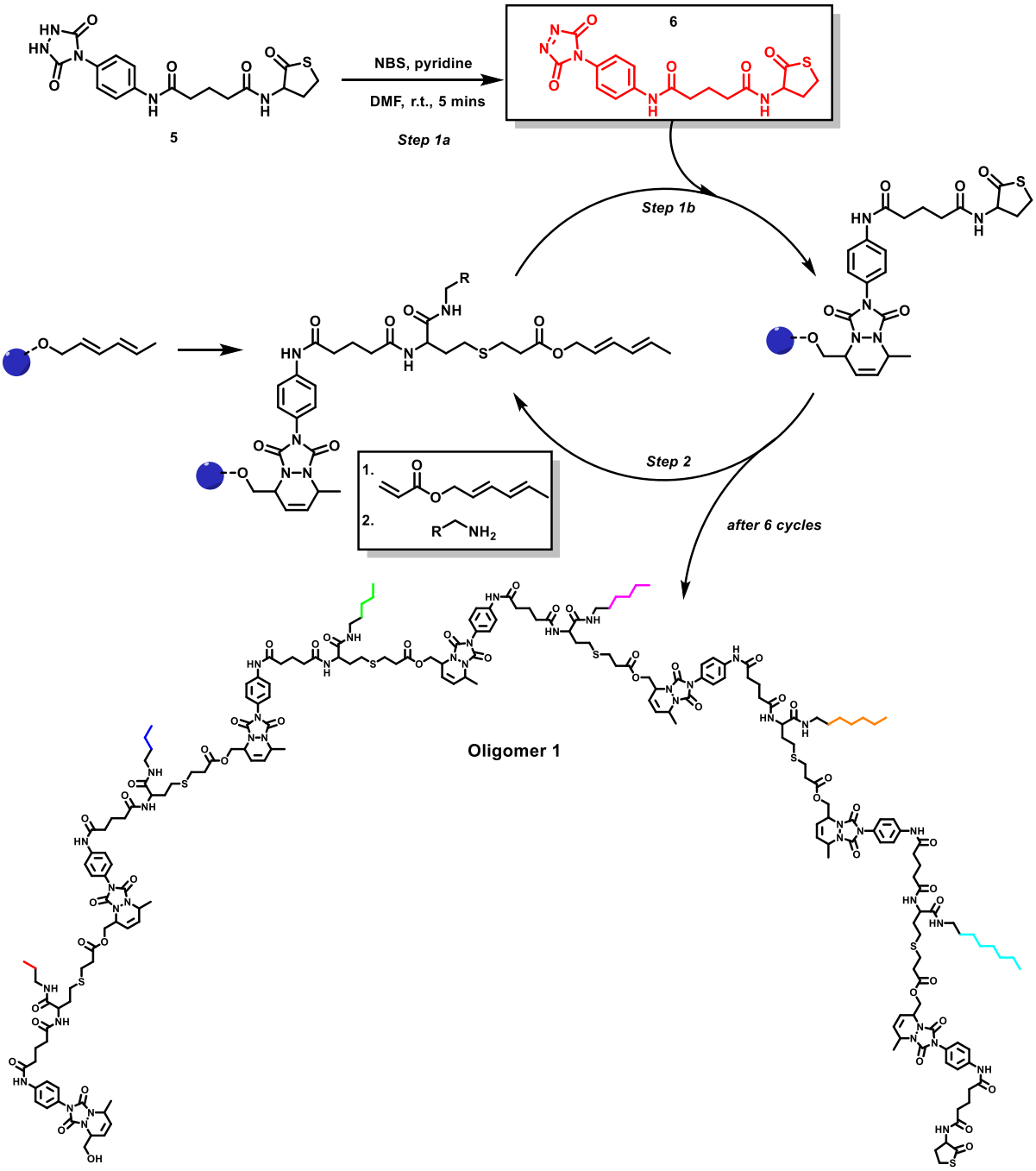
Scheme V 2: Proposed mechanism of possible double thiolactone addition to the 4-aniline urazole compound.

That, in combination with difficulties in separation during column chromatography meant that a low yield (26 %) was recorded for this reaction step. Nonetheless, 0.90 g of urazole thiolactone (**5**) was recovered and its purity analysed by LCMS (*Figure V 8*, Section V.4.3.6) and NMR spectroscopy. Regardless of the low yield, the small scale of solid-phase reactions and the high efficiency of TAD Diels-Alder reactions meant that only 2 equivalents of the TAD thiolactone molecule were needed per iterative cycle (*i.e.* 34 mg) to carry out the desired sequence-defined synthesis (*vide infra*). The urazole thiolactone molecule was finally oxidised to its corresponding TAD compound just before use. Urazoles are much more stable than TADs and have a shelf-life of years compared to hours/months (depending on storage) for TAD compounds.[39] The NBS/pyridine assisted oxidation reaction took 5 minutes and the resulting dark red reaction mixture was subsequently added to the solid-phase resin.

V.2.3 Implementation of TAD-thiolactone within a sequence-defined protocol

Following the synthesis of a compound containing both thiolactone and TAD functional groups, a multi-step solid-phase protocol was developed. 2-Chlorotrityl chloride resin was functionalised with sorbic alcohol, thus immobilising a conjugated diene directly onto a solid support. Urazole-thiolactone was oxidised, and the reaction mixture was added directly to the solid-phase resin. The ultra-fast reactivity of TAD meant that only 2 equivalents of reagent (notably low equivalents for solid-phase reactions)[60]

and 5 minutes of shaking were sufficient to achieve 100 % conversion (according to LCMS). The pendant thiolactone group was then available for modification *via* aminolysis. A range of different primary amines were used to introduce the sequence definition, and hexa-2,4-diene acrylate was synthesised, functioning both as a Michael acceptor for the released thiol during aminolysis and a as new conjugated diene for the subsequent addition of TAD-thiolactone. Hence, the continuation of the sequence-defined synthesis was enabled through an iterative protocol (see *Scheme V 3*).



Scheme V 3: Iterative solid-phase protocol for the synthesis of sequence-defined oligomers using the TAD-thiolactone molecule and the resulting oligomer ***1****.*

The protocol was implemented to synthesise a sequence-defined oligomer (**1**), using six different aliphatic amines (see *Table V 1*, Section V.4.4.3 for details). These non-functional aliphatic amines were selected in part because they are known to have relatively fast rates of thiolactone aminolysis (compared to other functionalised amines),[61] and also they do not contain functionalities that could react inadvertently with TAD.

For both the urazole thiolactone oxidation (step 1a, *Scheme V 3*) and the reaction of the TAD thiolactone with the conjugated diene (step 1b), 5 minutes was enough to achieve full conversion. As described previously in Chapter IV, the thiolactone aminolysis step was followed by LCMS to assess when the reaction had reached 100 % conversion. LCMS also enabled a quantitative assessment of purity as one could see the disappearance of the peak corresponding to the previous step in the chromatogram and the appearance of potential side products. During the first aminolysis with propylamine, it was observed that a reaction time of 30 minutes was not quite enough, but when filtering the reaction and adding fresh solvent and reagents and shaking for a further 30 minutes, one saw the complete disappearance of the unopened thiolactone from the previous step. However, in order to be sure and to compensate for slower reaction times in the case of longer aliphatic amines, 3 x 30 minutes was selected as the reaction time for this first step. From the 5th cycle, this was even increased to 4 x 30 minutes, as one observed a slowing down of the reaction kinetics, as also observed and discussed in Chapter IV and VII.

Figure V 7 below shows LCMS chromatograms recorded after each cycle (taken after the TAD-thiolactone addition reaction) in the synthesis of oligomer **1**. Whilst an LCMS was also taken after the thiolactone aminolysis steps to check conversion, only the chromatograms following the TAD thiolactone addition are displayed below. This is because the mildly acidic cleavage conditions (1 % TFA in CH_2Cl_2) were suspected to cause ester hydrolysis, resulting in the elimination of the conjugated diene group. Therefore, two peaks appeared in the LCMS chromatograms, one corresponding to the product mass, and one corresponding to the product mass minus that of the conjugated diene group (-80 Da). As can be seen in *Figure V 7*, minor impurities were visible in each cycle of the synthesis. An unavoidable side reaction that was observed to a lesser or greater degree was the partial oxidation of one of the thioether moieties to a sulfoxide, caused by the TFA present during cleavage and the difficulty in conducting this in an inert environment. In the first cycle, the presence of TFA is also seen to form an ester with the -OH group that is formed upon cleavage of the solid support.

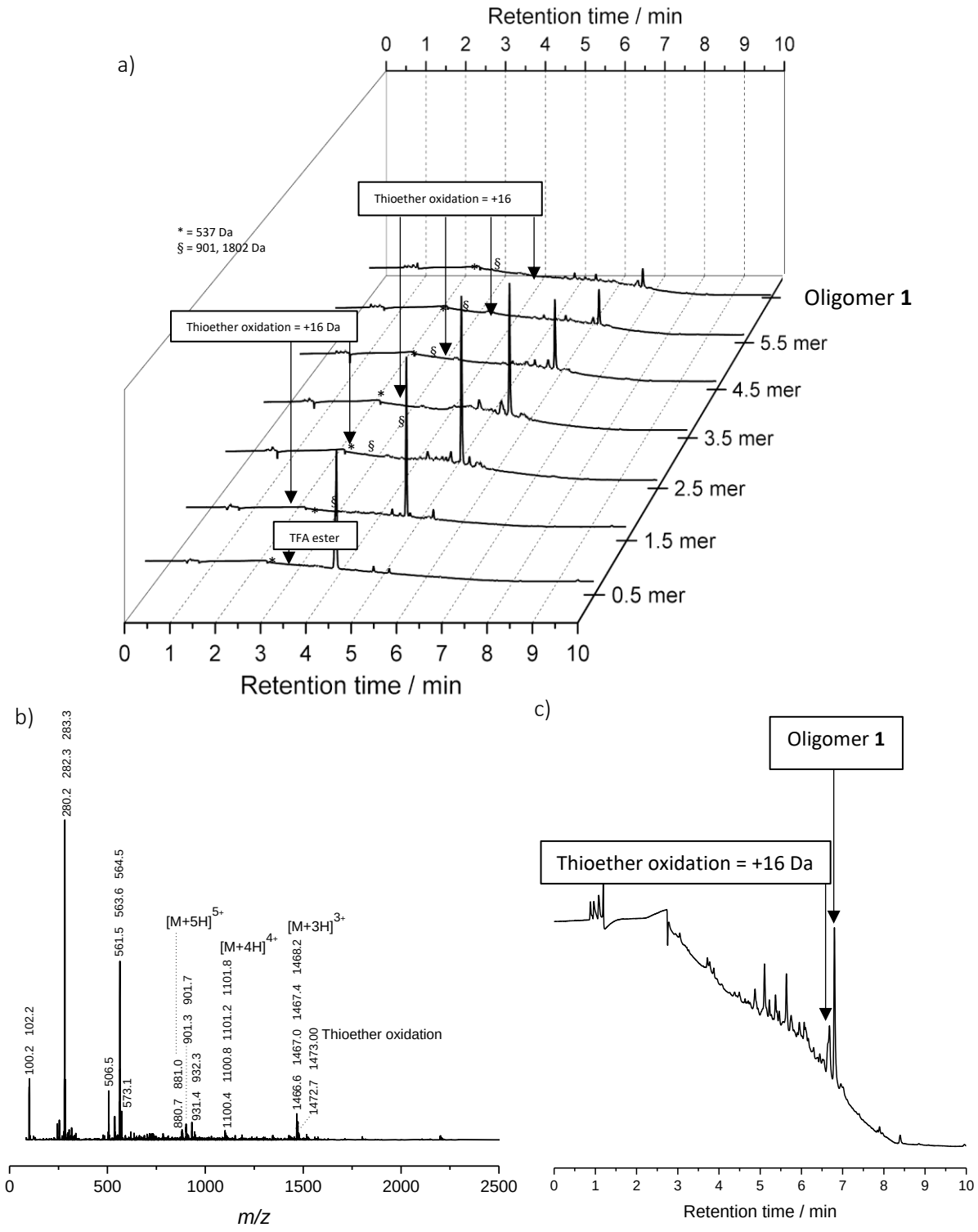


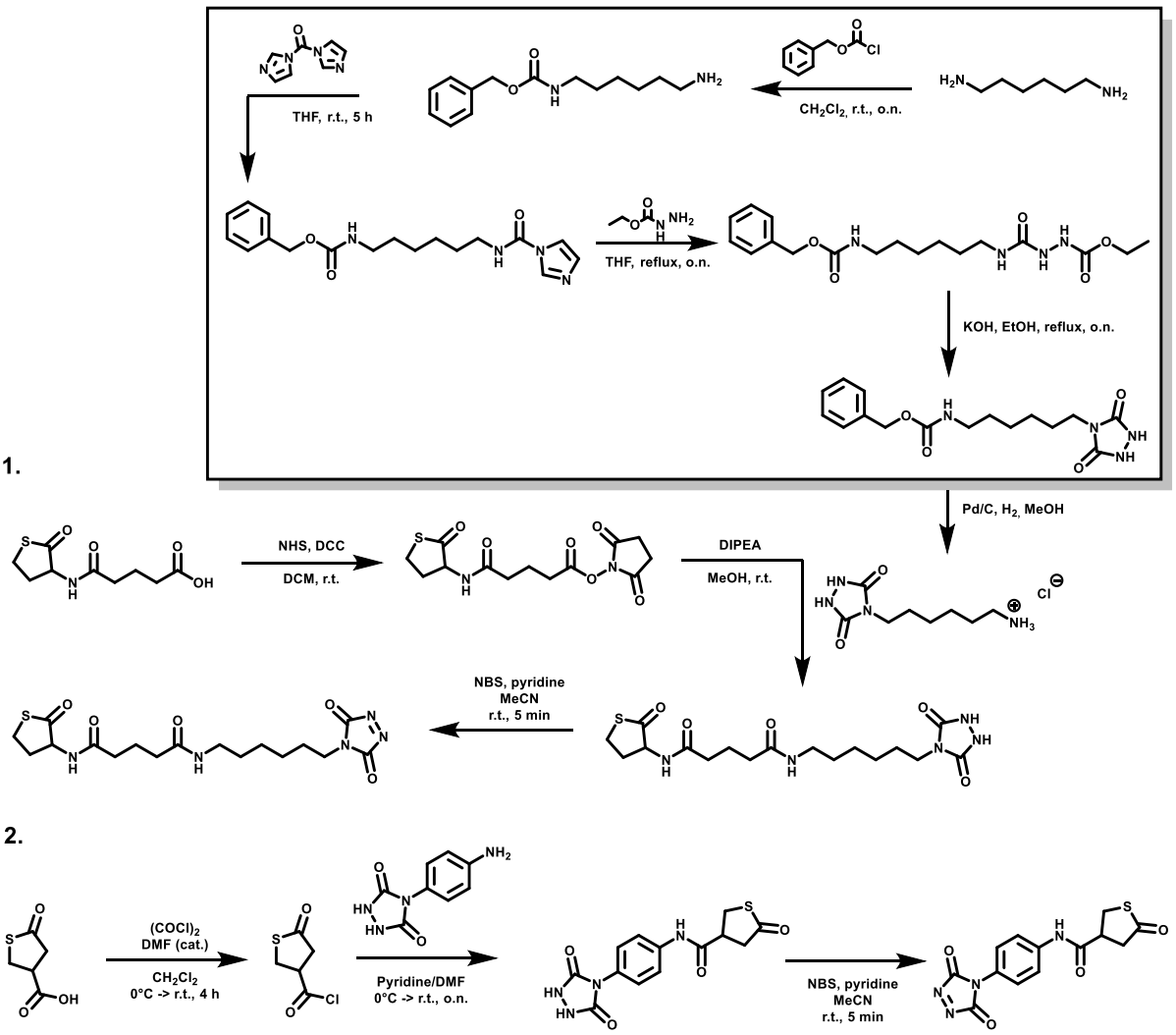
*Figure V 7: a) Stacked LCMS chromatograms (λ = 214 nm) displaying the oligomer after each TAD-thiolactone addition. The main peak in each step corresponds to the desired product. Side peaks include that of a partial oxidation of one of the thioether groups in the structure during cleavage from the resin using a 1 % TFA solution and ester formation with the TFA. * and § denote two unassignable recurring impurities/contaminations. b) ESI-MS spectrum (positive mode) of oligomer **1**. c) Zoom-in of LCMS chromatogram (λ = 214 nm) of oligomer **1**.*

Whilst the purity during the first five cycles of the synthesis remained relatively high, this was seen to drop during the following two. This suggested that the length and structure of the growing oligomer may have had an effect on the efficiency of the synthesis. Potentially the remaining impurities within the urazole thiolactone or the limited stability of the hexa-2,4-diene acrylate may have also influenced the resulting oligomer purity. The relative drop in the height of the peaks of the LCMS chromatograms of *Figure V 7* in the final cycles can be attributed to a reduction in relative sample concentration during analysis, despite the same amount of resin being cleaved for analysis each time (2 mg). Nonetheless, oligomer **1** was successfully synthesised, confirmed not only by LCMS but also by HRMS and NMR (see Section V.4.5).

V.2.4 Alternative routes to urazole thiolactone synthesis

Despite the imperfections and difficulties experienced during the synthesis of the TAD-thiolactone molecule, alternative routes towards the synthesis of such a functionalised molecule were also explored, but each of them proved to be either problematic during the synthesis or during their subsequent use within the sequence-defined protocol. *Scheme V 4* gives an overview of the alternative synthesis routes attempted, which are briefly discussed in this section.

Route 1 (*Scheme V 4*) bears resemblance to the method eventually used in the discussed protocol (*vide supra, Scheme V 1*). It required the synthesis of an activated ester (in this case using *N*-hydroxysuccinimide (NHS)), which was then coupled to an aliphatic urazole amine and oxidised using NBS and pyridine. Whilst the urazole was successfully synthesised and the oxidation appeared to be successful (as indicated by the colour change from a beige to dark red solution), the subsequent Diels-Alder reaction with a conjugated diene was not able to go to full completion. Considering the high and efficient reactivity of TAD species, this was an unexpected result. However, it was later concluded that the diisopropylethylamine (DIPEA) used to deprotonate the urazole amine salt was too difficult to remove, and its presence partially destroyed the TAD *in situ* as it was formed. Another disadvantage to this route was the tedious, 5-step synthesis towards the aliphatic urazole amine (in contrast, the 4-aniline urazole was synthesised in 3 steps, starting from the commercially available *p*-nitrophenol isocyanate). The synthesis resulted in a urazole amine chloride salt, and as mentioned above, its deprotonation led to further problems when oxidising the urazole to the corresponding TAD molecule.



Scheme V 4: Overview of alternative routes proposed for the synthesis of a TAD-thiolactone functional molecule.

A second alternative route explored a β-substituted thiolactone carboxylic acid molecule, prepared according to a previously published procedure (*Scheme V 4*).[58] This was transformed into an acid chloride, which provided a reactive site for nucleophilic attack with the 4-aniline urazole compound. The resulting urazole thiolactone compound was again oxidised to its corresponding TAD using NBS and pyridine. Whilst this strategy proved to be a higher yielding (i.e. 46 % instead of 26 % for the coupling reaction) and a more straightforward route with respect to synthesis and purification, it later transpired that the substitution at the β-position was far from ideal. Whilst the oxidation, subsequent TAD Diels-Alder reaction and the first thiolactone aminolysis step were successful, subsequent reaction steps were indeed problematic. Analysis by LCMS showed that in addition to the desired product being formed, side reactions occurred. The side group introduced by the aminolysis reaction appeared to be eliminated and it was suggested that the additional carbon atom, caused by the β- rather than γ-substitution facilitated the formation of a 5-membered ring intermediate, thus enabling the elimination.

This created problems for both the synthesis and analysis of the sequence-defined oligomer. Thus, this approach was not pursued any further.

V.3 Conclusion and outlook

Whilst this chapter does not present the most impressive, or purest sequence-defined oligomer described within this thesis, it does highlight the potential and advantage of using TAD chemistry within the context of sequence-defined synthesis. Through the successful yet challenging search to synthesise a TAD-thiolactone molecule, click and click-like reactions were nonetheless married together, resulting in a new, iterative, synthetic protocol, designed to be carried out on the solid-phase. This yielded a sequence-defined oligomer, carrying 6 different side groups. The developed protocol can be viewed as an improvement to the route discussed in Chapter IV, where although sequence-definition was again introduced *via* thiolactone aminolysis, the re-introduction of the functional thiolactone handle was much improved. Reaction times for this step were reduced from 2 hours to 5 minutes thanks to the highly efficient TAD Diels-Alder reaction, which was not accompanied by the complications that arose when using α-thiolactone-γ-isocyanate. The amount of reaction equivalents was also significantly reduced to just 2 equivalents of TAD-thiolactone compared with 20 equivalents of thiolactone isocyanate. Moreover, the bench-stable urazole was synthesised on a large enough scale and oxidised on demand, thus eliminating any long-life stability problems, which is the case with the isocyanate reagent.

The length of the oligomer backbone may be something to consider for the future, as the one presented here is quite long. This could cause too much flexibility in the macromolecular chain and movement of the pendant side-groups, thus losing the advantage of controlling the sequence definition. Also, whilst it was assumed that the slight excess of TAD would be completely washed away during the reaction work-up, residual TAD-thiolactone may have led to some of the impurities observed. The quenching of excess TAD was investigated in the work in the following chapter. As a result of the findings of this study, it was decided to change direction for the remainder of this PhD and to focus further on the use of TAD chemistry in favour of thiolactones in the pursuit of developing new, sequence-defined synthesis protocols as this reaction step was deemed to be much quicker and more robust. However, despite the imperfections of the protocol discussed within this chapter, the potential that the herein reported TAD-thiolactone molecule has for polymer post-modification is currently being explored by another colleague. If the synthesis and purification of this molecule could be further optimised, the potential to easily modify the backbone of any alkene-containing polymer such as polyisoprene, or the end-group of a diene or alkene-terminated polymer with the TAD-thiolactone molecule could be of

interest. Such a post-modification would therefore facilitate a further double modification of the polymer, by means of the newly installed thiolactone functionality and could enable one to alter the physical properties of the polymer (*e.g.* the introduction of a hydrophilic group to a hydrophobic polymer). Although interesting, these ongoing investigations fall outside the scope of sequence-defined chemistry and the present thesis.

V.4 Experimental details

This research was carried out in collaboration with Dr Hannes Houck (UGent), who is currently exploring the use of TAD-thiolactone in the post-modification of polydienes. The development and synthesis of the TAD-thiolactone molecule was therefore a joint effort.

V.4.1 Materials and separation techniques

All chemicals were used as supplied, unless otherwise stated. DMSO-d_6 ≥ 99.8 % and $CDCl_3$, ≥ 99.8 % were purchased from Euriso-top. D,L-Homocysteine thiolactone hydrochloride, 99 % was purchased from Haihang Industry (Jinan City, China). Magnesium sulfate, dried, ≥ 99 %, potassium carbonate, ≥ 99 %, sodium hydrogen carbonate, ≥ 99 % and sodium chloride, ≥ 99 % were purchased from Carl Roth. Acetic acid 99-100 % and hydrochloric acid, 36 % was purchased from Chem Lab NV. Trifluoroacetic acid, peptide grade and 2-chlorotrityl chloride resin (100-200 mesh, 1 % DVB, 1.6 mmol/g) were purchased from Iris Biotech GmbH. Acryloyl chloride, 96 % with phenothiazine stabiliser was purchased from abcr GmbH, Germany. Anhydrous dichloromethane, 99.8 %, anhydrous *N,N'*-dimethylformamide, 99.8 %, anhydrous tetrahydrofuran, 99.5 %, extra dry, over molecular sieves, anhydrous pyridine, 99.5 %, extra dry, ethyl carbazate, 97 %, hydroquinone inhibitor and methanol, HPLC grade, 99.8 % were purchased from Acros Organics. Dicyclohexylcarbodiimide (DCC) 99% and sorbic alcohol 98 % were purchased from Alfar Aesar. Acetonitrile and chloroform, HPLC grade ≥ 99.9 %, DL-*N*-acetylhomocysteine thiolactone 98 %, *N*-bromosuccinimide, ReagentPlus® 99 %, ethyl acetate, HPLC grade, ≥ 99.7 %, 4-nitrophenyl isocyanate 97 %, octylamine 99 %, potassium hydroxide 90 % and anhydrous triethylamine, ≥ 99.5 % were purchased from Sigma Aldrich. Hexane, HPLC grade was purchased from VWR. *N,N'*-dimethylformamide, dichloromethane, diethyl ether and toluene, HPLC grade, ≥ 99.8 % were purchased from Fischer Scientific. Amylamine 98.0 %, butylamine 99.0 %, dimethyl aminopyridine > 99.0 %, heptylamine 98.0 %, hexylamine 99.0 %, palladium hydroxide on carbon, wetted with ca. 50 % water, pentafluorophenol 98.0 % and propylamine 98.0 % were purchased from Tokyo Chemical Industry (Europe). Water, when used in the synthesis, was de-ionised. Silicagel (60 Å, 40-63 μm) was supplied by ROCC and used for purification of compounds by column chromatography. Thin Layer Chromatography (TLC) was performed using Merck Kieselgel 60 F254 coated aluminium plates.

V.4.2 Analytical methods

Nuclear Magnetic Resonance (NMR): ^{1}H- and ^{13}C-NMR Attached Proton Test (APT) spectra were recorded on a Bruker Avance 300, a Bruker Avance 400, Bruker Avance 500 or a Bruker Avance II 700. ^{19}F NMR was recorded on a Bruker Avance 500. Chemical shifts are presented in parts per million (δ) relative to DMSO-d_6 or $CDCl_3$ (2.50 ppm or 7.26 ppm in ^{1}H- and 39.51 ppm or 77.24 ppm in ^{13}C-NMR, respectively) as internal standard. Coupling constants (J) are reported in Hertz (Hz). All measurements were recorded in a standard fashion at 25 °C unless otherwise stated. Full assignment of structures was aided by 2D NMR analysis (COSY, HSQC and HMBC).

Electrospray Ionisation Mass Spectrometry (ESI-MS) and Liquid Chromatography Mass Spectrometry (LCMS): An Agilent technologies 1100 series LC/MSD system equipped with a diode array detector and single quad MS detector (VL) with an electrospray source (ESI-MS) was used for classic reversed phase LCMS and MS analysis. Analytic reversed phase HPLC (high-performance liquid chromatography) was performed with a Phenomenex Kmetex C18 (2) column with a solid core at 35 °C and a flow rate of 1.5 mL/min (5 µ, 150 x 4.6 mm) using a solvent gradient (0 → 100 % acetonitrile in H_2O in 6 min) and the eluting compounds were detected via UV-detection (λ = 214 nm). LCMS spectra were analysed using ACD/Spectrus software and the purity of compounds was assessed by integrating the LC peaks (λ = 214 nm) using the in-software function.

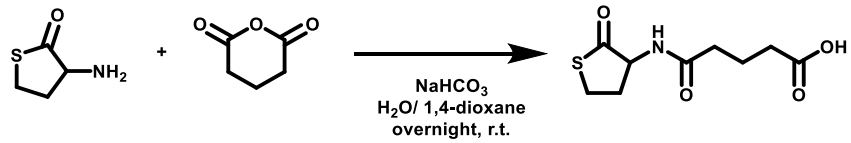
High Resolution Mass Spectroscopy (HRMS): HRMS spectra were collected using an Agilent 6220 Accurate-Mass time-of-flight (TOF) equipped with a multimode ionization (MMI) source.

Infrared spectra were recorded with Attenuated Total Reflection (ATR) with a PIKE Miracle ATR unit and a Perkin Elmer FTIR SPECTRUM 1000 spectrometer.

V.4.3 Synthesis of thiolactone and urazole functional building blocks

V4.3.1 Synthesis of thiolactone carboxylic acid

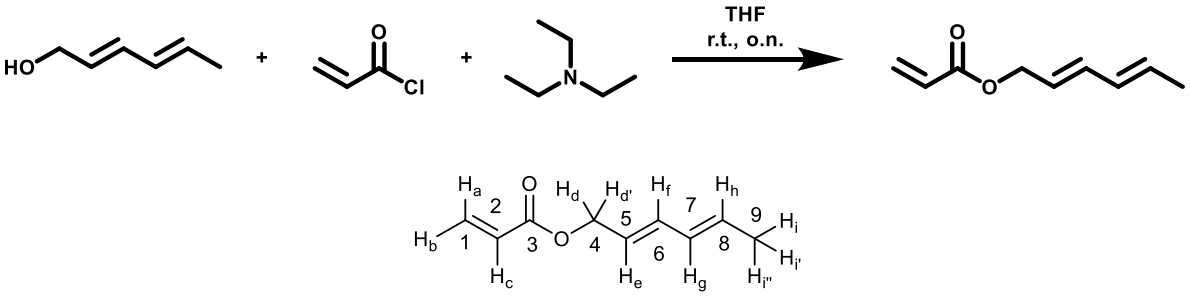
Thiolactone-carboxylic acid was prepared by a modified version of the previously reported procedure,[59] *as schematised below.*



See Chapter III.4.3.1 for experimental procedure and full characterisation.

V.4.3.2 Synthesis of hexa-2,4-diene acrylate

This was synthesised according to an adapted version of a previously reported procedure.[62]



NMR Assignment

Sorbic alcohol (6.39 g, 0.065 mol, 1.0 equiv.) was dissolved in anhydrous THF (100 mL) and triethylamine (13.8 mL, 0.0975 mols, 1.5 equiv.) was added. The reaction was stirred for 5 minutes at 0 °C, under an inert atmosphere, before acryloyl chloride (6.4 mL, 0.078 mols, 1.2 equiv.) was added dropwise. Once added, the reaction was allowed to warm to room temperature and then left to stir overnight. The reaction was then diluted with water (60 mL) and extracted with diethyl ether (3 x 60 mL). The organic phases were combined and dried over Mg_2SO_4, filtered and following the addition of hydroquinone inhibitor, the solvent was removed *in vacuo*. The resulting yellow oil was purified by column chromatography (1:9, ethyl acetate:hexane), R_f = 0.53, resulting in a colourless liquid. Yield = 58 % (m = 5.75 g). **^{1}H NMR (400 MHz, DMSO-*d*$_6$):** δ = 6.42-6.01 (m, 4H, $H_{b,c,f,g}$), 5.94 (dd, *J* = 10.2, 1.8 Hz, 1H, H_a), 5.85-5.53 (m, 2H, $H_{e,h}$), 4.63 (d, *J* = 6.4 Hz, 2H, $H_{d,d'}$), 1.72 (d, *J* = 7.0 Hz, 3H, $H_{i,i',i''}$). **^{13}C NMR APT (100 MHz, DMSO-*d*$_6$):** δ = 168.18 (C_3), 134.33 (C_6), 131.52 (C_1), 130.80 (C_8), 130.48 (C_7), 128.25 (C_2), 124.07 (C_5), 64.36 (C_4), 17.86 (C_9). **HRMS (ESI) *m/z*:** $[M + H]^+$ calculated for $C_9H_{13}O_2^+$, 153.0910; found, 153.0905. **IR** (ATR platinum diamond): ν [cm^{-1}] = 3024 & 2937 (C-H), 1721 (C=O), 1662 & 1635 (C=C), 1444 & 1406 (C-H), 1294, 1266, 1178 & 1044 (C-O), 984, 965 & 809 (C=C). It was observation that the lifetime of the hexa-2,4-diene acrylate, despite being stored under N_2, in the fridge and with hydroquinone inhibitor, was little more than 4-5 months before degradation of the molecule began to influence the experimental results.

V.4.3.3 Synthesis of 4-butyl TAD

This was synthesised according an adapted version of a previously reported procedure.[63] *4-*n*-Butyl-1,2,4-triazolidine-3,5-dione was synthesised according to a previously reported procedure,*[38] *as was the DABCO-Br.*[64]

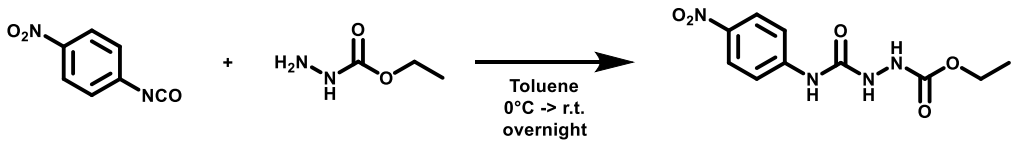
A mixture of 4-*n*-butyl-1,2,4-triazolidine-3,5-dione (2.0 g, 12.7 mmol, 1.0 eq.) and DABCO-Br (4.0 g, 2.54 mmol, 0.2 eq.) in 60 mL dichloromethane was placed under inert atmosphere and stirred at room temperature in the dark for 2 h. The resulting mixture was filtered, washed with CH_2Cl_2 (2 x 60 mL)

and the solvent was removed *in vacuo* at 35 °C. The resulting carmine red crystals (72 %, 1.41 g) were stored in the dark at -18 °C and regularly checked for purity prior to use. **^{1}H-NMR (400 MHz, DMSO-*d*$_6$):** δ = 3.47 (t, *J* = 7.0 Hz, 2H, N-C<u>H</u>$_2$,), 1.56 (quint, *J* = 7.3 Hz, 2H, N-CH$_2$-C<u>H</u>$_2$,), 1.30 (sext, *J* = 7.3 Hz, 2H, C<u>H</u>$_2$-CH$_3$,), 0.88 (t, *J* = 7.3 Hz, 3H, C<u>H</u>$_3$). **^{13}C-NMR (100 MHz, DMSO-*d*$_6$):** δ = 160.15 (C), 40.34 (CH$_2$), 28.72 (CH$_2$), 19.11 (CH$_2$), 13.32 (CH$_3$)**.**

V.4.3.4 Synthesis of 4(4-aminophenyl) urazole

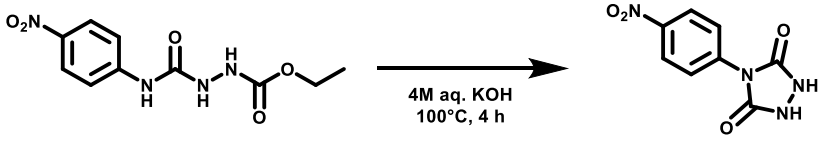
This was synthesised according to an adapted version of a previously reported procedure.[65]

Step 1:



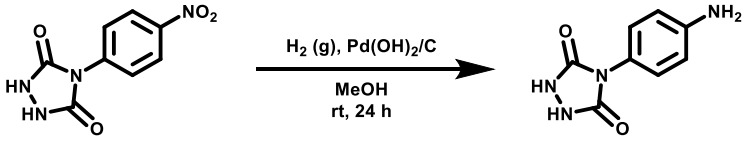
A solution of 4-nitrophenyl isocyanate (10.0 g, 0.061 mol, 1 eq.) was dissolved in toluene (100 mL) and placed under an inert atmosphere and cooled in a water-ice bath to 0 °C. To this, a solution of ethyl carbazate (6.34 g, 0.061 mol, 1 eq.) in toluene (100 mL) was added dropwise at 0 °C. The reaction was then left to stir overnight at room temperature. The reaction mixture was then cooled to 0 °C for 30 minutes and filtered. The solid residue was washed with 2 x 50 mL toluene and dried overnight under vacuum at 40 °C, yielding 4-(4-nitrophenyl)-1-(ethoxycarbonyl) semicarbazide as an off-white powder, 98 % (m = 16.1 g). **^{1}H NMR (400 MHz, DMSO-*d*$_6$):** δ = 9.52 (s, 1H, Ar-NH-C(O)-NH-N<u>H</u>), 8.66 + 9.04 (s, 1H, Ar-NH-C(O)-N<u>H</u>), 8.39 (s, 1H, Ar-N<u>H</u>), 8.11-8.20 (m, 2H, Ar<u>H</u>), 7.60-7.81 (m, 2H, Ar<u>H</u>), 4.07 (q, 2H, C<u>H</u>$_2$, *J* = 14.1, 7.2 Hz), 1.20 (t, 3H, C<u>H</u>$_3$, *J* = 6.9 Hz).

Step 2:



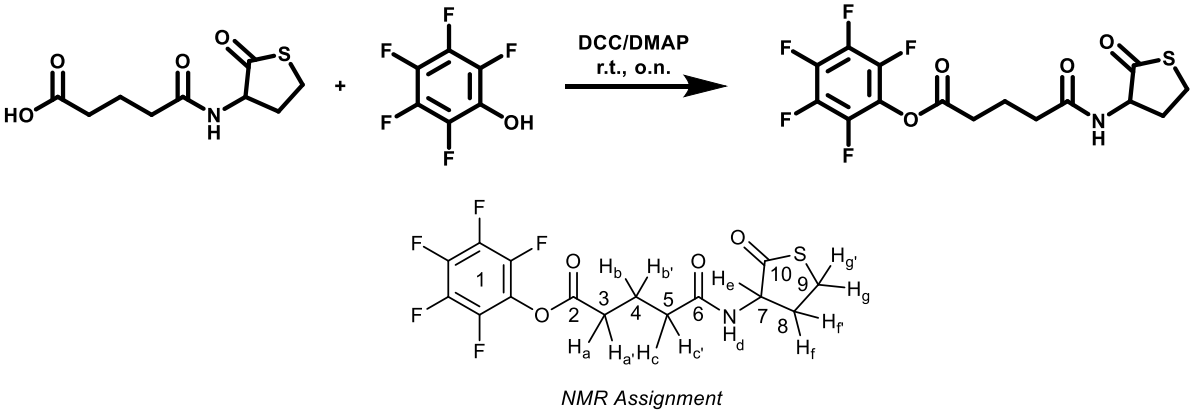
4-(4-nitrophenyl)-1-(ethoxycarbonyl) semicarbazide (11.3 g, 42.1 mmol, 1 eq.) was added to as solution of 4 M aqueous potassium hydroxide (27.5 mL) and placed under an inert atmosphere and heated to reflux at 100 °C for 4 h. The resulting reaction mixture was filtered warm and then cooled to room temperature before acidifying to pH = 1 by the slow addition of a 1 M aqueous hydrochloric acid solution. The formed precipitate was filtered off, washed with water (10 mL) and dried overnight under vacuum at 40 °C, yielding 4-(4-nitrophenyl) urazole as a yellow powder, 99 % (m = 9.28 g). **^{1}H NMR (400 MHz, DMSO-*d*$_6$):** δ = 10.83 (s, 2H, N<u>H</u>), 8.31-8.38 (m, 2H, Ar<u>H</u>), 7.85-7.92 (m, 2H, Ar<u>H</u>).

Step 3:



4-(4-nitrophenyl) urazole (9.28 g, 41.8 mmol, 1 eq.) was dissolved in methanol (185 mL) and a catalytic amount of palladium hydroxide on carbon (20 wt% loading, wet support) was added. The heterogeneous mixture was placed under a hydrogen atmosphere and stirred at room temperature for 24 h. The resulting reaction mixture was purged with a nitrogen gas stream, filtered over celite and washed with methanol (50 mL). The solvent was then removed *in vacuo* and dried overnight under vacuum at 40 °C, yielding 4-(4-aminophenyl) urazole as a beige/green powder, 84 % (m = 6.77 g). **^{1}H NMR (400 MHz, DMSO-*d*$_6$):** δ = 10.11 (s, 2H, NH), 6.92-7.00 (m, 2H, ArH), 6.54-6.64 (m, 2H, ArH), 5.28 (s, 2H, Ar-NH$_2$).

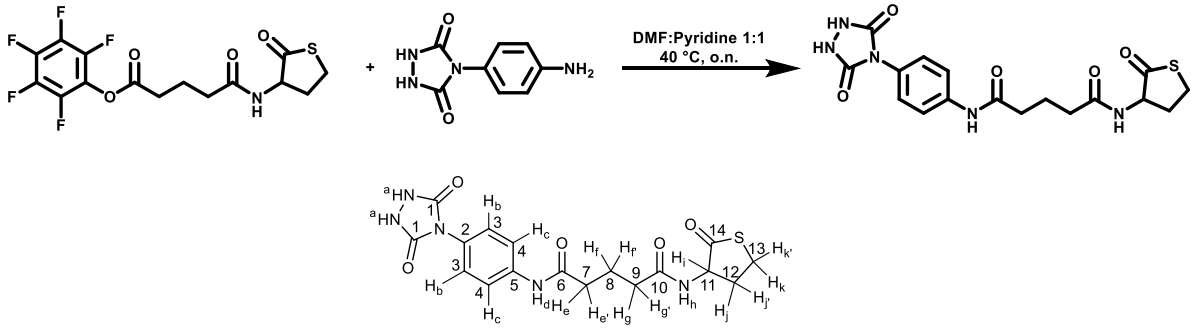
V.4.3.5 Synthesis of thiolactone pentafluorophenol



Thiolactone carboxylic acid (4.00 g, 0.0173 mols, 1.0 equiv.), pentafluorophenol (3.52 g, 0.0190 mols, 1.1 equiv.) and DMAP (423 mg, 0.00346 mols, 0.2 equiv.) were dissolved in anhydrous CH_2Cl_2 (200 mL) and anhydrous DMF (20 mL). DCC (4.28 g, 0.0208 mols, 1.2 equiv.) was dissolved in anhydrous CH_2Cl_2 (100 mL) and added dropwise at 0 °C. The reaction was then stirred for 1 week at room temperature under an inert atmosphere. The reaction was then filtered and washed with CH_2Cl_2. The filtrate was washed with saturated $NaHCO_{3\,(aq)}$ solution (50 mL), then with brine solution (50 mL), before being dried over Mg_2SO_4, filtered and the solvent was removed *in vacuo*, resulting in a brown oil. The product was purified by column chromatography (99:1, CH_2Cl_2:Acetone → 98:2, CH_2Cl_2:Acetone), resulting in a white, crystalline solid. Yield = 36 %, (m = 2.467 g), R_f = 0.1 (99:1, CH_2Cl_2:Acetone). **^{1}H NMR (500 MHz, $CDCl_3$):** δ = 5.97 (d, *J* = 4.5 Hz, 1H, H_d), 4.53 (p, *J* = 6.7, 5.8 Hz, 1H, H_e), 3.37 (td, *J* = 11.3, 5.1 Hz, 1H, $H_{g'}$), 3.26 (dd, *J* = 11.4, 6.9 Hz, 1H, H_g), 2.94 (p, *J* = 6.9, 5.2 Hz, 1H, H_f), 2.78 (t, *J* = 7.2 Hz, 2H, $H_{a,a'}$), 2.40 (td, *J* = 7.3, 2.9 Hz, 2H, $H_{c,c'}$), 2.12 (p, *J* = 7.2 Hz, 2H, $H_{b,b'}$), 1.99-1.88 (m, 1H, $H_{f'}$). **^{13}C NMR APT (100 MHz, $CDCl_3$):** δ = 205.47 (C_{10}), 172.22 (C_6), 169.18 (C_2), 59.68 (C_7), 34.54 (C_5), 32.35 (C_3), 32.07 (C_8), 27.70 (C_9), 20.41 (C_4). **^{19}F NMR (471 MHz,**

$CDCl_3$): δ = -152.56 - -152.89 (m, 2F), -157.87 (t, *J* = 22.1 Hz, 1F), -162.08 - -162.33 (m, 2F). **IR** (ATR platinum diamond): ν [cm^1] = 3292 (N-H), 1780 (C=O), 1698 (C=O), 1645 (C=O), 1518 (N-H), 1367 (C-O), 1111 (C-F), 1004 (C-F), 923, 882, 851, 641. **HRMS (ESI) *m/z*:** $[M + H]^+$ calculated for $C_{15}H_{13}F_5NO_4S^+$, 398.0480; found, 398.0488.

V.4.3.6 Synthesis of thiolactone phenyl urazole



4-(4-aminophenyl) urazole (1.66 g, 0.0086 mol, 1.0 equiv.) and thiolactone pentafluorophenol (4.59 g, 0.0086 mols, 1.0 equiv.) were dissolved in a 1:1 mixture of anhydrous DMF and pyridine (70 mL). The reaction was stirred overnight under an inert atmosphere at 40 °C. The reaction was then cooled to room temperature and the solvent was removed *in vacuo*. The product was loaded on silica and purified by column chromatography (1:9 MeOH:CH_2Cl_2 + 1 % AcOH → 2:8 MeOH:CH_2Cl_2 + 1 % AcOH), yielding a brown solid. The product was dried overnight under vacuum at 40 °C. Yield = 26 % (m = 0.898 g) and its purity checked by LCMS (*Figure V 8*). **^{1}H NMR (400 MHz, DMSO-d_6):** δ = 10.43 (s, 2H, H_a), 10.05 (d, *J* = 6.2 Hz, 1H, H_d), 8.20 (d, *J* = 8.3 Hz, 1H, H_h), 7.68 (dd, *J* = 9.0, 2.9 Hz, 2H, H_c), 7.41-7.30 (m, 2H, H_b), 4.70-4.53 (m, 1H, H_i), 3.47-3.21 (m, 2H, $H_{k,k'}$), 2.97-2.82 (m, 1H, H*), 2.48-2.31 (m, 2H, $H_{j,}$*), 2.27-2.16 (m, 2H, H*), 2.13-1.98 (m, 1H, $H_{j'}$), 1.90-1.78 (m, 2H, $H_{f,f'}$). * = $H_{e,e',g,g'}$ – could not be assigned to specific proton resonance. Integrals for the ^{1}H NMR were estimated because of impurities still present – see *Figure V 8*. **13C NMR APT (100 MHz, DMSO-d_6):** δ = 205.51 (C_{14}), 172.01§, 171.77 (C_{10}), 170.99 (C_6), 153.57 (C_1), 138.64 (C_2), 127.08§, 126.57 (C_3), 126.48 (C_5), 119.15 (C_4), 58.09 (C_{11}), 35.51, 34.42 ($C_{7,9}$), 30.17 (C_{12}), 26.72 (C_{13}), 21.00 (C_8), 19.84§. § ^{13}C resonances unattributable to the structure, presumably arising from traces of impurities such as double thiolactone adduct. **IR** (ATR platinum diamond): ν [cm^{-1}] = 3317 (N-H), 1692, 1662 & 1602 (C=O), 1517 (N-H), 1437 & 1410 (C-H), 1251, 1057 & 1016 (C-N), 920, 845, 789 & 755 (C-H_{Ar}). **HRMS (ESI) *m/z*:** $[M + H]^+$ calculated for $C_{17}H_{20}N_5O_5S^+$, 405.1227; found, 406.1187.

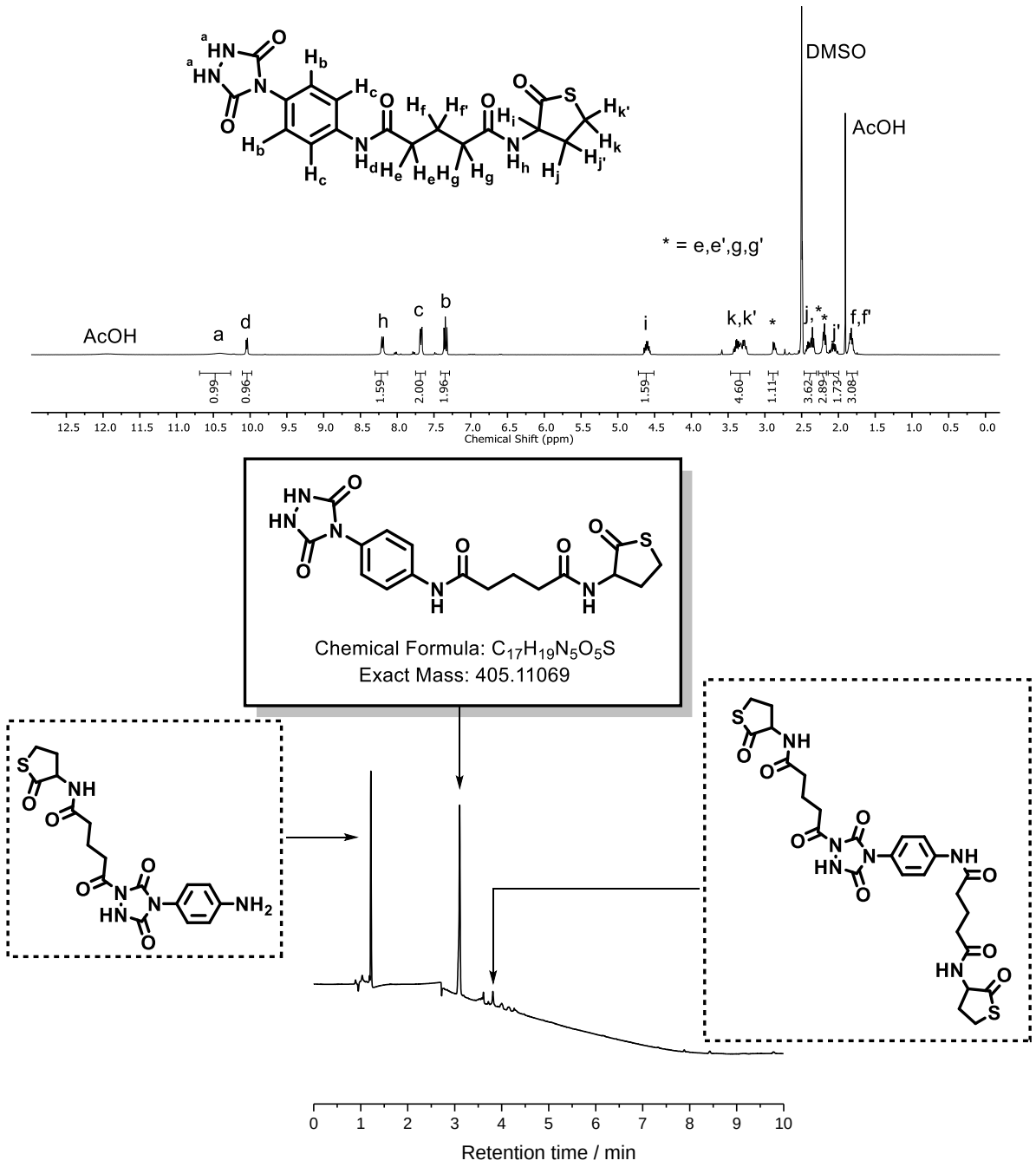


Figure V 8: Top) [1]H NMR spectrum of urazole thiolactone. Bottom) LCMS chromatogram at λ=214 nm, showing the purity of the obtained fraction of urazole thiolactone, following column chromatography, and highlighting two proposed side products that remained.

V.4.4 Synthesis of sequence-defined oligomer 1

V.4.4.1 Manipulation of the solid-phase resin

Swelling: The resin for each reaction was swollen for at least 10 minutes in the reaction solvent (1 mL of solvent per 100 mg of resin).

Washing: The solid phase resin was extensively washed, under filtration, after each reaction to ensure removal of remaining unreacted starting chemicals or unwanted side-products formed such as precipitates. Washing was done sequentially with DMF (x4), MeOH (x4), $CHCl_3$ (x4) and Et_2O (x4).

Cleavage: For analysis by LCMS, the sequence was cleaved from the resin by suspension in a solution of 1% TFA (trifluoroacetic acid) in CH_2Cl_2 for 5 minutes before filtration of the sample and then concentration by evaporation. During cleavage, a colour change of the beads could be observed from yellow to red because of the trityl cation formed on the resin.

Analysis: This was predominantly carried out using LCMS and HRMS. Once the complete oligomer was synthesised, the remainder of the compound was recovered from the resin and diluted in DMSO-d_6 for ^{1}H NMR and ^{13}C analysis.

V.4.4.2 Loading of the 2-chlorotrityl chloride resin with sorbic alcohol[8]

2-Chlorotrityl chloride resin (100-200 mesh, 1 % DVB, 1.6 mmol/g) (1.5 g, 2.4 mmol, 1.0 equiv.) was suspended in anhydrous THF (15 mL) and then sorbic alcohol (355 mg, 3.6 mmol, 1.5 equiv.) and pyridine (0.58 mL, 7.2 mmol, 3.0 equiv.) were added and the reaction was placed under an inert atmosphere. The reaction was shaken vigorously at 60 °C overnight. The reaction was then filtered and the resin was shaken three times for 10 minutes with a 17:2:1 solution of CH_2Cl_2:MeOH:DIPEA (3 x 30 mL) at room temperature. The reaction was then filtered and the resin wash washed with DMF (3 x 30 mL), CH_2Cl_2 (3 x 30 mL) and Et_2O (3 x 30 mL). The resin was finally dried under vacuum at room temperature for 4 hours.

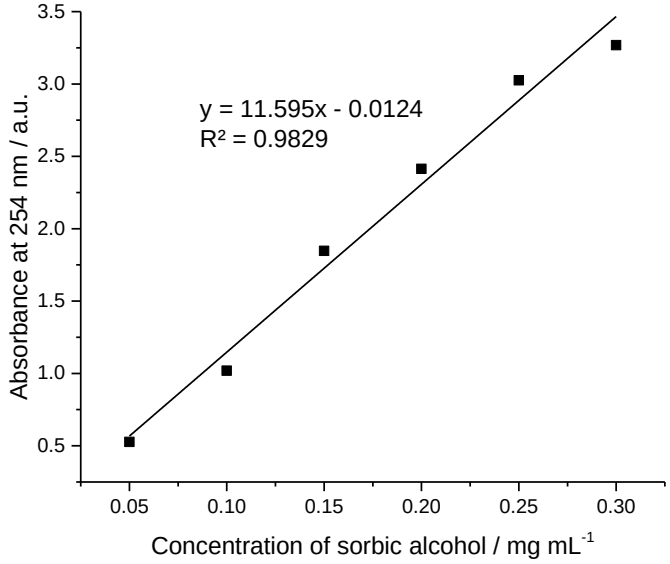


Figure V 9: UV-calibration curve of sorbic alcohol.

The loading efficiency was determined by UV-Vis spectroscopy at 254 nm with a calibration curve prepared (*Figure V 9*) for the sorbic alcohol. The loading was determined to be 1.13 mmol of sorbic alcohol per gram of resin, giving a loading efficiency of 71 %.

V.4.4.3 General solid-phase protocol

Step 1a – thiolactone phenyl urazole oxidation: Thiolactone phenyl urazole (46 mg, 0.113 mmol, 2 equiv.) was solubilised in anhydrous DMF (500 µL). Then *N*-bromosuccinimide (20 mg, 0.113 mmol, 2 equiv.) and anhydrous pyridine (9 µL, 0.113 mmol, 2 equiv.) were solubilised in anhydrous DMF (200 µL) and this solution was added to the urazole solution, which went immediately carmine red. This was stirred at room temperature for 5 min, before being directly used in the following step.

Step 1b – thiolactone phenyl TAD addition: The sorbic alcohol functionalised resin (50 mg, 0.0565 mmol, 1.0 equiv.) was swollen in DMF, before the newly formed TAD-thiolactone molecule (0.113 mmol, 2 equiv.) was added directly in solution following its oxidation. The reaction was shaken vigorously at room temperature for 5 minutes. The resin was then filtered and washed.

Step 2 – thiolactone ring opening: The solid-phase resin was then swollen in $CHCl_3$, before the addition of hexa-2,4-diene acrylate (172 mg, 1.13 mmol, 20 equiv.) and the appropriate primary amine (0.565 mmol, 10 equiv.) (see *Table V 1*). The reaction was shaken at room temperature for 30 min. The reaction was then filtered, and new solvent and reagents were added and the reaction was shaken for a further 30 min. This was repeated once more, before the resin was filtered and washed.

Table V 1: Table of the primary amines used in this sequence-defined protocol.

Primary Amine	Mw (g mol^{-1})	µL used	Density (g mL^{-1})
Propylamine	59.11	46.5	0.719
Butylamine	73.14	55.8	0.740
Amylamine (pentylamine)	87.16	65.2	0.755
Hexylamine	101.19	74.6	0.766
Heptylamine	115.22	83.8	0.777
Octylamine	129.24	93.4	0.782

V.4.5 Analysis of sequence-defined oligomer 1

Oligomer 1 was obtained as a red film with an overall yield over the 6 cycles of 3.4 % (m = 8.5 mg). Product was identified *via* LCMS and HRMS. ^{1}H NMR was too difficult for detailed assignment, on account of peak broadening and signal overlap. There was too little material to give a good enough resonance for ^{13}C NMR.

V.4.5.1 NMR analysis of oligomer 1

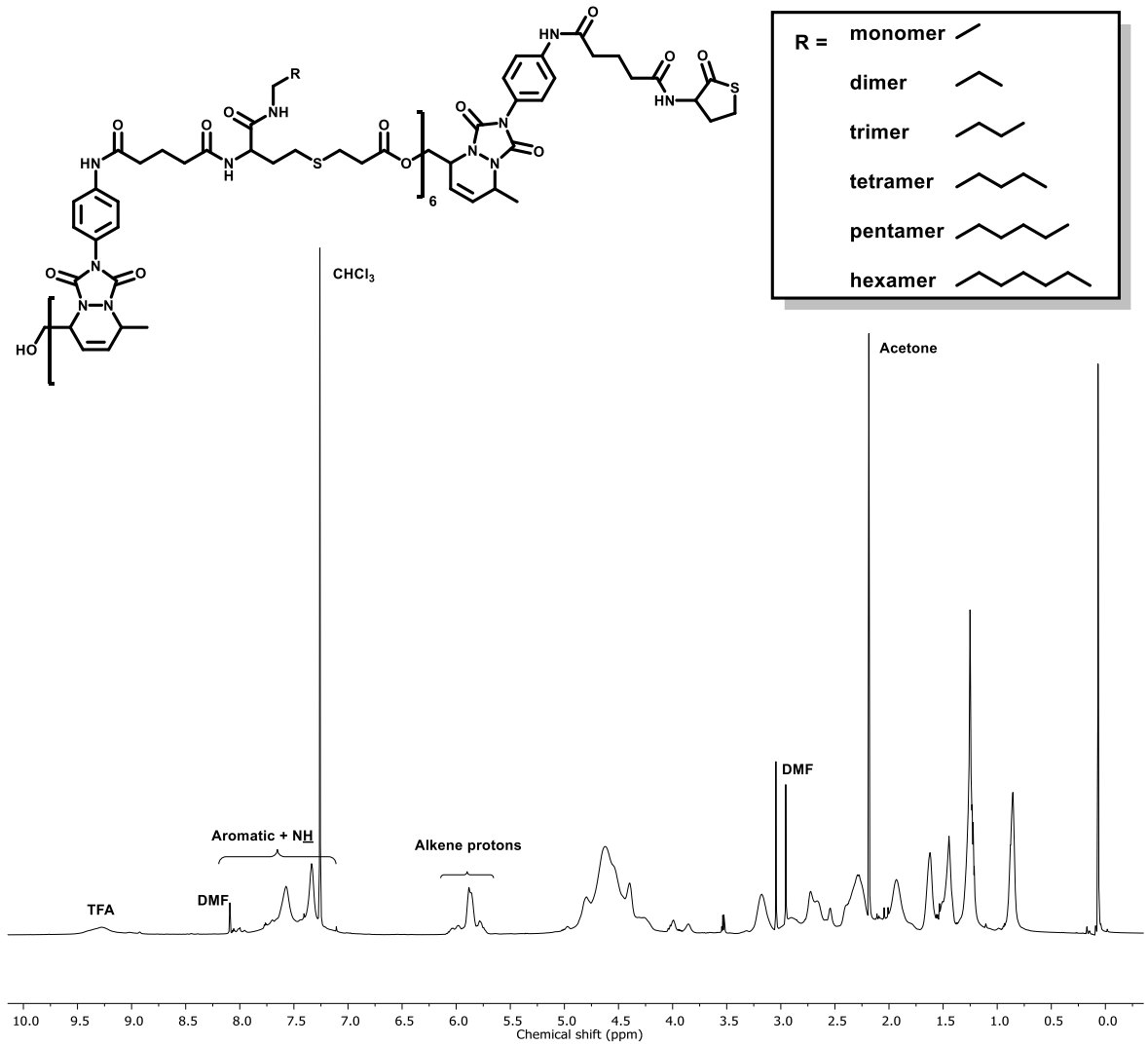


Figure V 10: ^{1}H NMR spectrum ($CDCl_3$) recorded at 700 MHz.

V.4.5.2 HRMS analysis of oligomer 1

*Table V 2: HRMS data of oligomer **1**.*

	***m/z* exp.**	**Formula**	***m/z* theo.**	**Δ *m/z***
1st TAD addition	502.1765	$[C_{23}H_{28}N_5O_6S]^+$	502.1755	0.0010
1st aminolysis	713.3339	$[C_{35}H_{49}N_6O_8S]^+$	713.3327	0.0012
2nd TAD addition	1116.4283	$[C_{52}H_{66}N_{11}O_{13}S_2]^+$	1116.4277	0.0006
2nd aminolysis	1341.5993	$[C_{65}H_{89}N_{12}O_{15}S_2]^+$	1341.6006	0.0013
3rd TAD addition	1744.6883	$[C_{82}H_{106}N_{17}O_{20}S_3]^+$	1744.6957	0.0074
3rd aminolysis*	1903.8216	$[C_{90}H_{123}N_{18}O_{22}S_3]^+$	1903.8231	0.0015
4th TAD addition	2386.9858	$[C_{113}H_{148}N_{23}O_{27}S_4]^+$	2386.9792	0.0066
4th aminolysis	1320.5893	$[C_{128}H_{176}N_{24}O_{29}S_4]^{2+}$	1320.5954	0.0061
5th TAD addition	1015.0943	$[C_{145}H_{194}N_{29}O_{34}S_5]^{3+}$	1015.0977	0.0034
5th aminolysis	1655.7600	$[C_{161}H_{222}N_{30}O_{36}S_5]^{2+}$	1655.7528	0.0072
6th TAD addition	1857.2994	$[C_{178}H_{239}N_{35}O_{41}S_6]^{2+}$	1857.3003	0.0009
6th aminolysis	1997.9102	$[C_{195}H_{270}N_{36}O_{43}S_6]^{2+}$	1997.9181	0.0079
7th TAD addition	2199.4550	$[C_{212}H_{287}N_{41}O_{48}S_7]^{2+}$	2199.4656	0.0106

**Acid induced hydrolysis of the conjugated diene ester means that only a mass -80 Da was detected.*

V.5 References

1 D. Frank, P. Espeel, S. Claessens, E. Mes and F. E. Du Prez, *Tetrahedron*, 2016, **72**, 6616–6625.

2 S. Reinicke, P. Espeel and F. E. Du Prez, *Polym. Chem.*, 2014, **5**, 5461–5470.

3 P. Espeel, F. Goethals, M. M. Stamenović, L. Petton and F. E. Du Prez, *Polym. Chem.*, 2012, **3**, 1007–1015.

4 M. M. Stamenović, P. Espeel, E. Baba, T. Yamamoto, Y. Tezuka and F. E. Du Prez, *Polym. Chem.*, 2013, **4**, 184–193.

5 P. Espeel and F. E. Du Prez, *Eur. Polym. J.*, 2015, **62**, 247–272.

6 S. Montolio, O. Zagorodko, R. Porcar, M. Isabel Burguete, S. V. Luis, H. Tenhu and E. García-Verdugo, *Polym. Chem.*, 2017, **8**, 4789–4797.

7 S. Mommer, K. Truong, H. Keul and M. Möller, *Polym. Chem.*, 2016, **7**, 2291–2298.

8 S. Martens, J. Van Den Begin, A. Madder, F. E. Du Prez and P. Espeel, *J. Am. Chem. Soc.*, 2016, **138**, 14182–14185.

9 S. Martens, A. Landuyt, P. Espeel, B. Devreese, P. Dawyndt and F. E. Du Prez, *Nat. Commun.*, 2018, **9**, 4451.

10 J. O. Holloway, S. Aksakal, F. E. Du Prez and C. Remzi Becer, *Macromol. Rapid Commun.*, 2017, **38**, 1700500.

11 J. O. Holloway, C. Mertens, F. E. Du Prez and N. Badi, *Macromol. Rapid Commun.*, 2019, **40**, 1800685.

12 F. Goethals, D. Frank and F. E. Du Prez, *Prog. Polym. Sci.*, 2017, **64**, 76–113.

13 P. Espeel and F. E. Du Prez, *Macromolecules*, 2015, **48**, 2–14.

14 S. Martens, J. O. Holloway and F. E. Du Prez, *Macromol. Rapid Commun.*, 2017, **38**, 1700469.

15 S. Martens, J. O. Holloway and F. E. Du Prez, in *Sequence-Controlled Polymers*, ed. J.-F. Lutz, Wiley VCH, Weinheim, 2018, pp. 379–416.

16 H. C. Kolb, M. G. Finn and K. B. Sharpless, *Angew. Chemie - Int. Ed.*, 2001, **40**, 2004–2021.

17 C. R. Becer, R. Hoogenboom and U. S. Schubert, *Angew. Chemie Int. Ed.*, 2009, **48**, 4900–4908.

18 J. E. Moses and A. D. Moorhouse, *Chem. Soc. Rev.*, 2007, **36**, 1249–1262.

19 V. K. Tiwari, B. B. Mishra, K. B. Mishra, N. Mishra, A. S. Singh and X. Chen, *Chem. Rev.*, 2016, **116**, 3086–3240.

20 M. D. Best, *Biochemistry*, 2009, **48**, 6571–6584.

21 W. H. Binder and R. Sachsenhofer, *Macromol. Rapid Commun.*, 2008, **29**, 952–981.

22 P. L. Golas and K. Matyjaszewski, *Chem. Soc. Rev.*, 2010, **39**, 1338–1354.

23 M. J. Robb and C. J. Hawker, in *Materials Science and Technology*, Wiley-VCH Verlag GmbH & Co. KGaA, Weinheim, Germany, 2012, pp. 923–972.

24 W. H. Binder and C. Kluger, *Macromolecules*, 2004, **37**, 9321–9330.

25 H. Nandivada, X. Jiang and J. Lahann, *Adv. Mater.*, 2007, **19**, 2197–2208.

26 M. Meldal, *Macromol. Rapid Commun.*, 2008, **29**, 1016–1051.

27 C. Barner-Kowollik and A. J. Inglis, *Macromol. Chem. Phys.*, 2009, **210**, 987–992.

28 W. Xi, T. F. Scott, C. J. Kloxin and C. N. Bowman, *Adv. Funct. Mater.*, 2014, **24**, 2572–2590.

29 C. Barner-Kowollik, F. E. Du Prez, P. Espeel, C. J. Hawker, T. Junkers, H. Schlaad and W. Van Camp, *Angew. Chemie Int. Ed.*, 2011, **50**, 60–62.

30 C. D. Hein, X.-M. Liu and D. Wang, *Pharm. Res.*, 2008, **25**, 2216–2230.

31 A. Marechal, R. El-Debs, V. Dugas and C. Demesmay, *J. Sep. Sci.*, 2013, **36**, 2049–2062.

32 O. Diels, J. H. Blom and W. Koll, *Justus Liebigs Ann. Chem.*, 1925, **443**, 242–262.

33 N. Zydziak, W. Konrad, F. Feist, S. Afonin, S. Weidner and C. Barner-Kowollik, *Nat. Commun.*, 2016, **7**, 1–10.

34 N. Zydziak, F. Feist, B. Huber, J. O. Mueller and C. Barner-Kowollik, *Chem. Commun.*, 2015, **51**, 1799–1802.

35 X. Elduque, A. Sánchez, K. Sharma, E. Pedroso and A. Grandas, *Bioconjug. Chem.*, 2013, **24**, 832–839.

36 O. Brun, X. Elduque, E. Pedroso and A. Grandas, *J. Org. Chem.*, 2015, **80**, 6093–6101.

37 C. Paris, O. Brun, E. Pedroso, A. Grandas, C. Paris, O. Brun, E. Pedroso and A. Grandas, *Molecules*, 2015, **20**, 6389–6408.

38 S. Billiet, K. De Bruycker, F. Driessen, H. Goossens, V. Van Speybroeck, J. M. Winne and F. E. Du Prez, *Nat. Chem.*, 2014, **6**, 815–821.

39 K. De Bruycker, S. Billiet, H. A. Houck, S. Chattopadhyay, J. M. Winne and F. E. Du Prez, *Chem. Rev.*, 2016, **116**, 3919–3974.

40 J. Thiele and O. Stange, *Justus Liebig's Ann. der Chemie*, 1894, **283**, 1–46.

41 R. C. Cookson, S. S. H. Gilani and I. D. R. Stevens, *J. Chem. Soc. C*, 1967, 1905–1909.

42 R. C. Cookson, S. S. H. Gilani and I. D. R. Stevens, *Tetrahedron Lett.*, 1962, **3**, 615–618.

43 R. C. Cookson, S. S. Gupte, I. D. R. Stevens and C. T. Watts, *Org. Synth.*, 1971, **51**, 121–127.

44 O. Türünç, S. Billiet, K. De Bruycker, S. Ouardad, J. M. Winne and F. E. Du Prez, *Eur. Polym. J.*, 2015, **65**, 286–297.

45 H. A. Houck, K. De Bruycker, S. Billiet, B. Dhanis, H. Goossens, S. Catak, V. Van Speybroeck, J. M. Winne and F. E. Du Prez, *Chem. Sci.*, 2017, **8**, 3098–3108.

46 S. Chattopadhyay and F. E. Du Prez, *Eur. Polym. J.*, 2016, **81**, 77–85.

47 N. Van Herck and F. E. Du Prez, *Macromolecules*, 2018, **51**, 3405–3414.

48 O. Roling, K. De Bruycker, B. Vonhören, L. Stricker, M. Körsgen, H. F. Arlinghaus, B. J. Ravoo and F. E. Du Prez, *Angew. Chemie - Int. Ed.*, 2015, **54**, 13126–13129.

49 G. Becker, L. Vlaminck, M. M. Velencoso, F. E. Du Prez and F. R. Wurm, *Polym. Chem.*, 2017, **8**, 4074–4078.

50 C. C. Cheng, C. A. Seymour, M. A. Petti, F. D. Greene and J. F. Blount, *J. Org. Chem.*, 1984, **49**, 2910–2916.

51 H. Ban, J. Gavrilyuk and C. F. Barbas, *J. Am. Chem. Soc.*, 2010, **132**, 1523–1525.

52 D. M. Bauer, I. Ahmed, A. Vigovskaya and L. Fruk, *Bioconjug. Chem.*, 2013, **24**, 1094–1101.

53 M. Shimizu, T. Takahashi, S. Uratsuka and S. Yamada, *J. Chem. Soc. Chem. Commun.*, 1990, **0**, 1416.

54 J. F. W. Keana, A. P. Guzikowski, D. D. Ward, C. Morat and F. L. Van Nice, *J. Org. Chem.*, 1983, **48**, 2654–2660.

55 H. Ban, M. Nagano, J. Gavrilyuk, W. Hakamata, T. Inokuma and C. F. Barbas, *Bioconjug. Chem.*, 2013, **24**, 520–532.

56 A. Nilo, M. Allan, B. Brogioni, D. Proietti, V. Cattaneo, S. Crotti, S. Sokup, H. Zhai, I. Margarit, F. Berti, Q.-Y. Hu and R. Adamo, *Bioconjug. Chem.*, 2014, **25**, 2105–2111.

57 WO2013009564, 2013.

58 D. Frank, P. Espeel, S. Claessens, E. Mes and F. E. Du Prez, *Tetrahedron*, 2016, **72**, 6616–6625.

59 P. Espeel, L. L. G. Carrette, K. Bury, S. Capenberghs, J. C. Martins, F. E. Du Prez and A. Madder, *Angew. Chemie - Int. Ed.*, 2013, **52**, 13261–13264.

60 J. O. Holloway, K. S. Wetzel, S. Martens, F. E. Du Prez and M. A. R. Meier, *Polym. Chem.*, 2019, **10**, 3859–3867.

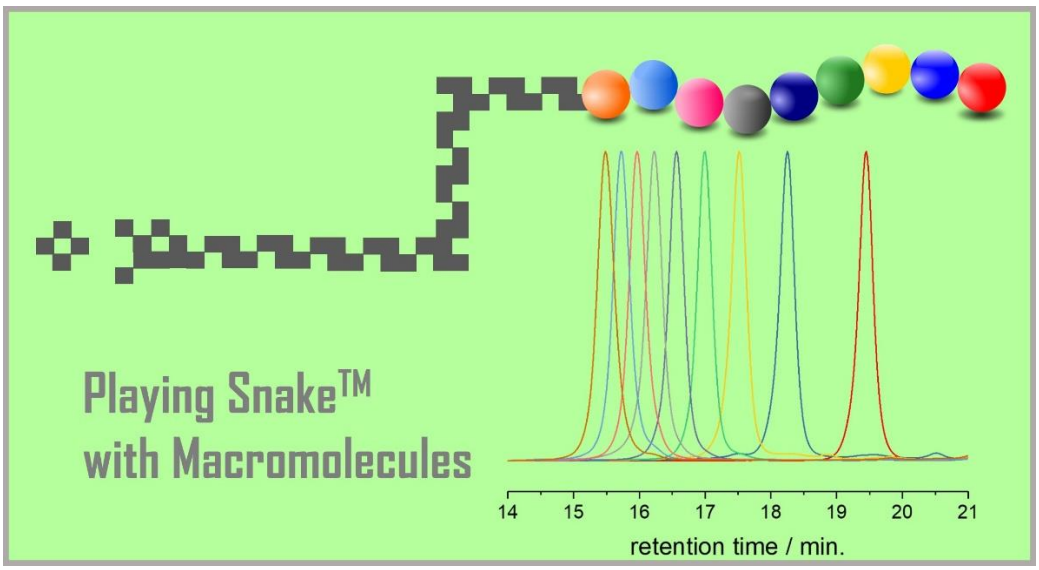
61 P. Espeel, F. Goethals, F. Driessen, L.-T. T. Nguyen and F. E. Du Prez, *Polym. Chem.*, 2013, **4**, 2373–2616.

62 A. Bousquet, C. Barner-Kowollik and Martina H. Stenzel, *J. Polym. Sci. Part A Polym. Chem.*, 2010, **48**, 1773–1781.

63 H. A. Houck, K. De Bruycker, C. Barner-Kowollik, J. M. Winne and F. E. Du Prez, *Macromolecules*, 2018, **51**, 3156–3164.

64 M. M. Heravi, F. Derikvand, M. Ghassemzadeh and B. Neumüller, *Tetrahedron Lett.*, 2005, **46**, 6243–6245.

65 O. Türünç, S. Billiet, K. De Bruycker, S. Ouardad, J. Winne and F. E. Du Prez, *Eur. Polym. J.*, 2015, **65**, 286–297.



This chapter is adapted with permission from:

J. O. Holloway, K. S. Wetzel, S. Martens, F. E. Du Prez and M. A. R. Meier, *Polym. Chem.*, 2019, **10**, 3859-3867.

Abstract

The synthesis of perfectly defined, monodisperse macromolecules is one of the challenges faced by polymer chemists today. Such precision synthesis requires a fundamentally different approach to conventional polymer synthesis, but in turn can unlock the door to many new applications. Therefore, the combination of ultra-fast "click" reactions using 1,2,4-triazoline-3,5-diones (TAD) with the highly efficient and versatile Passerini three-component reaction is introduced here. This new approach not only resulted in the synthesis of monodisperse, sequence-defined macromolecules of both high purity and molecular weight (> 7 kDa), but also offered new insights into the iterative synthesis of sequence-defined macromolecules in general. This chapter presents a detailed comparative study of the same chemistry protocols carried out on solid-phase as well as in solution and was carried out in collaboration with the Karlsruhe Institute of Technology (KIT), Germany.

Chapter VI
Direct comparison of solution and solid-phase sequence-defined synthesis using a combined click chemistry and multicomponent reaction approach

VI.1 Introduction

Chapter II introduced how the field of sequence-control and sequence-definition in polymer chemistry has evolved over the last decade into a hot research topic, as researchers worldwide strive to take inspiration from nature to synthesise macromolecules with precisely controlled structures.[1–6] As such, this field is now rapidly growing and resulting in various new routes towards precision macromolecular synthesis and potential applications thereof.[7–21] In Chapter II.2, the differences between the terms *"sequence-controlled"* and *"sequence-defined"* were distinguished, outlining that only the latter results in unique, monodisperse macromolecules, while sequence-controlled systems still show dispersity in many aspects.[22,23] Most sequence-defined macromolecules tend to be oligomers as opposed to polymers and thus extending degrees of polymerisation as well as scalability are issues of high relevance. Conventional polymerisation techniques on the other hand are up-scalable, but lead to irregularity and dispersity and thus, at best, can be considered to be sequence-controlled, depending on the polymerisation mechanism.[6,24]

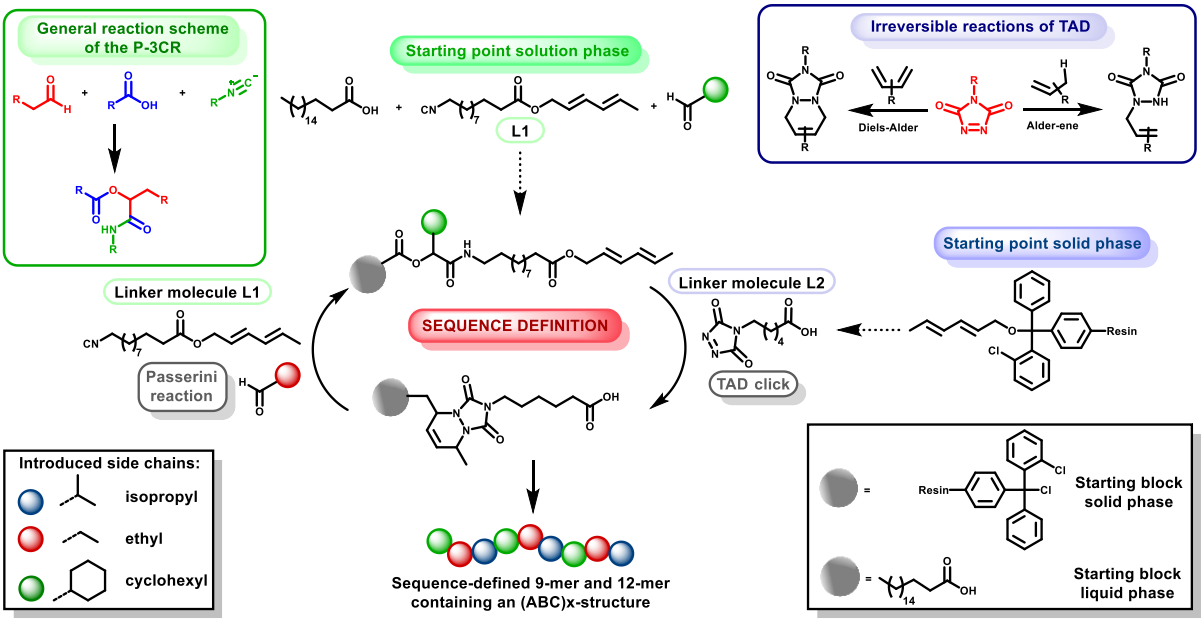
A common route towards sequence-defined oligomers, offering full control over each monomer unit, is the iterative synthesis approach, as used in the work discussed in the previous chapters.[7,25–32] This step-by-step growth of the macromolecule is necessary to ensure a perfectly defined sequence as well as monodispersity. Whilst many different approaches exist, the use of multi-component reactions (MCRs) seems a logical choice within this area and such reactions have indeed been shown to be highly effective tools for the synthesis of sequence-defined macromolecules.[17,18,33–40] In particular, the Passerini three-component reaction (P-3CR,*Scheme VI 1*, top left) between an acid, an aldehyde and an isocyanide, first discovered in 1921,[41] has been reported to be a highly effective technique in sequence-defined oligomer synthesis and is discussed in detail in Chapter II.6.2.[33–36]

On the other hand, click chemistry[42] is also an ideal concept for sequence-defined synthesis,[1,2] as elaborated in the previous chapter, where click and click-like chemistry was used together in one protocol and where the click reaction, in particular, was shown to be highly effective. The main

principles of click chemistry: high yields, being wide in substrate scope, production of inoffensive by-products and easy purification are all desirable to an iterative approach towards synthesising highly defined, monodisperse macromolecules. The work described in Chapter V highlighted one notable example of click chemistry: 1,2,4-triazoline-3,5-dione (TAD) chemistry.[43] The research discussed in Chapter V, led to the conclusion being made that the TAD reaction step was far more efficient than the thiolactone reaction. Moreover, when considering the work discussed in Chapters III and IV, certain difficulties were also observed with the thiolactone-based protocols discussed there. These were either side reactions or inefficiencies, on account of either the thiolactone ring-opening and subsequent Michael addition,[31] or the re-installation of thiolactone units using α-thiolactone-γ-isocyanate.[44] Therefore, the highly efficient reactions of TAD chemistry were pursued in place of thiolactone chemistry for the remaining work of this thesis.

The fast and efficient irreversible reactions of TAD (*Scheme VI 1*, top right), signified by a visual feedback on account of the vivid red colour of the TAD molecule,[43,45,46] has already led to it being used in a widening range of applications[47–49] and now also as a suitable reaction partner for sequence-defined chemistry, as introduced within this thesis for the first time. Depending on the substrate, the irreversible reactions of TAD can vary from less than one second to several hours.[43,45] Thus, by synthesising a carboxylic acid functionalised TAD compound, click chemistry - in this case *via* the Diels-Alder reaction - could be combined with the P-3CR. This enabled the development of a new, highly effective, strategy for the synthesis of sequence-defined macromolecules as outlined in*Scheme VI 1*.

The use of the Diels-Alder reaction in sequence-defined chemistry remains very limited to date, with only a few examples existing.[16,40,50,51] This chapter not only discusses the powerful combination of MCRs with click chemistry, but simultaneously introduces a comprehensive comparative study between solution and solid-phase chemistry approaches, which has not been done before in this field. These two techniques are undoubtedly both valuable tools for chemists in the pursuit of precise macromolecular control and sequence definition and it was felt that their direct comparison was long overdue. Herein, the advantages and disadvantages of both techniques are discussed and the combination of TAD Diels-Alder chemistry with the P-3CR is demonstrated to be a powerful tool for achieving high molecular weight, high purity, multi-functional, monodisperse macromolecules. Moreover, it is shown here that the introduction of TAD chemistry to the P-3CR has a profound effect on both its efficiency and speed of the synthesis.



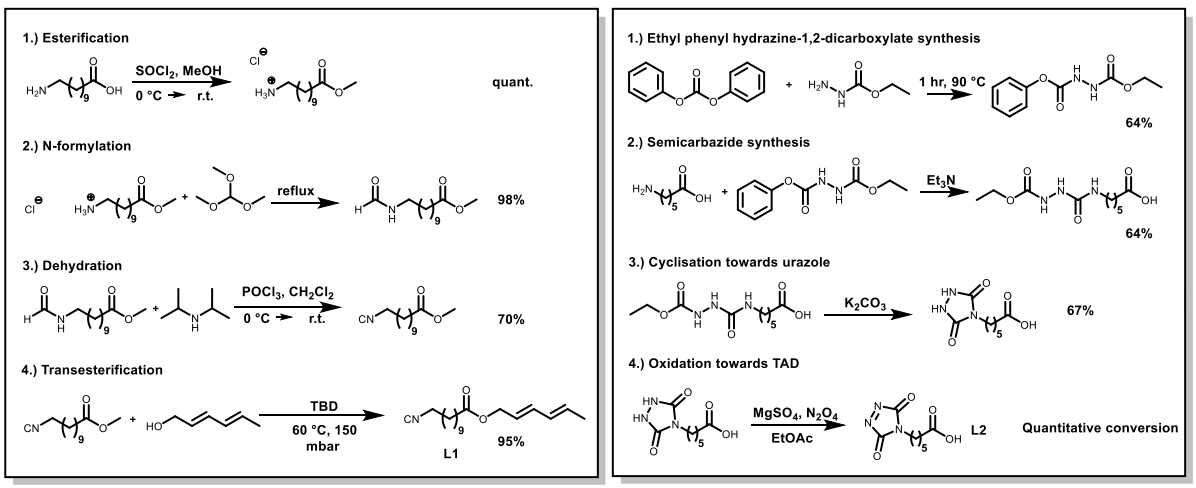
Scheme VI 1: Two-step iterative reaction cycle consisting of the P-3CR and the TAD Diels-Alder reaction, which can be applied to synthesise sequence-defined macromolecules on solid-phase and in solution. Box; top left) General reaction scheme of the P-3CR. Box; top right) Irreversible reactions of TAD.

As mentioned above, sequence-defined iterative synthesis protocols can be carried out in two ways. One possibility is *via* a Merrifield inspired[52] solid-phase approach, whereby polymer resins are functionalised with a typically acid sensitive cleavable linker, thus allowing the sequence to be grown on the resin before being recovered at the end.[7] Although usually limited in scale, this approach is particularly advantageous because of simple purification by washing and the potential to automate such a method.[7,31,44] The other possibility is solution phase chemistry. Whilst this more up-scalable approach facilitates easier characterisation and thus optimisation of each reaction step, purification can be more time-consuming. Additionally, the synthesis can be carried out using soluble polymer supports,[53–55] such as polystyrene and purified each time *via* precipitation. Also, the sequence can be synthesised in solution without any support and purification can be done, for example, by column chromatography.[17,33–35] Whilst a few reports exist of the use of similar chemistries on both solid and solution phase approaches, to the best of our knowledge, none make a full and direct comparison of the two, showcasing both the advantages and disadvantages.[53,56–58] Such a study was therefore needed in the field, as the choice of whether to opt for solid or solution phase synthesis when referring to sequence-defined protocols is always difficult, because it is highly dependent on the end goal of the work and the desired scale, purity and length of the macromolecule.

VI.2 Results and discussion

VI.2.1 Synthesis of AB-type linker molecules

To combine the P-3CR with TAD Diels-Alder reactions, two AB-type linker molecules (**L1** and **L2**) were synthesised (see *Scheme VI 2* and Section VI.4.3 for experimental details) and applied in a two-step iterative cycle (see *Scheme VI 1*), resulting in sequence-defined macromolecules. **L1**, functionalised with an isocyanide and a conjugated diene, was synthesised *via* a four-step protocol. The synthesis was carried out on a 15-gram scale with an overall yield of 65 %. **L2**, containing both the TAD and carboxylic acid moieties, was synthesised on a 2-gram scale, also *via* a four-step synthesis route, with an overall yield of 27 % of the corresponding urazole compound (the precursor to TAD). Because TAD is formed from the oxidation of its respective bench-stable urazole compound, **L2** was obtained by oxidising the urazole carboxylic acid molecule in small batches, as required, to avoid any unwanted degradation, as the stability of the TAD-functionality can vary from hours to months, depending on its structure and purity.[43] The linker molecules both contained one moiety that reacts in the Diels-Alder reaction (TAD and a diene) and a second one that is active in the P-3CR (carboxylic acid and isocyanide), allowing a protecting group-free, iterative approach, benefiting from the two orthogonal reactions. As the third component in the P-3CR, three aldehydes were used from commercially available sources to provide different functionalities and thus resulting in the desired sequence-definition. As it was already demonstrated previously that a large variety of side chains can be introduced to the oligomeric backbone by varying the aldehyde component in the P-3CR, this study was limited to three different aldehydes to generate "$[ABC]_x$"-sequences.[29,30,34,35]



*Scheme VI 2: General overview of the synthesis of AB-type linker molecules **L1** (left) and **L2** (right).*

Using **L1** and **L2,** a two-step, iterative cycle was developed, consisting of a TAD-based Diels-Alder reaction, followed by the P-3CR (*Scheme VI 1*). Both reactions reached quantitative conversions and

yields and were carried out both on solid-phase and in solution. As a result, a sequence-defined dodecamer and nonamer were obtained, respectively, *via* the two different synthesis methods. Apart from the starting block (which was different because of practical considerations), almost identical sequences were synthesised in both cases. Stearic acid was used as the starting molecule for the solution phase synthesis to make subsequent purifications easier. For the solid-phase, the resin was first loaded with hexadiene-1-ol to provide a suitable reaction site for the first Diels-Alder reaction. The obtained products were carefully compared regarding yield, purity (or sequence fidelity), reaction time, degree of polymerisation, purification method and scale (*vide infra*, *Table VI 1*).

VI.2.2 Solid-phase approach

For the solid-phase reactions, a 2-chlorotrityl chloride functionalised resin was used. This resin was selected because of its very mild cleavage conditions (1 % TFA in CH_2Cl_2), thus preventing unwanted potential side reactions such as degradation of ester bonds formed by the P-3CR, which would be problematic. Functionalisation of this resin with sorbic alcohol was adapted from an earlier reported method.[7] The conjugated diene structure was a suitable reaction partner for the irreversible TAD Diels-Alder reaction as it is known to be extremely fast and efficient (as discussed in Chapter II.7.3).[43,45] For the subsequent cycles, the conjugated diene, necessary for this step, was provided by the diene-isocyanide linker molecule **L1**. Starting from this functionalised resin and applying the protocol outlined in*Scheme VI 1*, a monomer and sequence defined dimer and trimer were first synthesised to confirm the success of the protocol, as confirmed by LCMS analysis (*Figure VI 1a*) and complete characterisation by NMR and HRMS was also conducted (see Section VI.4.5 and VI.4.6). The protocol was then repeated to synthesise longer sequences, thus resulting in an $[ABC]_3$-nonamer and an $[ABC]_4$-dodecamer. Propanal, isobutyraldehyde and cyclohexanal were used alternatively to introduce the side groups.

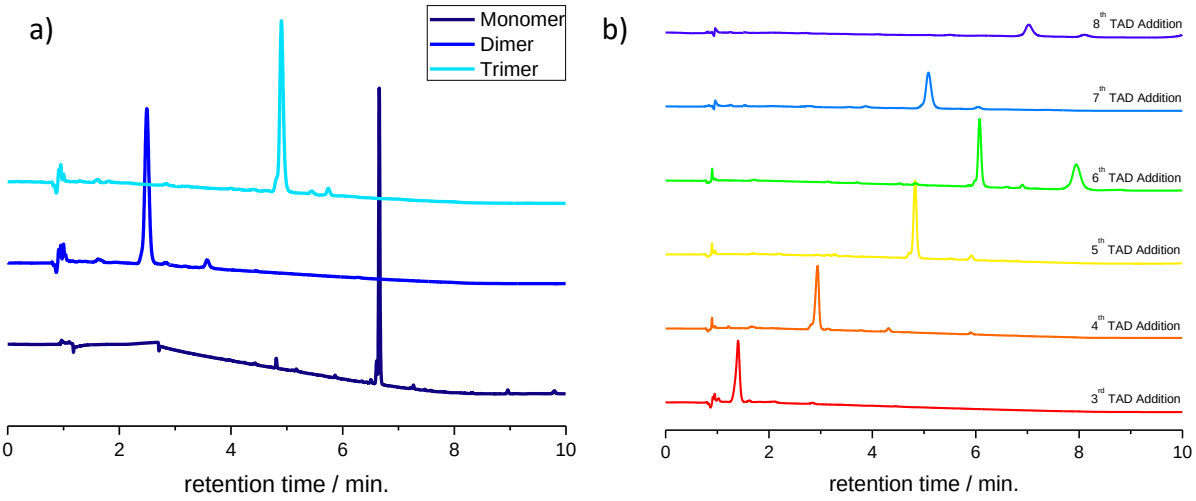


*Figure VI 1: a) LCMS chromatograms (λ=214 nm) of phenyl TAD capped monomer, dimer and trimer, demonstrating excellent conversion and purity. The monomer was analysed at a solvent gradient of 0 → 100 % acetonitrile → water, the dimer and trimer at a 75 → 100 % gradient because of their decreased polarity. The reduced gradient results in a lower retention time for the molecule. b) LCMS chromatograms (λ=214 nm) after each TAD molecule (**L2**) addition step. The increased polarity resulting from the carboxylic acid end-group made this step much easier to analyse by LCMS than after the P-3CR step. By following the same step in the cycle, one can see a shift in retention time as the molecular weight increases. It should be noted that this does not continue in a linear fashion because the solvent gradient was changed from 75-100 % to 90-100 % after the 6th cycle.*

One of the main advantages of solid-phase chemistry is the ability to work with large excesses of reagents to ensure 100 % conversion, as unwanted starting material can be simply washed away, thus massively simplifying purification. This is particularly advantageous for sequence-definition, as sequences often require a high number of iterative synthesis steps. It can also be a time or labour-saving approach as the purification can be much faster than, for example, column chromatography and one can, in principle, automate the reactions.[7,44] For the TAD addition step, the high reactivity of TAD molecules required only 2 equivalents (notably low for solid-phase synthesis, compared to other reported methods)[7,25,31] with shaking for 5 minutes at room temperature to ensure 100 % conversion, as quantified by LCMS.[59]

Despite a limited number of previous reports of the P-3CR being carried out on solid-phase,[60–62] the speed of the synthesis was of great importance to investigate here, thus the P-3CR step in the cycle was followed kinetically by LCMS. These results showed that the reaction was complete within 30 minutes[59] and was compared later with the reaction kinetics obtained in solution (*vide infra*). The reaction was much faster than anticipated and up to twelve times faster than in solution. The equivalents of reagents were increased 10-fold with respect to the solution phase experiments and in line with previous solid-phase reactions of our group.[7,25,31] The speed of the solid-phase reaction is a result of the high excess of reagents and thus effective concentration. The reaction time was increased every 3-4 cycles by a further

30 minutes in response to observations from LCMS analysis after each cycle, which showed a slowing down of the reaction as the oligomer grew larger. This was to be expected as it was known from the solution phase kinetics by online IR (*vide infra*) that the reaction slows down because of increasing oligomer chain length.

One disadvantage of solid-phase chemistry is typically its low scale, although large-scale (~10 kg) solid-phase synthesis has been reported.[63] Reactions described in this chapter were carried out on 50 mg of resin, yielding 14.4 mg (from 25 mg of resin in the case of the dodecamer) of oligomer, once cleaved from the resin. Automation of this approach could circumvent problems with scale, as use of a peptide-synthesiser allows up to 72 reactions to be carried out in parallel.[7,19,44] Nonetheless, the small scale used in this work resulted in a limited range of tandem characterisation techniques being available to use.

As previously reported,[7,31] LCMS was used as the most appropriate technique to unambiguously follow the progress of the reaction after each step, as only 2 mg of resin needed to be taken from the reaction for quantitative analysis. Furthermore, the LCMS sample itself could be diluted for HRMS analysis. However, after the P-3CR step in each cycle, acid induced hydrolysis of the conjugated diene ester group during cleavage from the resin resulted in the partial cleavage of the ester bond, hence two peaks appeared in the chromatogram. Therefore, *Figure VI 1b* displays only the LCMS chromatogram after the TAD Diels-Alder reaction, as the conjugated diene structure is no longer present, thus eliminating this cleavage effect and assisting the analysis. Also, following the addition of the TAD carboxylic acid molecule, the retention time was reduced compared to the preceding P-3CR because of the increased polarity, thus further helping the analysis. By comparison, after the P-3CR step of the 4th cycle, analysis by LCMS became too difficult as the long, apolar carbon chain from the linker molecule **L1** resulted in a too high retention time for accurate and quantitative analysis, even with a reduced solvent gradient from acetonitrile to water of 75-100 % and eventually 90-100 % instead of the more preferred 0-100 %. Because of the high molecular weight oligomers achieved here (7200 Da), compared to our previous reported works (around 4000 Da),[7,25,31,33] the limitations of the LCMS equipment became apparent by the 7th TAD addition step (ca. 3800 Da), as displayed in *Figure VI 1b*. Thus, the sequence was eventually continued without intermediate analysis and the final dodecamer was fully analysed by IR, NMR and SEC. Half of the reaction sample (25 mg resin) at the nonamer stage was used for intermediate analysis and remaining 25 mg was used to synthesise the dodecamer.

Periodic analysis of the solid-phase synthesised oligomers was also conducted by SEC for reasons of comparison with the solution approach (see *Figure VI 2*). This was the preferred method of analysis for

the oligomers synthesised in solution, as a minimal amount of product was required for analysis and the above-mentioned problems of the LCMS analysis could be overcome. The SEC measurements were performed using refractive index detectors and the columns used were specifically designed for low molecular weight molecules (100-60,000 Da). Thus, one could easily compare both the purity (or sequence fidelity, as determined by SEC) and dispersity of the obtained oligomers. In order to not lose material during the synthesis of the nonamer and dodecamer, a separate trimer was synthesised for SEC analysis, as this could be quickly done within just three hours *via* the solid-phase approach. For each of the oligomers, the conjugated diene chain end was "end-capped" with phenyl-TAD (PhTAD) before analysis, to prevent any further side reaction or cleavage of the ester bond induced by acid hydrolysis during cleavage from the solid-phase resin. A small amount of impurity could be seen in the SEC trace of the nonamer and dodecamer, amounting to a small percentage of dead chains (14 %) and a polymerisation side-product (12 %). Thus, the final product was obtained with a purity of 74% (calculated by deconvolution of the peak using the SEC software). An additional monomer, dimer and trimer were also separately synthesised, and the structures were fully resolved by ^{1}H and ^{13}C NMR techniques with the aid of 2D analysis (see Section VI.4.6). This, together with SEC and (LC)MS techniques ensured complete proof of the structures of the sequence-defined oligomers obtained and aided the final analysis of the dodecamer by NMR.

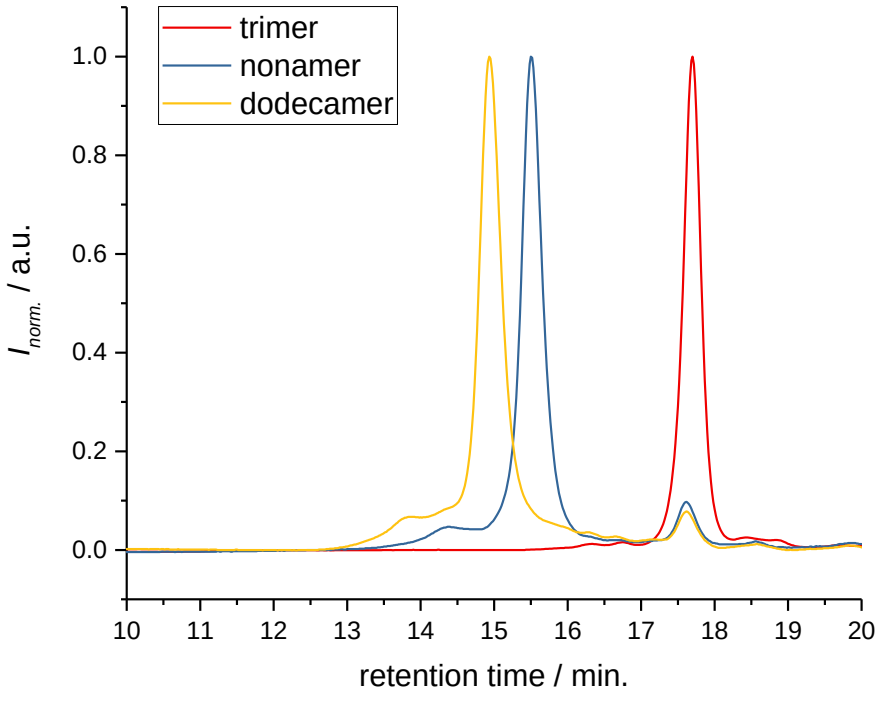


Figure VI 2: Evolution of the solid-phase synthesised oligomer from the trimer to the nonamer and dodecamer. In the nonamer, and even more in the dodecamer, a minor high molecular weight side-product is observed (left of the main peak), while a dead chain from the trimer level of the synthesis (right of the main peak) is also present.

The side reaction was later observed to a much greater extent in the solution phase (*vide infra*) and was concluded to be an unwanted polymerisation between excess TAD species, the aldehyde and isocyanide of the multicomponent reaction. Therefore, the focus was shifted there to optimise the synthesis to obtain a higher purity. The larger scale of solution phase synthesis and the increased prevalence of impurities enabled better understanding of this side reaction because full characterisation after each reaction step was possible (*vide infra*), thus enabling optimisation of the procedure. After having improved the reaction in solution (*vide infra*), the optimised conditions were then applied to the solid-phase approach. A new nonamer was synthesised to verify that these new conditions (quenching any excess un-reacted TAD with 2,3-dimethylbutene) worked for both approaches. A significant increase in the purity was observed by SEC (*Figure VI 3*). Additionally, the product was analysed by SEC-ESI-MS to further confirm the structure. The purity of the sequence-defined nonamer increased to 84 % (*vs.* 74 %) following optimisation, as determined by deconvoluting the SEC elugrams. The previously observed, polymerisation side reaction was successfully prevented. However, minor impurities were still observed (the SEC columns used were very sensitive) and could be attributed to the fact that whilst theoretically solid-phase synthesis facilitates 100 % conversion, in practice it is often slightly lower, depending on the shaking and handling of the resin. That combined with the multi-step, iterative nature of this protocol, meant that a negligible amount of lower molecular weight products was still present, as can be seen in *Figure VI 3*. One could potentially attribute this to human error, as it has been reported that automation introduces more consistency into iterative approaches, thus improving purity and reproducibility.[44]

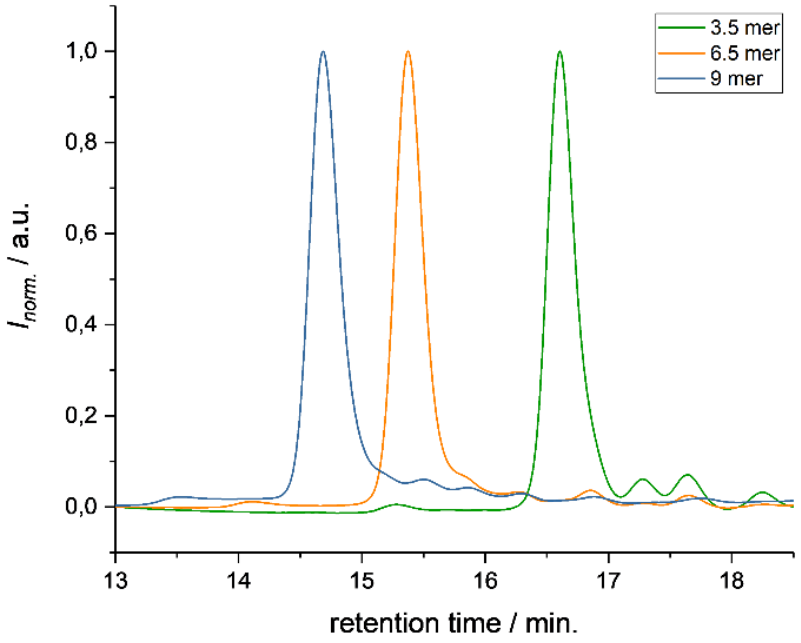


*Figure VI 3: SEC analysis of the solid-phase synthesised oligomers, depicting the 3.5mer (product from halfway through the 4th cycle), 6.5mer (product from halfway through the 7th cycle) and Ph-TAD capped nonamer. The P-3CR polymerisation side product was significantly reduced (*c.f. Figure VI 2*) following the successful application of the optimised conditions.*

VI.2.3 Solution-phase approach

For the solution phase synthesis, stearic acid was used as starting substrate. This long, aliphatic compound was used to help subsequent purification *via* column chromatography by lowering the polarity of the resulting molecules, thus aiding separation. This acid compound was first reacted with an aldehyde and with the isocyanide of linker molecule **L1** in a P-3CR. The same three aldehydes used in the solid-phase approach were used alternatively in the sequences to build monodisperse $[ABC]_x$ structures.

First, the kinetics of the P-3CR were investigated. Earlier works on the P-3CR never investigated this and typically reported reactions for 24 hours to ensure full conversion.[33–35] To study this, the three different aldehyde compounds were reacted with stearic acid and linker molecule **L1** and the reactions were followed by online IR (an example is shown in *Figure VI 4a* and *b*). The peak of the isocyanide at around 2145 cm^{-1} was the clearest one in the spectrum to identify and thus was used for monitoring the reaction. Since the isocyanide was used in excess, full conversion was indicated when the absorbance intensity of the isocyanide peak reached a plateau. After four to six hours of reaction time, the plateau was reached for all aldehydes. The Passerini product was purified by column chromatography, whereby a yield of 98 % was achieved. In further P-3CRs, the reaction was thus typically stirred for eight to ten hours to ensure full conversion, thus offering a significant time advantage over previous approaches.

Subsequently, the first TAD Diels-Alder reaction was performed. Since TAD compounds have an intense pink/red colour, which disappears as they are consumed, a visual feedback was observed during the reaction. Hence, linker molecule **L2** was added in small stoichiometric excess to the reaction mixture and the reaction was conducted as a titration. As soon as the colour slightly remained, the conversion was considered to be complete and the crude product was directly used for the subsequent P-3CR. This also resulted in a significant advance in time and ease of procedure. Most importantly, a purification step is saved in the new combination of TAD with P-3CR. By iterating this cycle several times, sequence-defined oligomers were synthesised.

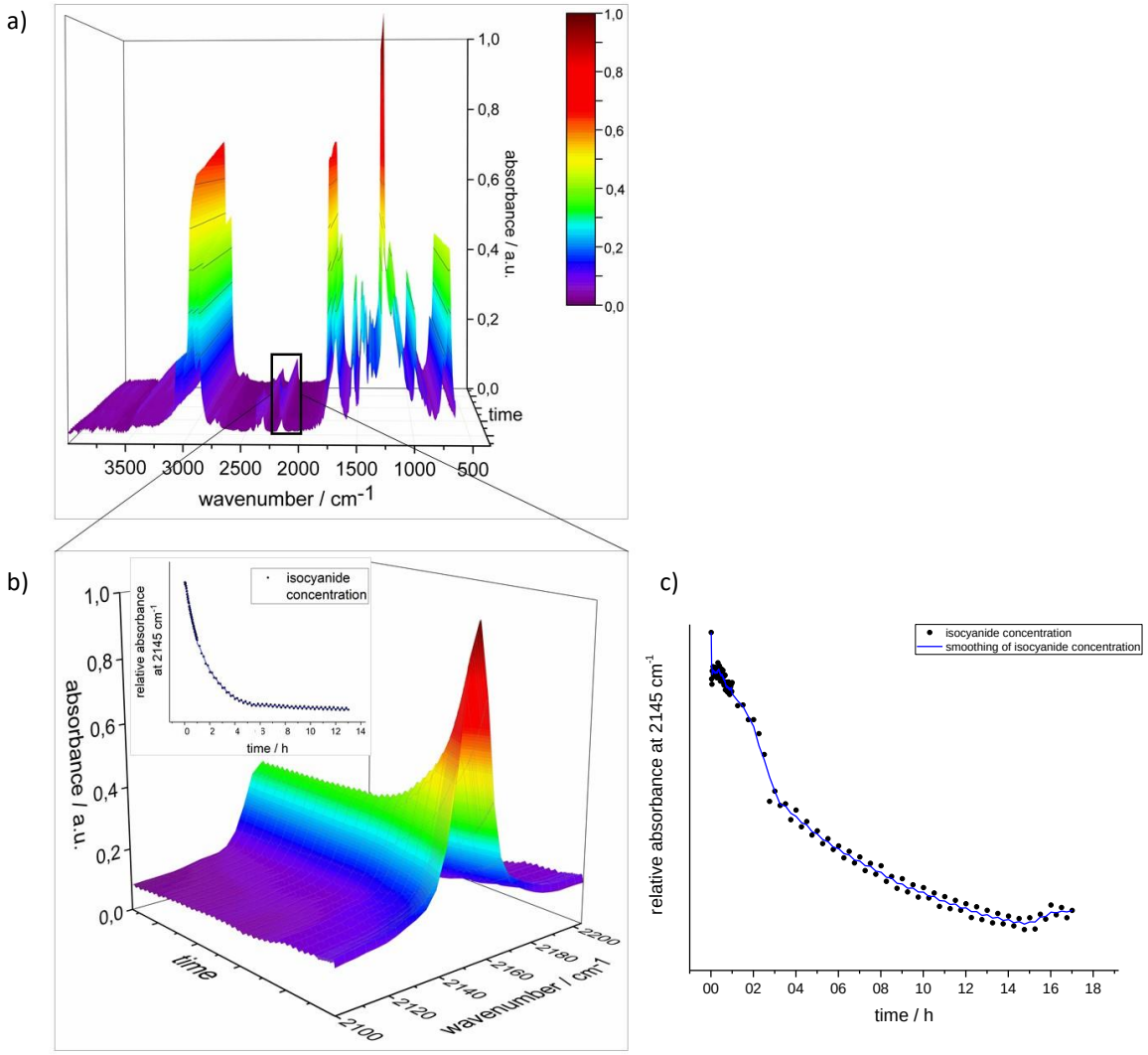
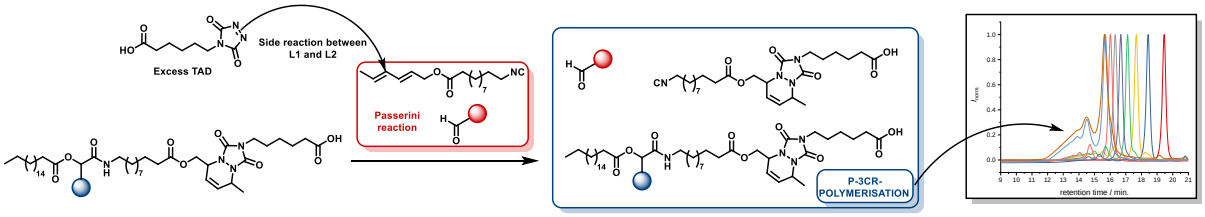


Figure VI 4: a) Example of an online IR measurement during a P-3CR, highlighting the isocyanide absorption band at 2145 cm^{-1}. b) By zooming in, the decrease of the absorbance of the isocyanide peak is clearly observed. Online IR analysis of the kinetics of the other aldehydes used can be found in the published supporting information.[59] *c) Online IR analysis of the P-3CR during the fifth reaction cycle depicting the decrease of isocyanide peak at 2145 cm^{-1} with time. The reaction was complete after 15 h..*

During the fifth reaction cycle, the online IR measurement was repeated (*Figure VI 4c*), showing an expected slowing-down of the reaction because of potential increasing chain entanglement and thus less accessible end groups. The following reaction was left for 16 hours, and for subsequent P-3CRs, the reaction time was systematically extended to 24 and eventually to 48 hours for higher molecular weight oligomers, to ensure reaction completion. By applying these reaction conditions, a sequence-defined nonamer was obtained. However, SEC analysis (*Scheme VI 3*) revealed that a side reaction had occurred in parallel to the nonamer formation.



*Scheme VI 3: Proposed side reaction that occurred between the excess TAD-COOH molecule, **L2** and the diene isocyanide linker molecule, **L1** to afford an uncontrolled Passerini-3CR polymerisation with present aldehydes and the SEC elugrams of the obtained oligomers and P-3CR polymerisation products.*

After each P-3CR, the obtained product was carefully characterised by ^{1}H and ^{13}C NMR, IR, MS, SEC, SEC-MS and LCMS. SEC was key to confirming the (mono)dispersity and thus purity of the products, as the side reaction was not observable by NMR nor LCMS analysis, whereas even traces of impurities were clearly visible in the SEC elugram. Starting from the trimer stage, side products of lower retention time, thus higher molecular weight, were observed, which could not be separated from the product. Over the course of the following reactions, the amount of polymeric side product increased drastically and at the final stage the reaction product consisted of 46 % side product and only 54 % sequence-defined nonamer. This side reaction was also observed, albeit to a much lesser extent, on the solid-phase synthesised oligomer (as already discussed above), but initial focus was given to optimising the solution phase reactions as the impurity was much more pronounced there, before later applying this to the solid-phase approach. Furthermore, the larger scale of solution synthesis allowed for full characterisation after each reaction step which helped to identify and understand the recurring side reaction. The side product was analysed by SEC-ESI-MS and was proposed to be the product of a P-3CR polymerisation, occurring because of the small excess of TAD compound present after each reaction cycle (*Scheme VI 3*), which was still present after evaporation of the solvent from the reaction mixture. Therefore, the two linker molecules **L1** and **L2** underwent a click reaction with each other, forming a new monomer carrying a carboxylic acid and isocyanide containing moiety, which reacted in a P-3CR polymerisation, together with the aldehyde compounds and the sequence-defined oligomer.

To prevent this side reaction, the reaction conditions were adjusted by adding a non-functional alkene (20 µL, 0.2 mmol of dimethylbut-2-ene) after the TAD addition reaction to quench the excess of linker **L2** *via* an Alder-ene reaction. This resulted in an immediate disappearance of the remaining pink colour and the reaction was then continued with the subsequent P-3CR. Because of the better scalability of the reactions in solution, the optimisation was first performed for the solution phase approach, as it offered the possibility to check the dispersity after every iterative cycle, and afterwards this optimisation was transferred to the solid-phase synthesis. By applying these optimised reaction conditions, the side reaction was prevented and a sequence-defined nonamer of very high purity was successfully

synthesised in solution. This oligomer, with a molecular weight of 5340 g mol^{-1}, was synthesised in 17 reaction steps with an overall yield of 18 % (180 mg). SEC analysis verified the high purity of the final product (*Figure VI 5*). In SEC-ESI-MS analysis, the doubly (*m/z* 2670.97), triply (*m/z* 1780.99) and quadruply (*m/z* 1335.86) charged protons as well as the sodium ions were observed and the isotopic pattern was compared with the calculated one, confirming the structure of the product. The product was further analysed by NMR- and IR spectroscopy, as well as by HRMS, all confirming the high purity of the macromolecule.

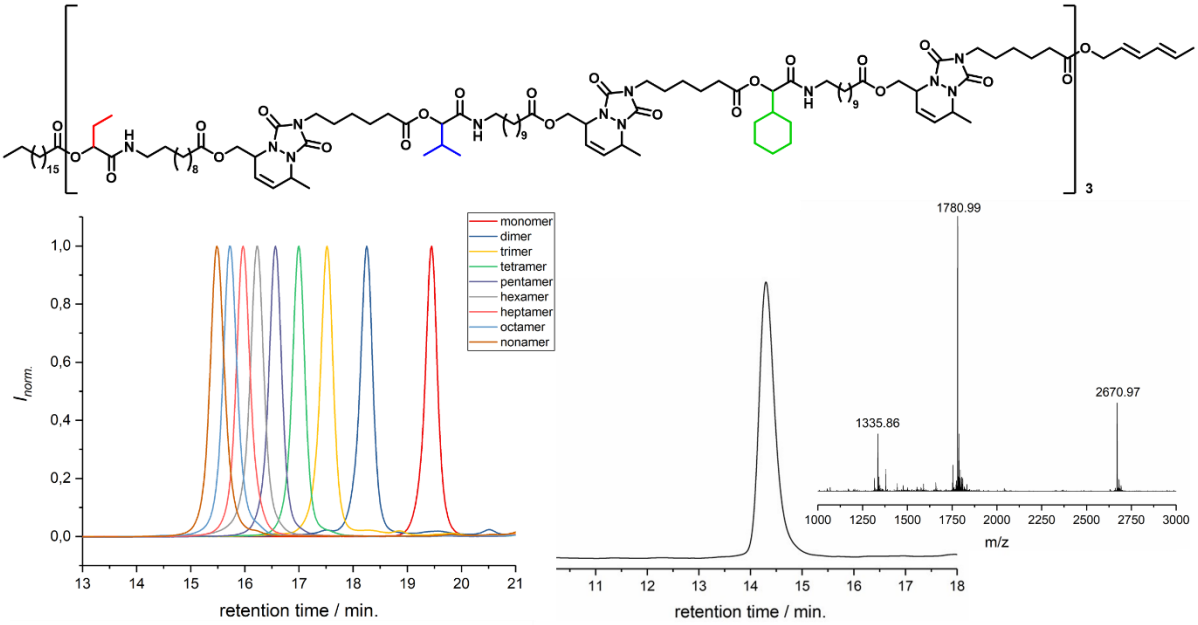


Figure VI 5: Top) Structure of the [ABC]$_3$ sequence-defined nonamer with three different side chains. Bottom left) SEC analysis of the obtained products from the optimised iterative synthesis cycle. The SEC results show the successful prevention of the side reaction and verify the high purity of the products. Bottom right) SEC-ESI-MS analysis of the nonamer showing the chromatogram and the corresponding mass spectrum at a retention time of 14 min 30 s. The assigned peaks correspond to the masses of the doubly, triply and quadruply charged protons.

VI.3 Conclusion and outlook

Through this work, a new approach towards sequence-defined macromolecules was introduced, combining the advantages of the P-3CR with the very efficient and ultra-fast TAD chemistry. A careful comparison of this approach carried out on solid-phase and in solution is given in *Table VI 1*. Originally, a dodecamer was synthesised in 25 steps with an overall yield of 5 % (14.4 mg) using the solid-phase approach. The synthesis was performed using 50 mg of loaded resin and the final product was obtained with a purity, or sequence fidelity, of only 74 % (as determined by SEC), because of occurrence of a P-3CR polymerisation side reaction. This was originally observed to a much greater extent with the solution phase approach. However, reaction optimisation showed how this could be successfully prevented, leading to a very practical and quick build-up of oligomers. The optimised reaction

conditions were later successfully applied to the solid-phase approach, resulting in a sequence-defined nonamer, where the purity, or sequence fidelity, was increased to 84 % (as determined by SEC) and the polymerisation side reaction was avoided. The most important advantage of the solid-phase approach highlighted in this comparative study is the time required, not only for the reaction itself, but also for the purification. On solid-phase, the P-3CRs were performed within 30 to 120 minutes and the TAD Diels-Alder reaction reached full conversions in less than five minutes. The products were purified by simple washing procedures. Thus, in comparison to solution phase chemistry, working with a solid support simplifies and accelerates the synthesis and workup procedure significantly. The synthesis of a nonamer in solution required approximately three weeks, whereas the same molecule synthesised on a solid support was obtained within two days. The solid-phase synthesis could also, in principle, be automated using a peptide synthesiser (as demonstrated in Chapter IV) to potentially result in not only vast libraries of different sequences in tandem but also to obtain the product in gram-scale.

Table VI 1: Direct comparison of the two synthesis techniques (i.e. solid-phase and solution phase chemistries).

	Solid-phase	**Solution phase**
Yield (%)	5	18
*** "Purity" (%)**	84	>99
Scale (mg)	50	200
Degree of polymerisation	9*	9
Purification method	Washing	Column chromatography
Reaction time	<5 min.,[a] 30-120 min[b]	5 min.,[a] 8-48 h[b]
Overall required time	2 days	3 weeks

*Reaction time for [a] TAD Diels-Alder reaction and [b] P-3CR. * Prior to optimisation, a degree of polymerisation of 12 was achieved. *Purity, or sequence-fidelity, was determined by SEC and thus refers to the % of monodisperse product.*

For the reactions carried out in solution, 180 mg of a monodisperse nonamer with a purity, or sequence fidelity, of >99 % (as determined by SEC) was obtained in 17 reaction steps, with an overall yield of 18 %. P-3CRs were carried out over a reaction time of eight to 48 hours, while TAD Diels-Alder reactions were again complete in less than five minutes. The products were purified by column chromatography, which was very effective, but time consuming. Automated column chromatography was investigated, but the yield was significantly lower than doing it manually, so this was not pursued

further. Here, the reactions were typically carried out in 200 mg scale but, theoretically, the synthesis could easily be scaled up to multigram scale.

The comprehensive study discussed here clearly demonstrates the power of combining click chemistry with multicomponent reactions and the potential that TAD chemistry holds within the field of sequence-defined synthesis. This combination facilitated the synthesis of multifunctional macromolecules *via* iterative growth, significantly improving already reported procedures in terms of purity, time and transferability between approaches for scalability. Through this comparative study, it was also demonstrated that many different and versatile chemistries could be carried out on both the solid-phase and in solution. The user choice for the appropriate procedure should be guided by decisions of synthesis speed, potential for library synthesis and necessary scale.

VI.4 Experimental details

This work was carried out in collaboration with Katharina Wetzel (KIT, Germany) whereby the work was equally divided. Functional TAD synthesis and solid-phase synthesis was carried out by myself and functional isocyanide synthesis and solution-phase synthesis was carried out by Katharina. Analysis and conclusion of the work was carried out together.

VI.4.1 Chemicals

The following chemicals were used as received from the suppliers unless otherwise described. CD_3CN-d_3 ≥ 99.8 %, DMSO-d_6 ≥ 99.8 %, CD_3OD-d_4 ≥ 99.8 % and $CDCl_3$ ≥ 99.8 % were purchased from Euriso-top. Ethyl carbazate 97 %, Stearic acid 98 %, hydrochloric acid in 1,4-dioxane ca. 4 mol/L, isobutyraldehyde >98 %, propanal >98 %, and cyclohexanal >98 % were purchased from the Tokyo Chemical Industry (Europe). Anhydrous ethyl acetate 99.8 %, 11-aminoundecanoic acid 97 %, thionyl chloride 99 %, trimethyl orthoformate 99 %, diisopropylamine (DIPEA) > 99.5 %, phosphorous (V) oxychloride 99 %, TLC silica gel F_{254}, cerium(IV)-sulfate 99 %, phosphomolybdic acid hydrate 99 %, sodium carbonate 98 %, sodium hydrogen carbonate > 95 %, sodium sulfate > 99 % (anhydrous), 2,3-dimethylbut-2-ene ≥ 99.9 %, and 1,5,7-triazabicyclo[4.4.0]dec-5-ene 98 % (TBD) were purchased from Sigma-Aldrich. Hydrochloric acid 36 wt% was purchased from Chem Lab NV. *Trans,trans*-2,4-hexadien-1-ol (sorbic alcohol) was purchased from both Sigma-Aldrich (97 %) and Alfa Aesar (98 %). Silica gel 60 (0.040 - 0.063) was purchased from both Sigma-Aldrich and Rocc S.A. Potassium Carbonate ≥ 99 % and magnesium sulfate ≥ 99 % were purchased from Carl Roth. Trifluoroacetic acid (TFA, peptide grade) and 2-chlorotrityl chloride resin (100-200 mesh, 1 % DVB, 1.6 mmol/g) were purchased from Iris Biotech GmbH. 1-Aminocaproic acid 99+ % and diphenyl carbonate 99 % was

purchased from Acros Organics. Acetonitrile (HPLC grade ≥ 99.9 %), chloroform (HPLC grade ≥ 99.9 %), and dichloromethane (DCM, HPLC grade ≥ 99.9 %) were purchased from Sigma-Aldrich. Methanol (HPLC grade 99.8 %), triethylamine (99 %, anhydrous), dimethylformamide (DMF, 99.8 %, anhydrous), pyridine (99.5 %, anhydrous), and tetrahydrofuran (THF, 99.5 %, extra dry over molecular sieves) were purchased from Acros Organics. Ethanol and diethyl ether, both analytical reagent grade, were purchased from Fisher Scientific. Technical grade hexane and ethyl acetate, supplied by Univar, were used for purifications by column chromatography. All solvents were used without further purification, unless otherwise noted. Water, when used in the synthesis, was de-ionised. N_2O_4 gas was supplied by Gerling Holz & Co, Germany.

VI.4.2 Analytical methods

Nuclear Magnetic Resonance (NMR): ^{1}H spectra were recorded at the Karlsruhe Institute of Technology (KIT, Germany) at 500 MHz and ^{13}C-NMR Attached Proton Test (APT) spectra were recorded at 125 MHz on a Bruker Avance DRX. Chemical shifts are presented in parts per million (δ) relative to the resonance signal of $CDCl_3$ or CD_3OD-d_4 (7.26 ppm or 3.31 ppm in ^{1}H- and 77.16 ppm or 49.00 ppm in ^{13}C NMR respectively). ^{1}H spectra were recorded at Ghent University (UGent, Belgium) on a Bruker Avance 300, a Bruker Avance 400, Bruker Avance 500 or a Bruker Avance II 700. ^{13}C-NMR Attached Proton Test (APT) spectra were recorded on a Bruker Avance 400. Chemical shifts are presented in parts per million (δ) relative to DMSO-d_6, $CDCl_3$ or MeCN-d_3 (2.50 ppm, 7.26 ppm or 1.94 ppm in ^{1}H- and 39.51 ppm, 77.24 ppm or 118.26 ppm in ^{13}C-NMR respectively) as internal standard. Coupling constants (J) are reported in Hertz (Hz). All measurements were recorded in a standard fashion at 25 °C. Full assignment of structures was aided by 2D NMR analysis (COSY, HSQC and HMBC).

Size Exclusion Chromatography (SEC): Oligomers were characterized at UGent on a Waters SEC system equipped with a Waters 1515 isocratic pump, Waters 2410 refractive index detector (24 °C), Waters 717plus autosampler and a Waters 2487 dual λ absorbance UV detector and column oven. For separation, a three-column setup was used with one SDV 3 µm, 8×50 mm precolumn and two SDV 3 µm, 1000 Å, 8×300 mm columns supplied by PSS, Germany. Tetrahydrofuran (THF) stabilized with butylated hydroxytoluene (BHT, HPLC-SEC grade) supplied by Biosolve was used at a flow rate 1.0 mL min^{-1}. Calibration was carried out by three injections of a mixture of narrow polystyrene standards ranging from 162 to 38640 kDa. SEC measurements were performed at the KIT on a SHIMADZU Size Exclusion Chromatography (SEC) system equipped with a SHIMADZU isocratic pump (LC-20AD), a SHIMADZU refractive index detector (24°C) (RID-20A), a SHIMADZU autosampler (SIL-20A) and a VARIAN column oven (510, 50°C). For separation, a three-column setup was used with one SDV 3 µm,

8×50 mm precolumn and two SDV 3 µm, 1000 Å, 3×300 mm columns supplied by PSS, Germany. Tetrahydrofuran (THF) stabilized with 250 ppm butylated hydroxytoluene (BHT, ≥99.9%) supplied by Sigma-Aldrich was used at a flow rate of 1.0 mL min^{-1}.

Electrospray Ionisation Mass Spectrometry (ESI-MS) and Liquid Chromatography Mass Spectrometry (LCMS): An Agilent technologies 1100 series LC/MSD system equipped with a diode array detector and single quad MS detector (VL) with an electrospray source (ESI-MS) was used for classic reversed phase LCMS and MS analysis. Analytic reversed phase HPLC (high-performance liquid chromatography) was performed with a Phenomenex Kmetex C18 (2) column with a solid core at 35 °C and a flow rate of 1.5 mL/min (5 µ, 150 x 4.6 mm) using a solvent gradient (0 → 100 % acetonitrile in H_2O in 6 min) and the eluting compounds were detected via UV-detection (λ = 214 nm). LCMS spectra were analysed using ACD/Spectrus software and the purity of compounds was assessed by integrating the LC peaks (λ = 214 nm) using the in-software function.

High Resolution Mass Spectroscopy (HRMS): HRMS spectra were collected using an Agilent 6220 Accurate-Mass time-of-flight (TOF) equipped with a multimode ionization (MMI) source.

Fast atom bombardment (FAB) mass spectra were recorded on a *Finnigan* MAT 95 instrument. The protonated molecule ion is expressed by the term: $[(M+H)]^+$.

Infrared (IR): Measurements were recorded at the KIT on a Bruker Alpha-p instrument in a frequency range from 3998 to 374 cm^{-1} applying KBr and Attenuated Total Reflection (ATR) technology or at UGent on a Perkin Elmer FTIR SPECTRUM 1000 spectrometer with ATR with a PIKE Miracle ATR unit.

Online FT-IR: Measurements were performed on a ReactIR 4000 instrument (Mettler Toledo) with the use of a silicon probe (SiComp, optical range 4400-650 cm^{-1}).

Thin layer chromatography (TLC): Experiments were performed on silica gel coated aluminium foil (silica gel 60 F_{254}, Sigma-Aldrich). Compounds were visualized by staining with Seebach-solution (mixture of phosphomolybdic acid hydrate, cerium(IV)-sulfate, sulfuric acid and water).

SEC-ESI-MS spectra were recorded on a Q Exactive (Orbitrap) mass spectrometer (Thermo Fisher Scientific, San Jose, CA, USA) equipped with an HESI II probe. The instrument was calibrated in the *m/z* range 74–1822 using premixed calibration solutions (Thermo Scientific). A constant spray voltage of 4.6 kV, a dimensionless sheath gas of 8, and a dimensionless auxiliary gas flow rate of 2 were applied. The capillary temperature and the S-lens RF level were set to 320 °C and 62.0, respectively. The Q Exactive was coupled to an UltiMate 3000 UHPLC System (Dionex, Sunnyvale, CA, USA) consisting of a pump (LPG 3400SD), autosampler (WPS 3000TSL), and a thermostated column department (TCC 3000SD). Separation was performed on two mixed bed size exclusion chromatography columns

(Polymer Laboratories, Mesopore 250 × 4.6 mm, particle diameter 3 µm) with precolumn (Mesopore 50 × 4.6 mm) operating at 30 °C. THF at a flow rate of 0.30 mL·min^{-1} was used as eluent. The mass spectrometer was coupled to the column in parallel to a RI-detector (RefractoMax520, ERC, Japan). 0.27 mL·min^{-1} of the eluent were directed through the RI-detector and 30 µL·min^{-1} infused into the electrospray source after post-column addition of a 100 µM solution of sodium iodide in methanol at 20 µL·min^{-1} by a micro-flow HPLC syringe pump (Teledyne ISCO, Model 100DM). A 20 µL aliquot of a polymer solution with a concentration of 2 mg·mL^{-1} was injected onto the HPLC system.

Orbitrap Electrospray-Ionisation Mass Spectrometry (ESI-MS) mass spectra were recorded on a Q Excative (Orbitrap) mass spectrometer (Thermo Fisher Scientific, San Jose, CA, USA) equipped with an atmospheric pressure ionisation source operating in the nebuliser assisted electrospray mode. The instrument was calibrated in the *m/z*-range 150-2000 using a standard containing caffeine, Met-Arg-Phe-Ala acetate (MRFA) and a mixture of fluorinated phosphazenes (Ultramark 1621, all from Sigma Aldrich). A constant spray voltage of 3.5 kV, a dimensionless sheath gas of 6, and a sweep gas flow rate of 2 were applied. The capillary voltage and the S-lens RF level were set to 68.0 V and 320 °C, respectively.

Electron ionisation (EI) For the measurements that were performed with the electron ionisation (EI) method, an instrument by Finnigan, model MAT 90 (70 eV), was used with 3-nitrobenzyl alcohol (3-NBA) as matrix. For the interpretation of the spectra, molecular peaks $[M]^+$, peaks of pseudo molecules $[M+H]^+$ and characteristic fragment peaks are indicated with their mass to charge ratio (*m/z*) and their intensity in percent, relative to the most intense peak (100%).

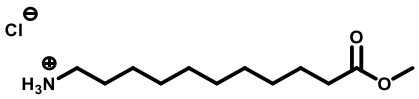
VI.4.3 Synthesis of linker molecules

VI.4.3.1 Synthesis of diene-isocyanide, L1

A schematic overview of the synthesis steps is shown above in Scheme VI 2.

Step 1: Synthesis of 11-methoxy-11-oxoundecan-1-ammonium chloride

This was synthesised according to a previously reported procedure.[64]

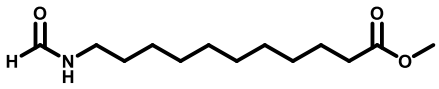


11-Aminoundecanoic acid (15.0 g, 74.5 mmol, 1.0 eq.) were suspended in 150 mL methanol and the suspension was cooled in an ice bath to 0 °C. Subsequently, thionyl chloride (18.9 mL, 31.0 g, 0.26 mol, 3.5 eq.) was added dropwise. The reaction was then allowed to warm to room temperature and was stirred overnight. The yellowish solution was then poured into cold diethyl ether (500 mL) and stored in the freezer for one hour. The product was filtered off and dried under high vacuum. 11-Methoxy-11-

oxoundecan-1-ammonium chloride was obtained as a white powder in a yield of 99 % (m = 18.6 g). The crude product was used without further purification. **^{1}H-NMR (300 MHz, CD_3OD-*d_4*):** δ = 3.62 (s, 3H, OCH_3), 2.91 (t, *J* = 7.0 Hz, 2H, $CH_2NH_3^+$), 2.34–2.20 (t, *J* = 7.4 Hz, 2H, CH_2COOCH_3), 1.75–1.47 (m, 4H, $CH_2CH_2COOCH_3$, $CH_2CH_2NH_3^+$), 1.46-1.15 (m, 12H, CH_2,). **^{13}C NMR (101 MHz, CD_3OD-*d_4*):** δ = 175.98, 51.95, 40.79, 34.78, 30.39, 30.37, 30.29, 30.15, 30.13, 28.55, 27.42, 25.99. **HRMS (EI) *m/z:*** $[M - H]^+$ calculated for $[C_{12}H_{26}NO_2^+]$: 215.1885, found: 215.1885. **HRMS (EI) *m/z:*** $[M]^+$ calculated for $[C_{12}H_{26}NO_2^+]$: 216.1964, found: 215.1964. **IR** (ATR platinum diamond): ν [cm^{-1}] = 2920, 2849, 1723, 1609, 1562, 1511, 1468, 1444, 1420, 1376, 1361, 1334, 1306, 1277, 1245, 1211, 1174, 1115, 1098, 1043, 1001, 971, 938, 886, 792, 742, 723, 703, 594, 504, 450, 426.

Step 2: Synthesis of methyl 11-formamidoundecanoate

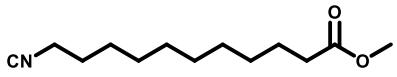
This was synthesised according to a previously reported procedure.[64]



11-Methoxy-11-oxoundecan-1-aminium chloride (18.8 g, 74.9 mmol, 1.0 eq.) was dissolved in trimethyl orthoformate (81 mL, 78.5 g, 0.74 mol, 10.0 eq.) and was heated to reflux (100 °C) and stirred for 12 hours. The solvent was removed *in vacuo*, yielding a white solid. Yield = 86 % (m = 15.6 g, 0.64 mol). The crude product was used without further purification. **^{1}H-NMR (300 MHz, $CDCl_3$):** δ = 8.19–7.87 (m, 1H, HCO), 6.08 (m, 1H, NH), 3.61 (s, 3H, OCH_3), 3.38–3.01 (m, 2H, CH_2), 2.24 (t, *J* = 7.5 Hz, 2H, CH_2), 1.69–1.36 (m, 4H, CH_2), 1.22 (s, 12H, CH_2). **^{13}C NMR (101 MHz, $CDCl_3$):** δ = 174.32, 155.78, 155.70, 155.62, 51.48, 41.69, 41.61, 41.52, 34.12, 29.32, 29.22, 29.14, 28.71, 26.35, 24.97. **HRMS (EI) *m/z:*** $[M]^+$ calculated for $[C_{13}H_{25}NO_3^+]$: 243.1834, found: 243.1835. **IR** (ATR platinum diamond): ν [cm^{-1}] = 3260, 2916, 2849, 1735, 1683, 1638, 1537, 1464, 1436, 1379, 1335, 1301, 1269, 1227, 1205, 1170, 1113, 1058, 1002, 980, 905, 883, 738, 721, 519, 449.

Step 3: Synthesis of methyl 11-isocyanoundecanoate

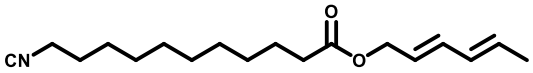
This was synthesised according to a previously reported procedure.[64]



Methyl 11-formamidoundecanoate (12.8 g) was dissolved in CH_2Cl_2 (180 mL) and diisopropylamine (22.3 mL, 16.1 g, 0.16 mol, 3.0 eq.) was added to the solution. The mixture was then cooled with an ice bath to 0 °C and phosphorus oxychloride (6.3 mL, 10.5 g, 68.8 mmol, 1.3 eq.) was added dropwise. After the addition, the ice bath was removed and the solution was allowed to warm to room temperature

and was stirred for two hours. The reaction was then quenched by addition of sodium carbonate solution (75 mL, 20 %) at 0 °C. The mixture was stirred for another 30 minutes at room temperature and subsequently, CH_2Cl_2 (80 mL) and water (80 mL) was added. The phases were separated and the organic layer was washed with water (3 x 80 mL) and brine (80 mL). The combined organic layers were dried over sodium sulfate, the solvent was evaporated under reduced pressure and the crude product was purified by column chromatography (hexane:ethyl acetate 19:1 → 10:1). The product was obtained as a yellowish liquid. Yield = 70 % (8.4 g, 37.1 mmol). **^{1}H-NMR (400 MHz, $CDCl_3$):** δ = 3.65 (s, 3H, OC$\underline{H}_3$), 3.44–3.26 (m, 2H, C$\underline{H}_2$), 2.29 (t, *J* = 7.5 Hz, 2H, C$\underline{H}_2$), 1.77–1.56 (m, 4H, C$\underline{H}_2$), 1.48–1.18 (m, 12H, C$\underline{H}_2$). **^{13}C NMR (75 MHz, $CDCl_3$):** δ = 174.32, 155.70, 51.48, 41.69, 41.61, 41.52, 34.12, 29.32, 29.22, 29.14, 28.71, 26.35, 24.97. **HRMS (EI)** ***m/z:*** $[M]^+$ calculated for $[C_{13}H_{23}NO_2^+]$: 225.1729, found: 225.1729. **IR** (ATR platinum diamond): *ν* [cm^{-1}] = 2926, 2855, 2147 (isocyanide), 1736, 1436, 1353, 1195, 1170, 1105, 1011, 849, 722, 428. **R_F** (hexane / ethyl acetate (5:1)) = 0.51.

Step 4: Synthesis of (2*E*,4*E*)-hexa-2,4-diene-1-yl 11-isocyanoundecanoate



To a mixture of methyl 11-isocyanoundecanoate (8.3 g, 36.3 mmol, 1.0 eq.) and sorbic alcohol (7.2 g, 73.3 mmol, 2.0 eq.), TBD (25.5 mg, 1.8 mmol, 5.0 mol%) was added as a catalyst and the reaction mixture was heated to 60 °C under a reduced pressure of 175 mbar at the rotavapor for 1 hour. Subsequently, the pressure was further decreased to 6 mbar and the temperature was decreased to 50 °C for another two and a half hours. Methanol was distilled off during the reaction. The crude product was purified by column chromatography (hexane:ethyl acetate 19:1→15:1) and was obtained as a slightly yellow liquid. Yield = 95 % (m = 10.1 g, 34.6 mmol). **^{1}H-NMR (400 MHz, $CDCl_3$):** δ = 6.28-6.15 (m, 1H, $\underline{H}$C=C, ^{1}), 6.08-5.97 (m, 1H, $\underline{H}$C=C, ^{2}), 5.79-5.65 (m, 1H, $\underline{H}$C=C, ^{3}), 5.65–5.53 (m, 1H, $\underline{H}$C=C, ^{4}), 4.54 (d, *J* = 6.6 Hz, 2H, COOC$\underline{H}_2$, ^{5}), 3.40-3.30 (m, 2H, C$\underline{H}_2$, ^{6}), 2.28 (t, *J* = 7.5 Hz, 2H, C$\underline{H}_2$, ^{7}), 1.74 (d, *J* = 6.7 Hz, 3H, C$\underline{H}_3$, ^{8}), 1.69–1.53 (m, 4H, C$\underline{H}_2$, ^{9}), 1.46–1.19 (m, 12H, C$\underline{H}_2$, ^{10}). **^{13}C NMR (75 MHz, $CDCl_3$):** δ = 173.57, 134.77, 131.15, 130.51, 123.91, 64.75, 41.66, 41.58, 41.49, 34.33, 29.30, 29.20, 29.13, 29.11, 28.70, 26.33, 24.94, 18.15. **HRMS (EI)** ***m/z:*** $[M]^{+\cdot}$ calculated for $[C_{18}H_{29}NO_2^+]$: 292,2198, found: 292.2198. **IR** (ATR platinum diamond): *ν* [cm^{-1}] = 2926, 2855, 2146 (isocyanide), 1732, 1662, 1453, 1378, 1351, 1231, 1164, 1104, 988, 925, 723, 506. **R_F** (hexane / ethyl acetate (5:1)) = 0.66.

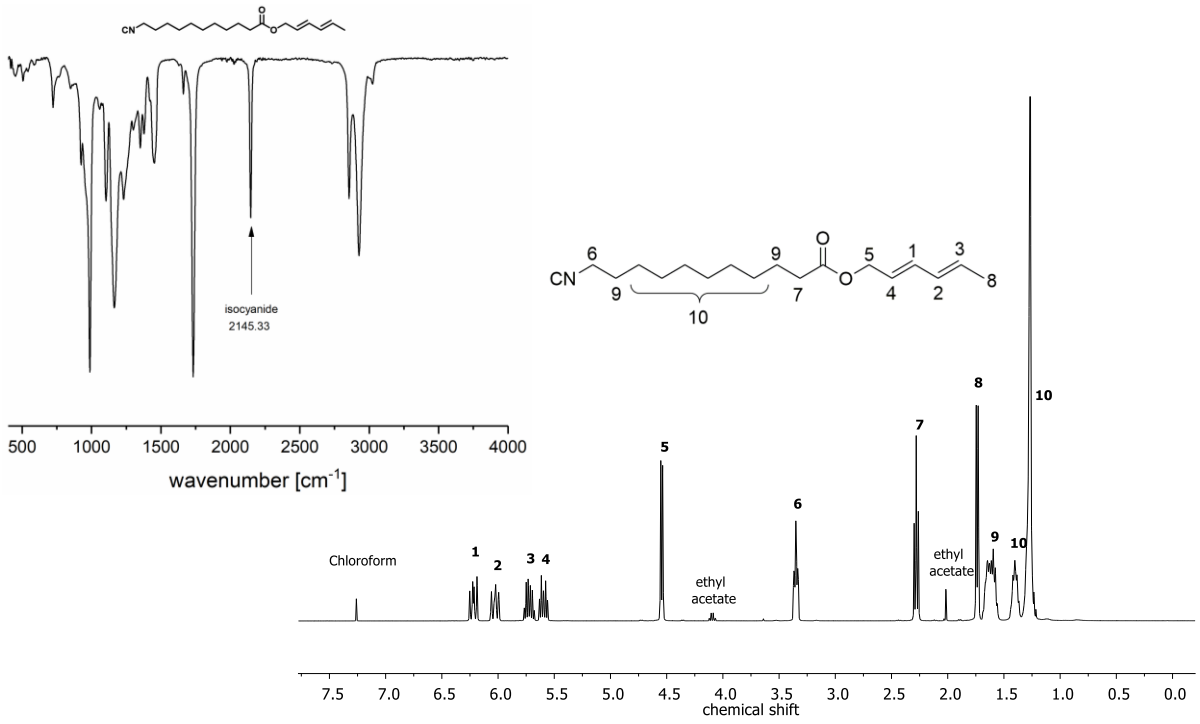


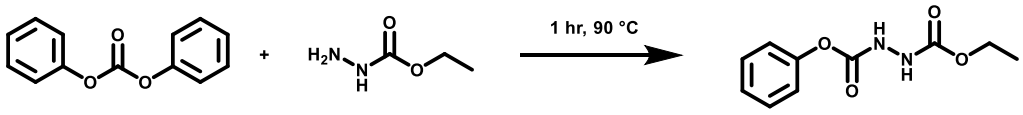
Figure VI 6: Right) IR spectrum of the same product, highlighting the peak selected for the online IR experiments. Left) [1]H NMR spectrum of (2E,4E)-hexa-2,4-diene-1-yl 11-isocyanoundecanoate.

VI.4.3.2 Synthesis of 1,2,4-triazoline-3,5-dione hexanoic acid (TAD-COOH), L2

A schematic overview of the synthesis steps is shown above in Scheme VI 2

Step 1: Synthesis of ethyl phenyl hydrazine-1,2-dicarboxylate

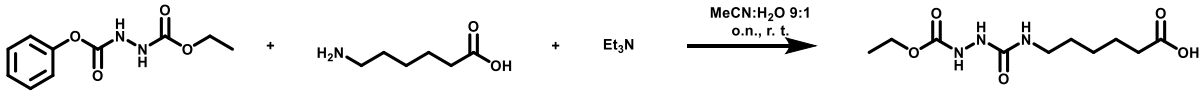
This was synthesised according to a previously reported procedure.[65]



Diphenyl carbonate (60.02 g, 0.280 mol, 1.0 equiv.) and ethyl carbazate (58.37 g, 0.560 mol, 2.0 equiv.) were heated and stirred in bulk at 90 °C for 1 hour. The reaction was then precipitated into water (1.5 L) resulting in an emulsion. The precipitation was stirred fast for several hours and a white solid formed. The precipitation was filtered off and the precipitate was dried overnight under vacuum at 40 °C, resulting in a white, crystalline solid. Yield = 64 % (m = 40.21 g). **^{1}H NMR (300 MHz, DMSO-d_6):** δ = 9.67 (s, 1H, PhOC=ONH), 9.24 (s, 1H, NHC=OOCH$_2$CH$_3$), 7.46-7.35 (m, 2H, Ph), 7.30-7.21 (m, 1H, Ph), 7.14-7.08 (m, 2H, Ph), 4.07 (q, 2H, *J* = 7.09, 7.09, CH$_2$CH$_3$), 1.19 (t, 3H, *J* = 7.08, CH$_2$CH$_3$). **^{13}C NMR (APT, 100 MHz, DMSO-d_6):** δ = 156.43 (C), 154.86 (C), 150.61 (C), 129.48 (CH), 125.39 (CH), 121.47 (CH), 60.70 (CH$_2$), 14.52 (CH$_3$). **HRMS (ESI) *m/z*:** [M + H]$^+$ for [$C_{10}H_{13}N_2O_4^+$];

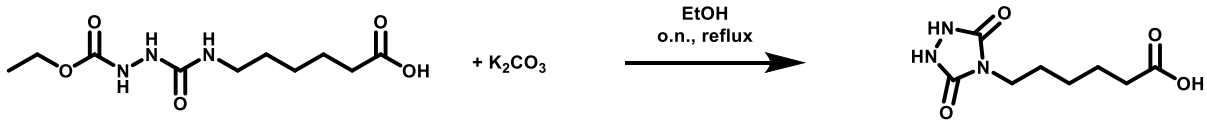
calculated: 225.08698, found: 225.0872. **IR** (ATR platinum diamond): ν [cm^{-1}] = 3225 (N-H), 1742 & 1699 (C=O), 1519 (N-H), 1489 (C-H), 1224, 1189, 1160, 1094 & 1045 (C-O), 907, 792, 723, 688.

Step 2: Synthesis of hexanoic acid semicarbazide



Aminocaproic acid (5.854 g, 44.6 mmol, 1.0 equiv.) and ethyl phenyl hydrazine dicarboxylate (10.0 g, 44.6 mmol, 1.0 equiv.) were dissolved in a 9:1 solution of acetonitrile:H_2O (150 mL). Triethylamine (12.4 mL, 89.2 mmol, 2.0 equiv.) was added and the reaction was stirred for at least 24 hours at room temperature. The acetonitrile was then removed *in vacuo* and then the residual water phase was diluted further with water (400 mL) and extracted three times with ethyl acetate to remove the phenol by-product from the reaction. The aqueous phase was then acidified to pH 1 with HCl in water (36 %) before removal of the water *in vacuo*. Water (20 mL) was then added and the product was stirred vigorously at room temperature overnight to extract any residual, unreacted aminocaproic acid. The reaction mixture was then filtered and the white precipitate dried overnight under vacuum at 40 °C. Yield = 64 % (m = 7.40 g). **^{1}H NMR (300 MHz, DMSO-*d*$_6$):** δ = 11.96 (s, 1H, COO<u>H</u>), 8.70 (s, 1H, OC=ON<u>H</u>), 7.61 (s, 1H, HNN<u>H</u>C=ONH), 6.29 (s, 1H, HNNHC=ON<u>H</u>), 4.02 (q, 2H, *J* = 7.08, 7.09, HNC=ONHC<u>H$_2$</u>), 2.97 (q, 2H, *J* = 6.61, 6.65, $CH_3C\underline{H_2}O$), 2.18 (t, 2H, *J* = 7.38, C<u>H$_2$</u>COOH), 1.48 (p, 2H, *J* = 7.40, 7.40, NHC=ONHCH$_2$C<u>H$_2$</u>), 1.41-1.31 (m, 2H, C<u>H$_2$</u>CH$_2$COOH), 1.28-1.20 (m, 2H, $(CH_2)_2C\underline{H_2}(CH_2)_2$), 1.17 (t, 3H, *J* = 7.09, C<u>H$_3$</u>). **^{13}C NMR (APT, 100 MHz, DMSO-*d*$_6$):** δ = 174.44 (C), 158.22 (C), 156.89 (C), 60.30 (CH_2), 38.96 (CH_2), 33.64 (CH_2), 29.58 (CH_2), 25.81 (CH_2), 24.25 (CH_2), 14.54 (CH_3). **HRMS (ESI) *m/z*:** $[M + H]^+$ for $[C_{10}H_{20}N_3O_5^+]$; calculated: 262.1403, found: 262.1396. **IR** (ATR platinum diamond): ν [cm^{-1}] = 3283 (N-H), 2939 (O-H), 1728, 1711 & 1662 (C=O), 1560 & 1531 (N-H), 1474 & 1365 (C-H), 1272, 1229, 1201 & 1056 (C-O), 898, 738, 648.

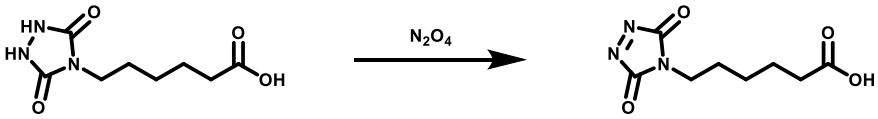
Step 3: Ring closure of hexanoic acid semicarbazide



The semicarbazide (6.05 g, 23.2 mmol, 1.0 equiv.) was solubilised in ethanol (100 mL). K_2CO_3 (12.7 g, 91.9 mmol, 4.0 equiv.) was added and the reaction was stirred at reflux for 24 hours. The reaction was then cooled to room temperature, filtered and the filtrate was evaporated *in vacuo* to complete dryness. The resulting solid was then solubilised in a minimum volume of 1,4-dioxane and then

acidified at room temperature to pH = 1 with HCl in 1,4-dioxane. The precipitate was then filtered off and the solvent was removed *in vacuo*, yielding a white, crystalline solid. Yield = 67 % (m = 3.304 g). **^{1}H NMR (400 MHz, DMSO-*d*$_6$):** δ = 11.99 (s, 1H, COOH), 10.02 (s, 2H, HN-NH), 3.39-3.30 (m, 2H, UrCH$_2$), 2.18 (t, 2H, *J* = 7.33, CH$_2$COOH), 1.50 (h, 4H, *J* = 6.07, 8.87, 7.47, CH$_2$CH$_2$CH$_2$CH$_2$CH$_2$), 1.28-1.18 (m, 2H, (CH$_2$)$_2$CH$_2$(CH$_2$)$_2$). **^{13}C NMR (100 MHz, DMSO-*d*$_6$):** δ = 174.38 (C), 155.06 (C), 37.75 (CH$_2$), 33.49 (CH$_2$), 27.27 (CH$_2$), 25.59 (CH$_2$), 24.02 (CH$_2$). **HRMS** (**ESI)** ***m/z*:** [M + H]$^+$ for [$C_8H_{15}N_3O_4^+$]; calculated: 216.0984, found: 216.0981. **IR** (ATR platinum diamond): ν [cm^{-1}] = 3166 (N-H), 2931 (O-H), 1668 (C=O), 1474 (N-H), 1415 & 1348 (C-N), 1225, 1190, 1116 & 1030 (C-O), 895, 849, 791, 767, 735, 639, 617.

Step 4: Oxidation of urazole to corresponding TAD hexanoic acid compound, L2



The urazole carboxylic acid (0.920 g, 4.27 mmols, 1.0 equiv.) was suspended in anhydrous ethyl acetate (100 mL). $MgSO_4$ (5.15 g, 42.8 mmols, 10 equiv.) was added. The reaction mixture was flushed for approximately 5 minutes with N_2O_4 gas, during which the white suspension became vividly pink in colour. The reaction mixture was then filtered and the solvent from the filtrate was removed *in vacuo*. The isolated TAD moiety was used stored under inert atmosphere at -20 °C because of the inherent high reactivity and instability of TAD compounds. ^{1}H NMR was used to determine the disappearance of the urazole proton resonances, but the yield was not quantified. **^{1}H NMR (400 MHz, DMSO-*d*$_6$):** δ = 11.99 (s, 1H, COOH), 3.46 (t, 2H, *J* = 7.09, TADCH$_2$), 2.18 (t, 2H, *J* = 7.34, CH$_2$COOH), 1.66-1.43 (m, 4H, CH$_2$CH$_2$CH$_2$CH$_2$CH$_2$), 1.36-1.21 (m, 2H, (CH$_2$)$_2$CH$_2$(CH$_2$)$_2$). **^{13}C NMR (100 MHz, DMSO-*d*$_6$):** δ = 174.34 (C), 160.15 (C), 40.50 (CH$_2$), 33.42 (CH$_2$), 26.39 (CH$_2$), 25.38 (CH$_2$), 23.89 (CH$_2$). **HRMS (ESI) *m/z*:** [M + H]$^+$ for [$C_8H_{12}N_3O_4^+$]; calculated: 214.0822, found: 214.1879. **HRMS (ESI) *m/z*:** [M + Na]$^+$ for [$C_8H_{11}N_3O_4Na^+$]; calculated: 236.0642, found: 236.1720. **IR** (ATR platinum diamond): ν [cm^{-1}] = 2934 (O-H), 1742 & 1698 (C=O), 1393 (O-H), 1336 1270, 1212, 1176 & 1137 (C-O & C-N). The following IR absorption bands were unassignable: 2357, 1525, 946, 853, 728, 677. They were proposed to be related to oxidation by-products or less well-known absorption frequencies related to the TAD structure.

VI.4.4 Solid-phase synthesis of sequence-defined oligomers

VI.4.4.1 Manipulation of the solid-phase resin

Swelling: The resin for each reaction was swollen for at least 10 minutes in the reaction solvent (1 mL of solvent per 100 mg of resin).

Washing: The solid-phase resin was extensively washed, under filtration, after each reaction to ensure removal of remaining unreacted starting chemicals or unwanted side-products formed such as precipitates. Washing was done sequentially with DMF (x4), MeOH (x4), $CHCl_3$ (x4) and Et_2O (x4).

Cleavage: For analysis by LCMS, the sequence was cleaved from the resin by suspension in a solution of 1% TFA (trifluoroacetic acid) in CH_2Cl_2 for 5 minutes before filtration of the sample and then concentration by evaporation. During cleavage, a colour change of the beads could be observed from yellow to red because of the trityl cation formed on the resin.

Analysis: This was predominantly carried out using LCMS and HRMS. Once the complete oligomer was synthesised, the remainder of the compound was recovered from the resin and diluted in DMSO-d_6 for ^{1}H NMR and ^{13}C analysis.

VI.4.4.2 Loading of the 2-chlorotrityl chloride resin

2-Chlorotrityl chloride resin was loaded with sorbic alcohol according to the procedure described in *Chapter V.4.4.2* which was adapted from a previously reported procedure.[7]

VI.4.4.3 General solid-phase synthesis protocol

Step 1 – TAD COOH Diels-Alder reaction

The diene functionalised resin (50.0 mg, 1.0 equiv.) was swollen for at least 10 min. in anhydrous DMF (500 µL). This was then filtered off. TAD-COOH (34 mg, 2.0 equiv.) solubilised in anhydrous DMF (500 µL) was added and the reaction was shaken vigorously at room temperature for 5 minutes. The reaction was then filtered and the resin subsequently washed with DMF (×4), $CHCl_3$ (×4), MeOH (×4) and Et_2O (×4). The reaction was analysed by LCMS (see Figure S1). To do this, 2 mg of the reaction resin was removed and suspended for 5 minutes in a 1 % TFA solution (in DCM). This was then filtered, concentrated by evaporation and then diluted with acetonitrile.

Step 2 – P-3CR

The resin from step 1 was swollen for at least 10 minutes in CH_2Cl_2 (500 µL). Then, the diene isocyanide linker molecule **L1** (0.350 g, 15 equiv.) and propanal, isobutyraldehyde or cyclohexanal (20 equiv.) were added. The reaction was shaken vigorously at room temperature for 30 minutes. After the 4th, 7th and 9th cycles, the reaction time was increased by a further 30 minutes as the reaction was slower as the chains lengthened (see IR monitoring results). The reaction was then filtered and the resin subsequently washed with DMF (×4), $CHCl_3$ (×4), MeOH (×4) and Et_2O (×4). A 2 mg sample was again prepared for LCMS analysis after each cycle as described above up until the 8th cycle when the molecular weight of the oligomer was beyond the measurable limits of the instrument, thus thereafter no intermediate analysis via LCMS or HRMS was done.

This iterative, two-step protocol was repeated up to 12 times and was then capped as described below, resulting in a sequence-defined dodecamer. Overall yield = 5 % (m = 14.4 mg).

Terminating step – Diene capping with Phenyl TAD

A separate monomer, dimer, trimer and dodecamer were synthesised and capped with phenyl TAD (synthesised according to previously reported work)[66] to prevent further reaction of the conjugated double bond and to prevent partial hydrolysis of the conjugated ester bond during the mild cleavage conditions. The capping was done by first swelling the resin for at least 10 mins in anhydrous DMF (500 µL). This was then filtered off. Afterwards, PhTAD (5.0 equiv.) was dissolved in anhydrous DMF (500 µl) and added to the resin. The reaction was shaken vigorously at room temperature for 5 minutes. The reaction was then filtered, and the resin subsequently washed with DMF (×4), $CHCl_3$ (×4), MeOH (×4) and Et_2O (×4). The oligomer was cleaved entirely from the resin by suspension for 5 minutes in a 1 % TFA solution (in DCM). This was then filtered and concentrated by evaporation. The resulting colourless-yellow film was dried under vacuum at room temperature for several hours.

LCMS and HRMS measurements were taken after each intermediate reaction step (TAD Diels-Alder reaction and P-3CR) for the synthesis of the sequence-defined nonamer. Details of which can be found in the supporting information of the related article.[59]

VI.4.5 HRMS analysis of the solid-phase synthesised sequence-defined oligomers

Table VI 2: HRMS data of solid-phase sequence-defined oligomers.

Sample name	m/z exp.	formula	m/z theo.	Δ m/z
Monomer	872.4503	$[C_{44}H_{63}N_7O_{10}Na]^+$	872.4529	0.0026
Monomer	850.4689	$[C_{44}H_{63}N_7O_{10}H]^+$	850.4709	0.0020
Dimer	1429.8302	$[C_{73}H_{109}N_6O_7NH_4]^+$	1429.8341	0.0038
Trimer	2051.1721	$[C_{106}H_{161}N_{15}O_{24}Na]^+$	2051.1731	0.0010
Trimer	1037.0803	$[C_{106}H_{161}N_{15}O_{24}Na_2]^{2+}$	1037.0812	0.0009
Trimer	2029.1907	$[C_{106}H_{161}N_{15}O_{24}H]^+$	2029.1912	0.0005
Trimer	1015.0980	$[C_{106}H_{161}N_{15}O_{24}H_2]^{2+}$	1015.0992	0.0012
Nonamer	2704.6421	$[C_{282}H_{448}N_{36}O_{64}Na_2]^{2+}$	2704.6346	0.0075
Nonamer	1810.7606	$[C_{282}H_{448}N_{36}O_{64}Na_3]^{3+}$	1810.7528	0.0078
Nonamer	1363.8164	$[C_{282}H_{448}N_{36}O_{64}Na_4]^{4+}$	1363.8119	0.0045
Nonamer	1095.6492	$[C_{282}H_{448}N_{36}O_{64}Na_5]^{5+}$	1095.6475	0.0017
Nonamer	2682.6045	$[C_{282}H_{448}N_{36}O_{64}H_2]^{2+}$	2682.6527	0.0482
Dodecamer	3669.7145	$[C_{382}H_{599}N_{51}O_{87}Na_2]^{2+}$	3669.6900	0.0245
Dodecamer	2454.1257	$[C_{382}H_{599}N_{51}O_{87}Na_3]^{3+}$	2454.1231	0.0026
Dodecamer	1846.3446	$[C_{382}H_{599}N_{51}O_{87}Na_4]^{4+}$	1846.3396	0.0050
Dodecamer	1481.6702	$[C_{382}H_{599}N_{51}O_{87}Na_5]^{5+}$	1481.6695	0.0007
Dodecamer	1238.5566	$[C_{382}H_{599}N_{51}O_{87}Na_6]^{6+}$	1238.5561	0.0005
Dodecamer	1064.9032	$[C_{382}H_{599}N_{51}O_{87}Na_7]^{7+}$	1064.9037	0.0005
Dodecamer	2432.1402	$[C_{382}H_{599}N_{51}O_{87}H_3]^{3+}$	2432.1411	0.0009
Dodecamer	1824.3595	$[C_{382}H_{599}N_{51}O_{87}H_4]^{4+}$	1824.1411	0.0018
Dodecamer	1459.6874	$[C_{382}H_{599}N_{51}O_{87}H_5]^{5+}$	1459.6876	0.0004
Dodecamer	1216.5735	$[C_{382}H_{599}N_{51}O_{87}H_6]^{6+}$	1216.5742	0.0007
Dodecamer	1043.0632	$[C_{382}H_{599}N_{51}O_{87}H_7]^{7+}$	1042.9218	0.1414

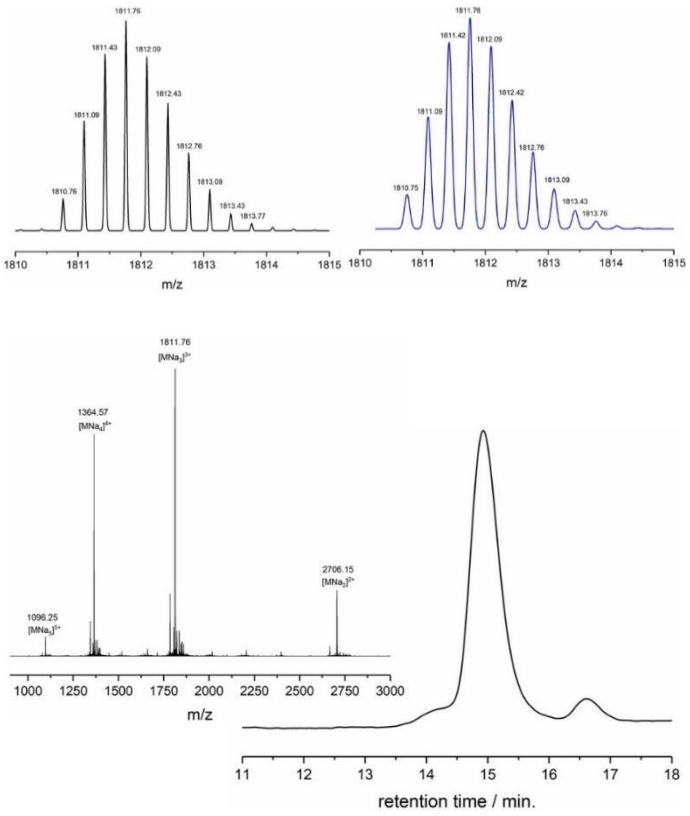


Figure VI 7: SEC-ESI-MS chromatogram and corresponding mass spectrum as well as isotopic pattern at 14.90 min retention time of the nonamer synthesised on solid-phase.

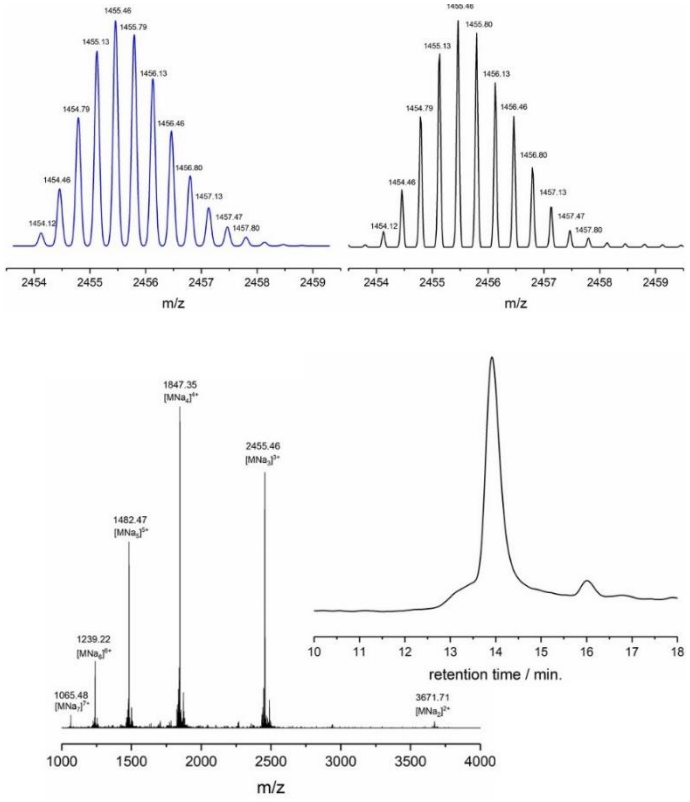


Figure VI 8: SEC-ESI-MS chromatogram and corresponding mass spectrum as well as isotopic pattern at 13.91 min retention time of the dodecamer synthesised on solid-phase.

VI.4.6 NMR analysis of the solid-phase synthesised sequence-defined oligomers

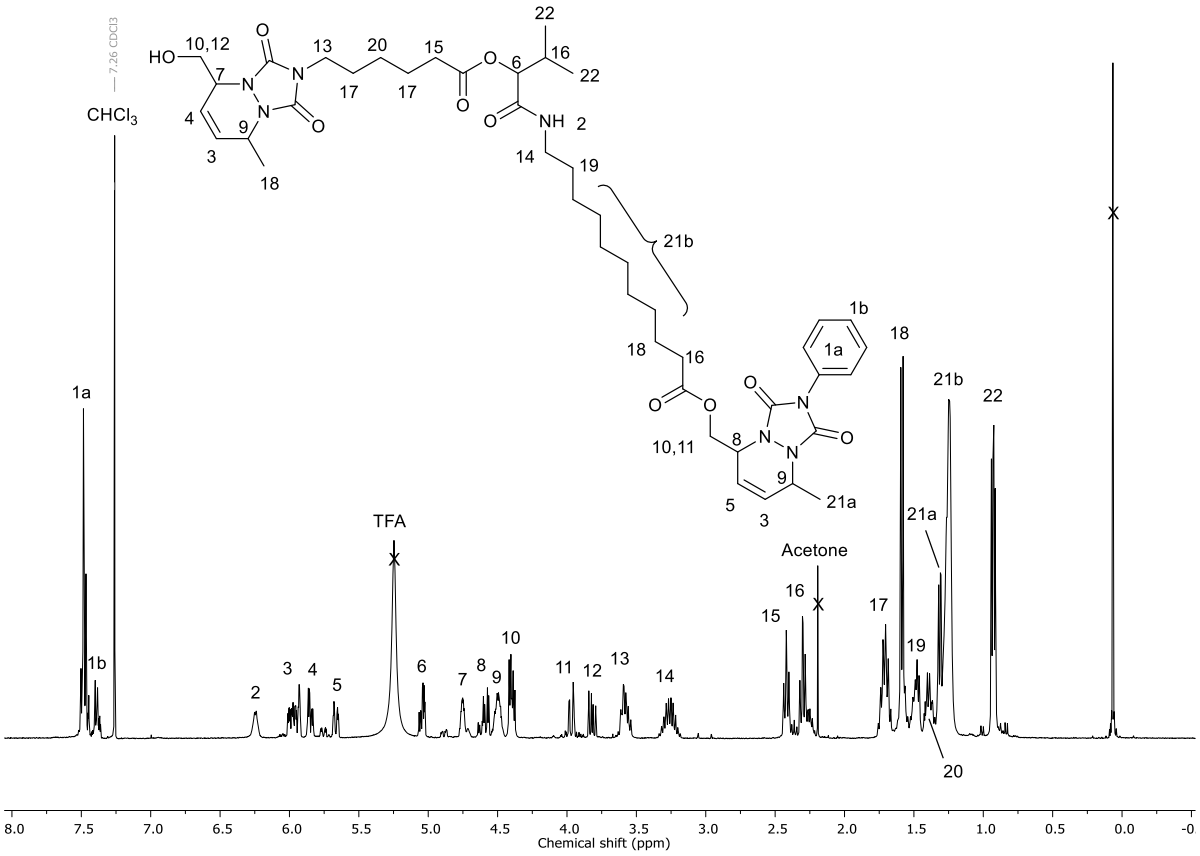


Figure VI 9: [1]H NMR spectrum in $CDCl_3$ of the PhTAD capped monomer.

[1]H NMR (300 MHz, $CDCl_3$): δ = 7.58-7.44 (m, 4H, [1a]), 7.43-7.35 (m, 1H, [1b]), 6.24 (s, 1H, [2]), 6.02-5.92 (m, 2H, [3]), 5.88-5.82 (m, 1H, [4]), 5.70-5.64 (m, 1H, [5]), 5.03 (dd, 1H, *J* = 1.65, 4.76, [6]), 4.75 (s, 1H, [7]), 4.66-4.55 (m, 1H, [8]), 4.49 (s, 2H, [9]), 4.40 (dd, 2H, *J* = 5.13, 11.60, [10]), 3.94 (d, 1H, *J* = 9.94, [11]), 3.82 (dd, 1H, *J* = 7.51, 12.39, [12]), 3.65-3.53 (m, 2H, [13]), 3.41-3.13 (m, 2H, [14]), 2.42 (t, 2H, *J* = 7.45, [15]), 2.33-2.21 (m, 3H, [16]), 1.78-1.65 (m, 4H, [17]), 1.59 (d, 5H, *J* = 6.59, [18]), 1.53-1.45 (m, 2H, [19]), 1.45-1.35 (m, 2H, [20]), 1.35-1.16 (m, 14H, [21a,b]), 0.93 (dd, 5H, *J* = 4.21, 6.77, [22]). **[13]C NMR (APT, 100MHz, $CDCl_3$):** δ = 173.80, 172.47, 170.90, 158.85, 158.44, 155.67, 1525.60, 151.56, 131.02, 129.89, 29.34, 129.06, 128.58, 126.00, 121.17, 120.90, 77.96, 65.77, 64.90, 62.70, 59.11, 53.14, 51.33, 49.65, 39.81, 39.34, 34.12, 33.93, 30.71, 29.49, 29.40, 29.17, 27.53, 26.87, 26.00, 24.78, 24.31, 19.69, 18.79, 17.95, 1711.

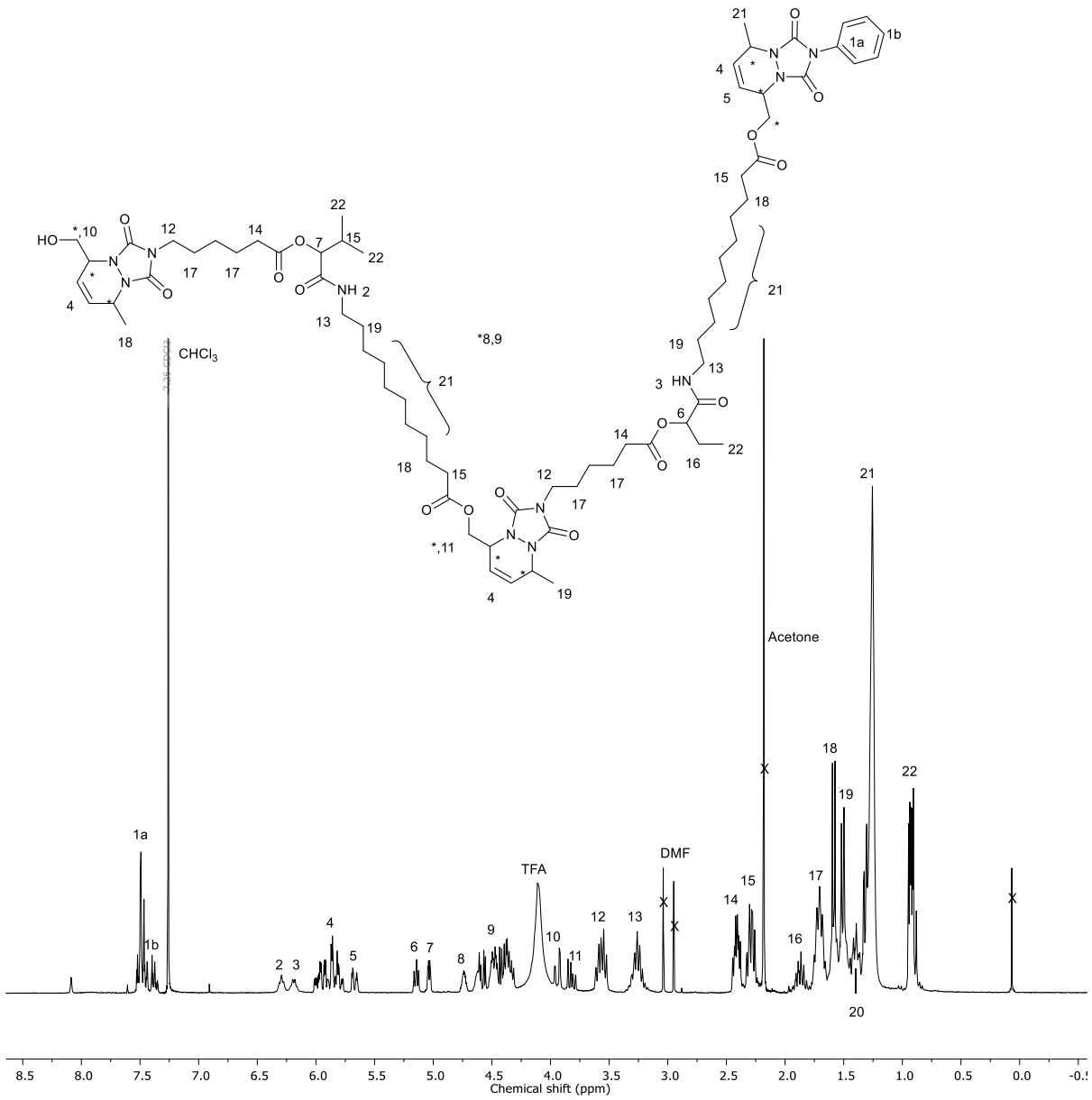


Figure VI 10: [1]H NMR spectrum in $CDCl_3$ of the PhTAD capped dimer.

[1]H NMR (300 MHz, $CDCl_3$): δ = 7.56-7.44 (m, 4H, [1a]), 7.42-7.33 (m, 1H, [1b]), 6.30 (t, 1H, *J* = 5.90, 5.63, [2]), 6.19 (d, 2H, *J* = 5.59, [3]), 6.04-5.75 (m, 5H, [4]), 5.71-5.64 (m, 1H, [5]), 5.14 (dd, 1H, *J* = 5.02, 6.47, [6]), 5.03 (dd, 1H, *J* = 1.69, 4.69, [7]), 4.78-4.29 (m, 10H, [8,9]), 3.94 (dd, 1H, *J* = 2.33, 12.40, [10]), 3.82 (ddd, 1H, *J* = 0.70, 7.27, 12.37, [11]), 3.63-3.50 (m, 4H, [12]), 3.36-3.17 (m, 4H, [13]), 2.47-2.36 (m, 4H, [14]), 2.29 (ddd, 5H, *J* = 5.03, 6.99, 8.18, [15]), 1.95-1.80 (m, 2H, [16]), 1.70 (p, 8H, *J* = 7.11, 6.94, [17]), 1.59 (d, 7H, *J* = 6.59, [18]), 1.55-1.46 (m, 7H, [19]), 1.46-1.36 (m, 4H, [20]), 1.36-1.11 (m, 27H, [21]), 0.99-0.87 (m, 9H, [22]). **[13]C NMR (APT, 100MHz, $CDCl_3$):** δ = 173.64, 173.56, 170.61, 170.21, 129.96, 129.29, 129.00, 128.41, 125.88, 121.53, 121.11, 121.05, 78.07, 74.83, 65.11, 62.74, 62.68, 59.35, 59.30, 53.16, 52.93, 51.31, 51.08, 49.65, 39.63, 39.26, 38.99, 34.13, 34.10, 31.08, 30.70, 29.57, 29.46, 29.34, 29.30, 29.23, 29.20, 27.67, 27.57, 26.94, 26.94, 26.11, 26.06, 25.25, 24.81, 24.39, 19.64, 19.51, 18.85, 17.96, 17.94, 17.14.

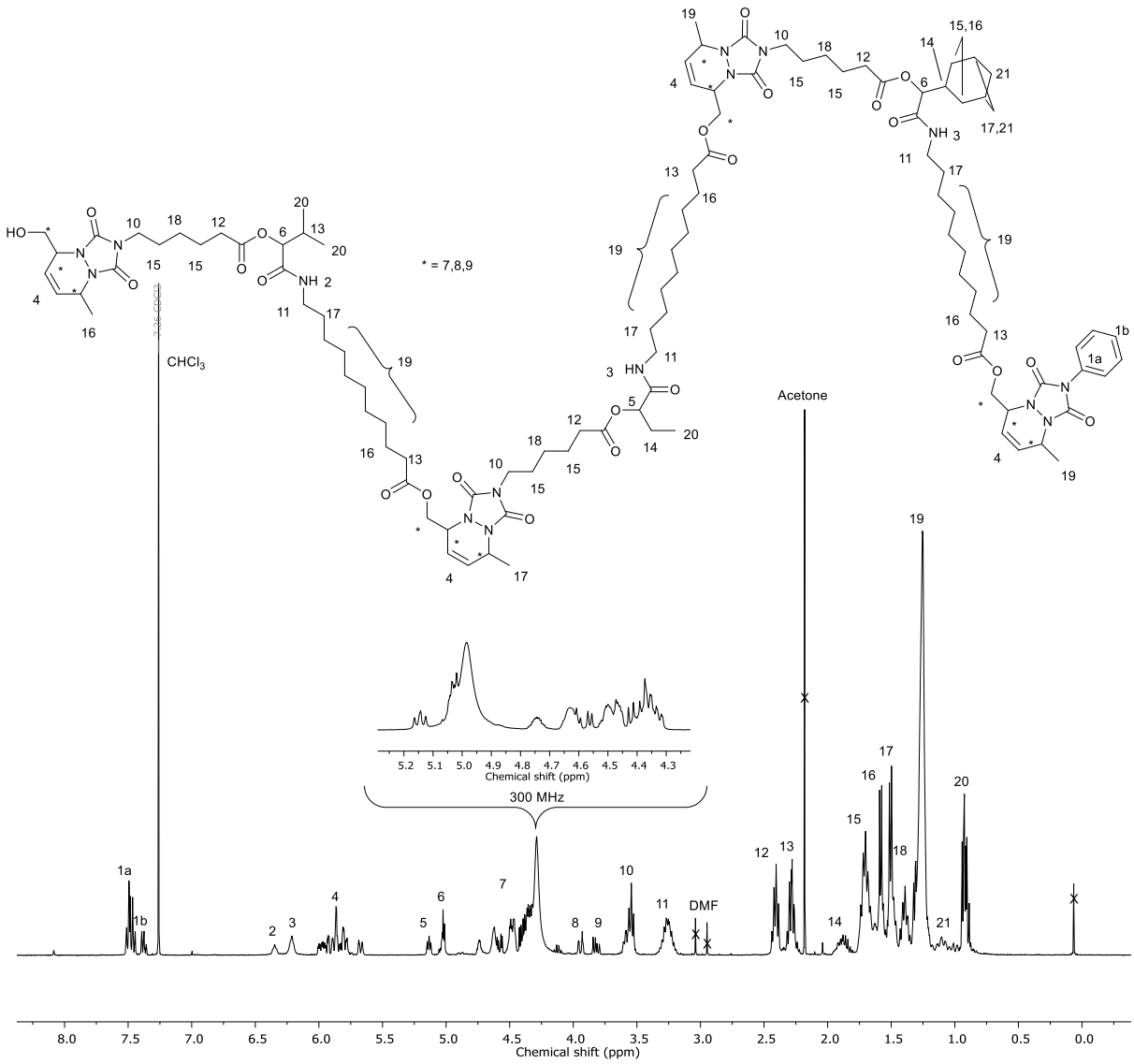


Figure VI 11: ^{1}H NMR spectrum in $CDCl_3$ of the PhTAD capped trimer.

^{1}H NMR (400 MHz, $CDCl_3$): δ = 7.54-7.43 (m, 4H, ^{1a}), 7.41-7.34 (m, 1H, ^{1b}), 6.35 (s, 1H, ^{2}), 6.21 (s, 2H, ^{3}), 6.03-5.61 (m, 8H, ^{4}), 5.18-5.09 (m, 1H, ^{5}), 5.09-4.99 (m, 1H, ^{6}), 4.77-4.17 (m, 14H, ^{7}), 3.93 (dd, 1H, J = 2.31, 9.76, 2.05, ^{8}), 3.84 (dd, 1H, J = 6.80, 4.88, 7.32, ^{9}), 3.64-3.49 (m, 6H, ^{10}), 3.38-3.16 (m, 6H, ^{11}), 2.40 (t, 6H, ^{12}), 2.37-2.22 (m, 7H, ^{13}), 1.99-1.81 (m, 3H, ^{14}), 1.80-1.65 (m, 14H, ^{15}), 1.58 (d, 11H, J = 6.59, ^{16}), 1.51 (d, 11H, J = 6.59, ^{17}), 1.43-1.34 (m, 6H, ^{18}), 1.34-1.17 (m, 42H, ^{19}), 1.14-1.00 (m, 4H, ^{21}), 1.00-0.78 (m, 9H, ^{20}). **^{13}C NMR (APT, 100MHz, $CDCl_3$):** δ = 173.59, 172.39, 170.88, 170.45, 170.42, 158.83, 158.41, 152.75, 129.93, 129.87, 129.29, 129.02, 128.45, 125.91, 121.42, 121.06, 121.00, 78.02, 77.64, 74.77, 65.02, 62.75, 62.68, 59.26, 59.22, 53.15, 52.92, 51.31, 51.09, 39.70, 39.67, 39.27, 39.02, 34.12, 34.10, 34.04, 33.99, 30.70, 29.84, 29.54, 29.47, 29.45, 29.43, 29.35, 29.33, 29.31, 29.27, 29.22, 29.19, 27.67, 26.92, 26.13, 26.09, 26.04, 24.80, 24.40, 24.37, 19.65, 19.50, 18.83.

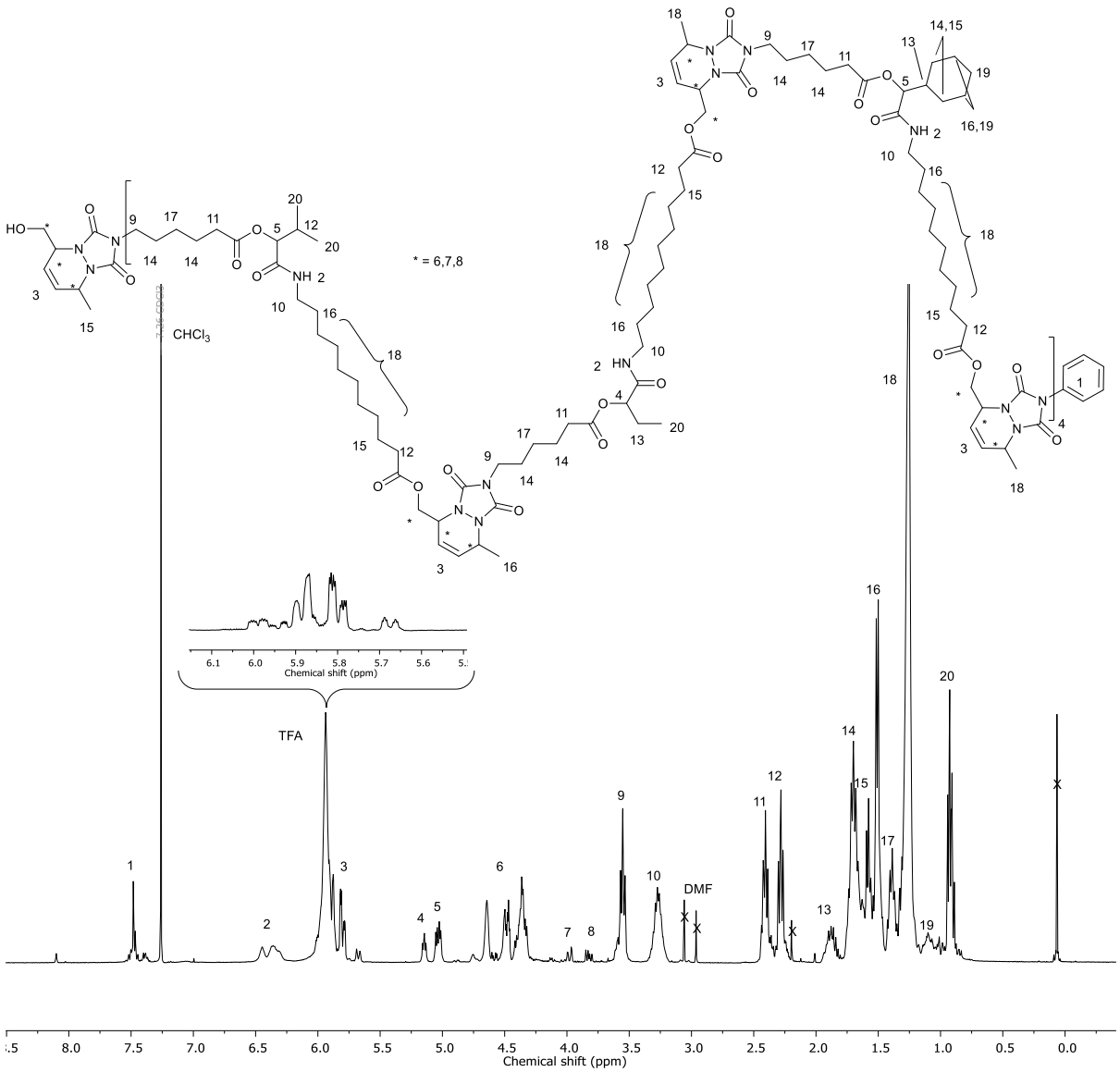


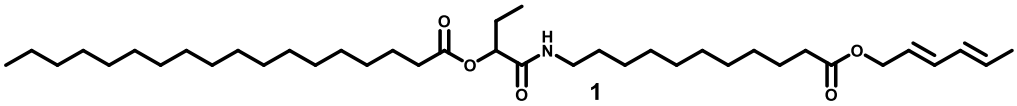
Figure VI 12: [1]H NMR spectrum in $CDCl_3$ of the PhTAD capped dodecamer.

[1]H NMR (400 MHz, $CDCl_3$): δ = 7.55-7.35 (m, 5H, [1]), 6.50-6.27 (m, 12H, [2]), 6.07-5.63 (s, 26H, [3]), 5.18-5.10 (m, 4H, [4]), 5.08-4.98 (m, 8H, [5]), 4.80-4.24 (m, 50H, [6]), 3.97 (dd, 1H, *J* = 2.06, 10.44, 1.76, [7]), 3.85 (dd, 1H, *J* = 7.23, 4.57, 7.73, [8]), 3.55 (t, 24H, *J* = 7.26 [9]), 3.34-3.18 (m, 24H, [10]), 2.48-2.33 (m, 24H, [11]), 2.33-1.21 (m, 25H, [12]), 1.97-1.78 (m, 12H, [13]), 1.78-1.61 (m, 56H, [14]), 1.58 (t, 35H, *J* = 6.90, [15]), 1.51 (d, 44H, *J* = 6.47, [16]), 1.45-1.35 (m, 24H, [17]), 1.35-1.17 (m, 168H, [18]), 1.16-0.97 (m, 16H, [19]), 0.96-0.82 (m, 36H, [20]). **[13]C NMR (APT, 100MHz, $CDCl_3$):** δ = 173.73, 172.49, 172.29, 171.45, 171.07, 171.00, 158.93, 158.52, 153.82, 152.70, 129.87, 129.76, 129.34, 129.07, 128.61, 126.01, 121.13, 120.93, 116.35, 113.51, 77.84, 74.67, 64.85, 62.77, 53.14, 52.92, 51.08, 40.12, 39.85, 39.09, 34.09, 33.96, 30.72, 29.54, 29.45, 29.42, 29.33, 29.25, 29.21, 27.63, 27.50, 26.90, 26.09, 26.05, 26.02, 25.90, 25.26, 24.79, 24.34, 19.70, 19.55, 18.79, 17.08. **IR** (ATR platinum diamond): ν [cm^{-1}] = 3355, 2930, 2856, 1740, 1692, 1555 1461, 1427, 1372 1209, 1154, 891, 805, 780, 766, 693, 646.

VI.4.7 Solution-phase synthesis of sequence-defined nonamer

Full ^{1}H and ^{13}NMR, IR and HRMS analysis following each P-3CR can be found in the published supporting information.[59]

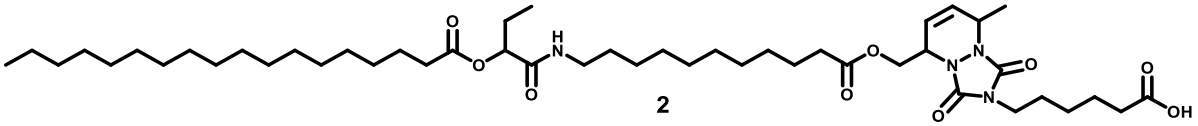
VI.4.7.1 1st P-3CR



1

Stearic acid (0.20 g, 0.70 mmol, 1.0 eq.) was dissolved in CH_2Cl_2 (2.0 mL, 0.35 M). Propanal (100 µL, 1.40 mmol, 2.0 eq.) and **L1** (0.31 g, 1.05 mmol, 1.5 eq.) were added and the reaction mixture was stirred at room temperature for 12 hours. Subsequently, the solvent was removed *in vacuo* and the crude product was purified by column chromatography (hexane:ethyl acetate 15:1 → ethyl acetate), **R_F:** (hexane:ethyl acetate (4:1)) = 0.56, resulting in product **1** as a white solid. Yield = 97 % (m = 433 mg, 0.68 mmol). Furthermore, the excess of the monomer was recovered (67 mg, 0.23 eq.) and could be reused.

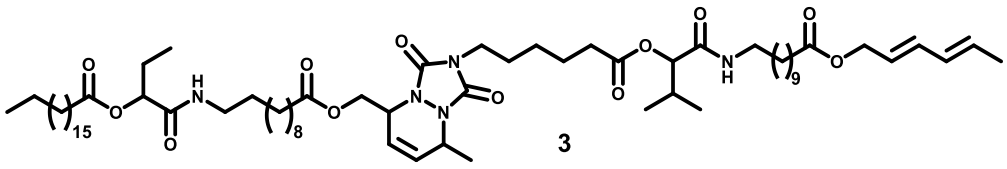
VI.4.7.2 1st TAD Diels-Alder reaction



2

0.402 g of **1** (0.634 mmol, 1.0 eq.) was dissolved in anhydrous ethyl acetate (3.0 mL) and **L2** (0.150 g, 0.697 mmol, dissolved in 1 mL anhydrous ethyl acetate) was added dropwise to the solution, until it stayed pink, indicating that **1** was fully converted to **2**. 2,3-dimethylbut-2-ene (20 µL, 0.20 mmol) was added to the reaction mixture in order to quench the excess of the TAD compound **L2**. The solvent was removed *in vacuo* and the crude product **2** was used without further purification or analysis.

VI.4.7.3 2nd P-3CR

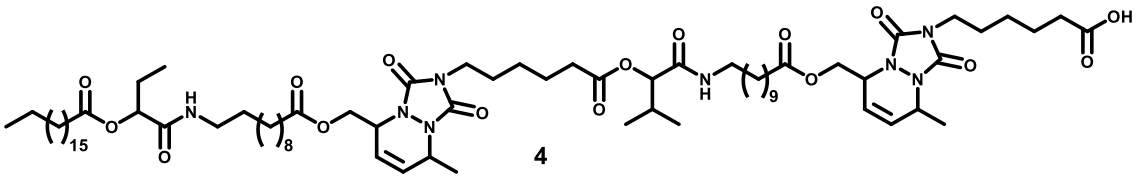


3

0.516 g of **2** (0.609 mmol, 1.0 eq.) was dissolved in CH_2Cl_2 (3.0 mL). Subsequently, isobutyraldehyde (110 µL, 1.218 mmol, 2.0 eq.) and **L1** (0.266 g, 0.914 mmol, 1.5 eq.) were added. The reaction was stirred for 12 hours at room temperature and the crude product was purified by column chromatography (hexane:ethyl acetate 10:1→1:2), **R_F:** (hexane:ethyl acetate (1:1)) = 0.42. Product **3** was obtained as a

yellowish, highly viscous oil. Yield of 88 % (m = 648 mg, 0.535 mmol, overall yield over two reaction steps).

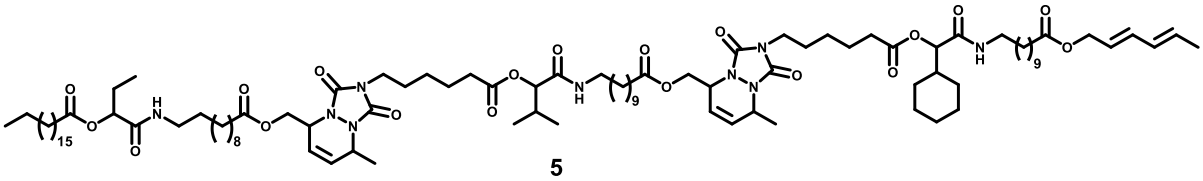
VI.4.7.4 2nd TAD Diels-Alder reaction



4

0.568 g of **3** (0.469 mmol, 1.0 eq.) was dissolved in anhydrous ethyl acetate (3.0 mL) and **L2** (0.110 g, 0.516 mmol, 1.1 eq., dissolved in 1 mL anhydrous ethyl acetate) was added dropwise to the solution, until it stayed pink, indicating that **3** was fully converted. 2,3-dimethylbut-2-ene (20 µL, 0.20 mmol) was added to the reaction mixture in order to quench the excess of the TAD compound **L2**. The solvent was removed *in vacuo* and the crude product **4** was used without further purification or analysis.

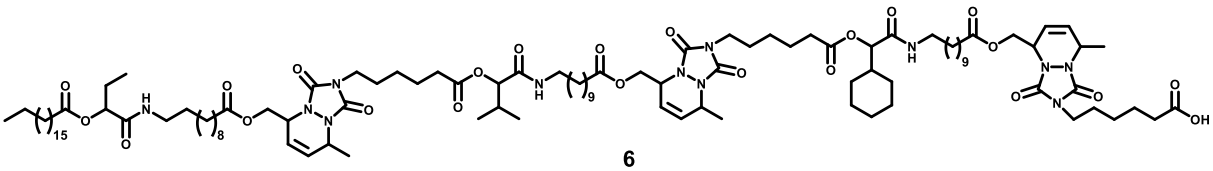
VI.4.7.5 3rd P-3CR



5

0.647 g of **4** (0.454 mmol, 1.0 eq.) was dissolved in CH_2Cl_2 (3.0 mL). Subsequently, cyclohexanal (110 µL, 0.908 mmol, 2.0 eq.) and **L1** (0.198 g, 0.681 mmol, 1.5 eq.) were added. The reaction was stirred for 12 hours at room temperature and the crude product was purified by column chromatography (hexane:ethyl acetate 5:1→1:3), $\mathbf{R_F}$**:** (hexane:ethyl acetate (1:2)) = 0.28. Product **5** was obtained as a yellowish, highly viscous oil. Yield = 73 % (m = 591 mg, 0.323 mmol, overall yield over two reaction steps).

VI.4.7.6 3rd TAD Diels-Alder reaction

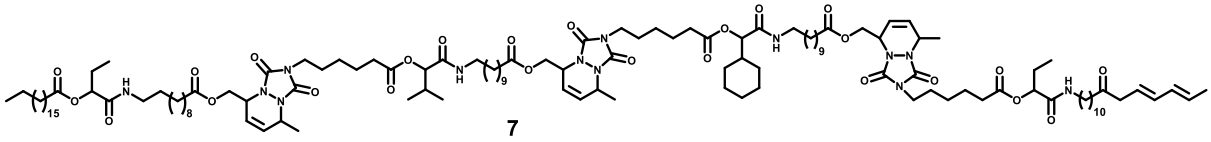


6

0.545 g of **5** (0.298 mmol, 1.0 eq.) was dissolved in anhydrous ethyl acetate (3.0 mL) and **L2** (73 mg, 0.343 mmol, 1.1 eq., dissolved in 2 mL anhydrous ethyl acetate) was added dropwise to the solution,

until it stayed pink, indicating that **5** was fully converted. 2,3-dimethylbut-2-ene (20 µL, 0.20 mmol) was added to the reaction mixture in order to quench the excess of the TAD compound **L2**. The solvent was removed *in vacuo* and the crude product **6** was used without further purification or analysis.

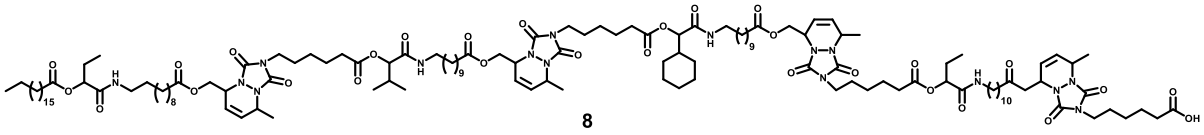
VI.4.7.7 4th P-3CR



7

0.571 g of **6** (0.282 mmol, 1.0 eq.) was dissolved in CH_2Cl_2 (2.0 mL). Subsequently, propanal (110 µL, 1.69 mmol, 6.0 eq.) and **L1** (0.370 g, 0.681 mmol, 4.5 eq.) was added. The reaction was stirred for 18 hours at room temperature and the crude product was purified by column chromatography (hexane:ethyl acetate 2:1→1:6), $\mathbf{R_F}$**:** (hexane:ethyl acetate (1:6)) = 0.68. Product **7** was obtained as a yellowish, highly viscous oil. Yield of 82 % (m = 472 mg, 0.231 mmol, overall yield over two reaction steps).

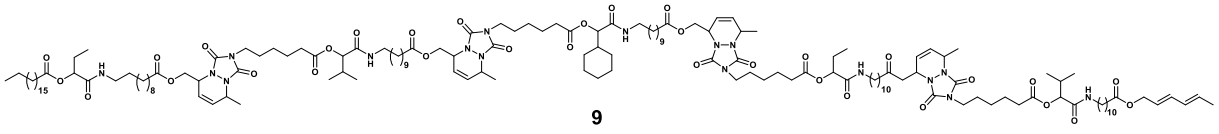
VI.4.7.8 4th TAD Diels-Alder reaction



8

0.419 g of **7** (0.175 mmol, 1.0 eq.) was dissolved in anhydrous ethyl acetate (3.0 mL) and **L2** (43 mg, 0.202 mmol, 1.1 eq. dissolved in 2 mL anhydrous ethyl acetate) was added dropwise to the solution, until it stayed pink, indicating that **7** was fully converted. 2,3-dimethylbut-2-ene (20 µL, 0.20 mmol) was added to the reaction mixture in order to quench the excess of the TAD compound **L2**. The solvent was removed *in vacuo* and the crude product **8** was used without further purification or analysis.

VI.4.7.9 5th P-3CR

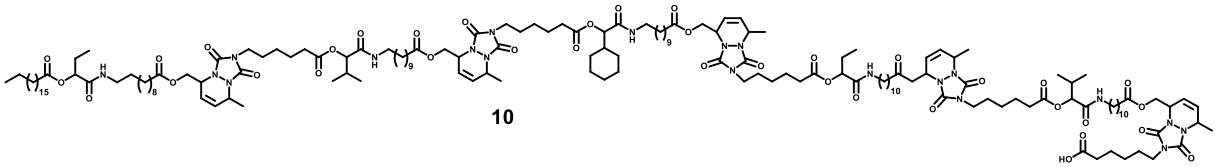


9

0.455 g of **8** (0.175 mmol, 1.0 eq.) was dissolved in CH_2Cl_2 (2.0 mL). Subsequently, isobutyraldehyde (95 µL, 1.05 mmol, 6.0 eq.) and **L1** (0. 229 g, 0.787 mmol, 4.5 eq.) was added. The reaction was stirred for 24 hours at room temperature and the crude product was purified by column chromatography (hexane:ethyl acetate 3:2→ethyl acetate), $\mathbf{R_F}$**:** (ethyl acetate) = 0.50. Product **9** was obtained as a

yellowish, highly viscous oil. Yield = 94 % (m = 486 mg, 0.164 mmol, overall yield over two reaction steps).

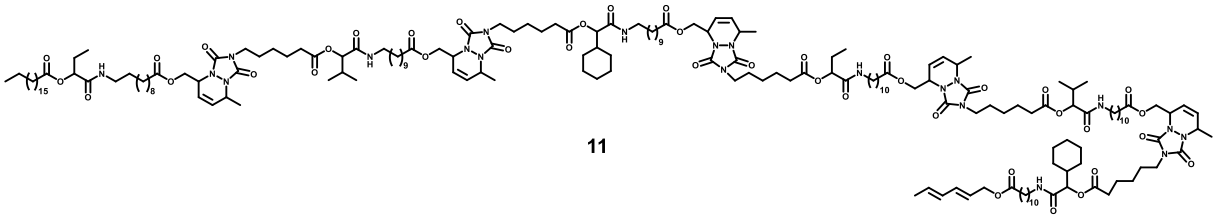
VI.4.7.10 5th TAD Diels-Alder reaction



10

0.471 g of **9** (0.159 mmol, 1.0 eq.) was dissolved in anhydrous ethyl acetate (3.0 mL) and **L2** (39 mg, 0.343 mmol, 1.1 eq. dissolved in 2 mL anhydrous ethyl acetate) was added dropwise to the solution, until it stayed pink, indicating that **9** was fully converted. 2,3-dimethylbut-2-ene (20 µL, 0.20 mmol) was added to the reaction mixture in order to quench the excess of the TAD compound **L2**. The solvent was removed *in vacuo* and the crude product **10** was used without further purification or analysis.

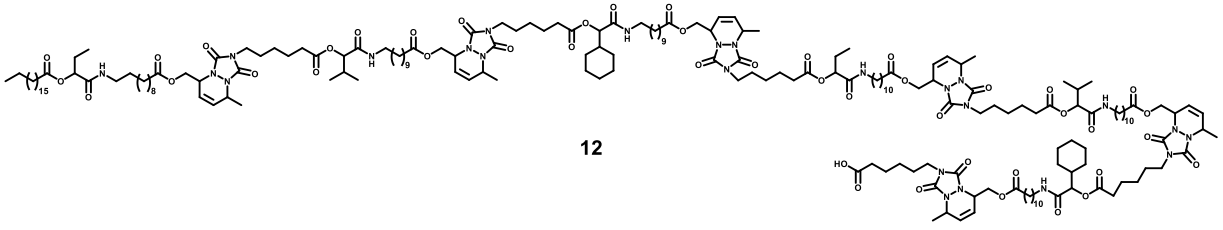
VI.4.7.11 6th P-3CR



11

0.505 g of **10** (0.159 mmol, 1.0 eq.) was dissolved in CH_2Cl_2 (2.0 mL). Subsequently, cyclohexanal (120 µL, 0.954 mmol, 6.0 eq.) and **L1** (0.209 g, 0.702 mmol, 4.5 eq.) were added. The reaction was stirred for 24 hours at room temperature and the crude product was purified by column chromatography (hexane:ethyl acetate 2:1→ethyl acetate), $\mathbf{R_F}$: (ethyl acetate) = 0.68. Product **11** was obtained as a yellowish, highly viscous oil. Yield = 70 % (m = 400 mg, 0.112 mmol, overall yield over two reaction steps).

VI.4.7.12 6th TAD Diels-Alder reaction

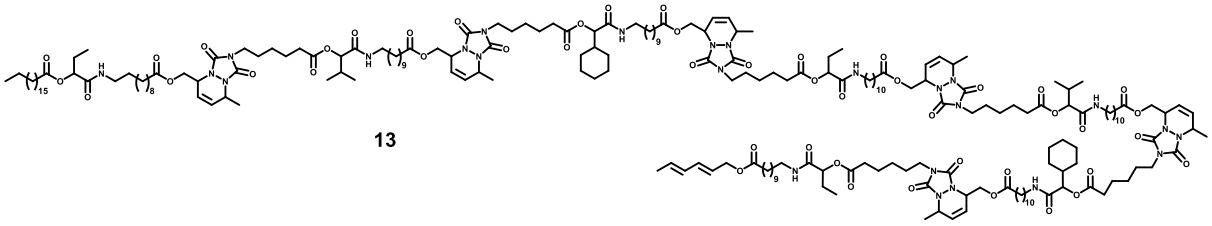


12

0.360 g of **11** (0.100 mmol, 1.0 eq.) was dissolved in anhydrous ethyl acetate (3.0 mL) and **L2** (25 mg, 0.115 mmol, 1.15 eq. dissolved in 2 mL anhydrous ethyl acetate) was added dropwise to the solution,

until it stayed pink, indicating that **11** was fully converted. 2,3-dimethylbut-2-ene (20 µL, 0.20 mmol) was added to the reaction mixture in order to quench the excess of the TAD compound **L2**. The solvent was removed *in vacuo* and the crude product **12** was used without further purification or analysis.

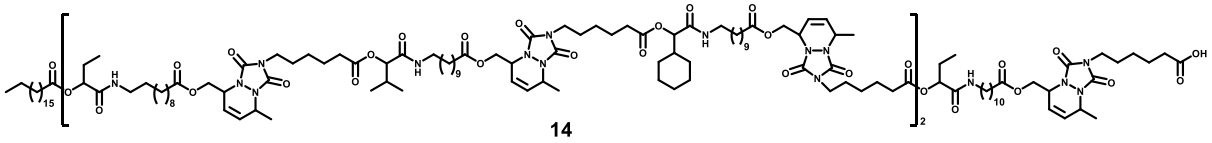
VI.4.7.13 7th P-3CR



13

0.379 g of **12** (0.10 mmol, 1.0 eq.) was dissolved in CH_2Cl_2 (2.0 mL). Subsequently, propanal (43 µL, 0.60 mmol, 6.0 eq.) and **L1** (0.131 g, 0.45 mmol, 4.5 eq.) was added. The reaction was stirred for 24 hours at room temperature and the crude product was purified by column chromatography (hexane:ethyl acetate 1:2→ethyl acetate), $\mathbf{R_F}$: (ethyl acetate) = 0.37. Product **13** was obtained as a yellowish, highly viscous oil. Yield = 75 % (m = 277 mg, 0.067 mmol, overall yield over two reaction steps).

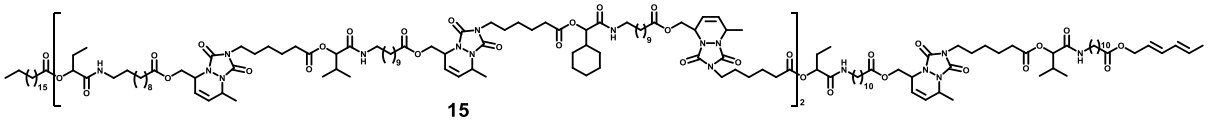
VI.4.7.14 7th TAD Diels-Alder reaction



14

0.236 g of **13** (0.056 mmol, 1.0 eq.) was dissolved in anhydrous ethyl acetate (3.0 mL) and **L2** (14 mg, 0.066 mmol, 1.15 eq. dissolved in 2 mL anhydrous ethyl acetate) was added dropwise to the solution, until it stayed pink, indicating that **13** was fully converted. 2,3-dimethylbut-2-ene (20 µL, 0.20 mmol) was added to the reaction mixture in order to quench the excess of the TAD compound **L2**. The solvent was removed *in vacuo* and the crude product **14** was used without further purification or analysis.

VI.4.7.15 8th P-3CR

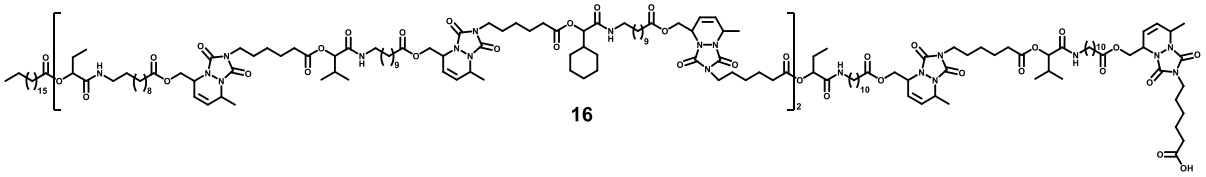


15

0.249 g of **14** (0.057 mmol, 1.0 eq.) was dissolved in CH_2Cl_2 (2.0 mL). Subsequently, isobutyraldehyde (13 µL, 0.342 mmol, 6.0 eq.) and **L1** (75 mg, 0.260 mmol, 4.5 eq.) was added. The reaction was stirred

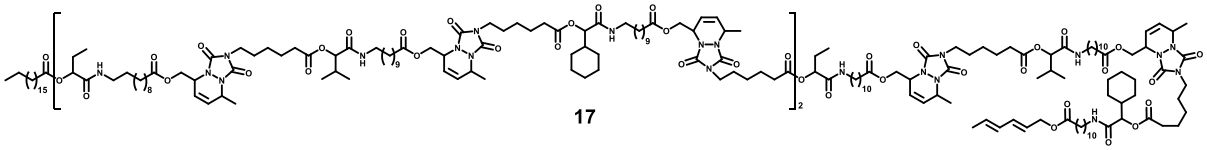
for 24 hours at room temperature and the crude product was purified by column chromatography (hexane:ethyl acetate 1:2→ethyl acetate+6 % MeOH), $\mathbf{R_F}$: (ethyl acetate) = 0.125. Product **14** was obtained as a yellowish, highly viscous oil. Yield = 94 % (m = 253 mg, 0.053 mmol, overall yield over two reaction steps).

VI.4.7.16 8th TAD Diels-Alder reaction



0.202 g of **15** (0.043 mmol, 1.0 eq.) was dissolved in anhydrous ethyl acetate (3.0 mL) and **L2** (11 mg, 0.049 mmol, 1.15 eq. dissolved in 2 mL anhydrous ethyl acetate) was added dropwise to the solution, until it stayed pink, indicating that **15** was fully converted. 2,3-dimethylbut-2-ene (20 µL, 0.20 mmol) was added to the reaction mixture in order to quench the excess of the TAD compound **L2**. The solvent was removed *in vacuo* and the crude product **16** was used without further purification or analysis.

VI.4.7.17 9th P-3CR



0.211 g of **16** (0.043 mmol, 1.0 eq.) was dissolved in CH_2Cl_2 (2.0 mL). Subsequently, cyclohexanal (32 µL, 0.257 mmol, 6.0 eq.) and **L1** (56 mg, 0.193 mmol, 4.5 eq.) was added. The reaction was stirred for 24 hours at room temperature and the crude product was purified by column chromatography (hexane:ethyl acetate 1:2.5→ethyl acetate+10 % MeOH), $\mathbf{R_f}$: (ethyl acetate) = 0.19. Product **17** was obtained as a yellowish, highly viscous oil. Yield = 78 % (m = 179 mg, 0.0335 mmol, overall yield over two reaction steps).

^{1}H NMR (500 MHz, $CDCl_3$): δ = 6.27–5.53 (m, 29H, [1]), 5.06-5.14 (m, 3H, [2]), 5.03–4.95 (m, 6H, [3]), 4.59 (s, 8H, [4]), 4.55 (d, *J* = 6.6 Hz, 2H, [5]), 4.48–4.41 (m, 8H, [6]), 4.38–4.27 (m, 16H, [7]), 3.59–3.45 (m, 16H, [8]), 3.30–3.13 (m, 18H, [9]), 2.46–2.34 (m, 18H, [10]), 2.32–2.18 (m, 21H, [11]), 1.97–1.78 (m, 9H, [12]), 1.77–1.52 (m, 70H, [13]), 1.49 (d, *J* = 6.6 Hz, 27H, [14]), 1.42–0.94 (m, 182H, [15]), 0.94–0.76 (m, 30H, [16]). **^{13}C NMR (126 MHz, $CDCl_3$):** δ = 173.40, 172.55, 172.31, 172.18, 169.75, 169.69, 169.33, 169.27, 153.91, 153.88, 152.78, 152.77, 134.85, 131.25, 130.56, 129.90, 123.96, 121.20, 78.09, 77.79, 74.97, 74.87, 64.83, 62.69, 52.93, 52.91, 51.02, 50.99, 40.11, 39.33, 39.29, 38.91, 34.43, 34.11, 34.06, 32.01, 30.65, 29.78, 29.73, 29.71, 29.55, 29.45, 29.35, 29.32, 29.31, 29.21, 27.68, 27.43, 26.96, 26.93, 26.16, 26.12, 26.08, 25.98, 25.20, 25.18, 25.09, 25.03, 24.78, 24.47, 24.45, 24.42, 22.78,

19.39, 18.87, 18.22, 17.10, 14.21, 9.11. **IR** (ATR platinum diamond): ν [cm^{-1}] = 3336.7, 2925.2, 2853.6, 1737.1, 1700.5, 1533.9, 1453.6, 1422.0, 1377.3, 1237.0, 1157.5, 1116.1, 765.5, 722.3, 5371, 423.1.

ESI-MS:

m/z exp.	formula	m/z theo.	Δ m/z
2691.2043	$[C_{286}H_{463}N_{33}O_{61}Na_2]^{2+}$	2691.1963	0.0080
1801.7965	$[C_{286}H_{463}N_{33}O_{61}Na_3]^{3+}$	1801.7940	0.0025
1357.0934	$[C_{286}H_{463}N_{33}O_{61}Na_4]^{4+}$	1357.0928	0.0006
2669.2178	$[C_{286}H_{463}N_{33}O_{61}H_2]^{2+}$	2669.2144	0.0034
1779.8157	$[C_{286}H_{463}N_{33}O_{61}H_3]^{3+}$	1779.8120	0.0037
1335.1125	$[C_{286}H_{463}N_{33}O_{61}H_4]^{4+}$	1335.1108	0.0017
1068.2902	$[C_{286}H_{463}N_{33}O_{61}H_5]^{5+}$	1068.2901	0.0001

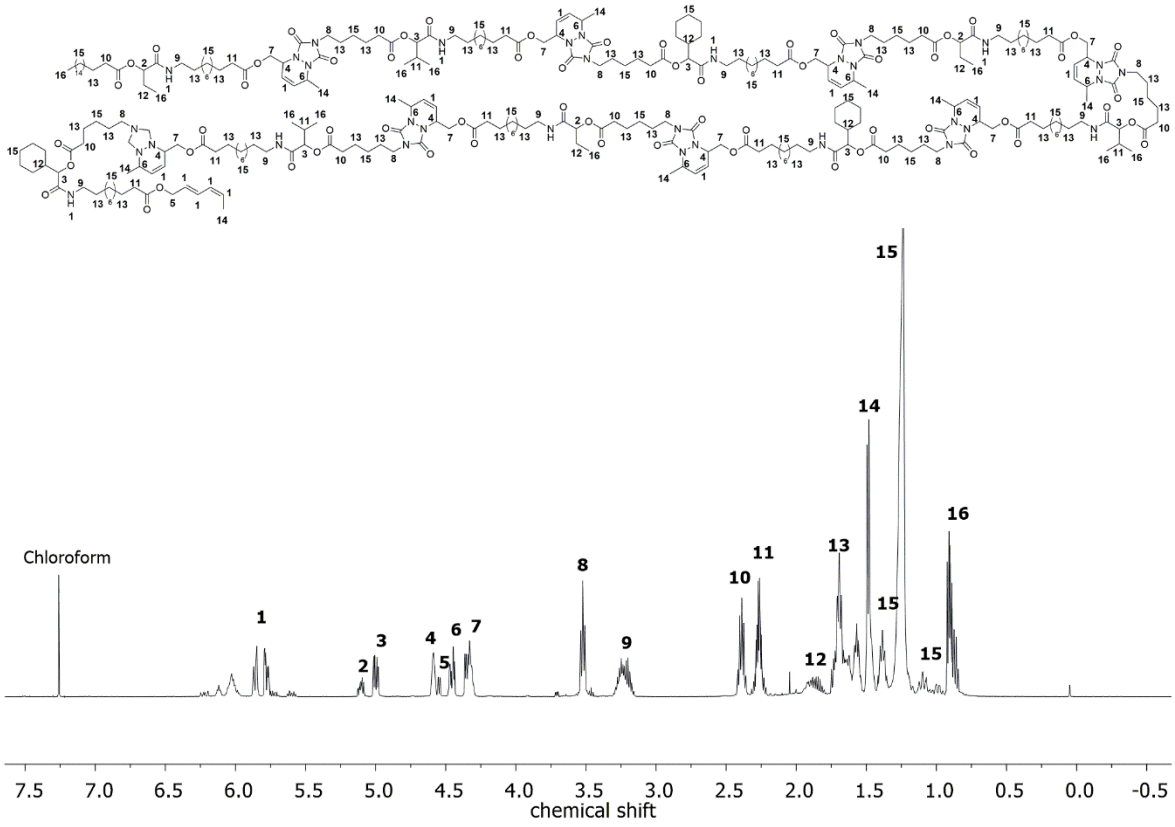


*Figure VI 13:[1]H NMR spectrum in $CDCl_3$ of solution-phase synthesised sequence-defined nonamer, **17**.*

VI.4.8 SEC-ESI-MS analysis of solution phase sequence-defined nonamer 17

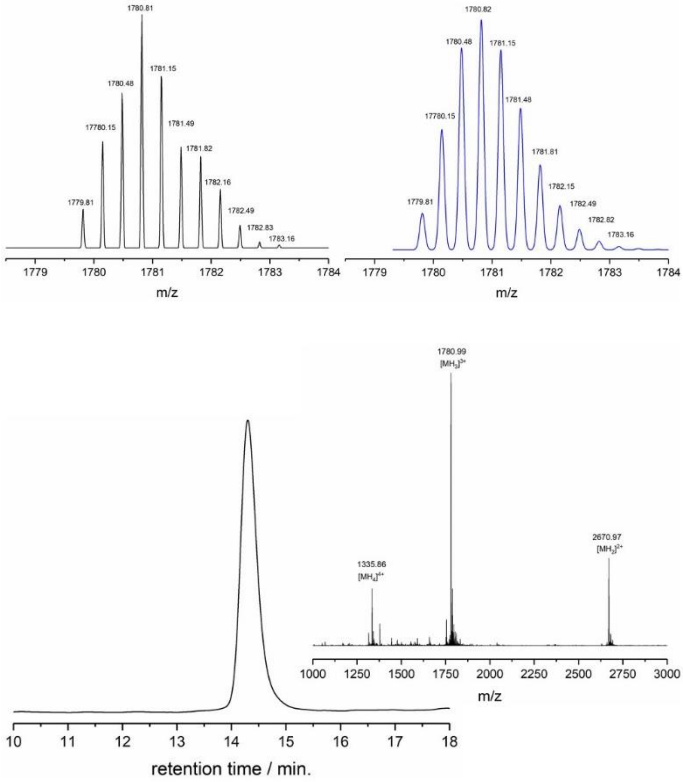


Figure VI 14: Top black) Measured ESI-MS spectrum. Top blue) The isotope pattern was theoretically calculated with the program mmass. The measured isotope pattern is in very good agreement with the theoretical one for the assumed chemical formula. Bottom) GPC chromatogram of the sequence-defined nonamer prepared in solution and the corresponding ESI-MS spectrum at a retention time of 14.30 minutes. The doubly- (2670.97 m/z), triply- (1780.99 m/z) and quadruply (1335.86 m/z) charged cations were clearly observed.

IV.5 References

1 S. Martens, J. O. Holloway and F. E. Du Prez, in *Sequence-Controlled Polymers*, ed. J.-F. Lutz, Wiley VCH, Weinheim, 2018, pp. 379–416.

2 S. Martens, J. O. Holloway and F. E. Du Prez, *Macromol. Rapid Commun.*, 2017, **38**, 1700469.

3 S. C. Solleder, R. V. Schneider, K. S. Wetzel, A. C. Boukis and M. A. R. Meier, *Macromol. Rapid Commun.*, 2017, **38**, 1600711.

4 N. Badi and J.-F. Lutz, *Chem. Soc. Rev.*, 2009, **38**, 3383–3390.

5 J.-F. Lutz, J.-M. Lehn, E. W. Meijer and K. Matyjaszewski, *Nat. Rev. Mater.*, 2016, **1**, 1–14.

6 J. A. De Neve, J. J. Haven, L. Maes and T. Junkers, *Polym. Chem.*, 2018, **9**, 4692–4705.

7 S. Martens, J. Van Den Begin, A. Madder, F. E. Du Prez and P. Espeel, *J. Am. Chem. Soc.*, 2016, **138**, 14182–14185.

8 C. Gerke, F. Jacobi, L. E. Goodwin, F. Pieper, S. Schmidt and L. Hartmann, *Macromolecules*, 2018, **51**, 5608–5619.

9 C. Fu, Z. Huang, C. J. Hawker, G. Moad, J. Xu and C. Boyer, *Polym. Chem.*, 2017, **8**, 4637–4643.

10 B. N. Norris, S. Zhang, C. M. Campbell, J. T. Auletta, P. Calvo-Marzal, G. R. Hutchison and T. Y. Meyer, *Macromolecules*, 2013, **46**, 1384–1392.

11 H. Zhang, X. Li, Q. Shi, Y. Li, G. Xia, L. Chen, Z. Yang and Z.-X. Jiang, *Angew. Chemie Int. Ed.*, 2015, **54**, 3763–3767.

12 Y. Hibi, M. Ouchi and M. Sawamoto, *Nat. Commun.*, 2016, **7**, 11064.

13 D. de Rochambeau, M. Barłóg, T. G. W. Edwardson, J. J. Fakhoury, R. S. Stein, H. S. Bazzi and H. F. Sleiman, *Polym. Chem.*, 2016, **7**, 4998–5003.

14 A. Al Ouahabi, M. Kotera, L. Charles and J.-F. Lutz, *ACS Macro Lett.*, 2015, **4**, 1077–1080.

15 M. Porel, D. N. Thornlow, N. N. Phan and C. A. Alabi, *Nat. Chem.*, 2016, **8**, 590–596.

16 N. Zydziak, F. Feist, B. Huber, J. O. Mueller and C. Barner-Kowollik, *Chem. Commun.*, 2015, **51**, 1799–1802.

17 S. C. Solleder, K. S. Wetzel and M. A. R. Meier, *Polym. Chem.*, 2015, **6**, 3201–3204.

18 A. C. Boukis, K. Reiter, M. Frölich, D. Hofheinz and M. A. R. Meier, *Nat. Commun.*, 2018, **9**, 1439.

19 S. Martens, A. Landuyt, P. Espeel, B. Devreese, P. Dawyndt and F. E. Du Prez, *Nat. Commun.*, 2018, **9**, 4451.

20 R. L. Kanasty, A. J. Vegas, L. M. Ceo, M. Maier, K. Charisse, J. K. Nair, R. Langer and D. G. Anderson, *Angew. Chemie Int. Ed.*, 2016, **55**, 9529–9533.

21 J. W. Grate, K.-F. Mo and M. D. Daily, *Angew. Chemie Int. Ed.*, 2016, **55**, 3925–3930.

22 J.-F. Lutz, in *Sequence-Controlled Polymers*, ed. J.-F. Lutz, Wiley VCH, Weinheim, 1st edn., 2018, pp. 1–26.

23 J.-F. Lutz, *Macromol. Rapid Commun.*, 2017, **38**, 1700582.

24 G. Gody, T. Maschmeyer, P. B. Zetterlund and S. Perrier, *Nat. Commun.*, 2013, **4**, 2505–2514.

25 P. Espeel, L. L. G. Carrette, K. Bury, S. Capenberghs, J. C. Martins, F. E. Du Prez and A. Madder, *Angew. Chemie - Int. Ed.*, 2013, **52**, 13261–13264.

26 C. Alabi, in *Sequence-Controlled Polymers*, ed. J.-F. Lutz, Wiley VCH, Weinheim, 1st edn., 2018, pp. 159–181.

27 T. T. Trinh, C. Laure and J.-F. Lutz, *Macromol. Chem. Phys.*, 2015, **216**, 1498–1506.

28 J. C. Barnes, D. J. C. Ehrlich, A. X. Gao, F. A. Leibfarth, Y. Jiang, E. Zhou, T. F. Jamison and J. A. Johnson, *Nat. Chem.*, 2015, **7**, 810–815.

29 D. Van Lysebetten, S. Felissati, E. Antonatou, L. Carrette, P. Espeel, E. Foquet, F. E. Du Prez and A. Madder, *ChemBioChem*, 2018, **19**, 641–646.

30 D. Chan-Seng, J. Louwsma, J.-F. Lutz and S. Joly, *Macromol. Rapid Commun.*, 2018, **38**, 1700764.

31 J. O. Holloway, S. Aksakal, F. E. Du Prez and C. Remzi Becer, *Macromol. Rapid Commun.*, 2017, **38**, 1700500.

32 M. R. Golder, Y. Jiang, P. E. Teichen, H. V.-T. Nguyen, W. Wang, N. Milos, S. A. Freedman, A. P. Willard and J. A. Johnson, *J. Am. Chem. Soc.*, 2018, **140**, 1596–1599.

33 S. C. Solleder, S. Martens, P. Espeel, F. E. Du Prez and M. A. R. Meier, *Chem. - A Eur. J.*, 2017, **23**, 13906–13909.

34 S. C. Solleder and M. A. R. Meier, *Angew. Chemie - Int. Ed.*, 2014, **53**, 711–714.

35 S. C. Solleder, D. Zengel, K. S. Wetzel and M. A. R. Meier, *Angew. Chemie - Int. Ed.*, 2016, **55**, 1204–1207.

36 Y.-H. Wu, J. Zhang, F.-S. Du and Z.-C. Li, *ACS Macro Lett.*, 2017, **6**, 1398–1403.

37 R. Kakuchi, *Angew. Chemie - Int. Ed.*, 2014, **53**, 46–48.

38 L. Yang, Z. Zhang, B. Cheng, Y. You, D. Wu and C. Hong, *Sci. China Chem.*, 2015, **58**, 1734–1740.

39 Z. Zhang, Y. You and C. Hong, *Macromol. Rapid Commun.*, 2018, **1800362**, 1800362.

40 W. Konrad, F. R. Blößer, K. S. Wetzel, A. C. Boukis, M. A. R. Meier and C. Barner-Kowollik, *Chem. - A Eur. J.*, 2018, **24**, 3413–3419.

41 M. Passerini, *Gazz. Chim. Ital.*, 1921, **51**, 126–129.

42 H. C. Kolb, M. G. Finn and K. B. Sharpless, *Angew. Chemie - Int. Ed.*, 2001, **40**, 2004–2021.

43 K. De Bruycker, S. Billiet, H. A. Houck, S. Chattopadhyay, J. M. Winne and F. E. Du Prez, *Chem. Rev.*, 2016, **116**, 3919–3974.

44 J. O. Holloway, C. Mertens, F. E. Du Prez and N. Badi, *Macromol. Rapid Commun.*, 2019, **40**, 1800685.

45 S. Billiet, K. De Bruycker, F. Driessen, H. Goossens, V. Van Speybroeck, J. M. Winne and F. E. Du Prez, *Nat. Chem.*, 2014, **6**, 815–821.

46 P. Espeel and F. E. Du Prez, *Macromolecules*, 2015, **48**, 2–14.

47 O. Roling, K. De Bruycker, B. Vonhören, L. Stricker, M. Körsgen, H. F. Arlinghaus, B. J. Ravoo and F. E. Du Prez, *Angew. Chemie - Int. Ed.*, 2015, **54**, 13126–13129.

48 H. A. Houck, F. E. Du Prez and C. Barner-Kowollik, *Nat. Commun.*, 2017, **8**, 1869.

49 N. Van Herck and F. E. Du Prez, *Macromolecules*, 2018, **51**, 3405–3414.

50 X. Elduque, A. Sánchez, K. Sharma, E. Pedroso and A. Grandas, *Bioconjug. Chem.*, 2013, **24**, 832–839.

51 N. Zydziak, W. Konrad, F. Feist, S. Afonin, S. Weidner and C. Barner-Kowollik, *Nat. Commun.*, 2016, **7**, 1–10.

52 R. B. Merrifield, *J. Am. Chem. Soc.*, 1963, **85**, 2149–2154.

53 M. I. Amrane, D. Chouikhi, N. Badi and J.-F. Lutz, *Macromol. Chem. Phys.*, 2014, **215**, 1984–1990.

54 A. Meszynska, N. Badi, H. G. Börner and J.-F. Lutz, *Chem. Commun.*, 2012, **48**, 3887–3889.

55 S. Pfeifer, Z. Zarafshani, N. Badi and J.-F. Lutz, *J. Am. Chem. Soc.*, 2009, **131**, 9195–9197.

56 G. Li, X. Wang, J. Li, X. Zhao and F. Wang, *Tetrahedron*, 2006, **62**, 2576–2582.

57 J.-J. Hwang and J. M. Tour, *Tetrahedron*, 2002, **58**, 10387–10405.

58 M. Landa, M. Kotera, J. S. Remy and N. Badi, *Eur. Polym. J.*, 2016, **84**, 338–344.

59 J. O. Holloway, K. S. Wetzel, S. Martens, F. E. Du Prez and M. A. R. Meier, *Polym. Chem.*, 2019, **10**, 3859–3867.

60 R. W. Armstrong, A. P. Combs, P. A. Tempest, S. D. Brown and T. A. Keating, *Acc. Chem. Res.*, 1996, **29**, 123–131.

61 L. Banfi, A. Basso, G. Guanti and R. Riva, *Mol. Divers.*, 2003, **6**, 227–235.

62 A. Basso, L. Banfi, R. Riva, P. Piaggio and G. Guanti, *Tetrahedron Lett.*, 2003, **44**, 2367–2370.

63 B. L. Bray, *Nat. Rev. Drug Discov.*, 2003, **2**, 587–593.

64 S. Oelmann and M. A. R. Meier, *RSC Adv.*, 2017, **7**, 45195–45199.

65 L. Vlaminck, B. Van De Voorde and F. E. Du Prez, *Green Chem.*, 2017, **19**, 5659–5664.

66 O. Türünç, S. Billiet, K. De Bruycker, S. Ouardad, J. M. Winne and F. E. Du Prez, *Eur. Polym. J.*, 2015, **65**, 286–297.



Abstract

Sequence-defined chemistry research today is now targeting a range of potential applications, including biomedical usage, long-term data storage and anticounterfeiting technologies. This final results chapter builds upon the use of functional 1,2,4-triazoline-3,5-dione (TAD) species in combination with multicomponent reactions, to yield sequence-defined oligomers that can serve as macromolecular pin codes. Importantly, TAD chemistry also offers the possibility to introduce dynamic behaviour into these precision macromolecules. Here, the reversible reaction of TAD with indole moieties was utilised to synthesise sequence-defined oligomers that carry a code, which could be de-coded or encrypted upon heating as a result of TAD-indole bond-shuffling. Eventually, the contained information could later be read-out or decrypted by only the intended person. This work improved upon the more complex sequence-defined decryption strategies that are currently employed, by using Liquid Chromatography Mass Spectroscopy (LCMS) as a more straightforward technique in comparison to tandem Mass Spectroscopy (MS/MS) to analyse and decipher the macromolecular pin code. Finally, a sequence-defined tetramer was synthesised and imbedded into a polymer material to demonstrate a potential real-world application of product tagging for anti-counterfeiting purposes.

Chapter VII
Dynamic sequence-defined macromolecular pin codes: The next generation of data encryption

VII.1 Introduction

Whilst the last decade has been mostly dedicated to developing an ever-widening range of synthesis routes towards sequence-defined oligomers (as comprehensively outlined in Chapter II),[1–3] researchers are now turning more towards the potential applications of sequence-defined chemistry.[4,5] Sequence-defined chemistry is already being investigated in a number of potential areas, including biomedical and biomimicking applications,[6–10] (bio)catalysis,[11] long-term or 'cold' data storage[12–16] and product coding/tagging for anti-counterfeiting applications.[8,17–20] These are all applications where the precise, monodisperse nature of sequence-defined structures is key, either because it mimics biological macromolecules or because there are no imperfections in the chain which would make information recovery difficult. For many of these applications, inspiration is once again drawn from Nature. For example, DNA uses four base pairs, allowing it to encode information on a quaternary level, which is already vastly superior to computers which work on a binary system.[4] Although DNA has already been used to store information,[21,22] there are limitations when considering it as a viable medium for data storage, namely its susceptibility to degradation, limited availability and cost.[12,23,24] However, by considering synthetic discrete macromolecules - which depending on the synthesis route chosen can be comprised of a wide range of monomers - the data storage density can be greatly enhanced.[4,25]

The use of sequence-defined chemistry to not only store but also encrypt data is of interest, as people are now seeking for more complex and fraud-resistant ways to protect and identify goods. Within this context, Lutz and co-workers have reported the decoding and erasing of encrypted data, through the synthesis of poly(alkoxyamine amides) which could be read-out *via* MS/MS analysis and then irreversibly erased by heating above 60 °C.[26] Alternatively, the use of sequence-defined (oligo)urethanes as readable, molecular barcodes or tags that are incorporated within a polymer matrix have been investigated as potential ways to combat the ever-growing counterfeiting of products.[17–19] Alternatively, Meier and co-workers recently reported the use of the Ugi four-component reaction (U-4CR)[27] to synthesise sequence-defined macromolecules for secret communication.[14] They used perfluorinated acids within the U-4CR, enabling simple purification *via* Fluorous Solid-Phase Extraction (F-SPE), along with a wide range of amines, aldehydes and isocyanides for the other components of the reaction to store encoded information in the form of sequence-defined molecules.

Using these molecules, they were able to write secret messages, deposit them in miniscule quantities on mediums such as an envelope (concealed behind the postage stamp), and then later extract the sequence-defined oligomers from the envelope using methanol and dichloromethane. These were then purified *via* F-SPE and deciphered using MS/MS, where the fragmentation patterns were used to read out the information by means of a script to generate an alpha-numeric code. Although the concept is interesting and elegantly uses multicomponent reactions to encrypt data, it might be regarded as an overly complex approach to store data on a synthetic medium.

An equally important aspect of both data storage and encryption is the read-out or decryption of this information, which should preferentially be fast and straightforward in order for it to be useful.[4] To date, data decryption of sequence-defined oligomers is exclusively carried out by tandem MS/MS techniques.[4,12,13,28,29] Nonetheless successful, important limitations are in place when using MS/MS as a read-out tool. Besides being an expensive technique, it relies on specific and easily fragmentable bonds in order to give distinct fragmentation patterns that can be easily resolved, as highlighted in the work of Lutz and co-workers, where a weak alkoxyamine bond leads to predictable fragmentation patterns.[30,31] However, in order to be applicable to more elaborate encoded data, MS/MS sequence read-out requires additional computer software and algorithms (as mentioned above).[32] Within our own research group, for example, thiolactone chemistry has been used to synthesise libraries of sequence-defined oligomers, using 15 different side-chain functionalities, which could both be encoded and decoded using specially designed computer software, resulting in the ground-breaking storage of a complete QR code in a chemical powder containing sequence-defined oligomers.[12] It is hoped that the future chemical storage of data will offer solutions to long-term storage in a space-saving manner, however it needs to be less complex (to make it more affordable) and for short-term storage, the read-out speed also needs to much simpler and faster than what currently exists.[12]

Whilst the work described thus far in the current thesis has focussed upon further developing synthetic protocols, using either thiolactone chemistry (Chapters III, IV and V) or by introducing 1,2,4-triazoline-3,5-dione (TAD) chemistry to this field (Chapters V, VI), the work described in this last chapter was designed to target a specific application of product coding/tagging. Chapter VI introduced the powerful combination of the irreversible TAD-based Diels-Alder reaction and the Passerini three-component reaction (P-3CR).[33] Based on this highly efficient, click-based protocol introduced, that was applicable to both solid and solution phase synthesis, this present chapter sought to further expand the scope of the protocol by combining multicomponent reactions (MCRs) with a dynamic, thermoreversible TAD-based chemistry to write a sequence-defined macromolecule or *macromolecular pin code* (see *Figure VII* 1).[34–36] A range of commercially available isocyanides were used to provide a chemical alphabet, in

order to write a macromolecular pin code by means of the P-3CR. Moreover, different indole compounds were used to mark the position in the sequence (*i.e.* A-D) that corresponds to the specific isocyanide "number" (*i.e.* 1-4). Only those who knew the order of the indole marker compounds would hence be able to extract the coded information and read the pin code (*vide infra*).

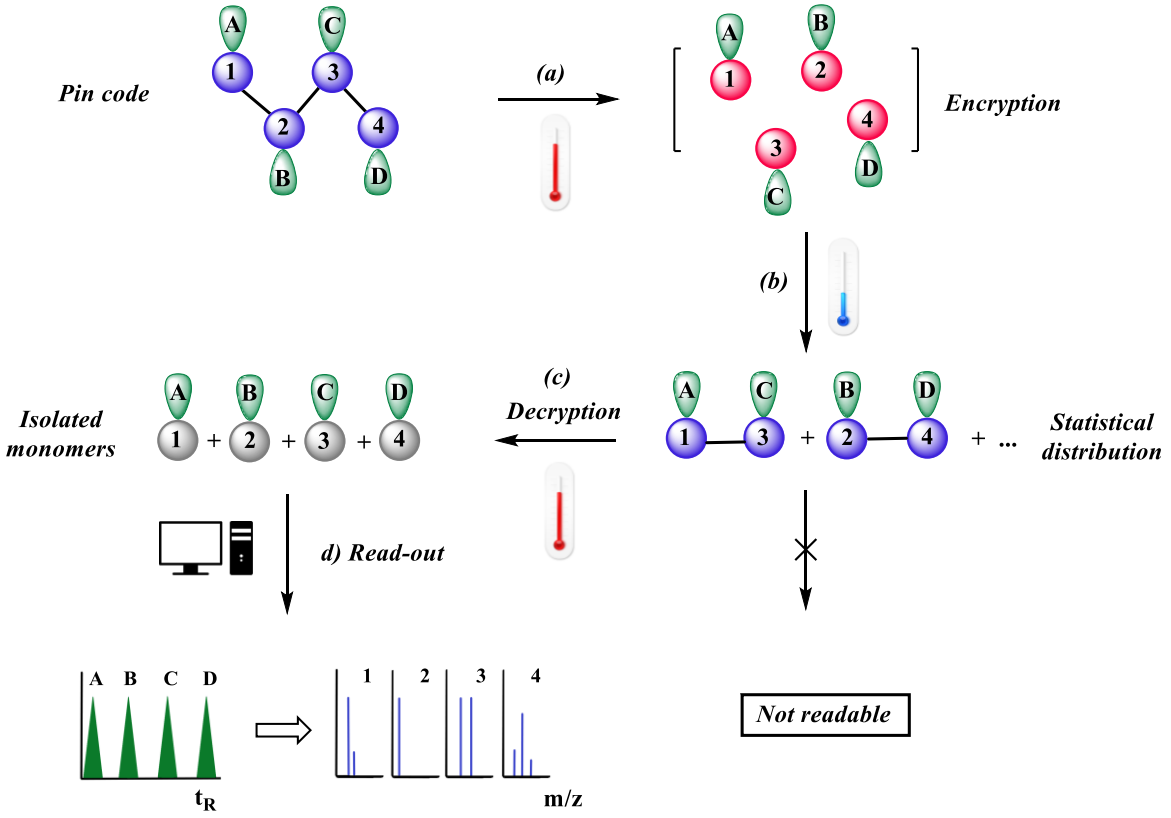


Figure VII 1: Schematic overview of the synthesis, encryption and decryption of thermoreversible macromolecular pin codes. *Sequence-defined oligomers were synthesised via a combination of TAD-indole chemistry and MCRs. These pin codes consist of an indole "marker" (i.e. A to D), which is paired to different isocyanide side-groups which make up the "chemical code" (e.g. 1-4). a) Firstly, the reversible TAD-indole covalent bonds are dissociated when heat is applied. b) Upon cooling, a random mix of oligomers is obtained, which could not be subsequently read out, thereby encrypting the encoded information c) To decrypt the information, the sequence was heated in the presence of a trapping agent (a conjugated diene), resulting in the isolation of the different monomers of the sequence. d) This mix of monomers can finally be read out via LCMS analysis to determine the original order of the building blocks, hence revealing the true macromolecular pin code.*

Incorporating TAD-indole bonds into the backbone of the sequence-defined oligomers offers the possibility to erase or encrypt the information contained within the sequence simply upon heating. Indeed, the covalent TAD-indole bonds in the macromolecular pin codes can be thermally broken, thereby resulting in the different monomers to be released and their order of connectivity to be lost (*Figure VII 1a*). When the resulting monomer mixture is then cooled down, the TAD and indole moieties will recombine, however now not in a defined but in a random fashion, leading to a statistical distribution of various oligomers and the loss of the coded information (*Figure VII 1b*). Only upon heating, the thermoreversible oligomers dissociate a second time in the presence of a conjugated diene,

the released TAD moieties can be irreversibly trapped in a Diels-Alder reaction whereby the liberated monomers can be isolated from the oligomer mixture (*Figure VII 1c*). An important aspect and considerable advancement within the field, is that the isolated monomers can now be read out using a much simpler technique, *i.e.* LCMS, to recover the encrypted information (*Figure VII 1d*). Indeed, a careful selection of functional monomers ensured a difference in polarity of the individual monomer units, whilst the indole markers were chosen to carry a specific element that has a distinct isotopic pattern, thus allowing the separation of the different monomers on the LC column and their subsequent read-out via ESI-MS.

VII.2 Results and discussion

Before investigating the potential of thermoreversible sequence-defined oligomers, the thermostability of a similar yet irreversible structure that was synthesised from Passerini products was first investigated. Because the herein proposed oligomers would need to be heated from between 90 and 150 °C to induce the retro-TAD-indole reaction, analysis *via* TGA was first performed in order to assess the thermal stability of Passerini-based macromolecules.[34,35] For this, the sequence-defined nonamer synthesised in Chapter VI (VI.4.7.17) was taken as a reference, as this also combined the P-3CR with TAD chemistry in the oligomer backbone, with the only major difference being the presence of an irreversible TAD-diene Diels-Alder covalent linkage instead of the dynamic TAD-indole Alder-ene adduct. The TGA thermogram shown in *Figure VII 2* revealed the structure to be stable until 205 °C (2 % mass loss) and even stable up to 310 °C if one considers 5 % mass loss to be the standard polymer degradation temperature, thus suggesting this to be an appropriate chemical platform to design thermoreversible precision macromolecules.

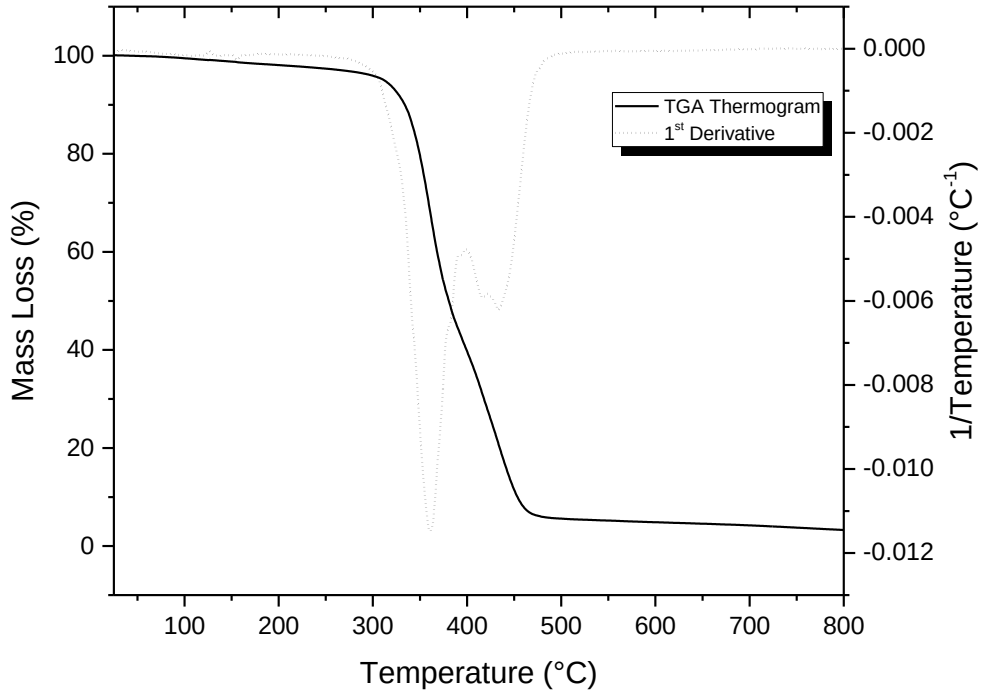
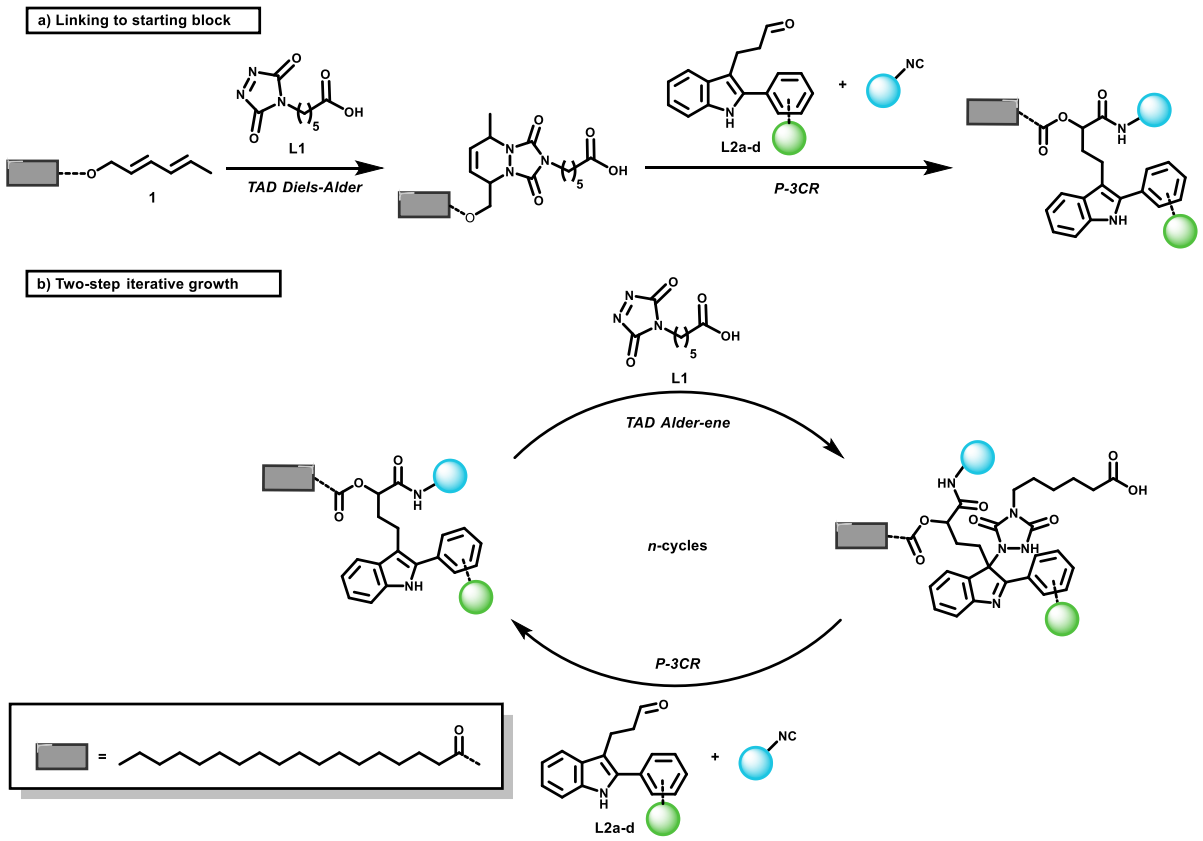


Figure VII 2: TGA of the sequence-defined nonamer synthesised in Chapter VI, used to determine the thermostability of TAD-Passerini-based macromolecules. The oligomer was thermally stable ($T_{d\,5\,\%}$) until 310 °C.

VII.2.1 Sequence-defined protocol

Having confirmed the appropriate temperature window, the successful protocol described in Chapter VI was next adapted to combine the reversible TAD-indole Alder-ene reaction with the P-3CR. Hence, the TAD-carboxylic acid molecule **L1** (TAD-COOH) that was introduced in Chapter VI was used as the first linker molecule to initiate the iterative growth of the macromolecular pin code (*Scheme VII 1a*). **L1** was synthesised according to the procedure outlined in Chapter VI, however the oxidation step which converted the urazole to the TAD species was changed to a less toxic approach with easier handling. Previously, gaseous N_2O_4 was used,[33] however this poses an acute toxicity to humans and so trichloroisocyanuric acid was used as an *in situ* halogen-mediated approach.[37] In contrast to the irreversible TAD/P-3CR protocol in which a diene isocyanide was used as the second linker to re-instate a TAD-reactive group, the thermoreversible sequence-defined oligomer targeted here employed four different indole-aldehyde linker compounds (**L2a-d**) to provide a dynamic TAD-adduct formation (*Scheme VII 1b*). Moreover, the indole moieties serve as position markers to locate the varying isocyanides that introduce the molecular information. From the knowledge obtained in Chapter VI, it was further decided to focus primarily on a solution phase synthesis approach, as it could be monitored more easily with a wider range of analytical techniques (*i.e.* not only SEC and LCMS but also NMR) and was much more up-scalable, which was considered an important advantage in view of the targeted application.

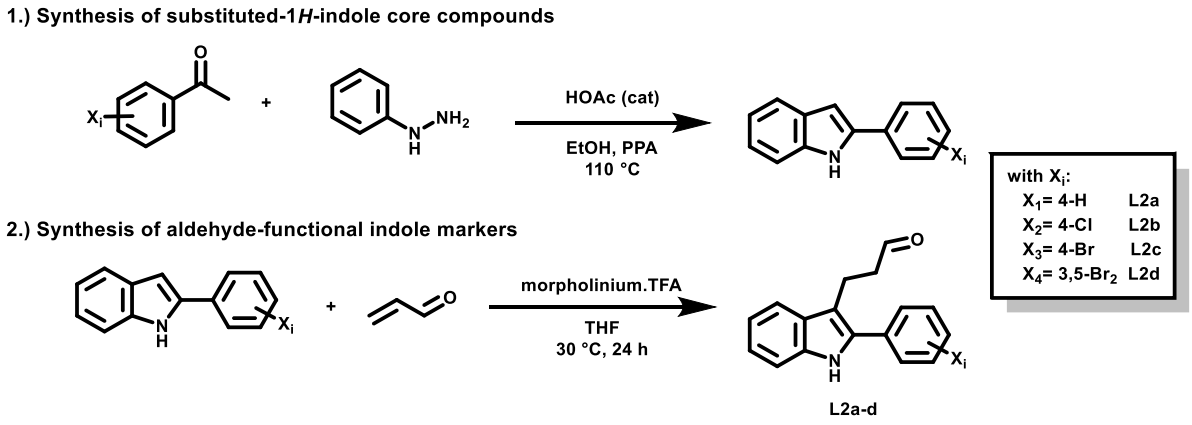


*Scheme VII 1: Solution phase, sequence-defined protocol combining the P-3CR and TAD Alder-ene reactions. a) Stearic acid was modified with sorbic alcohol to create the apolar starting block **1**, which facilitates purification by column chromatography. TAD Diels-Alder reaction with the TAD-COOH **L1** followed by a P-3CR with an indole aldehyde (**L2a-d**) and isocyanide enables the introduction of the first position marker and digit, respectively. b) Continuation of this two-step iterative protocol allows for a sequence-defined oligomeric growth to obtain the macromolecular pin code.*

Specifically, stearic acid was first functionalised with sorbic alcohol to create the apolar conjugated diene **1** that served as the starting block for the two-step iterative growth (see *Scheme VII 1a* and VII.4.5.1). As described in Chapter VI, the long alkyl chain was again exploited to facilitate separation and purification of the oligomer from the excess reagents after each cycle *via* column chromatography. Two AB-type linker molecules were necessary, each containing one functionality that would react in a P-3CR and the other that would undergo a TAD Alder-ene conjugation. **L1** first reacted in a Diels-Alder reaction with **1** and subsequently the carboxylic acid group underwent the first P-3CR with the first of the indole-aldehydes and one of a range of commercially available isocyanides, which were used as both the third component of the P-3CR and to introduce the sequence-definition or macromolecular pin code (*Scheme VII 1a*). Now that an indole species was introduced, the two-step cycle of TAD Alder-ene and P-3CR could continue (*Scheme VII 1b*), to yield sequence-defined oligomers.

VII.2.2 Synthesis of indole position markers

Whilst the sequence-defined code would be written using the differing isocyanide compounds, it was necessary to couple them with position markers, so that following encryption, the original order of the code could still be determined by the intended users. If the order of the isocyanides (the code) changed, it could still be read-out by keeping the indole order the same. Therefore, substituted indole aldehydes were introduced as they provided one of the necessary functionalities for both the P-3CR (along with the carboxylic acid and isocyanide) and the thermoreversible TAD Alder-ene reaction. The four aldehyde-functionalised indole markers **L2a-d** were synthesised by means of a nucleophilic substitution reaction of the appropriate indole precursor to an aldehyde acceptor. In particular plain, chloro-, bromo- and dibromo-substituted indole compounds were targeted since this would facilitate LCMS identification at a later stage, whereby each locator indole has a characteristic isotopic pattern that can be used as its "chemical fingerprint".[38] Whereas the plain 2-phenylindole is commercially available, the Cl- and Br-containing indole building blocks first had to be synthesised *via* a Fischer indolisation (*Scheme VII 2*).[39] Subsequent reaction with acrolein afforded the four aldehyde-functionalised indoles.[40] The indole locator compounds were intended so that both the person who synthesised the sequence and the person for whom the information was intended, would know the order of the indole compounds. However, only the person who synthesised the sequence would know the order of the isocyanides, or *macromolecular pin code*, thus once heated the information would be encrypted, as the original pin code could only be determined by the indole locater bound to the specific isocyanide.



*Scheme VII 2: Generic two-step synthesis route towards the indole-aldehyde position markers **L2a-d***

VII.2.3 Synthesis of a four-digit macromolecular pin code

Once the indole position markers were synthesised, a four-digit macromolecular pin code could be written using the protocol outlined in *Scheme VII 1*. The apolar starting block **1** (see *Scheme VII 1a*)

was first reacted with TAD-COOH (**L1**) to undergo a Diels-Alder reaction in solution. **L1** was added in a titration-type experiment until a pink colour persisted. This indicated the presence of a slight excess of the TAD linker and thus ensured quantitative conversion of the diene starting block. The excess TAD was then quenched by adding a small amount of 2,3-dimethylbut-2-ene until the pink colour disappeared to avoid any uncontrolled TAD-reactivity that might occur during the next step (see Chapter VI). The first P-3CR was then directly carried out without prior purification, using the first isocyanide digit (i.e. cyclohexyl isocyanide encoding '1', *Figure VII 3*) and indole-aldehyde position marker **L2a**. The resulting monomer **A1** was then purified *via* column chromatography, before continuing to the next cycle to remove traces of a second Passerini by-product that originated from the previously quenched excess of TAD-COOH. Once isolated, the monomer underwent a second TAD addition to re-instate the carboxylic acid, only this time through reaction with the indole in an Alder-ene conjugation. Following a second Passerini reaction with *tert*-butyl isocyanide 'digit 2' and indole **L2b**, the dimer derivative **A1-B2** was obtained. This iterative protocol was carried out for a total of four cycles, resulting in 360 mg of the sequence-defined tetramer **A1-B2-C3-D4** that formed the macromolecular pin code (*Figure VII 3*). The Alder-ene reaction between the indole and TAD was found to be slower for the Cl and Br substituted indoles, which can be attributed to the electron withdrawing effect of the halogen species. Each cycle during the synthesis was followed by LCMS and SEC (see *Figure VII 4*), to assess the purity and conversion obtained during the iterative sequential growth. In addition, full structural characterisation using 1D and 2D NMR techniques as well as HRMS confirmed the structure of the macromolecular pin code.

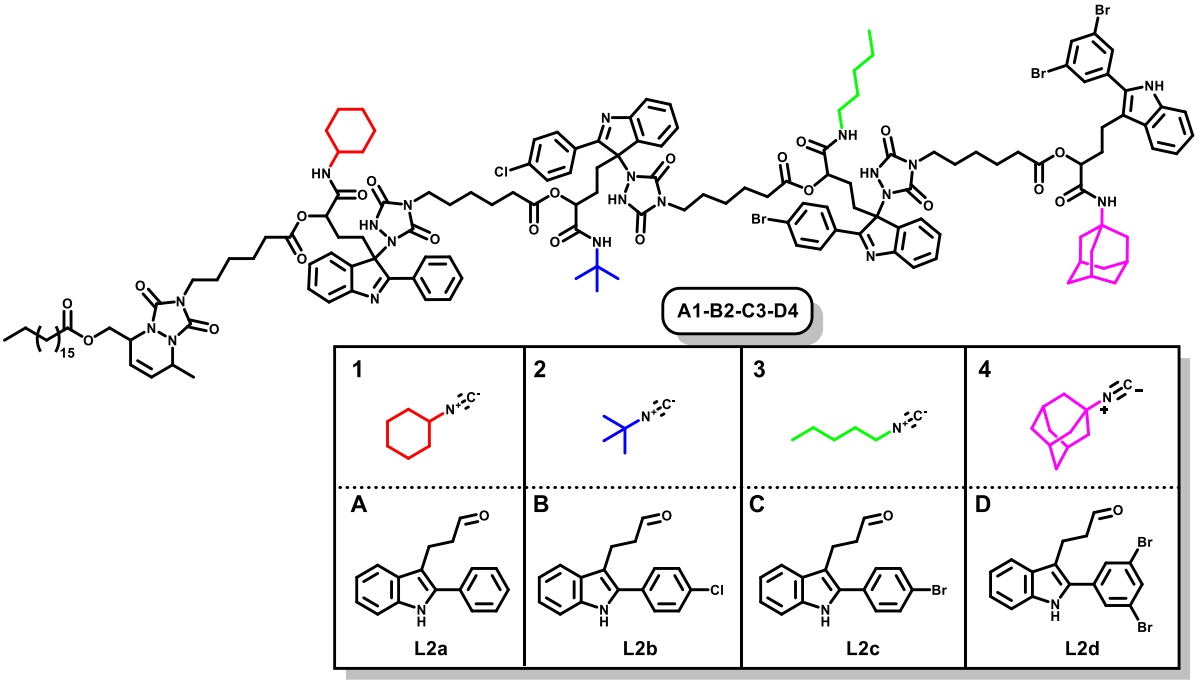
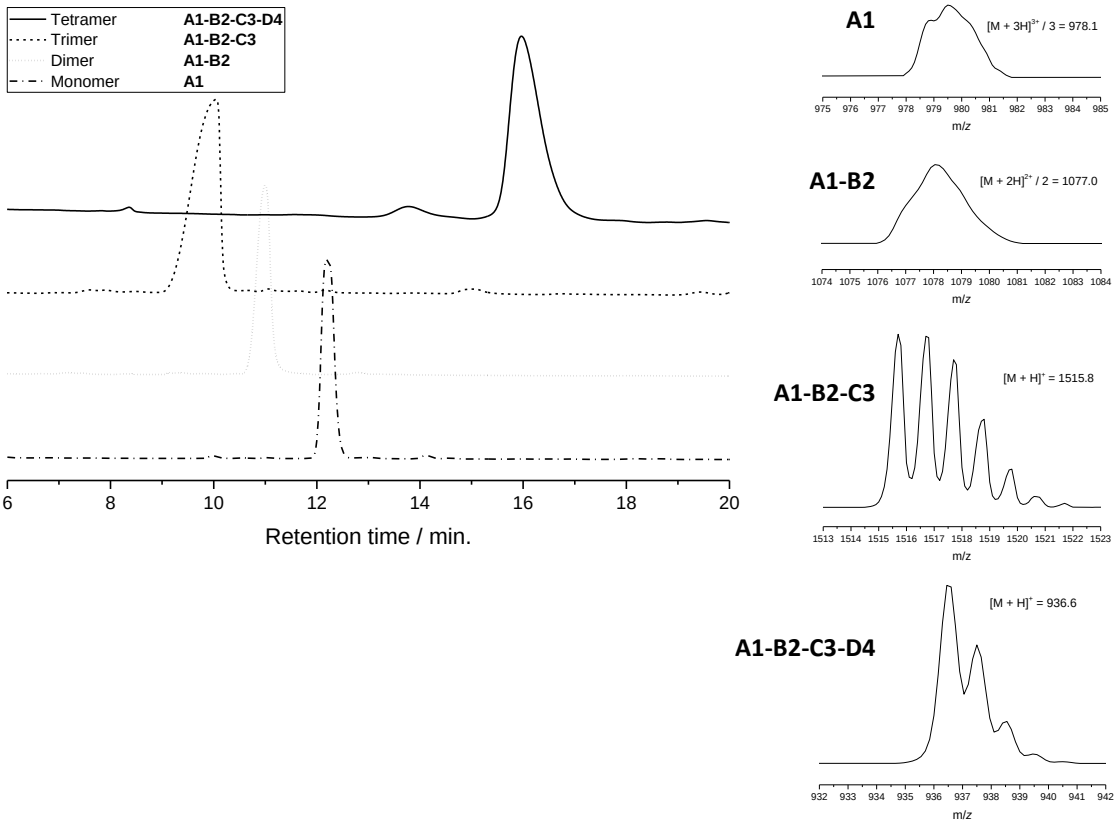


*Figure VII 3: Structure of the sequence-defined tetramer **A1-B2-C3-D4** that makes up the four-digit macromolecular pin code.*



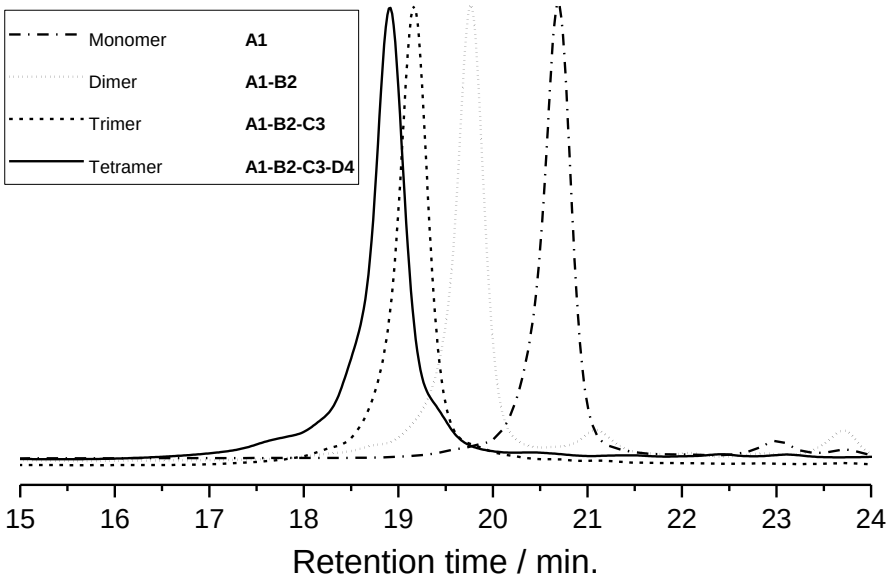


*Figure VII 4: Top) Stacked LCMS chromatograms (λ = 214 nm) and mass spectra obtained after each complete cycle during the synthesis of the macromolecular pin code **A1-B2-C3-D4**. Bottom) Corresponding SEC elugrams.*

VII.2.4 Encryption and decryption of macromolecular pin codes

In the interest of time at the end of the PhD research, the encryption and decryption of the sequence-defined oligomer was first tested using a 3-bit macromolecular pin code (*i.e.* the trimer **A1-B2-C3**). At first, the pin code was encrypted by heating a solution of the trimer to 150 °C for 15 minutes, in the absence of any co-reactant (*cf. Figure VII 1*). During the heating step, the retro-Alder-ene reaction of the TAD-indole covalent bond was initiated, which led to the dissociation of the monomer units from the oligomer. Since there was no trapping agent present during the encryption that can quench the liberated TAD moieties, subsequent cooling of the monomer mixture resulted in their recombination in a random order. Hence, a disperse mix of unreadable oligomers was formed, as shown below in *Figure VII 5*, whereby the information that they were carrying was encrypted.

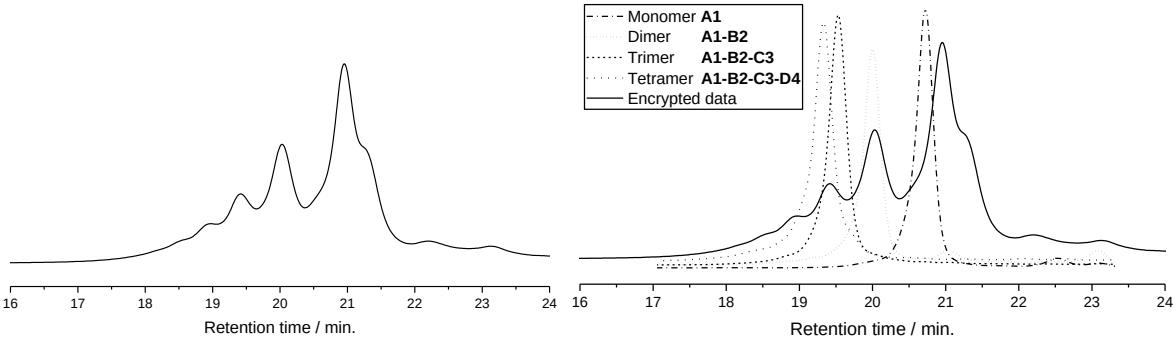


Figure VII 5: Left) SEC elugram after data encryption, showing a disperse mix of random oligomers (Đ = 1.49). Right) Overlay of SEC elugrams of the individual monomer units (Đ = 1.00) on top of that of the encrypted data. ***A1-D4*** *are shown for reference, although the encryption was only tested using* ***A1-B2-C3*** *trimer.*

In a second reheating step, this time in the presence of a trapping agent (i.e. sorbic alcohol), the TAD-indole bonds in the unreadable oligomer mix were again disociated into the corresponding monomer units in solution (*Figure VII 6a*). Because the TAD Diels-Alder reaction is kinetically more favourable than the TAD-indole Alder-ene adduct formation,[35,36] the TAD moieties were irreversibly capped with the diene from which the separate monomer units could be isolated and read-out or decrypted (*vide infra*). As can be seen in *Figure VII 6b*, there are several key proton resonances that provided confirmation of the dissociation – and thus successful decryption – of the Alder-ene adducts in the trimer. Notably, the appearance of new *NH* proton resonances associated with the release of the indole moieties of monomers **A1** and **B2** (*i.e.* the new signal *a* and increase of *b*, respectively), and the disappearance of the urazole *NH* proton resonances (*c*) as the TAD is being transformed from an indole-Alder-ene to a diene-Diels-Alder adduct. The formation of the Diels-Alder adduct in turn was evidenced by the introduction of a new, distinct resonance as the cyclic C=C bond is formed (g). Finally, a shift in the aromatic proton resonances from (*d*) to (*e*) of the indole structure is observed as the indole unit rearranges during the TAD-indole dissociation.

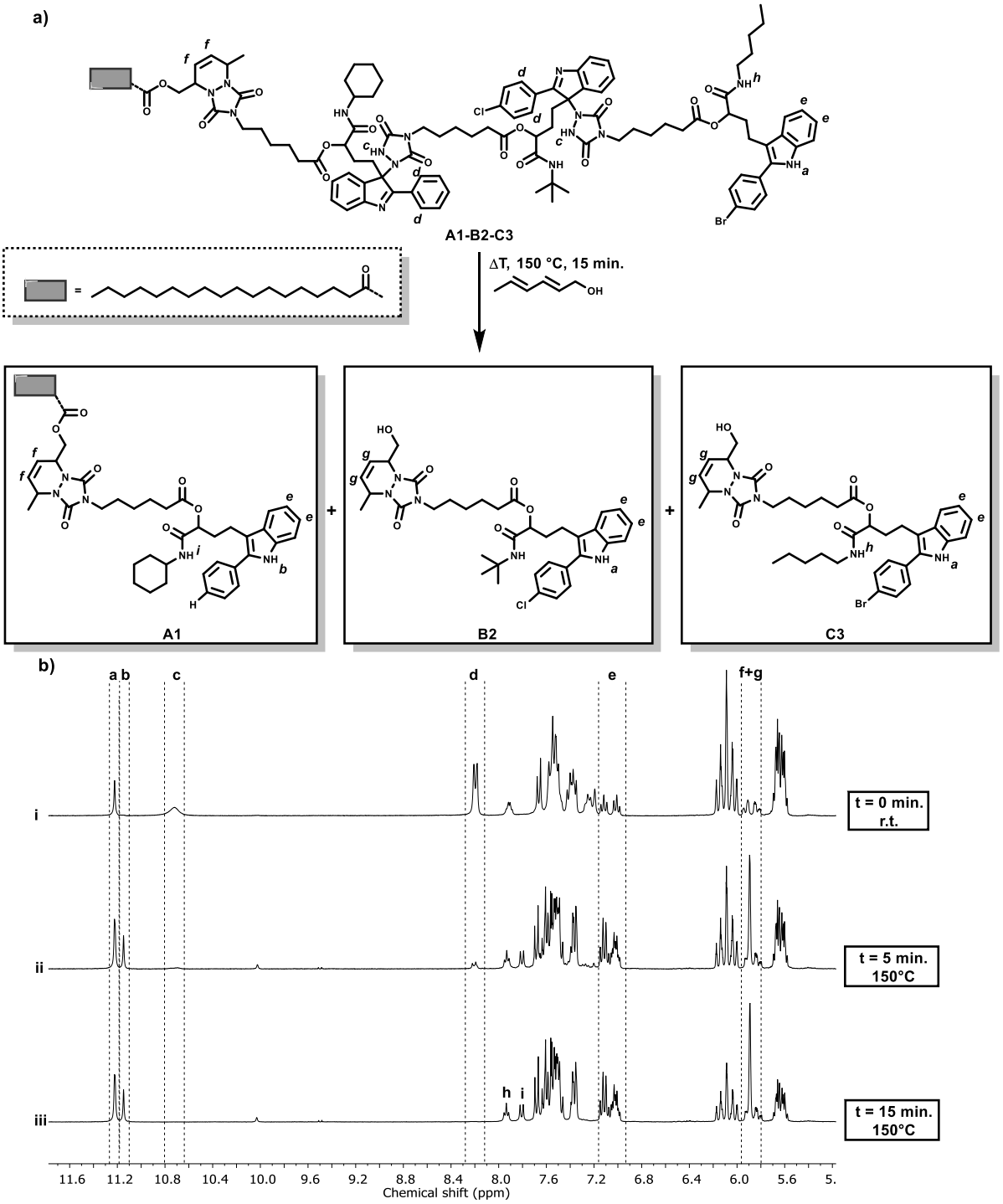


*Figure VII 6: a) Heating of trimer **A1-B2-C3** in the presence of sorbic alcohol results in the isolation of the three separate monomer units as the liberated TAD moiety is irreversibly trapped. b) ^{1}H NMR spectra in DMSO-d_6 i) before heating and after ii) 5 min and iii) 15 min. of heating at 150 °C. The encryption is indicated by the increase of signal 'a' arising from the initial bromo- **(C3)** and released chloroindole NH **(B2)**, as well as the new proton resonance 'b' of the released indole NH of **A1**. Moreover, the urazole N-H proton signal 'c' disappears as the Alder-ene adducts dissociate with the formation of the TAD-diene Diels-Alder adduct (signal 'g'). As a result of the retro-Alder-ene reaction, the indole aromatic proton resonances shift upfield from 'd' to 'e' as the structure rearranges.*

To determine the best conditions for the macromolecular pin code decryption, the dissociation of the trimer was studied at different temperatures over time. Thus, a solution of **A1-B2-C3** in DMSO-d_6 (0.023 M) was heated in an oil bath at 120 °C, 135 °C and 150 °C in the presence of sorbic alcohol (see VII.4.7.2 for experimental details). At regular time intervals during heating, the sample was removed from the oil bath and quickly cooled to room temperature to enable quantitative analysis of the thermal dissociation kinetics by means of ^{1}H NMR. Indeed, through the changes in integration of the indole proton resonances (*d*) & (*e*) (see *Figure VII 6b*), the progress of the thermoreversibility could be monitored and the percentage of reversibility over time could be plotted for the different temperatures investigated (*Figure VII 7*). As expected, the temperature was observed to have a significant effect on the rate of oligomer dissociation, with complete conversion into the diene-capped monomers and hence full encryption reached within 15 minutes at 150 °C, 45 minutes at 135 °C and 180 minutes at 120 °C. The analysis at three distinct temperatures enabled the determination of the activation energy of the overall decryption, as described in detail in VII.4.7.2. Indeed, the experimental data was used to create an Arrhenius plot (*Figure VII 31*, VII.4.7.2) based on the Arrhenius equation (where k = rate of reaction, A = pre-exponential factor, E_a = activation energy, R = molar gas constant and T = temperature), from which the activation energy was found to be 107.0 kJ mol^{-1}, ± 4.7 kJ mol^{-1}. This value is in accordance to previously reported TAD-indole retro-Alder-ene reactions[34,35] and should be interpreted as the superimposed energy barrier that is required to completely release the three differently substituted indoles.

Arrhenius equation: $k = A \exp(\frac{-E_a}{RT})$

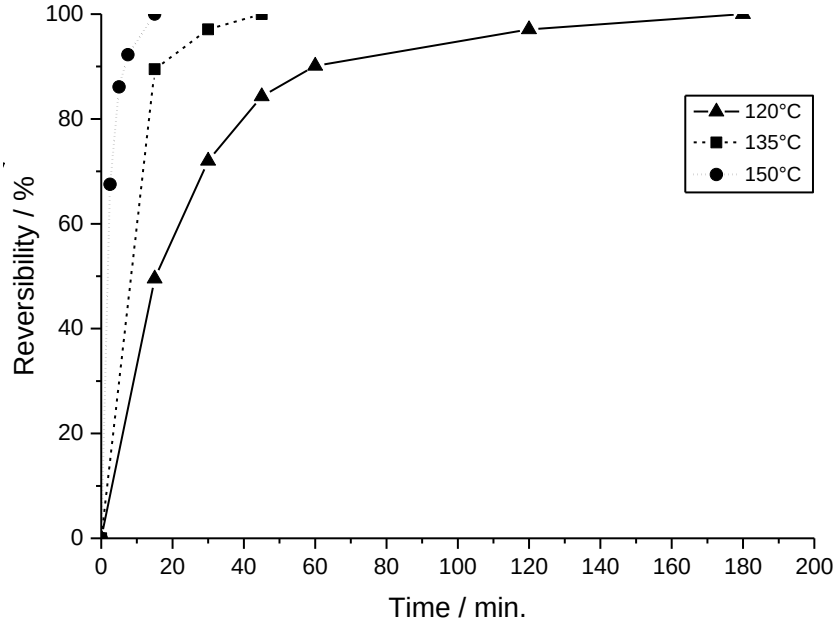


*Figure VII 7: Effect of temperature on the rate and efficiency for the decryption of trimer **A1-B2-C3** (0.023 M, DMSO-*d_6*).*

Having identified the conditions required to achieve complete decryption of the sequence-defined oligomer *via* ^{1}H NMR, the mixture of isolated monomers, obtained after heating **A1-B2-C3** for 15 minutes at 150 °C in the presence of sorbic alcohol, was next decoded by means of LCMS analysis. Indeed, the different monomer units could be separated based on polarity by LC (*Figure VII 8b*) and their corresponding masses could be read out by MS (*Figure VII 8d*). Additionally, SEC analysis was also performed but the differences in hydrodynamic volume were too small to obtain good separation of **B2** and **C3** (*Figure VII 8c*). The specific isotopic patterns that were incorporated via the substituents onto the different indole markers were used to identify the original location of the monomer within the sequence (*Figure VII 10*). Based on the differences in molecular mass, the correct isocyanide digit could then be assigned to this position so that one could reconstruct and finally read-out the original encoded information.

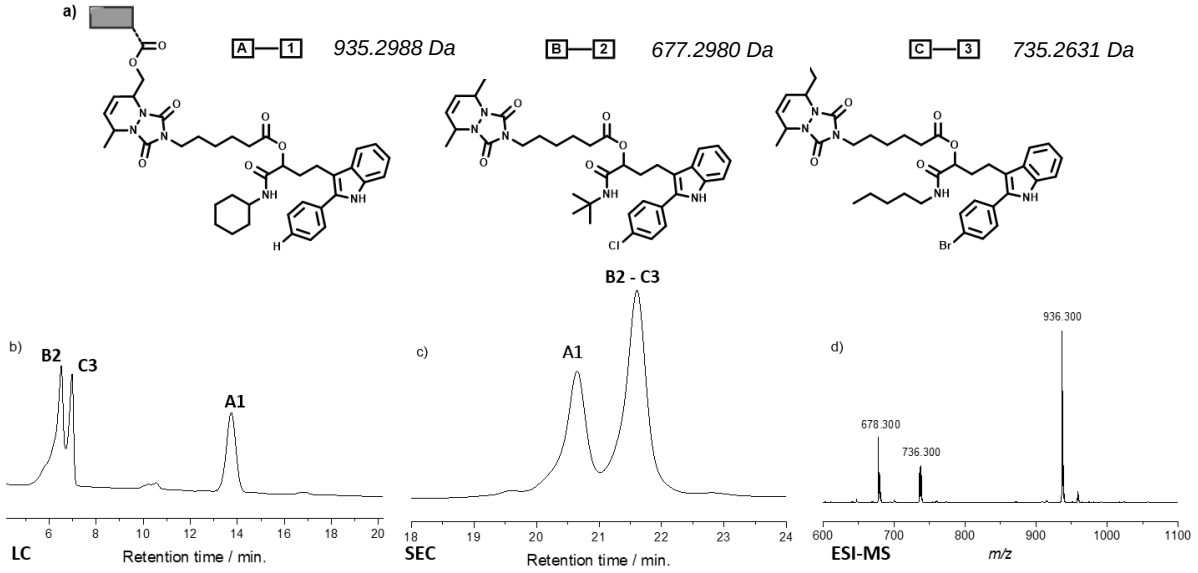


*Figure VII 8: a) Structures of the isolated monomers obtained after decryption of the macromolecular pin code **A1-B2-C3** (15 mins at 150 °C), with A, B & C denoting the indole locator compounds and 1, 2 & 3 corresponding to the different isocyanide digits. b) LC chromatogram (λ = 214 nm), indicates the separation of the three different monomer units, with **A1** attached to the apolar starting block **1**, thus resulting in a much higher retention time compared to its sorbic alcohol-capped analogues **B2** and **C3**. c) SEC elugram of the isolated monomer mix, following decryption at 135 °C for 45 min. d) The masses of the three monomer fragments can be obtained from the ESI-MS spectrum, which enabled the assignment of the isocyanide digit to the respective position in the sequence based on the specific isotopic patterns of the substituted indoles. The order of the indoles thus here reveals the macromolecular pin code to be 1-2-3.*

In a later phase of the current chapter, the decryption experiments were repeated using the apolar starting block **1** as a trapping agent instead of sorbic alcohol in a successful attempt to decrease the polarity and thereby facilitate better LCMS separation, as shown below in *Figure VII 9*. This also meant that the mass and retention time of the first unit (**A1**) was not vastly different from the rest. The isotopic patterns also corresponded well with the theoretical predictions shown in *Figure VII 10*.

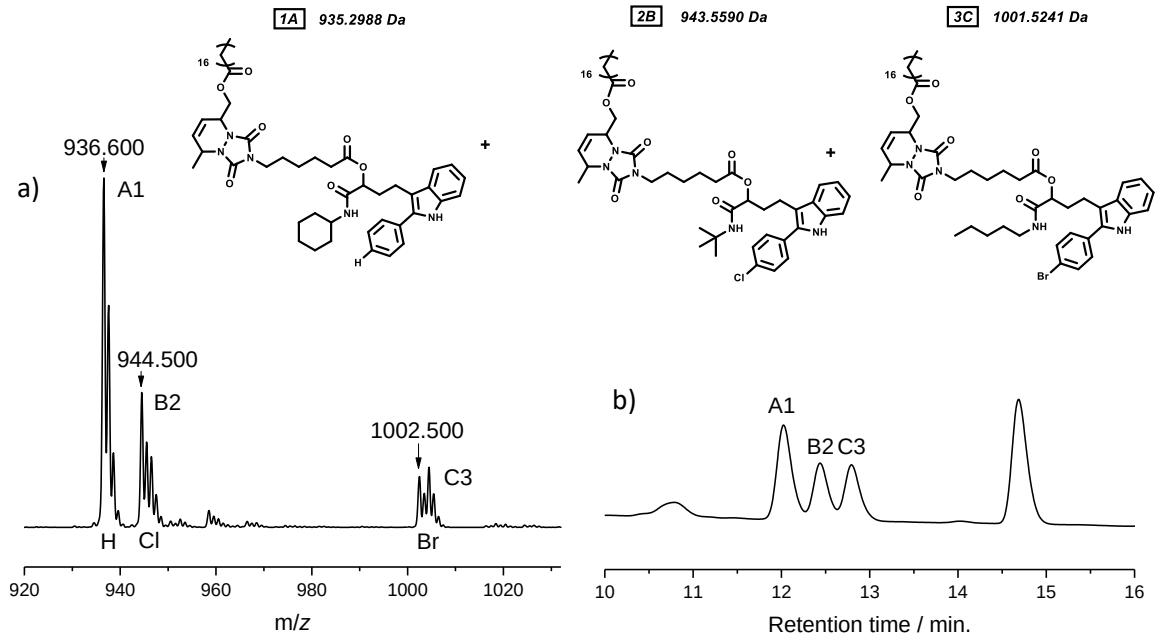


*Figure VII 9: Top) Structures of the isolated monomers obtained after decryption of the macromolecular pin code **A1-B2-C3** using starting compound **1** as trapping agent, with A, B & C denoting the indole locator compounds and 1, 2 & 3 corresponding to the different isocyanide digits. a) ESI-MS spectrum following the decryption, showing the mass of the three monomer units. Their original order can be determined using the isotopic pattern of the indole-markers. b) LC chromatogram (λ = 214 nm) using C5 columns, resulting in a clearer separation of the three monomer units of the macromolecular pin code. Decryption was carried out by heating in anhydrous butyl acetate at 120 °C for 5 hours (boiling point of butyl acetate = 126 °C).*

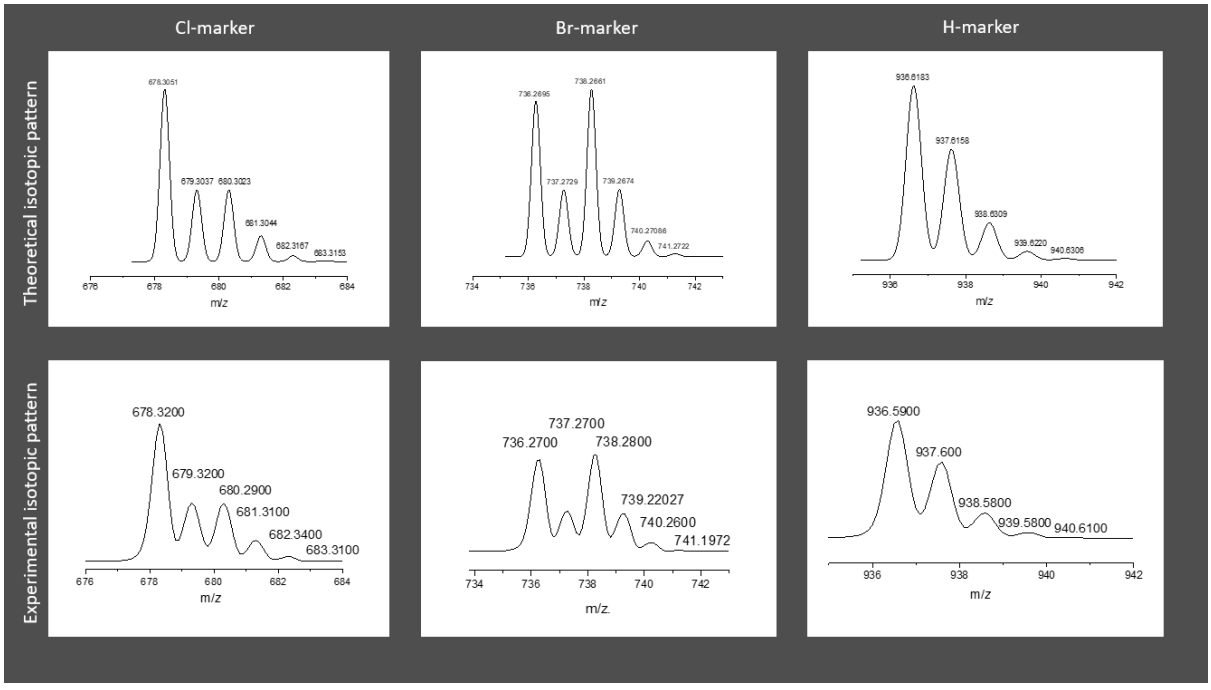


*Figure VII 10: Comparison of the theoretically predicted and experimentally obtained isotopic patterns of the three monomers obtained after decryption of the sequence-defined trimer **A1-2B-3C**, enabling the easy identification of the appropriate indole marker compound and therefore position of the isocyanide digit within the macromolecular pin code.*

VII.2.5 Incorporation of dynamic sequences onto polymer materials

As suggested above, one potential application for these macromolecular pin codes is for anti-counterfeiting purposes. As a proof-of-concept, the encrypted oligomers were applied to the new generation of Bank of England polymer (polypropylene) banknotes, which have recently been introduced into circulation in the United Kingdom to counter fraudulent activities and contain multiple layers of printing and security features. However, central banks are always looking at new ways to further protect their currency and sequence-defined macromolecules could be one potential solution.

As a demonstrator, a £5 and £10 polymer note were secured with encrypted sequence-defined oligomers (*Figure VII 11a*). Before coating the notes with the macromolecular pin codes, the £5 note was first suspended overnight in ethanol to verify that it did not dissolve or discolour in the solvent (*Figure VII 11b*) and ESI-MS was measured following evaporation of the ethanol to serve as a reference spectrum of background signals. Ethanol was chosen here as a practical, non-toxic solvent, which could be easily and safely used in a real-world application. Following this, approximately 10 mg of the encrypted trimer **A1-B2-C3** as well as the tetramer **A1-B2-C3-D4** were dissolved in a minimal amount of ethanol and deposited on the surface of the £5 and £10 banknotes, respectively (*Figure VII 11c*). Mild heating was applied to evaporate the solvent and the notes were then left to dry further overnight. The encoded banknotes had a similar appearance to the pristine ones (*Figure VII 11d*) and were placed again in ethanol for 5 hours to re-extract the encrypted oligomer from the surface (*Figure VII 11e* and *f*). Following extraction, the banknotes still retained their pristine look (*Figure VII 11g*) After solvent evaporation under reduced pressure, the recovered sequences were finally decrypted by heat treatment for 4 h 30 min. at 120 °C in the presence of **1**, followed by ESI-MS analysis.

ESI-MS analysis (*Figure VII 12*) was chosen as the LCMS chromatogram was inconclusive as a result of potential background contamination from the banknote itself and the apolarity of the individual monomers. This meant that with a regular C18 or even a C5 column at reduced solvent gradient, the monomers were too apolar to see a visible separation in the LC as their retention times were too high and at the limit of the column. However, by using straightforward ESI-MS analysis of the mixture extracted from the £5 note, the mass signals of the three distinct monomers (**A1, B2** and **C3**) were distinguishable and their original order was identified using the specific isotopic pattern associated with the varying indoles (**L2a-c**). However, the ion count was very low and in the mass spectrum of the monomers extracted from the £10 note, which had been encoded with the tetramer, only **A1** was visible. Closer examination of the baseline suggested the presence of the other isotopic patterns, but the signal response was too low to be conclusive.

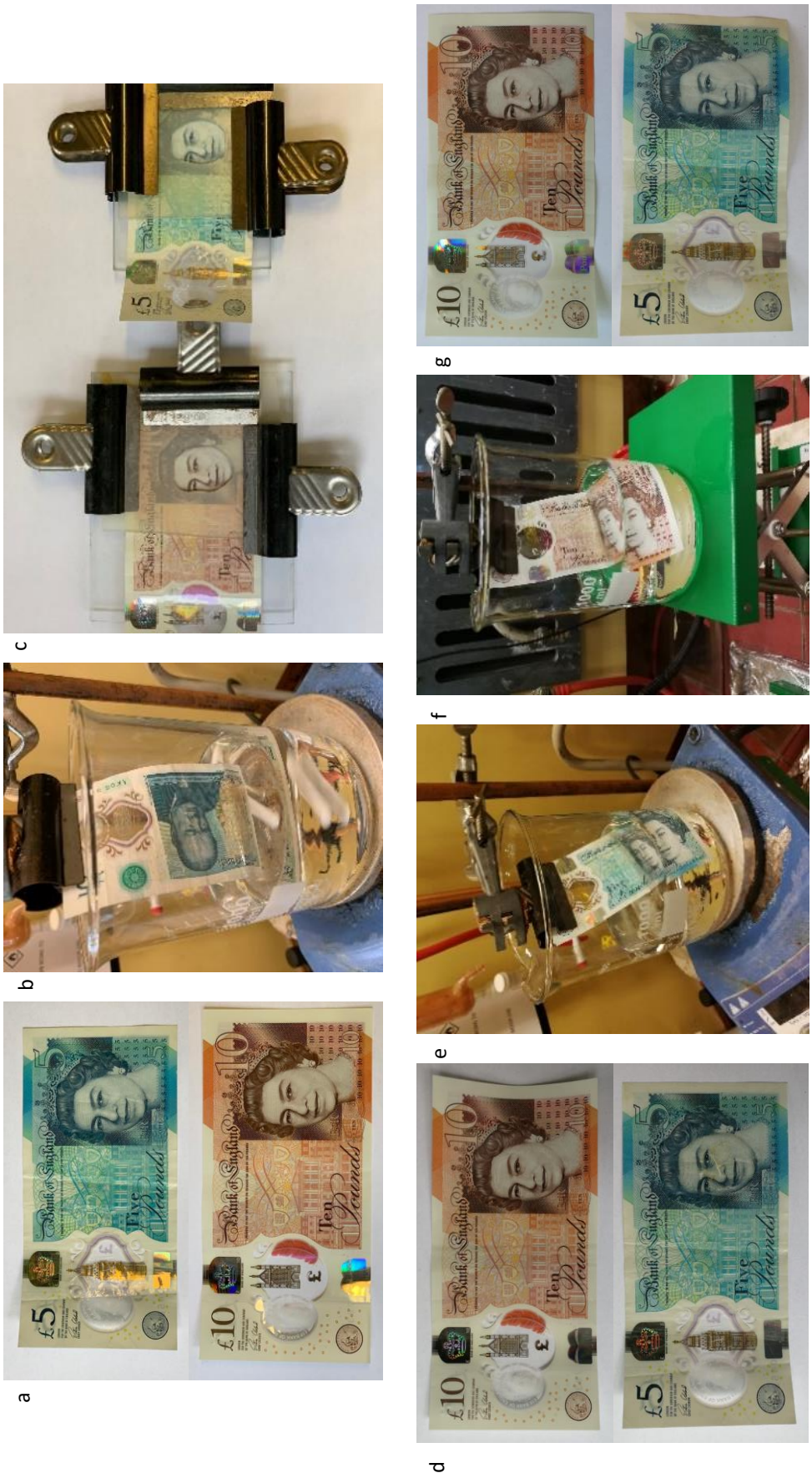


Figure VII 11: Images displaying the application of encrypted macromolecular pin codes to pound sterling banknotes. a) The pristine banknotes. b) Testing that the banknote did not dissolve or discolour when placed in ethanol overnight. c) Templates were made to allow application of the solution containing the encrypted pin code to a specific area of the banknote's surface. ***A1-B2-C3*** *was applied to the £5 and* ***A1-B2-C3-D4*** *was applied to the £10 note. d) The banknotes following application of the encrypted pin code to the surface, with the deposited sequences barely visible. e-f) Extraction of the encrypted pin code from the surface of the banknote in ethanol. g) The banknotes following the extraction of the macromolecular pin code in their original pristine condition.*

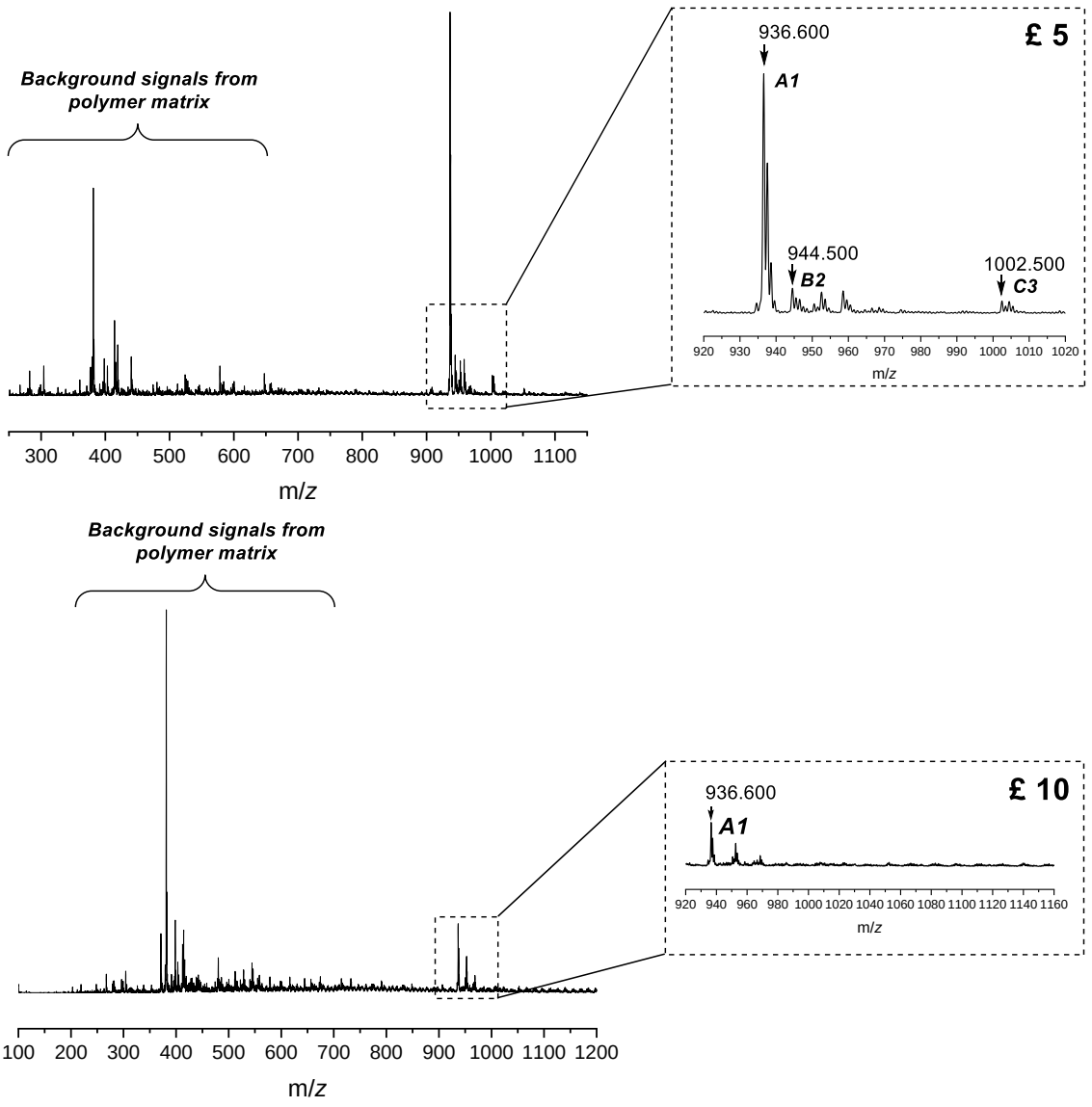


Figure VII 12:ESI-MS spectrum following decryption of the extracted macromolecular pin code from the surface of the £5 note (top) and the £10 (bottom). In the case of the £5 note, the 3-bit code was distinguishable in the MS spectrum and the original order identifiable because of the isotopic pattern associated with the indole marker compounds. For the £10 note was the ion count too low to decisively read out the whole code.

In the future, the read-out could be improved by fine-tuning the mass spectroscopy techniques used. For example, by using Selected Ion Monitoring techniques one could scan a more specific mass-to-charge ratio (m/z) range, thus removing the effect of the polymer matrix background interference by narrowing the analysis range. Background signals were to be expected as many other components are used within the banknotes (additives, colourants, etc.). Increasing the sample concentration may help to ensure a high enough ion count during ESI-MS. Alternatively, MALDI-TOF could be investigated for analysis and read-out. This wasn't considered initially as MALD-TOF is known to fragment TAD-Indole bonds, however, when only decryption is desired only TAD-Diels-Alder adducts are present, which are more stable towards MALDI-TOF, thus this could be further investigated.

VII.2.6 Solid-phase synthesis of macromolecular pin codes

As with the work outlined in Chapter VI, the protocol described herein was also investigated for solid-phase synthesis, the results of which will be briefly outlined here as they were less promising than those carried out in solution. Moreover, the solution-phase experiments meant that a more up-scalable amount of sequence-defined oligomer could be produced, thus enabling its testing in a material application (*vide supra*). Nonetheless, solid-phase synthesis was of interest to consider, as future potential applications of this protocol may require the synthesis of large libraries of varying macromolecular pin codes, thus, an automated and time-saving synthesis approach might be more attractive.

Firstly, 2-chlorotrityl chloride resin was functionalised with sorbic alcohol, and the protocol outlined in *Scheme VII 1* was adapted for solid-phase synthesis (see Experiment VII.4.4.6). Despite pure monomers and dimers being obtained, from the third cycle onwards, impurities were observed in the LCMS spectra, presumably because of an increasing steric crowding on the solid support (*Figure VII 13a*). Replacing the solid support to a rink-amide resin with a lower loading capacity, only resulted in a slight increase of the trimer purity although barely significant (*Figure VII 13b*). As a final experiment to grow macromolecular pin codes on solid supports, the rink-amide resin was further treated to cap unreacted secondary amine groups during the resin functionalisation with sorbic alcohol to prevent any potential side reactions with the TAD or during the P-3CR and then the sequence-defined synthesis was repeated. However, this was found to have no improvement on the sequence purity.

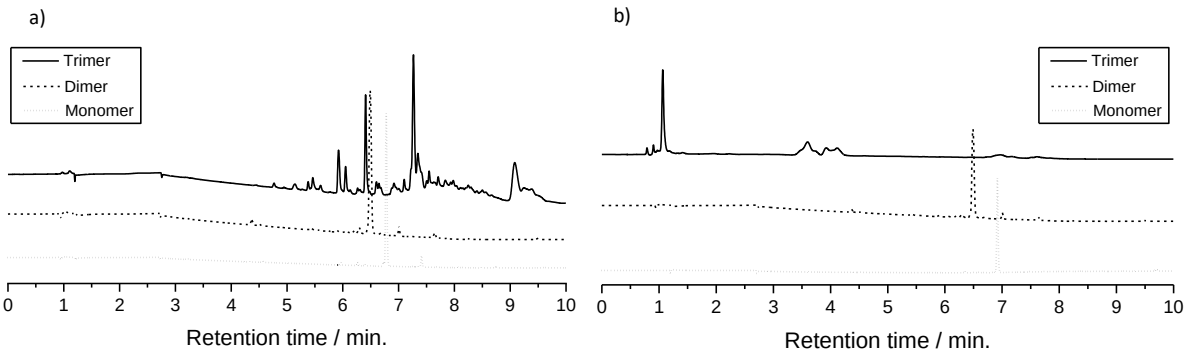
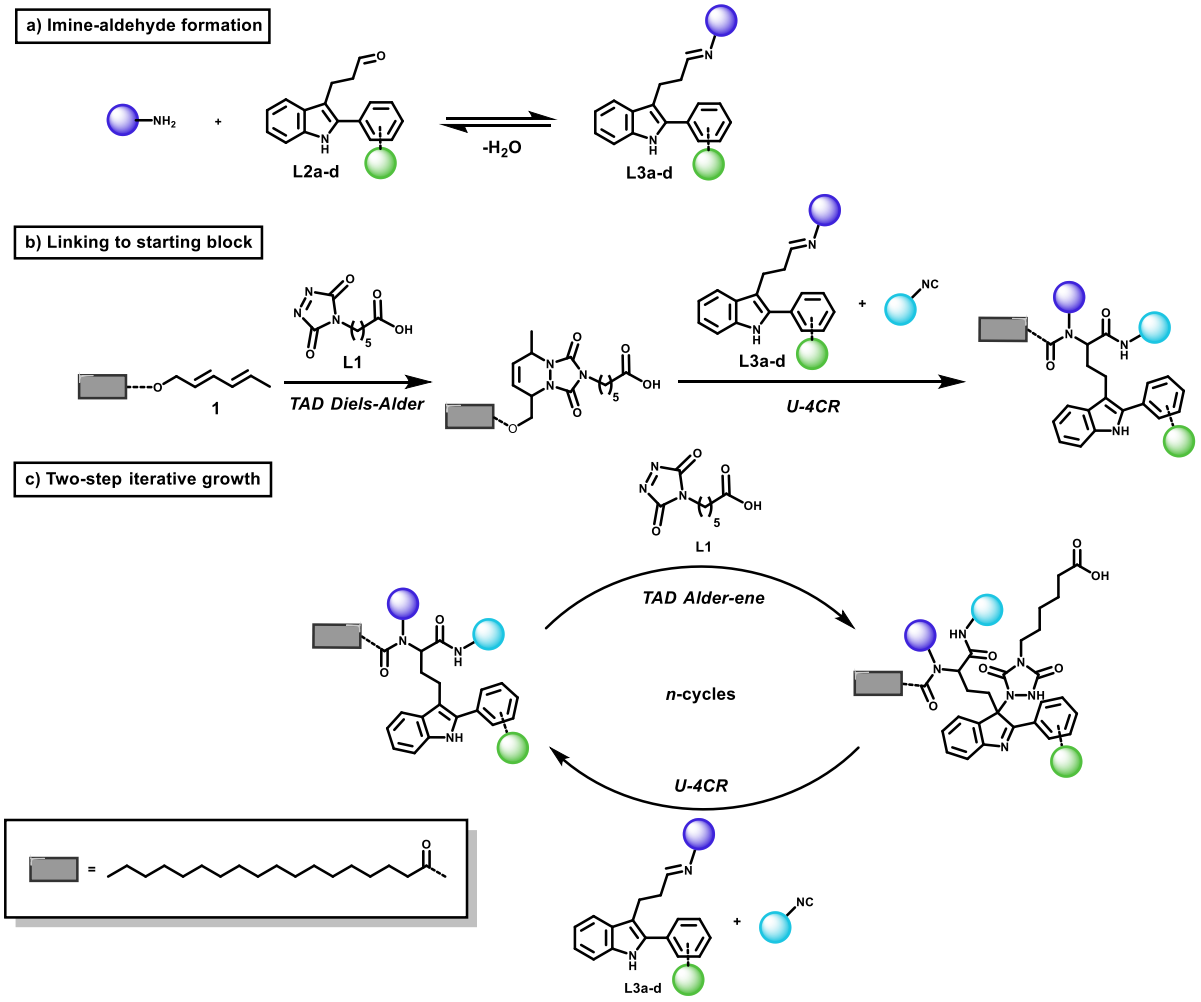


*Figure VII 13: a) LCMS chromatograms (λ = 214 nm) of the monomer, dimer and trimer synthesised using the 2-chlorotriytl chloride resin. b) LCMS chromatograms (λ = 214 nm) of the monomer, dimer and trimer synthesised using the rink-amide resin. In both cases, the indole aldehyde position marker (**L2a**) was used in each step to simplify the reaction parameters.*

VII.2.7 Expanding the chemical toolbox with the U-4CR

In a final experiment (VII.4.6), the Ugi four-component reaction (U-4CR)[27] (which is described in Chapter II.6.3) was also investigated, as this was a way to vastly increase the amount of information that could be stored on short oligomers, as it provided a double modification of the structure after each iterative addition.[14,41] Moreover, the U-4CR requires almost no additional chemical effort than the P-3CR. The U-4CR additionally introduces a primary amine to the reaction (as discussed in detail in Chapter II.6.3) by forming an imine (**L3$_{a-d}$**) upon reaction with the aldehyde which is then added to the MCR. Using a modified version of the protocol outlined in *Scheme VII 1*, (see Scheme *VII 3*) the U-4CR reaction was tested in combination with TAD chemistry, resulting in monomer **11** (see *Figure VII 14*)**.** Time prevented this being investigated further during this doctoral thesis, but nonetheless, this confirmed the compatibility of the U-4CR with the protocol described herein for future work.



*Scheme VII 3: Solution phase, sequence-defined protocol combining the U-4CR and TAD Alder-ene reactions. a) Indole-imine formation by reacting the indole-aldehyde with a primary amine, resulting in **L3$_{a-d}$**. b) Stearic acid was modified with sorbic alcohol to create the apolar starting block **1**. TAD Diels-Alder reaction with the **L1** followed by a U-4CR with an indole-imine (**L3a-d**) and isocyanide enables the introduction of the first position marker and digit, respectively. c) Continuation of this two-step iterative protocol allows for a sequence-defined oligomeric growth to obtain the macromolecular pin code.*

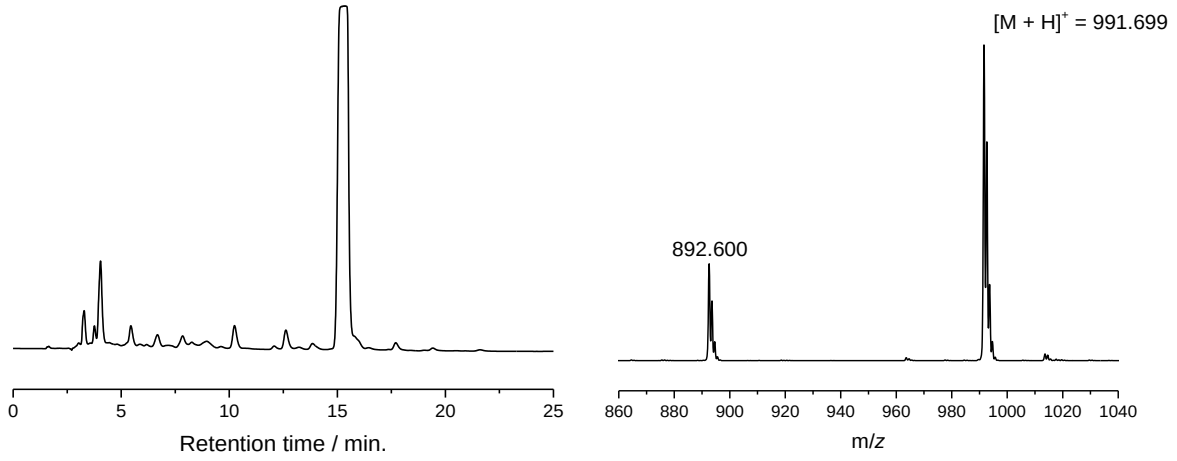


*Figure VII 14: Left) LCMS chromatogram of the U-4CR, showing the predominant formation of **11** (λ = 214 nm). Right) ESI-MS spectrum, indicating the successful generation of **11** by its protonated mass along with fragmentation side-product corresponding to the elimination of cyclohexylamine.*

VII.3 Conclusion and outlook

TAD chemistry has once again been demonstrated as a highly useful chemical platform for sequence-defined oligomer synthesis and in this chapter has projected this work towards a potential application with the synthesis of macromolecular pin codes for potential in anti-counterfeiting applications. The ability to encrypt the macromolecular pin codes by simply heating, highlights the unique advantage of using TAD-indole chemistry and furthermore, the ability to decrypt them by heating in the presence of a co-reactant led to their easy read-out using LCMS. The speed of decryption was found to be significantly influenced by the temperature applied and it was found that 15 minutes at 150 °C led to complete isolation of the monomer units of the macromolecular pin code. The investigation of different temperatures also allowed the activation energy of the overall decryption to be calculated and compared with the literature. Future work will hopefully investigate whether altering the structure of the TAD-COOH to contain an aromatic instead of an aliphatic spacer will enable one to significantly reduce the temperature of reversibility, without having a dramatic effect on the reaction kinetics.

The introduction of TAD-indole reactions in place of TAD-diene reactions in combination with the P-3CR was successful resulting in the synthesis of a sequence-defined tetramer (**A1-B2-C3-D4**). This meant that there was enough material to study the encryption and decryption of the macromolecular pin codes at a range of temperatures, use a wide range of analytical techniques and to test their use on a material level, thus investigating their potential towards a real-world application. The synthesis of four different indole-aldehydes (**L2a-d**) facilitated not only the TAD-indole reaction and P-3CR, but were highly effective as location markers, allowing one to determine the original order of the macromolecular

pin code following encryption and decryption, using their distinct isotopic patterns. This meant analysis could easily be carried out using LCMS, which represents a significant improvement compared with existing tandem MS/MS techniques. Moreover, thanks to the isotopic pattern of the indole markers, the code could even be deciphered using simple ESI-MS, as demonstrated by the polymer material test in *Figure VII 12*, reducing analysis time even further and under certain conditions this could even be applied online. Future work could expand the potential of these macromolecular pin codes by increasing the range of indole-aldehydes and isocyanides to write longer codes for added security. Alternatively, the use of the U-4CR offers the possibility to vastly increase the amount information or complexity of the code within relatively short oligomers, thanks to the introduction of primary amines to the MCR and should be further investigated in future work. By coating encrypted versions of **A1-B2-C3** and **A1-B2-C3-D4** on the surface of polymer banknotes, followed by their extraction and read-out by ESI-MS without damaging the polymer material, provided an easy demonstration to how these thermoreversible macromolecular pin codes could be used as a real-world anti-counterfeiting technology. Although, the envisaged read-out technique of LCMS proved difficult in this test, promising results were obtained *via* ESI-MS, although the ion count for the one sample was too low for clear analysis. One potential alternative could be to use MALDI-TOF analysis. Future work should also examine embedding the macromolecular pin codes within the polymer matrix and testing them on a range of other often counterfeited products.

VII.4 Experimental details

This work was carried out within the framework of the master's thesis of Filip Van Lysebetten, who worked jointly under the guidance of myself and Dr Hannes Houck.

VII.4.1 Chemicals

The following chemicals were used as received from the suppliers unless otherwise described. DMSO-d_6 ≥ 99.8 % and $CDCl_3$ ≥ 99.8 % were purchased from Euriso-top. 1-Adymantyl isocyanide 97 %, 4-chloroacetophenone >97 %, 1-(3-dimethylaminopropyl)-3-ethylcarbodiimide hydrochloride (EDC.HCl) >98 %, *t*-butyl isocyanide >95 %, cyclohexyl isocyanide >98 %, ethyl carbazate 97 %, 2,3-dimethylbut-2-ene ≥ 96 %, morpholine >99 %, 2-phenylindole, phenylhydrazine >98 %, stearic acid 98 % and hydrochloric acid in 1,4-dioxane ca. 4 mol/L were purchased from the Tokyo Chemical Industry (Europe). Acetic anhydride ≥98 %, acrolein 90 % with hydroquinone inhibitor, butyl acetate (anhydrous, ≥99 %), ethyl acetate (anhydrous, 99.8 %), n-butyl isocyanide 97 %, diisopropylamine (DIPEA) > 99.5 %, 1-pentyl isocyanide 97 %, phosphomolybdic acid hydrate 99 % and succinic anhydride ≥99 % were purchased from Sigma-Aldrich. Acetic acid 99-100 % and hydrochloric acid 36 wt% were purchased from Chem Lab NV. *Trans,trans*-2,4-hexadien-1-ol (sorbic alcohol) was

purchased from both Sigma-Aldrich (97 %) and Alfa Aesar (98 %). 4-Bromoacetophenone 98 % was purchased from Alfa Aesar. 3,5-dibromoacetophenone was purchased from Fluorochem. Silica gel 60 (0.040 - 0.063) was purchased from Rocc S.A. Magnesium sulfate ≥ 99 %, potassium Carbonate ≥ 99 %, sodium chloride ≥ 99 % and sodium hydrogen carbonate ≥ 99 % were purchased from Carl Roth. Trifluoroacetic acid (TFA, peptide grade) and 2-chlorotrityl chloride resin (100-200 mesh, 1 % DVB, 1.6 mmol/g) were purchased from Iris Biotech GmbH. Fmoc-protected rink-amide resin (100-200 mesh, 1 % DVB, 0.72 mmol/g) and citric acid were purchased from Merck – Novabiochem. Polyphosphoric acid (PPA) was purchased from Merck KGaA, Darmstadt, Germany. 1-Aminocaproic acid 99+ %, diphenyl carbonate 99 %, hydroquinone inhibitor, piperidine 99 % extra pure, pyridine 99+ % and trichloroisocyanuric acid 99 %, were purchased from Acros Organics. Acetonitrile (HPLC grade ≥ 99.9 %), ethyl acetate (HPLC grade, 99.7 %) chloroform (HPLC grade ≥ 99.9 %), and dichloromethane (CH_2Cl_2, HPLC grade ≥ 99.9 %) were purchased from Sigma-Aldrich. Methanol (HPLC grade 99.8 %), triethylamine (99 %, anhydrous), dichloromethane (99.8 %, anhydrous), *N,N'*-dimethylformamide (DMF, 99.8 %, anhydrous), pyridine (99.5 %, anhydrous) were purchased from Acros Organics. Ethanol and diethyl ether, both analytical reagent grade and *N,N'*-dimethylformamide (DMF) > 99.8 % were purchased from Fisher Scientific. Technical grade hexane and ethyl acetate, supplied by Univar, were used for purifications by column chromatography. All solvents were used without further purification, unless otherwise noted. Water, when used in the synthesis, was de-ionised.

VII.4.2 Analytical methods

Nuclear Magnetic Resonance (NMR): ^{1}H spectra were recorded on a Bruker Avance 300, a Bruker Avance 400, Bruker Avance 500 or a Bruker Avance II 700 and ^{13}C-NMR Attached Proton Test (APT) spectra were recorded on a Bruker Avance 400. Chemical shifts are presented in parts per million (δ) relative to DMSO-d_6 or $CDCl_3$ (2.50 ppm or 7.26 ppm in ^{1}H- and 39.51 ppm or 77.24 ppm in ^{13}C-NMR respectively) as internal standard. Coupling constants (J) are reported in Hertz (Hz). All measurements were recorded in a standard fashion at 25 °C unless otherwise stated. Full assignment of structures was aided by 2D NMR analysis (*i.e.* COSY, HSQC and HMBC).

Size Exclusion Chromatography (SEC): Oligomers were characterised on a Waters SEC system equipped with a Waters 1515 isocratic pump, Waters 2410 refractive index detector (24 °C), Waters 717plus autosampler and a Waters 2487 dual λ absorbance UV detector and column oven. For separation, a three-column setup was used with one SDV 3 µm, 8×50 mm precolumn and two SDV 3 µm, 1000 Å, 8×300 mm columns supplied by PSS, Germany. Tetrahydrofuran (THF) stabilized with butylated hydroxytoluene (BHT, HPLC-SEC grade) supplied by Biosolve was used at a flow rate 1.0

mL min^{-1}. Calibration was carried out by three injections of a mixture of narrow polystyrene standards ranging from 162 to 38640 kDa.

Electrospray Ionisation Mass Spectrometry (ESI-MS) and Liquid Chromatography Mass Spectrometry (LCMS): An Agilent technologies 1100 series LC/MSD system equipped with a diode array detector and single quad MS detector (VL) with an electrospray source (ESI-MS) was used for classic reversed phase LCMS and MS analysis. Analytic reversed phase HPLC (high-performance liquid chromatography) was performed with a Phenomenex Kmetex C18 (2) column with a solid core at 35 °C and a flow rate of 1.5 mL/min (5 µ, 250 x 4.6 mm) using a solvent gradient (0 → 100 % acetonitrile in H_2O in 6 min, unless otherwise stated). Alternatively, for more apolar compounds, a Phenomenex Luma C5 or Cyano porous column was used with a flow rate of 1 mL/min (5µm, 250 x 4.6 mm) using a solvent gradient of 50 → 100 % (Cyano) and 90 → 100 % (C5) acetonitrile in H_2O in 15 min, unless otherwise stated). The eluting compounds were detected via UV-detection (λ = 214 nm). LCMS spectra were analysed using ACD/Spectrus software and the purity of compounds was assessed by integrating the LC peaks (λ = 214 nm) using the in-software function.

High Resolution Mass Spectroscopy (HRMS): HRMS spectra were collected using an Agilent 6220 Accurate-Mass time-of-flight (TOF) equipped with a multimode ionization (MMI) source.

Infrared (IR): Measurements were recorded on a Perkin Elmer FTIR SPECTRUM 1000 spectrometer with Attenuated Total Reflection (ATR) with a PIKE Miracle ATR unit in a frequency range from 4000 to 600 cm^{-1}.

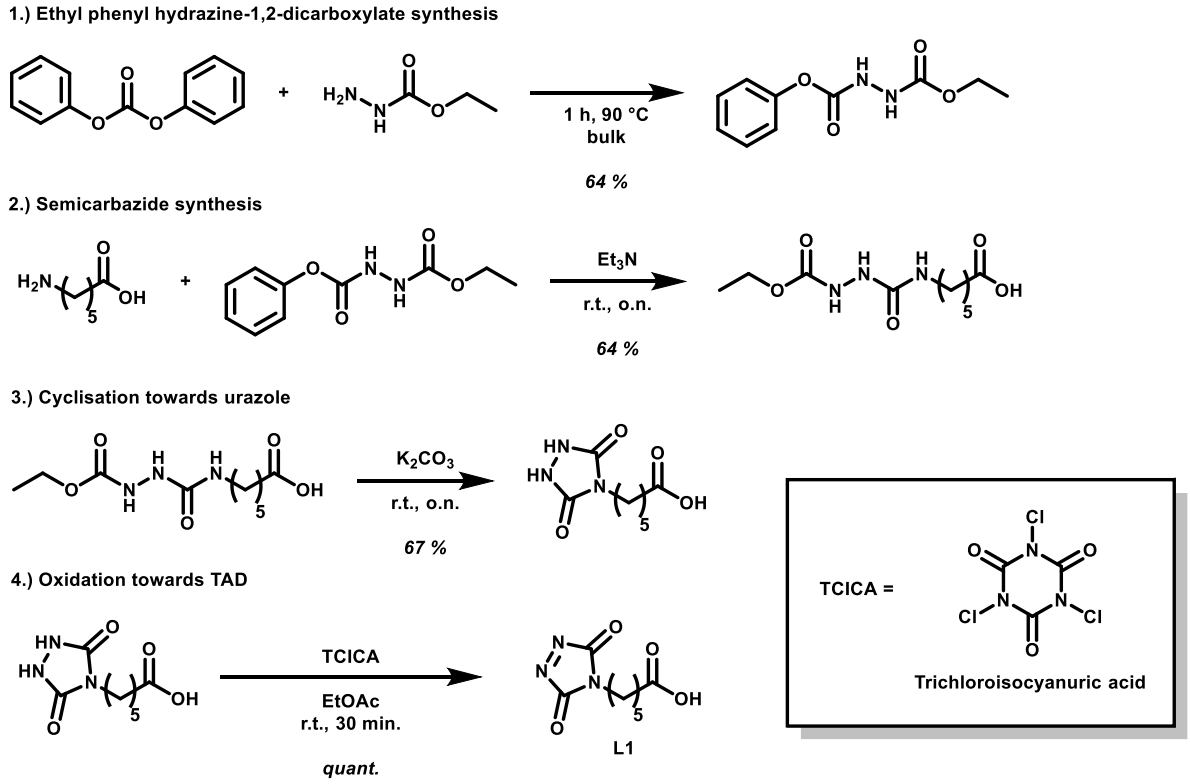
Thin layer chromatography (TLC): Experiments were performed on silica gel coated aluminium foil (silica gel 60 F_{254}, Sigma-Aldrich). Compounds were visualised by staining with phosphomolybdic acid (PMA).

Thermo Gravimetric Analysis (TGA): was performed on a Mettler Toledo TGA/SDTA851^e in a temperature window of 25−800 °C at a heating rate of 10 °C min^{-1} under a nitrogen atmosphere.

VII.4.3 Synthesis of multicomponent reaction building blocks

VII.4.3.1 Synthesis of 1,2,4-triazoline-3,5-dione hexanoic acid (TAD-COOH)

Urazole hexanoic acid was prepared as described and characterised in Chapter VI.4.3.2. See below for an overview of the reaction scheme. The oxidation to the corresponding urazole was altered in this chapter and is described in full below.



The urazole carboxylic acid (1.50 g, 6.94 mmol, 1.0 equiv.) was suspended in anhydrous ethyl acetate (100 mL). Trichloroisocyanuric acid (TCICA, 0.54 g, 2.31 mmol, 1/3 equiv.) was added. The reaction mixture was stirred vigorously for 30 min at room temperature. Then the solution was filtered and the filtrate was concentrated *in vacuo*, yielding **L1** as a vivid pink powder. Yield = 100% (m = 1.5 g). **^{1}H NMR (300 MHz, DMSO-*d*$_6$)**: δ = 12.01 (s, 1H, COO<u>H</u>, H^1), 3.46 (t, *J* = 7.09, 2H, N-C<u>H$_2$</u>, H^2), 2.18 (t, *J* = 7.34, 2H, C<u>H$_2$</u>COOH, H^3), 1.64-1.43 (m, 4H, N-CH$_2$C<u>H$_2$</u>CH$_2$C<u>H$_2$</u>, H^4), 1.34-1.22 (m, 2H, N-(CH$_2$)$_2$C<u>H$_2$</u>, H^5). **HRMS (ESI) *m/z*:** $[M + H]^+$ for $[C_8H_{12}N_3O_4^+]$; calculated: 214.0822, found: 214.1879; $[M+Na]^+$ for $[C_8H_{11}N_3O_4Na^+]$; calculated: 236.0642, found: 236.1720. Characterisation was in good accordance with that reported for **L1** in Chapter VI.4.3.2.

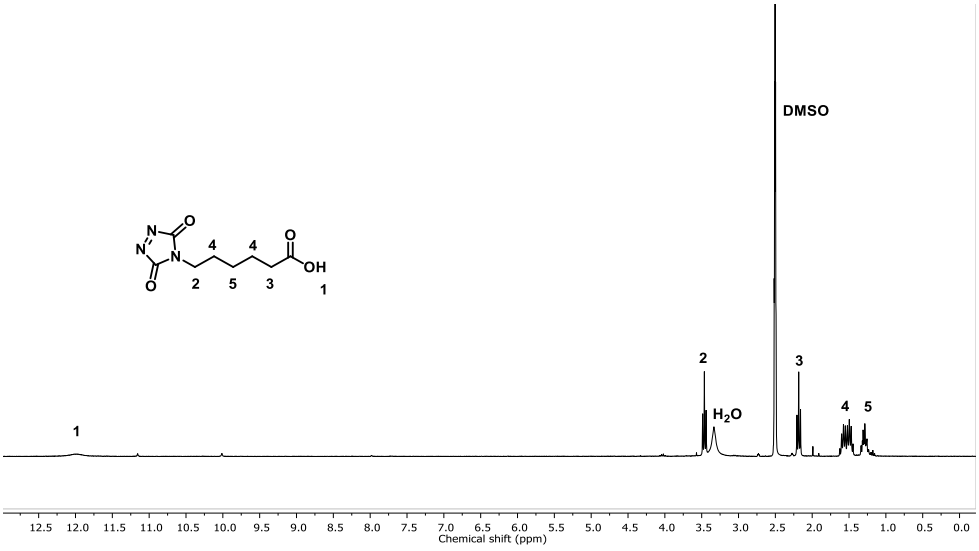
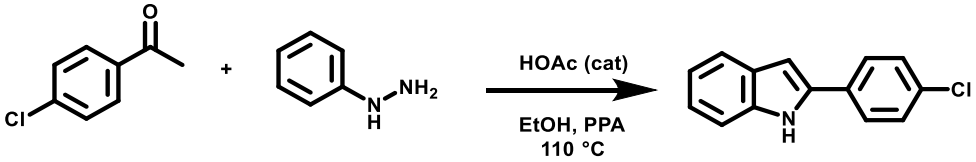


*Figure VII 15: ^{1}H NMR spectrum (DMSO-d_6) of TAD carboxylic acid **L1**.*

VII.4.3.2 Synthesis of 2-(4-chlorophenyl)-1*H*-indole



4-Chloroacetophenone (5.19 mL, 40.0 mmol, 1.0 equiv.) and phenylhydrazine (4.33 mL, 44.0 mmol, 1.1 equiv.) were solubilised in ethanol:HOAc (9:1; 10 mL). The reaction was stirred at reflux (80 °C) overnight and then cooled to room temperature prior to solvent removal *in vacuo*. The resulting yellow solid was then suspended in polyphosphoric acid (PPA) (25 mL) and the reaction mixture was stirred at reflux (110°C) for 4 hours. The crude reaction mixture was precipitated in ice-water (1.5 L) and stirred vigorously overnight at room temperature. The resulting brown precipitate was filtered and dried overnight under vacuum at 40 °C, yielding a grey powder that was used without further purification. Yield = 97 % (m = 8.81 g). **^{1}H-NMR (400 MHz, DMSO-d_6):** δ = 11.58 (s, 1H, NH, H^{1}), 7.85-7.92 (m, 2H, ArH, H^{2}), 7.49-7.56 (m, 3H, ArH, H^{3+4}), 7.38-7.43 (m, 1H, ArH, H^{5}), 7.11 (ddd, *J* = 8.1, 7.0, 1.2 Hz, 1H, ArH, H^{6}), 7.00 (ddd, *J* = 7.9, 7.0, 1.0 Hz, 1H, ArH, H^{7}), 6.93 (dd, *J* = 2.2, 0.7 Hz, 1H, ArH, H^{8}). **^{13}C-NMR (APT, 100 MHz, DMSO-d_6):** δ = 137.21 (C^{1}), 136.35 (C^{2}), 131.74 (C^{3}), 131.12 (C^{4}), 128.89 (CH^{5}), 128.52 (C^{6}), 126.60 (CH^{7}), 121.86 (CH^{8}), 120.15 (CH^{9}), 119.50 (CH^{10}), 111.34 (CH^{11}), 99.31 (CH^{12}). **HRMS (ESI) *m/z*:** [M + H]$^{+}$ for [$C_{14}H_{11}ClN^{+}$]; calculated: 228.0575, found: 228.0566. **IR** (ATR platinum diamond): ν [cm^{-1}] = 3316 (N-H), 3080 ($_{Ar}$C-H), 1570 (N-H), 1450 (C=C), 1228 (C-N), 735 & 699 (C-Cl).

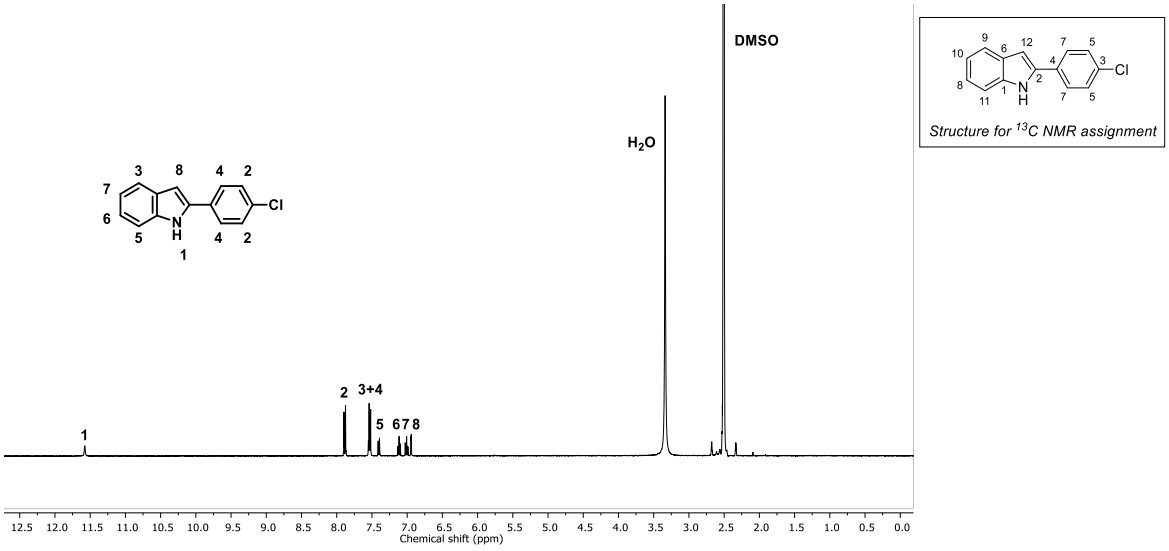
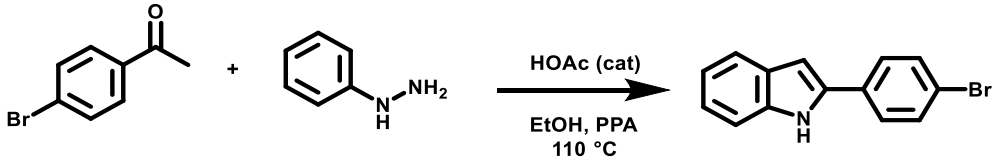


Figure VII 16: ^{1}H NMR spectrum (DMSO-d_6) of 2-(4-chlorophenyl)-1H-indole.

VII.4.3.3 Synthesis of 2-(4-bromophenyl)-1*H*-indole



4-Bromoacetophenone (9.95 g, 50.0 mmol, 1.0 equiv.) and phenylhydrazine (4.92 mL, 55.0 mmol, 1.1 equiv.) were solubilised in ethanol:HOAc (9:1; 10 mL). The reaction was stirred at reflux (80 °C) overnight and then cooled to room temperature prior to solvent removal *in vacuo*. The resulting yellow solid was then suspended in polyphosphoric acid (PPA) (25 mL) and the reaction mixture was stirred at reflux (110°C) for 30 minutes. The crude reaction mixture was precipitated in ice-water (1.5 L) and stirred vigorously overnight at room temperature. The resulting brown precipitate was filtered and dried overnight under vacuum at 40 °C, yielding a grey powder that was used without further purification. Yield = 57 % (m = 7.81 g). **^{1}H-NMR (400 MHz, DMSO-d_6):** δ = 11.58 (s, 1H, NH, H^{1}), 7.82 (m, 2H, ArH, H^{2}), 7.65 (m, 2H, ArH, H^{3}), 7.53 (d, *J* = 7.9 Hz, 1H, ArH, H^{4}), 7.40 (dd, *J* = 8.1, 0.9 Hz, 1H, ArH, H^{5}), 7.11 (ddd, *J* = 8.1, 7.0, 1.2 Hz, 1H, ArH, H^{6}), 7.00 (ddd, *J* = 7.9, 7.0, 1.0 Hz, 1H, ArH, H^{7}), 6.94 (dd, *J* = 2.2, 0.7 Hz, 1H, ArH, H^{8}). **^{13}C-NMR (APT, 100 MHz, DMSO-d_6):** δ = 137.23 (C^{1}), 136.35 (C^{2}), 131.77 (CH^{3}), 131.46 (C^{4}), 128.48 (C^{5}), 126.87 (CH^{6}), 121.90 (CH^{7}), 120.26 (C^{8}), 120.15 (CH^{9}), 119.49 (CH^{10}), 111.35 (CH^{11}), 99.34 (CH^{12}). **HRMS (ESI) *m/z*:** [M+H]$^{+}$ for [$C_{14}H_{11}BrN^{+}$]; calculated: 272.1450, found: 272.0064. **IR** (ATR platinum diamond): ν [cm^{-1}] = 3413 (N-H), 3100 ($_{Ar}$C-H), 1570 (N-H), 1449 & 1421(C=C), 1242 (C-N), 793, 754, 703 & 658 (C-Br).

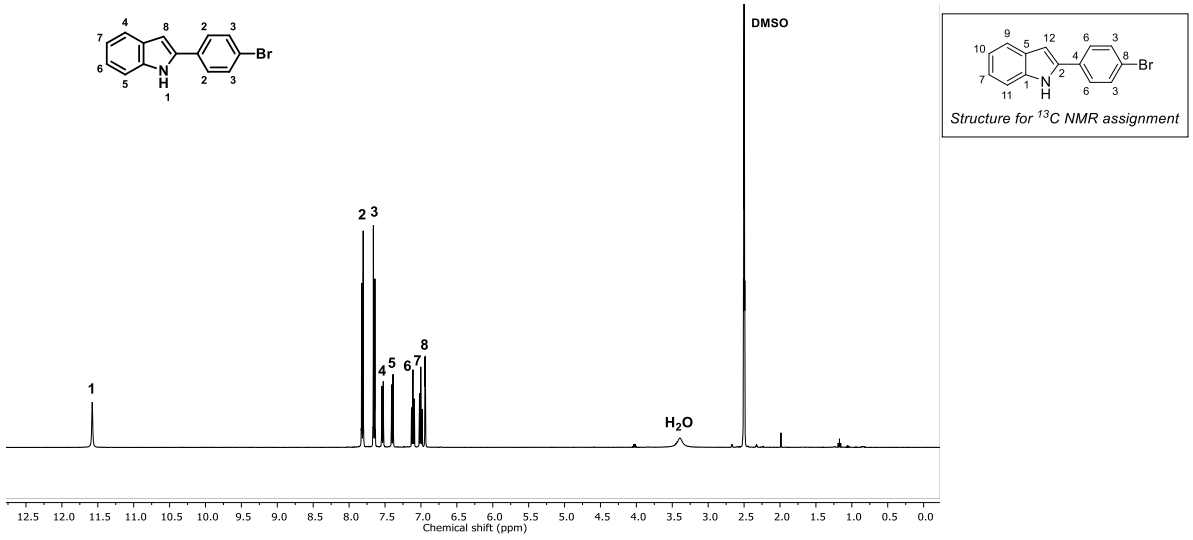
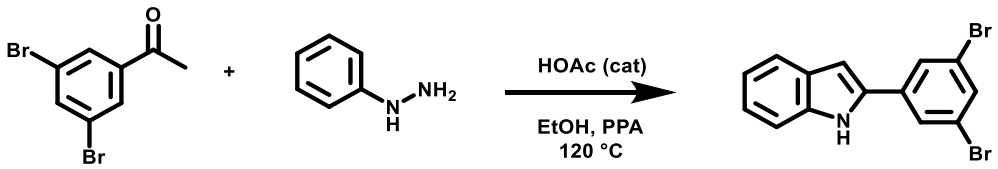


Figure VII 17: ^{1}H NMR spectrum (DMSO-d_6) of 2-(4-bromophenyl)-1H-indole.

VII.4.3.3 Synthesis of 2-(3,5-dibromophenyl)-1*H*-indole



3',5'-dibromoacetophenone (3.50 g, 12.6 mmol, 1.0 equiv.) and phenylhydrazine (1.70 mL, 17.3 mmol, 1.2 equiv.) were solubilised in ethanol:acetic acid (9:1 v/v; 10 mL). The reaction was stirred at reflux (80°C) overnight and cooled to room temperature prior to solvent removal *in vacuo*. The resulting yellow solid was then solubilised in polyphosphoric acid (PPA, 25 mL) and the reaction mixture was stirred at reflux (110°C) for 4 hours. The crude reaction mixture was precipitated in an ice-water mixture (1.5 L) and stirred vigorously overnight at room temperature. The resulting brown precipitate was filtered and dried overnight under vacuum at 40 °C, yielding a grey powder (approximately 1 g). The residue was dissolved in ethyl acetate and dried on silica *in vacuo*, after which it was purified by means of column chromatography (silica, eluent = ethyl acetate:hexane 1:9, R_F (EtOAc:hex 1:9) = 0.34) to give a pale yellow solid. Yield = 0.98 g (22.2 %). **^{1}H-NMR (400 MHz, DMSO-d_6):** δ = 11.67 (s, 1H, NH, H^{1}), 8.11 (d, *J* = 1.7 Hz, 2H, ArH, H^{2}), 7.74 (t, *J* = 1.6 Hz, 1H, ArH, H^{3}), 7.55 (d, *J* = 7.9 Hz, 1H, ArH, H^{4}), 7.40 (dd, *J* = 8.2, 0.9 Hz, 1H, ArH, H^{5}), 7.10-7.19 (m, 2H, ArH, H^{6+7}), 7.02 (ddd, *J* = 7.9, 7.0, 1.0 Hz, 1H, H^{8}). **^{13}C-NMR (APT, 100 MHz, DMSO-d_6):** δ = 137.41 (C^{1}), 136.14 (C^{2}), 134.27 (C^{3}), 131.60 (CH^{4}), 128.23 (C^{5}), 126.40 (CH^{6}), 123.14 (C^{7}), 122.56 (CH^{8}), 120.53 (CH^{9}), 119.74 (CH^{10}), 111.50 (CH^{11}), 101.12 (CH^{12}). **IR** (ATR platinum diamond): ν [cm^{-1}] = 3412 (N-H), 3070 (C-H), 1586 & 1551 (N-H), 1532 (C=C), 1433 & 1411 (C-H), 1348, 1300, 1241, 1101 & 1062 (C-N), 986 (C=C), 848, 802, 754, 742 & 658 (C-Br).

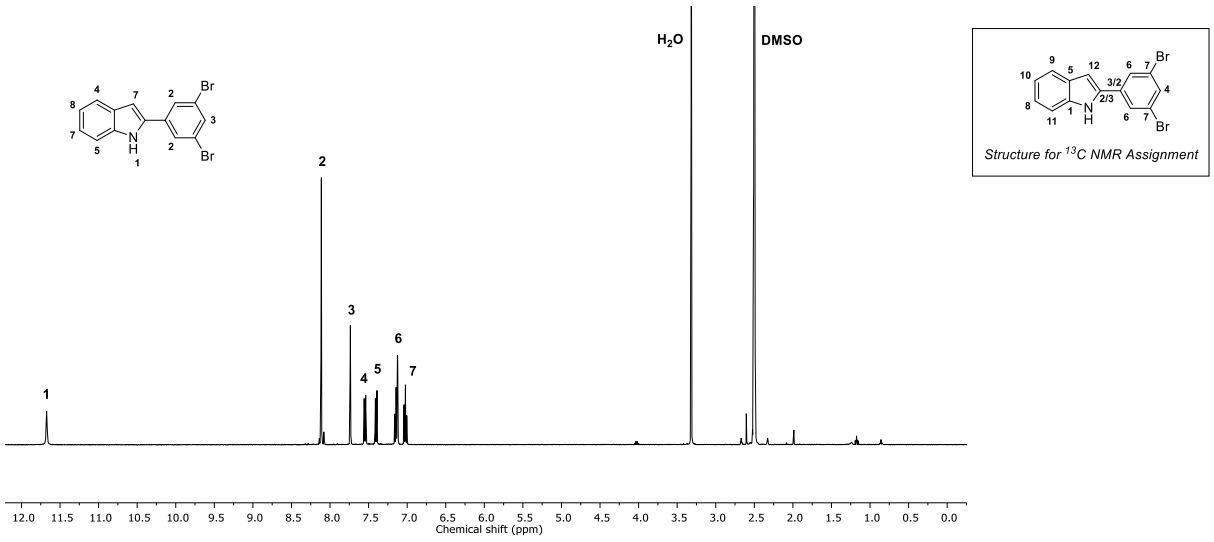
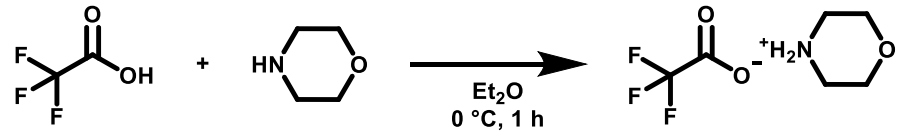


*Figure VII 18: ^{1}H and ^{13}C NMR spectra (DMSO-d_6) of 2-(3,5-dibromophenyl)-1*H*-indole.*

VII.4.3.4 Synthesis of morpholinum trifluoroacetate salt

Synthesised according to a previously reported procedure.[40]



A solution of morpholine (1.72 mL, 20.0 mmol, 1.0 equiv.) in 40 mL diethyl ether was cooled in an ice-water bath at 0 °C. To this, trifluoroacetic acid (TFA, 1.68 mL, 22.0 mmol, 1.1 equiv.) solubilised in 20 mL diethyl ether was added dropwise. After stirring for 1 hour, the reaction mixture was allowed to warm up to room temperature and the resulting white precipitate was filtered, washed with 2 x 10 mL diethyl ether and dried overnight under vacuum at 40°C, yielding a white powder. Yield = 95 % (m = 3.83 g). **^{1}H-NMR (400 MHz, DMSO-d_6):** δ = 9.02 (s, 1H, H^1), 3.83-3.69 (m, 2H, O-C$\underline{H}_2$, H^2), 3.19-3.01 (m, 2H, N-C$\underline{H}_2$, H^3). **^{13}C-NMR (APT, 100 MHz, DMSO-d_6):** δ = 203.06 (CH), 135.99 (C), 134.18 (C), 132.82 (C), 128.76 (CH), 128.24 (C), 127.83 (CH), 127.38 (CH), 121.57 (CH), 118.74 (CH), 118.53 (CH), 111.19 (CH), 110.12 (C), 44.11 (CH_2), 16.96 (CH_2). **HRMS (ESI) *m/z***: $[M+H]^+$ for $[C_4H_{10}NO^+]$; calculated: 88.0757 , found: 88.0759; $[M-H]^-$ for $[C_2F_3O_2^-]$; calculated: 112.9856, found: 112.9860. **IR** (ATR platinum diamond): ν [cm^{-1}] = 3340 (N-H), 3100-2500 (O-H), 1704 (C=O) 1439 (N-H), 1310 (C-O), 1172 (C-N), 1104 (C-F).

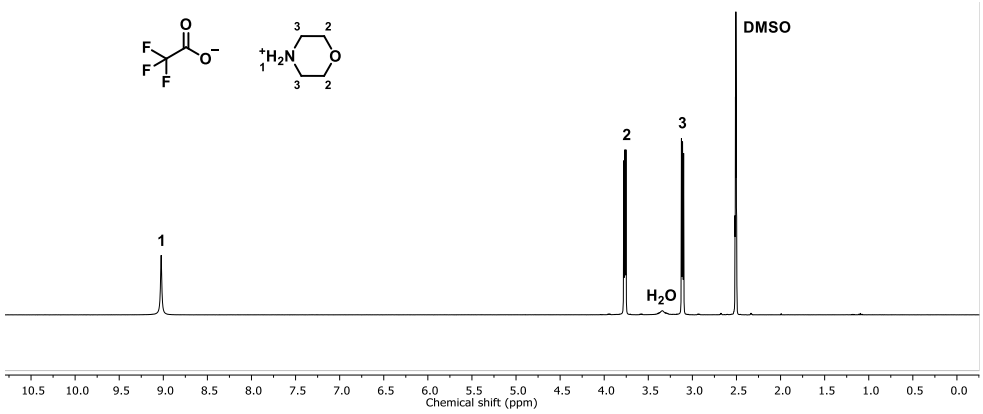
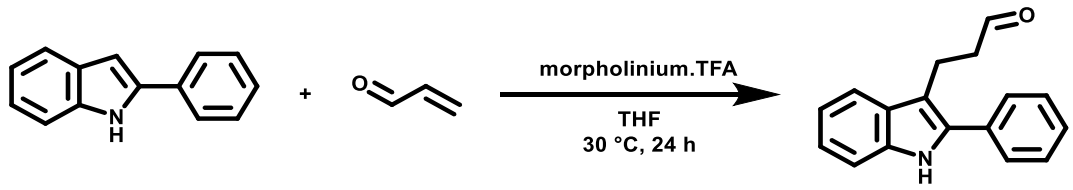


Figure VII 19: ^{1}H NMR spectrum in DMSO-d_6 of TFA morpholinium salt.

VII.4.3.5 Synthesis of 3-(2-phenyl-1*H*-indol-3-yl) propanal

Synthesis was carried out according to an adapted version of a previously reported procedure.[40]



2-Phenyl-1*H*-indole (6.00 g, 31.05 mmol, 1.0 equiv.) and acrolein (6.20 mL, 93.15 mmol, 3.0 equiv.) were solubilised in THF (200 mL). Morpholinium trifluoroacetate salt (1.26 g, 6.21 mmol, 0.2 equiv.) was added and the reaction was stirred until completion at 30 °C for 24 hours (monitored via thin layer chromatography). The resulting mixture was cooled to room temperature and the solvent was evaporated *in vacuo*. The resulting oil was dissolved in ethyl acetate (300 mL) and extracted with H_2O (30 mL), aqueous $NaHCO_3$ (2 x 30 mL) and brine (2 x 30 mL). Next, the combined organic phases were dried over $MgSO_4$, filtered and the filtrate was concentrated *in vacuo*. A small amount of hydroquinone was added as stabiliser prior to solvent removal. The resulting orange oil was purified by column chromatography (silica, hexane:ethyl acetate 4:1, R_F (hex:EtOAc 4:1) = 0.27). The product was obtained as an off-white powder. Yield = 61 % (m = 3.66 g). **^{1}H-NMR (400 MHz, DMSO-d_6):** δ = 11.19 (s, 1H, NH, H^1), 9.72 (t, *J* = 1.5 Hz, 1H, CHO, H^2), 7.45-7.67 (m, 5H, ArH, H^{3+4+5}), 7.31-7.45 (m, 2H, ArH, H^{6+7}), 7.12 (dd, *J* = 8.1, 7.0, 1.3 Hz, 1H, ArH, H^8), 7.02 (ddd, *J* = 7.9, 7.0, 1.1 Hz, 1H, ArH, H^9), 3.13 (m, 2H, CH_2-CH_2-CHO, H^{10}), 2.80 (m, 2H, CH_2-CHO, H^{11}). **^{13}C-NMR (APT, 100 MHz, DMSO-d_6):** δ(ppm) = 203.06 (CH^1), 135.99 (C^2), 134.18 (C^3), 132.82 (C^4), 128.76 (CH^5), 128.24 (C^6), 127.83 (CH^7), 127.38 (CH^8), 121.57 (CH^9), 118.74 (CH^{10}), 118.53 (CH^{11}), 111.19 (CH^{12}), 110.12 (C^{13}), 44.11 (CH_2^{14}), 16.96 (CH_2^{15}). **HRMS (ESI) *m/z*:** $[M+H]^+$ for $[C_{17}H_{16}NO^+]$; calculated: 250.1226, found: 250.1215 **IR** (ATR platinum diamond): *v* [cm^{-1}] = 3329 (N-H), 3058 ($_{Ar}$C-H), 2824 & 2725 (C-H), 1703 (C=O), 1602 (N-H), 1486 (C-H), 1448 (C=C) 1071 (C-N).

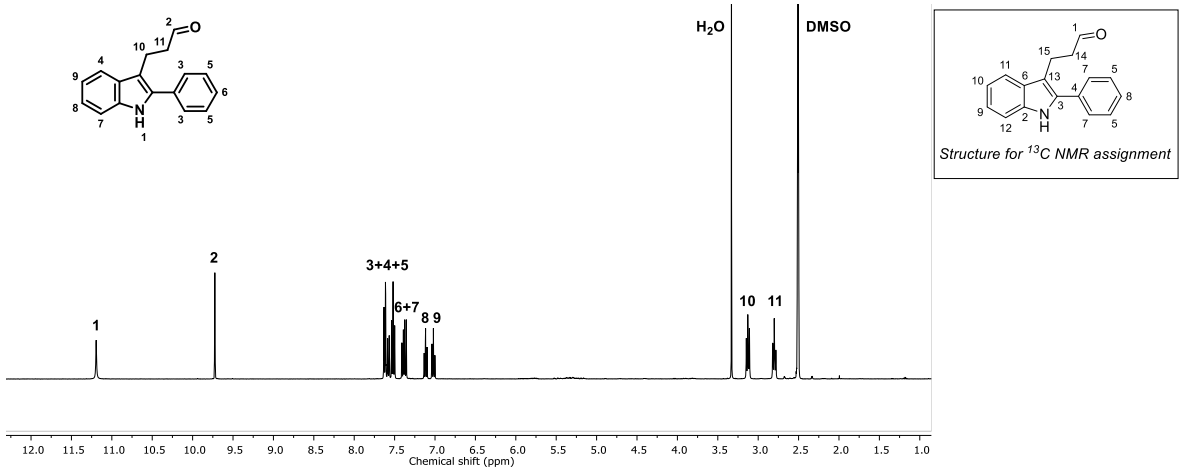
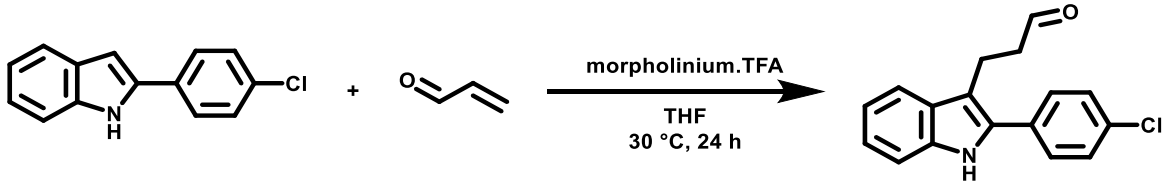


Figure VII 20: ^{1}H NMR spectrum in DMSO-d_6 of 3-(2-phenyl-1H-indol-3-yl) propanal.

VII.4.3.6 Synthesis of 3-(2-(4-chlorophenyl)-1*H*-indol-3-yl) propanal



2-(4-Chlorophenyl)-1*H*-indole (5.00 g, 22.0 mmol, 1.0 equiv.) and acrolein (4.41 mL, 66.0 mmol, 3.0 equiv.) were solubilised in THF (160 mL). Morpholinium trifluoroacetate salt (0.89 g, 4.4 mmol, 0.2 equiv.) was added and the reaction was stirred until completion at 30 °C for 24 hours (monitored via thin layer chromatography). The resulting mixture was then cooled to room temperature and the solvent was evaporated *in vacuo*. The resulting oil was dissolved in ethyl acetate (300 mL) and extracted with H_2O (30 mL), aqueous $NaHCO_3$ (2 x 30 mL) and brine (2 x 30 mL). Next, the combined organic phases were dried over $MgSO_4$, filtered and the filtrate was concentrated *in vacuo*. A small amount of hydroquinone was added as stabiliser prior to solvent removal. The resulting orange oil was purified by column chromatography (silica, hexane:ethyl acetate 4:1, R_F (hex:EtOAc 4:1) = 0.29). The product was obtained as an off-white powder. Yield = 40 % (m = 2.50 g). **^{1}H-NMR (400 MHz, DMSO-d_6):** δ = 11.25 (s, 1H, NH, H^{1}), 9.71 (t, *J* = 1.4 Hz, 1H, CHO, H^{2}), 7.67-7.61 (m, 2H, ArH, H^{3}), 7.61-7.53 (m, 3H, ArH, H^{4+5}), 7.36 (dt, *J* = 8.0, 0.9 Hz, 1H, ArH, H^{6}), 7.12 (ddd, *J* = 8.1, 7.0, 1.1 Hz, 1H, ArH, H^{7}), 7.02 (ddd, *J* = 7.9, 7.0, 1.0 Hz, 1H, ArH, H^{8}), 3.11 (m, 2H, CH_2-CH_2-CHO, H^{9}), 2.79 (m, 2H, CH_2-CHO, H^{10}). **^{13}C-NMR (APT, 100 MHz, DMSO-d_6):** δ = 202.97 (CH^{1}), 136.05 (C^{2}), 132.87 (C^{3}), 131.99 (C^{4}), 131.65 (C^{5}), 129.48 (CH^{6}), 128.79 (CH^{7}), 128.16 (C^{8}), 121.86 (CH^{9}), 118.88 (CH^{10}), 118.66 (CH^{11}), 111.25 (CH^{12}), 110.75 (C^{13}), 43.98 (CH_2^{14}), 16.88 (CH_2^{15}). **HRMS (ESI) *m/z*:** $[M+H]^+$ for $[C_{17}H_{15}ClNO^+]$; calculated: 284.0837, found: 284.0828. **IR** (ATR platinum diamond): *v* [cm^{-1}] = 3304 (N-H), 3054 ($_{Ar}$C-H), 2836 & 2740 (C-H), 1704 (C=O), 1483 (N-H), 1448 (C-H), 1309 (C=C), 721, 698 & 658 (C-Cl).

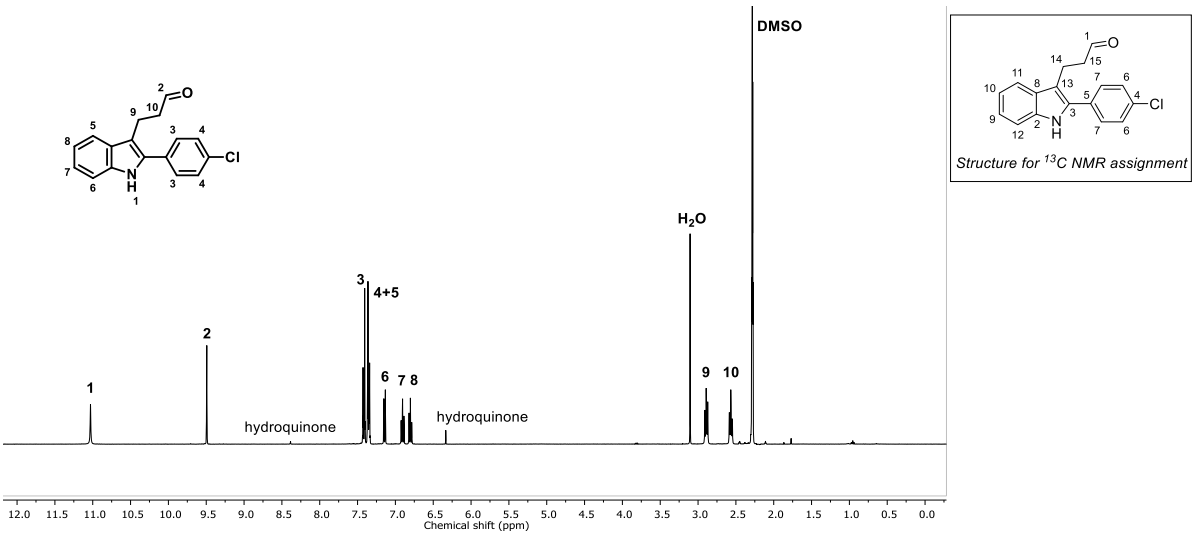
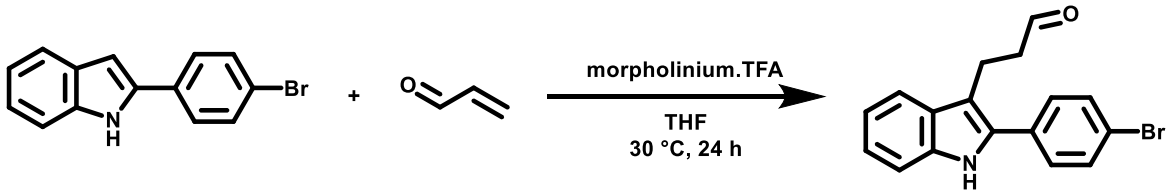


Figure VII 21: ^{1}H NMR spectrum in DMSO-d_6 of 3-(2-(4-chlorophenyl)-1H-indol-3-yl) propanal.

VII.4.3.7 Synthesis of 3-(2-(4-bromophenyl)-1*H*-indol-3-yl) propanal



2-(4-Bromophenyl)-1*H*-indole (7.05 g, 25.9 mmol, 1.0 equiv.) and acrolein (5.20 mL, 77.7 mmol, 3.0 equiv.) were solubilised in THF (200 mL). Morpholinium trifluoroacetate salt (1.05 g, 5.18 mmol, 0.2 equiv.) was added and the reaction was stirred until completion at 30 °C for 24 hours (monitored via thin layer chromatography). The resulting mixture was then cooled to room temperature and the solvent was evaporated *in vacuo*. The resulting oil was dissolved in ethyl acetate (300 mL) and extracted with H_2O (30 mL), aqueous $NaHCO_3$ (2 x 30 mL) and brine (2 x 30 mL). Next, the combined organic phases were dried over $MgSO_4$, filtered and the filtrate was concentrated *in vacuo*. A small amount of hydroquinone was added as stabiliser prior to solvent removal. The resulting orange oil was purified by column chromatography (silica, hexane:ethyl acetate 4:1, R_F (hex:EtOAc 4:1) = 0.31). The product was obtained as a yellow powder. Yield = 41 % (m = 3.49 g). **^{1}H-NMR (400 MHz, DMSO-*d*$_6$):** δ = 11.26 (s, 1H, NH, H^{1}), 9.72 (t, *J* = 1.4 Hz, 1H, CHO, H^{2}), 7.74-7.68 (m, 2H, ArH, H^{3}), 7.61-7.55 (m, 3H, ArH, H^{4+5}), 7.37 (dt, *J* = 8.1, 0.9 Hz, 1H, ArH, H^{6}), 7.13 (ddd, *J* = 8.1, 7.0, 1.2 Hz, 1H, ArH, H^{7}), 7.03 (ddd, *J* = 8.0, 7.0, 1.1 Hz, 1H, ArH, H^{8}), 3.13 (m, 2H, CH$_2$-CH$_2$-CHO, H^{9}), 2.80 (m, 2H, CH$_2$-CHO, H^{10}). **^{13}C-NMR (APT, 100 MHz, DMSO-*d*$_6$):** δ = 202.97 (CH^{1}), 136.05 (C^{2}), 132.87 (C^{3}), 131.99 (C^{4}), 131.65 (CH^{5}), 129.48 (CH^{6}), 128.16 (C^{7}), 121.86 (CH^{8}), 120.57 (C^{9}), 118.88 (CH^{10}), 118.66 (CH^{11}), 111.25 (CH^{12}), 110.75 (C^{13}), 43.98 (CH$_2$^{14}), 16.88 (CH$_2$^{15}). **HRMS (ESI) *m/z*:** $[M+H]^+$ for $[C_{17}H_{15}BrNO^+]$; calculated: 328.0332 , found: 328.0323. **IR** (ATR platinum diamond): ν [cm^{-1}] = 3339

(N-H), 3044 ($_{Ar}$C-H), 2854 & 2752 (C-H), 1697 (C=O), 1596 (N-H), 1440 (C-H), 1309 (C=C), 1072 (C-N), 737, 704 & 560 (C-Br).

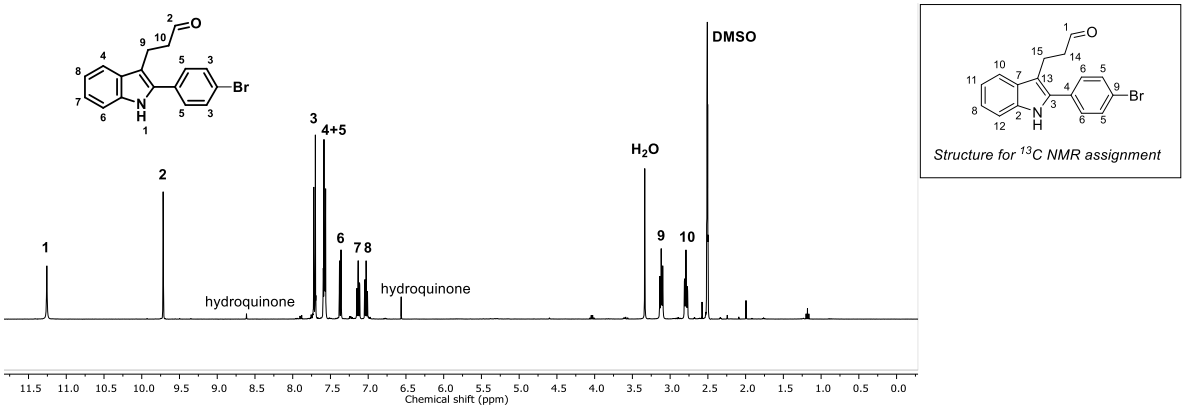
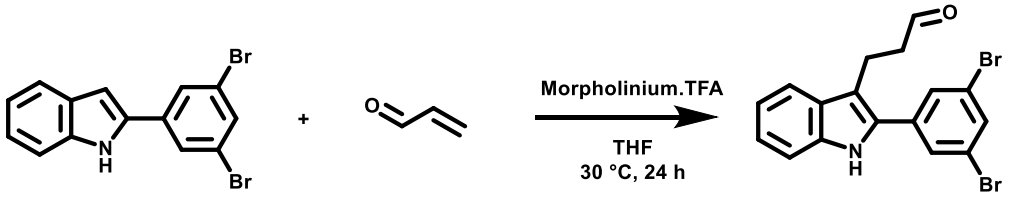


Figure VII 22: ^{1}H NMR spectrum (DMSO-d_6) of 3-(2-(4-bromophenyl)-1H-indol-3-yl) propanal.

VII.4.3.8 Synthesis of 3-(2-(3,5-dibromophenyl)-1H-indol-3-yl) propanal



2-(3,5-Dibromophenyl)-1*H*-indole (0.95 g, 2.71 mmol, 1.0 equiv.) and acrolein (0.54 mL, 8.1 mmol, 3.0 equiv.) were solubilised in THF (20 mL). Morpholinium trifluoroacetate salt (0.11 g, 0.54 mmol, 0.2 equiv.) was added and the reaction was stirred until completion at 30 °C for 24 hours (monitored via thin layer chromatography). The resulting mixture was then cooled to room temperature and the solvent was evaporated *in vacuo*. The resulting oil was dissolved in ethyl acetate (50 mL) and washed with H_2O (10 mL), aqueous $NaHCO_3$ (2 x 10 mL) and brine (2 x 10 mL). Next, the combined organic phases were dried over $MgSO_4$, filtered and the filtrate was concentrated *in vacuo* (keeping the temperature below 30 °C). The resulting yellow-brown oil was purified by column chromatography (silica, ethyl acetate:hexane 1:9, R_F (EtOAc:hex 1:9) = 0.12) to give the title compound as a pale yellow solid. Yield = 38 % (m = 0.42 g). **^{1}H-NMR (400 MHz, DMSO-d_6):** δ = 11.37 (s, 1H, N<u>H</u>, H^{1}), 9.71 (t, *J* = 1.3 Hz, 1H, C<u>H</u>O, H^{2}), 7.85 (t, *J* = 1.7 Hz, 1H, Ar<u>H</u>, H^{3}), 7.81 (d, *J* = 1.7 Hz, 2H, Ar<u>H</u>, H^{4}), 7.61 (d, *J* = 8.1 Hz, 1H, Ar<u>H</u>, H^{5}), 7.37 (d, *J* = 8.2 Hz, 1H, Ar<u>H</u>, H^{6}), 7.15 (ddd, *J* = 8.1, 7.0, 1.1 Hz, 1H, Ar<u>H</u>, H^{7}), 7.04 (ddd, *J* = 8.0, 7.0, 1.0 Hz, 1H, H^{8}), 3.12 (t, *J* = 7.6 Hz, 2H, C<u>H$_2$</u>-CH$_2$-CHO, H^{9}), 2.82 (t, *J* = 7.6 Hz, 2H, C<u>H$_2$</u>-CHO, H^{10}). **^{13}C-NMR (APT, 100 MHz, DMSO-d_6):** δ = 202.84 (CH^{1}), 136.67 (C^{2}), 136.22 (C^{3}), 131.91 (CH^{4}), 130.79 (C^{5}), 129.27 (CH^{6}), 127.95 (C^{7}), 122.84 (C^{8}), 122.50 (CH^{9}), 119.10 (CH^{10}), 119.04 (CH^{11}), 112.28 (C^{12}), 111.42 (CH^{13}), 43.72 (CH$_2$^{14}), 16.72 (CH$_2$^{15}). **IR** (ATR platinum diamond): ν [cm^{-1}] = 3411 (N-H), 1719 (C=O), 1582 (N-H), 1537 (C=C), 1442 & 1409 (C-

H), 1337, 1303, 1269, 1369, 1096 & 1040 (C-N), 987 (C=C), 854, 741, 694, 653 & 624 (C-Br).

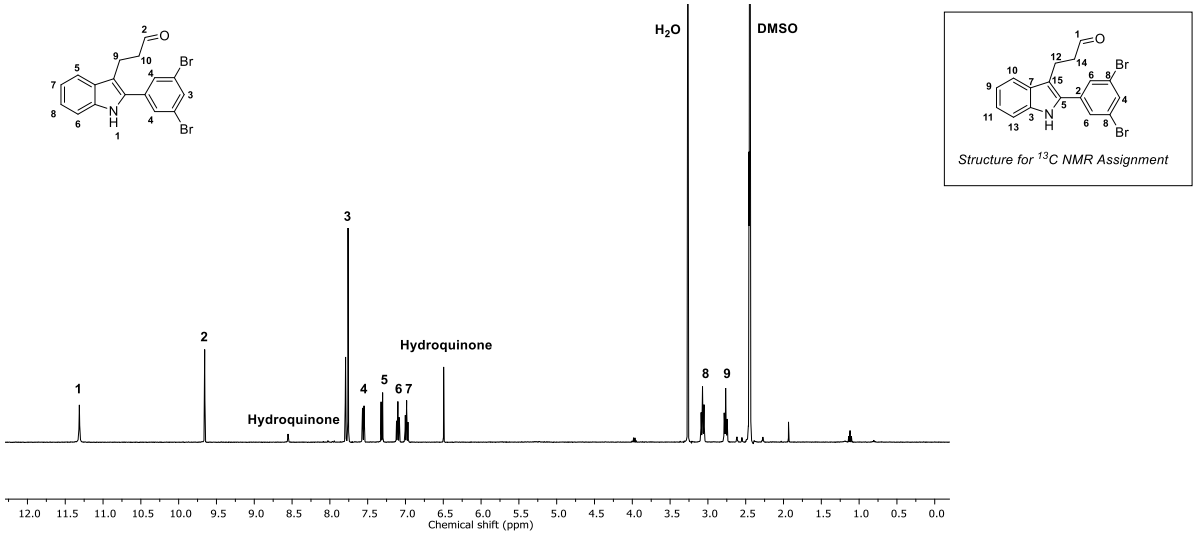


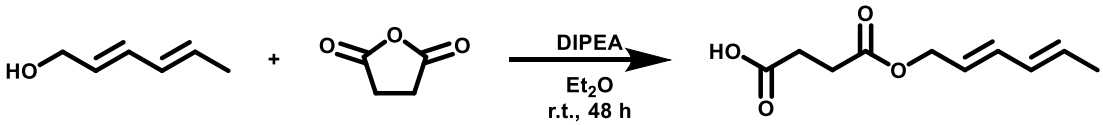
Figure VII 23: ^{1}H NMR spectrum (DMSO-d_6) of 3-(2-(3,5-dibromophenyl)-1H-indol-3-yl) propanal.

VII.4.4 Solid-phase synthesis of sequence-defined oligomers *via* the P-3CR

VII.4.4.1 Loading of the 2-chlorotrityl chloride resin

The loading of the 2-chlorotrityl chloride resin was carried out according to the procedure described in Chapter V.4.4.2.

VII.4.4.2 Synthesis of 4-(((2E,4E)-hexa-2,4-dien-1-yl)oxy)-4-oxobutanoic acid



A mixture of *trans*,*trans*-2,4-hexadien-1-ol (2.55 g, 26.0 mmol, 1.0 equiv.), succinic anhydride (3.00 g, 30.0 mmol, 1.15 equiv.) and *N*,*N*-diisopropylethylamine (DIPEA, 3.40 g, 26.0 mmol, 1.0 equiv.) in diethyl ether (10 mL) was stirred for 48 hours at room temperature. The solvent was evaporated *in vacuo* and the residue dissolved in CH_2Cl_2 and washed with an aqueous solution of 5% w/w citric acid. The organic layer was dried over $MgSO_4$, filtered and the solvent was removed *in vacuo*. Yield = 80 % (m = 14.3 g). **^{1}H-NMR (300 MHz, $CDCl_3$):** δ = 9.86 (s, 1H, COO<u>H</u>, ^{1}), 6.25 (dd, *J* = 15.2, 10.5 Hz, 1H, CH_2-CH-C<u>H</u>, H^2), 6.0.5 (ddd, *J* = 14.7, 10.5, 1.4 Hz, 1H, C<u>H</u>-CH-CH_3, H^3), 5.84-5.68 (m, 1H, C<u>H</u>-CH_3, H^4), 5.67-5.53 (m, 1H, CH_2-C<u>H</u>, H^5), 4.60 (d, *J* = 6.7 Hz, 2H, O-C<u>H_2</u>, H^6), 2.75-2.57 (m, 4H, C<u>H_2</u>-C<u>H_2</u>, H^7), 1.76 (d, *J* = 6.7 Hz, 3H, C<u>H_3</u>, H^8). **^{13}C-NMR (APT, 100 MHz, $CDCl_3$):** δ = 178.30 (C^1), 172.05 (C^2), 135.24 (C^3), 131.56 (C^4), 130.50 (C^5), 123.48 (C^6), 65.51 (C^7), 29.04 (C^8), 29.00 (C^9), 18.25 (C^{10}). Characterisation was in good accordance with previously published data.

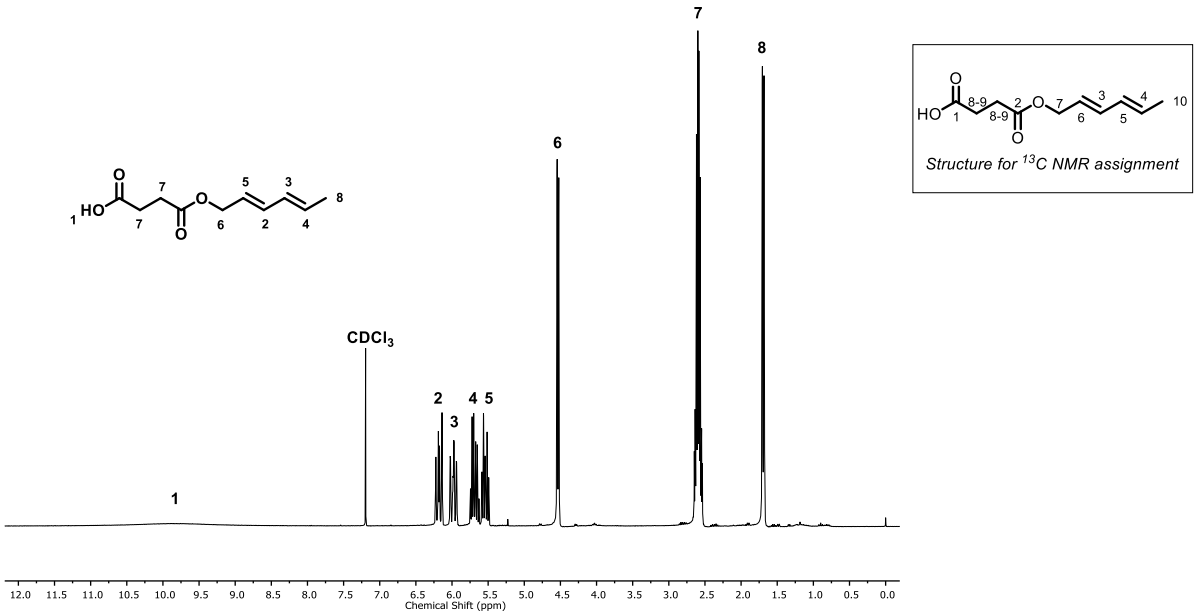
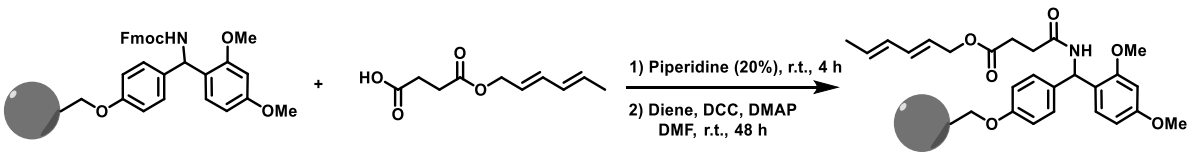


Figure VII 24: ^{1}H NMR spectrum ($CDCl_3$) of 4-(((2E,4E)-hexa-2,4-dien-1-yl)oxy)-4-oxobutanoic acid.

VII.4.4.3 Loading of the Rink-Amide resin

Loading of the rink-amide resin was carried out using an adapted version of the procedure described in Chapter IV.4.3.3.1.



Fmoc-protected Rink Amide resin (100-200 mesh, 0.4 mmol/g) (2.5 g, 1.0 mmol, 1.0 equiv.) was swollen in CH_2Cl_2 for 5 min. Then, piperidine (20%) solution in CH_2Cl_2 (20 mL) was added and the reaction mixture was shaken vigorously at room temperature for 4 hours. The reaction was then filtered and the resin was washed with DMF (3 x 30 mL) and CH_2Cl_2 (3 × 30 mL). Subsequently, the resin was swollen for 5 min in CH_2Cl_2 and 4-(((2E,4E)-hexa-2,4-dien-1-yl)oxy)-4-oxobutanoic acid (0.992 g, 5.0 mmol, 5.0 equiv.), *N*,*N*'-dicyclohexylcarbodiimide (DCC, 1.032 g, 5.0 mmol, 5.0 equiv.) and 4-(dimethylamino)pyridine (DMAP, 12.22 mg, 0.1 mmol, 0.1 equiv.) dissolved in dry DMF (4 mL) were added. The reaction mixture was placed under an inert N_2 atmosphere and shaken vigorously at room temperature for 48 hours. The resin was then filtered and washed with DMF (3 × 30 mL), CH_2Cl_2 (3 × 30 mL) and Et_2O (3 × 30 mL). The resin was then dried under vacuum at room temperature for 4 hours and used directly for the first reaction step (*vide infra*).

VII.4.4.4 Capping the loaded Rink Amide resin

The Rink Amide resin was shaken in a mixture of acetic anhydride:pyridine (3:2) for 30 minutes at room temperature. Subsequently, the resin was washed with DMF (3 x 30 mL) and dried under vacuum at room temperature for 4 hours. The resin was then used directly for the first reaction step (*vide infra*).

VII.4.4.5 Manipulation of the solid-phase resin

Swelling: The resin for each reaction was swollen for at least 10 minutes in the reaction solvent (1 mL of solvent per 100 mg of resin).

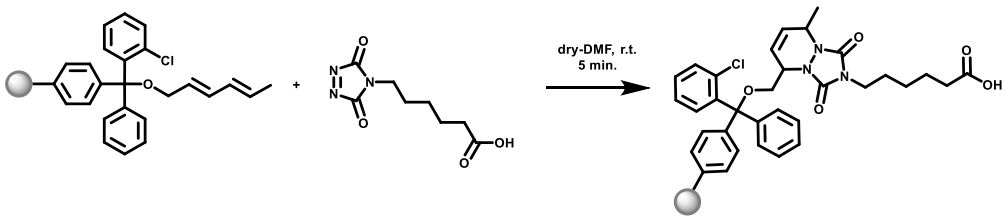
Washing: The solid phase resin was extensively washed, under filtration *in vacuo*, after each reaction step to ensure removal of remaining unreacted starting chemicals or unwanted side-products formed such as precipitates. Washing was done sequentially with DMF (x4), MeOH (x4), $CHCl_3$ (x4) and Et_2O (x4).

Cleavage: For analysis by LCMS, 2 mg of the sequence-containing beads was cleaved from the resin by suspending it in a solution of 1% trifluoroacetic acid (TFA) in CH_2Cl_2 for 5 minutes for the 2-chlorotrityl chloride resin or 10 % TFA in CH_2Cl_2 for 25 minutes for the Rink Amide resin. Filtration of the sample was finally followed by concentration through evaporation under a continuous N_2 stream.

Analysis: This was predominantly carried out using LCMS and HRMS. Once the complete oligomer was synthesised, the remainder of the compound was recovered from the resin and dissolved in DMSO-d_6 for ^{1}H and ^{13}C NMR analysis.

VII.4.4.6 General procedure of the solid-phase protocol

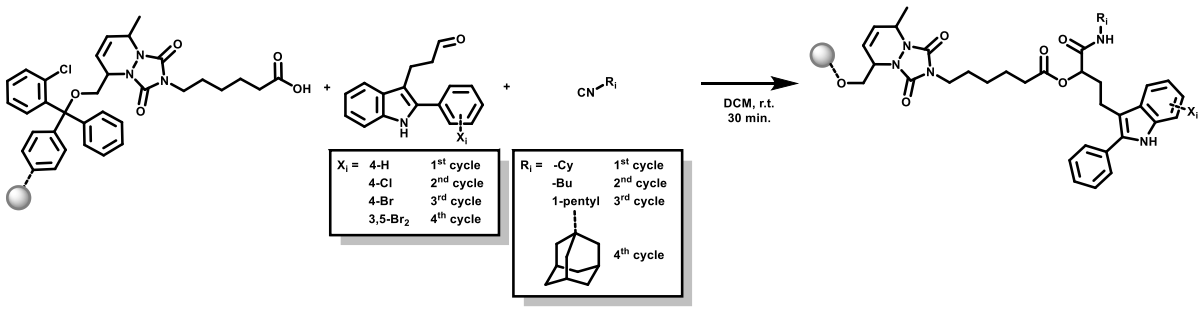
Diels-Alder addition of TAD-COOH to the diene-functionalised solid-phase resin:



The diene functionalised resin (50.00 mg, 1.0 equiv.) (0.02 mmol – rink-amide resin, 0.0565 mmol – 2-chlorotrityl resin) was swollen for at least 10 minutes in anhydrous DMF (500 µL) before filtering it off. TAD-COOH, **L1**, (3.0 equiv.) solubilised in anhydrous DMF (500 µL) was added to the resin, which was then shaken vigorously at room temperature for 5 minutes. 2,3-Dimethylbut-2-ene (10.0 equiv.) was next added to the reaction mixture and shaken vigorously at room temperature for 5 minutes

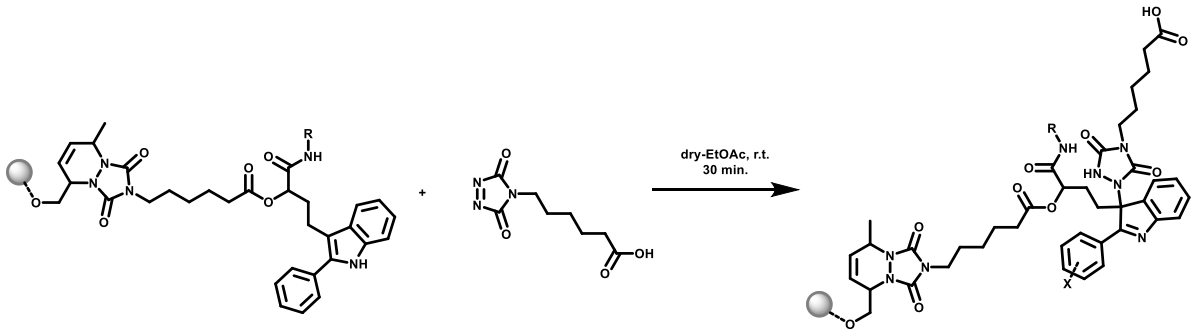
to quench the excess of unreacted TAD. The reaction was then filtered and the resin was subsequently washed and submitted for LCMS analysis according to the procedure described above VII.4.4.5.

Step 1 – P-3CR:



The carboxylic acid-functionalised resin (50.00 mg, 1.0 equiv.) (0.02 mmol – rink-amide resin, 0.0565 mmol – 2-chlorotrityl resin) was swollen for at least 10 minutes in CH_2Cl_2 (500 µL), before filtering it off. Then, a solution of the indole aldehyde (20.0 equiv.) in CH_2Cl_2 (500 µL) was added to the resin, followed by the isocyanide (15.0 equiv.). The reaction mixture was shaken vigorously at room temperature for 30 minutes, filtered and the resin was subsequently washed and submitted for LCMS analysis according to the procedure described above in VII.4.4.5.

Step 2 – Alder-ene addition of TAD-COOH:

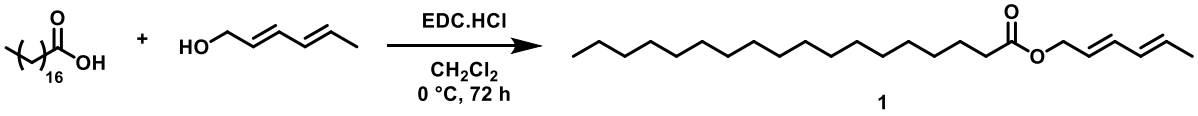


The resin was then swollen for at least 10 minutes in anhydrous ethyl acetate (500 µL) before filtering it off. A solution of TAD-COOH, **L1** (3.0 equiv.) in anhydrous ethyl acetate (500 µL) was added and the resin, which was shaken vigorously at room temperature for 30 minutes. 2,3-Dimethylbut-2-ene (10.0 equiv.) was added to the reaction mixture and shaken vigorously at room temperature for 5 minutes to quench the excess of unreacted TAD. The reaction mixture was then filtered and the resin subsequently washed and submitted for LCMS analysis according to the procedure described above in VII.4.4.5.

Steps 1 and 2 (*i.e.* the first cycle) were repeated three more times with different indole aldehyde and isocyanides (i.e. X_i and R_i, respectively) to synthesise a sequence-defined tetramer. The reaction was carried out on both a 2-chlorotrityl chloride and Rink Amide resin. For the 2-chlorotrityl chloride resin, the loading was determined to be 1.12 mmol/g, whereas for the Rink Amide resin the commercial loading was used (*i.e.* 0.4 mmol/g).

VII.4.5 Solution synthesis of sequence-defined oligomers *via* the P-3CR

VII.4.5.1 Synthesis of (2E, 4E)-hexa-2,4-dien-1-yl stearate starting block (1)



Stearic acid (5.69 g, 20.0 mmol, 1.0 equiv.), sorbic alcohol (2.36 g, 24.0 mmol, 1.2 equiv.) and 4-(dimethylamino)pyridine (DMAP, 0.50 g, 4.0 mmol, 0.2 equiv.) were solubilised in anhydrous CH_2Cl_2 (50 mL). The reaction mixture was cooled to 0 °C and a suspension of 1-(3-dimethylaminopropyl)-3-ethylcarbodiimide hydrochloride (EDC.HCl, 4.60 g, 24.0 mmol, 1.2 equiv.) in 30 mL anhydrous CH_2Cl_2 was added dropwise to the solution. Subsequently, the reaction was stirred for 72 hours in a water bath, after which the resulting colourless solution was extracted with water (2 x 50 mL) and brine (1 x 50 mL). Next, the combined organic phases were dried over $MgSO_4$, filtered and concentrated *in vacuo*. The residue was recrystallised from H_2O:EtOH (50 mL:250 mL) and dried overnight under vacuum at 40°C, yielding a white residue. Yield = 75 % (m = 5.49 g).

^{1}H-NMR (400 MHz, $CDCl_3$): δ = 6.26 (m, 1H, CH_3-CH=CH-C<u>H</u>, H^1), 6.06 (m, 1H, CH_3-CH=C<u>H</u>, H^2), 5.77 (m, 1H, CH_3-C<u>H</u>, H^3), 5.63 (m, 1H, O-CH_2-C<u>H</u>, H^4), 4.58 (d, *J* = 6.5 Hz, 2H, O-C<u>H_2</u>, H^5), 2.31 (t, *J* = 7.5 Hz, 2H, C(O)-C<u>H_2</u>, H^6), 1.77 (d, *J* = 6.6 Hz, 3H, CH-C<u>H_3</u>, H^7), 1.63 (m, 2H, C(O)-CH_2-C<u>H_2</u>, H^8), 1.26 (m, 28H, CH_3-(C<u>H_2</u>)$_{14}$, H^9), 0.89 (t, *J* = 6.8 Hz, 3H, CH_2-C<u>H_3</u>, H^{10}). **^{13}C-NMR (APT, 100 MHz, $CDCl_3$):** δ = 173.66 (C^1), 134.76 (CH^2), 131.16 (CH^3), 130.47 (CH^4), 123.87 (CH^5), 64.67 (CH_2^6), 34.38 (CH_2^7), 31.94 (CH_2^8), 29.69-29.14 (CH_2^9), 24.95 (CH_2^{10}), 22.68 (CH_2^{11}), 18.12 (CH_3^{12}), 14.14 (CH_3^{13}). **HRMS (ESI) *m/z*:** $[M+H]^+$ for $[C_{32}H_{56}N_3O_6^+]$; calculated: 578.4164 , found: 578.4183. Submitted as adduct upon reaction with TAD-COOH (**2**) because of stability during HRMS. **IR** (ATR platinum diamond): *v* [cm^{-1}] = 3342 & 2908 (C-H), 1729 (C=O), 1596 (N-H), 1462 & 1392 (C-H), 1175 (C-O), 984 & 963 (C=C), 730 (C-H).

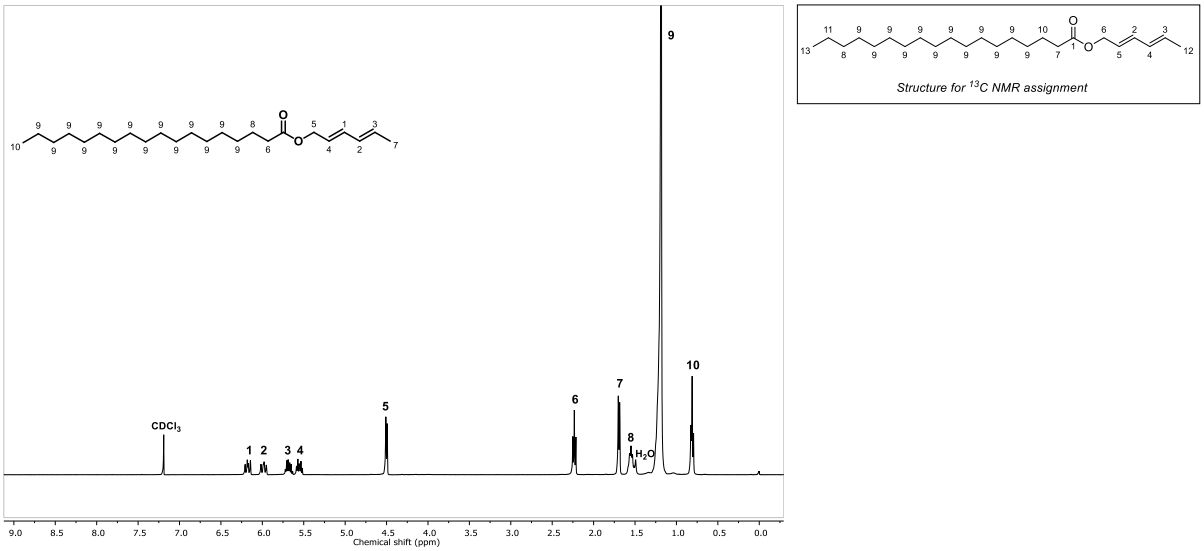
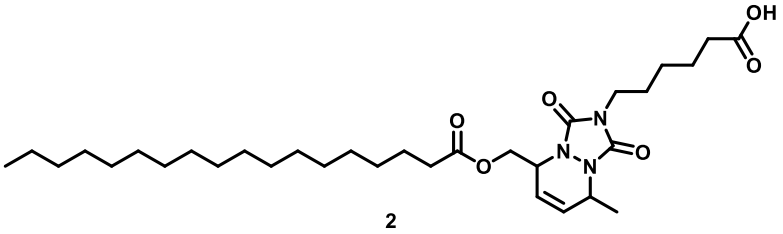


*Figure VII 25: ^{1}H NMR spectrum ($CDCl_3$) of **1**.*

VII.4.5.2 1st TAD addition

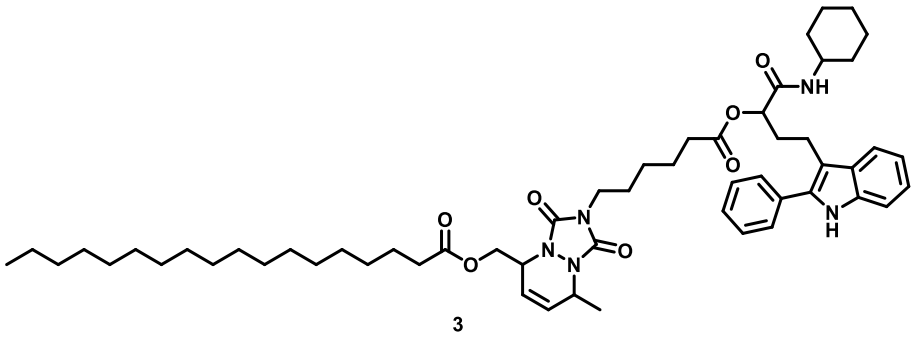
The synthesis was carried out according to an adapted version of the procedure outlined in Chapter VI.4.7[33]



2

1 (364.6 mg, 1.0 mmol, 1.0 equiv.) was dissolved in anhydrous ethyl acetate (3 mL), to which a solution of TAD-COOH, **L1** (256 mg, 1.20 mmol, 1.20 equiv.) in ethyl acetate (1 mL) was added dropwise to until a pink colour persisted, indicating that the diene was completely consumed. Next, 2,3-dimethylbut-2-ene (24 µL, 17 mg, 0.20 mmol, 0.20 equiv.) was added to the reaction mixture in order to quench the excess of unreacted TAD. The solvent was removed *in vacuo* at 35 °C and the crude product was used in the next step without further purification or analysis.

VII.4.5.3 1st P-3CR



3

2 (584 mg, 1.0 mmol, 1.0 equiv.) was dissolved in anhydrous CH_2Cl_2 (3 mL). Subsequently, 3-(2-phenyl-1*H*-indol-3-yl) propanal, **L2a** (499 mg, 2.0 mmol, 2.0 equiv.), was solubilised in CH_2Cl_2 (2 mL) and added to the reaction mixture, followed by cyclohexyl isocyanide (187 µL, 1.5 mmol, 1.5 equiv.). The reaction mixture was stirred for 24 hours at room temperature and the crude product was purified by column chromatography (silica, hexane:ethyl acetate 9:1→1:1, R_F (hex:EtOAc 2:1) = 0.23) to give **3** as a yellow viscous oil that solidified upon further drying *in vacuo*. Overall yield over two reaction steps: 90 % (m = 841 mg).

^{1}H NMR (400 MHz, DMSO-*d*$_6$): δ = 11.15 (s, 1H, H^1), 7.81 (d, *J* = 8.0 Hz, 1H, H^2), 7.62-7.58 (m, 2H, H^3), 7.53-7.47 (m, 3H, H^{4+5}), 7.40-7.34 (m, 2H, H^{6+7}), 7.10 (m, 1H, H^8), 7.00 (m, 1H, H^9), 5.91 (m, 1H, H^{10}), 5.82 (m, 1H, H^{11}), 4.89 (t, *J* = 6.0 Hz, 1H, H^{12}), 4.62 (m, 1H, H^{13}), 4.49 (dd, *J* = 11.7, 3.6 Hz, 1H, H^{14}), 4.29 (m, 1H, H^{15}), 4.19 (ddd, *J* = 11.6, 5.1, 0.9 Hz, 1H, $H^{14'}$), 3.58-3.51 (m, 1H, H^{16}), 3.40 (t, *J* = 7.1 Hz, 2H, H^{17}), 2.88 (m, 2H, H^{18}), 2.34 (m, 2H, H^{19}), 2.21 (t, *J* = 7.4 Hz, 2H, H^{20}), 2.04 (dt, *J* = 9.5, 6.4 Hz, 2H, H^{21}), 1.73-1.60 (m, 4H, $H^{22+23+24}$), 1.60-1.49 (m, 5H, $H^{23'+25}$), 1.45 (t, *J* = 7.0 Hz, 2H, H^{26}), 1.40 (dd, *J* = 6.6, 0.6 Hz, 3H, H^{27}), 1.37-1.03 (m, 35H, $H^{22'+24'+28+29}$), 0.88-0.81 (m, 3H, H^{30}). **^{13}C-NMR (APT, 100 MHz, DMSO-*d*$_6$):** δ = 172.56 (C), 172.14 (C), 168.05 (C), 153.74 (C), 151.90 (C), 136.02 (C), 133.96 (C), 132.83 (C), 129.74 (CH), 128.62 (CH), 128.40 (C), 127.63 (CH), 127.18 (CH), 121.50 (CH), 120.98 (CH), 118.66 (CH), 118.19 (CH), 111.19 (CH), 110.54 (C), 72.96 (CH), 61.86 (CH_2), 52.12 (CH), 50.61 (CH), 47.46 (CH), 38.11 (CH_2), 33.20 (CH_2), 32.79 (CH_2), 32.23 (CH_2), 31.28 (CH_2), 28.99-28.35 (CH_2), 27.07 (CH_2), 25.36 (CH_2), 25.15 (CH_2), 24.57 (CH_2), 24.09 (CH_2), 23.89 (CH_2), 22.07 (CH_2), 19.81 (CH_2), 18.89 (CH_3), 13.92 (CH_3). **HRMS** (ESI) m/z: $[M+H]^+$ for $[C_{56}H_{82}N_5O_7^+]$; calculated: 936.6209, found: 936.6192.

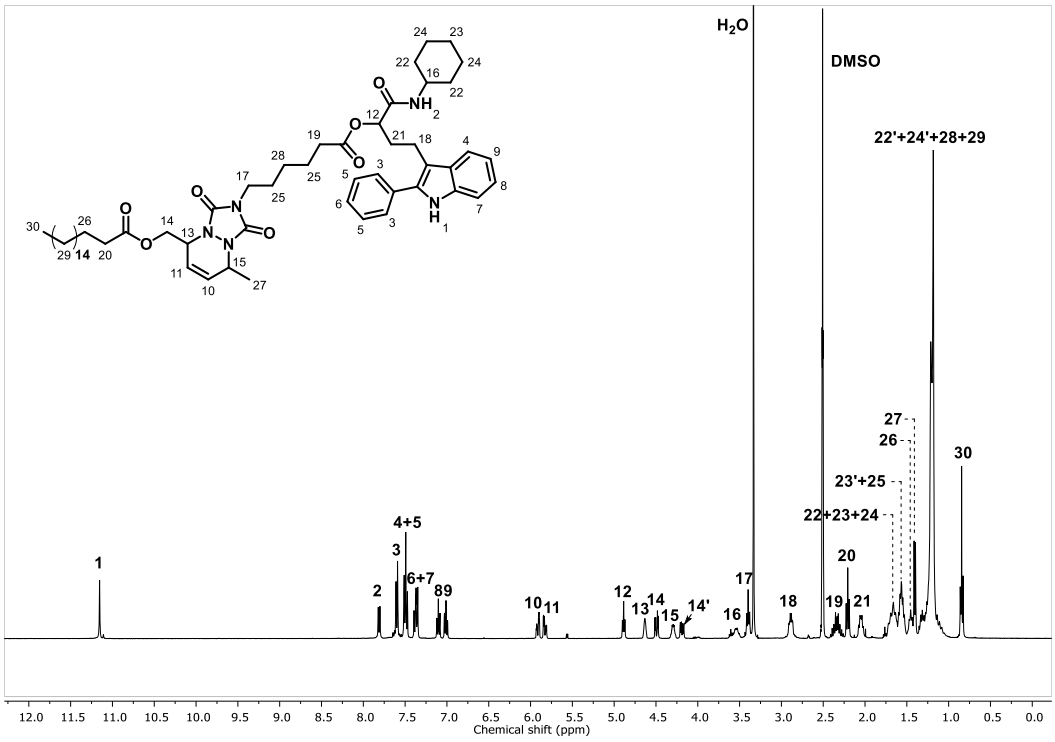
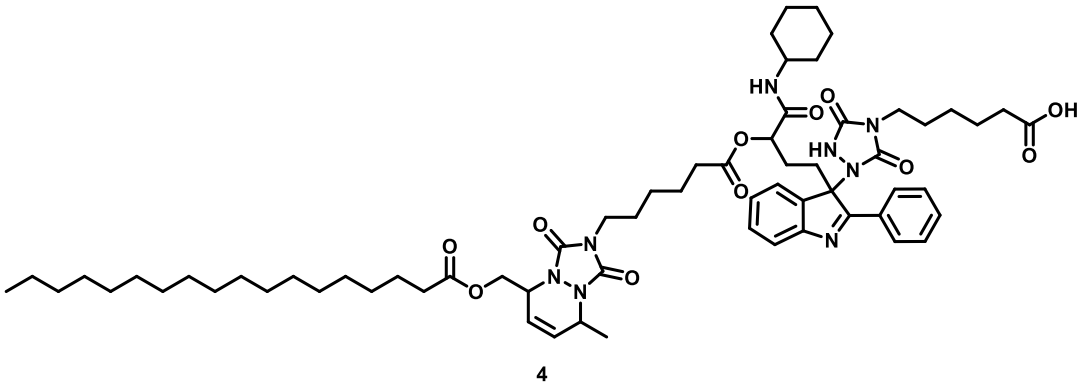


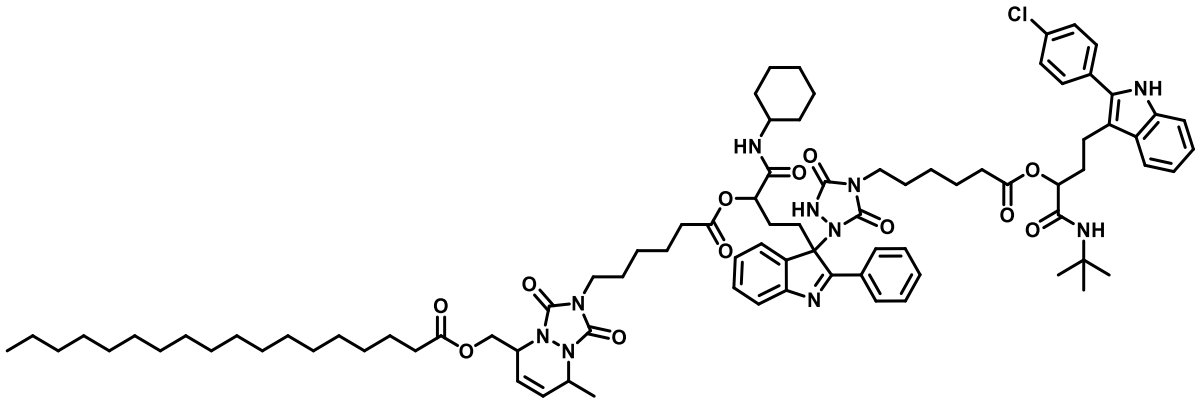
*Figure VII 26: ^{1}H NMR spectrum (DMSO-d_6) of **3**.*

VII.4.5.3 2nd TAD addition



3 (800 mg, 0.85 mmol, 1.0 equiv.) was dissolved in anhydrous ethyl acetate (3 mL) to which a solution of TAD-COOH **L1** (219 mg, 1.03 mmol 1.20 equiv.) in ethyl acetate (1 mL) was added dropwise until a pink colour persisted, indicating full consumption of the indole **L2a**. Next, 2,3-dimethylbut-2-ene (20 µL, 14 mg, 0.17 mmol, 0.20 equiv.) was added to the reaction mixture to quench the excess of unreacted TAD. The solvent was removed *in vacuo* at 35 °C and the crude product was used in the next step without further purification or analysis.

VII.4.5.4 2nd P-3CR



5

4 (1.02 g, 0.85 mmol, 1.0 equiv.) was dissolved in anhydrous CH_2Cl_2 (3 mL). Subsequently, a solution of 3-(2-(4-chlorophenyl)-1*H*-indol-3-yl) propanal, **L2b** (485 mg, 1.70 mmol, 2.0 equiv.) in anhydrous CH_2Cl_2 (2 mL) was added to the reaction mixture, followed by *tert*-butyl isocyanide (145 µL, 1.28 mmol, 1.5 equiv.). The reaction mixture was stirred for 24 hours at room temperature and the crude product was purified by column chromatography (silica, hexane:ethyl acetate 9:1→1:1, R_F (hex:EtOAc 2:1) = 0.21), to give **5** as a yellow viscous oil that solidified upon further drying *in vacuo*. Overall yield over two reaction steps: 88 % (m = 1.136 g).

^{1}H NMR (400 MHz, DMSO-*d*$_6$): δ =11.22 (s, 1H, H^1), 10.69 (s, 1H, H^2), 8.24-8.14 (m, 2H, H^3), 7.65-7.58 (m, 2H, H^4), 7.57-7.46 (m, 9H, H^5), 7.44-7.33 (m, 3H, H^6), 7.27-7.21 (m, 1H, H^7), 7.16-7.06 (m, 1H, H^8), 7.05-6.98 (m, 1H, H^9), 5.96-5.89 (m, 1H, H^{10}), 5.86-5.78 (m, 1H, H^{11}), 4.83 (t, *J* = 6.0 Hz, 1H, H^{12}), 4.67-4.61 (m, 1H, H^{13}), 4.58-4.53 (m, 1H, H^{14}) 4.49 (dd, *J* = 11.6, 3.6 Hz, 1H, H^{15}), 4.34-4.28 (m, 1H, H^{16}), 4.21 (dd, *J* = 11.6, 4.9 Hz, 1H, H^{17}), 3.40-3.34 (m, 2H, H^{18}), 3.30-3.07 (m, 3H, H^{19+20}), 2.86 (t, *J* = 8.3 Hz, 2H, H^{21}), 2.64-2.34 (m, 2H, H^{22}), 2.20 (t, *J* = 7.4 Hz, 2H, H^{23}), 2.17-2.1.98 (m, 6H, H^{24+25}), 1.65-1.42 (m, 9H, H^{26+27}), 1.42-1.37 (m, 3H, H^{28}), 1.37-1.09 (m, 51H, H^{29+30}), 1.09-0.87 (m, 3H, H^{31}), 0.86-0.80 (m, 3H, H^{32}). **^{13}C-NMR (APT, 100 MHz, DMSO-*d*$_6$):** δ =172.38 (C), 171.80 (C), 171.55 (C), 171.49 (C), 168.20 (C), 166.87 (C), 155.00 (C), 153.47 (C), 151.79 (C), 135.90 (C), 132.52 (C), 131.71 (C), 131.50 (C), 131.02 (CH), 129.61 (CH), 129.50 (CH), 129.13 (CH), 128.47 (CH), 128.14 (C), 127.46 (CH), 126.36 (CH), 121.63 (CH), 121.06 (CH), 120.82 (CH), 120.43 (CH), 118.62 (CH), 118.12 (CH), 111.09 (CH), 111.03 (C), 72.88 (CH), 71.26 (CH), 61.68 (CH_2), 59.53 (CH_2), 52.00 (CH), 50.37 (CH), 50.00 (CH_2), 47.11 (CH), 37.91 (CH_2), 33.06 (CH_2), 32.93 (CH_2), 32.50 (CH_2), 31.07 (CH_2), 28.82-26.42 (CH_2), 28.19 (CH_3), 25.09 (CH_2), 24.76 (CH_2), 24.26 (CH_2), 23.91 (CH_2), 23.45 (CH_2), 21.87 (CH_2), 20.54 (CH_3), 19.58 (CH_2), 18.68 (CH_3), 13.87 (CH_3), 13.72 (CH_3). **HRMS (ESI) *m/z*:** $[M+H]^+$ for $[C_{86}H_{116}ClN_{10}O_{12}^+]$; calculated: 1515.8457, found: 1515.8465.

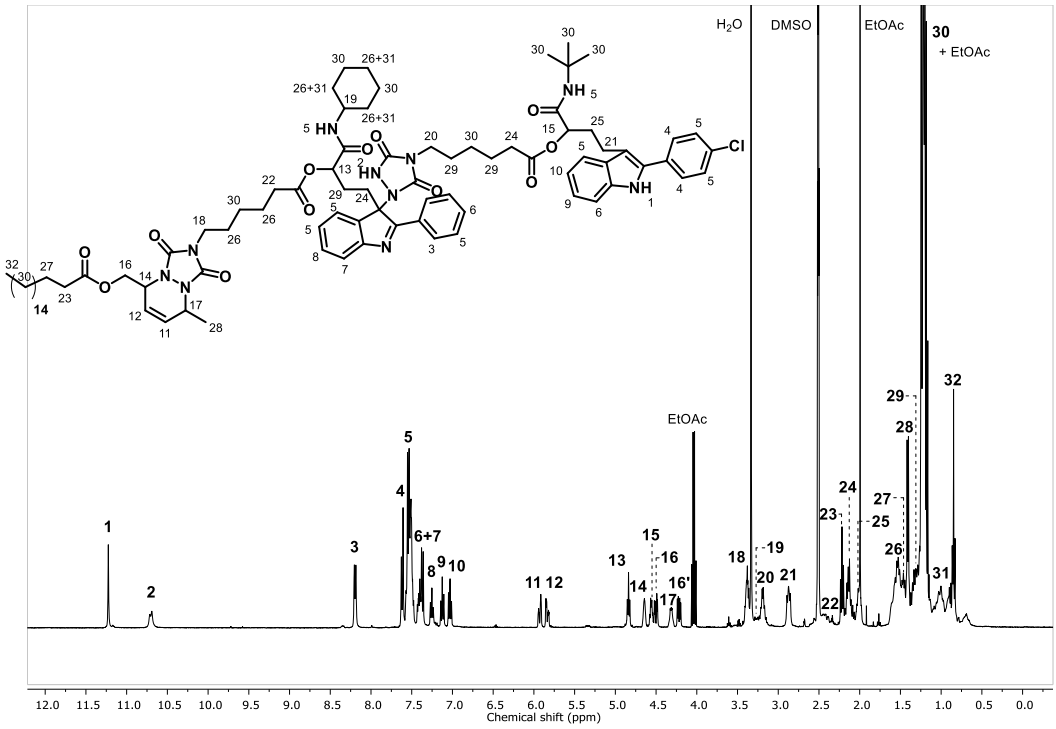
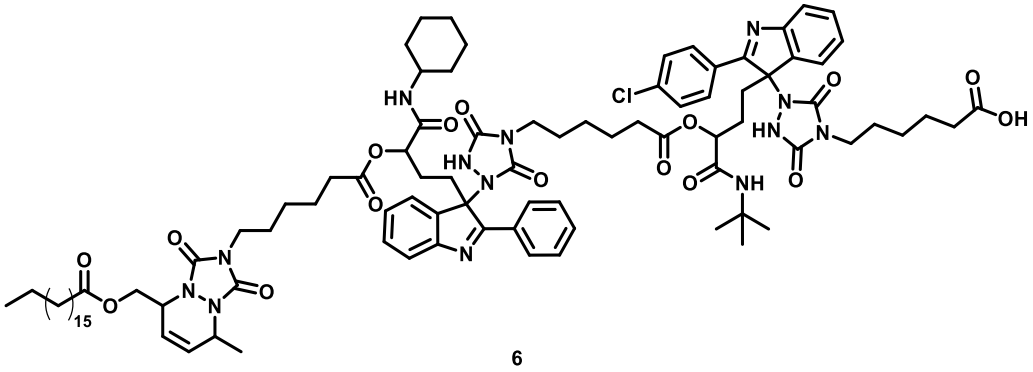


*Figure VII 27: ^{1}H NMR spectrum (DMSO-d_6) of **5**.*

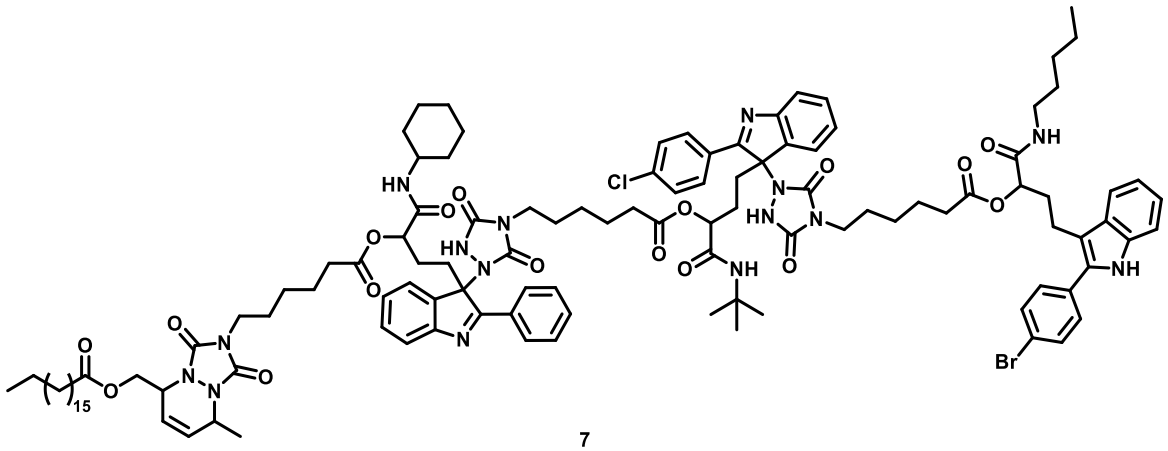
VII4.5.5 3rd TAD addition



6

5 (1.00 g, 0.66 mmol, 1.0 equiv.) was dissolved in anhydrous ethyl acetate (3 mL) to which a solution of TAD-COOH **L1** (169 mg, 0.79 mmol, 1.20 equiv.) in ethyl acetate (1 mL) was added dropwise, until a pink colour persisted, indicating full consumption of **5**. Next, 2,3-dimethylbut-2-ene (24 µL, 11 mg, 0.13 mmol, 0.20 equiv.) was added to the reaction mixture to quench the excess of unreacted TAD. The solvent was removed *in vacuo* at 35 °C and the crude product was used in the next step without further purification or analysis.

VII.4.5.6 3rd P-3CR



7

6 (1.14 g, 0.66 mmol, 1.0 equiv.) was dissolved in anhydrous CH_2Cl_2 (3 mL). Subsequently, a solution of 3-(2-(4-bromophenyl)-1*H*-indol-3-yl) propanal, **L2c** (433 mg, 1.32 mmol, 2.0 equiv.) in anhydrous CH_2Cl_2 (2 mL) was added to the reaction mixture, followed by 1-pentyl isocyanide (125 µL, 0.99 mmol, 1.5 equiv.). The reaction mixture was stirred for 24 hours at room temperature and the crude product was purified by column chromatography (silica, hexane:ethyl acetate 2:1→0:1, R_F (EtOAc) = 0.52) to give **7** as a yellow viscous oil that solidified upon further drying *in vacuo*. Overall yield over two reaction steps: 60 % (m = 853 mg).

^{1}H NMR (400 MHz, DMSO-*d*$_6$): δ = 11.22 (s, 1H, H^1), 10.69 (s, 2H, H^2), 8.19 (d, *J* = 8.3 Hz, 4H, H^3), 7.91 (q, *J* = 5.7 Hz, 1H, H^4), 7.73-7.60 (m, 2H, H^5), 7.60-7.46 (m, 11H, H^6), 7.46-7.30 (m, 5H, H^7), 7.29-7.17 (m, 3H, H^8), 7.16-7.06 (m, 1H, H^9), 7.04-6.94 (m, 1H, H^{10}), 5.97-5.89 (m, 1H, H^{11}), 5.87-5.79 (m, 1H, H^{12}), 4.88-4.77 (m, 1H, H^{13}), 4.67-4.61 (m, 1H, H^{14}), 4.59-4.45 (m, 3H, H^{15}), 4.34-4.28 (m, 1H, H^{16}), 4.21 (dd, *J* = 11.6, 4.9 Hz, 1H, H^{17}), 3.40-3.34 (m, 2H, H^{18}), 3.18-3.12 (m, 5H, H^{19}), 3.09-2.97 (m, 2H, H^{20}), 2.93-2.80 (m, 2H, H^{21}), 2.65-2.25 (m, 4H, H^{22}), 2.25-1.85 (m, 10H, H^{23}), 1.66-1.27 (m, 26H, H^{24}), 1.27-0.88 (m, 54H, H^{25}), 0.96-0.74 (m, 6H, H^{26}). **^{13}C-NMR (APT, 100 MHz, DMSO-*d*$_6$):** δ = 172.59 (C), 172.07 (C), 171.70 (C), 170.32 (C), 169.00 (C), 167.32 (C), 153.68 (C), 152.00 (C), 136.13 (C), 132.89 (C), 132.01 (C), 131.58 (CH), 129.65 (CH), 129.39 (CH), 128.83 (CH), 128.60 (CH), 128.33 (C), 127.67 (CH), 126.81 (CH), 126.57 (CH), 121.87 (CH), 121.32 (CH), 121.04 (CH), 120.49 (C), 118.84 (CH), 118.38 (CH), 111.31 (CH), 111.05 (C), 72.90 (CH), 71.45 (CH), 61.89 (CH_2), 59.74 (CH_2), 52.26 (CH), 50.58 (CH), 50.08 (CH_2), 49.96 (CH_2), 47.32 (CH), 38.27 (CH_2), 38.11 (CH_2), 33.28 (CH_2), 33.04 (CH_2), 31.28 (CH_2), 29.02-25.36 (CH_2), 22.08 (CH_2), 21.76 (CH_2), 20.75 (CH_3), 18.89 (CH_3), 14.08 (CH_3), 13.93 (CH_3), 13.85 (CH_3). **HRMS (ESI) *m/z*:** $[M+H]^+$ for $[C_{117}H_{152}BrClN_{15}O_{17}^+]$; calculated: 2153.0357, found: 2153.0265.

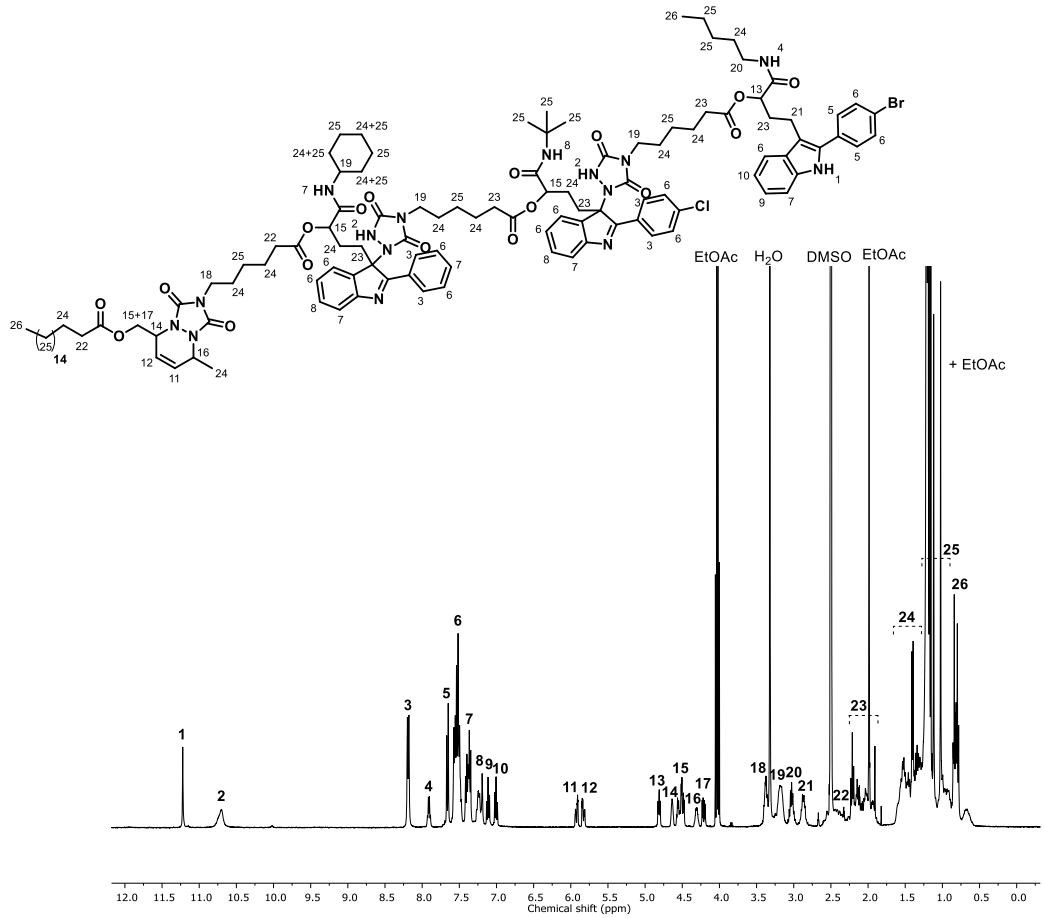
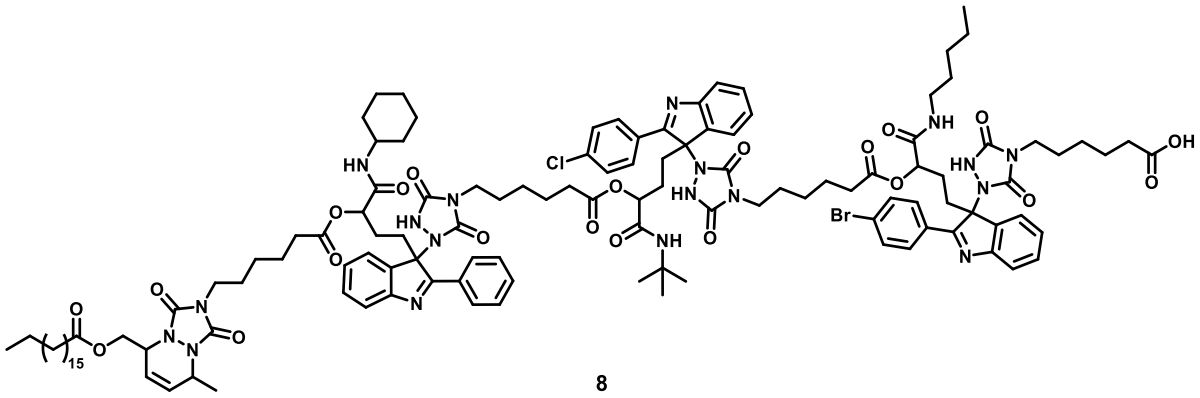


*Figure VII 28: ^{1}H NMR spectrum (DMSO-d_6) of **7**.*

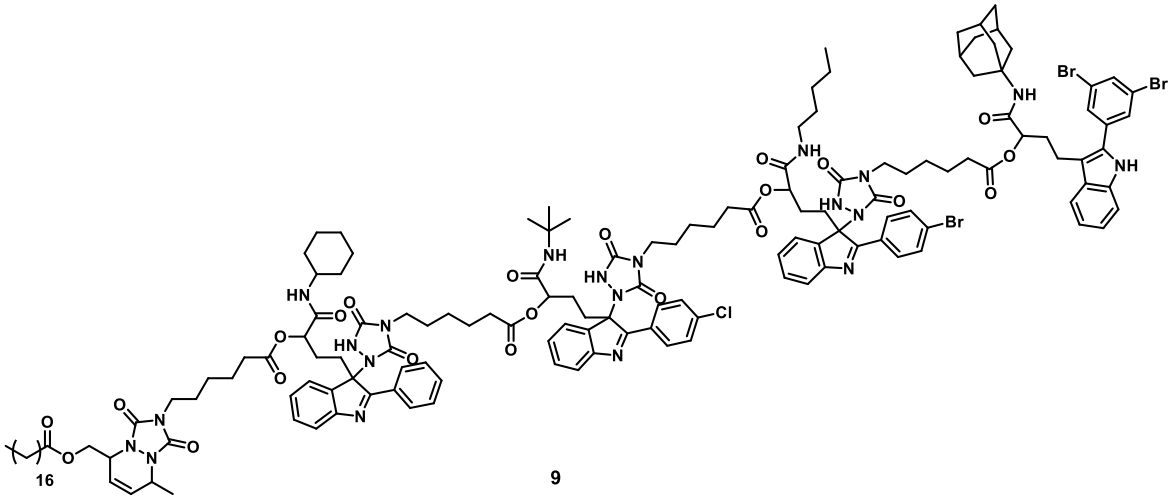
VII.4.5.7 4th TAD addition



8

7 (300.00 mg, 0.14 mmol, 1.0 equiv.) was dissolved in anhydrous dry ethyl acetate (3 mL) to which a solution of TAD-COOH **L1** (35.60 mg, 0.17 mmol, 1.20 equiv.) in ethyl acetate (1 mL) was added dropwise, until a pink colour persisted, indicating full conversion of **7**. Next, 2,3-dimethylbut-2-ene (3.3 µL, 2.4 mg, 0.028 mmol, 0.20 equiv.) was added to the reaction mixture to quench the excess of unreacted TAD. The solvent was removed *in vacuo* at 35 °C and the crude product was used in the next step without further purification or analysis.

VII.4.5.8 4th 3-PCR



8 (329 mg, 0.14 mmol, 1.0 equiv.) was dissolved CH_2Cl_2 (2 mL). Subsequently, a solution of 3-(2-(3,5-dibromophenyl)-1*H*-indol-3-yl) propanal, **L2d** (98 mg, 0.28 mmol, 2.0 equiv.) in CH_2Cl_2 (1 mL) was added to the reaction mixture, followed by 1-adamantyl isocyanide (34 mg, 0.21 mmol, 1.5 equiv.). The reaction was stirred for 24 hours at room temperature and the crude product was purified by column chromatography (silica, hexane:ethyl acetate 2:1→0:1, R_F (EtOAc) = 0.43) to give **9** as a yellow viscous oil that solidified upon further drying *in vacuo*. Overall yield over two reaction steps: 91 % (m = 360 mg).

^{1}H NMR (400 MHz, DMSO-*d*$_6$): δ = 11.33 (s, 1H, H^1), 10.83-10.61 (m, 3H, H^2), 8.19 (d, *J* = 7.9 Hz, 4H, H^3), 8.11 (d, *J* = 8.4 Hz, 2H, H^4), 7.83-7.74 (m, 3H, H^5), 7.74-7.60 (m, 3H, H^6), 7.60-7.45 (m, 10H, H^7), 7.45-7.30 (m, 8H, H^8), 7.30-7.18 (m, 4H, H^9), 7.15 (t, *J* = 7.5 Hz, 1H, H^{10}), 7.04 (t, *J* = 7.5 Hz, 1H, H^{11}), 5.97-5.89 (m, 1H, H^{12}), 5.87-5.79 (m, 1H, H^{13}), 4.88-4.77 (m, 1H, H^{14}), 4.67-4.61 (m, 1H, H^{15}), 4.60-4.45 (m, 4H, H^{16}), 4.36-4.26 (m, 1H, H^{17}), 4.21 (dd, *J* = 11.6, 5.0 Hz, 1H, H^{18}), 3.43-3.34 (m, 2H, H^{19}), 3.29-3.08 (m, 7H, H^{20}), 3.09-2.97 (m, 4H, H^{21}), 2.65-2.25 (m, 4H, H^{22}), 2.25-1.80 (m, 23H, H^{23}), 1.66-0.88 (m, 94H, H^{24}), 0.96-0.74 (m, 6H, H^{25}). **^{13}C-NMR (APT, 100 MHz, DMSO-*d*$_6$):** δ = 172.58 (C), 171.98 (C), 171.76 (C), 171.69 (C), 171.59 (C), 167.95 (C), 167.30 (C), 167.14 (C), 167.08 (C), 155.17 (C), 153.66 (C), 151.99 (C), 136.72 (C), 136.29 (C), 136.16 (C), 131.94 (C), 131.88 (CH), 131.77 (CH), 131.72 (CH), 131.58 (CH), 130.76 (C), 129.95 (CH), 129.69 (CH), 129.55 (CH), 129.37 (CH), 129.20 (CH), 128.82 (CH), 128.62 (CH), 128.10 (C), 127.67 (CH), 122.83 (C), 121.03 (CH), 120.84 (CH), 120.63 (CH), 119.05 (CH), 118.72 (CH), 117.99 (CH), 112.57 (C), 111.47 (CH), 76.06 (CH_2), 72.86 (CH), 71.57 (CH), 71.45 (CH_2), 61.88 (CH_2), 59.74 (CH_2), 52.25 (CH), 50.87 (CH_2), 50.57 (CH), 50.07 (CH_2), 49.96 (CH_2), 47.31 (CH), 40.84 (CH_2), 38.10 (CH_2), 35.96 (CH_2), 33.26 (CH_2), 32.96 (CH_2), 32.58 (CH_2), 31.96 (CH_2), 31.27 (CH_2), 29.00 (CH_2), 28.93 (CH_2), 28.78 (CH), 28.68 (CH_2), 28.63 (CH_2), 28.46 (CH_2), 28.37 (CH_2), 28.26 (CH), 28.11 (CH), 27.04-21.68 (CH_2), 20.74 (CH_3), 18.88 (CH_3), 14.07 (CH_3), 13.92 (CH_3), 13.84 (CH_3).

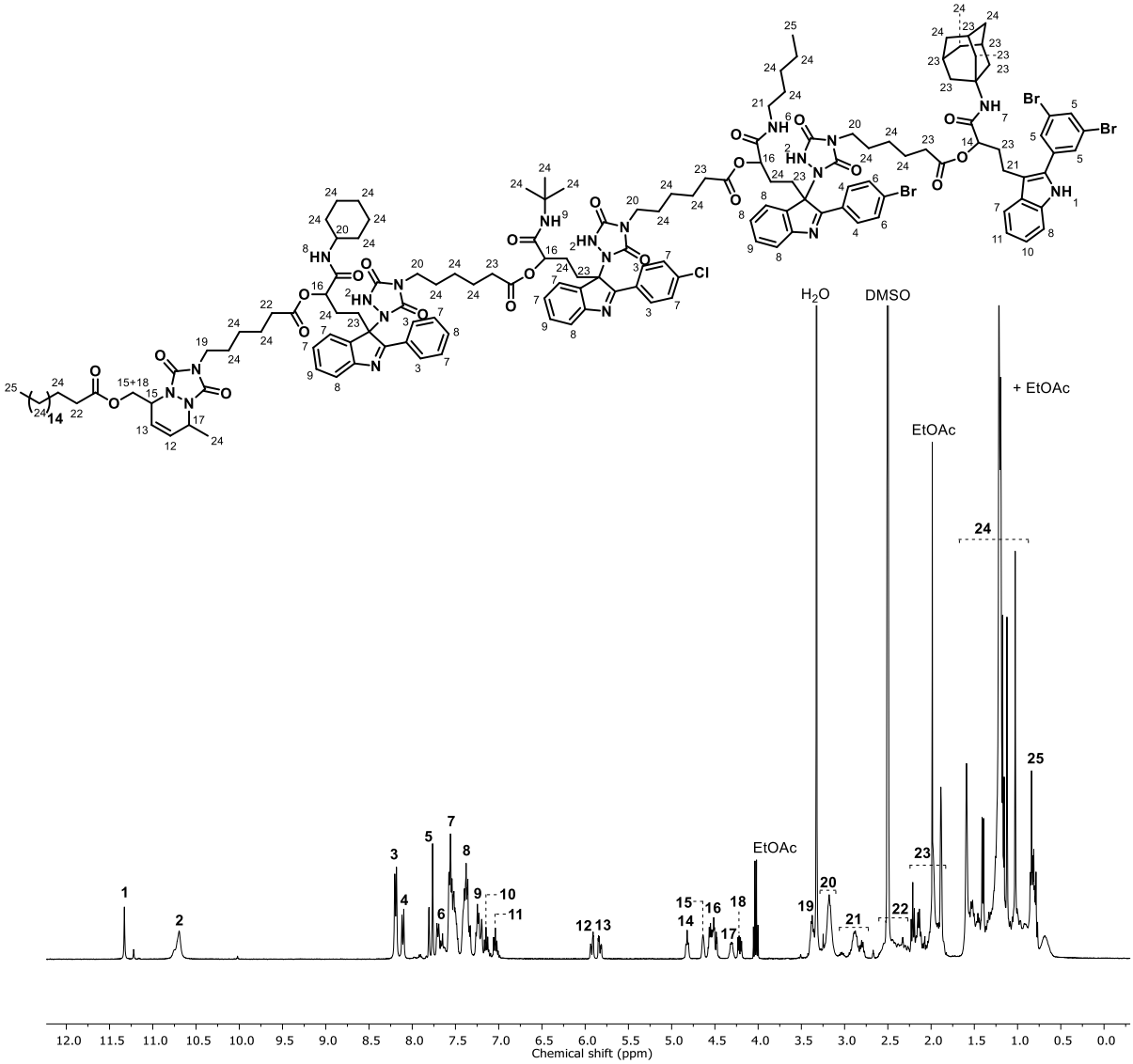
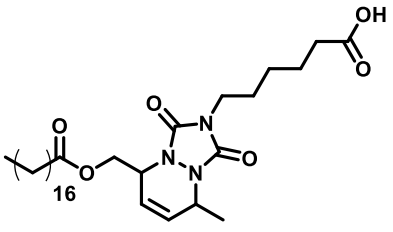


*Figure VII 29: ^{1}H NMR spectrum (DMSO-d_6) of **9**.*

VII.4.6 Solution synthesis of sequence-defined oligomers *via* the U-4CR

VII.4.6.1 1st TAD addition

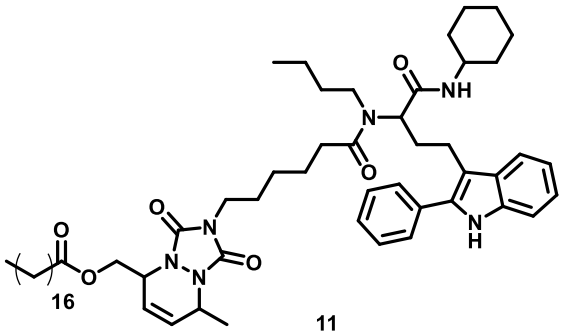


10

1 (365 mg, 1.0 mmol, 1.0 equiv.) was dissolved in anhydrous ethyl acetate (3 mL) to which a solution of TAD-COOH **L1** (256 mg, 1.20 mmol, 1.20 equiv.) in ethyl acetate (1 mL) was added dropwise, until

a pink colour persisted, indicating full conversion of **1**. Next, 2,3-dimethylbut-2-ene (24 µL, 17 mg, 0.20 mmol, 0.20 equiv.) was added to the reaction mixture to quench the excess of unreacted TAD. The solvent was removed *in vacuo* at 35 °C and the crude product was used in the next step without further purification or analysis.

VII.4.6.2 1st U-4CR



11

10 (584 mg, 1.0 mmol, 1.0 equiv.) was dissolved in MeOH (3 mL). To this, a premade solution of 3-(2-phenyl-1*H*-indol-3-yl) propanal**, L2a** (499 mg, 2.0 mmol, 2.0 equiv.) and butylamine (198 µL, 2.0 mmol, 2.0 equiv.) in MeOH (2 mL), stirred for 30 minutes at room temperature, was added followed by the addition of cyclohexyl isocyanide (187 µL, 1.5 mmol, 1.5 equiv.). The reaction mixture was stirred for 48 hours at room temperature and the crude product was purified by column chromatography (silica, hexane:ethyl acetate 9:1→1:1, R_F (hex:EtOAc 2:1) = 0.21) to give **11** as a yellow viscous oil that solidified upon further drying *in vacuo*. Overall yield over two reaction steps: 92 % (910 mg).

^{1}H NMR (400 MHz, DMSO-*d*$_6$): δ = 11.13 (d, *J* = 16.5 Hz, 1H, H^1), 7.85 (d, *J* = 7.3 Hz, 1H, H^2), 7.64-7.52 (m, 3H, H^3), 7.52-7.43 (m, 2H, H^4), 7.35 (dd, *J* = 12.0, 5.9 Hz, 2H, H^5), 7.09 (t, *J* = 7.5 Hz, 1H, H^6), 7.00 (t, *J* = 7.4 Hz, 1H, H^7), 5.96-5.87 (m, 1H, H^8), 5.86-5.79 (m, 1H, H^9), 4.76 (t, *J* = 6.6 Hz, 1H, H^{10}), 4.68-4.59 (m, 1H, H^{11}), 4.52-4.44 (m, 1H, H^{12}), 4.36-4.22 (m, 1H, H^{13}), 4.22-4.12 (m, 1H, $H^{12'}$), 3.62-3.49 (m, 1H, H^{14}), 3.38 (t, *J* = 6.9 Hz, 2H, H^{15}), 3.28-3.08 (m, 2H, H^{16}), 2.86-2.70 (m, 2H, H^{17}), 2.39-2.03 (m, 6H, H^{18}), 1.92-1.36 (m, 21H, H^{19}), 1.36-0.98 (m, 30H, H^{20}), 0.91-0.74 (m, 6H, H^{21}). **^{13}C-NMR (APT, 100 MHz, DMSO-*d*$_6$):** δ = 172.59 (C), 171.71 (C), 169.41 (C), 153.79 (C), 151.90 (C), 136.02, (C), 134.00 (C), 133.81 (C), 132.91 (C), 132.86 (C), 129.77 (CH), 128.61 (CH), 128.54 (CH), 127.74 (CH), 127.69 (CH), 127.22 (CH), 127.16 (CH), 121.45 (CH), 120.97 (CH), 118.58 (CH), 111.20 (CH_2), 111.12 (CH), 110.66 (CH_2), 61.85 (CH_2), 59.03 (CH), 57.26 (CH), 52.15 (CH), 50.69 (CH), 47.87 (CH), 47.49 (CH), 44.73 (CH_2), 38.28 (CH_2), 38.15 (CH_2), 33.26(CH_2), 32.39 (CH_2), 32.15 (CH_2), 31.98 (CH_2), 31.28 (CH_2), 30.61 (CH_2), 29.00 (CH_2), 28.98 (CH_2), 28.94 (CH_2), 28.83 (CH_2), 28.80 (CH_2), 28.69 (CH_2), 28.65 (CH_2), 28.38 (CH_2), 27.44 (CH_2), 27.27 (CH_2), 25.68 (CH_2), 25.19 (CH_2), 24.59 (CH_2), 24.45 (CH_2), 24.11 (CH_2), 22.08 (CH_2), 20.05 (CH_2), 19.69 (CH_2), 18.92 (CH_3), 13.92 (CH_3), 13.51 (CH_3).

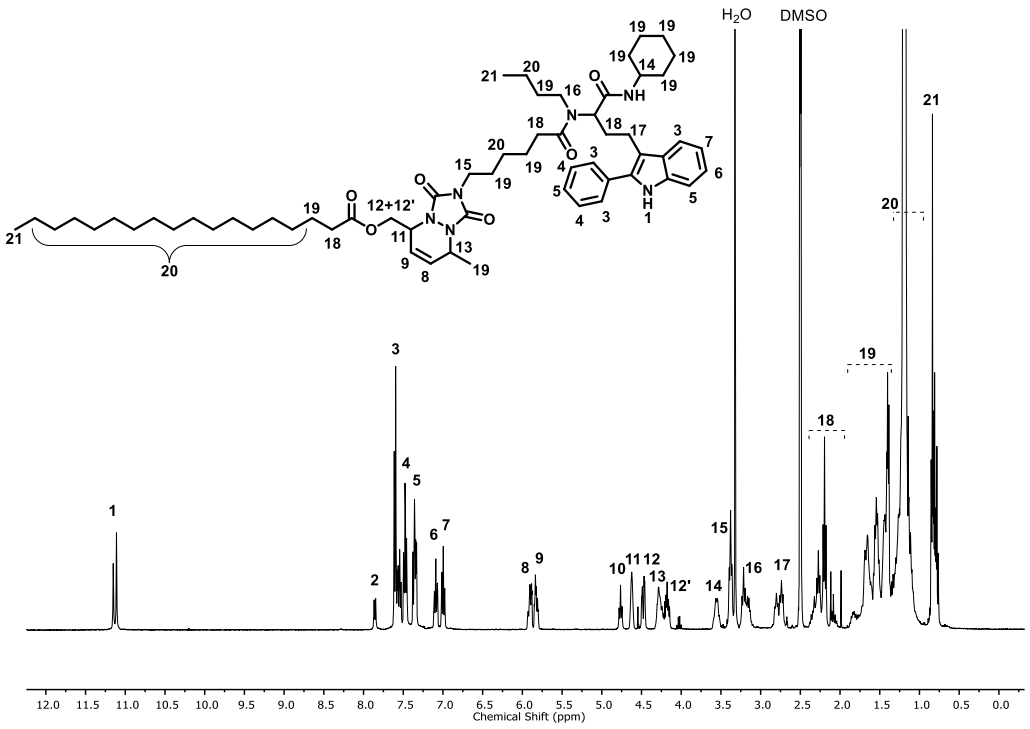


*Figure VII 30: ^{1}H NMR spectrum (DMSO-d_6) of **11**.*

VII.4.7 Encryption and decryption model studies

VII.4.7.1 Encryption model study

A solution of **7** (50 mg, 0.028 mmol, 1.0 equiv.) in DMSO-d_6 (1 mL) was transferred into a pressure tube and placed in a pre-heated oil bath at 120 °C. At distinct time intervals, *i.e.* 15, 30, 45, 60 and 120 minutes, 0.20 mL of the mixture was taken out and the sample was submitted to SEC analysis.

VII.4.7.2 Decryption model study

7 (50 mg, 0.028 mmol, 1.0 equiv.) and sorbic alcohol (5.0 mg, 0.062 mmol, 2.2 equiv.) were dissolved in DMSO-d_6 (1 mL). The solution was transferred into an NMR tube and placed in a pre-heated oil bath at **120 °C**. At distinct time intervals, *i.e.* 15, 30, 45, 60 and 120 minutes, 0.20 mL of the mixture was taken out and the sample was submitted to NMR analysis, from which the conversion was determined.

7 (25 mg, 0.014 mmol, 1.0 equiv.) and sorbic alcohol (2.5 mg, 0.031 mmol, 2.2 equiv.) were dissolved in DMSO-d_6 (0.5 mL). The solution was transferred into an NMR tube and placed in a pre-heated oil bath at **135 °C**. At distinct time intervals, *i.e.* 15, 30 and 45 minutes, 0.20 mL of the mixture was taken out and the sample was submitted to NMR analysis, from which the conversion was determined.

7 (25 mg, 0.014 mmol, 1.0 equiv.) and sorbic alcohol (2.5 mg, 0.031 mmol, 2.2 equiv.) were dissolved in DMSO-d_6 (0.5 mL). The solution was transferred into an NMR tube and placed in a pre-heated oil bath at **150 °C**. After 15 minutes, 0.20 mL of the mixture was taken out and the sample was submitted to NMR analysis, from which the conversion was determined to be 100 %, thus further measurements were not needed. This reaction was then repeated with **7** (50 mg, 0.028 mmol, 1.0 equiv.) and **1** (9.48 mg, 0.026 mmol, 2.2 equiv.) dissolved in anhydrous butyl acetate (1 mL). The solution was transferred into an NMR tube and placed in a pre-heated oil bath at 150 °C. After 15 minutes, 0.20 mL of the mixture was taken out and the sample was submitted to LCMS and SEC analysis.

The kinetics of the retro-Alder-ene reaction of the TAD-indole system (*Figure VII 7*) was analysed by calculating the percentage of indole moieties that have been released from their corresponding TAD-adduct at specific time intervals upon heating (120 °C, 135 °C and 150 °C). In order to enable offline NMR analysis to monitor the TAD-indole dissociation, sorbic alcohol was used as an *in situ* trapping agent, forming an irreversible Diels-Alder adduct with the released TAD. As this TAD-diene Diels-Alder reaction is ultrafast, first-order reaction kinetics can be assumed, which results in a simplified expression of the observed first-order rate coefficient (k_{obs}) (*vide infra*). By calculating k_{obs} of the TAD-indole dissociation at the three different temperatures of reversibility, the activation energy (E_a) of the retro-Alder-ene reaction could eventually be determined by means of an Arrhenius plot.

$$Rate = -\frac{d[A]}{dt} = k_{obs}[A]$$

$$\ln[A]_t - \ln[A]_0 = \frac{[A]_t}{[A]_0} = -k_{obs}t$$

From the fraction of TAD-indole adducts remaining at specific time intervals, $\ln\frac{[A]_t}{[A]_0}$ was determined *via* integration of the ^{1}H NMR spectra. The observed rate coefficient, k_{obs} was hence calculated at each of the three temperatures. Using the rearranged Arrhenius equation below, the observed activation energy ($E_{a,\ obs}$) of the TAD-indole system could be calculated.

$$lnk_{obs} = \frac{-E_{a,\ obs}}{RT} + \ln A$$

By plotting ln k_{obs} as a function of temperature (T^{-1}), an Arrhenius plot was obtained (*Figure VII 31*) and the best-fit linear interpolation of the three data points was determined. The equation of the linear fit (*vide infra*) could be applied to calculate the activation energy from the slope, using the molar gas constant, R = 8.314 J mol^{-1} K^{-1}.

$$y = ax + b$$

$$a = \frac{-\mathrm{E_{a,obs}}}{R}$$

$$\mathrm{E_{a,obs}} = -aR = 107.0 \pm 4.7\ kJ\ mol^{-1}$$

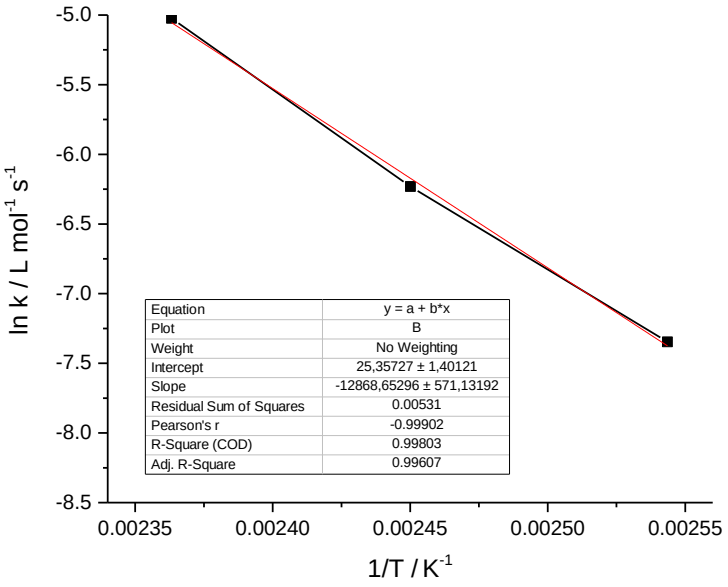


*Figure VII 31: Arrhenius plot from the temperature dependent reversibility study, enabling one to calculate the activation energy of the retro-Alder-ene reaction of the sequence-defined trimer **A1-B2-C3**.*

VII.5 References

1 S. Martens, J. O. Holloway and F. E. Du Prez, *Macromol. Rapid Commun.*, 2017, **38**, 1700469.

2 S. C. Solleder, R. V. Schneider, K. S. Wetzel, A. C. Boukis and M. A. R. Meier, *Macromol. Rapid Commun.*, 2017, **38**, 1600711.

3 J. A. De Neve, J. J. Haven, L. Maes and T. Junkers, *Polym. Chem.*, 2018, **9**, 4692–4705.

4 M. A. R. Meier and C. Barner-Kowollik, *Adv. Mater.*, 2019, **31**, 1806027.

5 J.-F. Lutz, M. Ouchi, D. R. Liu and M. Sawamoto, *Science*, 2013, **341**, 1238149.

6 L. Hartmann, *Macromol. Chem. Phys.*, 2011, **212**, 8–13.

7 L. Hartmann and H. G. Börner, *Adv. Mater.*, 2009, **21**, 3425–3431.

8 D. Karamessini, B. E. Petit, M. Bouquey, L. Charles and J.-F. Lutz, *Adv. Funct. Mater.*, 2017, **27**, 1604595.

9 M. Porel, D. N. Thornlow, C. M. Artim and C. A. Alabi, *ACS Chem. Biol.*, 2017, **12**, 715–723.

10 M. Porel, D. N. Thornlow, N. N. Phan and C. A. Alabi, *Nat. Chem.*, 2016, **8**, 590–596.

11 P. Chandra, A. M. Jonas and A. E. Fernandes, *J. Am. Chem. Soc.*, 2018, **140**, 5179–5184.

12 S. Martens, A. Landuyt, P. Espeel, B. Devreese, P. Dawyndt and F. E. Du Prez, *Nat. Commun.*, 2018, **9**, 4451.

13 N. Zydziak, W. Konrad, F. Feist, S. Afonin, S. Weidner and C. Barner-Kowollik, *Nat. Commun.*, 2016, **7**, 1–10.

14 A. C. Boukis, K. Reiter, M. Frölich, D. Hofheinz and M. A. R. Meier, *Nat. Commun.*, 2018, **9**, 1439.

15 H. M. Colquhoun and J.-F. Lutz, *Nat. Chem.*, 2014, **6**, 455–456.

16 J.-F. Lutz, *Macromolecules*, 2015, **48**, 4759–4767.

17 U. S. Gunay, B. E. Petit, D. Karamessini, A. Al Ouahabi, J. A. Amalian, C. Chendo, M. Bouquey, D. Gigmes, L. Charles and J.-F. Lutz, *Chem*, 2016, **1**, 114–126.

18 D. Karamessini, T. Simon-yarza, S. Poyer, E. Konishcheva, L. Charles, D. Letourneur and J.-F. Lutz, *Angew. Chemie Int. Ed.*, 2018, **57**, 10574–10578.

19 D. Karamessini, S. Poyer, L. Charles and J.-F. Lutz, *Macromol. Rapid Commun.*, 2017, **38**, 1700426.

20 C. Laure, D. Karamessini, O. Milenkovic, L. Charles and J.-F. Lutz, *Angew. Chemie - Int. Ed.*, 2016, **55**, 10722–10725.

21 G. M. Church, Y. Gao, S. Kosuri, H. H. Wang, A. W. Briggs, J. Lee, T. Wu and D. B. Goodman, *Nucleic Acids Res*, 2010, **38**, 372.

22 C. Bancroft, T. Bowler, B. Bloom and C. T. Clelland, *Science*, 2001, **293**, 1763–1765.

23 J. Bonnet, M. Colotte, D. Coudy, V. Couallier, J. Portier, B. Morin and S. Tuffet, *Nucleic Acids Res.*, 2010, **38**, 1531–1546.

24 T. Lindahl, *Nature*, 1993, **362**, 709–715.

25 J. A. Amalian, T. T. Trinh, J.-F. Lutz and L. Charles, *Anal. Chem.*, 2016, **88**, 3715–3722.

26 R. K. Roy, A. Meszynska, C. Laure, L. Charles, C. Verchin and J.-F. Lutz, *Nat. Commun.*, 2015, **6**, 7237–7239.

27 I. K. Ugi, *Angew. Chemie*, 1959, **71**, 373–388.

28 L. Charles, C. Laure, J.-F. Lutz and R. K. Roy, *Macromolecules*, 2015, **48**, 4319–4328.

29 R. K. Roy, C. Laure, D. Fischer-Krauser, L. Charles and J.-F. Lutz, *Chem. Commun.*, 2015, **51**, 15677–15680.

30 G. Cavallo, A. Al Ouahabi, L. Oswald, L. Charles and J.-F. Lutz, *J. Am. Chem. Soc.*, 2016, **138**, 9417–9420.

31 G. Cavallo, S. Poyer, J.-A. Amalian, F. Dufour, A. Burel, C. Carapito, L. Charles and J.-F. Lutz, *Angew. Chemie Int. Ed.*, 2018, **130**, 6374–6377.

32 A. Burel, C. Carapito, J.-F. Lutz and L. Charles, *Macromolecules*, 2017, **50**, 8290–8296.

33 J. O. Holloway, K. S. Wetzel, S. Martens, F. E. Du Prez and M. A. R. Meier, *Polym. Chem.*, 2019, **10**, 3859–3867.

34 H. A. Houck, K. De Bruycker, C. Barner-Kowollik, J. M. Winne and F. E. Du Prez, *Macromolecules*, 2018, **51**, 3156–3164.

35 H. A. Houck, K. De Bruycker, S. Billiet, B. Dhanis, H. Goossens, S. Catak, V. Van Speybroeck, J. M. Winne and F. E. Du Prez, *Chem. Sci.*, 2017, **8**, 3098–3108.

36 S. Billiet, K. De Bruycker, F. Driessen, H. Goossens, V. Van Speybroeck, J. M. Winne and F. E. Du Prez, *Nat. Chem.*, 2014, **6**, 815–821.

37 K. De Bruycker, S. Billiet, H. A. Houck, S. Chattopadhyay, J. M. Winne and F. E. Du Prez, *Chem. Rev.*, 2016, **116**, 3919–3974.

38 D. H. Williams and I. Fleming, *Spectroscopic Methods in Organic Chemistry*, McGraw-Hill Education (UK), Maidenhead, 6th edn., 2008.

39 A. Geetika, S. Sunita and J. Sukesha, *Asian J. Chem.*, 2017, **29**, 20315.

40 S.-K. Xiang, B. Zhang, L.-H. Zhang, Y. Cui and N. Jiao, *Chem. Commun.*, 2011, **47**, 8097.

41 S. C. Solleder, K. S. Wetzel and M. A. R. Meier, *Polym. Chem.*, 2015, **6**, 3201–3204.

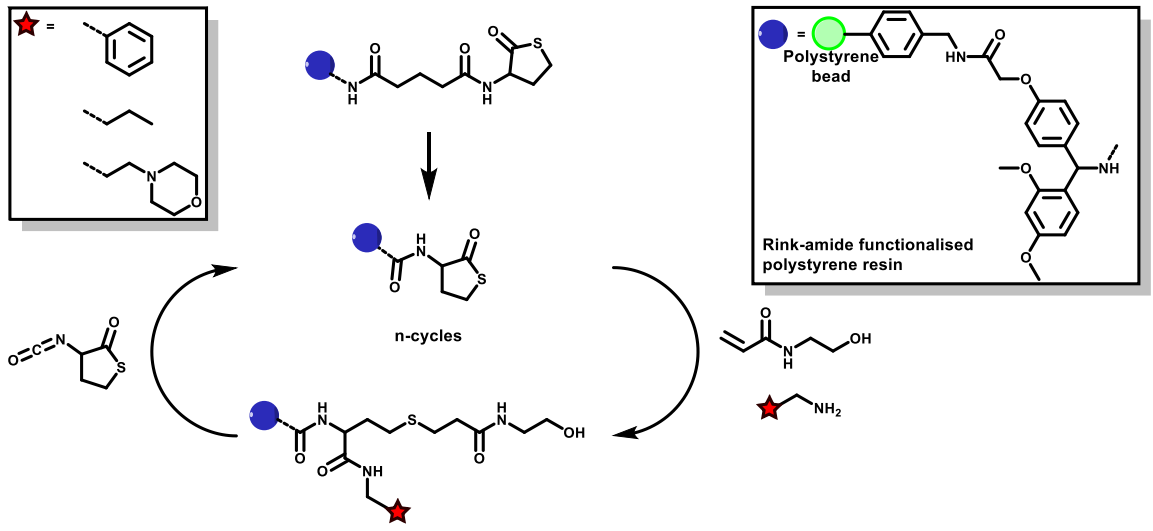
Chapter VIII
Conclusion and outlook

VIII.1 Conclusion

The initial aim of this doctoral work was to further build upon and expand the thiolactone-based, sequence-defined protocols already developed within our group[1–3] in order to further increase the monomer toolbox and diversify the potential macromolecular structures. It was proposed that altering the macromolecular structures may have had a beneficial effect on the thiolactone-based oligomer properties. By increasing the monomer toolbox, it was envisaged that one could begin to introduce specific functional groups to target certain sequence-defined applications or examine how the defined order of functionalities could alter their effectiveness. Moreover, by altering the way that thiolactone moieties were functionalised in a sequence-defined protocol, it was thought that this may bring benefits (*e.g.* improved reaction time or purity) to the synthesis approach. Expansion of the thiolactone-based protocol was initially achieved using thioacrylates as modifiable Michael acceptors in a sequence-defined protocol,[4] and later on a simplified version of this protocol was developed through the use of varying primary amines and a hydroxy-functionalised acrylamide.[5] The latter led to the automation of the solid-phase protocol using a peptide synthesiser.[5] The work later shifted from the use of thiolactone chemistry to the use of 1,2,4-triazoline-3,5-dione (TAD) chemistry as a click chemistry platform,[6] in combination with multicomponent reactions (MCRs).[7] This enabled the development of completely new, iterative chemical protocols, which could be applied to both the solid and solution phase, resulting in both a full comparative study and the introduction of thermoreversible chemistry to target potential applications of sequence defined oligomers.

Sequence-defined chemistry is a relatively young research field within polymer science, yet since its inception (ca. 2005),[8] it has become a hot topic and an area of intense research activity.[9,10] Following a short introduction and overview of the aims of this doctoral thesis in **Chapter I**, the recent advances in sequence-defined research, some important terminology and an introduction into the specific chemistries used during this PhD thesis were described in detail in **Chapter II**. Within each results chapter, a detailed conclusion is given. These will be summarised below, followed by a conclusion of this doctoral work and an outlook on the future work and perspectives related both to this research field and this PhD thesis.

In **Chapter III**, the use of thioacrylates within a solid-phase, iterative protocol was introduced, expanding the monomer toolbox of existing thiolactone-based protocols, which had been previously limited to acrylates and a small number of acrylamides.[1–3] Following careful studies of the reactivity and modification of thioester containing moieties, a four-step, protecting group-free protocol was devised, which incorporated thioacrylates and their thiophenol-catalysed modification with primary amines, resulting in multifunctional, sequence-defined oligomers.[4] The higher reactivity of thioacrylates towards other chemical functionalities compared to acrylates lead to unforeseen side reactions (reactions of amines and alcohols directly with the thioacrylate), thus a more complex protocol was required than other previously reported approaches.[1–3] The results obtained from this protocol highlighted how even the most complex, multi-step synthesis strategy can be carried out using solid-phase synthesis. Whilst a selection of primary amines with varying functionalities were used to demonstrate the versatility of the approach, their wide availability both from commercial sources and through organic synthesis, holds the potential to increase the monomer alphabet even further. This is of potential interest for applications such as data storage and encryption[1,3,11–13] or for introducing targeted functionalities such as bioactive moieties.[14–18] However, the complexity of a four-step approach resulted in certain limitations, regarding time efficiency and the potential for automation. Therefore, in **Chapter IV**, an improved, two-step protocol (*Scheme VIII 1*) was proposed, which involved the direct aminolysis of thiolactone moieties immobilised on a solid-phase resin by primary amines, followed by an immediate thiol-Michael addition with *N*-hydroxyethyl acrylamide.[5]



Scheme VIII 1: Iterative protocol for the (automated) synthesis of sequence-defined oligo-urethane-amides.

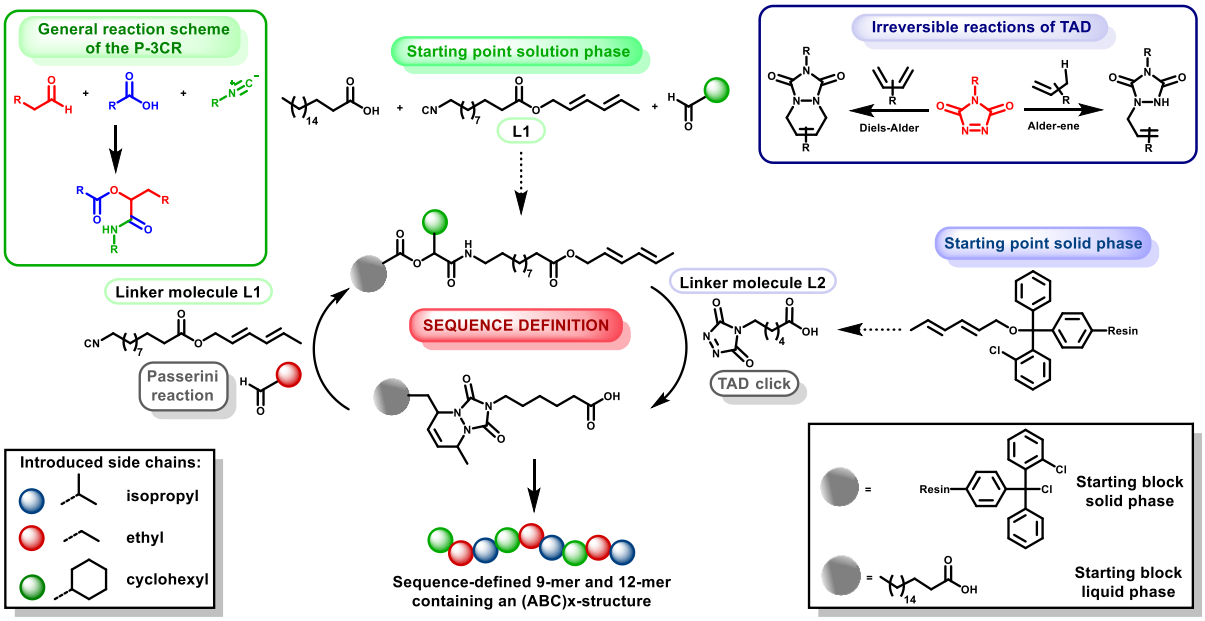
The protocol was successfully automated, enabling a time and labour-saving approach towards sequence-defined synthesis. Automation also offers the potential to synthesise large libraries of sequence-defined macromolecules concurrently, which can be particularly appealing if one wishes to study the effect of varying the position of specific functionalities on the polymer backbone, or to store

large amounts of data on sequence-defined oligomers.[3,12,13,19] Furthermore, the synthesis was expanded to different solid-phase resins, which were sensitive to differing concentrations of acid (1 %, 10 % and 50 %), to demonstrate the possibilities regarding solid-phase synthesis, as some sequence-defined structures might be more or less sensitive to acid.

Chapter V described the efforts undertaken during this doctoral thesis to combine TAD chemistry with thiolactones. Difficulties were observed in obtaining the TAD-thiolactone molecule with a high purity. Within Chapter II, the synthesis of TAD compounds was extensively discussed, where it was highlighted that the incorporation of specific functional groups during TAD synthesis can be challenging and that post-modification is often the best route. However, a range of model studies were first conducted to confirm the compatibility of TAD and thiolactone functionalities. Following the successful synthesis of a TAD-thiolactone molecule, the advantages of both a TAD moiety and a solid-support became quickly apparent. The impurities can usually be removed by simple washing and filtration and the ultra-fast, irreversible reaction of TAD in a Diels-Alder reaction meant that the thiolactone unit could be reinstalled for the subsequent cycle in just 5 minutes, as opposed to 2 hours with the automated approach described within Chapter IV. Despite the problems observed with the TAD-thiolactone synthesis, with further optimisation, this molecule could lead to an easy route for polymer modification. The TAD unit can react selectively and rapidly with alkene-containing polymers, thus immobilising a thiolactone unit on either the backbone or polymer end-group, which is available for further double modification. This would allow one to modify the polymer properties or install certain functionalities that could not be directly installed during the initial polymerisation. The success of the TAD addition step during the protocol developed within this chapter, led the research direction to change for the remainder of this PhD thesis, focussing more exclusively on TAD chemistry, as click-chemistry platform for sequence-defined synthesis.

In **Chapter VI**, a carboxylic acid functionalised TAD molecule (TAD-COOH) was synthesised for use within the Passerini three-component reaction (P-3CR).[20–23] Additionally the synthesis of a diene-isocyanide meant that an iterative, two-step protocol could be designed, alternating between a TAD Diels-Alder reaction and a P-3CR. This was facilitated by the orthogonal reaction groups of the TAD-COOH and diene isocyanide molecules and was carried out both on solid-phase and in solution (*Scheme VIII 2*).[7] The ultra-fast and efficient reaction of the TAD molecule with the diene isocyanide, in combination with the reliable and chemoselective P-3CR, meant that high molecular weight (> 7 kDa), sequence-defined oligomers could be synthesised. Initially a polymerisation side reaction was observed because of an excess of TAD remaining and reacting in the following P-3CR. This was successfully and easily avoided by quenching the TAD after each cycle with the addition of a non-functional alkene,

resulting in an increase in the purity of the obtained products, particularly for the solution-phase experiments. The purity and conversion were analysed not only using Liquid Chromatography Mass Spectroscopy (LCMS) as in previous chapters but also using Size Exclusion Chromatography (SEC). Because this protocol was applied to both solid and solution-phase synthesis, a unique and comprehensive study was conducted, comparing and highlighting the advantages and disadvantages of the two different techniques, which are both often used in sequence-defined chemistry. The two routes were carefully compared on yield, purity, scale, purification method and time with the conclusion made that the choice to opt for solid or solution-phase synthesis should be guided by the potential application and whether the user favours rapid or up-scalable synthesis.



Scheme VIII 2: Two-step iterative reaction cycle consisting of the P-3CR and the TAD Diels-Alder reaction, which can be applied to synthesise sequence-defined macromolecules on solid-phase and in solution. Box top left) General reaction scheme of the P-3CR. Box top right) Irreversible reactions of TAD.

Finally, in **Chapter VII** the protocol introduced in the previous chapter (*Scheme VIII 2*) was developed further to introduce the dynamic, thermoreversible TAD Alder-ene reaction in place of the Diels-Alder reaction. This was again combined with the P-3CR to synthesise reversible, sequence-defined oligomers for use as macromolecular pin codes. The introduction of Alder-ene linkages between the different monomer units was achieved using four specific indole-aldehyde compounds as position markers and the sequence-defined code was written using four different isocyanides. This meant that upon heating, the sequence could be encrypted, as the monomer units dissociated (*Figure VIII 1a*) and upon cooling, they formed a randomly ordered statistical distribution of oligomers, where the code contained within was unreadable (*Figure VIII 1b*). Upon heating this mixture again, this time in the presence of a trapping agent, the retro-Alder-ene reaction was again initiated. Upon cooling, the liberated TAD moieties favoured reaction with the trapping agent over the indole units,[24–26] thus forming a mixture of isolated

monomers, decrypting the information (*Figure VIII 1c*). The decrypted information could then be easily read-out using ESI-MS and LCMS, with the substitution of the specific indole-aldehyde compounds aiding their identification thanks to unique isotopic patterns (*Figure VIII 1d*). This is considered to be a very significant improvement compared with existing techniques, which used tandem MS/MS analysis, often requiring complex computer software and algorithms to decipher the information.[3,12,13,16,19,27–32] The order of the indole-aldehyde compounds therefore enabled one to work out the original order of the sequence, thus determining the original isocyanide-based code. Based upon the findings reported in Chapter VI, this work was carried out primarily using solution-phase synthesis to increase the scale of material produced. This ensured enough product for reversibility tests at a range of temperatures and to carry out characterisation using a range of analytical techniques. The macromolecular pin codes were finally encrypted and coated onto the surface of one of the new generations of pound sterling polymer banknotes as a demonstration towards their potential application in anti-counterfeiting applications. The encrypted oligomer was later extracted with ethanol and decrypted, thus enabling the successful read-out of the code, thus adding a further layer of protection to the currency.

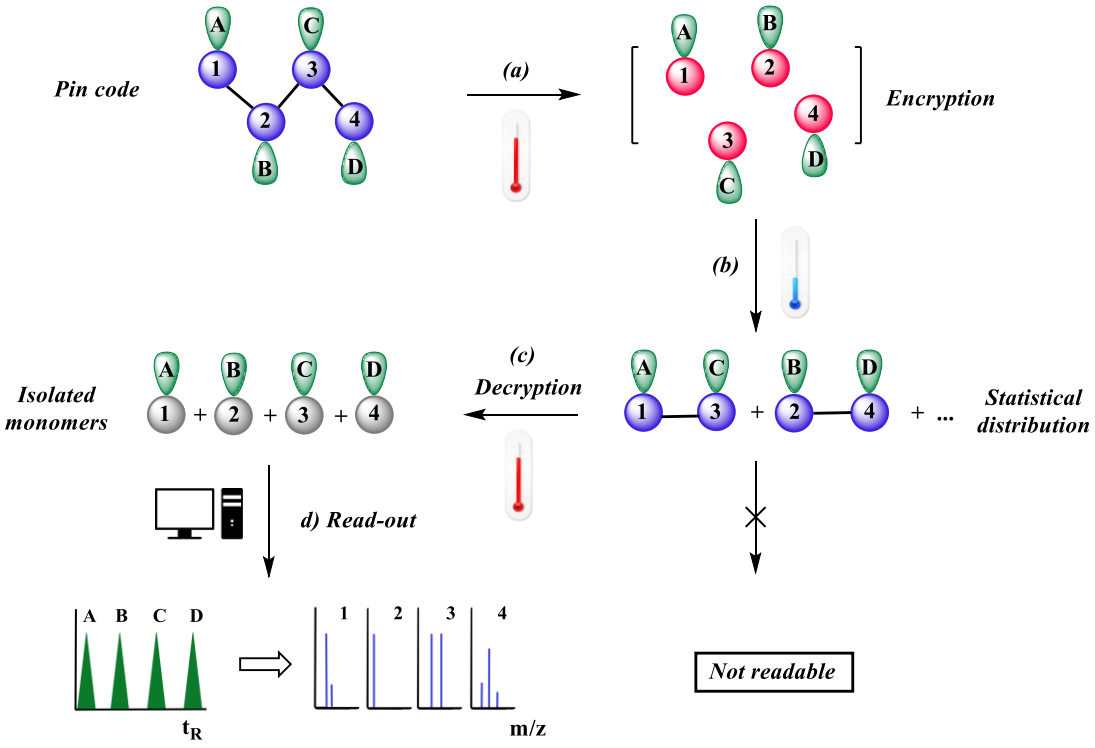


Figure VIII 1: Schematic overview of the encryption and decryption of thermoreversible sequence-defined oligomers (macromolecular pin codes) synthesised via a combination of TAD-indole chemistry and MCRs. These pin codes consist of an indole "marker" (i.e. A to D), which is paired to different isocyanide side-groups or "chemical digits" (e.g. 1,2,3 or 4). a) The reversible TAD-indole covalent bonds are dissociated when heat is applied, thereby encrypting the encoded information b) Upon cooling, a random mix of oligomers is obtained, which could not be subsequently read out. c) To decrypt the information, the sequence was heated in the presence of a trapping agent (a conjugated diene), resulting in the isolation of the different monomers of the sequence. d) This mix of monomers could be read out via LCMS to determine the original order of the building blocks, revealing the pin code.

VIII.2 Outlook and future work

This PhD thesis has explored the use of both thiolactone and TAD chemistry for the synthesis of sequence-defined oligomers, as described above. Whilst thiolactone chemistry was already known to our research group within sequence-defined synthesis,[1,2] this thesis introduced alternative thiolactone-based protocols, whereby sequence-definition was installed using primary amines. Importantly, different Michael acceptors were used to expand the monomer toolbox and alter the oligomer backbone.[4,5] However, the introduction of TAD chemistry immediately highlighted its many advantages compared with thiolactone chemistry for sequence-defined synthesis. It provided a visual feedback when the reaction was complete, the speed of reactions was much faster and up-scalable synthesis was possible thanks to the ease of transferring the chemical protocol from solid-phase to solution phase synthesis. Although TAD chemistry has its disadvantages, particularly with regard to functional TAD synthesis and shelf-life, it still proved to be the more successful chemical platform used within this thesis (in combination with multicomponent reactions (MCRs)), leading to the synthesis of sequence-defined oligomers of a higher molecular weight, yield and purity (or sequence fidelity).

The traditional route of reinstalling the thiolactone moiety using α-thiolactone-γ-isocyanate was challenged[1,3–5] with the introduction of a TAD-thiolactone molecule. Despite the difficulties encountered here, this paved the way towards further pursuing the use of TAD chemistry as the main chemical method for the synthesis of sequence-defined oligomers. The TAD/P-3CR protocol introduced in Chapter VI (*Scheme VIII 2*) further strengthened the concept of using TAD-based click reactions in sequence-defined synthesis approaches and the combination with MCRs proved highly effective. Therefore, the work described in Chapter VII, which moved towards potential applications of the herein reported chemistry holds the highest potential for future research. Although briefly investigated, the use of MCRs could be further extended to the Ugi four-component reaction as the double modification possible with this approach enables even greater data storage capacity in a condensed manner. The synthesis *via* the combination of the P-3CR and the TAD retro-Alder-ene reactions was limited to just very short oligomers, and longer oligomer synthesis should be further investigated, although this must be in combination with the synthesis of a wider range of substituted indole marker compounds with specific isotopic patterns. The use of a TAD-carboxylic acid molecule with an aromatic ring as a spacer between the functionalities rather than a 6-carbon aliphatic chain will also be investigated soon. This will not only control to the conformation of the oligomer but should have a positive effect on the temperature of reversibility of the TAD retro-Alder-ene reaction. The first test of coating the macromolecular pin codes on a polymer banknote gave promising results, demonstrating the potential of this approach towards anti-counterfeiting applications. This concept should be further investigated

and extended to a range of other substrates or within the polymer matrix instead of surface coating. Whilst read-out of only one of the macromolecular pin codes was successful *via* ESI-MS, this read-out should be further developed (for example, using - Selected Ion Monitoring) to avoid any interference from background signals from the polymer banknote itself.

Nonetheless, the use of thiolactone chemistry enabled the automation of sequence-defined synthesis, demonstrating a great advantage over the manual approach. The time and labour-saving benefits of using an automated synthesiser meant that automated synthesis was preferred, despite optimisation and minor technical issues in the beginning of the project. In view of the successful automation of the protocol described in Chapter IV, further work should be performed to examine whether much longer sequences can be made (> nonamer) in this fashion, thus exploring the limits of solid-phase automation. This would also enable one to determine what the ideal or maximum sequence length would be in terms of synthesis and whether the analysis of thiolactone-based sequence-defined macromolecules above a certain number of repeating units would become too difficult. This work was also limited to just two different thiolactone compounds, thus future research could explore the use of other thiolactone structures in sequence-defined approaches, such as thiolactone azides[39] and maleimides[40] or combining the amine-thiol-ene conjugation reaction of thiolactones with other conjugations such as the alkyne-azide-amine coupling.[41]

Furthermore, only racemic thiolactone compounds were used, thus it would be interesting to investigate whether the of introduction of chiral compounds would influence structure-property relationships such as folding and primary structure.[33,34] This could become more relevant when expanding the work to install functionalities such as sugar-containing molecules onto the backbone. Another important point to consider is the length of the backbone compared with the number of side-chain functionalities. For example, the oligomer synthesised in Chapter V, despite being a well-defined structure, has many atoms between each side chain and so the conformational arrangement and flexibility of the backbone could cause the sequence to essentially loose its definition as the functionalities move closer to or further away from one another in space. One possible solution to this is to design the backbone to be as rigid as possible, although this could have a negative influence on solubility.

One potential future direction for the sequence-defined synthesis protocols developed in this thesis, could be to investigate how the precise positioning of sugar moieties along the oligomer backbone would influence their interaction and binding with lectin,[35–38] thus providing further proof as to the importance of controlling the sequenced order of monomers within macromolecular structures and

further confirming the importance of defining the spacing between functionalities. Using an automated synthesis approach would enable the easy synthesis of a range of oligomers, thus allowing one to make an effective screening of the spacing versus binding effect.

Finally, throughout this thesis it has been discussed and shown that within a relatively short period of time, sequence-defined chemistry and the broader area of sequence-control, has proved to be of extreme interest within polymer chemistry and holds the key to projecting the field towards new, ground-breaking and ever more interesting applications. Amongst the many challenges that are currently facing chemists working in the area of sequence-defined synthesis (and have been highlighted in this outlook section), bringing this topic to a broader audience and into real-world applications remains the biggest challenge yet.

VIII.3 References

1 S. Martens, J. Van Den Begin, A. Madder, F. E. Du Prez and P. Espeel, *J. Am. Chem. Soc.*, 2016, **138**, 14182–14185.

2 P. Espeel, L. L. G. Carrette, K. Bury, S. Capenberghs, J. C. Martins, F. E. Du Prez and A. Madder, *Angew. Chemie - Int. Ed.*, 2013, **52**, 13261–13264.

3 S. Martens, A. Landuyt, P. Espeel, B. Devreese, P. Dawyndt and F. E. Du Prez, *Nat. Commun.*, 2018, **9**, 4451.

4 J. O. Holloway, S. Aksakal, F. E. Du Prez and C. Remzi Becer, *Macromol. Rapid Commun.*, 2017, **38**, 1700500.

5 J. O. Holloway, C. Mertens, F. E. Du Prez and N. Badi, *Macromol. Rapid Commun.*, 2019, **40**, 1800685.

6 K. De Bruycker, S. Billiet, H. A. Houck, S. Chattopadhyay, J. M. Winne and F. E. Du Prez, *Chem. Rev.*, 2016, **116**, 3919–3974.

7 J. O. Holloway, K. S. Wetzel, S. Martens, F. E. Du Prez and M. A. R. Meier, *Polym. Chem.*, 2019, **10**, 3859–3867.

8 C. J. Hawker and K. L. Wooley, *Science*, 2005, **309**, 1200–1205.

9 S. Martens, J. O. Holloway and F. E. Du Prez, *Macromol. Rapid Commun.*, 2017, **38**, 1700469.

10 S. C. Solleder, R. V. Schneider, K. S. Wetzel, A. C. Boukis and M. A. R. Meier, *Macromol. Rapid Commun.*, 2017, **38**, 1600711.

11 J.-F. Lutz, *Macromolecules*, 2015, **48**, 4759–4767.

12 R. K. Roy, A. Meszynska, C. Laure, L. Charles, C. Verchin and J.-F. Lutz, *Nat. Commun.*, 2015, **6**, 7237–7239.

13 A. C. Boukis, K. Reiter, M. Frölich, D. Hofheinz and M. A. R. Meier, *Nat. Commun.*, 2018, **9**, 1439.

14 L. Hartmann, *Macromol. Chem. Phys.*, 2011, **212**, 8–13.

15 L. Hartmann and H. G. Börner, *Adv. Mater.*, 2009, **21**, 3425–3431.

16 D. Karamessini, B. E. Petit, M. Bouquey, L. Charles and J.-F. Lutz, *Adv. Funct. Mater.*, 2017, **27**, 1604595.

17 M. Porel, D. N. Thornlow, C. M. Artim and C. A. Alabi, *ACS Chem. Biol.*, 2017, **12**, 715–723.

18 M. Porel, D. N. Thornlow, N. N. Phan and C. A. Alabi, *Nat. Chem.*, 2016, **8**, 590–596.

19 A. C. Boukis and M. A. R. Meier, *Eur. Polym. J.*, 2018, **104**, 32–38.

20 M. Passerini, *Gazz. Chim. Ital.*, 1921, **51**, 126–129.

21 S. C. Solleder, D. Zengel, K. S. Wetzel and M. A. R. Meier, *Angew. Chemie - Int. Ed.*, 2016, **55**, 1204–1207.

22 S. C. Solleder, S. Martens, P. Espeel, F. E. Du Prez and M. A. R. Meier, *Chem. - A Eur. J.*, 2017, **23**, 13906–13909.

23 S. C. Solleder and M. A. R. Meier, *Angew. Chemie - Int. Ed.*, 2014, **53**, 711–714.

24 S. Billiet, K. De Bruycker, F. Driessen, H. Goossens, V. Van Speybroeck, J. M. Winne and F. E. Du Prez, *Nat. Chem.*, 2014, **6**, 815–821.

25 H. A. Houck, K. De Bruycker, S. Billiet, B. Dhanis, H. Goossens, S. Catak, V. Van Speybroeck, J. M. Winne and F. E. Du Prez, *Chem. Sci.*, 2017, **8**, 3098–3108.

26 H. A. Houck, K. De Bruycker, C. Barner-Kowollik, J. M. Winne and F. E. Du Prez, *Macromolecules*, 2018, **51**, 3156–3164.

27 G. Cavallo, A. Al Ouahabi, L. Oswald, L. Charles and J.-F. O. Lutz, *J. Am. Chem. Soc*, 2016, **138**, 2.

28 L. Charles, C. Laure, J.-F. Lutz and R. K. Roy, *Macromolecules*, 2015, **48**, 4319–4328.

29 L. Charles, in *Sequence-Controlled Polymers*, ed. J.-F. Lutz, Wiley VCH, Weinheim, 1st edn., 2018, pp. 479–504.

30 C. Laure, D. Karamessini, O. Milenkovic, L. Charles and J.-F. Lutz, *Angew. Chemie - Int. Ed.*, 2016, **55**, 10722–10725.

31 U. Saim Gunay, B. Eric Petit, D. Karamessini, D. Gigmes, L. Charles and J.-F. Lutz, *Chem*, 2016, **1**, 23–24.

32 J. A. Amalian, T. T. Trinh, J.-F. Lutz and L. Charles, *Anal. Chem.*, 2016, **88**, 3715–3722.

33 European Patent Office, EP1964838A1, 2008.

34 D. Van Lysebetten, S. Felissati, E. Antonatou, L. Carrette, P. Espeel, E. Foquet, F. E. Du Prez and A. Madder, *ChemBioChem*, 2018, **19**, 641–646.

35 Y. Abdouni, G. Yilmaz and C. R. Becer, *Macromol. Rapid Commun.*, 2017, **38**, 1700212.

36 G. Yilmaz and C. R. Becer, *Eur. Polym. J.*, 2013, **49**, 3046–3051.

37 D. Ponader, F. Wojcik, F. Beceren-Braun, J. Dernedde and L. Hartmann, *Biomacromolecules*, 2012, **13**, 1845–1852.

38 C. Gerke, M. F. Ebbesen, D. Jansen, S. Boden, T. Freichel and L. Hartmann, *Biomacromolecules*, 2017, **18**, 787–796.

39 R. R. Wang, J. J. Yan, R. L. Yang, D. H. Pan, W. Li, Y. P. Xu, L. Z. Wang, X. Y. Wang and M. Yang, *J. Polym. Sci. Part A Polym. Chem.*, 2017, **55**, 2053–2060.

40 T. Rudolph, P. Espeel, F. E. Du Prez and F. H. Schacher, *Polym. Chem.*, 2015, **6**, 4240–4251.

41 Z. Zhang, Y. You, D. Wu and C. Y. Hong, *Macromolecules*, 2015, **48**, 3414–3421.

Hoofdstuk IX
Nederlandstalige samenvatting

IX.1 Inleiding

De ontwikkeling van het allereerste volledig gesynthetiseerd polymeer door de Gentenaar Leo Bakeland in 1907 (beter bekend als Bakeliet®),[1] was het startpunt van een onderzoeksveld dat vandaag de dag is uitgegroeid tot een enorm, wereldwijd industrieel niveau. Dagelijks worden er enorme hoeveelheden aan polymeermaterialen gebruikt, meestal in de vorm van verbruiksvoorwerpen, zoals PET flessen of verpakkingen, maar ook in meer high-end toepassingen, zoals in computers of auto's. In totaal produceert de polymeerindustrie meer dan 340 miljoen ton kunststoffen per jaar. Ook in België vertegenwoordigt de polymeersector een aanzienlijk deel van de lokale economie, dit vooral in Vlaanderen wat vertaald wordt in baanbrekend onderzoek in dit veld in zowel onze maatschappij en universiteiten. Gedurende de afgelopen 30 jaar is polymeeronderzoek uitgebreid van de productie van bulkmaterialen, gemaakt uit eenvoudige bouwstenen, naar polymeren met meer specifieke en unieke structuren en eigenschappen, zoals blok co-polymeren, graft-polymeren en dendrimeren.[2] De ontdekking van een aantal gecontroleerde radicalaire polymerisaties[3–6] in de jaren 80 en 90,[7–9] bood nieuwe kansen om meer precieze structuren te verkrijgen met beperkte dispersiteit voor specifieke toepassingen. Deze ontdekking stimuleerde het onderzoek naar nieuwe materialen en mogelijkheden binnen de industrie en academia wereldwijd.[2]

In vergelijking met natuurlijke biopolymeren, (bv. DNA),[10] zijn deze "gecontroleerde" polymeren eigenlijk niet altijd zo gecontroleerd. Biomacromoleculen in ons lichaam (bv. DNA, enzymen, ezv) hebben een exact gedefinieerde primaire structuur én een bepaalde en vaste monomeervolgorde. Deze specifieke moleculaire eigenschappen en complexe structuren zijn belangrijk voor hun biologische functie zoals het opslaan van de genetische code of katalyse van essentiële biochemische reacties.[11] Ter illustratie, alle genetische informatie is opgeslagen in ons DNA. De combinatie en volgorde van de monomeren in het DNA schrijft een leesbare code van informatie dat door ons lichaam uitgelezen kan worden. Dit is enkel mogelijk dankzij de strikt gedefinieerde eigenschappen van deze biomacromoleculen en is niet gelimiteerd tot informatieopslag. Een andere categorie van biomacromoleculen met bepaalde belangrijke functies in ons lichaam zijn de proteïnen en enzymen. Chemici wereldwijd hebben hun inspiratie uit dit biologisch concept van streng gedefinieerde biomacromoleculen gehaald om hun onderzoek verder uit te breiden om synthetisch, gecontroleerde macromoleculen te ontwikkelen. Dit leidde de laatste 10-15 jaar tot een nieuw gebied in

chemisch/polymeer onderzoek; de *sequentie gecontroleerde chemie*. Het werd voor het eerst opgemerkt in 2005 door Hawker en Wooley,[12] maar het onderzoeksveld werd beter geïntroduceerd en ondersteund door Jean-François Lutz in 2010.[13] Dit gebied binnen de polymeerchemie wordt gezien als één van de volgende "hot topics" van onze tijd, zoals gecontroleerde radicalaire polymerisaties 20 jaar geleden.

Binnen *sequentie controle* bestaan er twee verschillende en belangrijke categorieën: de zogenaamde *sequentie gecontroleerde* en *sequentie gedefinieerde* macromoleculen. Veel wetenschappers gebruiken deze twee termen op een onachtzame manier, maar er is een subtiel en belangrijk verschil tussen beide.[14–17] *Sequentie gecontroleerde chemie* verwijst naar macromoleculen waarbij hun monomeervolgorde vaststaat, maar de ketens zijn niet van één bepaalde lengte, wat leidt tot dispersiteit. Vaak zijn deze *sequentie gecontroleerde polymeren* gemaakt door technieken zoals gecontroleerde radicalaire polymerisaties.[14–18] Anderzijds zijn er *sequentie gedefinieerde macromoleculen*. Hier ligt niet alleen de monomeervolgorde vast, maar de structuur is discreet en uniform, dus hebben alle ketens exact dezelfde lengte.[14–17] Een andere eigenschap van sequentie gedefinieerde macromoleculen is dat zij vaak oligomeren zijn i.p.v. polymeren, omdat hun synthese meestal praktisch beperkt is tot een stapsgewijze aanpak en geen polymerisatie.[14] De klasse van sequentie gedefinieerde macromoleculen is de focus van dit onderzoek, wat besproken wordt in deze thesis.

Een sequentie gedefinieerd oligomeer wordt vaak gerealiseerd door efficiënte en orthogonale reacties, dit omdat een stapsgewijze aanpak gehanteerd wordt voor de synthese van zulke structuren.[19,20] De introductie van het concept van "klik"chemie door Sharpless *et. al.* in 2001[21] had een diepgaand effect op zowel organisch en polymeer onderzoek wereldwijd.[22–28] Klikreactie is een term die gehanteerd wordt voor een aantal chemische reacties die aan een aantal strikte voorwaarden voldoen. Sharpless heeft hiervoor 10 voorwaarden gedefinieerd om een reactie echt klik te noemen:

⇒ *Stereospecifiek*
⇒ *Brede toepasbaarheid*
⇒ *Modulair*
⇒ *Vormt alleen onschadelijke bijproducten (die gemakkelijk kunnen verwijderd worden via niet-chromatografische technieken)*
⇒ *Hoge opbrengst*
⇒ *Beginnen van gemakkelijk verkrijgbare startmaterialen*
⇒ *Eenvoudige reactieomstandigheden*
⇒ *Geen of onschadelijke oplosmiddelen*
⇒ *Stabiele reactieproducten*

⇒ *Bij voorkeur enkel één reactietraject.*

Deze voorwaarden werden later uitgebreid om meer toepasbaar op polymeerniveau te zijn.[29] Equimolariteit, grootschalige opzuivering en een snelle reactietijd zijn belangrijk voor efficiënte polymeer-polymeer koppelingen. Andere reacties die efficiënt zijn maar niet aan alle klikvoorwaarden voldoen, zijn de zogenaamde "klikgeïnspireerde" reacties. Klikchemie en klikgeïnspireerde reacties bleken cruciaal in de vooruitgang van sequentie controle en voor veel van de reacties die besproken werden binnen deze thesis.

Binnen dit doctoraat werden er twee specifieke soorten van klikgeïnspireerde en klikreacties onderzocht: thiolactonchemie en 1,2,4-triazoline-3,5-dione (TAD) chemie. Thiolacton is een beschermde thiol functionaliteit[30] die door een ring-opening reactie met een amine vrijgelaten wordt. Hierdoor is deze thiol beschikbaar voor een onmiddellijke thiol-een reactie met een acrylaat of acrylamide. Deze tweestaps reactie (een amine-thiolacton-ene conjugatie) leidt tot een dubbele modificatie van de thiolactongroep.[30] Hoewel de mogelijke nevenreacties het moeilijk maken om thiolactonchemie als echte klikchemie te bestempelen, wordt het door zijn efficiëntie een klikgeïnspireerde reactie genoemd.

Veel onderzoek binnen de Polymer Chemistry Research Group aan Universiteit Gent gaat naar thiolactonchemie en sequentie controle maar ook polymeersynthese en postmodificatie.[31–40] TAD is een heel interessante molecule dat tijdens dit doctoraat voor de eerste keer in het gebied van sequentie controle gebruikt werd. Hoewel TAD reeds sinds 1894 bestaat,[41] duurde het tot de jaren 1960-1970 dat veel onderzoek gedaan werd op deze molecule door o.a. Cookson *et. al*.[42–44]. Vanaf 2014 begon onze groep te werken op TAD chemie.[45–52] Door de hoge reactiviteit, kan TAD bijna onmiddellijk een heel efficiënte reactie ondergaan. De twee belangrijkste hierin zijn de Diels-Alder[53] en Alder-een reacties.[52] De reactiesnelheid en evenwicht zijn afhankelijk van substraat en reactieomstandigheden. Reacties met indolen, bijvoorbeeld, zijn thermoreversibel.

Binnen deze thesis werd TAD-chemie gebruikt om nieuwe dynamische protocollen te ontwikkelen waardoor zowel irreversibele en reversibele reacties kunnen gebruikt worden om onze kennis rond TAD-chemie verder uit te breiden en nieuwe toepassingen van sequentie gedefinieerde macromoleculen te ontdekken.

IX.2 Overzicht van de resultaten

Hoofdstuk I is een Engelstalige inleiding tot de polymeerwetenschap en zijn evolutie naar sequentie controle waarin kort het doel binnen elk project van dit doctoraat worden besproken. Bovendien is er een overzicht van alle hoofdstukken in deze thesis. **Hoofdstuk II** gaat dieper in op de theoretische achtergrond van dit gebied binnen de polymeerchemie. Beginnen wordt gedaan met de evolutie van de polymeerchemie naar meer gecontroleerde polymerisaties zoals vrije radicalaire polymerisaties en hoe wetenschappers hun inspiratie genomen hebben uit de Natuur om specifieke macromoleculen te ontwikkelen. Het verschil tussen *sequentie gecontroleerde* en *sequentie definieerde macromoleculen* wordt hier in meer detail uitgelegd en de verschillende beschikbare technieken zoals reacties in vaste fase of vloeistoffase aangeduid worden. Een aantal bio-geïnspireerde routes om sequentie gedefinieerde macromoleculen te maken, worden hier tevens ook beschreven. Vervolgens is er een uitgebreid overzicht aan klik en klikgeïnspireerde routes binnen sequentie controle met de focus op thiolactonchemie en Diels-Alder reacties omdat deze meer relevant zijn voor de thesis. Daarnaast is er ook een inleiding tot multicomponent reacties (vooral op de Passerini en Ugi reacties). Tenslotte, wordt TAD-chemie geïntroduceerd waarin de synthese en reactiviteit van TAD-moleculen beschreven wordt.

Hoofdstuk III beschrijft een project dat in samenwerking met het Polymer Chemistry Laboratory van Queen Mary, University of London uitgevoerd werd. Deze groep is gespecialiseerd in thioacrylaatchemie[54,55] en samen met onze kennis van thiolactonchemie, hebben wij een nieuwe sequentie gedefinieerd vierstaps protocol ontwikkeld.[40] In dit onderzoek werd de thiolacton met ethanolamine geopend en vervolgens was er een Michael-additie reactie met een ethyl thioacrylaat molecule. Deze functionaliteit kon later met verschillende primaire amines gemodificeerd werden door een gekatalyseerde reactie. Tenslotte werd een α-thiolacton-γ-isocyanaat molecule gebruikt om de protocol cyclus opnieuw te beginnen en zo gedefinieerde oligomeren te maken.

Hoofstuk IV rapporteert onze voortdurende inspanningen om een thiolactonchemie gebaseerde protocol te ontwikkelen waardoor de vooropgestelde sequentie met verschillende primaire amines geïntroduceerd kon worden. Ten opzichte van het protocol in hoofdstuk III, was het mogelijk om de volledige synthetische cyclus binnen twee stappen in plaats van vier te vervolledigen.[39] De thiolacton werd met drie verschillende primaire amines geopend met een daaropvolgende thiol-een reactie met *N*-hydroxyethyl acrylaat in een tweestaps reactie. Een nieuwe thiolacton molecule werd aan de keten gekoppeld door de reactie tussen de eindstandige hydroxy groep en een zelfgemaakt α-thiolacton-γ-isocyanaat molecule. Bovendien was het mogelijk om dit protocol te automatiseren door een

gemodificeerde peptide robot. Het protocol was eerst manueel geoptimaliseerd en kon tot lange sequenties met de robot worden gemaakt. Bij langere sequenties (van zes herhalende monomeren of meer) was het noodzakelijk om een opzuivering te doen met prep-HPLC. Ook waren verschillende vaste-fase resins gebruikt om de veelzijdigheid van het protocol aan te tonen. Dit hoofdstuk toont zowel de voordelen van vaste-fase reacties als van thiolactonchemie. Voornamelijk de eenvoudig dubbele modificatie van thiolacton, gecombineerd met het gebruiksgemak van vaste-fase reacties betekent dat er een mogelijkheid is om een bibliotheek van verschillende sequenties tegelijkertijd te maken.

Hoofdstuk V introduceert de combinatie van TAD-chemie met thiolacton. Het concept was deze klik en klik-geïnspireerde functionaliteiten op één molecule te brengen als een multifunctionele bouwsteen om sequentie gedefinieerde oligomeren te maken. Een vaste-fase resin werd met een geconjugeerde dieen structuur gefunctionaliseerd. De additie van een TAD-thiolacton molecule *via* een Diels-Alder reactie aan het dieen is een eenvoudigere en snellere manier dan met thiolacton isocyanaat. Vervolgens was de thiolactongroep beschikbaar voor een ring-opening reactie met een primair amine en een onmiddellijke thiol-een reactie met een geconjugeerde dieenacrylaat. Dit geeft opnieuw een vrij dieen waarbij de cyclus opnieuw kan worden gestart en zo uiteindelijk een sequentie gedefinieerde structuur te bekomen. De grootste uitdaging van dit werk was de TAD-thiolacton molecule te maken en dit omdat gefunctionaliseerde urazoles (de precursor van TAD-moleculen) moeilijk zijn om te maken.[52] Daarom werd gestart met een aantal model studies om de compatibiliteit van TAD en thiolacton functionaliteiten te testen. Hoewel uiteindelijk de gewenste molecule bereid werd, was de opbrengst en zuivering van de reacties heel moeilijk. Tenslotte was een multigefunctionaliseerd oligomeer gemaakt met zes verschillende repeterende eenheden, maar met lagere zuiverheid dan verwacht. De problemen tijdens de synthese en opzuivering van de TAD-thiolacton molecule en mogelijk nevenreacties met de thiolacton aminolyse konden oorzaken hiervan zijn.

Door de resultaten van Hoofdstuk V is het traject van dit doctoraat veranderd. Dit wordt beschreven in **Hoofdstuk VI.** Er werd beslist om verder met TAD-chemie te werken en niet met thiolacton omwille van zijn eenvoud en hogere snelheid. Hoofdstuk V toonde aan dat de TAD-reactie supersnel en efficiënt was en dat thiolactonchemie nevenreacties en begrenzingen hadden. Door een samenwerking met de Karlsruhe Instituut voor Technologie (KIT) in Duitsland, werd TAD-chemie gecombineerd met de Passerini drie-component reactie (P-3CR).[14] De P-3CR is een orthogonale reactie tussen een aldehyde, isocyanide en een carbonzuur. Om een sequentie gedefinieerd protocol te maken, hadden wij een TAD-carbonzuur en een geconjugeerde dieen molecule gemaakt. Met het gebruik van verschillende aldehyden was het mogelijk om oligomeren met een hoogmoleculair gewicht (> 7 kDa) te bekomen met een goede zuiverheid. Met dit protocol werd in oplossing en op vaste-fase gewerkt om de twee

strategieën te vergelijken. Hierin werd opbrengst, tijd, zuiverheid, opzuiveringen en polymerisatiegraad bekeken.

Dankzij de goede resultaten van de combinatie van TAD-chemie en de P-3CR, werd dit onderzoek verder uitgebreid door meer dynamische TAD-chemie te gebruiken, zoals in **hoofdstuk VII** beschreven is. Hier werd de thermoreversible reactie tussen TAD-moleculen en indolen onderzocht om kleine gedefinieerde sequenties te maken om codes te schrijven die later uitgelezen kunnen worden. Opnieuw wordt hier gebruik gemaakt van hetzelfde TAD-carbonzuur, samen met verschillende indool-aldehyden en isocyaniden. De sequentie werd geschreven door de verschillende isocyaniden en de verschillende indool-aldehyden markeerden de locatie van de isocyanide. Wanneer de sequentie wordt opgewarmd tot 150 °C, worden de dynamische TAD-indoolverbindingen verbroken. Terwijl de reactie terug naar kamertemperatuur gebracht werd, ontstond er een onleesbaar mengsel van verschillende oligomeren. Na een tweede opwarming reageerde TAD echter opnieuw met het aanwezige dieen via een Diels-Alder reactie waardoor nu wel een leesbaar mengsel van monomeren verkregen werd. De originele volgorde van de code (geïntroduceerd door de verschillende isocyaniden) was enkel leesbaar voor mensen wie de juiste volgorde van de indool-aldehyden locatie moleculen kent. De codes kunnen uitgelezen worden *via* Liquid Chromatography Mass Spectroscopy (LCMS). De reacties waren meestal in oplossing om een hogere opbrengst van materiaal te verkrijgen. De chemie werd verder uitgebreid naar de Ugi vier-component reactie (U-4CR) om nog meer informatie te encrypteren.

In **hoofdstuk VIII** is er een Engelstalige conclusie en vooruitblik die hieronder kort samengevat wordt.

IX.3 Conclusie en vooruitblik

Chemici hopen dat de ontwikkeling van sequentie gedefinieerde macromoleculen nieuwe toepassingen in de polymeerwetenschap zullen toelaten.[56] De vooruitgang die al binnen de laatste 10 jaren werd gemaakt, leidde tot veel verschillende synthetische routes om gedefinieerde macromoleculen op te bouwen.[19,57] Een aantal toepassingen worden nu al gepubliceerd.[56] Bijvoorbeeld, met gebruik van sequentie gedefinieerde oligomeren is het nu mogelijk om data op te slaan,[33,58–61] zoals in de vorm van een QR-code[33] of voor de encryptie of bescherming van informatie.[59,62] Toepassingen zoals anti-fraude zien een toekomst in het gebruik van sequentie gedefinieerde oligomeren.[63–67] Andere gebieden binnen het onderzoek naar sequentie controle, liggen meer in het veld van biomedische[67–71] of biokatalytische toepassingen.[72]

In onze onderzoeksgroep werd thiolactonchemie al geïntroduceerd als een belangrijke molecule voor polymeersynthese en post-modificaties.[36–38,73–75] Bovendien werd het ook met succes gebruikte om sequenties op te bouwen.[31,33,34] In het begin van dit doctoraat werd thiolactonchemie verder onderzocht als hulpmiddel in de opbouw van een sequentie dankzij de mogelijkheden van eenvoudige modificaties door de amine-thiol-een geconjugeerde reactie. Binnen dit doctoraat werden thioacrylaten gebruikt in combinatie met de thiolactonchemie binnen het veld van sequentiecontrole.[40] Hun gekatalyseerde modificatie met primaire amines leidt tot een nieuw vierstapsprotocol. Hoewel succesvol multifunctionele oligomeren gemaakt konden worden, was het protocol te lang en te complex in vergelijking met andere thiolacton protocollen.[34] Uiteindelijk werd er een eenvoudigere tweestaps protocol ontwikkeld waardoor de thiolactoneenheid met verschillende primaire amines werd geopend, waarop een thiol-een reactie met een hydroxyacrylamide-eenheid op volgde. Verder was het mogelijk om dit protocol te automatiseren en de verkregen oligomeren op te zuiveren door prep-HPLC. Hoewel het interessant is om de gedefinieerde sequentie te introduceren door verschillende amines te gebruiken met een andere oligomeerstructuur, was het protocol uit hoofdstuk IV uiteindelijk niet zo snel, betrouwbaar en gemakkelijk in vergelijking met eerder onderzoek binnen onze onderzoeksgroep.[34] Wanneer snelheid van minder belang is maar een sterke backbone nodig is of als bepaalde functionaliteiten enkel mogelijk zijn om te introduceren als een amine, kan dit protocol uit Hoofdstuk IV wel aangewend worden.

Ten slotte, door de combinatie van TAD en thiolactonchemie binnen één protocol (hoofdstuk V), werd beslist om enkel verder te werken met TAD-chemie. Dankzij een productieve samenwerking met KIT, werd TAD-chemie en P-3CR gecombineerd.[14] De ultrasnelle reactiviteit van TAD met een geconjugeerd dieen, in combinatie met de orthogonaliteit en veelzijdigheid van multicomponentreacties, leidde tot een nieuwe tweestaps protocol dat zowel in de vloeistof- als vaste-fase mogelijk was. Hierdoor was het mogelijk om een vergelijking te maken tussen deze twee methodes wat betreft opbrengst, tijd, zuiverheid, opzuiveringen en polymerisatiegraad, wat nooit eerder in het veld van sequentie controle gepubliceerd werd. Deze resultaten gaven de inspiratie voor het werk dat binnen hoofdstuk VI beschreven werd. Door de reversibele reactie tussen TAD en indool componenten werd het mogelijk om sequentie gedefinieerde moleculen te maken met een dynamische covalente binding waarop een code geschreven werd aan de hand van verschillende isocyaniden. Door verwarmen bij 150 °C, was het mogelijk om de TAD- indool verbinding te breken en de code te beveiligen. Enkel na een tweede behandeling bij hoge temperatuur in de aanwezigheid van een dieen kon de sequentie gedefinieerde molecule worden ontcijferd en uitgelezen door LCMS, enkel door de personen die de initiële volgorde van de indolen kende.

Het succesvol gebruik van TAD-chemie, in combinatie met multicomponentreacties, toont de voordelen en nadelen tussen vloeistoffase en vaste-fase reacties voor sequentie-definitie. Het onderzoek op dynamische sequenties is momenteel in de proof-of-concept fase. Het idee hier is dat dit concept verder wordt uitgebreid naar steeds langere en meer complexe sequenties die het mogelijk maken om grotere hoeveelheden informatie op te slaan. Hierin zal ook worden gekeken om deze sequenties in te brengen in materialen voor bepaalde toepassingen zoals anti-fraude.

IX.4 Referenties

1 L. H. Baekeland, *J. Ind. Eng. Chem.*, 1909, **1**, 149–161.

2 J.-F. Lutz, J.-M. Lehn, E. W. Meijer and K. Matyjaszewski, *Nat. Rev. Mater.*, 2016, **1**, 1–14.

3 K. Matyjaszewski and T. P. Davis, Eds., *Handbook of Radical Polymerization*, John Wiley & Sons, 2003.

4 K. Matyjaszewski, *Advances in Controlled/Living Radical Polymerization*, American Chemical Society, Vol. 854., 2003.

5 W. A. Braunecker and K. Matyjaszewski, *Prog. Polym. Sci.*, 2007, **32**, 93–146.

6 K. Matyjaszewski, *Curr. Opin. Solid State Mater. Sci.*, 1996, **1**, 769–776.

7 G. Moad, E. Rizzardo and D. H. Solomon, *Macromolecules*, 1982, **15**, 909–914.

8 J.-S. Wang and K. Matyjaszewski, *J. Am. Chem. Soc.*, 1995, **117**, 5614–5615.

9 M. Kato, M. Kamigaito, M. Sawamoto and T. Higashimura, *Macromolecules*, 1995, **28**, 1721–1723.

10 J. D. Watson and F. H. C. Crick, *Nature*, 1953, **171**, 737–738.

11 J.-F. Lutz, T. Y. Meyer, M. Ouchi and M. Sawamoto, Eds., *Sequence-Controlled Polymers: Synthesis, Self-Assembly and Properties*, American Chemical Society, Washington DC, 2014.

12 C. J. Hawker and K. L. Wooley, *Science*, 2005, **309**, 1200–1205.

13 J.-F. Lutz, *Polym. Chem.*, 2010, **1**, 55–62.

14 J. O. Holloway, K. S. Wetzel, S. Martens, F. E. Du Prez and M. A. R. Meier, *Submitted*.

15 J.-F. Lutz, in *Sequence-Controlled Polymers*, ed. J.-F. Lutz, Wiley VCH, Weinheim, 1st edn., 2018, pp. 1–26.

16 J.-F. Lutz, *Macromol. Rapid Commun.*, 2017, **1700582**, 1–12.

17 J. A. De Neve, J. J. Haven, L. Maes and T. Junkers, *Polym. Chem.*, 2018, **9**, 4692–4705.

18 G. Gody, T. Maschmeyer, P. B. Zetterlund and S. Perrier, *Nat. Commun.*, 2013, **4**, 2505–2514.

19 S. Martens, J. O. Holloway and F. E. Du Prez, *Macromol. Rapid Commun.*, 2017, **38**, 1700469.

20 S. Martens, J. O. Holloway and F. E. Du Prez, in *Sequence-Controlled Polymers*, ed. J.-F. Lutz, Wiley VCH, Weinheim, 2018, pp. 379–416.

21 H. C. Kolb, M. G. Finn and K. B. Sharpless, *Angew. Chemie - Int. Ed.*, 2001, **40**, 2004–2021.

22 B. Helms, J. L. Mynar, C. J. Hawker and J. M. J. Fréchet, *J. Am. Chem. Soc.*, 2004, **126**, 15020–15021.

23 N. V. Tsarevsky, K. V. Bernaerts, B. Dufour, F. E. Du Prez and K. Matyjaszewski, *Macromolecules*, 2004, **37**, 9308–9313.

24 P. Wu, A. K. Feldman, A. K. Nugent, C. J. Hawker, A. Scheel, B. Voit, J. Pyun, J. M. J. Fréchet, K. B.

Sharpless and V. V. Fokin, *Angew. Chemie Int. Ed.*, 2004, **43**, 3928–3932.

25 D. D. Díaz, S. Punna, P. Holzer, A. K. McPherson, K. B. Sharpless, V. V. Fokin and M. G. Finn, *J. Polym. Sci. Part A Polym. Chem.*, 2004, **42**, 4392–4403.

26 W. H. Binder and C. Kluger, *Macromolecules*, 2004, **37**, 9321–9330.

27 C. Barner-Kowollik and A. J. Inglis, *Macromol. Chem. Phys.*, 2009, **210**, 987–992.

28 P. Espeel and F. E. Du Prez, *Macromolecules*, 2015, **48**, 2–14.

29 C. Barner-Kowollik, F. E. Du Prez, P. Espeel, C. J. Hawker, T. Junkers, H. Schlaad and W. Van Camp, *Angew. Chemie Int. Ed.*, 2011, **50**, 60–62.

30 P. Espeel and F. E. Du Prez, *Eur. Polym. J.*, 2015, **62**, 247–272.

31 P. Espeel, L. L. G. Carrette, K. Bury, S. Capenberghs, J. C. Martins, F. E. Du Prez and A. Madder, *Angew. Chemie - Int. Ed.*, 2013, **52**, 13261–13264.

32 S. C. Solleder, S. Martens, P. Espeel, F. E. Du Prez and M. A. R. Meier, *Chem. - A Eur. J.*, 2017, **23**, 13906–13909.

33 S. Martens, A. Landuyt, P. Espeel, B. Devreese, P. Dawyndt and F. E. Du Prez, *Nat. Commun.*, 2018, **9**, 4451.

34 S. Martens, J. Van Den Begin, A. Madder, F. E. Du Prez and P. Espeel, *J. Am. Chem. Soc.*, 2016, **138**, 14182–14185.

35 D. Frank, P. Espeel, S. Claessens, E. Mes and F. E. Du Prez, *Tetrahedron*, 2016, **72**, 6616–6625.

36 S. Reinicke, P. Espeel and F. E. Du Prez, *Polym. Chem.*, 2014, **5**, 5461–5470.

37 P. Espeel, F. Goethals, F. Driessen, L.-T. T. Nguyen and F. E. Du Prez, *Polym. Chem.*, 2013, **4**, 2373–2616.

38 P. Espeel, F. Goethals, M. M. Stamenović, L. Petton and F. E. Du Prez, *Polym. Chem.*, 2012, **3**, 1007–1015.

39 J. O. Holloway, C. Mertens, F. E. Du Prez and N. Badi, *Macromol. Rapid Commun.*, 2018, **40**, 1800685.

40 J. O. Holloway, S. Aksakal, F. E. Du Prez and C. Remzi Becer, *Macromol. Rapid Commun.*, 2017, **38**, 1700500.

41 J. Thiele and O. Stange, *Justus Liebig's Ann. der Chemie*, 1894, **283**, 1–46.

42 R. C. Cookson, S. S. H. Gilani and I. D. R. Stevens, *J. Chem. Soc. C*, 1967, **0**, 1905–1909.

43 R. C. Cookson, S. S. H. Gilani and I. D. R. Stevens, *Tetrahedron Lett.*, 1962, **3**, 615–618.

44 R. C. Cookson, S. S. Gupte, I. D. R. Stevens and C. T. Watts, *Org. Synth.*, 1971, **51**, 121–127.

45 O. Türünç, S. Billiet, K. De Bruycker, S. Ouardad, J. Winne and F. E. Du Prez, *Eur. Polym. J.*, 2015, **65**, 286–297.

46 S. Billiet, K. De Bruycker, F. Driessen, H. Goossens, V. Van Speybroeck, J. M. Winne and F. E. Du Prez, *Nat. Chem.*, 2014, **6**, 815–821.

47 S. Chattopadhyay and F. E. Du Prez, *Eur. Polym. J.*, 2016, **81**, 77–85.

48 H. A. Houck, K. De Bruycker, S. Billiet, B. Dhanis, H. Goossens, S. Catak, V. Van Speybroeck, J. M. Winne and F. E. Du Prez, *Chem. Sci.*, 2017, **8**, 3098–3108.

49 O. Roling, K. De Bruycker, B. Vonhören, L. Stricker, M. Körsgen, H. F. Arlinghaus, B. J. Ravoo and F. E. Du Prez, *Angew. Chemie - Int. Ed.*, 2015, **54**, 13126–13129.

50 G. Becker, L. Vlaminck, M. M. Velencoso, F. E. Du Prez and F. R. Wurm, *Polym. Chem.*, 2017, **8**, 4074–4078.

51 N. Van Herck and F. E. Du Prez, *Macromolecules*, 2018, **51**, 3405–3414.

52 K. De Bruycker, S. Billiet, H. A. Houck, S. Chattopadhyay, J. M. Winne and F. E. Du Prez, *Chem. Rev.*, 2016, **116**, 3919–3974.

53 O. Diels and K. Alder, *Justus Liebig's Ann. der Chemie*, 1928, **460**, 98–122.

54 S. Aksakal and C. R. Becer, *Polym. Chem.*, 2016, **7**, 7011–7018.

55 S. Aksakal, R. Aksakal and C. R. Becer, *Polym. Chem.*, 2018, **9**, 4507–4516.

56 M. A. R. Meier and C. Barner-Kowollik, *Adv. Mater.*, 2019, 1806027.

57 S. C. Solleder, R. V. Schneider, K. S. Wetzel, A. C. Boukis and M. A. R. Meier, *Macromol. Rapid Commun.*, 2017, **38**, 1600711.

58 N. Zydziak, W. Konrad, F. Feist, S. Afonin, S. Weidner and C. Barner-Kowollik, *Nat. Commun.*, 2016, **7**, 1–10.

59 A. C. Boukis, K. Reiter, M. Frölich, D. Hofheinz and M. A. R. Meier, *Nat. Commun.*, 2018, **9**, 1439.

60 H. M. Colquhoun and J.-F. Lutz, *Nat. Chem.*, 2014, **6**, 455–456.

61 J.-F. Lutz, *Macromolecules*, 2015, **48**, 4759–4767.

62 R. K. Roy, A. Meszynska, C. Laure, L. Charles, C. Verchin and J.-F. Lutz, *Nat. Commun.*, 2015, **6**, 7237–7239.

63 U. S. Gunay, B. E. Petit, D. Karamessini, A. Al Ouahabi, J. A. Amalian, C. Chendo, M. Bouquey, D. Gigmes, L. Charles and J.-F. Lutz, *Chem*, 2016, **1**, 114–126.

64 D. Karamessini, T. Simon-yarza, S. Poyer, E. Konishcheva, L. Charles, D. Letourneur and J.-F. Lutz, *Angew. Chemie Int. Ed.*, 2018, **57**, 10574–10578.

65 D. Karamessini, S. Poyer, L. Charles and J.-F. Lutz, *Macromol. Rapid Commun.*, 2017, **1700426**, 1700426.

66 C. Laure, D. Karamessini, O. Milenkovic, L. Charles and J.-F. Lutz, *Angew. Chemie - Int. Ed.*, 2016, **55**, 10722–10725.

67 D. Karamessini, B. E. Petit, M. Bouquey, L. Charles and J.-F. Lutz, *Adv. Funct. Mater.*, 2017, **27**, 1604595.

68 L. Hartmann, *Macromol. Chem. Phys.*, 2011, **212**, 8–13.

69 L. Hartmann and H. G. Börner, *Adv. Mater.*, 2009, **21**, 3425–3431.

70 M. Porel, D. N. Thornlow, C. M. Artim and C. A. Alabi, *ACS Chem. Biol.*, 2017, **12**, 715–723.

71 M. Porel, D. N. Thornlow, N. N. Phan and C. A. Alabi, *Nat. Chem.*, 2016, **8**, 590–596.

72 P. Chandra, A. M. Jonas and A. E. Fernandes, *J. Am. Chem. Soc.*, 2018, **140**, 5179–5184.

73 M. M. Stamenović, P. Espeel, E. Baba, T. Yamamoto, Y. Tezuka and F. E. Du Prez, *Polym. Chem.*, 2013, **4**, 184–193.

74 F. Driessen, S. Martens, B. De Meyer, F. E. Du Prez and P. Espeel, *Macromol. Rapid Commun.*, 2016, **37**, 947–951.

75 F. Driessen, F. E. Du Prez and P. Espeel, *ACS Macro Lett.*, 2015, **4**, 616–619.

List of publications

Publications included (in full or in part) within this thesis

Click and click-inspired chemistry for the design of sequence-controlled polymers

S. Martens, J. O. Holloway and F. E. Du Prez, *Macromol. Rapid Commun.*, 2017, **38**, 1700469.

Tailored modification of thioacrylates in a versatile, sequence-defined procedure

J. O. Holloway, S. Aksakal, F. E. Du Prez and C. R. Becer, *Macromol. Rapid Commun.*, 2017, **38**, 1700500.

Automated synthesis protocol of sequence-defined oligo-urethan-amides using thiolactone chemistry

J. O. Holloway, C. Mertens, F. E. Du Prez and N. Badi, *Macromol. Rapid Commun.*, 2019, **40**, 1800685.

Direct comparison of solution and solid phase synthesis of sequence-defined macromolecules

J. O. Holloway, K. S. Wetzel, S. Martens, F. E. Du Prez and M. A. R. Meier, *Polym. Chem.*, 2019, **10**, 3859-3867.

Book chapter

Click and click-inspired chemistry for the design of sequence-controlled polymers

S. Martens, J. O. Holloway and F. E. Du Prez, in *Sequence-Controlled Polymers*, ed. J. -F. Lutz, Wiley VCH, Weinheim, 2018, pp. 379-416.



Over the last 15 years, chemists have taken inspiration from the many highly complex biopolymers found in Nature, such as DNA, to synthesise non-natural macromolecular architectures which exhibit precise control over both the chain length and sequenced order of monomers. This has led to the introduction of the area of sequence-defined chemistry, which has become labelled as one of the latest 'hot topics' within polymer science. Research groups worldwide have been investigating various synthesis strategies and chemical platforms to result in a diverse range of well-defined macromolecular structures. It is hoped that this synthetic approach will unlock new applications of polymer chemistry, from biomedical advances to long-term data storage solutions and anti-counterfeiting.

Thiolactone and 1,2,4-triazoline-3,5-dione (TAD) chemistries have been the focus of much research activity within the Polymer Chemistry Research group over the last decade. The possible one-pot double modification reaction of thiolactone moieties *via* an amine-thiol-ene conjugation has led to their use not only in polymer modification but also within precision chemistry, where they have been incorporated into solid-phase, iterative protocols for the synthesis of sequence-defined oligomers. Within this thesis, thiolactone chemistry is further explored for the development of new, solid-phase, sequence-defined protocols and the synthesis was carried out in both a manual and automated fashion. TAD moieties have found use in polymer modification on account of their ultrafast reactivity towards certain substrates and the visual feedback they provide as they go from red to colourless upon reaction. Interestingly, their reaction with certain substrates can also be thermoreversible. However, this PhD thesis describes, for the first time, the use of TAD chemistry towards sequence-defined macromolecular synthesis. Its combination with multicomponent reactions resulted first in a comparative study between sequence-defined synthesis using solid- or solution-phase chemistry. Later, exploration of the thermoreversible reactivity of TAD led to the synthesis of dynamic, thermoreversible sequence-defined oligomers which could be both scrambled upon heating and later read-out using mass spectrometry techniques, thus allowing one to encrypt and decrypt a chemical-based code. This resulted in the synthesis of macromolecular pin codes for potential product labelling and anti-counterfeiting applications.

This project has received funding from the European Union's Horizon 2020 research and innovation programme under the Marie Skłodowska-Curie grant agreement No *642083.*

This project was also partially funded by the Ghent University Special Research Fund-ITN (BOF-ITN).

www.pcr.ugent.be

www.cmac.ugent.be

Polymer Chemistry Research Group (PCR)
Centre of Macromolecular Chemistry (CMaC)
Department of Organic and Macromolecular Chemistry
Faculty of Sciences
Ghent University, Campus Sterre
Krijgslaan 281 S4-bis
B-9000, Ghent
Belgium

UNIVERSITEIT GENT